

# Carnegie Mellon University

CARNEGIE INSTITUTE OF TECHNOLOGY

THESIS

SUBMITTED IN PARTIAL FULFILLMENT OF THE REQUIREMENTS

FOR THE DEGREE OF Doctor of Philosophy

**TITLE Oxyfuel Carbon Capture for Pulverized Coal: Techno-Economic Model Creations and Evaluation Amongst Alternatives**

**PRESENTED BY Kyle James Borgert**

**ACCEPTED BY THE DEPARTMENT OF**

**Engineering and Public Policy**

Edward S. Rubin  
ADVISOR, MAJOR PROFESSOR

May 5, 2015  
DATE

Douglas Sicker  
DEPARTMENT HEAD

May 5, 2015  
DATE

**APPROVED BY THE COLLEGE COUNCIL**

Vijayakumar Bhagavatula  
DEAN

May 12, 2015  
DATE

# OXYFUEL CARBON CAPTURE FOR PULVERIZED COAL: TECHNO-ECONOMIC MODEL CREATION AND EVALUATION AMONGST ALTERNATIVES

SUBMITTED IN PARTIAL FULFILLMENT OF THE REQUIREMENTS FOR

THE DEGREE OF

DOCTOR OF PHILOSOPHY

IN

ENGINEERING & PUBLIC POLICY

KYLE JAMES BORGERT

B.S.E., MECHANICAL ENGINEERING, UNIVERSITY OF MICHIGAN

M.S., ENGINEERING & PUBLIC POLICY, CARNEGIE MELLON UNIVERSITY

CARNEGIE MELLON UNIVERSITY

PITTSBURGH, PENNSYLVANIA

MAY 2015

Copyright © by Kyle J. Borgert, 2015

All rights reserved

# ACKNOWLEDGEMENTS

“No man holding a strong belief on one side of a question, or even wishing to hold a belief on one side, can investigate it with such fairness and completeness as if he were really in doubt and unbiased: so that the existence of a belief, not founded on fair inquiry, unfits a man for the performance of this necessary duty.”

-W.K. Clifford-

Throughout this endeavor I have attempted to follow these words and produce a fair, technically sound assessment of one of the carbon capture technologies under consideration for reducing carbon emissions from electricity generation. As we collectively move forward, as a species inhabiting the only planet we have ever known, it is my hope that we have the resolve necessary to ensure our continued existence upon it. If I have here fulfilled my duty, perhaps Sisyphus will be one step closer to eventually finding rest.

I must first thank the woman who has stood beside me as I have struggled through completion. Nicole, I love you, and could not have made it through this without you. I only hope that I may one day return the favor for your patience and continued grace throughout this process. To my parents, my admiration and thanks for all you have given and the opportunities you have afforded me in my brief life is truly beyond words. This is as much your accomplishment as it is my own. To my sister Jamie, with whom I was fortunate enough to share a passion for learning and restlessness for achievement which refused to be confined by the trappings of a humble rural upbringing. To all my friends and family who suffered my ethereal thoughts, occasional arrogance, and youthful exuberance; many thanks. This would not have been possible, and I would not be who I am, without all of your love and support. Thank You.

Next, I would like to thank my committee chair Professor Edward S. Rubin. This effort would not have been possible without your support. I have always appreciated your continued patience and faith in my abilities. To committee member Allen L. Robinson, I would like to thank you for your time and intellectual support. You were a wonderful teacher and I relished the opportunity to take your courses. Also, thank you for always making time, it meant the world to me. To committee member M. Granger Morgan, thanks for your personal investment in the EPP Department. I always felt like EPP was home for me; whether I was in Pittsburgh, or literally in your childhood home. To committee member H. Scott Matthews, I have taken many courses in my life, but none have left more pleasant memories of fantastic discourse than yours. You are an excellent teacher and I have been fortunate to have you as a resource these past few years. To committee member Michael Matuszewski, I appreciate your willingness to help and be a part of this project. Lastly, I owe a huge thank you to Haibo Zhai and Karen Kietzke. This project would not have reached completion without you. Thanks for your long hours and patience.

This work was supported by the National Energy Technology Laboratory’s Regional University Alliance (NETL-RUA), a collaborative initiative with technical efforts performed under contract number 24905.913.ER.1041723.

# ABSTRACT

Today, and for the foreseeable future, coal and other fossil fuels will provide a major portion of the energy services demanded by both developed and developing countries around the world. In order to reduce the emissions of carbon dioxide associated with combustion of coal for electricity generation, a wide range of carbon capture technologies are being developed. This thesis models the oxyfuel carbon capture process for pulverized coal and presents performance and cost estimates of this system in comparison to other low-carbon fossil fuel generators.

Detailed process models for oxygen production, flue gas treatment, and carbon dioxide purification have been developed along with the calculation strategies necessary to employ these components in alternative oxyfuel system configurations for different types of coal-fired power plants. These new oxyfuel process models have been implemented in the widely-used Integrated Environmental Control Model (IECM) to facilitate systematic comparisons with other low-carbon options employing fossil fuels.

Assumptions about uncertainties in the performance characteristics of gas separation processes and flue gas duct sealing technology, as well as plant utilization and financing parameters, were found to produce a wide range of cost estimates for oxyfuel systems. In case studies of a new 500 MW power plant burning sub-bituminous Powder River Basin coal, the estimated levelized cost of electricity (LCOE) 95% confidence interval (CI) was 86 to 150 [\$/MWh] for an oxyfuel system producing a high-purity [99.5 mol% CO<sub>2</sub>] carbon dioxide product while capturing 90% of the flue gas carbon dioxide. For a CoCapture oxyfuel system capturing 100% of the flue gas CO<sub>2</sub> together with all other flue gas constituents, the estimated LCOE 95% CI was 90 to 153 [\$/MWh] (all costs in constant 2012 US Dollars).

Using the IECM, an oxyfuel system for CO<sub>2</sub> capture also was compared under uncertainty to an existing amine-based post-combustion capture system for a new 500 MW power plant, with both systems capturing 90% of the CO<sub>2</sub> and producing a high-purity stream for pipeline transport to a geological sequestration site. The resulting distribution for the cost of CO<sub>2</sub> avoided showed the oxyfuel-based system had a 95% CI of 44 to 126 [\$/tonne CO<sub>2</sub>] while the amine-based system cost 95% CI ranged from 50 to 133 [\$/tonne CO<sub>2</sub>]. The oxyfuel cost distribution had a longer tail toward more expensive configurations but over 70% of the distribution showed the oxyfuel-based system to be ~10[\$/tonne CO<sub>2</sub>] lower in cost compared to the amine-based capture system.

An evaluation of several low-carbon generation options fueled by coal and natural gas further considered both direct and indirect greenhouse gas emissions. This analysis showed oxyfuel to be economically competitive with all capture system considered, and also indicated oxyfuel to be the preferred carbon capture technology for minimizing overall carbon intensity. Combined, these results suggest that oxyfuel is a promising carbon capture technology, and the only one which offers the unique ability to capture all the combustion gases to become a truly zero emission coal plant. Realization of the latter option, however, is contingent on the development of new regulatory policies for underground injection of mixed flue gas streams that is outside the scope of this thesis.

# TABLE OF CONTENTS

## Contents

ACKNOWLEDGEMENTS.....	iii
ABSTRACT.....	iv
TABLE OF CONTENTS.....	v
LIST OF FIGURES.....	xi
LIST OF TABLES.....	xxii
Chapter 1 An Introduction .....	1
1.1.    U.S. Electricity Generation and Carbon Emissions.....	1
1.2.    Technology Options for Carbon Capture and Storage for Electrical Generation Units .....	6
1.3.    Storage Options .....	9
1.4.    CCS Development and Deployment.....	9
1.4.1.    The Potential Role of Enhanced Oil Recovery.....	11
1.5.    Objectives and Scope of this Thesis .....	11
1.6.    Organization of this Thesis.....	12
Chapter 2 Oxyfuel Carbon Capture Systems and Components for Pulverized Coal Plants .....	14
2.1    Commonalities with Air-Fired Pulverized Coal Electricity Generation .....	14
2.1.1    Common Components and Retrofit Suitability.....	16
2.2    Proposed Pulverized Coal Oxyfuel Systems .....	16
2.2.1    Potential System Configurations.....	20
2.2.2    Cycle Selection Update Rationale .....	20
2.3    Oxyfuel Plant Components .....	21
2.3.1    Oxyfuel Boilers .....	21
2.3.2    Oxygen Separation Technologies.....	22
2.3.3    Criteria Pollutant Treatment and Removal Systems.....	24
2.3.4    Second Generation Pollution Removal Technologies.....	25
2.3.5    Carbon Dioxide Purification Technologies .....	31
2.3.6    CO <sub>2</sub> Product Transport Pressure Requirements.....	42
2.3.7    Storage Concerns for Impure Carbon Dioxide Products .....	43
Chapter 3 Pulverized Coal Oxyfuel Model Configurations and Conceptual Operation .....	45
3.1    New Oxyfuel Plant Configurations.....	46
3.1.1    Oxyfuel Cycle for Medium-High Sulfur Coals .....	46

3.1.2	Oxyfuel Cycle for Low-Medium Sulfur Coals.....	47
3.1.3	Oxyfuel Cycle for Low Sulfur Coals.....	48
3.2	Detailed Stream Flow Diagrams.....	48
3.3	Carbon Handling System Options .....	52
3.4	Conceptual Calculation Strategy.....	52
3.4.1	Mass Balance.....	53
Chapter 4	Pulverized Coal Oxyfuel Performance Model .....	66
4.1	Performance Model Input and Output Parameters .....	66
4.1.1	Explanation of Key Oxyfuel Specific Parameters .....	67
4.1.2	Key Input Parameter Characterization.....	68
4.1.3	Key Model Outputs .....	69
4.2	Fuel Composition and Normalized Combustion Moisture .....	70
4.3	Oxyfuel Base Plant Performance .....	73
4.3.1	Boiler and Steam Cycle .....	74
4.4	Flue Gas Mass Balance.....	75
4.4.1	Base Flue Gas Recycle Configurations.....	76
4.4.2	General Calculation Algorithm.....	77
4.4.3	Coal Flow Rate.....	78
4.4.4	Oxidant Handling.....	78
4.4.5	Carbon Dioxide and Moisture Mass Balance .....	81
4.4.6	Remaining Flue Gas Constraints .....	86
4.5	Energy Balance.....	87
4.5.1	Gas Thermodynamic Property Calculations.....	87
4.5.2	Combining the Recycle Streams.....	89
4.5.3	Recycle Preheater Energy Balance Model .....	93
4.5.4	Recycle Heat Energy Correction.....	93
4.5.5	ASU and CPU Heat Integration.....	96
4.6	Net Plant Performance .....	99
4.6.1	Flue Gas Recycle Fan.....	99
4.6.2	Net Plant Electrical Output .....	100
Chapter 5	Air Separation Unit Performance Model .....	101
5.1	Application .....	101
5.2	Modeling Approach and Development.....	102

5.3	Summary of Input and Output Parameters .....	106
5.4	Mass and Energy Balance Calculations .....	107
5.4.1	Oxidant Production .....	108
5.4.2	Water Production from Compression.....	108
5.4.3	Nitrogen Vent Stream and Oxidant Balance .....	109
5.4.4	Cooling and Heat Integration .....	111
5.4.5	Electrical Load Requirement .....	112
5.4.6	Oxidant Compressor Electrical Load Requirement .....	113
Chapter 6 Direct Contact Cooler and Polishing Scrubber Performance Model.....		115
6.1	General Power Plant Applications .....	115
6.2	Oxyfuel Application.....	116
6.3	Modelling Approach.....	117
6.4	Saturation Pressure of Water .....	119
6.5	Latent Heat of Water Condensation .....	120
6.6	Sulfur Removal Calculation .....	121
6.7	Summary of Input and Output Parameters .....	121
6.8	Mass and Energy Balance Calculations .....	122
6.8.1	Gas Stream Flow Rate Calculations.....	123
6.8.2	Reagent Stream Flow Rate Calculations .....	125
6.8.3	Precipitant Stream Flow Rate Calculations .....	125
6.8.4	Calculating the Required Cooling Load .....	126
6.8.5	Latent Heat of Water .....	127
6.9	Cooling Water Requirement Calculation .....	128
6.9.1	Water Balance.....	128
6.9.2	Auxiliary Electrical Load Requirements.....	129
Chapter 7 Carbon Processing Unit Performance Model.....		130
7.1	Model Objectives .....	130
7.2	Carbon Handling System Configurations .....	131
7.3	Carbon Handling Bypass .....	131
7.3.1	CoCapture Bypass .....	132
7.3.2	CPU Bypass.....	133
7.4	CoCapture Performance Model .....	135
7.4.1	Summary of Input and Output Parameters .....	135

7.4.2	Mass and Energy Balance Calculations .....	136
7.5	High-Purity Carbon Processing Unit Performance Model .....	141
7.5.1	General Application .....	141
7.5.2	Oxyfuel Application.....	142
7.5.3	Modelling Approach.....	142
7.5.4	Model Structure and Theoretical Foundation .....	143
7.5.5	MATLAB CPU Exergy Analysis Model .....	148
7.5.6	Summary of Input and Output Parameters .....	159
7.5.7	Mass and Energy Balance Calculations .....	159
Chapter 8	Pulverized Coal Oxyfuel Cost Model .....	167
8.1	Plant Costing Method .....	167
8.1.1	Cost Model Terminology.....	167
8.1.2	Total Capital Requirement .....	169
8.1.3	General Component Size and Cost Year Adjustment.....	170
8.1.4	General Operations and Maintenance Cost .....	171
8.2	Base Plant.....	173
8.3	Criteria Pollution Control Units.....	173
8.4	Air Separation Unit.....	174
8.4.1	Capital Cost .....	174
8.4.2	Fixed and Variable Operations and Maintenance Cost .....	175
8.5	Oxidant Compressor .....	176
8.5.1	Capital Cost .....	176
8.5.2	Fixed and Variable Operations and Maintenance Cost .....	177
8.6	Direct Contact Cooler and Polishing Scrubber .....	177
8.6.1	Capital Cost .....	177
8.6.2	Fixed and Variable Operations and Maintenance Cost .....	178
8.7	Carbon Processing Unit.....	180
8.7.1	Capital Cost .....	180
8.7.2	Fixed and Variable Operations and Maintenance Cost .....	181
8.8	Balance of Oxyfuel Plant .....	182
8.8.1	Flue Gas Recycle Fan.....	182
8.8.2	Flue Gas Recycle Ducting .....	183
8.9	Plant Water Usage and Cooling .....	183

8.10	Carbon Dioxide Transport and Storage.....	183
8.11	Incremental Cost of Electricity.....	184
8.12	Cost of Carbon Dioxide Captured and Avoided .....	185
Chapter 9 Applications of the Pulverized Coal Oxyfuel Model in the IECM .....		187
9.1	Technical Component Sensitivity.....	187
9.1.1	Air Separation Unit.....	187
9.1.2	Direct Contact Cooler and Polishing Scrubber.....	196
9.1.3	Carbon Processing Unit.....	201
9.1.4	CoCapture System.....	216
9.1.5	Flue Gas Recirculation Rate .....	223
9.1.6	Transport and Storage .....	226
9.1.7	Plant Size and Financial Parameters .....	228
9.2	Total Plant Analysis: Reference Air Fired Plants .....	230
9.3	Base Oxyfuel Plants for Sensitivity Analysis.....	232
9.4	Coal Composition Effects .....	236
9.5	Recycle Configuration Effects .....	238
9.5.1	Ideal Gas Separation Oxyfuel.....	240
9.6	Uncertainty Analysis .....	241
9.6.1	Financial Uncertainty .....	241
9.6.2	Performance Uncertainty.....	243
9.6.3	Total Uncertainty .....	245
9.6.4	Magnitude of Uncertainty Sources .....	249
Chapter 10 Comparison of PC Oxyfuel to Alternative Low-Carbon Fossil Fuel Generators .....		254
10.1	Oxyfuel and Amine Capture Under Uncertainty.....	254
10.1.1	Wyoming Powder River Basin Sub-bituminous Coal .....	255
10.1.2	Illinois #6 Bituminous Coal.....	258
10.1.3	North Dakota Lignite .....	260
10.2	Generation Alternatives: A Comparison including a Life-Cycle Perspective.....	262
10.2.1	Upstream Emissions Inventory .....	265
Chapter 11 Policy Analysis and Implications.....		268
11.1	New Source Performance Standards .....	268
11.2	Valuing Carbon Dioxide.....	271
11.3	Low Carbon Capacity Standard .....	275

Chapter 12 Summary and Conclusions .....	277
12.1 Thesis Summary .....	277
12.2 Future Research for Oxyfuel Systems .....	279
12.3 Concluding Remarks.....	280
REFERENCES.....	281
Appendix A Low-Carbon Capacity Standard .....	288
Appendix B Recycle Preheating and Energy Balance.....	300
Appendix C Matlab Code for Carbon Processing Unit .....	303
Appendix D Case Studies.....	312
Appendix E Illinois #6 IECM Base Plant: Full IECM Configuration.....	317

# LIST OF FIGURES

Figure 1.1 Annual generation of electricity in the United States by fuel type (10). .....	2
Figure 1.2. . The substantial increase in natural gas generating capacity in the past decade is very prominent and actually now exceeds the total installed capacity of coal (11). .....	3
Figure 1.3. U.S. electric power producer price for natural gas [\$/MCF] from 2002-2014 (12) .....	4
Figure 1.4. Annual carbon dioxide emissions from electricity generation from coal and natural gas (13).4	
Figure 1.5. Annual electricity generation with historical data and projections through 2040 (14) .....	5
Figure 1.6. Projected world coal consumption in Quadrillion BTU (3). Presents the essentially level continued consumption of coal by OECD countries while the Non-OECD consumption is expected to increase by 50 Quads over the next 20 years. ....	5
Figure 1.7. Representation of the three prominent forms of carbon dioxide capture for electricity generation units (15). ....	6
Figure 1.8. The installed capacity of CCS is far behind the goals outlined in the stabilization wedges emissions reduction scheme.....	10
Figure 1.9. Prices of crude oil for the West Texas Intermediate (WTI) over the past decade (25). .....	11
Figure 2.1 Simplified process flow diagram of a pulverized coal plant with the interaction between boiler and electricity generation shown. ....	14
Figure 2.2 Simplified process flow diagram of the oxyfuel process. The interaction with the steam cycle has been omitted for clarity. ....	15
Figure 2.3 Cold recycle oxyfuel process flow diagram designed by B&W. This process is suited to highly corrosive coals. ....	17
Figure 2.4 Cool recycle oxyfuel process flow diagram with wet flue gas desulfurization designed by B&W. This process is suited to highly corrosive coals and offers a heat rate advantage over the cold recycle process.....	18
Figure 2.5 Cool recycle oxyfuel process flow diagram with spray dry absorption designed by B&W. This process is suited for less corrosive coals and offers an improved heat rate compared to the WFGD variation. ....	18
Figure 2.6 Warm recycle oxyfuel process flow diagram with spray dry absorber bypass designed by B&W. This process is for the least corrosive coals and offers the most thermally efficiency oxyfuel configuration.....	19
Figure 2.7 Process flow diagram of the warm recycle oxyfuel configuration adapted for B&W with the Sour Compression Process being developed by Air Products. ....	20
Figure 2.8 Simplified layout of flue gas indirect contact cooler and the main compressors of the sour gas compression process (52). ....	27
Figure 2.9 Sour compression process layout diagram (45).....	28

Figure 2.10 Phase 1 test results showing very high levels of SO <sub>2</sub> and NO <sub>x</sub> removal using the test rig on slip-stream from the Alstom oxy-coal facility in Windsor, CT (52). .....	30
Figure 2.11 Process diagram for a dual flash system producing a gaseous CO <sub>2</sub> product at 110bar (19)..	32
Figure 2.12 . Comparison between distillation and 2-stage flash systems for a stipulated CO <sub>2</sub> recovery rate (54). .....	33
Figure 2.13 Process diagram for a single flash, single distillation column system producing gaseous CO <sub>2</sub> at a pressure of 110 bar (48).....	34
Figure 2.14 Process diagram for a single flash, single distillation column system with extensive heat integration producing gaseous CO <sub>2</sub> at a pressure of 110 bar (48).....	35
Figure 2.15 Process diagram for a dual flash system with membrane separation and permeate recycle (49). .....	36
Figure 2.16 Process diagram for a single flash, single distillation column system with membrane separation and permeate recycle (50).....	38
Figure 2.17 Process diagram for a dual flash, single distillation column system with 30 bar liquefied CO <sub>2</sub> product (45). .....	39
Figure 2.18 Process diagram for a triple flash, single distillation column system with 7 bar liquefied CO <sub>2</sub> product (45). .....	40
Figure 2.19 Minimum required pressure to avoid two-phase flow as calculated by Vattenfall (56) using GERG-2004 equation of state software at 285K. Avoidance of 2-phase flow is essential so that traditional pumps and pipeline materials may be used without fear of cavitation and accelerated corrosion, respectively.....	42
Figure 2.20 Normalized CO <sub>2</sub> storage capacity at 330K as calculated using the carbon dioxide impurity capacity adjustment equation, where the densities are calculated with Peng-Robinson Equation of State (57). At low purity oxyfuel operation (CoCapture) this analysis shows that geological capacity could be reduced nearly forty percent compared to pure carbon dioxide.....	43
Figure 3.1 Process flow diagram for the oxyfuel model utilized in IECM version 9 (and previous). All the flue gas is treated by the traditional pollution control technologies and is handled as a single recycle stream to the boiler. ....	45
Figure 3.2 Process flow diagram for coals with a sulfur content above 1.5 wt%. This process is most similar to the pre-existing oxyfuel model in that the entire gas stream is treated for particulates and sulfur. ....	46
Figure 3.3 Process flow diagram for coals with sulfur contents between 0.5 [wt%] and 1.5 [wt%] .....	47
Figure 3.4 Process flow diagram for coals with very low sulfur concentrations (<0.5 wt%). The warm recycle process allows for the secondary recycle stream to be split off prior to sulfur treatment. The advantage to this configuration is that it allows for a very high thermal energy recycle stream to be returned to the boiler and consequently enables higher plant efficiency. ....	48

Figure 3.5 Detailed stream flow diagram for the cool recycle configuration with wet flue gas desulfurization. This process configuration is recommended for coals with a sulfur mass fraction above 1.5%.....	49
Figure 3.6 Detailed stream flow diagram for the cool recycle configuration with spray dry absorption desulfurization. This process configuration is recommended for coals with a sulfur mass fraction that is between 0.5% and 1.5%.....	50
Figure 3.7 Detailed stream flow diagram for the warm recycle configuration with spray dry absorption desulfurization. This process configuration is recommended for coals with a sulfur mass fraction that is below 0.5%.....	51
Figure 3.8 Decision flow diagram of the generic oxyfuel plant layout. ....	54
Figure 3.9 The carbon dioxide flow rates from coal and that removed via the Z-stream reach convergence in less than 15 iterations in this example with a FGR of 60%.....	56
Figure 3.10 CO <sub>2</sub> convergence is accomplished very quickly with low flue gas recirculation rates. For 45% FGR less than ten iterations were required to reach steady state operation. ....	57
Figure 3.11 CO <sub>2</sub> convergence is accomplished quickly with moderate flue gas recirculation rates. For 60% FGR, the low end of expected FGR, less than fifteen iterations were required to reach steady state operation.....	58
Figure 3.12 CO <sub>2</sub> convergence is accomplished fairly quickly with elevated flue gas recirculation rates. For 75% FGR, a value near the higher end of anticipated FGR, just over twenty iterations were required to reach steady state operation.....	58
Figure 3.13 CO <sub>2</sub> convergence is accomplished much more slowly with high flue gas recirculation rates. Roughly 70 iterations were required to reach convergence for 90% FGR. This number is still computationally reasonable however despite 90% FGR being on the extreme high end of expected FGR's. ....	59
Figure 3.14 Iterations of FGR streams are not limited by the convergence of required oxygen. The amount of oxygen required can be determined in less than five iterations because many of the inputs can be calculated prior to the first iteration and are constant in value, being a multiple of the stoichiometric oxygen required based upon the chosen fuel composition. ....	60
Figure 3.15 Recycle moisture convergence is accomplished through increasing the amount of moisture removed from the bulk flue gas by the DCCPS. A larger fraction of the bulk recycle is assigned to the primary split (passes through DCCPS) until the maximum recycle moisture constraint can be satisfied. .	61
Figure 3.16. Initial recycle moisture is too great under an equivalent primary to secondary split regime for this example. As the split ratio is adjusted in favor of the primary, the overall recycle moisture is decreased until the MRM constraint is met; at which point the system is allowed to converge. ....	62
Figure 3.17 Moisture convergence is accomplished much more slowly with high flue gas recirculation rates. In this demonstration over 70 iterations were required to reach convergence for 80% FGR. This number is still computationally reasonable however a more efficient algorithm has been used for the IECM code. ....	63

Figure 3.18 Sulfur dioxide convergence in the recycle stream is accomplished by increasing the removal efficiency of the WFGD/SDA until the NSPS limit can be met in the bulk recycle stream. ....	64
Figure 4.1 The inverse proportionality of fuel and recycle moisture dictates as linear trade-off between the NCM and Maximum Recycle Moisture. The relation exhibits the anticipated result of lignite coals (high NCM) requiring relatively dry recycle conditions whereas bituminous coals (low NCM) can operate with higher recycle moisture levels. ....	72
Figure 4.2 IECM boiler efficiency for arbitrary fuel compositions .....	74
Figure 4.3 Simplified process flow diagram of the cool recycle process overlaid with the system boundary for determining the mass balance of the flue gas.....	75
Figure 4.4 Simplified process flow diagram for the warm recycle process of the pulverized coal oxyfuel model in the IECM. Only equipment which alters the gaseous composition of the flue gas streams has been shown for simplicity.....	76
Figure 4.5 Simplified process flow diagram for the cool recycle process of the pulverized coal oxyfuel model in the IECM. Only equipment which alters the gaseous composition of the flue gas streams has been shown for simplicity.....	76
Figure 4.6. Iterations of FGR streams are not limited by the convergence of required oxygen. The amount of oxygen required can be determined in less than five iterations because many of the inputs can be calculated prior to the first iteration and are constant in value, being a multiple of the stoichiometric oxygen required based upon the chosen fuel composition. ....	80
Figure 4.7 Walk of the recycle fractions (alpha and beta) as the recycle moisture constraint is met .....	84
Figure 4.8 Trajectory of the mass flow rate of moisture in the recycle stream as the system works toward convergence. ....	85
Figure 4.9 Diagram depicts the stream flows associated with the combining of the three feed streams which comprise the bulk recycle stream (1) and the heat exchange between the bulk recycle stream (2,3) and the flue gas (4,5). ....	90
Figure 4.10 Recycle heat input ratio as a function of the normalized combustion moisture of the fuel being burned.....	94
Figure 4.11 Example of the disparity in the recycle to input heat ratio (RIHR) which may result from the use of a wet flue gas desulfurization ratio.....	95
Figure 4.12 Plot of the steam cycle heat rate delta observed in the DOE cases as a function of the total reported heat integration duty.....	97
Figure 4.13 Simplified heat integration effect on gross turbine output for oxyfuel plants in the IECM. This relation allows the thermal benefits of heat integration with the ASU and CPU to be accounted for without needing to reiterate the mass balance across the entire plant. ....	98
Figure 5.1 The relation between specific separation work and single train capacity is best represented with an exponential regression equation. This regression equation is used to predict the base work requirements of single train ASU's with a capacity between 200 and 550 [tph]. ....	103

Figure 5.2 A piecewise correlation was developed for oxidant purity levels above and below the point where oxygen and argon are the two remaining atmospheric gases to be separated in the ASU. These correlation equations are used to adjust the specific work requirements to produce oxygen at a 95 [mol%] purity. ....	105
Figure 5.3 Comparison of the old and new ASU model performance across oxidant purity levels from a production rate of 400 tonnes of oxygen per hour. ....	106
Figure 5.4 Process flow diagram of all the gas and liquid streams entering and exiting the air separation unit. ....	108
Figure 6.1 Illustration of the physical working process utilized in the direct contact cooler polishing scrubber. ....	116
Figure 6.2 Block flow diagram representing the stream flows accounted for in the direct contact cooler and polishing scrubber model. ....	117
Figure 6.3 Saturation pressure of water vapor in air as a function of temperature between 0 and 300 degrees centigrade. ....	119
Figure 6.4 The latent heat of vaporization of water is temperature dependent. The decline in LHOV magnitude is very linear over the temperature window expected during operation of the DCCPS.....	120
Figure 7.1 Process flow diagram of the carbon handling system bypass. ....	132
Figure 7.2 Matrix of gamma fractions corresponding to CRR and CAP values for the CPU system with bypass. White cells represent the feasible region; red cells violate mass balance constraints. ....	134
Figure 7.3 Process flow diagram of all the gas and liquid streams entering and exiting the CoCapture unit. ....	136
Figure 7.4 Phase diagram of carbon dioxide which shows the path taken by carbon dioxide gas in the carbon processing unit, cooled at an elevated pressure and condensed out as a liquid, as the temperature approaches the triple point.....	142
Figure 7.5 Flow diagram of the CPU which represents how stream data is handled and presented in literature. ....	143
Figure 7.6 Depiction of the debiting of compression work required to produce the reported CO2 product stream from the reported CPU work data. This yielded the fraction of reported work assumed to be associated with the separation of gases in the feed stream. ....	144
Figure 7.7 The real separation work is the difference between the black box CPU work and the compression work on a per tonne entrained CO2 basis. The real separation work is comprised of the minimum work required to move from state 1 to 2 along with all work lost to process inefficiencies...	145
Figure 7.8 Diagram of the system used to conduct the exergy analysis as coded in MATLAB.....	148
Figure 7.9 Three dimensional plot of the ideal separation data from the MATLAB model for a 70% carbon dioxide inlet stream converted to a flowrate to the CPU basis [kWh/tonne].....	152
Figure 7.10 Plot of the reduced order model for ideal separation work along with the raw data from the MATLAB model. ....	154

Figure 7.11 Residual error plot of the raw data from the MATLAB exergy analysis model and the exponential reduced order model generated using DataFit Software. ....	154
Figure 7.12 Comparison of ROM predicted ideal separation work values to the raw data generated from the MATLAB thermodynamic model shows that the overall fit is very good, but lacks some accuracy at very low values.....	155
Figure 7.13 Three dimensional plot of the real separation work data from the MATLAB model for a 70% carbon dioxide inlet stream converted to a flowrate to the CPU basis [kWh/tonne] with the 2nd Law efficiency relation applied. ....	157
Figure 7.14 Three dimensional plot of the real (blue) and ideal (red) separation work response surfaces for a 70% carbon dioxide inlet stream.....	158
Figure 7.15 Process flow diagram of all the gas and liquid streams entering and exiting the CPU.....	160
Figure 8.1 Flow chart of how cost estimates get built up from the equipment cost to the total capital required for both plant components and the overall plant.....	169
Figure 8.2 Process facility cost of ASU's across various oxygen production rates presented in 2010 dollars. The correlation coefficient is relatively weak $\sim 0.65$ , however the data is relatively well represented by a 6/10ths scaling law .....	174
Figure 8.3 Oxygen compressor process facility cost curves for various exit pressures .....	176
Figure 9.1. Water produced by the main air compressor of the air separation unit across relative humidity levels for various ambient temperatures .....	188
Figure 9.2. ASU electrical power consumption across air ingress rates (5% typical) to the recycled flue gas stream.....	189
Figure 9.3. Electrical use of the ASU across excess air requirements (5% typical) for combustion in the boiler .....	189
Figure 9.4. Specific oxygen separation work of the ASU as a function of oxidant purity .....	190
Figure 9.5. Comparison of the pre-existing ASU model with the updated ASU model which reflects the real world specific separation work across oxidant purity levels.....	191
Figure 9.6 As the ASU transitions from removing nitrogen to separating oxygen from argon the net plant efficiency decreases substantially due to the large increase in ASU unit work.....	192
Figure 9.7 The levelized cost of electricity increases markedly in reverse proportion to the decrease in net plant efficiency at high oxidant purity levels.....	192
Figure 9.8. Effect of required oxidant delivery pressure on the ASU specific work .....	193
Figure 9.9. Number of ASU trains required across gross electrical output of the base plant .....	193
Figure 9.10. Specific oxygen separation work of the ASU across gross electrical output of the base plant .....	194
Figure 9.11. Electrical load of the ASU across the gross electrical output of the base plant .....	195
Figure 9.12. Process facilities cost of the ASU across the gross electrical output of the base plant.....	195

Figure 9.13. Annual operations and maintenance costs for the ASU across gross electrical output of the base plant.....	196
Figure 9.14. Mass flow rate of water in the flue gas stream exiting the DCCPS as a function of operating exit temperature .....	197
Figure 9.15. Cooling water flow rate requirement for the DCCPS as a function of operating exit temperature.....	197
Figure 9.16. Electrical load required to operate the DCCPS across operating exit temperature .....	198
Figure 9.17. Process facilities cost of the DCCPS as a function of operating exit temperature.....	199
Figure 9.18. Flue gas recirculation fan load across DCCPS operating exit temperature .....	200
Figure 9.19. Required DCCPS trains across gross electrical output. ....	200
Figure 9.20 Process facilities cost of the DCCPS as a function of the gross electrical output. ....	201
Figure 9.21. Unit carbon purification work of the CPU across carbon dioxide purity levels of the product stream. ....	202
Figure 9.22 Effect of CPP on the total load of the CPU for the base plant. ....	202
Figure 9.23 Net electrical output of the base plant is decreased as the CPP is increased. ....	203
Figure 9.24 The levelized annual cost of transport and storage declines slightly in erratic fashion with increasing CPP for the base plant. ....	203
Figure 9.25 Accelerating increase in the CPU unit work as the CRR is increased. ....	204
Figure 9.26 Steady decrease in the net electrical output of the base plant and the CRR is increased. ..	205
Figure 9.27 Intuitively, the carbon intensity of electricity generated by the base plant decreases as the CRR of the CPU is increased. ....	206
Figure 9.28 The PFC of the pipeline transport system for the base plant increases discretely as the CRR of the CPU is increased. ....	206
Figure 9.29 Transport and storage costs measured by two different metrics as a function of CPU CRR. ....	207
Figure 9.30 CPU load increases dramatically as the operating temperature of the DCCPS gets towards the high end of the spectrum. ....	208
Figure 9.31 The total electrical load of the flue gas recirculation and purification has a knee at around 50 centigrade for the base plant.....	208
Figure 9.32 The net electrical output of the plant reflects the knee identified in the flue gas recirculation and purification load as a function of DCCPS operating temperature. ....	209
Figure 9.33 CPU load increase about 10% as the product pressure is increased from 7 to 15 MPa.....	210
Figure 9.34 CPU load decreases as the CO2 compressor efficiency is increased. ....	210
Figure 9.35 The electrical power consumption of the CPU increases dramatically once the air ingress rate exceeds ~10%. ....	211

Figure 9.36 CPU load increased as excess air is provided to the boiler due to dilution of the flue gas. There is a knee in this curve that is the result of the carbon dioxide to oxygen ratio causing a change in the second law separation efficiency of the CPU. ....	212
Figure 9.37 Effect of 2nd Law Separation efficiency on the CPU load.....	213
Figure 9.38 CPU load is a linear function of plant size.....	213
Figure 9.39 The required number of CPU trains increased to two once the gross electrical output exceeds 900 [MW]. ....	214
Figure 9.40 PFC of the CPU has a discontinuity from the inclusion of a second train when gross electrical output exceeds 900 [MW]. ....	215
Figure 9.41 Levelized flue gas recirculation and purification costs are a muted reflection of the gross PFC for this umbrella system. ....	215
Figure 9.42 Excess air has little effect of the overall load of the CoCapture system.....	216
Figure 9.43 The effect of air ingress on CoCapture load is dramatic as a result of the added gas which must be compressed.....	217
Figure 9.44 Reduction in overall plant efficiency is just shy of 1.5 percentage points for an air ingress rate of 10%.....	217
Figure 9.45 Marked increase in LCOE result from increases in the air ingress rate. This is of potential concern as oxyfuel plants age and leaks form. ....	218
Figure 9.46 The overall PFC of the CoCapture system is actually decreased at high air ingress rates. This is because it allows for the ASU, the most capital intensive component, to be undersized.....	218
Figure 9.47 Condensed flue gas moisture is reduced to a quarter of its value at 20 centigrade when operating at 75 centigrade. ....	219
Figure 9.48 Operating the DCCPS at elevated temperatures results in a decrease in the net electrical output of the base plant. ....	220
Figure 9.49 CoCapture power use increases steadily as a function of plant size. ....	221
Figure 9.50 The number of required CoCapture trains increases to two at a gross plant output of 800 [MW]. ....	221
Figure 9.51 Process facilities cost of the CoCapture carbon handling system across gross electrical output. ....	222
Figure 9.52 The operations and maintenance costs associated with the total CoCapture system display a discontinuity in an otherwise constantly increasing function of plant size where the second train is added. ....	222
Figure 9.53 Total capital requirement of the base plant as the flue gas recycle rate is increased. There are two perturbations in the curve resulting from alterations to the TSP and FGD system to accommodate the change in gas volume. ....	223
Figure 9.54 Capital requirement of the TSP system as a function of flue gas recycle rate for the base plant. ....	224

Figure 9.55 Capital requirement of the FGD system as a function of the flue gas recycle rate for the base plant. ....	224
Figure 9.56 Increasing electrical loads to operate the gas handling and processing equipment at higher flue gas recycle rates reduces the net electrical output of the base plant. ....	225
Figure 9.57 LCOE increases at an increasing rate for the base plant as the flue gas recirculation rate is increased. ....	225
Figure 9.58 Required discrete pipe diameters required to handle the mass flow of carbon dioxide product as a function of gross electrical output. ....	226
Figure 9.59 The levelized cost of transporting the captured carbon dioxide decreases in a stepwise fashion as gross plant size is increased. ....	227
Figure 9.60 Levelized storage costs reduce with increasing plant size primarily due to high fixed operating costs which can only be reduced by spreading them over a larger base. ....	227
Figure 9.61 Specific total capital requirement of two plants with either carbon handling system as a function of gross electrical output. ....	228
Figure 9.62 Levelized cost of electricity for two plants with either carbon handling system as a function of the gross electrical output. The CPU system has the lower LCOE across the range examined for the nominal plant configurations. ....	229
Figure 9.63 The fixed charge factor plays an important role in determining the LCOE from a project. .	229
Figure 9.64 Assumed fuel cost can have a large effect on the LCOE of the nominal plant. In this instance, an increase in LCOE of 20% was observed as coal prices ranged from 30 to 70 [\$/tonne]. ....	230
Figure 9.65. Net plant efficiency [HHV %] across steam cycle performance levels (Sub Critical, Super Critical, and Ultra-Super Critical) for both CPU (Case 8) and CoCapture (Case 9) with Illinois #6 Coal. All costs are reported in constant 2012 dollars. ....	233
Figure 9.66. Specific carbon dioxide emissions for CPU (Case 8) and CoCapture (Case 9) for Illinois #6 Coal across steam cycle performance levels (Sub Critical, Super Critical, and Ultra-Super Critical). All costs are reported in constant 2012 dollars. ....	234
Figure 9.67. Cost of carbon dioxide avoidance cost for Illinois #6 Coal across steam cycle performance levels (Sub Critical, Super Critical, and Ultra-Super Critical) for CPU (Case 8) and CoCapture (Case 9). All costs are reported in constant 2012 dollars. ....	235
Figure 9.68. Cost of carbon dioxide capture cost for Illinois #6 Coal across steam cycle performance levels (Sub Critical, Super Critical, and Ultra-Super Critical) for CPU (Case 8) and CoCapture (Case 9). All costs are reported in constant 2012 dollars. ....	236
Figure 9.69 Cumulative distribution function of total revenue requirement (LCOE) for warm recycle oxyfuel using PRB coal. Revenue requirement for CPU system is below the CoCapture system for all probabilities. All costs are reported in constant 2012 dollars. ....	242
Figure 9.70 Cumulative distribution function of CO <sub>2</sub> avoidance cost for warm recycle oxyfuel using PRB coal. Avoidance cost for CPU system is above the CoCapture system for all probabilities. All costs are reported in constant 2012 dollars. ....	243

Figure 9.71 Cumulative distribution function of total revenue requirement (LCOE) for warm recycle oxyfuel using PRB coal. Revenue requirement for CPU system is below the CoCapture system by approximately 8 [\$ /MWh] for all probabilities. All costs are reported in constant 2012 dollars. .... 244

Figure 9.72 Cumulative distribution function of CO<sub>2</sub> avoidance cost for warm recycle oxyfuel using PRB coal. Avoidance cost for CPU system is above the CoCapture system for most all probabilities, but are indistinguishable for the high performing systems sampled. All costs are reported in constant 2012 dollars..... 245

Figure 9.73 Total uncertainty plot of the base, CPU, and CoCapture plant configurations for levelized cost of electricity (LCOE). Deterministic results have been shown for reference and indicate that the case studies generated in this work are optimistic. All costs are reported in constant 2012 dollars. .... 246

Figure 9.74 Total uncertainty plot of the base, CPU, and CoCapture plant configurations for carbon dioxide avoidance cost. Deterministic results have been shown for reference and indicate that the case studies generated in this work are optimistic. All costs are reported in constant 2012 dollars. .... 247

Figure 9.75 The uncertainty distributions for carbon intensity of the capture systems suggest that most of the variability in the cost metric of avoidance cost is due to cost parameters..... 248

Figure 9.76. Cumulative probability distribution for the PRB oxyfuel system for just the physical performance parameters produced by the Monte Carlo simulations. All costs are reported in constant 2012 dollars..... 249

Figure 9.77. Cumulative probability distribution function for PRB systems including process and project contingency and capital cost uncertainty in addition to performance parameters. All costs are reported in constant 2012 dollars..... 250

Figure 9.78. Cumulative probability distribution function for PRB systems including fuel cost uncertainty along with PFC and performance parameters. All costs are reported in constant 2012 dollars..... 251

Figure 9.79. Cumulative probability distribution function for PRB systems including capacity factor in addition to fuel cost, PFC, and performance parameters. All costs are reported in constant 2012 dollars. .... 252

Figure 9.80. Cumulative probability distribution function for PRB systems including the cost of borrowing money (FCF) in addition to capacity factor, fuel cost, PFC, and performance parameters. All costs are reported in constant 2012 dollars. .... 253

Figure 10.1 Cumulative probability functions for the warm oxyfuel and amine plants have similar LCOE ranges. The warm oxyfuel plant distribution has a longer tail than the amine system, displaying a skew toward higher LCOE values. All costs are reported in constant 2012 dollars..... 256

Figure 10.2 Cumulative probability functions for the warm oxyfuel and post-combustion amine system for carbon dioxide avoidance cost. The warm oxyfuel system has a lower expected avoidance cost across the distribution. All costs are reported in constant 2012 dollars..... 257

Figure 10.3 Cumulative probability functions for the carbon dioxide intensity of electricity produced from the warm oxyfuel and amine systems. The expected emissions from the warm oxyfuel system are approximately 15% lower than the amine system. .... 258

Figure 10.4. Cumulative probability distribution functions for the warm oxyfuel system and amine based capture for Illinois #6 Bituminous Coal. The systems are at near cost parity for this coal when the FCF ranges are similar. All costs are reported in constant 2012 dollars. .... 259

Figure 10.5. Cumulative probability distribution functions for the warm oxyfuel system and amine based capture for Illinois #6 Bituminous Coal. The avoidance cost of the oxyfuel system is stochastically dominate until about 85<sup>th</sup> percentile where amine and oxyfuel are essentially the same. All costs are reported in constant 2012 dollars. .... 260

Figure 10.6. Cumulative probability distribution functions for the cool recycle oxyfuel system and equivalent post combustion capture amine based systems for North Dakota Lignite. The oxyfuel system is stochastically dominant over amine based capture for the ND Lignite. All costs are reported in constant 2012 dollars..... 261

Figure 10.7. Cumulative probability distribution functions for cool oxyfuel and comparable amine based post combustion capture systems for North Dakota Lignite. The efficiency advantage of oxyfuel produces a significant advantage for oxyfuel over amine based PCC. All costs are reported in constant 2012 dollars..... 261

Figure 10.8 Comparison of direct carbon dioxide emission intensity for the six low-carbon fossil fuel generators. All costs are reported in constant 2012 dollars. .... 264

Figure 10.9 Comparison of the 100 year CO<sub>2</sub>e intensity of the six low-carbon fossil fuel generators. All costs are reported in constant 2012 dollars. .... 266

Figure 10.10 The rate of fugitive emissions assumed for the NGCC with Amine Capture facility determines whether it has the lowest or the highest CO<sub>2</sub>e intensity of any of the capture facilities. All costs are reported in constant 2012 dollars. .... 267

Figure 11.1. NSPS compliant carbon capture plants and their LCOE's as a function of enhanced oil recovery revenue. All costs are reported in constant 2012 dollars..... 270

Figure 11.2. A closer look at the interplay between EOR revenue and the three NSPS compliant carbon capture facilities. All costs are reported in constant 2012 dollars. .... 271

Figure 11.3. Levelized cost of electricity for the generation sources evaluated under a carbon dioxide tax. The U.S. social cost of carbon has also been plotted for comparison. All costs are reported in constant 2012 dollars..... 273

Figure 11.4. A zoomed in look at the levelized cost of electricity for the generation sources evaluated under a carbon dioxide tax. The U.S. social cost of carbon has also been plotted for comparison. All costs are reported in constant 2012 dollars. .... 274

Figure 11.5. Summary of Net Cost of New Entry (Net CONE) calculations for electricity generation sources evaluated for the low carbon capacity standard (23). .... 275

# LIST OF TABLES

Table 2-1 Summary of ASU cycles on an equal basis (34).....	23
Table 2-2 Trends in the SO <sub>x</sub> /NO <sub>x</sub> conversion efficiency from Air Products test rig at the Alstom oxy-coal facility (52). .....	31
Table 2-3 PRISM Membrane performance characteristics (49).....	37
Table 2-4 Summary of the seven Air Products purification processes (52). .....	40
Table 3-1 Enumeration of all oxyfuel configurations in the updated model with carbon dioxide handling, sulfur treatment technology, and flue gas recycle selection considered.....	52
Table 3-2 Constraints for the oxyfuel mass balance listed with the effect each has on determining either the primary and secondary recycle fractions or the required performance of criteria pollution control equipment.....	55
Table 3-3 Demonstration of the increase in boiler sulfur content for oxyfuel, relative to air-firing, across a range of fuel sulfur mass fractions.....	64
Table 4-1 Key input parameters for the pulverized coal oxyfuel model with default values and parameter ranges. This list applies once a fuel and recycle configuration have been stipulated.....	69
Table 4-2 Key model outputs of the pulverized coal oxyfuel performance model .....	70
Table 4-3 Normalized combustion moisture are corresponding recycle moisture limits for coals in the IECM Database.....	73
Table 4-4 Steam cycle heat rates for the IECM.....	75
Table 4-5 Example calculation of the stoichiometric oxygen requirement for Appalachian Medium Sulfur Coal .....	79
Table 4-6 Gas Phase Coefficients for the Shomate Relations (59).....	88
Table 4-7 Comparison between previously NIST coefficients and current NIST coefficients.....	89
Table 4-8 Calculated enthalpy values for the example oxidant stream. ....	91
Table 4-9 Thermal Input and Recycle Heat for the DOE Case Studies .....	94
Table 5-1 Summary of ASU performance from recent literature .....	102
Table 5-2 Relative ASU Separation Energy across Oxidant Purity Levels.....	104
Table 5-3 ASU Cooling Duty Information from DOE Oxyfuel Report .....	111
Table 6-1. The constants used in the Antoine Equation are temperature dependent across the range of expected operation of the DCCPS.....	122
Table 7-1 Co-Capture Cooling Duty Information .....	139
Table 7-2 Composition of the inlet gas streams used in MATLAB Exergy Analysis.....	150
Table 7-3 Composition of CO <sub>2</sub> Product Streams for Various CPP Values .....	151
Table 7-4 Ideal separation work values as calculated by the MATLAB model [kWh/tonne CO <sub>2</sub> ]. .....	151

Table 7-5 DOE Case Studies with Ideal Separation Work Values from MATLAB Exergy Analysis.....	156
Table 7-6 CPU Cooling Duty Information .....	163
Table 8-1 Capital Cost Elements and Valuation in the IECM .....	170
Table 8-2 Plant cost index (CEPCI (63)) for all years in which reference cost estimates were performed .....	171
Table 8-3 O&M Cost Elements for a WFGD Unit in the IECM v9 .....	172
Table 8-4 Default O&M Parameters for the ASU Model.....	175
Table 8-5 Default O&M Parameters for the DCCPS Model.....	179
Table 8-6 Default O&M Parameters for the DCCPS Model.....	181
Table 9-1 Summary of cost and performance data for air fired pulverized coal and natural gas combined cycle reference plants. All costs are reported in constant 2012 dollars.....	231
Table 9-2. Cost and performance summary for CPU (Case 8) and CoCapture (Case 9) oxyfuel reference plants with Illinois #6 Coal across steam cycle performance levels (Sub Critical, Super Critical, and Ultra-Super Critical). All costs are reported in constant 2012 dollars. ....	232
Table 9-3 Important parameters and results for Appalachian Low Sulfur and North Dakota Lignite modeled in the cool recycle configuration and utilizing a spray dry absorber. All costs are reported in constant 2012 dollars.....	237
Table 9-4 Important parameters and results for Powder River Basin coal utilizing the three (Cases 12-14) new oxyfuel recycle configurations. Case 15 explores the thermodynamic limits of the warm recycle configuration. All costs are reported in constant 2012 dollars. ....	239
Table 9-5 Thermodynamic limit gas separation values (73) for the air separation unit and carbon processing unit.....	240
Table 9-6 Financial uncertainty parameters and their chosen distributions.....	241
Table 9-7 Performance uncertainty parameters and their chosen distributions. ....	244
Table 9-8 Deterministic cases used to compare the uncertainty analysis results. The default IECM fixed charge factor (FCF) is 0.113 and has been used in all the base case studies. Cases 14 and 16 were duplicated with a FCF of 0.14 to demonstrate the importance of this parameter in the uncertainty analysis and are denoted Cases 14a and 16a. All costs are reported in constant 2012 dollars.....	246
Table 10-1 Uncertainty parameters and their chosen distributions for the comparison between warm recycle oxyfuel and post-combustion amine capture systems.....	255
Table 10-2. Cost and performance highlights from the low carbon fossil fuel case studies. All costs are reported in constant 2012 dollars. ....	263
Table 10-3 Emission factors used for converting from consumable flow rates to 100 Year Global Warming Potential [CO <sub>2</sub> e].....	265

Table 11-1. Carbon capture plants capable of meeting or exceeding the carbon dioxide new source performance standard proposed by the Environmental Protection Agency. All costs are reported in constant 2012 dollars..... 269

Table 11-2. Air fired and carbon capture plants evaluated on their economic value under a potential carbon dioxide tax. All costs are reported in constant 2012 dollars. .... 272

# Chapter 1 An Introduction

The combustion of fossil fuels results in the emission of carbon dioxide which is a major greenhouse gas contributing to climate change (1). Carbon dioxide capture and storage (CCS) is a potentially critical technology with which emissions from fossil fuels could be reduced and climate change mitigated. The process of CCS has the potential to reduce future world emissions from energy by 20% (2) and is considered vital to holding the global temperature increase below 2°C (3). Given this importance, information regarding the cost and performance of CCS is highly sought after by a variety of actors in government, industry and other organizations for purposes of policy analysis, investment decisions, technology assessments, R&D activities, and energy-environmental policy-making, including development of legislation and regulations involving CCS (4).

There are three general technological approaches to carbon capture: pre-combustion, post-combustion, and oxyfuel. Currently, none of these possess a distinct advantage with regard to both cost and efficiency (5). Given the lack of a single, preferred technological pathway, policy makers need access to cost and performance estimates for the most viable technologies which could be used for carbon capture in a particular situation. Unfortunately such estimates can be difficult to find or expensive and time consuming to produce. Furthermore, existing estimates can be challenging to modify if different financial, technological, or environmental conditions apply. For example, in 2010 the U.S. National Energy Technology Laboratory estimated that on a new supercritical coal-fired power plant with amine-based CO<sub>2</sub> capture and long term storage, would lower the plant efficiency by 11.9 percentage points and would increase the cost of electricity by \$52/MWh compared to a plant without CCS (6). This provides a valuable baseline, but it is also based on a large number of financial, technological and site specific assumptions. Thus, it can be challenging, if not impossible, to extend these results to alternate scenarios. The development of accessible analytical tools that can provide flexible estimates, such as the Integrated Environmental Control Model (IECM) (7), provides an important resource for analysts and policy makers concerned with energy and environmental policy. This work adds to the already robust capabilities of the IECM by updating and expanding the pulverized coal oxyfuel model.

## 1.1. U.S. Electricity Generation and Carbon Emissions

With the recent proposal of rules by the U.S. Environmental Protection Agency (EPA) regulating emissions from new and existing electricity generation sources, 111(b) (8) and 111(d) (9), the generation of electricity in the United States is heading towards uncharted waters. With history as our guide, the legality of these rules is sure to be challenged and the ultimate outcome for specific regulations to be faced by generators remains in doubt. Understanding the current state of the electricity generation industry in the United States is imperative to gaining insight into what technologies might be required to respond to regulations as well as where we stand as we progress toward an uncertain future.

For over a century, the generation of electricity in the U.S. has been anchored by coal. Although there have been changes in the source region, composition, and rank of the average coal burned by facilities

as the industry responded to criteria pollution legislation; coal has remained the stalwart producer. A culmination of factors have seen generation from natural gas make significant inroads on coal's market share, but for the time being coal remains king (Fig. 1.1).

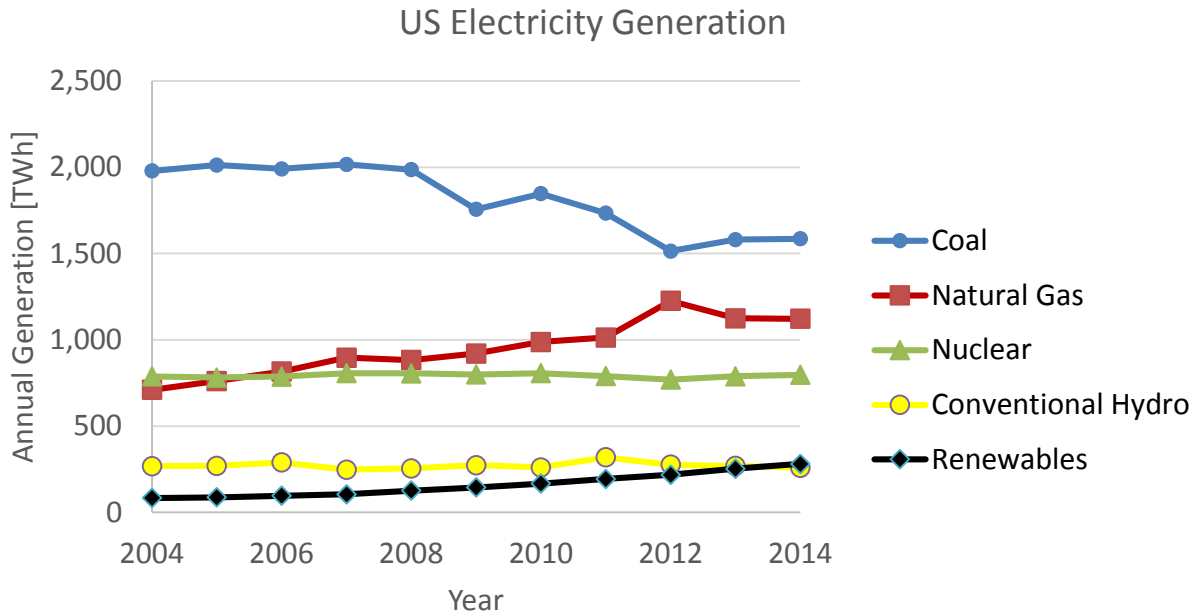


Figure 1.1 Annual generation of electricity in the United States by fuel type (10).

A few of the aforementioned factors which have led to an upsurge in natural gas generation are: installed generation capacity, attractive natural gas prices, and increasingly stringent air emission standards. Air emission standards, such as the Mercury and Air Toxics Standard (MATS), are putting pressure on operators to reduce (or eliminate) the number of operating hours for older coal generating facilities not equipped with emission control equipment. In many cases, decommissioning these assets, and making up for their generation with natural gas or renewables, makes greater financial sense than investing in the pollution control equipment which would be required to keep them in their generation portfolio. The macro result has been a reduction in the available coal generation capacity available.

The second factor eroding the market share of coal has been widespread investment in the installation of natural gas generation capacity. In the United States, the two decades since the release of the first IPCC report on climate change have seen little change in the overall percentage of electricity generated from fossil fuels (~70%); but the majority of the new generation capacity has been supplied by natural gas units (Fig. 1.2).

### U.S. Generation Capacity by Energy Source

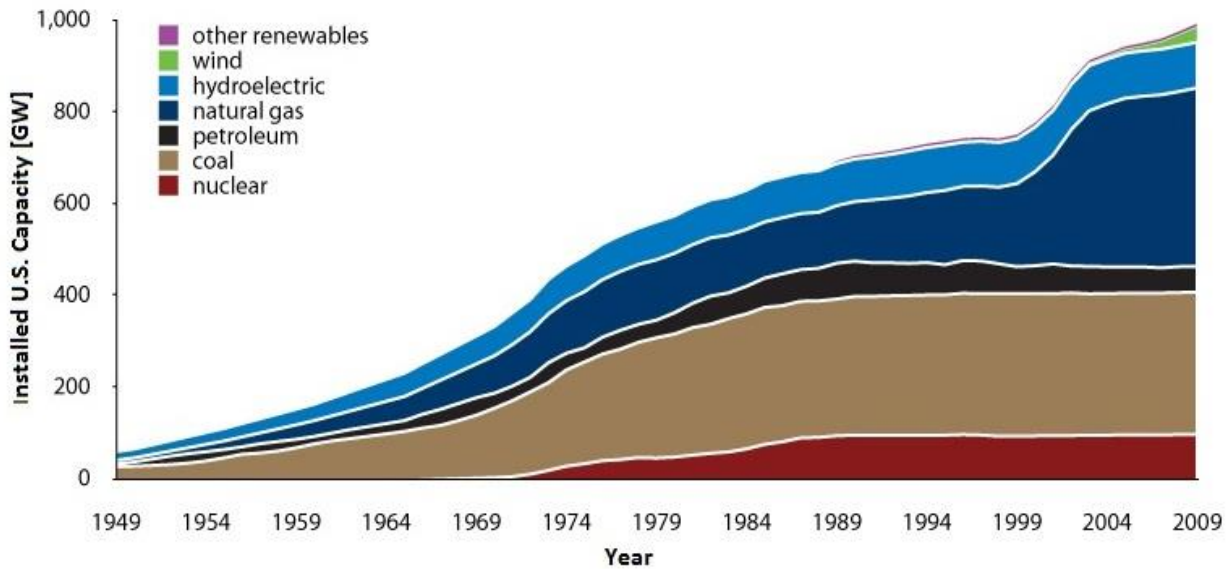


Figure 1.2. . The substantial increase in natural gas generating capacity in the past decade is very prominent and actually now exceeds the total installed capacity of coal (11).

The recent build out of natural gas generation capacity had been motivated by a large number of factors: relatively low capital intensity, low criteria pollutant generation, high ramp rates, social acceptance and ease of permitting. Arguably the singularly most important factor for capacity installations in the late 1990's and early 2000's (Fig. 1.3) was the low cost of natural gas. The low natural gas prices of the late nineties fostered enormous capital investment and the low prices of the past few years have led to higher natural gas plant capacity factors, the third factor in reducing coal's market share.

The production of natural gas from shale deposits through the use of hydraulic fracturing has lowered prices because of an influx of recoverable reserves. The use of natural gas has been so prolific the past few years that for the first time coal and natural gas contributed nearly identical generation to the U.S. grid in April, 2012. The annual generation statistics (Fig. 1.1) don't indicate that natural gas will continue its rapid ascendancy; the trend has returned to the steadier gain of the previous decade. The past two years natural gas has contributed closer to 70% of the megawatt-hours of coal; down from over 80% in 2012.

Coal fired generation has declined nearly 25% since 2009. Some of this decline may be attributed to reduced demand resulting from economic down turn, but the majority of the lost coal-fired megawatt-hours have been shifted to natural gas. Since the beginning of coal's slide in 2009, natural gas prices have been consistently attractive to power producers (Fig. 1.3); floating between 4 and 6 [\$/MCF]. Ultimately, as long as the cost of natural gas (accounting for disparity in plant HHV efficiency and O&M costs) remains below that of coal on a per unit energy basis, natural gas generation will continue to increase.

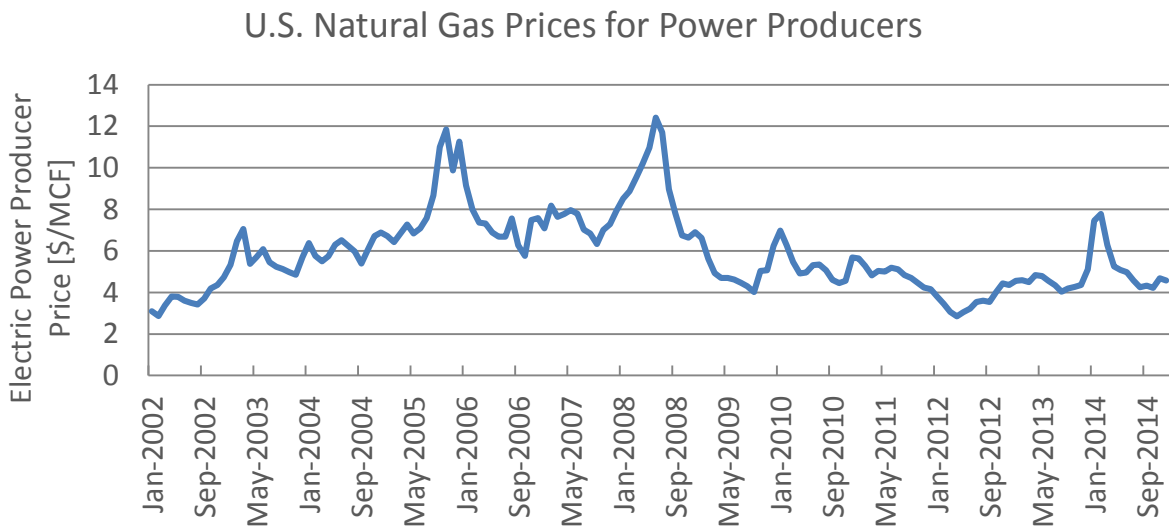


Figure 1.3. U.S. electric power producer price for natural gas [\$/MCF] from 2002-2014 (12)

For those seeking reductions in the rate at which carbon dioxide is released to the atmosphere; the specific reasons for the decrease in coal generation are secondary to the associated carbon emissions curtailed. The reduction in carbon dioxide emissions from coal generation between 2009 and 2014 has been substantial; close to 500 million tonnes per year. Meanwhile, the increase in carbon dioxide emissions from natural gas generation have increased by less than 100 million tonnes annually (Fig. 1.4).

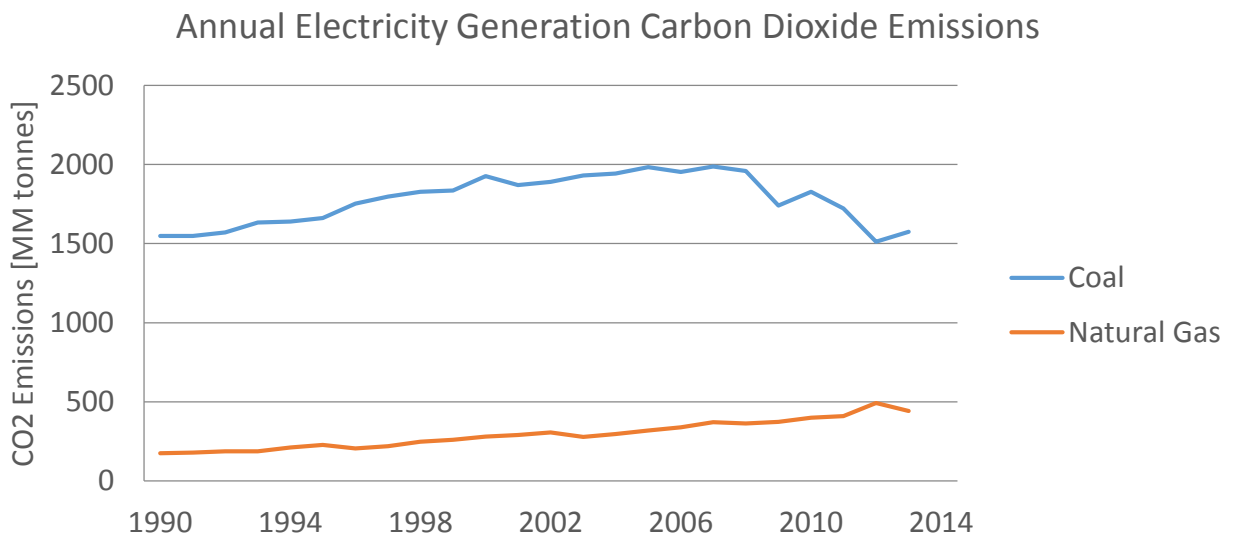


Figure 1.4. Annual carbon dioxide emissions from electricity generation from coal and natural gas (13)

This trade-off from a carbon intense generation source (coal) to one which is markedly less so (natural gas) has been welcome news. However, there are market principles (cost and supply of natural gas) which will prevent a wholesale conversion to natural gas as the singular form of fossil fuel generation in the near future. In the United States specifically, the Energy Information Administration (EIA) is

forecasting a slow increase in natural gas generation as overall electricity demand increases over the next few decades, but that coal will continue to provide a sizeable fraction (~1/3) of generation through 2040 (Fig. 1.5).

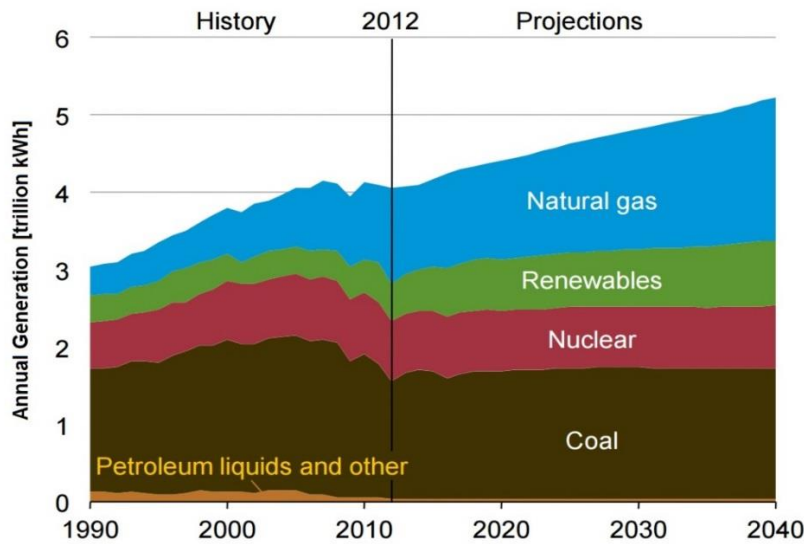


Figure 1.5. Annual electricity generation with historical data and projections through 2040 (14)

What's more alarming for those concerned with global climate change is that the international consumption of coal is anticipated to increase dramatically in developing countries while the developed nations will mirror the consistent use of coal in the United States (Fig. 1.6). Specifically, the International Energy Agency (IEA) is forecasting that consumption of coal will increase by ~50% in the non-OECD nations over the upcoming two decades.

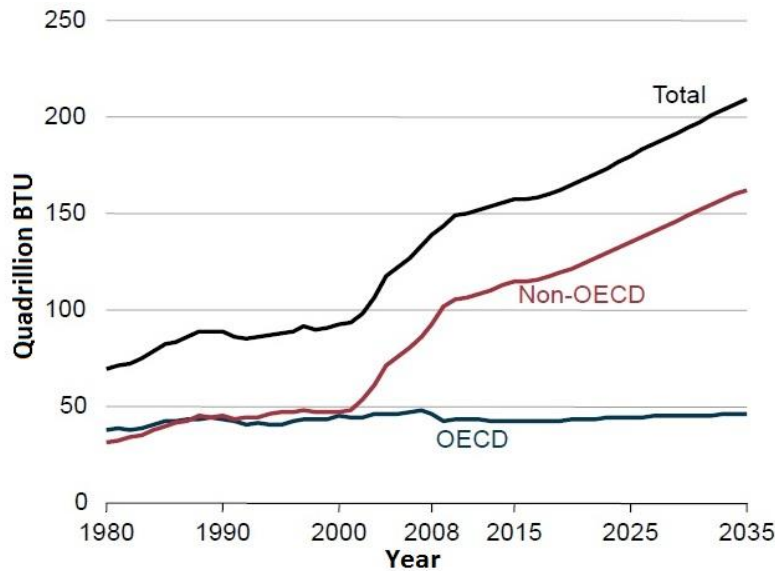


Figure 1.6. Projected world coal consumption in Quadrillion BTU (3). Presents the essentially level continued consumption of coal by OECD countries while the Non-OECD consumption is expected to increase by 50 Quads over the next 20 years.

This increase in coal consumption represents a potentially alarming increase in the annual emission rate of carbon dioxide to the Earth's atmosphere. Developing nations are seeking access to electricity essential to economic growth and cannot be faulted for aspiring to lift themselves out of poverty through utilizing the same cost-efficient fossil fuel technologies relied upon during the development of many OECD nations. To me, it follows that there is an imperative for those in OECD nations to not rest on the laurels of the modest progress made concerning intranational electricity carbon intensity and to continue to innovate and seek out technologies to further reduce emissions both at home and abroad in a cost-effective manner.

From the forecasts provided by EIA and IEA there seems little reason to posit that a sudden decrease in the use of fossil fuels will occur. It is also informative to observe the modest contribution of renewable generation in the United States (Fig. 1.1) even after decades of government funded research, state portfolio standards, and production and investment tax credits. It is in direct observance of these trends that the use of fossil fuels with carbon capture and sequestration is seen as vital to limiting the global increase in temperature to under 2°C (3). The following section focusses on the current carbon capture technologies available to potentially play a vital role in the reduction of carbon dioxide emissions from the continued use of fossil fuels.

## 1.2. Technology Options for Carbon Capture and Storage for Electrical Generation Units

There are three primary options for the capture of carbon dioxide from electrical generation units (EGUs). These options can be broadly defined by where the concentration of carbon dioxide gas occurs in the plant. Figure 1.7 shows a representation of the gas streams associated with each of the capture options along with depicting the interaction of the capture componentry with power generation.

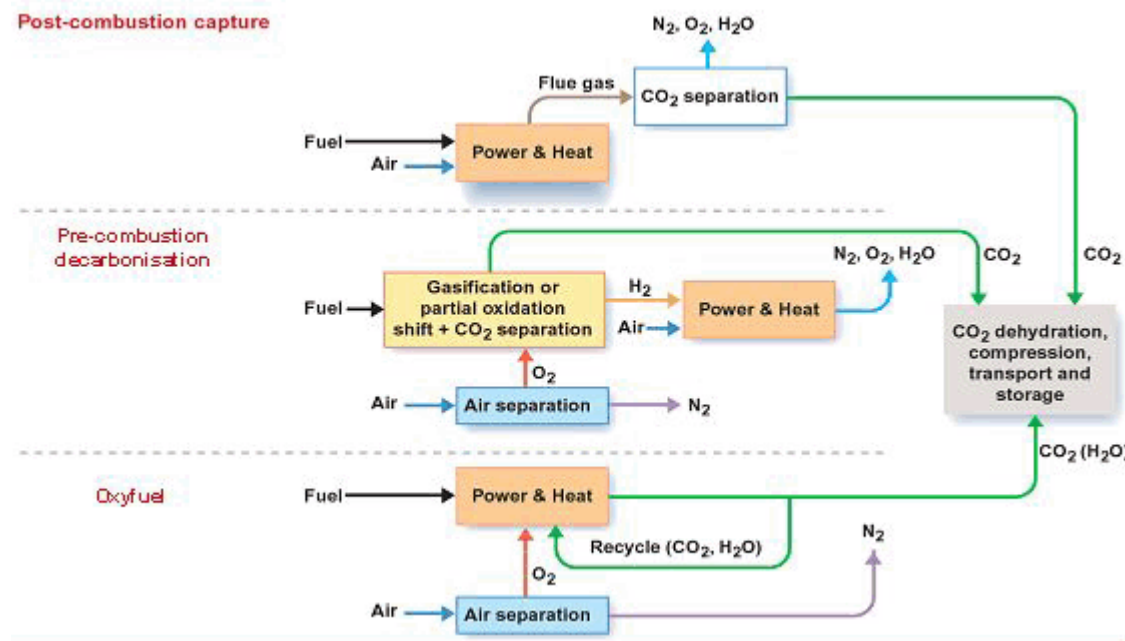


Figure 1.7. Representation of the three prominent forms of carbon dioxide capture for electricity generation units (15).

**Post-Combustion Capture** is essentially an add-on technology which is used to scrub the flue gas produced by a traditional, air-fired fossil fuel EGU. The most developed post-combustion technology (and carbon capture technology, generally) utilizes amines in solution to absorb carbon dioxide from the flue gas in a large contacting tower. This system has been used on smaller commercial projects for decades; typically to produce small quantities of high-grade carbon dioxide for industrial uses or the food industry. In October of 2014, the Boundary Dam facility in Saskatchewan, Canada began operation and is scheduled to capture one million tonnes of carbon dioxide annually (16). This facility is the largest commercial deployment of post-combustion capture to date and represents a substantial milestone for carbon capture.

There are several variations on the post-combustion capture theme including the use of ammonia, solid sorbents (fixed amines), membrane separation, and chemical-looping of limestone. These systems are at various stages of development from power plant slip-stream (ammonia) to bench scale (limestone chemical-looping). Substantial investigation of all these systems has been undertaken by current and former members of the IECM research team at Carnegie Mellon. Models of each of these systems can be found in the IECM and the details of their work can be found on the model website (7).

The systems which rely on absorption/adsorption of carbon dioxide (liquid amines, solid sorbents, and ammonia) all face a similar operational challenge. Once carbon dioxide had been removed from the flue gas and is bound to the solvent or sorbent work must be done to release the carbon dioxide. Energy may be provided in the form of a pressure or temperature swing, but the reduction in the substantial required energy to release the captured carbon dioxide is the general focus of continued development for this capture option.

**Pre-combustion decarbonization** relies on an alternative plant design known as integrated gasification combined cycle (IGCC). In this design a gasifier is used to convert the coal slurry to a hydrogen and carbon monoxide gas rich mixture known as syngas through partial oxidation with high-purity oxygen provided by an ASU. The partial oxidation process produces heat which partially operates a traditional Rankine cycle while the syngas is processed and then burned in a Brayton cycle before being passed through a heat recovery steam generator which augments the Rankine cycle.

Processing of the syngas involves removal of particulates, sulfur and nitrogen oxides, and the separation of carbon dioxide. A water gas shift reactor is utilized to increase the concentration of hydrogen and carbon dioxide in the syngas. The syngas is then passed through an absorber where a solvent strips the carbon dioxide from the syngas. This process is similar to the systems utilized in post-combustion capture except that the elevated pressure and concentration of carbon dioxide in the syngas make the stripping process much more efficient.

The Kemper County Energy Facility is a 582 megawatt IGCC facility owned by the Mississippi Power Company which is capable of capturing up to 67% of its carbon dioxide emissions (16). Slated to begin capture operation in 2016 the Kemper facility is anticipated to capture 3 million tonnes of carbon dioxide annually. This is a first-of-a-

kind facility capable of utilizing very cheap (1.25-1.50 [\$/MMBtu]) low-rank Mississippi lignite coal which over the lifetime of the plant will help offset the high capital intensity of the facility.

**Oxyfuel** capture differs from the other two capture options in that neither a solvent nor sorbent is used to separate carbon dioxide from the flue gas or syngas. Rather, the goal of oxyfuel is to create a carbon dioxide rich flue gas stream and then remove the remaining impurities to arrive at a high purity carbon dioxide product. The process relies on the separation of oxygen from atmosphere to produce oxidant with which to combust the fuel. The stoichiometric combustion products of burning carbonaceous fuels are almost completely carbon dioxide and water (plus trace species). However, the adiabatic flame temperatures of fuels combusted with pure oxygen are hot enough to destroy the boiler and steam generation components. To prevent mechanical failure, and to aid in heat transfer, a portion of the flue gas (~2/3) is recycled to the boiler to moderate temperatures.

The downstream treatment of criteria pollutants is similar to traditional air-fired EGUs, utilizing the same basic equipment for sulfur oxide treatment and total suspended particulate removal. Once the water is precipitated out of the flue gas, the remaining gas stream (~85 [CO<sub>2</sub> mol%]) can either be sequestered straight away or additional processing can be used to remove the remaining gas species (typically argon, oxygen, and nitrogen) to arrive at a near pure carbon dioxide product stream.

The flagship oxyfuel project was to be the FutureGen 2.0 project in Meredosia, Illinois. This project was cancelled in February 2015, but had been scheduled to be the largest operating oxyfuel plant with a net output of 168 megawatts and capable of capturing 1.1 million tonnes of carbon dioxide annually. The proposed 426 [MW] White Rose Carbon Capture and Storage project near Selby in North Yorkshire would be the first commercial oxyfuel plant if the project is carried to fruition. To date, several similar oxyfuel projects have been undertaken (16): Schwarze Pumpe (30 [MW-thermal]), Lacq CCS Pilot Project (30 [MW-thermal]), and CIUDEN Technology Development Center ( 20 [MW-thermal] PC boiler and 30 [MW-thermal] CFB boiler). The largest facility is the Callide Oxyfuel Project in Queensland, Australia. This 30 [MW] unit is capable of capturing 75 tonnes of carbon dioxide per day and has logged more than 7500 hours of operation as of September 2014 (15).

The three carbon dioxide capture options presented in Figure 1.7 and discussed briefly above have all been proven at the pilot plant size. Post-combustion capture with liquid amines is the only option proven to be commercially operational at the time of writing, but should be joined by pre-combustion within a few years. The cancellation of the FutureGen 2.0 project has set back commercial demonstration of oxyfuel for a few years, but the White Rose project may change that by 2020.

Determining which of these technologies would be the best option for a new EGU is currently rather opaque. The primary difficulty is that currently, none of these possess a distinct advantage with regard to both cost and efficiency (5). Disparities between the technologies exist with regard to: capital

investment, O&M cost, CO<sub>2</sub> recovery rate and CO<sub>2</sub> product purity. This work focusses on exploring the characteristics which are unique to oxyfuel and providing an accessible, robust resource for analysts and policy makers to gain insight into all the technological options for carbon capture.

### 1.3. Storage Options

No matter which carbon capture technology has been selected, every CCS project ultimately needs to have the “S”, storage<sup>1</sup>. There will be very little of this work devoted to the topic of storage, but the importance of this final step has not gone unnoticed by the geologic community. Extensive charting of all the formations suitable for the storage of carbon dioxide has been undertaken by the Regional Carbon Sequestration Partnerships in association with the Department of Energy, Office of Fossil Fuels, and the National Energy Technology Laboratory in the preparation of the U.S. Carbon Utilization and Storage Atlas. The formations identified for storage include: sedimentary basins, oil and gas reservoirs, unmineable coal seams, saline formations, basalt formations, and organic-rich shale basins. The total current storage resource identified between these formations is estimated to be between 2,380 and 20,353 billion metric tons (17).

To put the size of this storage capacity resource into perspective: stationary CO<sub>2</sub> emissions in the United States are ~3.3 billion metric tonnes per year, about ¾ of which is from electricity generation (13). Even if we were to assume that all the electricity generation carbon emissions could be captured (2.5 billion tonnes CO<sub>2</sub>/yr), the low end of the Carbon Atlas storage estimate would still afford a thousand years’ worth of storage for the electricity generation industry at the current rate of carbon dioxide output. Proximity and access to storage may remain issues to be resolved by an individual project, but storage capacity should not be an issue.

### 1.4. CCS Development and Deployment

Despite its potential, CCS development has not happened at the pace expected by the Intergovernmental Panel on Climate Change (IPCC) and other climate organizations (18) around the world. As an illustrative example consider the stabilization wedges (19) emission reduction scheme to stabilize global carbon emissions by 2050. This scenario, one of the less demanding of CCS, requires CCS to abate 25 gigatonnes of carbon (91.7 [GtCO<sub>2</sub>]) over fifty years and ramps linearly. The slightly less than 6 [MtC/y]r (20) we are currently capturing<sup>2</sup> amounts to less than 5% of what is required to satisfy the CCS wedge (Fig. 1.8) even at this early stage. The reasons for this shortfall include uncertainties about regulatory requirements and the maturity of CCS for power plants, in addition to high capital and operating costs (20).

---

<sup>1</sup> The term storage has recently gained prominence over sequestration; with the reasons for this being largely political. I have here taken storage to mean sequestration, i.e. long term, permanent containment.

<sup>2</sup> Of the 21.7 MtCO<sub>2</sub>/yr being captured as of 2012 nearly 90% is being used for enhanced oil recovery projects.

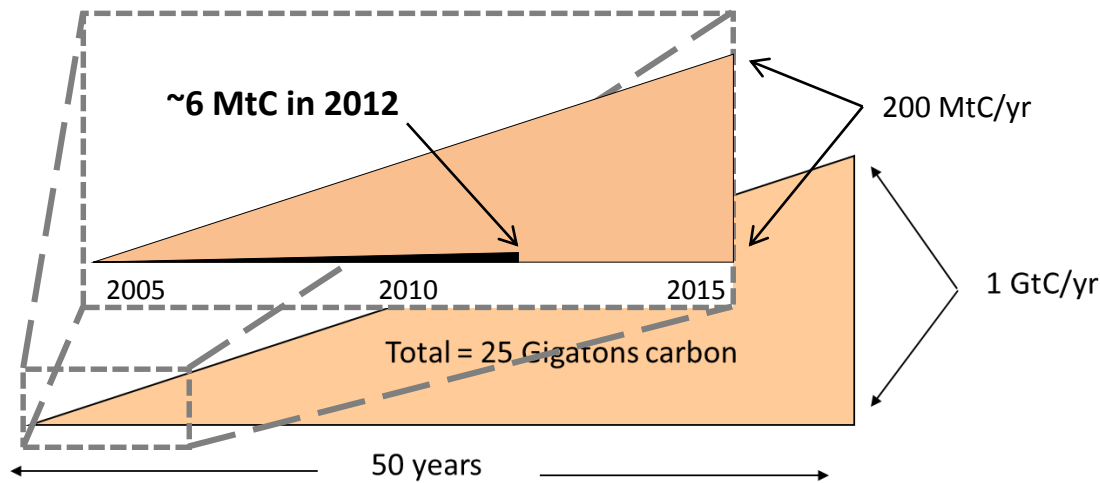


Figure 1.8. The installed capacity of CCS is far behind the goals outlined in the stabilization wedges emissions reduction scheme.

While the lack of installed CCS capacity can be attributed in large measure to failures to pass climate change legislation, the lack of large-scale demonstrations of all the capture technologies is another important factor. Thus, the excerpt below from “The Future of Coal” study is as prescient today as it was when written.

*“Today, and independent of whatever carbon constraints may be chosen, the priority objective with respect to coal should be the successful large-scale demonstration of the technical, economic, and environmental performance of the technologies that make up all of the major components of a large-scale integrated CCS system — capture, transportation and storage. Such demonstrations are a prerequisite for broad deployment at gigatonne scale in response to the adoption of a future carbon mitigation policy, as well as for easing the trade-off between restraining emissions from fossil resource use and meeting the world’s future energy needs” (21)*

This statement is both instructive and prudent, especially if we believe CCS component costs will mirror the experience curves of past emission reduction technologies such as selective catalytic reduction for nitrous oxides and wet flue gas desulfurization (22). However, the need for either a positive or negative economic force to provide impetus to such large-scale demonstrations remains. Absent climate policy, there are two other potentially positive economic forces available for furthering the development of carbon capture technology: enhanced oil recovery and the value of fossil generators equipped with CCS to provide capacity as an electric service (23). Neither revenue stream by itself would be sufficient to stimulate the build out of CCS capacity, but the combination of the two, along with additional tax incentives akin to those provided to renewables over the past decades might be.

### 1.4.1. The Potential Role of Enhanced Oil Recovery

The market price of crude has plummeted in the past few months (Fig. 1.9), but the sustained high-prices of the past decade have served to reinvigorate an oil production technique which had previously fallen out of favor. Enhanced oil recovery (EOR), a method by which developed oil wells can be brought back into production through the injection of carbon dioxide, becomes increasingly economically attractive as crude prices escalate. Historically, the low price of crude oil had kept this practice from being economically viable. However, that situation has begun to change in the past decade and, as of 2012, roughly 250,000 incremental barrels of oil were produced daily in the U.S. using CO<sub>2</sub>-EOR (24).

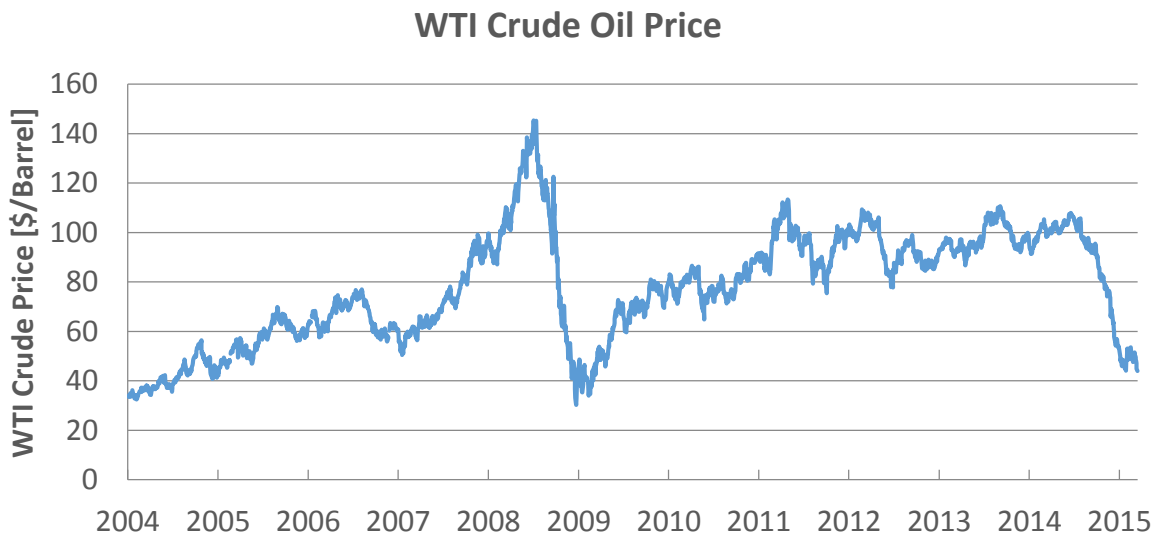


Figure 1.9. Prices of crude oil for the West Texas Intermediate (WTI) over the past decade (25).

The recent downturn in crude oil prices may have momentarily tempered the demand for carbon dioxide, but the long term prospects for EOR remain fundamentally strong. The creation of a market for carbon dioxide through EOR may provide a means of improving the economics of carbon capture, which could help foster development of carbon capture, utilization, and storage (CCUS) in the absence of climate policy (23).

## 1.5. Objectives and Scope of this Thesis

Of the three major carbon dioxide capture options, oxyfuel has been the least researched and least lauded, in contrast to the prominence of post-combustion capture systems. Reliable and detailed information about the technical and economic performance of oxyfuel systems thus has been relatively difficult to find. When this thesis was undertaken it was unclear whether oxyfuel had been marginalized because it was inferior to post-combustion capture or whether its lack of popularity was due simply to a

deficiency of quality information about the technology. Thus, this research has sought to provide honest, sober analysis, rooted in engineering principles, to address the following questions:

- What are the key parameters that affect the thermal performance, cost, and environmental emissions of oxyfuel systems?
- How does the composition of the fuel chosen affect the system configuration and traditional pollutant control equipment required?
- How do alterations in the system configuration affect the thermal performance of the system? How do they affect system cost?
- What are the thermodynamic limits of oxyfuel as a means of carbon dioxide control for electrical power generation?
- Compared to post-combustion capture are there circumstances where oxyfuel is a dominant technology with respect to performance and cost?
- Are there unique performance characteristics of oxyfuel which differentiate it from the other available capture technologies? Do these present policy and regulatory challenges?

These are mostly engineering questions with a strong focus on the technology itself rather than the broader context of how the technology may fit into the grander scheme of U.S. electricity generation. This thesis is dominated by the components and system which comprise the oxyfuel model in the Integrated Environmental Control Model. In Chapter 10 the scope is broadened to examine how oxyfuel compares to other low-carbon electrical generation technologies. In Appendix A, my co-authors and I examine a mechanism through which carbon capture, utilization, and storage (CCUS) may be incented in restructured utility markets. Chapters 10 and 11, along with Appendix A serve to provide context to the greater work of this thesis. Hopefully the labors undertaken serve to reduce the gap in the information availability of oxyfuel systems for analysts and energy policy decision makers.

## 1.6. Organization of this Thesis

The organization of this thesis is as follows. Chapter 2 provides a brief overview of proposed pollutant control technologies and system configurations for oxyfuel-based power generation, along with the rationale for the oxyfuel model. Chapter 3 introduces the oxyfuel configurations utilized in the IECM and provides a conceptual explanation of the model's development and operation. Chapter 4 documents the mass and energy balance of the oxyfuel system in the IECM. This chapter touches on convergence algorithms, methodology, parameters and performance equations. Chapter 5 provides technical documentation for the cryogenic air separation unit (ASU) and includes development, methodology, parameters and performance equations. Chapter 6 is the technical documentation for the direct contact cooler and polishing scrubber (DCCPS) model. Included in this chapter are

development, methodology, parameters and performance equations relevant to the DCCPS. Chapter 7 details the technical documentation for the carbon dioxide handling systems in the oxyfuel model. The Combined flue gas product Capture (CoCapture) and High-Purity Carbon Processing Unit (CPU) documentation includes development, methodology, parameters and performance equations specific to each carbon handling system. Chapter 8 provides cost model information for the overall oxyfuel system as well as the individual process components. This chapter outlines the costing methodology utilized in the creation of cost estimates including capital and operations and maintenance costs for all process components. Chapter 9 demonstrates the utilization of the completed component and oxyfuel models to show sensitivity and uncertainty in the cost and performance of these systems. Also included is the analysis of several case studies to identify options that maximize performance and minimize costs for various plant configurations and fuel blends. In Chapter 10 a comparison to other low-carbon electricity generation systems is performed to identify the circumstances under which various oxyfuel might be the preferred carbon mitigation technology. In Chapter 11 a few of the policy relevant aspects of this work are examined. Finally, Chapter 12 presents concluding remarks on this work and provides recommendations for further work. Details about potential future additions to the oxyfuel model, development of process models, case study details, and a co-authored paper on a potential mechanism for incenting the deployment of carbon capture, utilization, and storage are included as appendices (A-E).

# Chapter 2 Oxyfuel Carbon Capture Systems and Components for Pulverized Coal Plants

This chapter will provide an overview of the technological options for oxyfuel as a system for carbon dioxide capture from coal-fired electricity generation units. We will begin by comparing the layout of an oxyfuel plant to that of a traditional air-fired pulverized coal facility. From there, the proposed oxyfuel system configurations will be presented and discussed. Lastly, the component systems of oxyfuel for gas separation and criteria pollution control will be covered. As technical components are covered, rationale will be provided for the need to update critical process models in the Integrated Environmental Control Model. This chapter is intended to familiarize the reader with how oxyfuel works and what system components would comprise a functioning facility.

## 2.1 Commonalities with Air-Fired Pulverized Coal Electricity Generation

A traditional pulverized coal (PC) plant combines air and fuel in a boiler to generate steam and combustion gases. The steam drives a turbine to produce electricity while the combustion gases are cleaned to compliance and then released through the stack (Fig. 2.1)

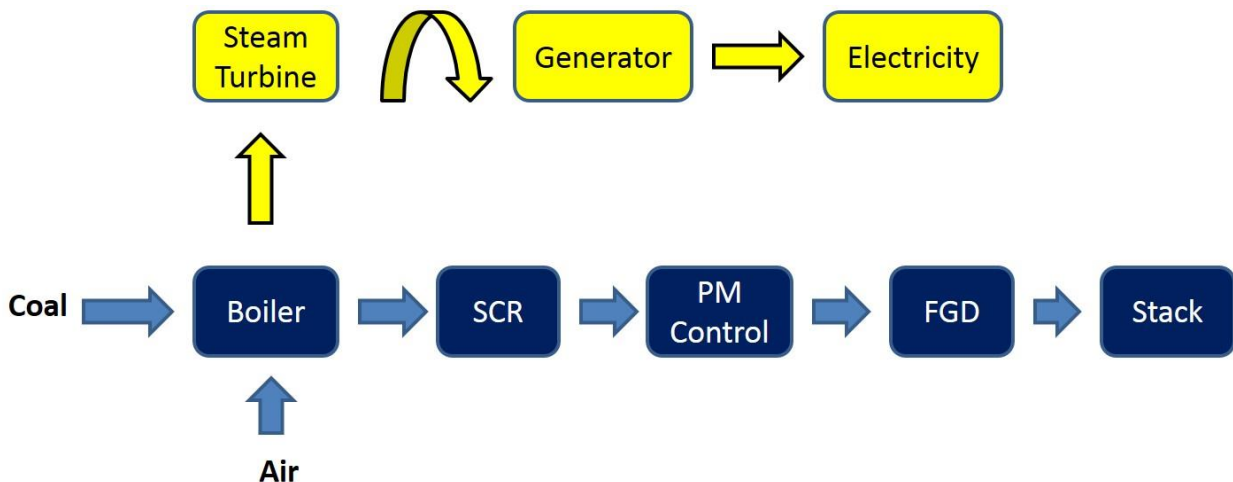


Figure 2.1 Simplified process flow diagram of a pulverized coal plant with the interaction between boiler and electricity generation shown.

The above diagram is heavily simplified and has sacrificed much detail for the sake of simplicity. Represented by just the boiler, steam turbine, and stack in Figure 2.1, the base plant additionally comprised of all the smaller pieces of equipment and systems required for the plant to function. The omitted systems include, but are not limited to, the following: coal conveyors, coal mills/pulverizers, steam cycle pumps, heat exchangers, forced/induced draft fans, air preheater, cooling water systems,

and ash handling systems. These integral components of the base plant rarely are represented in process flow diagrams, but should be remembered as the necessary balance of equipment when the term “base plant” is used.

In a traditional coal plant a selective catalytic reduction (SCR) is used to reduce the presence of nitrogen oxides in the flue gas formed during combustion. The flue gas is then passed through some device to capture particulate matter. Either an electrostatic precipitator (ESP) or fabric filter (FF) may be used to perform particulate control. The flue gas is then passed through a device to reduce the concentration of sulfur oxides. Depending on the percentage of sulfur in the coal being fired, a spray dry absorber (SDA) or wet flue gas desulfurization (WFGD) unit may be employed. From there the flue gas is readied to be sent to the stack where the flue gas will be emitted to the atmosphere.

An oxyfuel pulverized coal plant combines oxidant and fuel in a boiler to generate steam and combustion gases. The steam drives a turbine to produce electricity while the combustion gases are cleaned and then purified to produce a high-purity carbon dioxide stream for storage while the balance of gases are released from the stack.

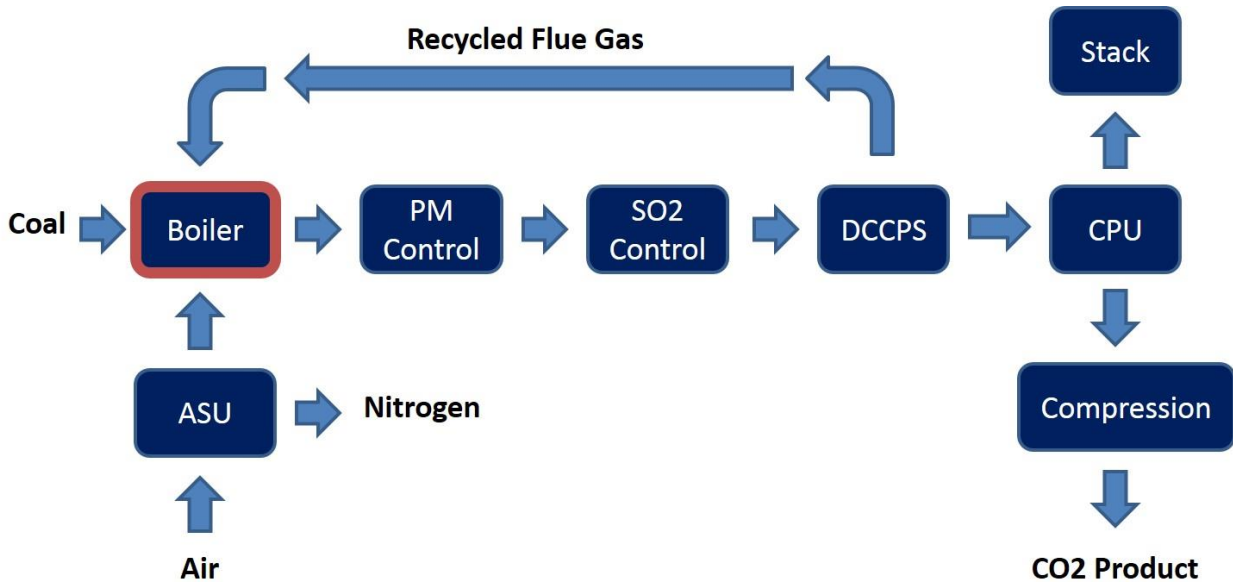


Figure 2.2 Simplified process flow diagram of the oxyfuel process. The interaction with the steam cycle has been omitted for clarity.

The steam and electricity generation portion of oxyfuel is essentially the same as a conventional plant and thus many of the required system components are identical and mature. The primary difference is that an air separation unit (ASU) is used to produce concentrated oxygen (known as oxidant) to combust the fuel inside a boiler. The combustion zone, like the rest of the plant, is sealed to the outside atmosphere. The advent of this is that nitrogen free combustion produces combustion gases which are almost entirely CO<sub>2</sub> and water. In order to avoid extreme temperatures from pure oxygen combustion roughly 2/3 of the flue gas is recycled back to the boiler as a diluent.

Once the combustion gases leave the boiler, pollution control equipment, similar to that used for air-fired PC, is used to clean particulate matter and sulfur oxides from the CO<sub>2</sub> and water rich gas. An additional piece of equipment, called a direct contact cooler and polishing scrubber (DCCPS) is then used

to remove moisture and remaining sulfur oxides and particulate matter from the flue gas. The dehydrated flue gas is then split between being sent back to the boiler to moderate combustion temperatures and the carbon processing unit (CPU). In the CPU, cryogenic gas separation is used to produce a high-purity carbon dioxide stream which can be compressed and stored. The balance of combustion gases that enter the CPU are vented from the plant's stack and are primarily oxygen, argon, and nitrogen.

### 2.1.1 Common Components and Retrofit Suitability

There are many common components between a traditional air-fired PC plant and a PC oxyfuel plant. This applicability of many of the air fired components for oxyfuel will be covered in greater depth in the following sections, but generally, many of the components could be used for either system with little required adaptation or changes in operating performance. The first generation of oxyfuel systems are also being designed to use traditional air-fired boilers and matching their originally designed heat transfer profiles through combustion control and adjusting the flue gas recirculation rate.

That having been said, the conversion from air-fire to oxyfuel is far from a "bolt on" technology. The need to seal the plant's process components from the atmosphere presents serious challenges for retrofitting an air-fired pulverized coal unit to oxyfuel. This is especially true of the boiler, air preheater, and flue gas ducting which typically operate below atmospheric pressure in an air-fired plant. The problem with this is that air leaks into the flue gas, dilutes the carbon dioxide concentration, and undermines the fundamental intent of oxyfuel. This leaking of atmosphere into the flue gas is called "air ingress". The alterations required to the boiler and air preheater systems to reduce air ingress rates to an acceptable level for an air fired plant are substantial. This capital investment, combined with the expense of the gas separation system (ASU and CPU) and the age of current coal fleet present very few potentially eligible projects in the United States. The number of eligible projects would likely be further reduced when the availability of other carbon dioxide capture systems (post-combustion) which require less modification to the base plant are considered. For this reason, the focus of this work is new installs.

## 2.2 Proposed Pulverized Coal Oxyfuel Systems

The current generation of oxyfuel PC boiler technology requires that a large fraction of the flue gas be recycled to the boiler in order to maintain heat transfer and mass flow parity with conventional air-fired PC boilers. This necessitates that the recycled combustion gases be cleaned to an adequate level to prevent the buildup of corrosive gas concentrations in the boiler which otherwise would exceed those found in air-firing. The following four process flow diagrams present plausible, near-term oxyfuel plant configurations, proposed by Babcock & Wilcox (26), covering a spectrum of coals from highly corrosive (Fig. 2.3) to ultra-low sulfur (Fig. 2.6).



## COOL RECYCLE PROCESS

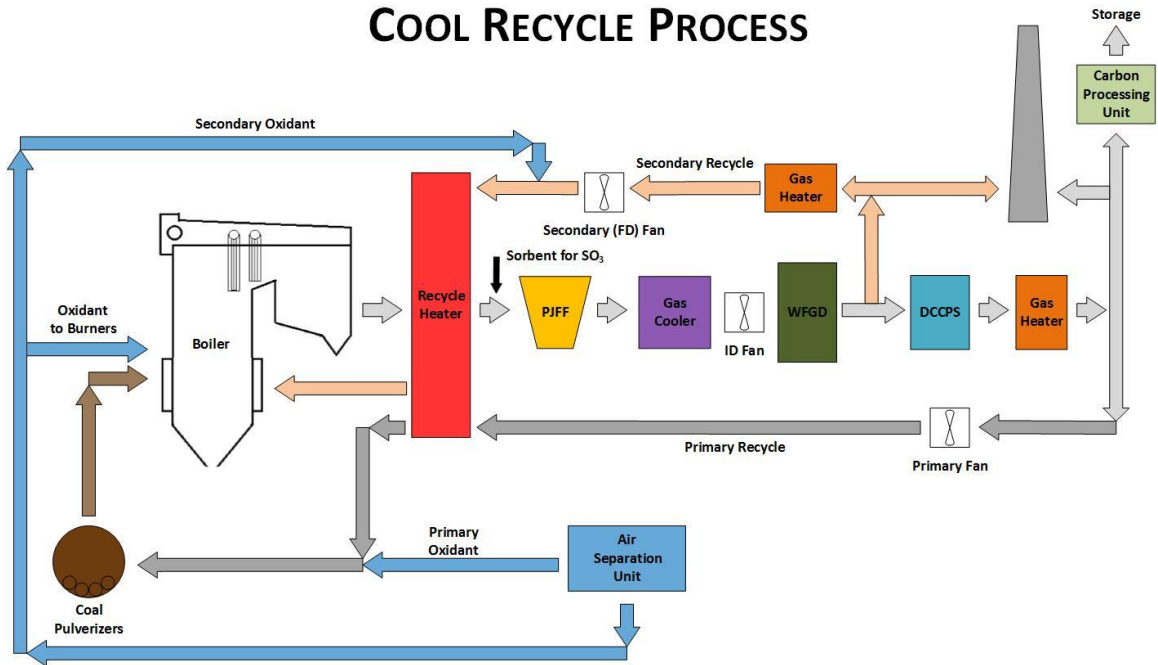


Figure 2.4 Cool recycle oxyfuel process flow diagram with wet flue gas desulfurization designed by B&W. This process is suited to highly corrosive coals and offers a heat rate advantage over the cold recycle process.

## COOL RECYCLE PROCESS

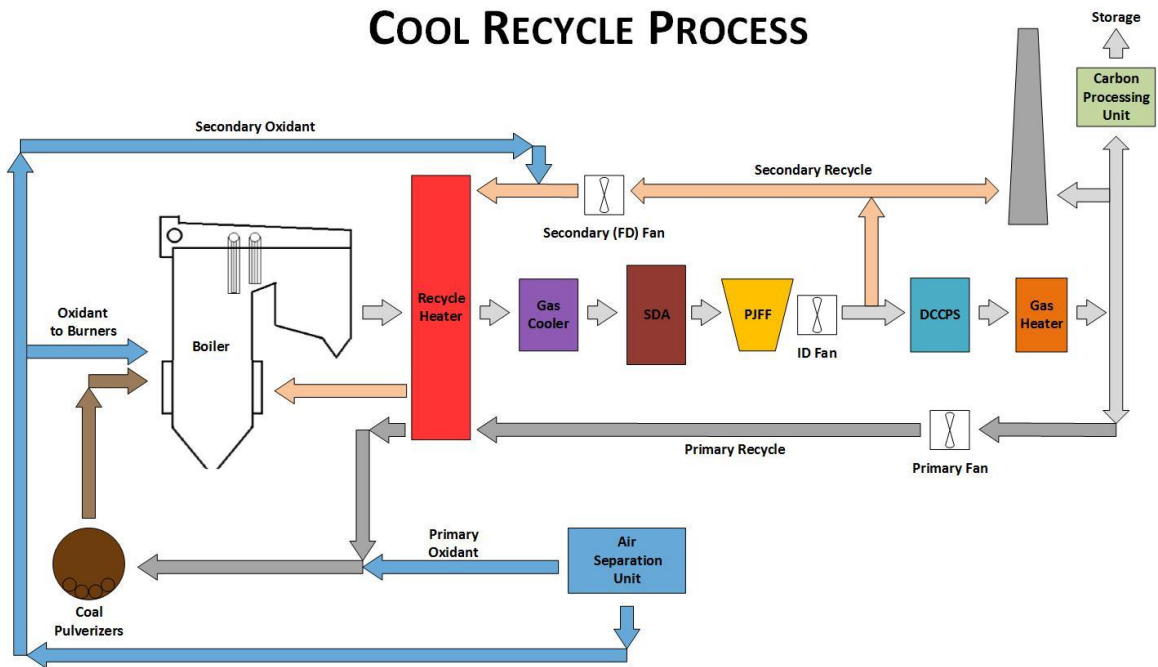


Figure 2.5 Cool recycle oxyfuel process flow diagram with spray dry absorption designed by B&W. This process is suited for less corrosive coals and offers an improved heat rate compared to the WFGD variation.

The cool recycle process can be adapted for use with both high sulfur (Fig. 2.4) and low sulfur (Fig. 2.5) coals. In cool recycle the secondary recycle is returned to the recycle heater after the primary scrubber.

For high sulfur coals the primary scrubber will be a WFGD and for medium or low sulfur coals a SDA may be used. The limitation on the use of an SDA is the maximum achievable sulfur removal is lower than with a WFGD and controlling the resulting furnace SO<sub>2</sub> concentration could become difficult if operated near the threshold. Since the flue gas in oxycombustion has higher moisture content than in air-firing, the amount of reagent that can be sprayed into the SDA while maintaining a safe approach to water saturation temperature at the outlet can be severely limited.

One of the major advantages of this process is that the DCCPS and gas heater downstream of the primary scrubber can be downsized because the secondary recycle loop need not be treated. Net plant heat rates are correspondingly reduced because the secondary recycle streams are cooled less and the power requirements of the downsized scrubbers are reduced.

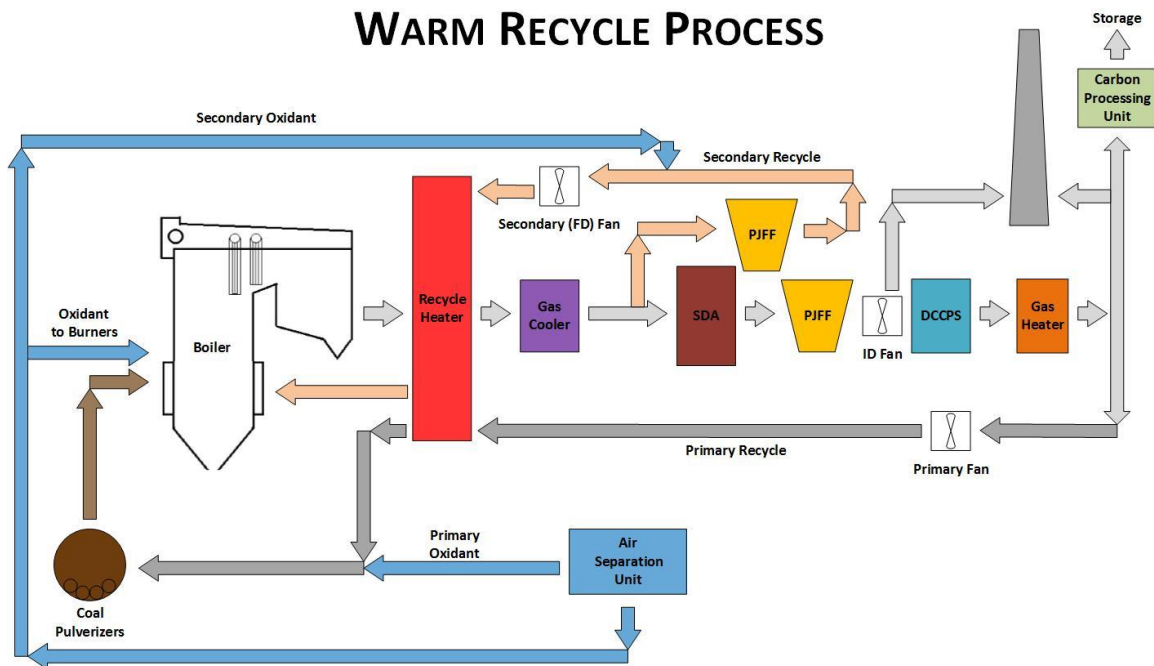


Figure 2.6 Warm recycle oxyfuel process flow diagram with spray dry absorber bypass designed by B&W. This process is for the least corrosive coals and offers the most thermally efficiency oxyfuel configuration.

For very low sulfur fuels, a warm recycle may be used. With warm recycle only particulate matter is removed from the secondary recycle stream before it re-enters the recycle heater. Here again, there is modest improvement in net plant heat rate due to the higher temperature of the secondary recycle upon entering the recycle heater in addition to the use of a smaller SDA. Application of this process requires fuels with exceedingly low corrosive potential so that boiler concentrations do not become elevated when lack of secondary recycle treatment is considered. This requirement limits the application of warm recycle in many regions in the United States where present-day coal blends maintained. It should also be noted that moisture levels also increase in the boiler under this cycle, which can further limit the effectiveness of the SDA as the saturation point of the flue gas will quickly be met upon the addition of lime slurry.

## 2.2.1 Potential System Configurations

There are several system configurations in addition to the four outlined above which were adopted from Babcock & Wilcox (25). Many of these configurations are contingent upon the commercial development of some alternative form of SO<sub>x</sub> and NO<sub>x</sub> removal. An example of one of these alternatives is the “Sour Gas Compression Process” being pursued by Air Products; which is outlined in detail in the Purification section. The need for auxiliary sulfur removal in addition to sour compression would be determined by the sulfur content of the chosen coal in a similar fashion to the limitations for using a SDA. Additionally, the sour compression process stoichiometry may necessitate the need to control the SO<sub>x</sub> to NO<sub>x</sub> ratio with auxiliary sulfur removal in order to assure high conversion efficiency. A representative process diagram, utilizing sour compression, analogous to the warm recycle process is presented below.

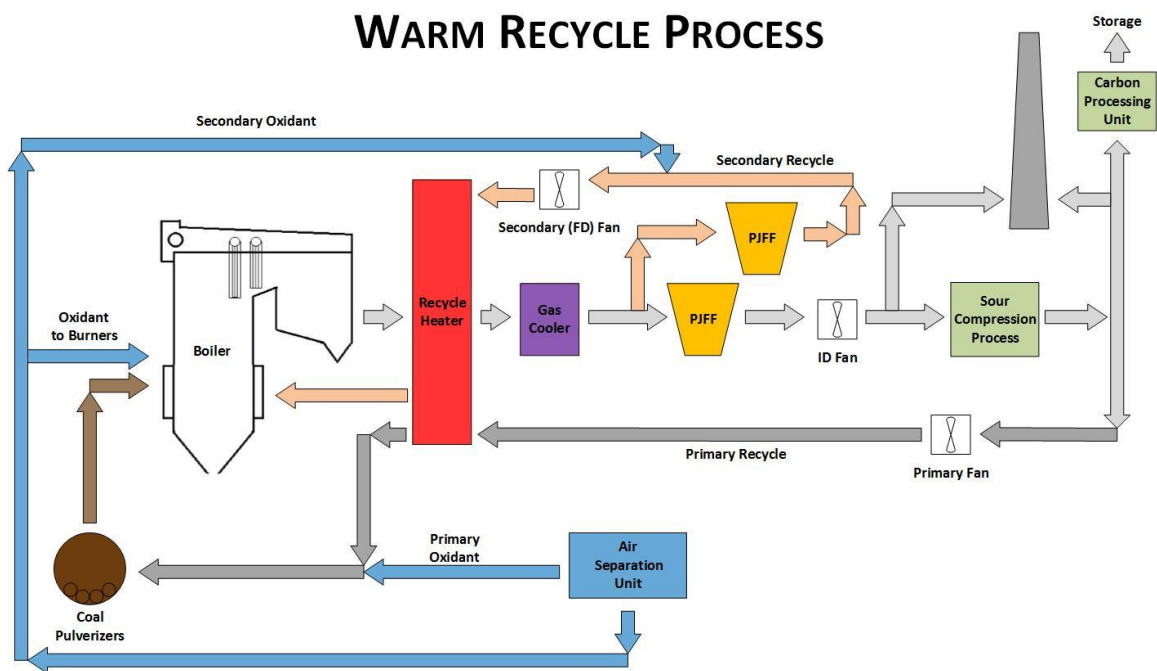


Figure 2.7 Process flow diagram of the warm recycle oxyfuel configuration adapted for B&W with the Sour Compression Process being developed by Air Products.

Other possible system configurations reflect assumptions about the intended operation of the completed plant. For example: laboratory and pilot testing (27) has demonstrated a reduction in NO<sub>x</sub> formation during oxyfuel operation sufficient to forego the use of dedicated NO<sub>x</sub> reduction equipment. The decision to not incorporate a SCR represents a tacit acceptance that the plant will only be operated under capture conditions. This assumption is representative of the current North American ethos but does not reflect the desire for mixed air-fired/capture operation being considered in Europe.

## 2.2.2 Cycle Selection Update Rationale

When the original oxyfuel model was created there was significantly less information publicly available about the potential layout of oxyfuel plants. As is detailed in the original technical documentation (28),

it was unclear whether recycled flue gas would be dried, what form of particulate removal should be used, whether and to what extent flue gas should be cooled, or whether flue gas desulfurization, selective catalytic reduction, or both would be needed. The answer to all of these questions is now known with a high enough degree of certainty to make a determination that both the warm and cool recycle processes should be adopted for this iteration of IECM updates. Because of the flexibility of these cycles to handle coals of varying levels of sulfur content depending on the addition and reconfiguration of just a few system components: PJFF, SDA, WFGD, and the DCCPS, the number of configurations to accommodate different coals is reduced to three. In the update, a high sulfur ( $>1.5$  [S mass%]), a medium sulfur ( $0.5 < [S \text{ mass\%}] < 1.5$ ) and a low sulfur ( $\leq 0.5$  [S mass%]), configuration is chosen based upon the ultimate analysis of the selected coal and then the pollution removal sub-modules (WFGD or SDA, respectively) are sized appropriately to limit the accumulation of sulfur in the boiler.

The selection of the warm and cool cycle processes will also be easily adaptable to future advances in the removal of criteria pollutants. Whether performance advancements come in the form of reductions to specific input power for pre-existing sub-modules or through the creation of novel sub-modules by future students/researchers; the framework of the warm and cool recycle process will provide a robust environment capable of adapting to changes in gas composition and energy content.

## 2.3 Oxyfuel Plant Components

This section will cover the individual components which comprise an oxyfuel system. The focus has been mostly to evaluate the process components most likely to be a part of the first generation oxyfuel plants which will be built. However, where information was available, potential second generation technologies have been described. For the process components which had a previous model version in the IECM, such as the ASU, rationale for their update has been provided if warranted.

### 2.3.1 Oxyfuel Boilers

The first generation oxyfuel systems will utilize boilers which were originally developed to be air-fired. Extensive laboratory and pilot scale work has been undertaken to evaluate the behavior of oxyfuel combustion. Topics considered include: Ignition, combustion, heat transfer, flame propagation and stability, startup and crossover of oxyfuel operation, and fuel burnout. A comprehensive summary of these studies have been completed by the Greenhouse Gas Division of IEA (29). The take-away message from this work is that the conventional boilers can and will be used for the first generation oxyfuel systems. Given the gravity of this assessment, it was deemed appropriate to utilizing the pre-existing IECM models for cost and performance of boilers.

One notable departure from air-fired systems is the low rate of nitrogen oxide formation in oxyfuel boilers. A recent review of the technological status of NO<sub>x</sub> control systems for oxyfuel combustion process reported that flue gas recirculation alone, an integral part of the technology, can achieve a 65% reduction in NO<sub>x</sub> emissions (29). They also note that high temperature combustion, achievable through oxyfuel conditions, could reduce NO<sub>x</sub> emissions by 95%. Contrary to air-firing where there is plentiful

diatomic nitrogen from which to form oxides, the near absence of diatomic nitrogen enables the reverse Zeldovich mechanism to destroy NO at high temperatures (31). The combination of these NO<sub>x</sub> eliminating features of oxyfuel prevents the need for a SCR system.

### 2.3.2 Oxygen Separation Technologies

There are several air separation processes which are commercially available for oxygen production. However, only cryogenic distillation is currently technically proven and economically viable at the scale required for commercial oxyfuel PC plants. Future advancements in ion transport membranes and pressure swing adsorption may reduce the required energy of separation, but for the time being cryogenics is assumed to be the oxidant production system. However, the prospect of these technologies becoming competitive in the near future (32) was taken into account when creating the ASU module for the IECM. To accommodate this concern, any specific energy of separation or reduction in capital cost relative to cryogenics may be specified by the user. Depending upon the degree to which one thermodynamically idealizes the separation process and what initial and end state assumptions are made of the air and oxidant product, respectively; the minimum ASU energy consumption is around 50 (33) kWh/tonne contained oxygen.

Within the broad umbrella of cryogenics there exists a great deal of variety with respect to the types of cycles employed for efficient and cost effective oxygen separation. Historically there has been little commercial need to produce large quantities of relatively low purity oxygen (<97 [mol%]). However, the increasing likelihood of carbon capture, both IGCC and oxyfuel, has begun to change this precedent. For this new application low specific energy of separation and minimizing capital cost are the seminal design criteria. The design strategies by which this can be achieved, and the accompanying cycle comparison table, are elucidated brilliantly by Higginbotham et al. (34) and have been reproduced in this sub-section with minimal alteration. There are broadly three approaches that can be taken to minimize net power input:

- 1) Minimize *total* power input by reducing the feed air pressure, producing each product at no more than its specified pressure and venting waste nitrogen to the atmosphere.
- 2) Minimize *net* power input by maintaining a normal feed air pressure but recovering some compression energy as a pressurized product, and if necessary recovering excess compression energy by expansion.
- 3) Minimize *net* power input by increasing the operating pressure of the ASU and producing all the waste nitrogen at high pressure and using or recovering the compression energy it contains.

In general, approaches 2 and 3 are only worthwhile when there is actually a need for the compressed oxidant stream (IGCC). In these cases the avoided product compression power can be credited against the input power to give a low net separation power and the capital cost of the product compressor can be reduced. If there is no use for the pressurized product, only part of the energy can normally be recovered by expansion, and additional capital equipment is required in the form of an expander. Although there is no consideration of capital cost, Table 2-1 compares the oxygen separation shaft power (i.e. the part of the shaft power for producing oxidant at 1.013 [bar(a)]) for the different cycles at

ISO conditions for a plant making 5400 TPD contained oxygen at 95% purity and 1.1 [bar(a)] pressure optimized for a high power cost. Motor and transformer losses, cooling system and molecular sieve regeneration energy are all excluded and there are no liquid or gaseous co-products, so that the basis is the same as Darde et al. (35).

Table 2-1 Summary of ASU cycles on an equal basis (34)

Cycle number		1a	1b	2a	2b	3a	3b	4	5
Description		Three column cycle	Three column cycle + MPGAN	2 column cycle	2 column cycle + MPGAN	2 column 2 reboiler	2 column 2 reboiler + MPGAN	EP Three column cycle + MPGAN	EP 2 column 2 reboiler + MPGAN
Low pressure column pressure	bar(a)	1.2	1.2	1.2	1.2	1.2	1.2	2.7	4.2
Oxygen recovery	%	97%	93%	99%	92%	90%	83%	89%	87%
Input Power	kW	36410	40900	42767	47960	38256	45351	58716	72586
GAN power credit	kW	0	7107	0	11540	0	10566	26907	42949
GAN power credit	% power in	0%	17%	0%	24%	0%	23%	46%	59%
Net GOX Power	kW	36410	33793	42767	36420	38257	34785	31809	29637
Specific shaft separation power	kWh/te	158	147	187	158	167	151	138	128
% credit to equal (1a)	%	N/A	63%	N/A	100%	N/A	85%	83%	84%

The above table shows that if the medium pressure gaseous nitrogen (MPGAN) could be adiabatically expanded to recover compression energy that there are more efficient cycles than the three column design. From a practical standpoint however, this is not typically feasible due to either economic or thermodynamic limitations. The take-away result of this analysis points toward a three column (dual high pressure) design being the best option because it is capable of achieving the best balance of shaft separation power, limited to no need for integration with the power cycle, and correspondingly no need for significant new machinery development. Another engineering study focused on just the three column and dual column designs and arrived at a similar conclusion: the three column system is marginally more efficient. After completing a thorough exergy (availability) analysis, Van der Ham et al. found the three column design to require 7% less input power (36). It has been assumed that it was in response to the enumerated reasons that the ASU designs employed by B&W (26), NETL/DOE (37), and IEA GHG (38) are all variations of the three column design.

### 2.3.2.1 ASU Update Rationale

Given the presence of several papers and case studies which used either a variation of the dual or three column cryogenic ASU designs we made the assessment that it would be worthwhile to update the two decade old ASU model being employed by public release v8.0.2 and earlier versions of the IECM. The updated ASU performance and cost models are explained in greater detail in those respective chapters, but an explanation of the simplifications and assumptions made in their construction will be briefly discussed here. The principle reasons for updating include:

- The large quantities of oxygen required for PC oxyfuel required an ASU model that would accurately reflect the number of trains likely to be employed in a modern oxidant production system.

- The relatively low oxygen purity (<97 [mol%]) requirements of oxyfuel or IGCC systems allow the use of ASU's specifically designed to produce large quantities of oxygen without co-production of other high purity industrial gases.
- Because of the high volumetric demand for oxygen, accurately understanding any reduction in specific net power input from increased train size is vital<sup>3</sup>.
- The previous ASU model wrongly characterized the functional relationship of the discontinuity in separation energy that occurs as the separation process transitions from removing nitrogen from an argon/oxygen mixture to separating argon from oxygen.
- Capital costs have changed as a result of technological progress and installed capacity.
  - a. Additionally, twenty years is far too long a time span to reliably update costs using the chemical engineering plant cost index.

For these reasons, the revised ASU performance model in Chapter 5 and cost model in Chapter 9 has been created. The intent was not to create a fully optimized cryogenic cycle for each volume of oxygen demanded by an IECM user. This practice would not only be computationally cumbersome and impractical, but would not be possible without a great deal more knowledge about the environment in which the proposed plant would theoretically be built. This degree of detail specificity falls outside the intended purpose of the IECM and was discarded in favor of a creating an “anticipated average cost and performance” model based upon the many case studies and academic papers detailing the process of cryogenic air separation.

In addition to the previously cited sources in the literature review data from the following sources has been used in constructing the updated air separation and carbon processing units: Cormos (39), Amann et al. (40), Huang et al. (41), Hu et al. (42), The Canadian Department for Business Enterprise & Regulatory Reform Report (43), The Department of Energy Report on Oxyfuel (37), and the Babcock & Wilcox Ultra-supercritical Oxyfuel Report (26).

### 2.3.3 Criteria Pollutant Treatment and Removal Systems

The flue gas produced from oxyfuel combustion in a pulverized coal boiler is comprised primarily of CO<sub>2</sub> and water vapor with minor amounts of oxygen, nitrogen and argon as a result of air ingress and the delivery of impure oxygen from the ASU. There are also acid gases formed as combustion by-products: SO<sub>3</sub>, SO<sub>2</sub>, HCl and NO<sub>x</sub>. The removal of these acid gases is essential to prevent downstream corrosion in the transport pipeline or the plant itself. Although there are a handful of alternative methods for removing acid gases, including the sour compression process detailed in a following section, the first generation of oxyfuel demonstration plants are likely to be built using more traditional, commercially available pollutant removal equipment.

#### 2.3.3.1 Pulse Jet Fabric Filter

The cool recycle process utilizes a pulse jet fabric filter, also known as a baghouse, to remove particulate matter and ash from the flue gas stream. The pre-existing IECM fabric filter cost and performance

---

<sup>3</sup> This was not possible given the old ASU model, as specific power input was solely a function of oxygen purity and scaled linearly with oxidant production.

models will be used in the updated PC oxyfuel model. Details on the performance and cost models for fabric filters can be found in Section 5 (44) of main technical documentation report for the Integrated Environmental Control Model.

#### *2.3.3.2 Wet Flue Gas Desulfurization*

The cool recycle process utilizes wet flue gas desulfurization (WFGD) to remove sulfur from the flue gas stream when a coal has a sulfur content exceeding 1 [S mass%]. The preexisting WFGD cost and performance models will be used in the updated PC oxyfuel model. Details on the performance and cost models for WFGD systems can be found in Section 6 (44) of main technical documentation report for the Integrated Environmental Control Model.

#### *2.3.3.3 Spray Dry Absorber*

The cool recycle process utilizes spray dry adsorption (SDA) to remove sulfur from the flue gas stream when a coal has a sulfur content equal to, or below 1 [mass%]. The preexisting SDA cost and performance models will be used in the updated PC oxyfuel model. Details on the performance and cost models for SDA systems can be found in Section 6 (44) of main technical documentation report for the Integrated Environmental Control Model.

#### *2.3.3.4 Selective Catalytic Reduction*

Selective catalytic reduction (SCR) is not utilized by the proposed form of the cool recycle process. As was mentioned previously, the deletion of the SCR reduces initial capital costs and is currently perceived as a redundancy for air-fired operation by North American centered studies and analysis. However, in the future, due either to stringent plant startup air quality regulations or the desire to examine scenarios involving mixed capture and air-fired modes of operation; it may be necessary to add the ability to equip a SCR unit. If and or when this ability is added the preexisting SCR cost and performance models will be used in the updated PC oxyfuel model. Details on the performance and cost models for SCR systems can be found in Section 3 (44) of main technical documentation report for the Integrated Environmental Control Model.

#### *2.3.3.5 Mercury Controls*

An unrecognized consideration for the previous oxyfuel model, the need for some form of mercury removal will most likely be necessary to ensure continued safe operation of the aluminum heat exchangers in the cryogenic section of the carbon processing unit (CPU). The process of liquid metal embrittlement occurs when mercury interacts with aluminum, resulting in a degradation of the material properties of the heat exchangers. The Moomba and Skikda gas processing plant disasters, which investigations determined were most likely caused by liquid metal embrittlement, serve to demonstrate the potentially devastating consequences of overlooking the presence of mercury in oxyfuel combustion systems. The preexisting carbon injection performance and cost model of mercury removal will be used by the updated oxyfuel model.

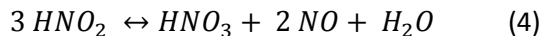
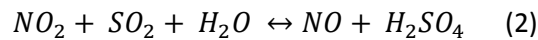
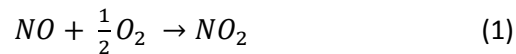
### **2.3.4 Second Generation Pollution Removal Technologies**

Air Products has been developing a novel process for CO<sub>2</sub> purification (45) (46) (47) (48) (49) (50) in conjunction with researchers at Imperial College London and now the University of Bath. The proposed sour compression process was first introduced at GHGT-8 and was followed at GHGT-9 with

experimental results from Doosan Babcock’s 160 [kW] coal-fired oxyfuel test rig which demonstrated the feasibility of removing 99% and 90% of SO<sub>2</sub> and NO<sub>x</sub> compounds, respectively. In a paper submitted for GHGT-10 Murciano et al. (51) investigated the effects of pressure, temperature, residence time and presence of water in a laboratory scale apparatus using synthetic flue gas in an effort to develop a reliable kinetic and process model. The aim of this section is to provide an account of the current state of sour compression development and evaluate its potential for incorporation in a future PC oxyfuel plant model.

#### 2.3.4.1 Proposed Reaction Mechanism

The primary NO<sub>x</sub> species formed during PC combustion is NO which is expected to be converted to NO<sub>2</sub> via Reaction 1. At low temperature, equilibrium favors the production of NO<sub>2</sub> but, kinetics remain slow at low pressures. In accordance with Le Chatelier’s Principle: the kinetics of Reaction 1 can be accelerated though increasing pressure, but temperature must be controlled to achieve an acceptable NO conversion rate. Reaction 1 is a third order reaction, therefore kinetics increase proportional to pressure to the 3<sup>rd</sup> power allowing equilibrium to be reached within a matter of seconds at the anticipated operating condition of 15 [bar]. The reaction of NO<sub>2</sub> with SO<sub>2</sub> to form sulfuric acid (reaction 2), known widely as the Lead Chamber process for sulfuric acid production, is a well understood process with fast kinetics. NO<sub>2</sub> not consumed in the production of sulfuric acid would be used in reactions 3 and 4 to produce nitric acid. The NO formed through reactions 2 and 4 would then be expected to be reconverted to NO<sub>2</sub> through reaction 1.



This series of reactions facilitates the removal of SO<sub>2</sub> as sulfuric acid and NO<sub>x</sub> as nitric acid through a two stage, wet compression process known as “Sour Gas Compression”. Additionally, mercury present in the flue gas is anticipated to be removed by the created nitric acid either by reaction or dissolution.

#### 2.3.4.2 Proposed Technology for Sour Compression

A process for the removal of NO<sub>x</sub> and SO<sub>x</sub> by compression was first introduced by Air Products at GHGT-8 (46). This process has since become the most developed second generation system yet proposed to meet the effluent purifications stipulated for flue gas entry into the CO<sub>2</sub> purification system. The below schematic and process description was adopted from the report produced by Air Products for NETL award DE-NT0005309.

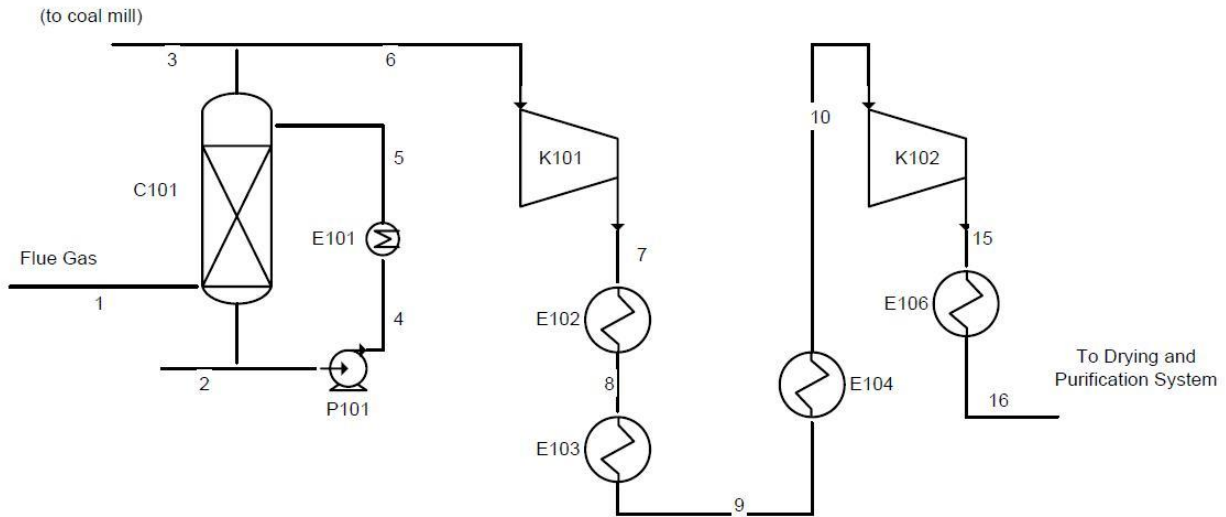


**Figure 2.8 Simplified layout of flue gas indirect contact cooler and the main compressors of the sour gas compression process (52).**

The above figure shows the raw flue gas entering from any prior effluent treatment: initial cooling, particulate removal, and desulfurization (if necessary). The gas enters an indirect contact cooler (ICC), C101, to condense water vapor, remove traces of ash and dissolve soluble gases such as SO<sub>2</sub>, SO<sub>3</sub> and HCl. The ICC is a direct contact, packed tower, water scrubber wherein the circulating water system used for scrubbing is cooled by indirect heat transfer with a cooling water stream in E101. The net condensed water is first filtered and then, together with the soluble impurities, is sent to a water treatment system for further purification.

The flue gas now is split between entering the Sour Compression process (6) and being sent to the coal mills before entering the boiler as the primary recycle stream (3). The first step of the compression process is a pressure change to 15 bar via compressor 1, K101. The compressed gas is then cooled through a two stage heat exchanger process where heat is recovered for boiler feed water heating and condensate preheating in E102 and E103, respectively. Prior to entering the first reactor chamber, C102, the gas undergoes a further temperature reduction as it is passed through a heat exchanger, E104, using cooling water.

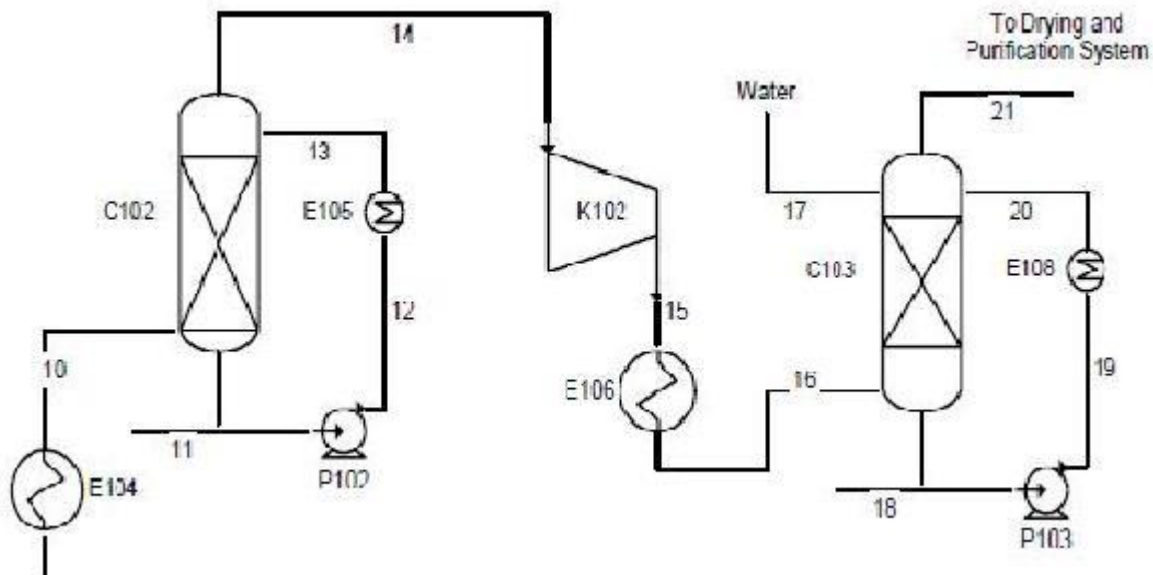


Figure 2.9 Sour compression process layout diagram (45).

At this point some form of hold-up is introduced, by, for instance, the use of a packed bed contacting column with pumped-around liquid condensate. The final production form of the two reactors, C102 and C103, is uncertain. Little to no work has been done to attempt to optimize this step of the process with respect to either performance or cost. The  $\text{SO}_2$ -free gas is then compressed to 30 [bar] in K102. The 30 [bar] point is considered the ideal location to remove NO and  $\text{NO}_2$  from the process. Once cooled in E106 using cooling water the gas enters the second reactor, C103. At this point, a few seconds of hold-up will be provided to ensure the reactions proceed until all  $\text{SO}_2$  and the bulk of the NO is removed. Little  $\text{HNO}_2$  or  $\text{HNO}_3$  will be formed until most of the  $\text{SO}_2$  has been consumed. Some  $\text{NO}_2$  formed by reaction 1 will be consumed by reaction 3, but the latter reaction produces NO, thus resulting in zero net  $\text{NO}_x$  removal. Therefore, reaction 4 is the dominant route for  $\text{NO}_x$  removal, producing  $\text{HNO}_2$  or  $\text{HNO}_3$ . In this way, about 90% of the  $\text{NO}_x$  and all of the  $\text{SO}_2$  can be removed from the  $\text{CO}_2$  before the removal of the non-condensable gases.

#### 2.3.4.3 Laboratory Testing

Although the conceptual design of the sour gas compression process has been more or less settled for some time; the real world operating conditions, and the performance expected from the process, have remained uncertain. In order to better understand the effects of pressure, residence time, and water contact Murciano et al. investigated these variables in a systematic fashion in the Imperial College London laboratory. The following section is a summary of these findings (51) with commentary on their implications.

##### Oxidation of $\text{SO}_2$ and NO Separately Under Dry Conditions

Synthetic flue gas was introduced into a dry reaction chamber with either pure  $\text{N}_2$  or a small fraction (3.5%) of oxygen. The degree of NO to  $\text{NO}_2$  oxidation was found to be positively correlated with both residence time and pressure. Under the test conditions no other  $\text{NO}_x$  species, such as  $\text{N}_2\text{O}$  or  $\text{N}_2\text{O}_4$ , were identified by mass spectroscopy. The tests showed that oxidation was near complete (87%) at pressures

of 15 [bar] and that the presence of SO<sub>2</sub> had the effect of increasing the fraction of NO oxidized by an additional 9 percentage points.

#### Oxidation of SO<sub>2</sub> and NO Separately Under Wet Conditions

Introduced to a wet reactor, free of oxygen, the NO composition in the flue gas remained constant; confirming the low solubility of NO in water predicted by theory. In the presence of oxygen, NO oxidized to NO<sub>2</sub> in the dry reactor, as described above, then was converted into acid liquid products (mainly HNO<sub>3</sub> and HNO<sub>2</sub>) when introduced to the wet reactor. Experiments confirmed that liquid acid formation was indeed a positive function of pressure. Acceptable NO conversion rates (~90%) were observed at 15 [bar]; indicating that a two stage commercial process operating at 15 and 30 [bar] should achieve at least this level of conversion.

Unlike NO, SO<sub>2</sub> was shown to readily dissolve into water forming sulfurous and sulfuric acids, both in oxygen rich and free environments. The rapid dissolution into water created the effect of an increase in the reactor concentration of SO<sub>2</sub> in time as the water was slowly saturated and liquid phase oxidation occurred. Experiments at 5 and 15 [bar] showed an order of magnitude increase in the initial molar transfer rate from 0.00577 to 0.0565 [mol SO<sub>2</sub>/h\*L]. These results indicate that under higher pressures, and elevated flow rates, the gas/liquid phase contact becomes very important; therefore mass-transfer limitations must be taken into consideration when progressing towards full scale operation.

#### Oxidation of Mixed SO<sub>2</sub> and NO

Under dry conditions there was no significant oxidation of SO<sub>2</sub> by NO at any pressure and temperature combination inclusive to the range of operating conditions being considered. Three wet scenarios were evaluated to test the effect of both liquid and vapor water on the reaction mechanisms. Under the large volume of liquid regime there was the anticipated high initial removal of SO<sub>2</sub> with gradual gaseous concentration increase discussed prior, but additionally a sizeable proportion of the formed NO<sub>2</sub> was also converted (~50% at 5 [bar] and ~80% at 15 [bar]) into nitric/nitrous acids. In the presence of a small volume of water the initial conversion of SO<sub>2</sub> was lower than the large volume however, the level of SO<sub>2</sub> conversion increased with time. As before the NO<sub>2</sub> concentration is reduced through the formation of liquid products but also due to reduction via reaction 2 to NO. Additional testing on the interplay between acid concentration and SO<sub>2</sub> removal indicated that a catalytic reaction between NO<sub>2</sub> and oxygen in the presence of strong acid facilitates the creation of sulfuric acid.

These experiments showed the importance of the presence of both water and oxygen in enabling the proposed reaction mechanisms to occur under the operating conditions appropriate for the sour compression process. The researchers did caution that more detailed interpretation of their data was complicated by the presence of small, highly acidic liquid droplets which were found in the cooler parts of the test rig downstream of the reactor. This phenomenon occurred as a result of the high dew point of sulfurous acids which condense out of the gaseous mixture at a higher temperature than pure water would due to the presence of SO<sub>2</sub>. The researchers elucidated this problem by noting that the measured SO<sub>2</sub> conversion rates were similar from 100 to 400 [°C] (mass-spec right after reactor) which implies both the importance of liquid acid droplet formation and the extent to which it will occur in practice. An effort is already underway to modify the test rig in order to obtain a more robust understanding of the role of acid precipitation in the sour compression process.

#### 2.3.4.4 Air Products Work at Alstom Facility

The Air Products Company has been performing small scale testing of the sour compression process at the Alstom Oxyfuel test facility in Windsor, Connecticut. The test rig, designed and assembled by Air Products, operated at 7 - 15 bar and received a slip stream of 0.25 – 0.33 [MW-thermal] equivalent flow rate from the 15 [MW-thermal] tangentially fired oxy-coal combustion unit. The test rig was comprised of three main units: scrubber/condenser, compressor, and reactor. The function of the latter two units is self-evident, but the first unit served to remove particulates and significant amounts of soluble acid gases in addition to cooling the flue gas. After compression the gas was cooled prior to entering the reactor. During testing the gas analyzer was cycled every fifteen minutes between the gas stream inlet to the reactor and the effluent stream. A plot of analyzer data for one of the runs with high conversion numbers is displayed below.

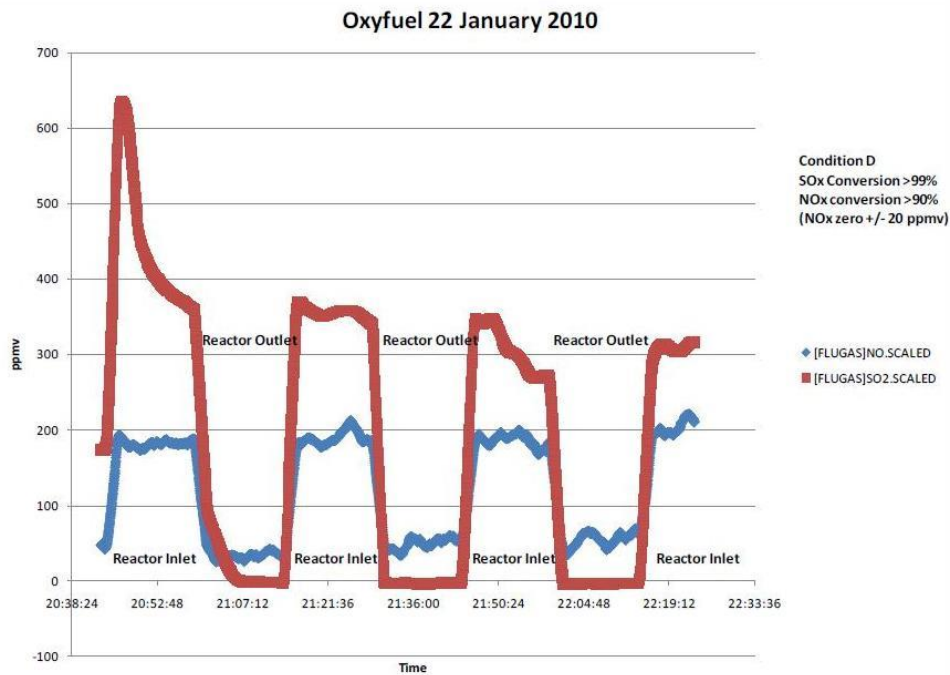


Figure 2.10 Phase 1 test results showing very high levels of SO<sub>2</sub> and NO<sub>x</sub> removal using the test rig on slip-stream from the Alstom oxy-coal facility in Windsor, CT (52).

In addition to identifying operating conditions in which the test rig performed admirably, it was necessary to test across a wide range of entry and processing conditions in an attempt to gain insight into how the rig would react under dynamic loading conditions. The program evaluated 24 different sets of conditions, including variations in the five primary reactor operating parameters: pressure, gas flow-rate, liquid recirculation flow-rate, fresh make-up water flow-rate, and reactor inlet SO<sub>x</sub>/NO<sub>x</sub> ratio. Table 2-2 summarizes the effects of these parameters on the conversion of NO<sub>x</sub> and SO<sub>x</sub>, with all other variables held constant.

Table 2-2 Trends in the SO<sub>x</sub>/NO<sub>x</sub> conversion efficiency from Air Products test rig at the Alstom oxy-coal facility (52).

↑ in Operating Parameter	SO <sub>x</sub> Conversion	NO <sub>x</sub> Conversion
Column pressure	↑	↑
Column gas flow-rate	↓	↓
Column recirculation liquid flow-rate	↑	↑
Column fresh make-up water flow-rate	↑	↑
Column inlet SO <sub>x</sub> /NO <sub>x</sub> ratio	↓	↑

Of the five parameters, four display mutual effects for the degree of SO<sub>x</sub> and NO<sub>x</sub> conversion. All of these (Column pressure, Column gas flow-rate, Column recirculation liquid flow-rate, and Column fresh make up water flow-rate) are all directly related to the gas/liquid phase contact and consequently the mass-transfer limitations discussed earlier. The appearance of these trends in empirical data verifies the theoretical calculations, and in doing so, lends credence to moving forward with a larger pilot program.

### 2.3.5 Carbon Dioxide Purification Technologies

The question of how to best further purify the CO<sub>2</sub> rich gas stream once it has gone through preliminary gas clean-up is still largely undecided. There are two primary reasons for this state of affairs: A.) It remains unresolved, by either regulatory agencies or commercial utilities, what the purity standards will be for any integrated pipeline network. B.) The nascent state of commercial development has left the door open to a myriad of competing ideas proposed by at least three vendors (Linde, Praxair, and Air Products). Of the three vendors just enumerated, the systems proposed by Air Products have been the most vetted and are thus the only systems analyzed in this section. The following section provides a brief introduction to the seven proposed systems by Air Products; which correspond to a range of different purity and capture rates.

The Air Products schemes all rely upon CO<sub>2</sub> condensation as the means of performing inert gas removal. In order to reach temperatures low enough to facilitate this process (-55°C) these systems all utilize the effects of Joule-Thompson expansion to provide the cooling duty required. This practice is referred to as an auto refrigeration cycle because the working fluid in the system is also the product stream being processed. It should be noted that the use of this cycle is by no means obligatory and preliminary work has been completed on evaluating external means of meeting the cooling duty (53). Also, a shared feature of all Air Products systems is the use of a pair of thermally regenerated desiccant driers to provide a dry waste gas stream to the cold box in order to prevent ice buildup.

#### 2.3.5.1 Carbon Dioxide Purity Dependency

The purity of the carbon dioxide exit product is a system design variable in a PC oxyfuel plant. The product stream can range from about 85% CO<sub>2</sub>, dry basis (depending on air ingress) to 99.9999% pure. This range corresponds to simple flue gas dehydration and compression on the low end to high purity, multi-stage cryogenic distillation producing a liquid CO<sub>2</sub> product on the other. The following subsections present technical details for several of the carbon dioxide processing unit cycles being considered to produce an oxyfuel product stream of varying degrees of purity.

## Dual Flash

The simplest system that has been proposed utilizes two flash drums inside the cold box to achieve an exit stream purity of 95.9 (46) [mol%] CO<sub>2</sub>. Air Products reports that this setup is capable of recovering 89% of CO<sub>2</sub> while producing a rich product containing 0.91 [mol%] oxygen. This high oxygen content would preclude this product from being used in enhanced oil recovery however as the risks of explosion are unacceptably high at such concentrations. Figure 2.11 shows the process diagram from the exit of the previous gas treatment process (stream 1) to the product exit and non-condensable vent (stream 20 and 12, respectively).

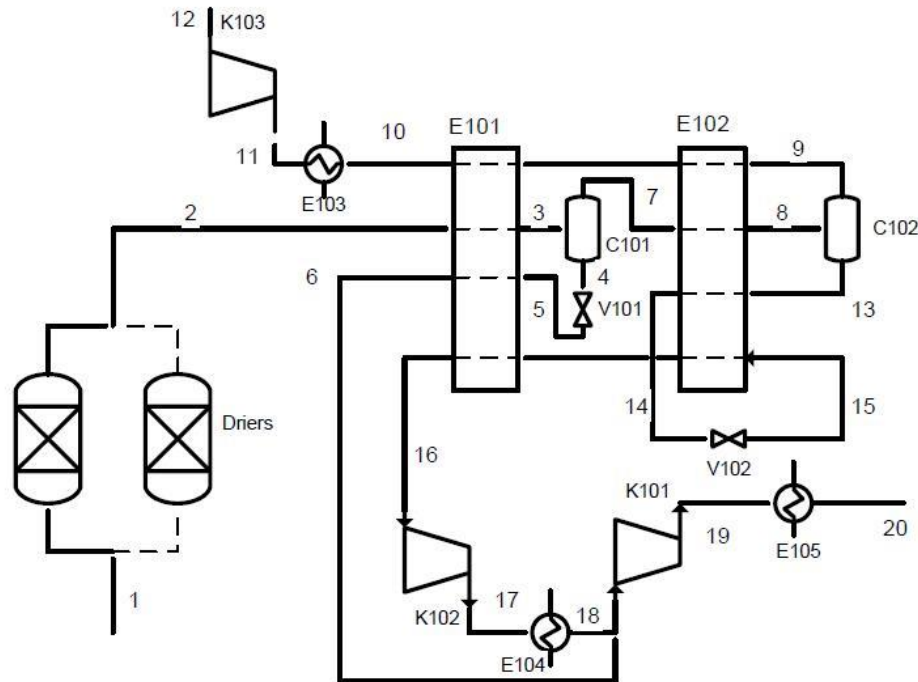


Figure 2.11 Process diagram for a dual flash system producing a gaseous CO<sub>2</sub> product at 110bar (19).

After leaving the cold box (stream 16) the product is pressurized to 110 bar (pipeline pressure assumed for all gaseous cases) via multistage compression with heat recovery through the boiler feed water heat exchangers (E104 & 105). At this point the CO<sub>2</sub> rich product is fully processed and ready to enter the pipeline through which it will be transferred and stored.

This process has currently been adopted as the “base case” in large part because the relative simplicity of its design provides that it has the cheapest CAPEX of the competing designs. It is unclear what the exact split will be between CAPEX and OPEX for purification systems, but OPEX is believed to account for over half. Because of the energy intensive nature of the process it is useful to consider what options might be available for reducing the energy of separation and consequently, OPEX.

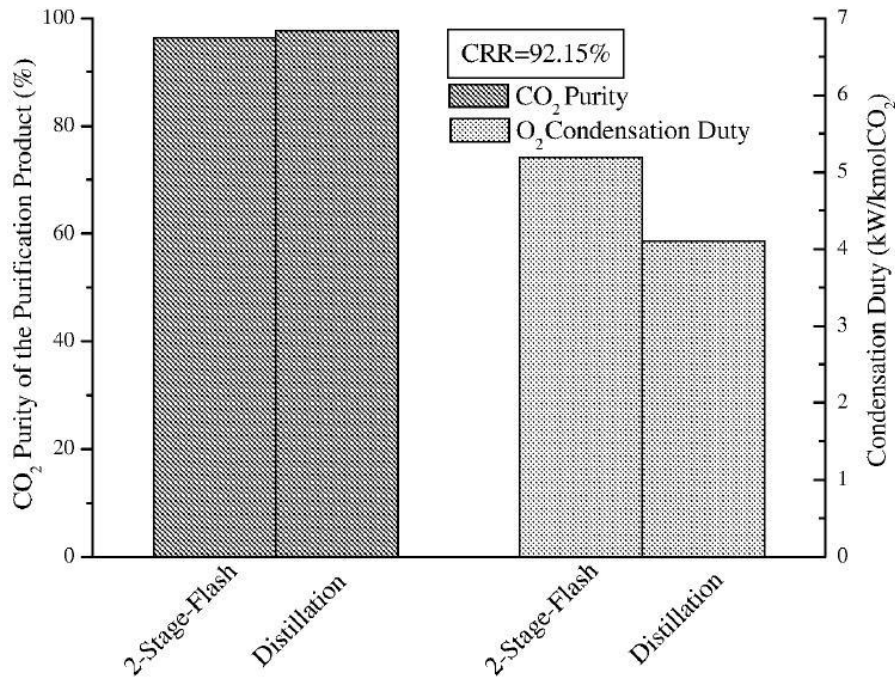


Figure 2.12 . Comparison between distillation and 2-stage flash systems for a stipulated CO<sub>2</sub> recovery rate (54).

As the above figure taken from Li et al. shows; for a specified CO<sub>2</sub> recovery rate a single stage distillation process requires less condensing duty and produces a product stream of superior purity. Although none of the designs from Air Products feature a single distillation process, distillation is utilized along with knock out drums in order to achieve a higher purity in some of the following designs without adversely effecting specific power consumption.



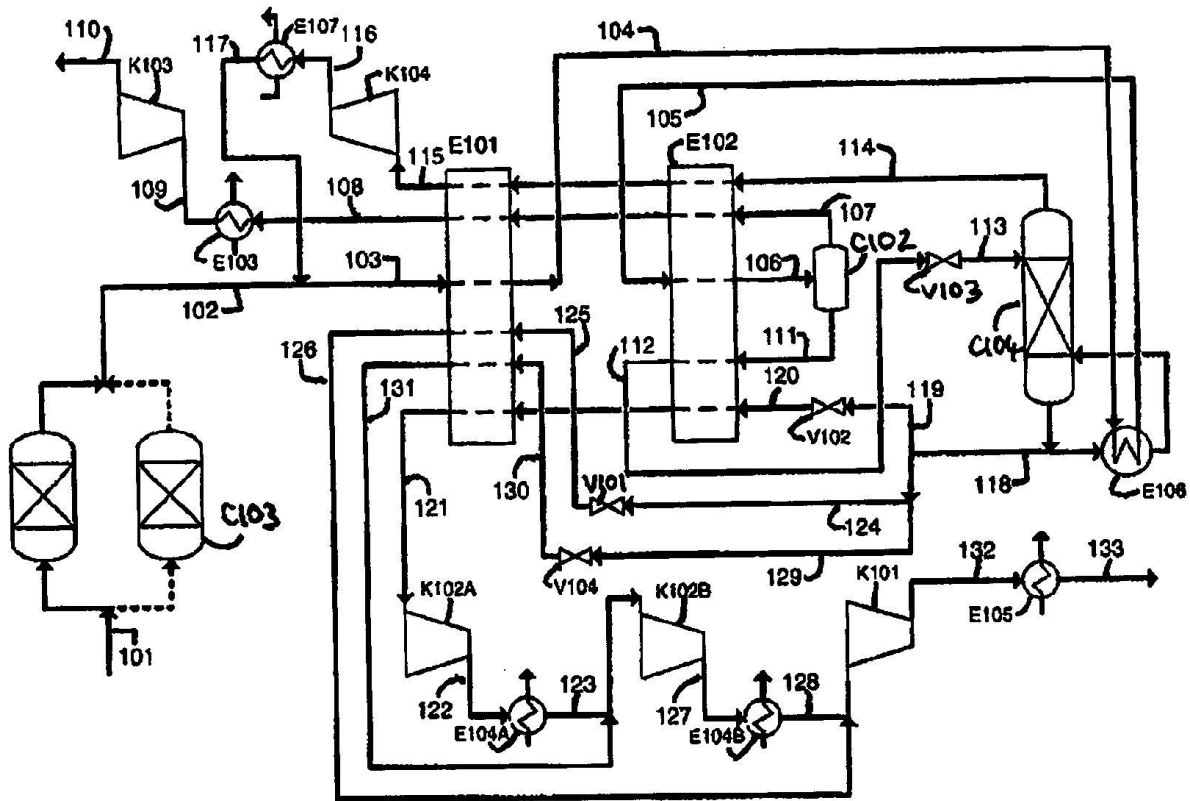


Figure 2.14 Process diagram for a single flash, single distillation column system with extensive heat integration producing gaseous CO<sub>2</sub> at a pressure of 110 bar (48).

Incorporating the changes outlined above allow this system to achieve 87.7% recovery at a purity of 99.98 [CO<sub>2</sub> mol %]. The product is EOR compatible and thanks to the altered compressor arrangement and heat integration the specific power is reduced by 1% relative to the baseline. Higher CAPEX prevents this system from strictly dominating the baseline but more will be said with respect to these plant-wide tradeoffs later on.

#### Dual Flash with Membrane

Similar in design to the base case, this design would incorporate the use of a permeable membrane in order to lessen the amount of oxygen and carbon dioxide being expelled from the vent along with the non-condensable gases. Conceptually, the use of a membrane would provide for a decrease in the ASU load as oxygen which would have been vented to the atmosphere is now circulated back into the combustion chamber. Although it has not yet been empirically tested, results from Aspen modeling completed using the following process layout have yielded specific power reductions of nearly 9%.



Table 2-3 PRISM Membrane performance characteristics (49).

Permeate Fraction		Non-permeate Fraction		Relative
CO <sub>2</sub>	O <sub>2</sub>	N <sub>2</sub>	Ar	Size
0.70	0.37	0.92	0.83	1.00
0.75	0.41	0.90	0.81	1.13
0.80	0.46	0.89	0.78	1.30
0.85	0.51	0.87	0.75	1.49
0.88	0.55	0.86	0.73	1.62
0.90	0.58	0.84	0.70	1.76
0.93	0.63	0.82	0.67	1.94
0.95	0.68	0.80	0.63	2.18

Using this membrane in their aforementioned model a CO<sub>2</sub> purity of 96.3 [mol%] with a CO<sub>2</sub> recovery rate of 97.7% was achieved. As before mentioned this system operated at a 9% lower specific power and delivered nearly 9% points higher capture rate at nearly an identical purity to the double flash base case.

#### Single Flash, Single Distillation with Membrane

This cycle is analogous to that presented in Figure 2.13 except that a membrane has been incorporated into the non-condensable vent of the system. Because of the inclusion of distillation this process is capable of very high CO<sub>2</sub> purity levels, 99.86 [mol%], with oxygen levels expected to be around 100 ppm. This means that this would be a suitable process when there is a chance of using your product CO<sub>2</sub> for EOR. This process would share in the same benefits of ASU duty reduction mentioned in the previous case thanks to a recirculation of excess oxygen. This energy reduction would be substantial enough to reduce specific power by three percent relative to the baseline while capturing 97.9% of CO<sub>2</sub> at a saleable purity. The schematic below illustrates the proposed system layout.

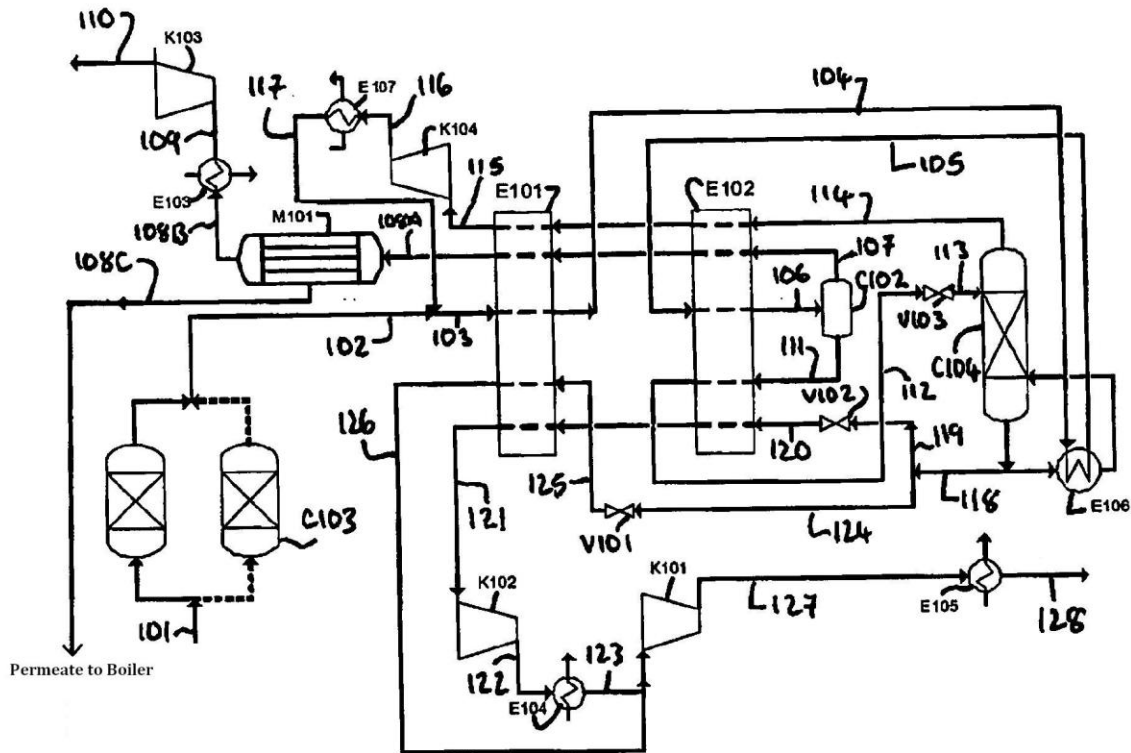


Figure 2.16 Process diagram for a single flash, single distillation column system with membrane separation and permeate recycle (50).

#### Double Flash, Single Distillation with Liquid Product

The following two systems are designated as “high purity” options by Air Products. They differ from the competing systems in that they produce liquid CO<sub>2</sub> as their end product. There are intrinsic advantages to pumping a fluid rather than compressing a gas, namely the mechanical work required to transport a given quantity of CO<sub>2</sub> product is reduced. Also, the collection of distillation bottoms allows for the collection of very high purity CO<sub>2</sub> at a comparatively low pressure for transport (7 or 30 [bar] v. 110 [bar]). Currently, there appears to be little reason to produce high purity CO<sub>2</sub> product in this manner. However, if extremely exacting levels of purity were required the liquefaction systems seem to hold the most promise for meeting these requirements in an economically viable manner.

The system detailed in the following figure would produce liquid CO<sub>2</sub> product at a pressure of 30 [bar]. The corresponding purity would be 99.98 [mol%] with a CO<sub>2</sub> recovery rate of 87.7%. The relative specific power consumption of this system is 2% lower than our baseline making it a more attractive option, with respect to this parameter, than the dual distillation column design discussed earlier. Further techno-economic analysis will need to be completed in order to flush out whether or not the liquefaction system is indeed the preferred option for CO<sub>2</sub> product purity of 99.98%.

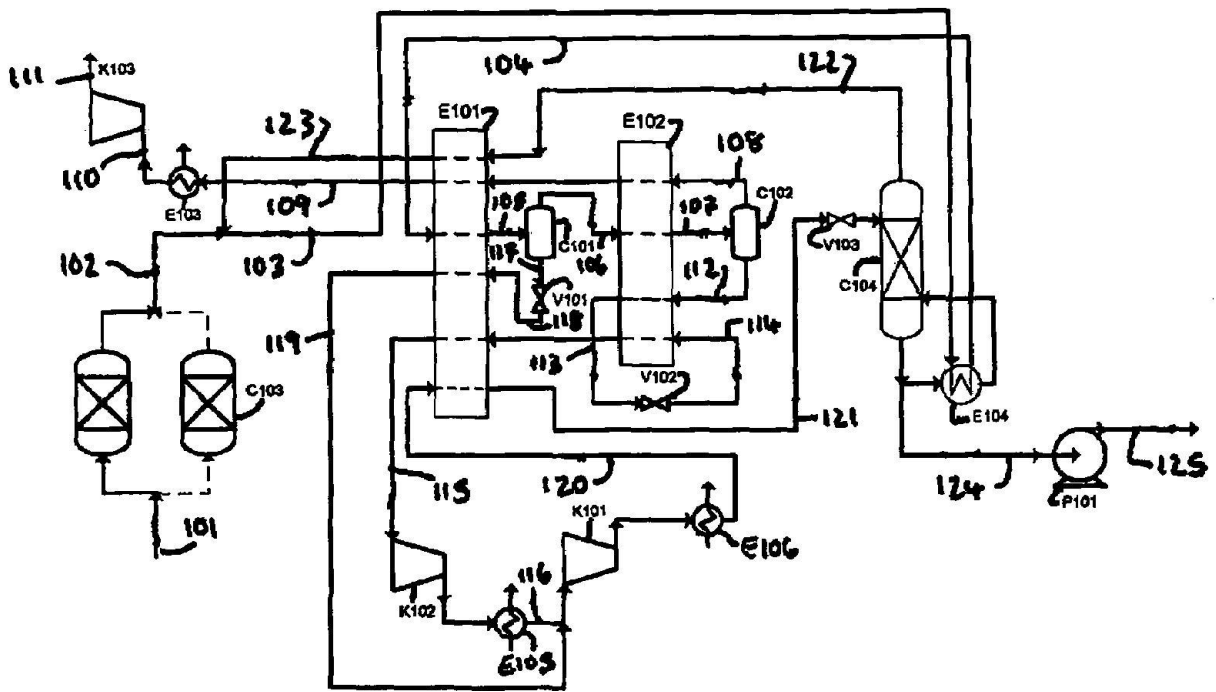


Figure 2.17 Process diagram for a dual flash, single distillation column system with 30 bar liquefied CO<sub>2</sub> product (45).

#### Triple Flash, Single Distillation with Liquid Oxygen Product

This system is very unlikely to see wide spread adoption in the CCS community simply because there currently exists a very limited market for the sale of food-grade carbon dioxide. Capable of producing 99.9999 [mol%] pure liquid product at a pressure of 7 [bar], this system is capable of purity levels that can't be achieved by any other system here enumerated. With oxygen levels in the 5 [ppm] range and recovery still at 87.7% it is understandable that efficiency sees a 2% decrease relative to our baseline. This is also the most complex system with respect to the quantity of equipment involved and is therefore likely to be very expensive with respect to both CAPEX and OPEX. It remains to be seen whether sufficient demand will emerge to warrant the level of investment required for this system on a commercial scale. Aspen modeling utilizing the process layout in the following diagram has at least theoretically demonstrated that meeting stringent purity requirements is possible if the economics of operation suggest that very high product purity is the Pareto optimum.

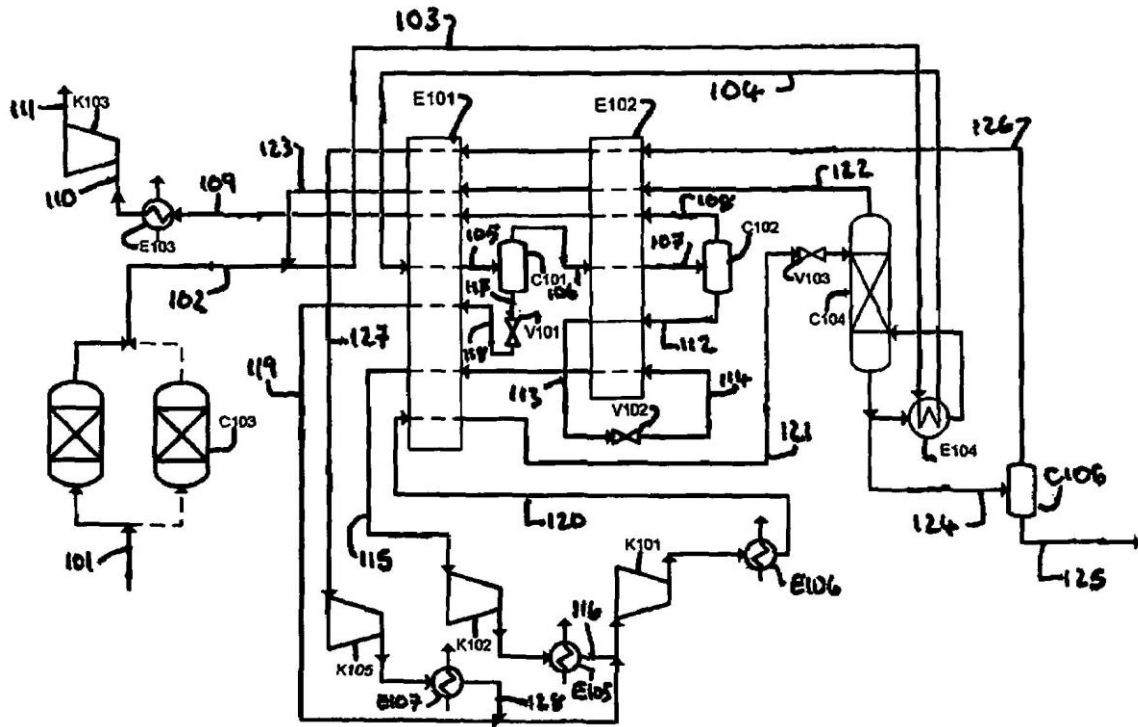


Figure 2.18 Process diagram for a triple flash, single distillation column system with 7 bar liquefied CO<sub>2</sub> product (45).

### 2.3.5.2 Relative CPU System Performance

There are several options for purification depending upon what purity of the CO<sub>2</sub> end product is required. Also, the above seven system variants are just those being offered by Air Products. For ease of comparison the following table of the seven systems and their most relative attributes has been compiled. A note to the reader: The widely acknowledged upper limit on oxygen concentration for the safe use of CO<sub>2</sub> product gas for enhanced oil recovery is 100 [ppm].

Table 2-4 Summary of the seven Air Products purification processes (52).

Description	CO <sub>2</sub> Purity	Oxygen Content	CO <sub>2</sub> Pressure	CO <sub>2</sub> Recovery	Relative Specific Power
Standard Cycle	95.90 mol%	0.91 mol%	110 bar	89.0%	1.00
High Purity Option 1	99.89 mol%	100.00 ppm	110 bar	87.4%	1.03
High Purity Option 2	99.98 mol%	100.00 ppm	110 bar	87.7%	0.99
30 bar liquid CO <sub>2</sub>	99.98 mol%	100.00 ppm	30 bar	87.7%	0.98
7 bar liquid CO <sub>2</sub>	100.00 mol%	5.01 ppm	7 bar	87.7%	1.02
Standard with membrane	96.30 mol%	0.73 mol%	110 bar	97.7%	0.91
High purity Option 1 with membrane	99.86 mol%	100.00 ppm	110 bar	97.9%	0.97

The systems outlined all have their specific merits which may qualify them to be the system of choice for any specific plant under the right circumstances. In the absence of any authoritatively derived purity standards, the circumstance most likely to be crucial will be that of cost. Determining the total cost incurred for the separation and transportation of a given quantity of carbon dioxide however, is a formula which includes more than just the CAPEX and OEPEX of the purification system downstream of criteria pollutant removal. Currently there seems to be consensus forming around the 96 [mol%] CO<sub>2</sub> purity level due to the balance of the economics of separation and the lack of severely deleterious effects on the transport and storage capacity required at lowered purity levels.

#### *2.3.5.3 CPU Update Rational*

Given the presence of several papers and case studies outlining the recent advances in CPU design we made the assessment that it would be worthwhile to update the CPU model being employed by public release v8.0.2 and earlier versions of the IECM. The updated CPU performance and cost models are explained in greater detail in those respective chapters, but an explanation of the simplifications and assumptions made in their construction will be discussed here. The principle reasons for updating include:

- The separation energy + compression energy values for high CO<sub>2</sub> exit purity configurations of the old model are not reflective of the performance reported for similar exit purity conditions by the aforementioned Air Products patents or the DOE oxyfuel case studies.
- There was no physical or function link between CO<sub>2</sub> product purity and the percent of CO<sub>2</sub> captured by the old CPU model. A detailed explanation of how this was amended in the new model is present in Chapter 7.
- Developing an accurate understanding of any reduction in specific net power input from increased train size was an important objective which it was unfortunately not possible to achieve in this work. In the future, this dimension should be added to the CPU model as additional performance studies become available which examine a wider array of flue gas throughput.
- Carbon purification equipment has matured enough that information about maximum train size can be inferred. This information has been used to improve the economic model of carbon handling systems and is presented in Chapter 8.

For these reasons the revised CPU model described in Chapter 7 was created. Carbon processing units are a unique technology to model in that they are designed specifically to process a given volume of flue gas to a predetermined level of exit purity which is essentially static. It is the author's opinion that if oxyfuel does develop as a major electricity production technology that the purity level of the CPU will either become dictated by environmental regulation or the industry will develop 2 or 3 standard purity outputs which will be selected based upon the intend use of the CO<sub>2</sub> product. However, for the sake of modeling from a limited number of available case studies across a variety of assumed exit purities the CPU model has been assumed to be continuous with respect to purity and capture rate. Future refinement to this assumption will likely be necessary but even in its current form the updated CPU model is a vast improvement upon its predecessor.

### 2.3.6 CO<sub>2</sub> Product Transport Pressure Requirements

Unlike post-combustion capture, the CO<sub>2</sub> product leaving an oxyfuel plant is often impure. This may lead to the need for special precautions when handling the mixture as well as a need to assess how the amount of inert impurities in the product affects the transportation system. Two-phase flow and the condensation of acid gases are the two main concerns when transporting impure CO<sub>2</sub> product. Two-phase flow can cause pump failure due to cavitation and the condensation of acid gases would either lead to increased levels of corrosion or the need for more expensive, corrosion resistant materials (55). Both issues can be mitigated if the mixture is kept at a sufficiently high pressure to ensure that all components of the mixture remain as super-critical fluids for the duration of transport through the pipeline network.

Equations of state can be used to compute theoretical thresholds for the pressures and temperatures required to ensure that a mixture will stay in a super-critical state (54). Figure 2.19 presents work completed by the Vattenfall Corporation (56) using the GERG-2004 Equation of State software to compute the minimum mixture pressures at normal subterranean pipeline temperatures to ensure that two-phase flow and condensation are avoided.

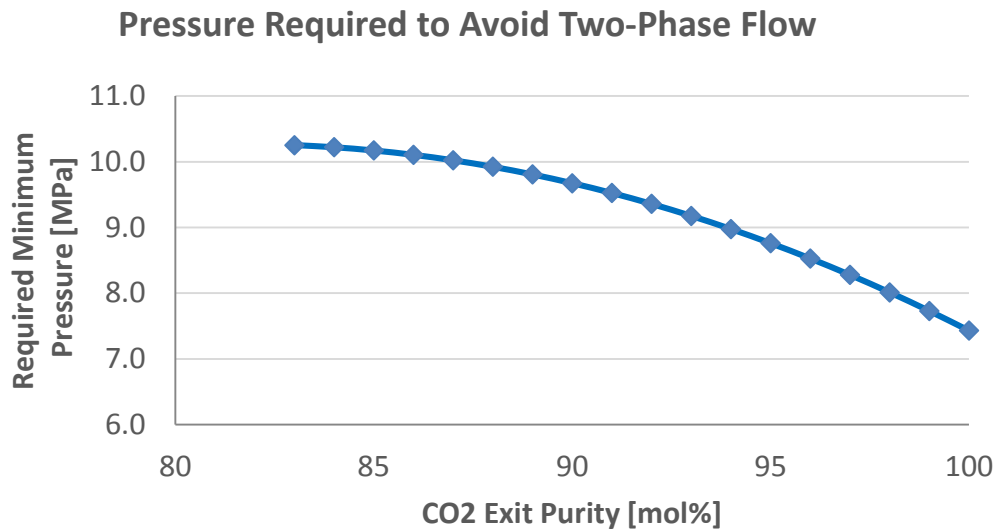


Figure 2.19 Minimum required pressure to avoid two-phase flow as calculated by Vattenfall (56) using GERG-2004 equation of state software at 285K. Avoidance of 2-phase flow is essential so that traditional pumps and pipeline materials may be used without fear of cavitation and accelerated corrosion, respectively.

The most commonly anticipated injection pressures for the sequestration of carbon dioxide range from 2000-2200 [psia] or about 13.8-15.2 [MPa]. This, in conjunction with Vattenfall's findings regarding minimum pressure requirements indicates that avoiding two-phase flow should not be a problem in the course of normal operation.

### 2.3.7 Storage Concerns for Impure Carbon Dioxide Products

Another issue of concern, were an oxyfuel plant to the point of being sited, would be the potential effect that impurities in the CO<sub>2</sub> product could have on the available geological storage capacity. Recent work completed through the IEA GHG Division has produced the formula below which provides an estimate of the relative CO<sub>2</sub> storage capacity adjusted for the effect of impurities in the CO<sub>2</sub> product (57).

$$\text{Carbon Dioxide Impurity Capacity Adjustment} = \frac{M}{M_0} = \frac{\bar{\rho}}{\rho_0(1 + \sum_i m_i/m_{CO_2})}$$

In this relation M and M<sub>0</sub> denote the mass of CO<sub>2</sub> in the mixture and the pure stream, given equal volume, respectively. The densities  $\bar{\rho}$  and  $\rho_0$ , denote the mixture and the pure stream, and  $m_i/m_{CO_2}$  is the ratio of the mass of impurity i to the mass of CO<sub>2</sub> in the mixture. The ratio of M/M<sub>0</sub>, which can be interpreted as the ratio of the mass of CO<sub>2</sub> per unit volume in the mixture to that in the pure state, represents a normalized storage capacity for the CO<sub>2</sub> product in the supercritical phase. For the pure state this ratio equals unity but even modest amounts of impurities can yield substantial changes in normalized storage capacity.

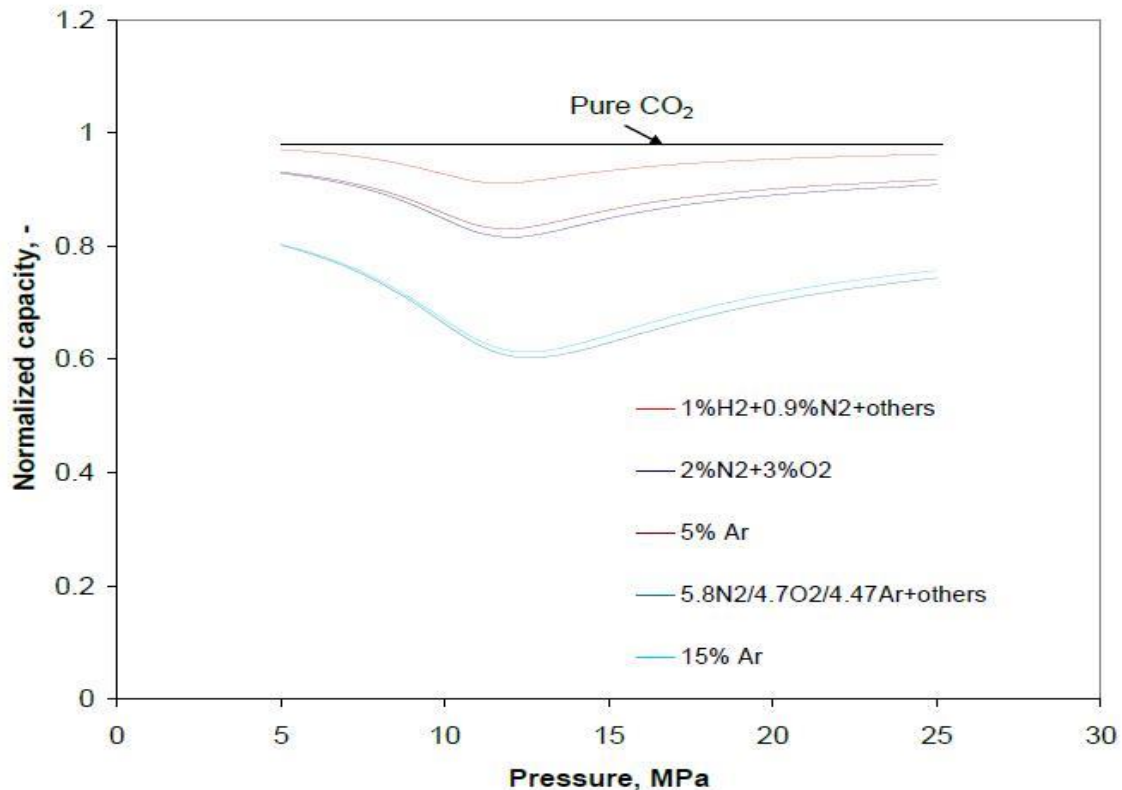


Figure 2.20 Normalized CO<sub>2</sub> storage capacity at 330K as calculated using the carbon dioxide impurity capacity adjustment equation, where the densities are calculated with Peng-Robinson Equation of State (57). At low purity oxyfuel operation (CoCapture) this analysis shows that geological capacity could be reduced nearly forty percent compared to pure carbon dioxide.

The consequences for reducing storage capacity by operating an oxyfuel plant at a low purity state could be substantial. Furthermore, the presence of impurities also impacts the injection properties of the supercritical fluid which can have either positive or negative ramifications depending on the constituency of the fluid. The capacity restrictions of a specific geographical area will clearly have implications for the exit purity chosen for any future oxyfuel installation, but each will have to be dealt with on a case by case basis and represent irreducible and falls outside the scope of this thesis.

In addition to the physical and engineering obstacles related to handling and storing impure carbon dioxide are the legal and regulatory concerns. With respect to Class IV well permits, questions remain about the applicability of the Resource Conservation and Recovery Act (RCRA) and the Comprehensive Environmental Response, Compensation, and Liability Act (CERCLA) for CO<sub>2</sub> streams. The U.S. Environmental Protection Agency has stated that a CO<sub>2</sub> stream is not itself listed as a RCRA hazardous waste (58). However, plant operators will need to determine whether the impurities of the CO<sub>2</sub> stream produced by a plant should cause that stream to be deemed hazardous under EPA's RCRA regulations, and if so, any and all injection of that stream must occur in a Class I hazardous waste inject well. This would potentially add considerable expense to any sequestration project, especially likely with CoCapture.

The EPA has also stated that CO<sub>2</sub> itself is not listed as a hazardous substance under CERCLA (58). A carbon dioxide product stream however may contain a listed hazardous substance (mercury) or may mobilize substances in the formation chosen for injection to produce listed hazardous substances (sulfuric acid). CERCLA may exempt from liability under CERCLA section 107, 42 U.S.C. 9607 certain "Federally permitted releases" (FPR) which would include the injectate stream from a carbon capture facility as long as it is injected and behaves in accordance with the permit requirements (58). However, this leaves the subject of accidental releases (and liability) to the discretion of the individual permit requirements as any releases from the well would be outside the scope of the Class VI well permit and thus would be no longer considered a federally permitted release. There remains appreciable uncertainty to the legal viability of CoCapture. Lastly, the associated additional cost of handling an impure CO<sub>2</sub> product stream remains largely unknown and is beyond the scope of this thesis.

# Chapter 3 Pulverized Coal Oxyfuel Model Configurations and Conceptual Operation

Prior to the uptake of this work, an oxyfuel model was available to users of the Integrated Environmental Control Model (IECM). The previous model was the product of work undertaken by PhD. Anand Rao more than a decade ago. The commercial development of oxyfuel at that time was not very advanced and there was considerable uncertainty about the cycle configuration to be used. Figure 3.1 is a representation of the oxyfuel system developed for the IECM at that time.

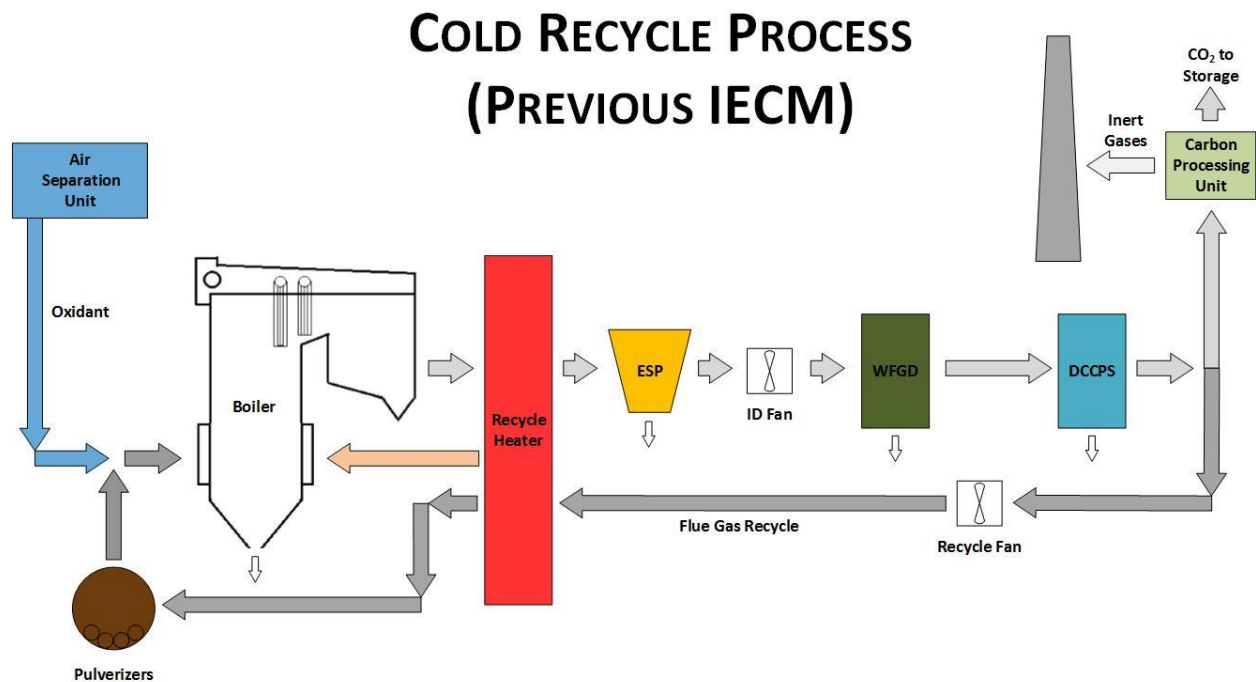


Figure 3.1 Process flow diagram for the oxyfuel model utilized in IECM version 9 (and previous). All the flue gas is treated by the traditional pollution control technologies and is handled as a single recycle stream to the boiler.

This oxyfuel cycle represents the most robust configuration to ensure compliance with all environmental regulations, material corrosion concerns, and fuel flexibility. What is sacrificed with this configuration, known as Cold Recycle, is thermodynamic efficiency. After particulate removal in the electrostatic precipitator (ESP), all the flue gas is passed through a wet flue gas desulfurization unit (WFGD) followed by a direct contact cooler and polishing scrubber (DCCPS). This ensures the flue gas sent to the carbon processing unit (CPU) and flue gas recycle will have very low sulfur oxide levels, relatively low moisture content, and be essentially free of particulate matter. The price paid is that all those gas handling systems must be large enough to handle the entire flue gas stream (capital intensive) and the flue gas recycled to the boiler is cold (thermally inefficient).

## 3.1 New Oxyfuel Plant Configurations

The updated oxyfuel model in the IECM consists of three configurations; each of these corresponds to a mass fraction range for sulfur in the fuel to be used. A coal with a very low sulfur content, say Wyoming Powder River Basin, could be used in any of the recycle configurations. However, using a cool recycle configuration with a WFGD would neglect the gain in thermal efficiency and reduction in capital costs which could be had by selecting the warm recycle configuration. Fuel sulfur is the determining factor for which of the three configurations is selected, but how the flue gas is ultimately divided is a function of the amount of contained fuel moisture. The conceptual details of how the flue gas is divided are presented in Section 3.4 and the algorithms used in the IECM are covered in detail in Chapter 4.

### 3.1.1 Oxyfuel Cycle for Medium-High Sulfur Coals

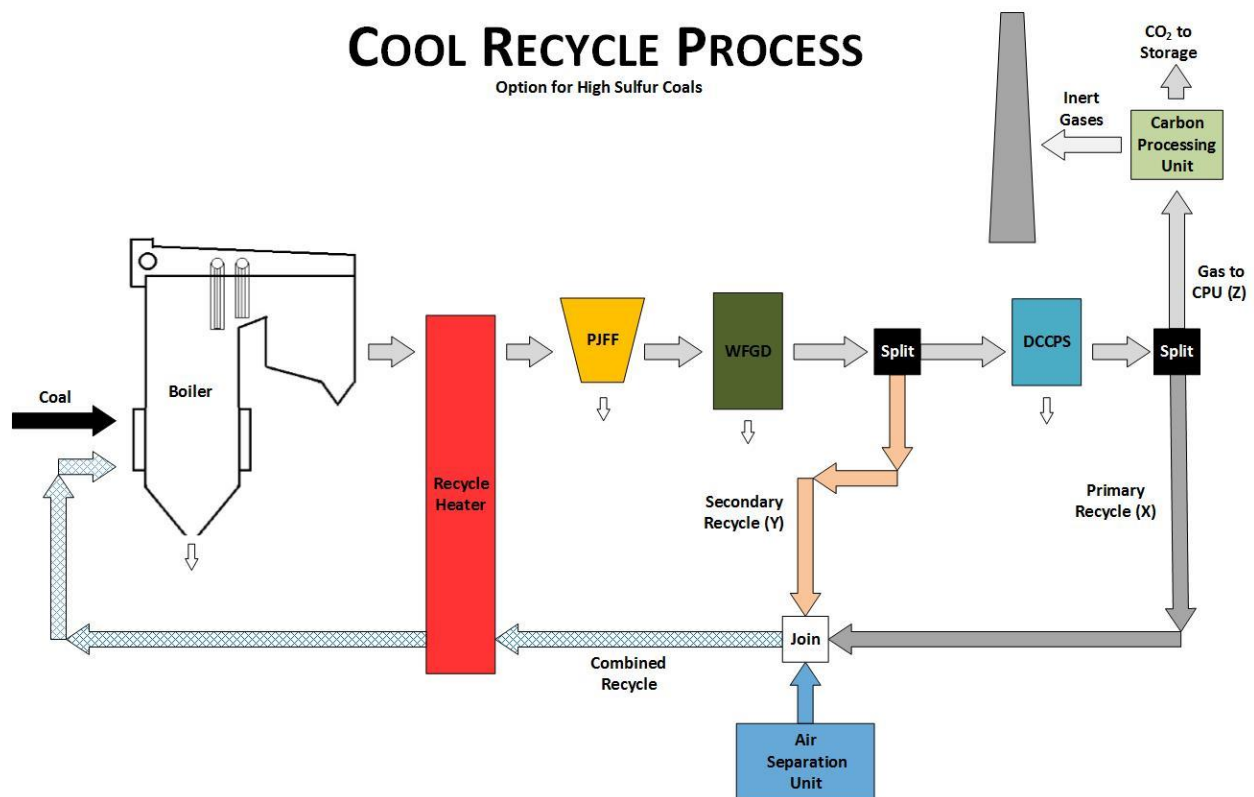


Figure 3.2 Process flow diagram for coals with a sulfur content above 1.5 wt%. This process is most similar to the pre-existing oxyfuel model in that the entire gas stream is treated for particulates and sulfur.

The cool recycle process with wet flue gas desulfurization above would produce efficiency results very close to the cold recycle system in IECM (v9 and previous) for all coals. The largest difference is that not all the flue gas must be passed through the DCCPS in the cool recycle configuration. In both the cool and warm recycle configurations there is a secondary recycle path in addition to the primary recycle. Two recycle pathways are used in order to maximize the thermal performance of the configuration for the fuel being fired; whilst still maintaining emission compliance and assuring acceptable levels of

corrosive gases within the plant. From a thermal performance perspective there is typically little difference between the two, but some small differences ( $\sim\pm 20$  M\$) in the cost of the DCCPS would be expected as a smaller absolute volume of flue gas is required to be processed.

### 3.1.2 Oxyfuel Cycle for Low-Medium Sulfur Coals

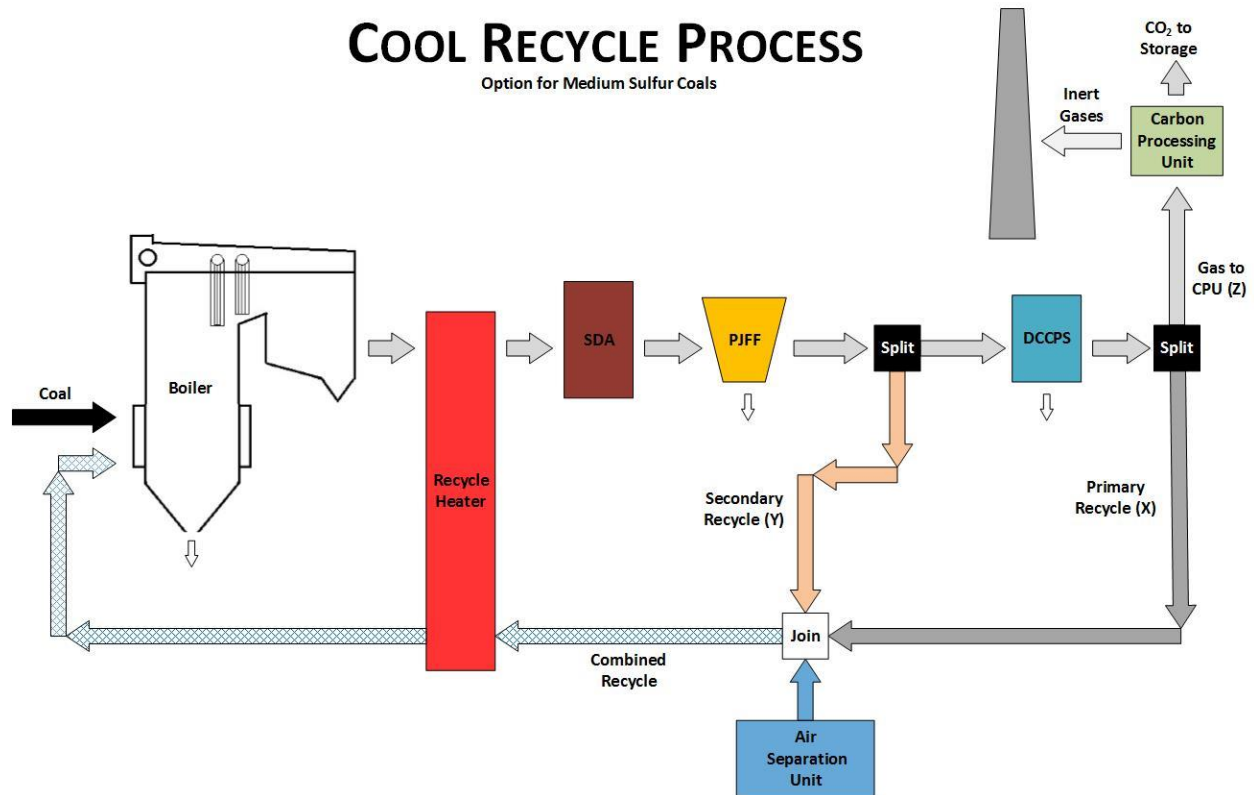


Figure 3.3 Process flow diagram for coals with sulfur contents between 0.5 [wt%] and 1.5 [wt%]

The cool recycle process with a spray dry absorption is appropriate for coals with sulfur levels between 0.5 and 1.5 [wt%]. Two such coals from the IECM database are: Appalachian Medium Sulfur and North Dakota Lignite. The primary and secondary recycle splits on those two coals would be very different because of the added moisture in lignite requiring a large fraction of the flue gas to pass through the DCCPS (primary). The performance difference from the cold recycle configuration will be dependent upon the size of the secondary recycle stream allowed by the moisture content of the coal.

### 3.1.3 Oxyfuel Cycle for Low Sulfur Coals

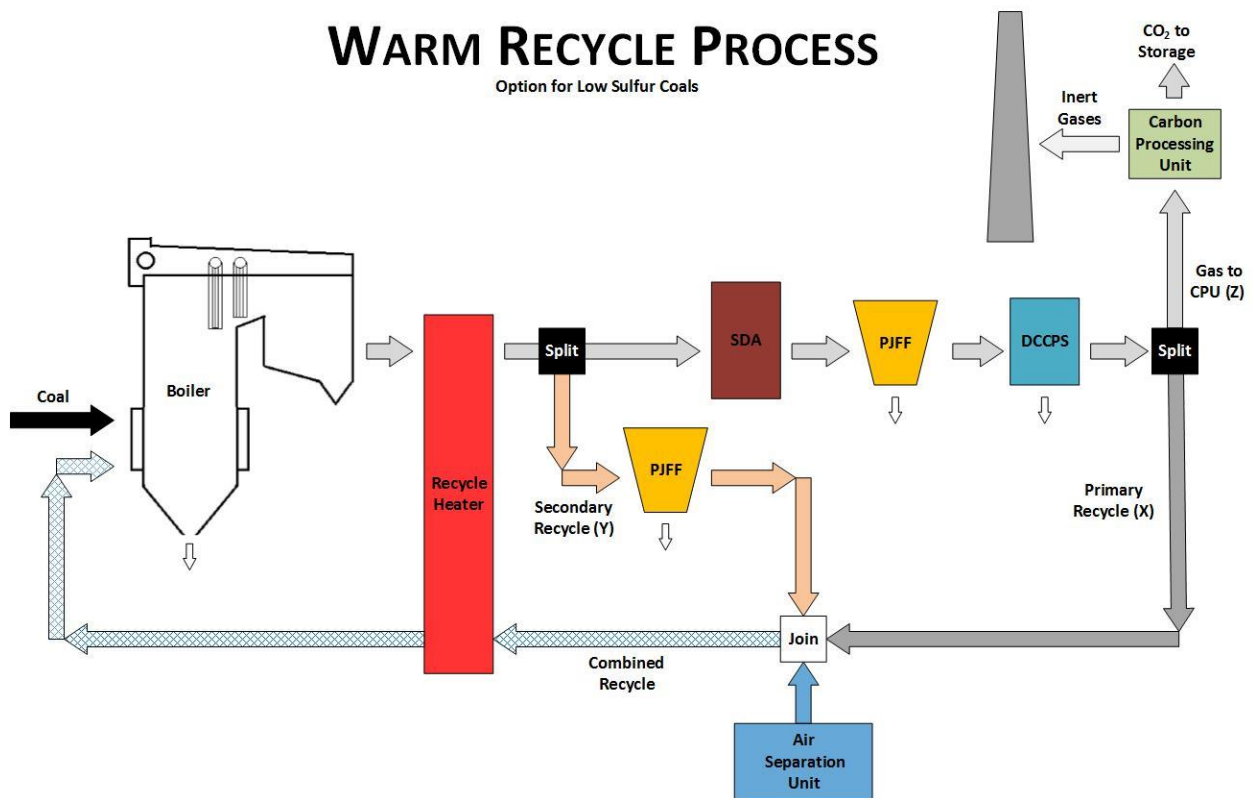


Figure 3.4 Process flow diagram for coals with very low sulfur concentrations (<0.5 wt%). The warm recycle process allows for the secondary recycle stream to be split off prior to sulfur treatment. The advantage to this configuration is that it allows for a very high thermal energy recycle stream to be returned to the boiler and consequently enables higher plant efficiency.

The warm recycle configuration is only suitable for coals with a sulfur mass below 0.5%. The secondary recycle stream is removed prior to any sulfur treatment and only is passed through a fabric filter prior to rejoining the primary recycle stream. The high enthalpy content of the secondary stream increases the temperature of the combined recycle stream resulting in the highest thermal efficiency of any of the oxyfuel configurations. Additionally, there are cost benefits due to the downsizing of the SDA, PJFF, and DCCPS as a result of a smaller fraction of the overall recycle gas being processed.

## 3.2 Detailed Stream Flow Diagrams

Presented in the respective sequence as they appeared in the previous section, the detailed stream flow diagram for each of the new oxyfuel system configurations can be found on the following three pages. The weight of the lines and size of the arrows used in the flue gas recycle stream is intended to be representative of mass flow rate.

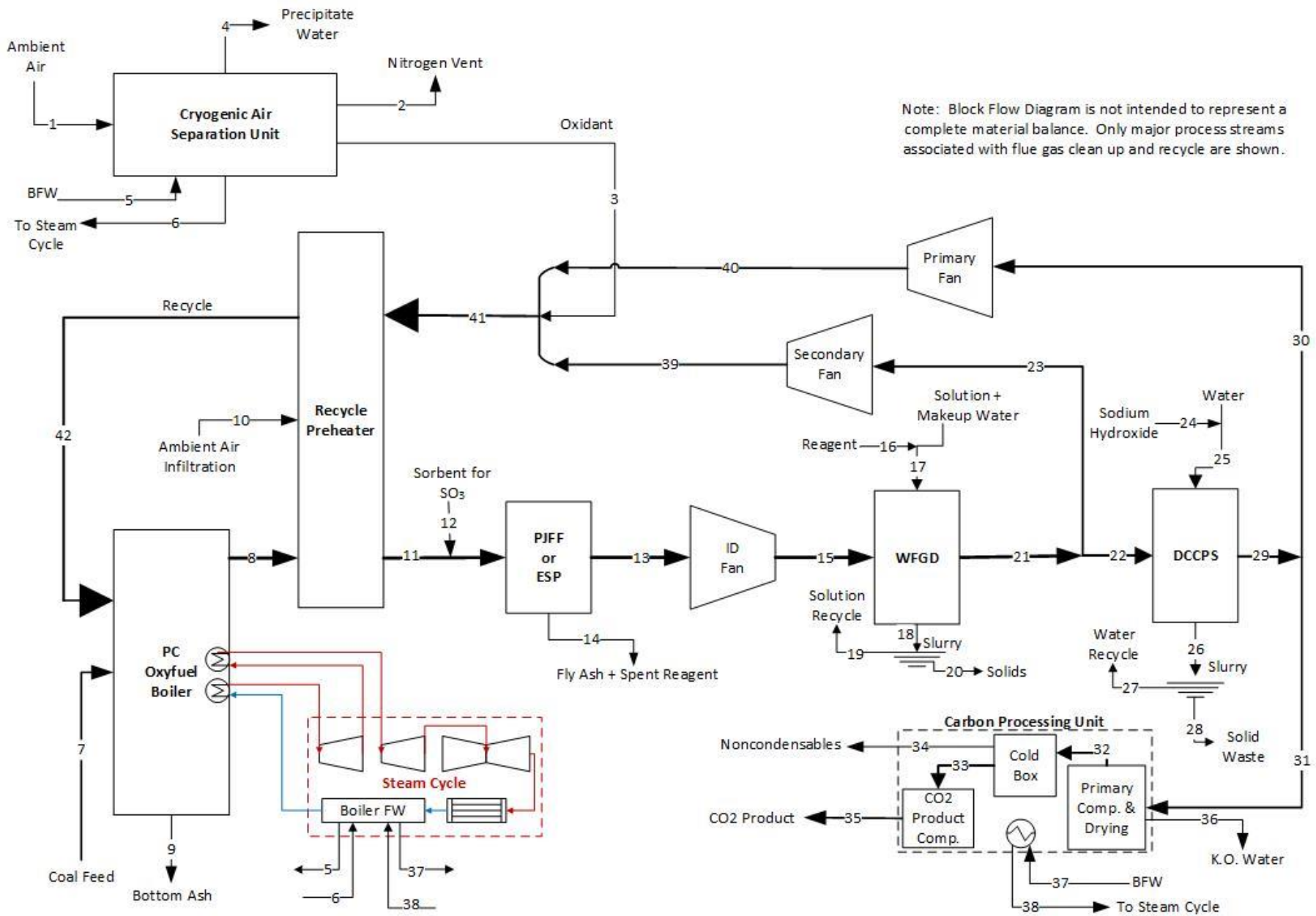


Figure 3.5 Detailed stream flow diagram for the cool recycle configuration with wet flue gas desulfurization. This process configuration is recommended for coals with a sulfur mass fraction above 1.5%

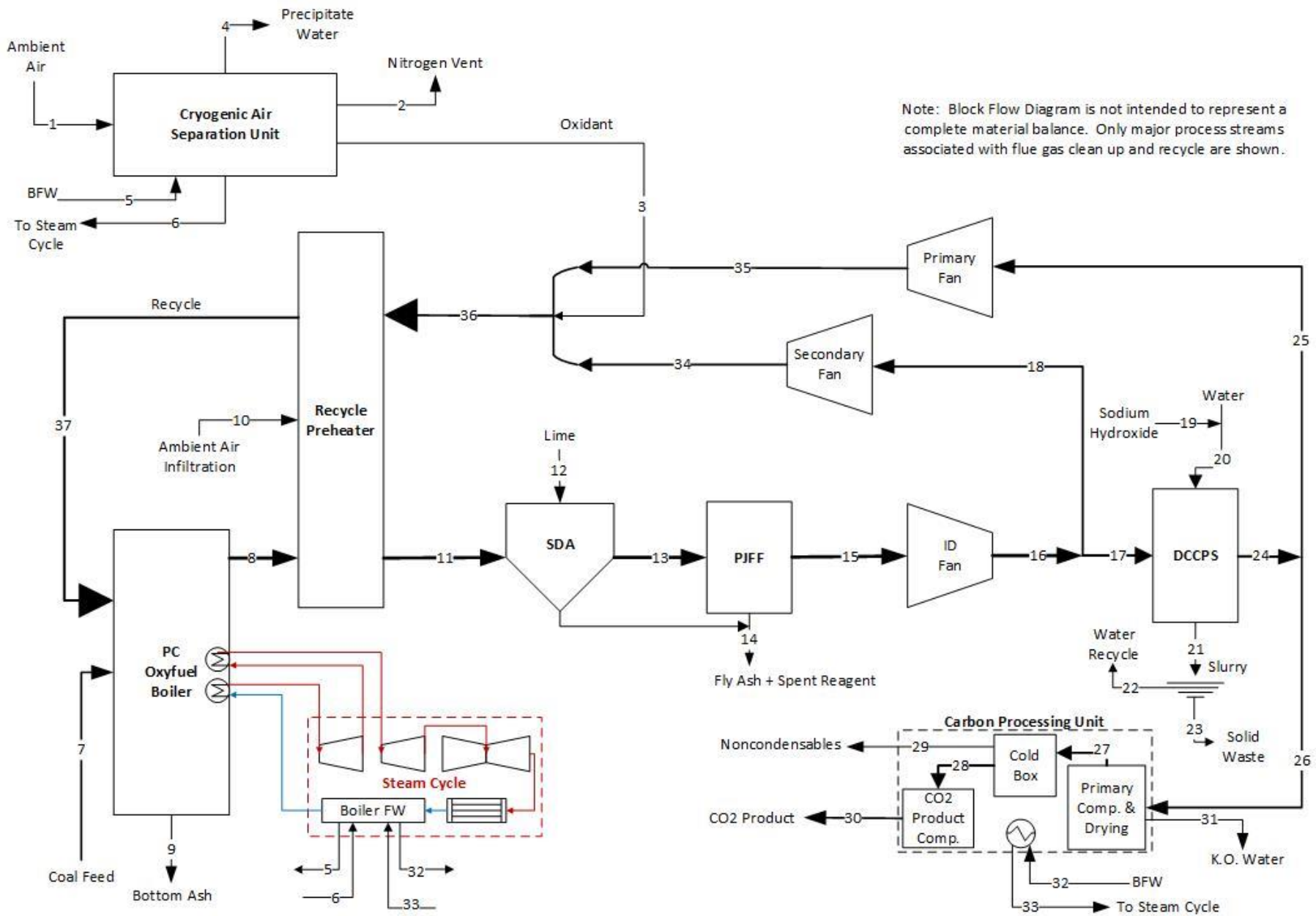


Figure 3.6 Detailed stream flow diagram for the cool recycle configuration with spray dry absorption desulfurization. This process configuration is recommended for coals with a sulfur mass fraction that is between 0.5% and 1.5%

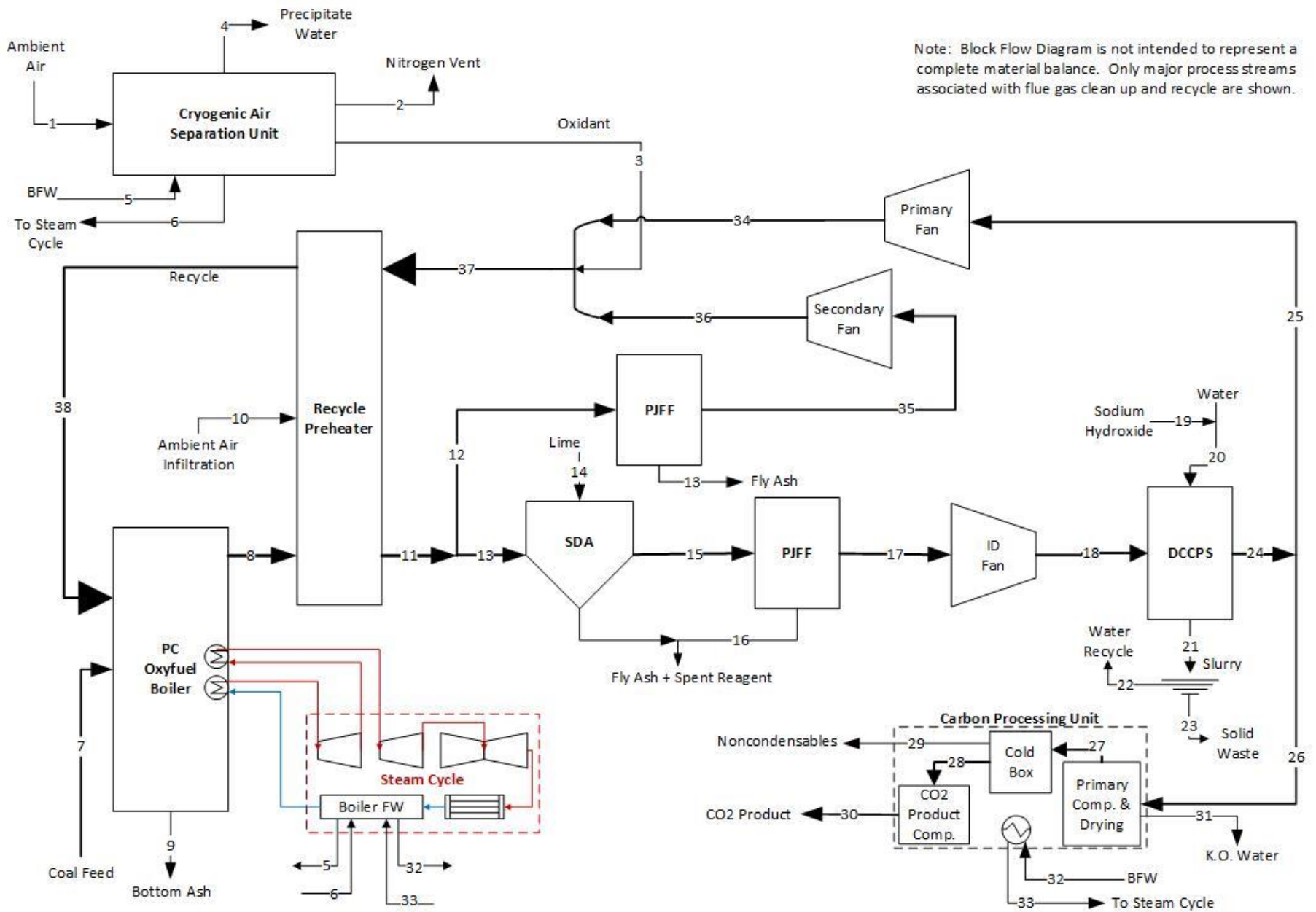


Figure 3.7 Detailed stream flow diagram for the warm recycle configuration with spray dry absorption desulfurization. This process configuration is recommended for coals with a sulfur mass fraction that is below 0.5%

### 3.3 Carbon Handling System Options

Each of the recycle configurations may also be paired with either of the carbon handling systems. The choice of carbon handling system is driven entirely by the desired purity of the carbon dioxide product produced by the plant. If a CoCapture system is chosen, the carbon handling system will only dehydrate the flue gas it receives from the DCCPS and then compress the entire stream to pipeline pressure. The user has no direct means of altering the carbon dioxide product purity with a CoCapture system. If a higher purity carbon dioxide product stream is desired, a cryogenic carbon processing unit (CPU) should be selected. The CPU allows purity levels up to 99.98 [CO<sub>2</sub> mol%] and as low as 90 [CO<sub>2</sub> mol%] as a function of user input.

**Table 3-1 Enumeration of all oxyfuel configurations in the updated model with carbon dioxide handling, sulfur treatment technology, and flue gas recycle selection considered.**

	<b>Recycle Configuration</b>	<b>Sulfur Treatment</b>	<b>Carbon Handling</b>
<b>Possible Oxyfuel Model Configurations</b>	Warm Recycle	Spray Dry Adsorption	Co-Capture
	Warm Recycle	Spray Dry Adsorption	Cryogenic CPU
	Cool Recycle	Spray Dry Adsorption	Co-Capture
	Cool Recycle	Spray Dry Adsorption	Cryogenic CPU
	Cool Recycle	Wet Flue Gas Desulfurization	Co-Capture
	Cool Recycle	Wet Flue Gas Desulfurization	Cryogenic CPU

### 3.4 Conceptual Calculation Strategy

This pulverized coal oxyfuel model has been created to become a module in the Integrated Environmental Control Model (IECM). The IECM is an integrated modeling software package which simulates the performance and cost of fossil fueled electricity generation systems with environmental controls. All major plant components, and the associated mass and energy flows, are taken into consideration. The remainder of this chapter seeks to familiarize the reader through an outline of the calculation strategy of the model. Technical detail is provided for the closure of the mass and energy balance of the flue gas cycle in Chapter 5 with technical detail for the major plant components (ASU, DCCPS, CPU) following in their own chapters. This organizational strategy has been adopted primarily to aid comprehension and ease of information access to the reader, but also highlights the independent nature of the sub-systems and their ability to operate outside the oxyfuel model in the IECM. Throughout the following chapters and sections many example calculations are provided to aid

explanation of the many model sub-systems. These examples are intended to be descriptive only and should not be taken as a comprehensive illustration of the model, this will be provided in the case studies of Chapter 10.

The interconnected nature of oxyfuel sub-systems necessitates that their mass flows be calculated iteratively and simultaneously across the entire plant. This requires that the mass and energy flows into and out of the boiler be balanced and reach a steady state capable of meeting or exceeding all operational and emission criteria. However, closing the mass and energy balance of an oxyfuel system is not as straight-forward as simply identifying a stable solution. As with any coal plant, there are criteria pollutant emission limits which must be satisfied. These include but are not limited to: sulfur oxides, nitrogen oxides, and particulate matter. Unique to oxyfuel are additional constraints on the amount of moisture and sulfur oxides which may be recycled to the boiler to ensure proper performance of sub-systems and limit material degradation, respectively. There is also a fundamental constraint that the mass flow of carbon out of the system be equivalent to the flow in with the fuel. The carbon constraint is straight-forward for once through air-fired systems, but is significantly complicated by recycling flue gas and the need to handle a diverse variety of fuels.

### 3.4.1 Mass Balance

An oxyfuel plant is, at the most basic level, an electricity generating steam cycle attached to a complex gas handling facility specifically designed to handle the flue gas produced by a single, chosen fuel. From a design perspective, this means that the fuel must be stipulated before all the gas handling equipment can be selected and sized. The same is true with respect to developing an oxyfuel model capable of handling arbitrary fuel compositions and generating plant configurations which contain the requisite equipment. There are a few heuristics and user options for determining the required design configuration, such as the >1.5 wt% sulfur boundary for requiring a WFGD rather than a SDA, but the vast majority of plant sizing and configuration is determined strictly by the mass balance.

#### 3.4.1.1 Calculation Strategy Overview

The iterative process is initiated in the boiler where fuel is ideally combusted in the presence of oxidant to produce an initial flue gas composition matrix. This matrix of element and compound mass flows is then passed throughout the system, updated by each process module, and then passed onto the next process. The matrix is passed around the loop according to the procedures outlined in Figure UU until all values in the matrix have reached steady-state and all mass constraints have been satisfied. The resolution of convergence, or steady-state, is 0.0005 for the IECM for all values.

$$Steady\ State_{IECM} = \frac{x_1 - x_0}{x_0} \leq 0.0005$$

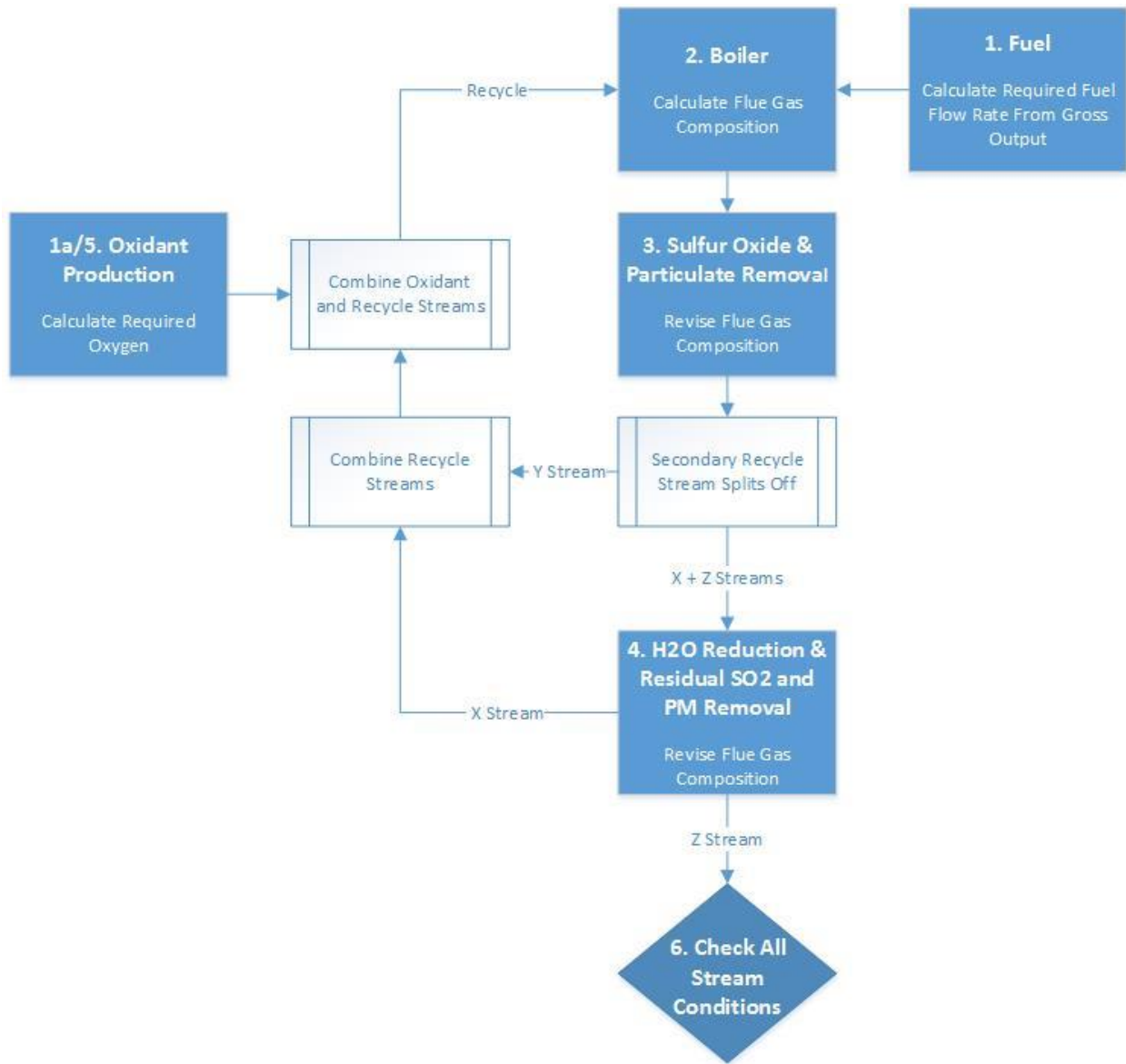


Figure 3.8 Decision flow diagram of the generic oxyfuel plant layout.

1. *FUEL AND OXYGEN*

The loop is initiated by a fuel flow rate being calculated for the gross electrical output specified.

- a. The mass flow rate of oxidant required to ideally combust the calculated fuel flow rate at stoichiometric conditions is produced and sent to the boiler.

2. *BOILER*

For the first iteration: fuel is combusted with the stoichiometric quantity of oxidant to generate flue gas.

Subsequent iterations: fuel is combusted with oxidant introduced with the recycled flue gas to generate a new flue gas.

3. *SULFUR OXIDE AND PARTICULATE MATTER REMOVAL*

These criteria pollutants are removed by their respective technology module in accordance with the removal efficiency specified. (function of mass flow constraints).

4. *FLUE GAS DRYING AND SULFUR OXIDE POLISHING*

Moisture and residual SO<sub>2</sub> are removed from the flue gas (less the secondary recycle stream) in accordance with the operating conditions specified for the DCCPS.

5. *OXIDANT PRODUCTION*

A quantity of oxygen slightly less than the stoichiometric value for combustion is produced and mixed with the flue gas recycle stream prior to boiler entry. Leakage of ambient air into the recycle stream is responsible for reducing combustion oxygen requirements.

6. *CHECK THE CURRENT UNMET HIERARCHY CONSTRAINT*

After all values in the flue gas matrix have reached steady-state, the model checks through a series of constraints to ensure that the current plant configuration is valid and able to meet all operational and criteria emission constraints. This step will be covered in greater detail in the following section, but if all constraints have been met the mass balance calculation is complete.

3.4.1.2 *Mass Balance Constraints*

To arrive at stable oxyfuel system balances for an arbitrary fuel, capable of meeting operational and criteria pollutant constraints in a computationally efficient manner, a hierarchy of constraints was created and utilized. In order of descending importance for constructing the oxyfuel system, these constraints are: carbon mass flow, flue gas moisture mass flow, flue gas sulfur oxide mass flow, and then nitrogen oxides and particulate matter. The effect on the configuration of the overall oxyfuel system for each of these constraints is summarized in Table 3-2.

Table 3-2 Constraints for the oxyfuel mass balance listed with the effect each has on determining either the primary and secondary recycle fractions or the required performance of criteria pollution control equipment.

Oxyfuel Constraint	Effect on System Configuration
Carbon Mass Flow	CPU fraction and total FGR fraction
Moisture Mass Flow	Primary and Secondary FGR fractions
Sulfur Dioxide Mass Flow	WFGD/SDA Removal Efficiency
Particulate Matter Emission Limit	PJFF/ESP Removal Efficiency
Nitrogen Oxide Emission Limit	N/A

In practice, the listed constraints interact in an iterative fashion while the model works towards a stable solution. For simplicity of explanation, examples of how each constraint independently may affect the system configuration during the process of finding a stable solution are provided in the following sections. However, these examples are provided for illustration purposes only and should not be viewed as part of a cohesive solution to a specific plant system.

### 3.4.1.3 Carbon Mass Flow

The first step towards fully defining the configuration and mass flows is to ensure that the amount of carbon entering the system is equal to the amount exiting. More specifically, the molar flow rate of carbon dioxide directed to the carbon processing unit (Z-stream in Figure 3.8) must be equivalent to the molar flow rate of carbon dioxide generated by the combustion of coal in the boiler.

$$\varphi_{CO_2_{Coal}} = \varphi_{CO_2_{Zstream}}$$

This carbon dioxide balance is arrived at in an iterative fashion by the model. For each iteration, a set quantity of coal is combusted in oxidant provided by the ASU (augmented by oxygen in the recycle stream) and the resulting flue gas is passed through the traditional pollutant control equipment. Once processed, the specified bulk flue gas recycle rate (FGR) is used to split the stream into recycle and removal streams. The fraction of flue gas removed (1-FGR) initially contains a much smaller amount of carbon dioxide than is entering from the coal. However, with each passing iteration, the net carbon dioxide in the system grows due to the recycle stream returning flue gas to the boiler. As the net carbon dioxide circulating in the system increases the amount of carbon dioxide removed increases proportionally. This increase in the quantity of carbon dioxide removed continues until a steady state condition is reached wherein the net carbon dioxide in the system stabilizes and the molar flow rates of carbon dioxide produced from coal and removed in the Z-stream are equivalent.

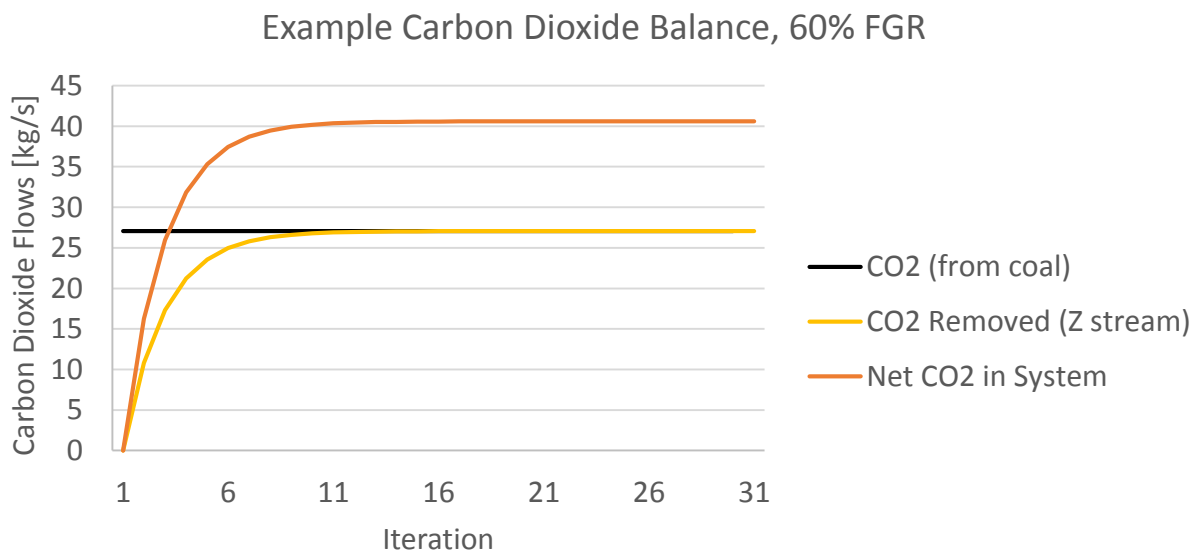


Figure 3.9 The carbon dioxide flow rates from coal and that removed via the Z-stream reach convergence in less than 15 iterations in this example with a FGR of 60%

The only constraint check required to ensure the carbon dioxide balance is completed is to allow the molar flow rate exiting the system in the Z-stream to reach steady state.

$$\Delta\varphi_{CO_2_{Zstream}} \leq 0.05\%$$

There is a furnace factor which allows the user to input a concentration of carbon that is collected in the fly and bottom ash which may be as large as 10% of the carbon entering with the coal. If a non-zero value is specified, the steady state constrain on the z-stream remains unchanged. However, the amount of carbon dioxide leaving in the z-stream will be reduced proportionately.

The IECM is intended to quickly produce results which may have uncertainty placed on key parameters. From a computational standpoint, this means that several hundred fully stable plant configurations need to be achieved for a single run with uncertainty. If a single plant configuration takes tens of thousands of iterations just to achieve convergence, the time to use uncertainty analysis could become prohibitive. To ensure that the number of iterations required for convergence was not excessive and would not balloon dramatically as critical parameters were put through their viable ranges, sample case studies were conducted. The following series of convergence examples illustrates the sensitivity of the number of iterations to the flue gas recirculation rate for carbon dioxide convergence.

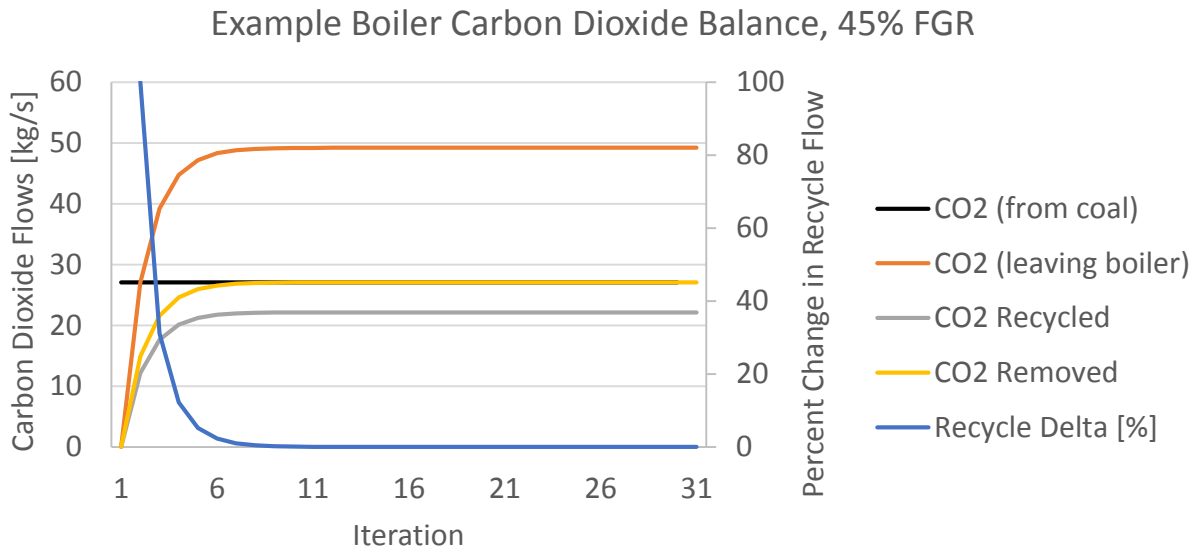


Figure 3.10 CO2 convergence is accomplished very quickly with low flue gas recirculation rates. For 45% FGR less than ten iterations were required to reach steady state operation.

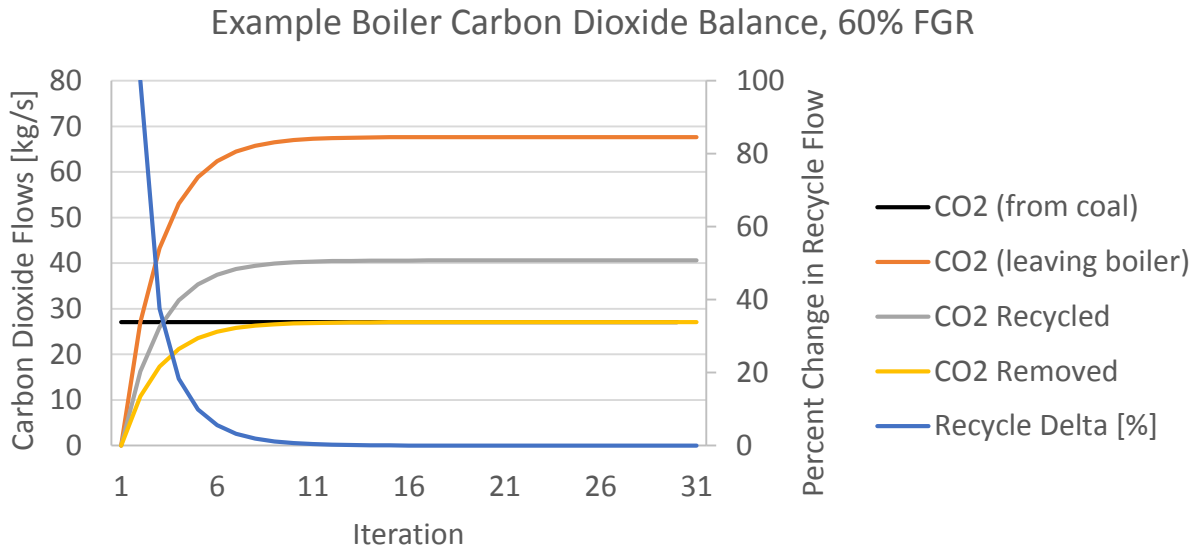


Figure 3.11 CO2 convergence is accomplished quickly with moderate flue gas recirculation rates. For 60% FGR, the low end of expected FGR, less than fifteen iterations were required to reach steady state operation.

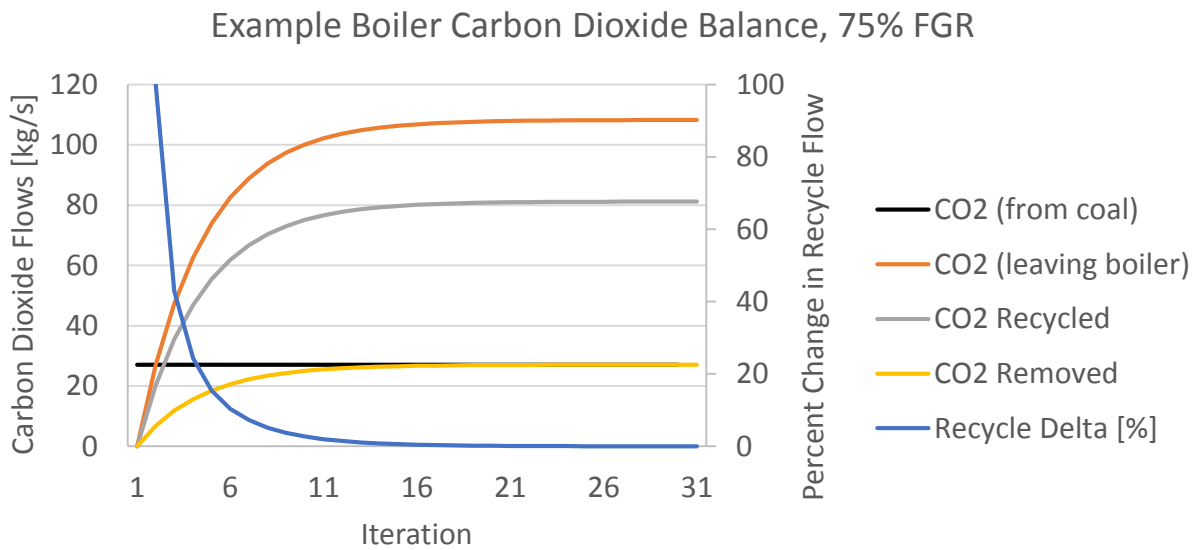


Figure 3.12 CO2 convergence is accomplished fairly quickly with elevated flue gas recirculation rates. For 75% FGR, a value near the higher end of anticipated FGR, just over twenty iterations were required to reach steady state operation.

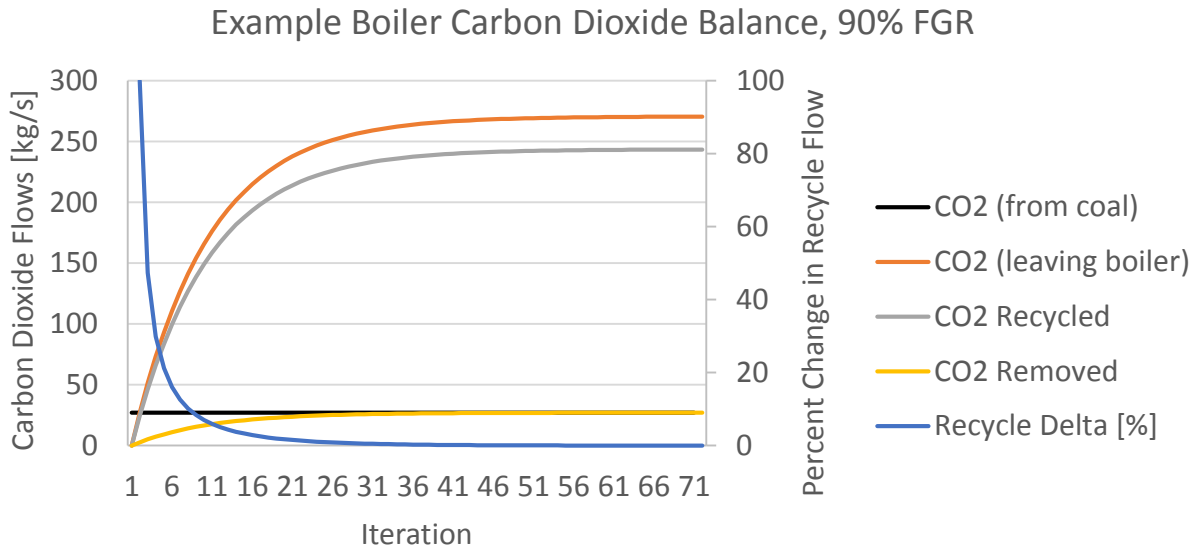


Figure 3.13 CO2 convergence is accomplished much more slowly with high flue gas recirculation rates. Roughly 70 iterations were required to reach convergence for 90% FGR. This number is still computationally reasonable however despite 90% FGR being on the extreme high end of expected FGR's.

Flue gas recirculation rates are anticipated to be somewhere between 60-65% for common fuel mixtures. The preceding analysis suggest that as we add complexity, and consider more mass flows and their constraints, the number of required iterations to close the carbon dioxide mass flow constraint is unlikely to rate limiting. FGR's greater than 75% are very atypical and would not represent plants likely to be constructed. In order to encourage users to examine realistic configurations and to prevent unnecessary iterations, the FGR is limited to a maximum value of 85% and a minimum value of 60%.

#### 3.4.1.4 Oxygen Mass Flow

The flow of oxygen in the mass balance is not part of the hierarchy of constraints. It is subject to the same convergence criteria as other species in the recycle stream however.

$$\Delta \dot{M}_{O_2\_Recycle} \leq 0.05\%$$

The algorithm for determining the quantity of oxygen required to be produced for combustion is based upon combustion stoichiometry and is therefore constant as long as the fuel flow rate remains unchanged. Similarly, the amount of air ingress into the recycle stream is defined as a percentage of the stoichiometric oxygen requirement. The result of framing the algorithm in this way is that the adjusted ASU oxidant load can be calculated within three iterations. This very fast convergence can be seen in Figure 3.14 below, which assumes that oxygen from air ingress "Recycle O2" was not calculated a priori and thus an extra iteration is shown for demonstration purposes only.

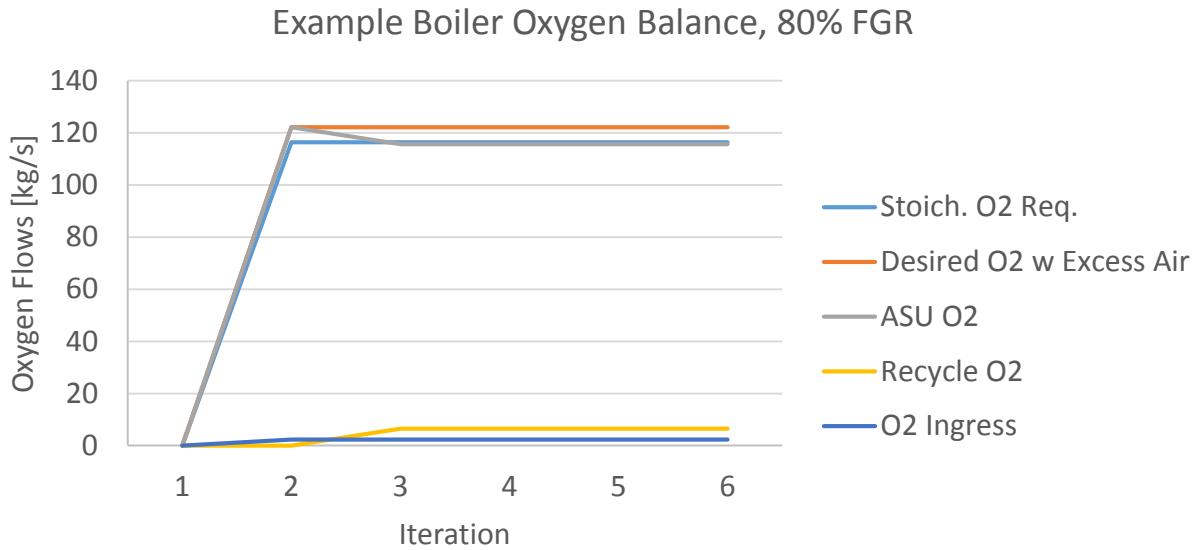


Figure 3.14 Iterations of FGR streams are not limited by the convergence of required oxygen. The amount of oxygen required can be determined in less than five iterations because many of the inputs can be calculated prior to the first iteration and are constant in value, being a multiple of the stoichiometric oxygen required based upon the chosen fuel composition.

#### 3.4.1.5 Moisture Mass Flow

With the total recycle fraction having been set by the user, and the carbon dioxide constraint satisfied, the percentage of the total recycle which will comprise the primary and secondary split needs to be determined. A constant amount of moisture is being introduced to the boiler from fuel combustion. Additional moisture is then added when the flue gas passes through the desulfurization process. The quantity of moisture taken up by the flue gas during the desulfurization process is the difference between entry composition and the saturation composition of the flue gas at the temperature which the flue gas leaves the desulfurization unit. For more information on this calculation please reference the IECM Documentation for the appropriate sulfur removal system for your chosen oxyfuel configuration. For economy of explanation, the desulfurization moisture uptake is not explicitly included in the example figures provided below. However, the effect of its inclusion would be to increase the magnitude of “Boiler Exit Moisture” and the affected balance streams (i.e. “DCCPS Precipitate”) would adjust in corresponding fashion.

As was the case with the carbon dioxide balance constraint, our initial constraint for the moisture balance is to ensure that the mass flow of moisture in the recycle stream to the boiler has reached steady-state prior to checking for further compliance.

$$\Delta \dot{M}_{H_2O\_Recycle} \leq 0.05\%$$

The model then checks to ensure that the quantity of moisture in the recycle stream, on a mass fraction basis, is less than the maximum recycle moisture fraction (MRM) for the fuel blend being combusted. As will be discussed in Section 4.2 on arbitrary fuel compositions, the normalized combustion moisture (NCM) of the fuel blend is used to calculate the maximum allowable recycle moisture fraction.

$$y_{H_2O\_Recycle} \leq \text{Max Recycle Moisture}$$

$$\text{Max Recycle Moisture } [y_{H_2O\_Recycle}] = 16.163 - 0.2043 * \text{Normalized Combustion Moisture}$$

If the mass fraction of moisture in the recycle stream is lower than the computed maximum recycle moisture, then the constraint is met and the global moisture mass flow constraint has been satisfied. Typically however, the initial values for the primary and secondary recycle splits will need to be adjusted iteratively until a solution is found which sends a large enough portion to the primary stream (and DCCPS) to achieve adequate moisture removal for the combined recycle stream. To demonstrate the iterative process of finding suitable primary and secondary recycle fractions and to show that the number of iterations is not excessive even using an inefficient algorithm; the following cases were created.

To initialize the iteration loop in this example, the primary and secondary fractions were set by simply splitting the total FGR in half. The primary and secondary fractions were then indexed by 1% + and -, respectively until a solution was found which met the max recycle moisture constraint and would reach steady state for moisture content in the bulk recycle stream back to the preheater/boiler. Assuming a representative 60% FGR, the initial iteration has primary and secondary recycle rates of 30% of the total flue gas exiting the boiler. As would be expected, the initial result of this split is that “Recycle Moisture” quickly exceeds the MRM for the fuel being combusted within a few iterations. As is illustrated in Figure 3.15, the water precipitated out by the DCCPS is increased until the MRM constraint is met and “Recycle Moisture” and “Boiler Exit Moisture” are steady-state.

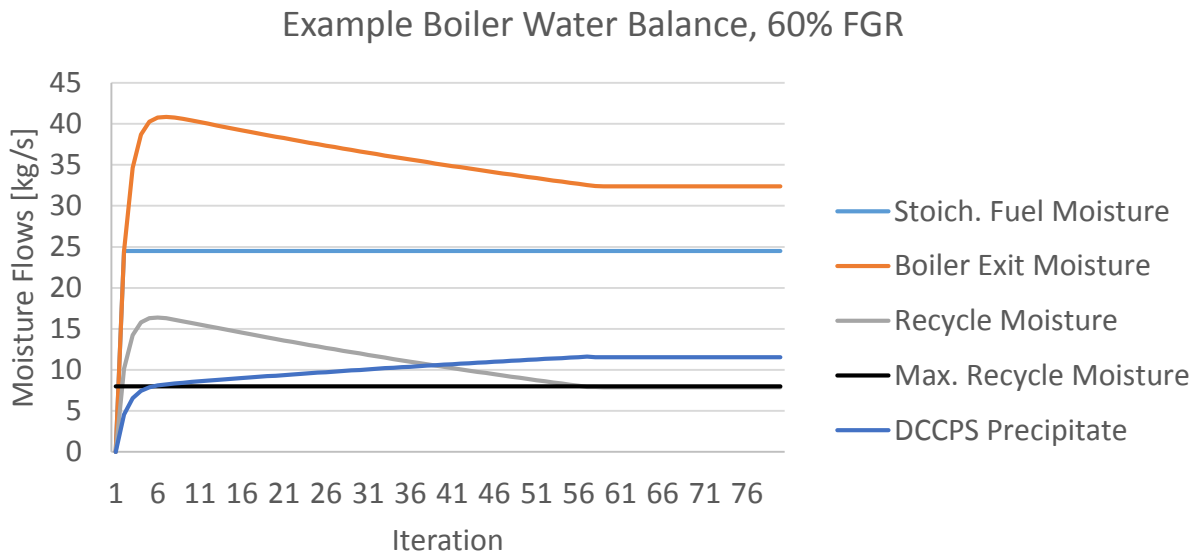


Figure 3.15 Recycle moisture convergence is accomplished through increasing the amount of moisture removed from the bulk flue gas by the DCCPS. A larger fraction of the bulk recycle is assigned to the primary split (passes through DCCPS) until the maximum recycle moisture constraint can be satisfied.

The increase in water precipitated out by the DCCPS is not due to a change in the performance characteristics of the DCCPS, but rather a reflection of the increase in volumetric flow rate of flue gas through the DCCPS. The orange line in Figure 3.16 shows that the actual total moisture coming from the primary recycle stream is increasing as the fraction of flue gas assigned to the primary split is increased. However, the relative moisture content of flue gas passed through the DCCPS is so greatly reduced that

the bulk recycle moisture content continues to decrease as the recycle split is more heavily weighted towards the primary and away from the secondary.

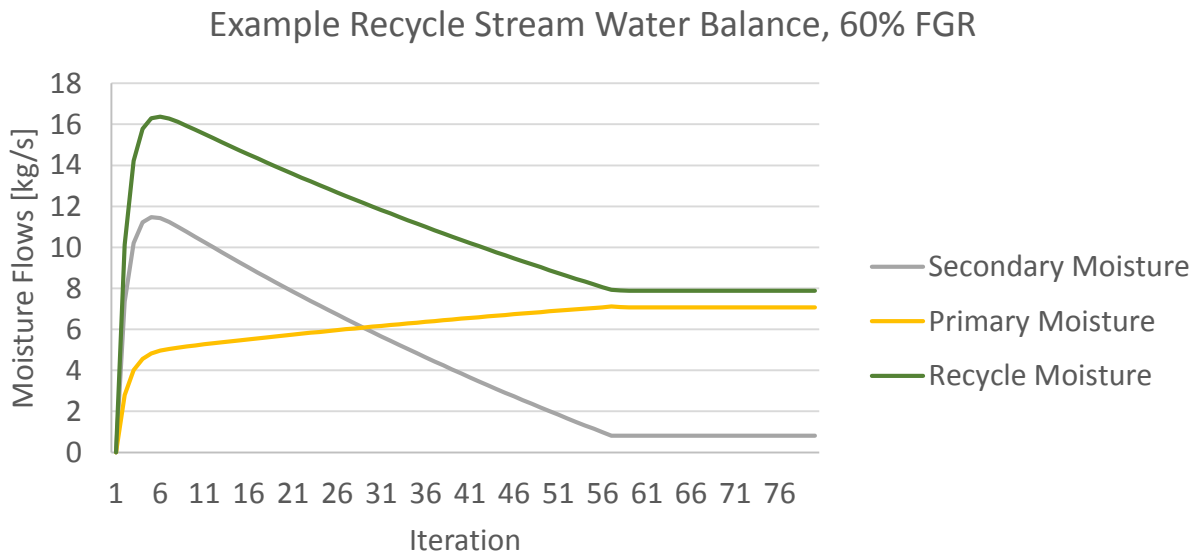


Figure 3.16. Initial recycle moisture is too great under an equivalent primary to secondary split regime for this example. As the split ratio is adjusted in favor of the primary, the overall recycle moisture is decreased until the MRM constraint is met; at which point the system is allowed to converge.

The number of iterations required to reach convergence using a basic indexing technique can be quite high (>50) for FGR's greater than about 70%. Since the FGR parameter is allowed to be specified up to a value of 85% by a user, it was important to ensure that the time to run the model would not become excessive under such specifications.

### Example Boiler Water Balance Across FGR Percentage

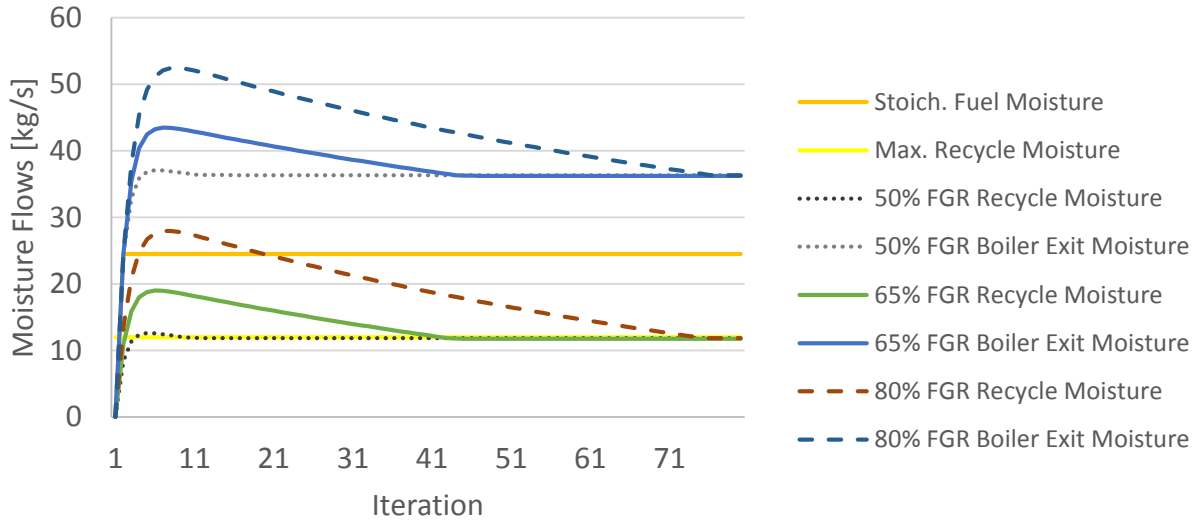


Figure 3.17 Moisture convergence is accomplished much more slowly with high flue gas recirculation rates. In this demonstration over 70 iterations were required to reach convergence for 80% FGR. This number is still computationally reasonable however a more efficient algorithm has been used for the IECM code.

#### 3.4.1.6 Sulfur Dioxide Mass Flow

With the total amount of flue gas to be recirculated to the boiler known and the splits for both primary and secondary recycle determined, we turn our attention to sulfur removal. The form of the sulfur removal system, be it a wet scrubber or a spray-dry absorption system, will already be known based upon the sulfur content of the fuel mixture. Also, for the system configurations being considered, the entire volume of the flue gas must pass through the absorber(s). Thus the only performance parameter which needs to be determined is the actual sulfur dioxide removal efficiency.

As before, we enforce our steady-state constraint on the mass flow rate of sulfur dioxide in the bulk recycle stream prior to checking further constraints.

$$\Delta \dot{M}_{SO_2\_Recycle} \leq 0.05\%$$

With the system having reached convergence, the model then checks to ensure that the amount of sulfur dioxide in the bulk recycle stream is at or below the New Source Performance Standard (NSPS) for sulfur dioxides. The reason for choosing NSPS as the upper bound for sulfur dioxide was that emission levels would not be exceeded in the event that flue gas needed to be vented during operation or while the plant was in the start-up phase.

$$\dot{M}_{SO_2\_Recycle} \leq NSPS\ Limit$$

Where the NSPS limit is fuel specific and is already calculated in the IECM once a fuel blend has been specified for combustion.

The actual algorithm used in the IECM for determining the sulfur dioxide removal efficiency is more optimal with regard to reducing the computations required for mass balance closure. However, as was

the case with the moisture balance, we walk through a basic linear iteration process for demonstration purposes. The initial iteration of the sulfur balance starts with an 80% sulfur removal efficiency. If the NSPS constraint is not met once steady-state was reached for SO<sub>2</sub> in the bulk recycle stream, then the sulfur dioxide removal efficiency is indexed up 0.5% until a solution which met both constraints can be found. This slow, step-wise movement of the removal efficiency upward towards an acceptable level can be seen below.

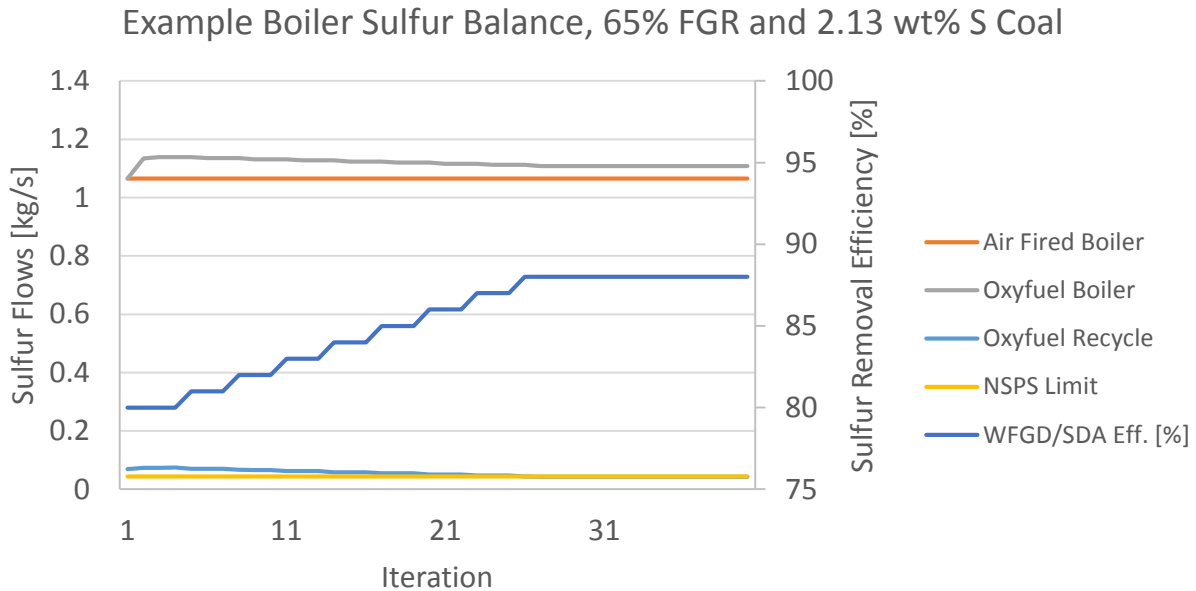


**Figure 3.18** Sulfur dioxide convergence in the recycle stream is accomplished by increasing the removal efficiency of the WFGD/SDA until the NSPS limit can be met in the bulk recycle stream.

An additional benefit of using the NSPS limit as the acceptable limit for sulfur dioxide concentration in the flue gas is that it so strictly limits the accumulation of sulfur in the recycle stream that concerns over material corrosion are largely abated. It should be noted that sulfur accumulation may still be an issue in oxyfuel systems and even in air-fired systems utilizing a high sulfur content coal. However, as can be seen in Table 3-3, using the NSPS limit ensures that there is a very slight absolute increase in the mass (not concentration) of sulfur leaving the boiler.

**Table 3-3** Demonstration of the increase in boiler sulfur content for oxyfuel, relative to air-firing, across a range of fuel sulfur mass fractions.

	Sulfur content of fuel [wt %]				
	1%	2%	3%	4%	5%
<b>WFGD/SDA Eff. to Meet NSPS* [%]</b>	75	87	92	94	95
<b>Increase in Boiler Sulfur [wt%]</b>	8.8	4.4	2.8	2.1	1.8

\*NSPS assumed to have a value of 0.134 lbSO<sub>2</sub>/MMBtu for all sulfur content levels

The other trend highlighted in Table 3-3 is the sulfur dioxide removal efficiency required to meet a NSPS standard of 0.134 [lbSO<sub>2</sub>/MMBtu]. The reported values are based on simplified assumptions but

represent a bottom-line sulfur dioxide removal performance which must be met by the sulfur control system. This baseline, in combination with real-world performance that can safely be expected from spray-dry absorption systems, lends further credence to our conservative SDA to WFGD cut-off level of 1.5% sulfur by mass.

Lastly, as with the carbon dioxide balance, there is a furnace factor which allows the user to input a concentration of sulfur that is collected in the fly ash which may be as large as 100% of the sulfur entering with the coal. If a non-zero value is specified, the steady state constrain on the recycle-stream remains unchanged. However, the amount of sulfur leaving through the FGD and DCCPS will be reduced proportionately.

#### 3.4.1.7 *Particulate Matter Emission Limits*

The control of particulate matter (PM) is managed by the oxyfuel model in the same manner as it has been handled for traditional pulverized coal systems in the IECM. For detailed information on the performance and cost models for electrostatic precipitators or fabric filters please see Sections 4 and 5, respectively, of the IECM base technical documentation (43). For the purposes of this model, we have assumed that both PM generation and the effectiveness of reduction equipment is at parity with air-fired pulverized coal systems. The oxyfuel model checks to ensure convergence in the mass flow rate of PM in the recycle stream before determining whether the NSPS limit has been met.

$$\Delta\dot{M}_{PM\_Recycle} \leq 0.05\%$$

$$\dot{M}_{PM\_Recycle} \leq NSPS\ Limit$$

Like sulfur oxides, particulate matter is subject to a mass flow constraint on a [lb/MMBtu] basis. The reason for choosing NSPS as the upper bound for particulate matter was that emission levels would not be exceeded in the event that flue gas needed to be vented during operation or while the plant was in the start-up phase. The NSPS limit is a function of the particular fuel blend and is calculated in the existing IECM.

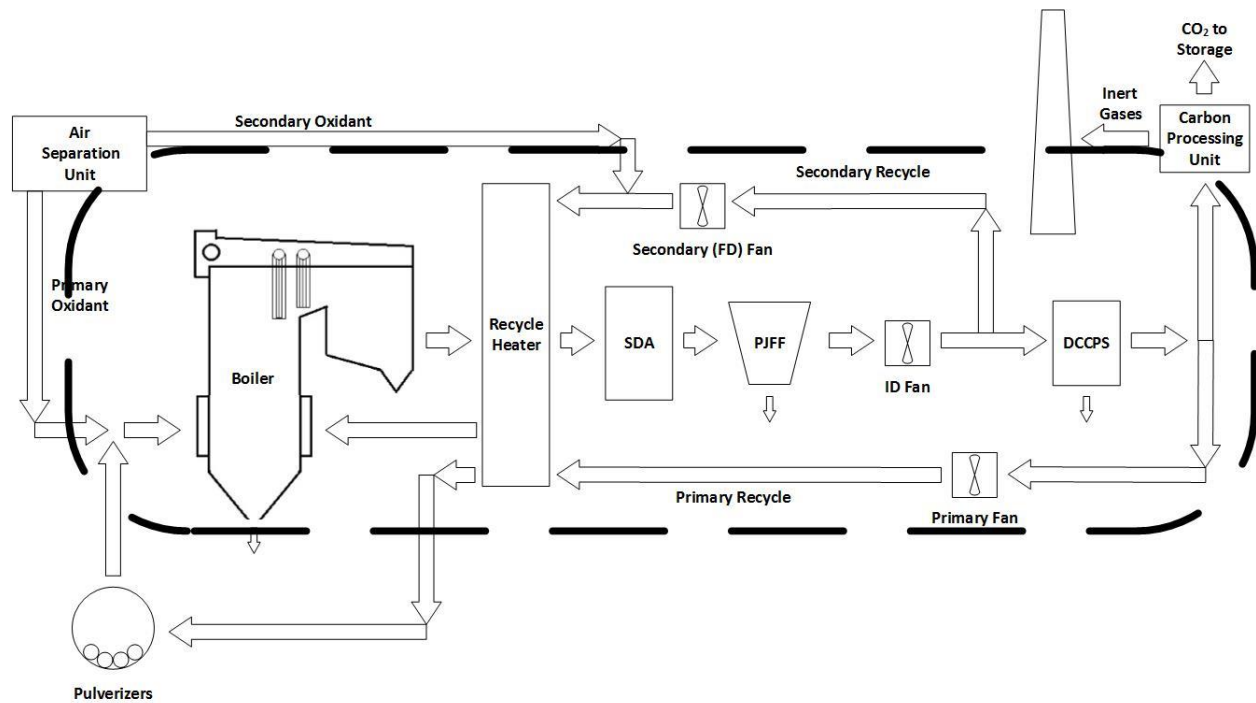
#### 3.4.1.8 *Nitrogen Oxide Emission Limits*

The creation and control of nitrogen oxides is managed by the oxyfuel model. Although it is listed as part of the hierarchy of constraints, the plant layout is not affected by any limit on nitrogen oxides. As has been previously discussed in Chapter 2, a ~70% reduction in nitrogen oxide formation is anticipated under oxyfuel conditions. This reduction is significant enough that emission limits are anticipated to be met without additional gas after treatment from a selective catalytic reduction (SCR) system.

Consequently there is no specific removal efficiency parameter which can be manipulated directly as was the case with an FGD or SDA and sulfur removal. The model instead checks to ensure convergence in z-stream and then reports the final value to the user in the “Get Results” section of the model.

$$\Delta\dot{M}_{NOx\_Zstream} \leq 0.05\%$$

# Chapter 4 Pulverized Coal Oxyfuel Performance Model



## 4.1 Performance Model Input and Output Parameters

The integral, plant-wide design altering nature of oxyfuel as a carbon dioxide control technology obfuscates the process of enumerating all the oxyfuel input parameters. A truncated list of the most prominent parameters for oxyfuel system performance are explained and characterized in this section. Also provided is a list of key model outputs from the pulverized coal oxyfuel model. The complete list of input and output parameters for the pulverized coal oxyfuel model in the Integrated Environmental Control Model (IECM) numbers in the hundreds. More thorough characterization of the input and output parameters for individual component models are provided in their respective chapters.

### 4.1.1 Explanation of Key Oxyfuel Specific Parameters

**Oxygen Purity:** Air contains about 21% oxygen on molar basis. The oxygen product obtained from an air separation unit (ASU) is typically in excess of 90 [mol%]. It may be noted that the unit energy penalty increases sharply with oxidant purity in excess of 97.5 [mol%]. However, at higher oxygen purity there are less non-condensable impurities in the CO<sub>2</sub> product obtained from the system. Many studies have reported that 95 [mol%] is an optimal level of oxygen purity but conversations with industry representatives has indicated that this value is slightly lower than the likely industry standard. The default value of 97 [mol%] oxygen (transition from removing nitrogen from an argon and oxygen mix to separating argon from oxygen) has been adopted for the updated model. At this purity level the main impurity in the oxygen product is argon, with trace amounts of nitrogen.

**Oxygen pressure:** This is the pressure at which the oxygen product is delivered from the air separation unit to either the PC oxyfuel boiler or to the IGCC gasifier. The total energy requirement for the ASU also depends on this pressure.

**Excess Air:** Excess air is generally provided to ensure complete combustion of the fuel and to avoid formation of carbon monoxide. Conventional coal combustion is carried out using about 15-20% excess air. Since pure oxygen is an expensive commodity as compared to air, minimizing the use of excess oxygen is desirable. The optimum level of excess oxygen needed to ensure complete combustion is not yet clear and will likely depend upon the composition of the coal being fired. Examined case studies have used values ranging from 2-15% with vendor derived estimates being in a slightly narrower 5-10% range. A default value of 5% excess air has been stipulated as the default value for the oxyfuel update. As a clarifying note: this 5% includes ingress and fuel based oxygen into the boiler.

**Leakage Air at Preheater:** Ideally, the oxyfuel system aims at using only pure oxygen for combustion. However, it may not be practically feasible to seal the boiler and flue gas ductwork completely to avoid air ingress. Such air infiltration into the system is termed as air ingress, but represented by the parameter name “Leakage Air at Preheater” in the IECM for consistency with air-fired units. Values in the range of 1-5% have been assumed by various studies, while many others tend to ignore this parameter and assume zero air leakage. In a conventional air-fired boiler, the amount of air leakage is typically 15-20% of the theoretical air requirement. It is expected that oxyfuel systems would be better sealed and the default value for air leakage is thus assumed to be 2% of theoretical (stoichiometric) oxygen.

**Flue Gas Recycled:** Oxyfuel combustion systems with flue gas recycle are also commonly referred to as “O<sub>2</sub>/CO<sub>2</sub> combustion systems”. The flue gas recycle ratio (FGRR) is the fraction of total flue gas generated that is recycled back into the boiler. Higher FGRR implies a lower oxygen mole fraction in the O<sub>2</sub>/CO<sub>2</sub> oxidant entering the boiler, whereas zero FGRR is the case of no flue gas recycle. Studies using flue gas recycle assume FGRR values in the range 0.6-0.85. The IECM uses a nominal value of 0.65. It should be noted that this is a simplification of the actual mechanics of the oxyfuel system as there is not one flue gas recycle loop but two. The primary recycle loop is always dried and used to convey the pulverized coal from the mills to the boiler. The secondary recycle loop can undergo varying degrees of cooling/pollutant treatment before returning to the boiler. The updated model handles the proper

balancing of the mass flow for the user automatically to limit increases in the plant heat rate whilst ensuring that acid gas concentrations within the boiler are maintained at acceptable levels.

**CPU/ASU Heat Integration:** Both the air separation unit and the carbon processing unit utilize very large compressor trains to elevate the pressure of their gas feed streams. A large quantity of heat is produced in both of these compression processes which require management through cooling. In an effort to increase net plant efficiency, a portion of the compressor cooling duty for each system may be supplied by boiler feed water rather than cooling water. The boiler feed water preheating provided reduces the steam cycle heat rate and results in slightly higher plant efficiency.

**CO<sub>2</sub> Product Purity:** The flue gas from oxyfuel combustion is a mixture of CO<sub>2</sub> with other compounds. Even after drying (i.e. removal of H<sub>2</sub>O, which is the second largest component in the flue gas), the concentrated CO<sub>2</sub> stream may contain various non-condensable gases (e.g. N<sub>2</sub>, O<sub>2</sub>, Ar) and pollutants (SO<sub>2</sub>, NO<sub>x</sub>, HCl), depending on the combustion conditions and various parameters discussed before. Some studies assume that the CO<sub>2</sub> product may be compressed and disposed together with all these impurities (co-capture), while other studies propose schemes for CO<sub>2</sub> product purification. The CO<sub>2</sub> product purity is a parameter that would dictate the kind of post-treatment required for the CO<sub>2</sub> stream. It would also affect the energy requirement for CO<sub>2</sub> purification and compression. A nominal purity of 99.95% is assumed in the IECM for purposes of similarity with the purity produced by competing carbon capture systems.

**CO<sub>2</sub> Recovery Rate:** Under ideal conditions, oxyfuel combustion system with flue gas recycle should be able to capture all the CO<sub>2</sub> present in the flue gas, i.e. the theoretical capture efficiency of this system is 100%. However, only the co-capture system is capable of complete capture of the CO<sub>2</sub> emissions. The addition of a CPU will reduce the fraction of CO<sub>2</sub> captured due to practical limits imposed by the design of cryogenic separation systems. Accounting for these currently economically unavoidable losses, the CO<sub>2</sub> capture efficiency of this system, as reported by various studies, is in the range of 50-99.5%.

**2<sup>nd</sup> Law Separation Efficiency:** The efficiency of gas separation in distillation systems is a function of the vapor pressure differential between the gases being separated. The two gases with the most similar vapor pressures in the CPU are oxygen and carbon dioxide. The ratio of these two gases [mol basis] is used along with a correlation developed from empirical systems to estimate the efficiency of the gas separation process in the CPU. For more information on this parameter please see Chapter 7.

**CO<sub>2</sub> product pressure:** This is the final pressure at which the CO<sub>2</sub> product is delivered at the plant boundary. A typical value is about 2000 psig (13.7 MPa). This parameter, along with the CO<sub>2</sub> compression efficiency, determines the total energy requirement for CO<sub>2</sub> compression, which is a major energy penalty item; second only to that of the air separation unit.

#### 4.1.2 Key Input Parameter Characterization

The key input parameters of the oxyfuel performance model are those which define the operation of the base plant and the gas separation and processing equipment. The 17 most important performance parameters are characterized in Table 4-1. One very important assumption of this list is that the fuel

blend has already been stipulated and the appropriate flue gas recycle configuration has been chosen based upon the sulfur content of the fuel.

**Table 4-1 Key input parameters for the pulverized coal oxyfuel model with default values and parameter ranges. This list applies once a fuel and recycle configuration have been stipulated.**

<b>Parameter</b>	<b>Units</b>	<b>Default value</b>	<b>Range</b>
Capacity Factor	Fraction	0.75	0-1
Gross Electrical Output	Megawatts	650	100-2500
Steam Cycle Heat Rate	kJ/kWh	7764 (Supercritical)	6300-15830
Boiler Efficiency	%	Calc (fuel dependent)	50-100
Oxygen Purity	%mole	97	90-100
Oxidant Pressure	MPa	0.14	0.14-6.0
Excess Air	% Stoich.	5	0-40
Leakage Air at Preheater	% Stoich.	2	0-50
ASU Heat Integration	Fraction	0.25	0-0.3
Flue Gas Recycled	%	65	60-85
CPU Heat Integration	Fraction	0.25	0-0.3
DCCPS Exit Temperature	Celsius	55	15.56-75
CO <sub>2</sub> Recovery Rate	%	90	50-99.5
CO <sub>2</sub> Product Purity	% mole	99.95	90-99.98
2 <sup>nd</sup> Law Separation Efficiency	%	Calc	0-100
CO <sub>2</sub> Product pressure	MPa	13.8	7.6-15.2
CO <sub>2</sub> Compressor Efficiency	%	85	75-100

### 4.1.3 Key Model Outputs

The key output parameters of the pulverized coal oxyfuel performance model in the IECM are all related to the efficiency and quantity of electricity produced on an annual basis. There are a number of outputs such as the gas and mass flows of all the process streams which are omitted from this list. Also emitted are all the parasitic loads of the base plant and components which determine the disparity between gross and net electricity generation.

Table 4-2 Key model outputs of the pulverized coal oxyfuel performance model

Parameter	Units
Gross Electrical Output	Megawatts
Net Electrical Output	Megawatts
Gross Plant Heat Rate	kJ/kWh
Net Plant Heat Rate	kJ/kWh
Coal Flow Rate	Tonne/hr
Annual Operating Hours	Hours
Annual Electricity Generation	BkWh/yr
Carbon Dioxide Emission Rate	Tonne/hr
Net Plant Efficiency	HHV %

## 4.2 Fuel Composition and Normalized Combustion Moisture

When constructing models for use in the Integrated Environmental Control Model, great care is taken to ensure that the model has adequate flexibility to handle any reasonable set of inputs a user could think to stipulate. Recent interest from IECM users in Biomass Energy with Carbon Capture and Storage (BECCS), as a potential means of achieving net-negative carbon emissions, has put pressure on the development of the oxyfuel model to handle biomass as a fuel. The fuel mixtures proposed for BECCS facilities can be comprised partially, or completely, of biomass from various sources. The irreducible uncertainty of biomass fuel mixtures, along with a desire to keep fidelity with the air-fired PC boiler and allow user-defined coals, meant that the oxyfuel model would need to be able to handle arbitrary fuel mixtures.

For oxyfuel systems, limiting the quantity of water returned to the boiler is essential to ensure proper operation. In practice, once a fuel composition has been chosen, the quantity of moisture returned to the boiler is controlled by the proportion of recycled flue gas which is processed through the DCCPS. To determine the quantity of flue gas recycle which must be processed for an arbitrary fuel mixture a method for determining the maximum acceptable quantity of moisture being returned to the boiler had to be created. The approach adopted ensures a maximum moisture concentration [wt%] for the flue gas exiting the boiler that is in accordance with the boiler exit conditions of the DOE case studies (36). Implicit in this technique is, the assumption adopted from DOE, that first generation oxyfuel systems will use pre-existing boiler designs and therefore operate at conditions to match the heat transfer profiles which would be present under air-fired conditions. This assumption is perfectly acceptable for the purposes of this model and allows the back-calculation of the maximum amount of moisture returned to the boiler in the recycled flue gas.

For a stipulated mass fraction of water to be present in the flue gas exiting the boiler; the amount of moisture being introduced by the recycle stream must be inversely proportional to the amount being introduced by fuel combustion. For an arbitrary fuel composition the amount of combustion moisture generated per unit mass of fuel combusted is given by the following:

$$\text{Combustion Moisture} \left[ \frac{g \text{ H}_2\text{O}}{kg \text{ Fuel}} \right] = 10 * (9 * y_{\text{Fuel}_H} + y_{\text{Fuel}_{\text{H}_2\text{O}}})$$

For convenience of comparison and to normalize for fuel blends with varied heating values combustion moisture is normalized using the following:

$$\text{Normalized Combustion Moisture} \left[ \frac{g \text{ H}_2\text{O}}{MJ} \right] = \frac{\text{Combustion Moisture} \left[ \frac{g \text{ H}_2\text{O}}{kg \text{ fuel}} \right]}{\text{HHV} \left[ \frac{MJ}{kg \text{ fuel}} \right]}$$

Calculating the Normalized Combustion Moisture (NCM) of the coals used in the DOE case studies and then plotting these values along with their corresponding moisture recycle mass fractions gives us just two data points. In this instance, two data points is sufficient because we know the functional form of the anticipated relation between fuel moisture and recycle moisture (inversely proportional on a mass basis). The inverse proportionality constraint allows us to draw a straight line that intersects both points and extends until it crosses both the x and y-axis. This line then defines the solution space boundary of possible combinations of recycle and fuel moisture which will yield an acceptable moisture concentration in the flue gas exiting the boiler. Those solutions lying upon the line represent the Maximum Recycle Moisture (MRM) constraint for the corresponding fuel blend.

## Maximum Recycle Moisture Determination for Arbitrary Fuel Composition

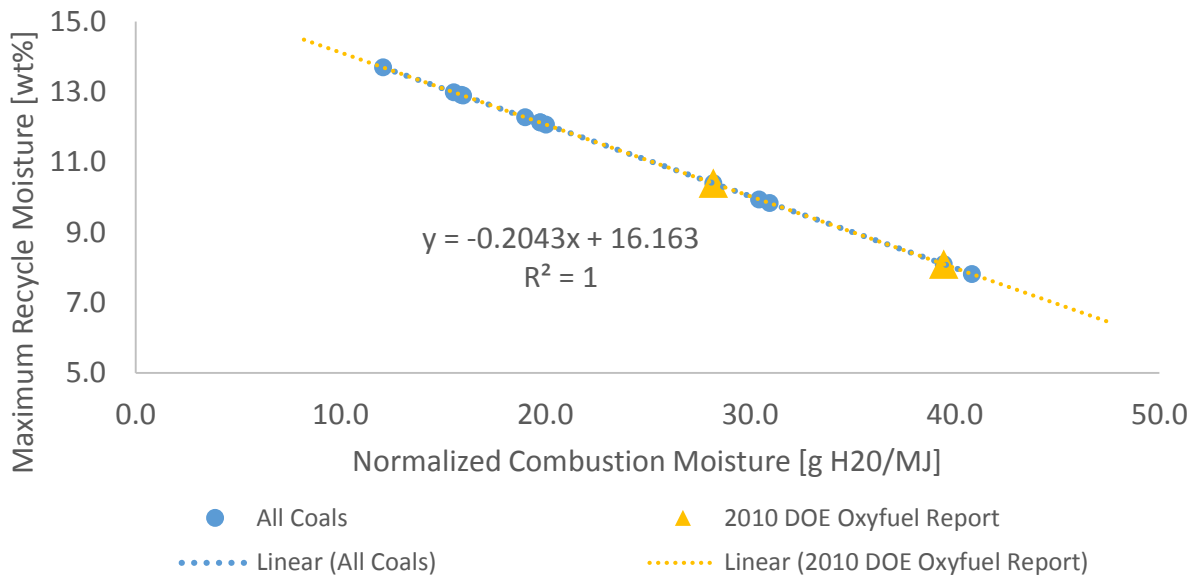


**Figure 4.1** The inverse proportionality of fuel and recycle moisture dictates as linear trade-off between the NCM and Maximum Recycle Moisture. The relation exhibits the anticipated result of lignite coals (high NCM) requiring relatively dry recycle conditions whereas bituminous coals (low NCM) can operate with higher recycle moisture levels.

The blue dots in Figure 4.1 are the standard coal compositions available in the IECM coal database. The constraint can be calculated for any arbitrary fuel composition using the following:

$$Max\ Recycle\ Moisture\ [y_{H_2O\_Recycle}] = 16.163 - 0.2043 * Normalized\ Combustion\ Moisture$$

Table 4-3 is provided to illustrate how NCM is calculated as well as to provide additional information to the reader so that individual coal blends may be identified in Figure 4.1.

Table 4-3 Normalized combustion moisture are corresponding recycle moisture limits for coals in the IECM Database.

Coal Type	HHV [MJ/kg]	Fuel Hydrogen [wt%]	Fuel Moisture [wt%]	Combustion Moisture [g H <sub>2</sub> O/kg fuel]	Normalized Combustion Moisture [g H <sub>2</sub> O/MJ]	Maximum Recycle Moisture [wt%]
DOE PRB (Montana Rosebud)	19.92	3.38	25.77	561.90	28.21	10.4
DOE Lignite (ND Beulah-Zap)	15.39	2.74	36.08	607.40	39.46	8.1
Pittsburgh #8	30.84	4.90	5.20	493.00	15.99	12.9
Illinois #6	25.54	4.25	12.20	504.50	19.75	12.1
Wyoming PRB	19.39	3.31	30.24	600.30	30.97	9.8
Appalachian Low Sulfur	30.40	4.62	5.63	472.10	15.53	13.0
Appalachian Medium Sulfur	30.82	4.88	5.05	489.70	15.89	12.9
Illinois #6	27.14	4.50	11.12	516.20	19.02	12.3
WPC Utah	26.13	4.85	7.95	516.00	19.75	12.1
North Dakota Lignite	13.99	2.68	33.03	571.50	40.84	7.8
Illinois #6 (EPRI)	25.35	4.20	13.00	508.00	20.04	12.1
Upper Freeport (NETL)	30.98	4.03	1.14	374.10	12.08	13.7
Wyodak-Andreson (NETL)	19.60	3.51	28.10	596.90	30.45	9.9

Using the NCM methodology allows the model to quickly determine the maximum mass fraction of moisture in the recycle stream regardless of fuel composition and heating value. As will be explained in greater depth in the following section on mass flow constraints, the maximum recycle moisture is used to determine the allocation of recycle flue gas between the primary and secondary loops.

### 4.3 Oxyfuel Base Plant Performance

The pulverized coal oxyfuel model utilizes the pre-existing base plant model in the IECM for handling many of the performance calculations related to basic plant operation. These calculations range in importance from major to minute and include systems such as coal handling, ash handling and disposal,

waste water treatment, cooling water supply, and boiler and steam cycle performance. Furthermore, the oxyfuel model also exercises the pollution control models for particulate removal and sulfur dioxide treatment. For more information on all of these systems please consult the applicable IECM documentation.

### 4.3.1 Boiler and Steam Cycle

The first generation of pulverized coal oxyfuel systems are expected to use traditional boilers designed for air-fired operation. Thermal management inside the boiler must be performed in order to ensure conductive and radiative heat transfer to the steam generator be maintained at nearly identical levels as would have been anticipated for the original air-fired operation. Consequently, the expected boiler efficiency for oxyfuel operation is nearly identical to air-fired operation. This is demonstrated in the DOE case study (36) for Wyoming PRB and North Dakota Lignite coals which were assumed to have boiler efficiencies of 85.8% and 83.5%, respectively. These efficiency values are identical to the boiler efficiencies currently reported in the IECM for these coals under air-fired operation.

We are able to accurately predict the boiler efficiency for arbitrary fuel mixtures by again employing our normalized combustion moisture methodology. Figure 4.2 shows a nearly perfect linear regression is held by plotting the reported boiler efficiency in the IECM of standard coals against the respective coals' NCM.

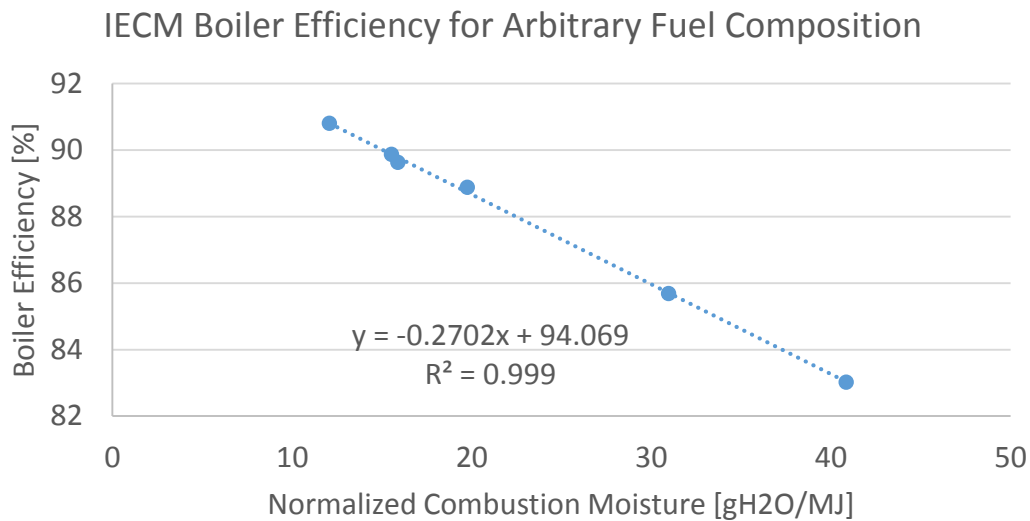


Figure 4.2 IECM boiler efficiency for arbitrary fuel compositions

For an arbitrary fuel blend, the boiler efficiency can be calculated using the normalized combustion moisture:

$$\eta_{Boiler}[\%] = -0.2702 * NCM + 94.069$$

The steam cycle heat rate is a measure of how efficiently the steam generator-turbine system is able to convert thermal energy into electrical output. Classically, there are a series of steam generator-turbine system performance classes identified loosely by the quality of the steam which is fed into the high

pressure side of the steam turbine. The term “loosely” is used in the previous sentence in recognition that there is no single steam quality (pressure and temperature) which canonically defines the class Supercritical. For example, in the IECM, the default steam cycle heat rate for Supercritical is 7,764 [kJ/kWh]. This is a higher heat rate (less efficient) than the Supercritical steam cycle heat rate of about 7,200 [kJ/kWh] which was back-calculated from the DOE case studies (36). The flexibility to accommodate various steam cycle heat rates has been built into the oxyfuel model by parameterizing the value. The model default is Supercritical, but the upper and lower bounds, along with typical class values are presented in Table 4-4.

Table 4-4 Steam cycle heat rates for the IECM

Existing IECM Defaults	Steam Cycle Heat Rate [kJ/kWh]
Maximum Value	15,830
Sub-critical	8,219
Supercritical	7,764
Ultra-Supercritical	7,074
Minimum Value	6,330

#### 4.4 Flue Gas Mass Balance

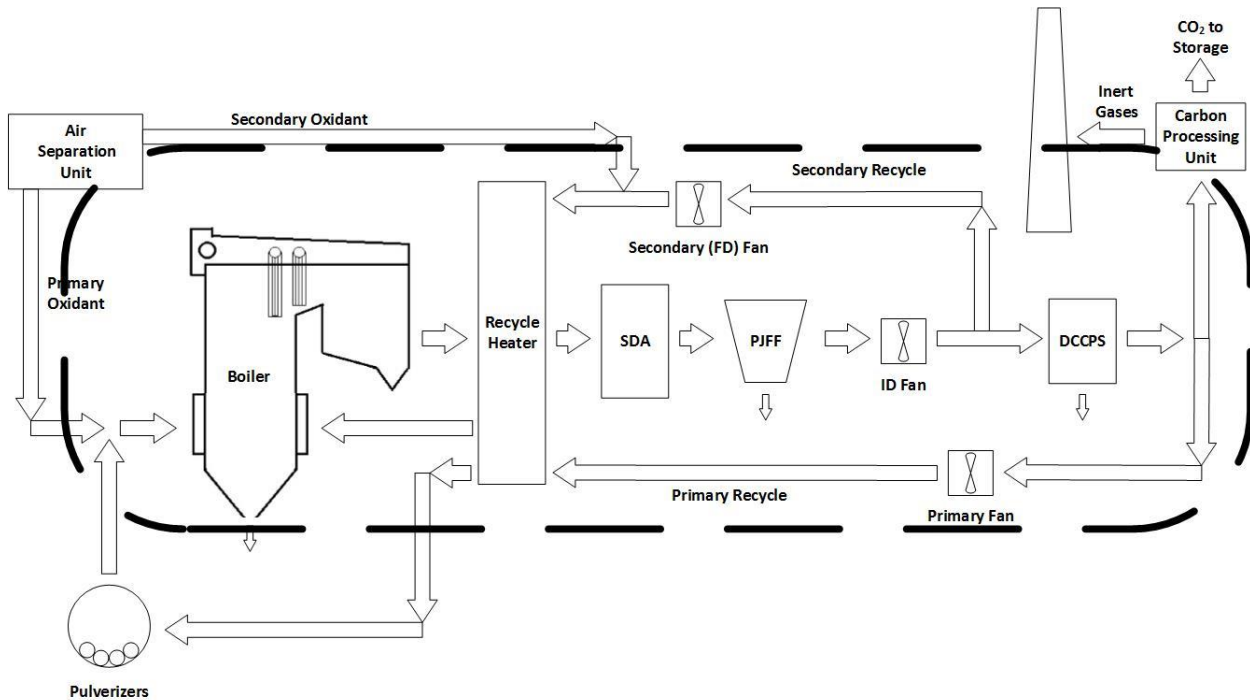


Figure 4.3 Simplified process flow diagram of the cool recycle process overlaid with the system boundary for determining the mass balance of the flue gas.

### 4.4.1 Base Flue Gas Recycle Configurations

Although there are three typical oxyfuel configurations to handle the various levels of sulfur content in the fuel being burned, there are only two configurations (warm and cool) for handling the recycle stream splits and determining the flue gas mass balance. Each of the configurations (Fig. 4.4 & 4.5) has been created specifically to facilitate the creation of algorithms for closing the mass balance.

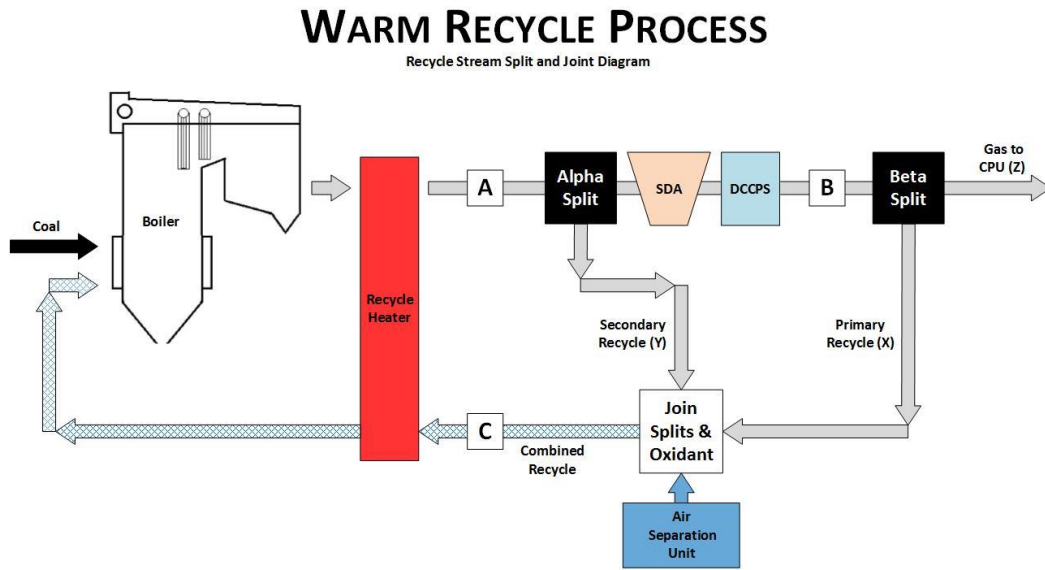


Figure 4.4 Simplified process flow diagram for the warm recycle process of the pulverized coal oxyfuel model in the IECM. Only equipment which alters the gaseous composition of the flue gas streams has been shown for simplicity.

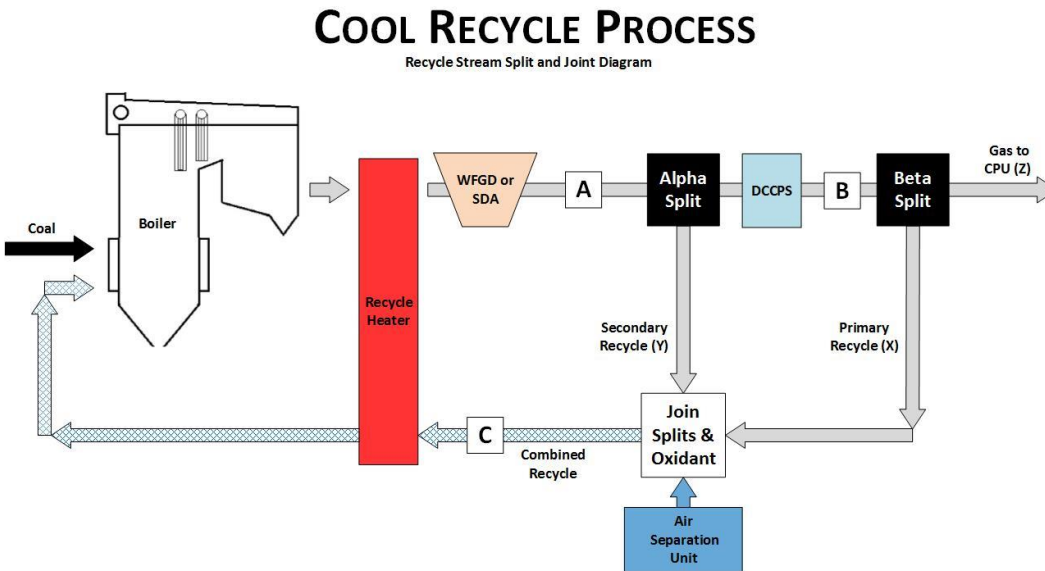


Figure 4.5 Simplified process flow diagram for the cool recycle process of the pulverized coal oxyfuel model in the IECM. Only equipment which alters the gaseous composition of the flue gas streams has been shown for simplicity.

The square, lettered boxes on the recycle process diagrams are locations where the molar flow rate of the flue gas is split. The alpha and beta split represent the creation of the secondary and primary flue gas recycle streams, respectively. The reasons for adopting this nomenclature and design will be elaborated further in section 4.4.5, but the flexibility provided by this design was essential in being able to create an integrated oxyfuel system from the individual process models in the IECM.

#### 4.4.2 General Calculation Algorithm

These are the steps required, each iteration, in the warm recycle process configuration:

- Determine molar flow rate of flue gas exiting the cool side of the recycle heater
  - Calculate combustion products from combustion reaction stoichiometry in the IECM
  - Calculate required oxidant flow rate to meet excess air requirements (less recycled oxygen)
  - Calculate air ingress to the flue gas across the recycle heater
  - Sum across the molar flow rates of each gas species in the above processes to arrive at a total gas flow rate for each species exiting the cool side of the recycle heater
- Create the secondary recycle stream
  - Split off the secondary recycle stream by applying the alpha fraction to the molar flow rate of each gas species at point A
  - Calculate main flue gas stream by applying the 1-alpha fraction to the molar flow rate of each gas species at point A
- Perform traditional pollutant control on the secondary recycle stream
  - Use the entered performance parameters for the PJFF to alter the molar flow rates of the secondary recycle stream
- Perform traditional pollutant control and moisture reduction on the main recycle stream
  - Use the entered performance parameters for the SDA, PJFF, and DCCPS to alter the molar flow rates of the main recycle stream
- Create the primary recycle stream
  - Split off the primary recycle stream by applying the beta fraction to the molar flow rate of each gas species at point B in the main recycle stream
  - Calculate the flue gas stream sent to the CPU (Z-stream) by applying 1-beta to the molar flow rate of each gas species at point B in the main recycle stream
- Calculate the combined recycle stream
  - The primary and secondary recycle streams must be joined with the oxidant stream by aggregating the molar flow rate across the three streams for each gas species
  - Thermal properties of the combined recycle stream are calculated as part of the stream joining process
- Verify whether constraints have been met, serially, in the following order:
  - The mass fraction of water in the combined recycle stream, at point C, must be less than the Maximum Recycle Moisture.

- If NO: index Alpha fraction down by the Alpha step from previous Alpha fraction (initial Alpha = Recycle Rate)
  - If YES: an acceptable system of recycle splits has been configured
- The molar flow rate of O<sub>2</sub> in the combined recycle stream (point C) has reached steady state
  - If NO: iterate again, up to the maximum number of allowable iterations
  - If YES: an stable quantity of oxidant is being generated
- The mole fraction of sulfur oxides in the combined recycle stream, at point C, must be less than the calculated NSPS for the chosen fuel
  - If NO: index the sulfur removal fraction 1 percentage point higher (initial 90%)
  - If YES: an acceptable level of sulfur removal is being performed
- The molar flow rate of CO<sub>2</sub> in the Z-stream has reached steady state
  - If NO: iterate again, up to the maximum number of allowable iterations
  - If YES: STOP

#### 4.4.3 Coal Flow Rate

The flow rate of fuel into the boiler is a function of the specified gross plant output, steam cycle heat rate, the boiler efficiency, and the higher heating value of the fuel to be fired. The relation below is used to determine the fuel flow rate necessary to provide the specified gross plant output, given the higher heating value of the fuel.

$$\dot{M}_{Fuel} [kg/s] = \frac{MW_{Gross} * HR_{Steam}}{3.6 * \eta_{Boiler} * HHV_{Fuel}}$$

Where

$MW_{Gross}$  is the specified gross output of the plant [MW]

$HR_{Steam}$  is the heat rate of the steam cycle [kJ/kWh]

$\eta_{Boiler}$  is the boiler efficiency [%]

$HHV_{Fuel}$  is the higher heating value of the fuel [kJ/kg]

It should be noted that the boiler efficiency is not an independent variable in the above relation for fuel flow rate; it is a function of the fuel composition.

#### 4.4.4 Oxidant Handling

The required oxygen flow rate for combustion is calculated through the following steps:

- Calculate the stoichiometric oxygen requirement based on the coal flow rate, coal composition, and emission factors for incomplete combustion reactants.
- Calculate the total oxygen requirement based on the excess oxygen specified

Table 4-5 Example calculation of the stoichiometric oxygen requirement for Appalachian Medium Sulfur Coal

Coal Component	Molecular Weight [g/mol]	Mass Fraction	Mass Flow Rate [t/hr]	Stoich. Oxygen [mass/mass]	Oxygen Mass Flow Requirement [t/hr]
Carbon	12	73.81	132.9	2.67	354.3
Hydrogen	2	4.88	8.78	8.0	70.3
Oxygen	32	5.41	9.74	-1	-9.74
Sulfur	32	2.13	3.83	1	3.83
Nitrogen	28	1.42	2.56	0.05*	0.13
Total (stoich.)					418.7

The table above is populated with values calculated from a 50 kg/s flow rate of Appalachian medium sulfur coal from the IECM coal database.

#### 4.4.4.1 Air Ingress

Air ingress (or leakage) is defined on the basis of theoretical air (oxygen) requirement and is assumed to enter into the flue gas stream at the recycle heater prior to any pollutant treatment or recycle streams being split-off. The default air ingress fraction is assumed to be 1% of theoretical oxygen requirement for combustion. So, the amount of oxygen in air ingress stream =  $0.01 \times 418.7 = 4.2$  [t/hr]. Air contains about 20.95 [wt%] oxygen. So, the ingress air mass flow rate is estimated to be  $4.2/0.2095 = 20.1$  [t/hr]. With the total mass flow rate of air ingress calculated, the corresponding molar flow rate of each gas species needs to be added to the combustion gases exiting the cool side of the recycle heater.

#### 4.4.4.2 ASU Oxidant Production

The algorithm for determining the quantity of oxygen required to be produced for combustion is based upon combustion stoichiometry and is therefore constant as long as the fuel flow rate remains unchanged. Similarly, the amount of air ingress into the recycle stream is defined as a percentage of the stoichiometric oxygen requirement. The result of framing the algorithm in this way is that the adjusted ASU oxidant load can be calculated within two iterations. The algorithm's very fast convergence as can be seen in Figure 4.6 below, which assumes that oxygen from air ingress "Recycle O2" was not calculated a priori and thus an extra iteration is shown for demonstration purposes only.

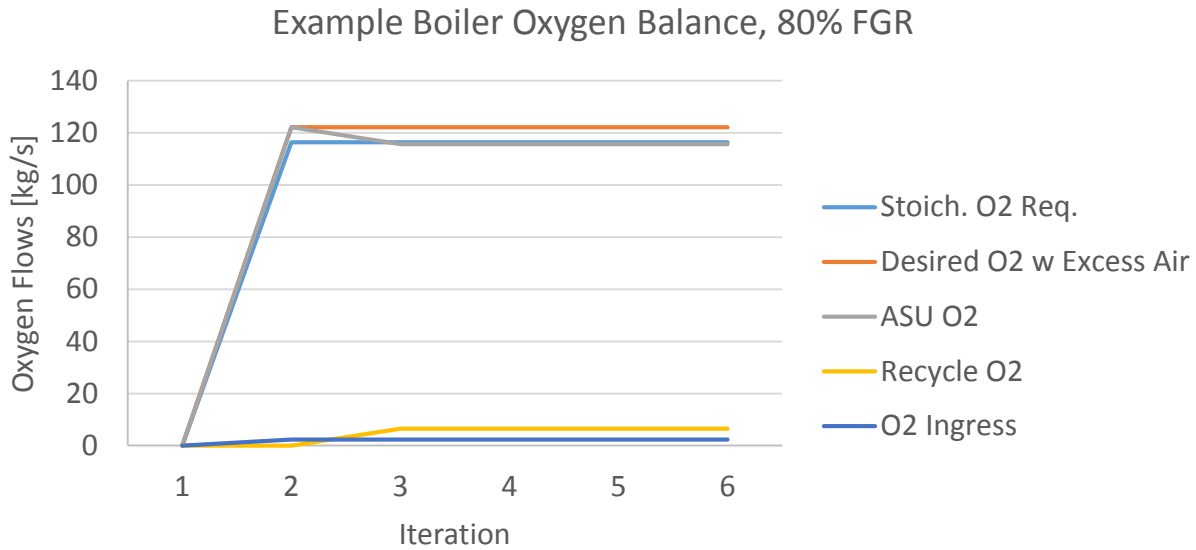


Figure 4.6. Iterations of FGR streams are not limited by the convergence of required oxygen. The amount of oxygen required can be determined in less than five iterations because many of the inputs can be calculated prior to the first iteration and are constant in value, being a multiple of the stoichiometric oxygen required based upon the chosen fuel composition.

The steps required to determine the oxygen production requirement from the ASU are:

Initial Iteration:

1. Calculate the stoichiometric oxygen required for combustion (ex. Table 4-4)
2. Calculate the desired excess oxygen for combustion
3. Add stoichiometric and excess oxygen quantities together for get total oxygen requirement
4. Add the calculated total quantity of oxygen to the boiler to combust the fuel (no need to use the ASU module for initial iteration)
5. Add the calculated ingress air to the combustion products
6. Perform recycle splits and pollutant control operations as dictated by plant configuration
7. Calculate the amount of oxygen present in the recycle streams

$$Oxygen_{Recycle} = Oxygen_{Primary} + Oxygen_{Secondary}$$

8. Calculate the required oxygen which must be produced by the ASU. This is the quantity of oxygen specified by the user, including excess oxygen, less all oxygen being recycled.

$$ASU_{Oxygen} = \left\{ \left( 1 + \frac{Excess\ Oxygen\ [\%]}{100} \right) * Oxygen_{Stoichiometric} \right\} - Oxygen_{Recycle}$$

9. Set the ASU model to produce the calculated mass flow of oxygen with the selected oxidant purity level.
10. Add the oxidant gas stream produced by the ASU to the primary and secondary recycle streams to create the Combined Recycle stream.

Subsequent Iterations:

1. Add the Combined Recycle stream to the boiler to combust the fuel.
2. Add the calculated ingress air to the combustion products.
3. Perform recycle splits and pollutant control operations as dictated by plant configuration.
4. Calculate the amount of oxygen present in the recycle streams

$$Oxygen_{Recycle} = Oxygen_{Primary} + Oxygen_{Secondary}$$

5. Calculate the required oxygen which must be produced by the ASU. This is the quantity of oxygen specified by the user, including excess oxygen, less all oxygen being recycled.

$$ASU_{Oxygen} = \left\{ \left( 1 + \frac{Excess\ Oxygen\ [\%]}{100} \right) * Oxygen_{Stoichiometric} \right\} - Oxygen_{Recycle}$$

6. Set the ASU model to produce the calculated mass flow of oxygen with the selected oxidant purity level.
7. Add the oxidant gas stream produced by the ASU to the primary and secondary recycle streams to create the Combined Recycle stream.
8. Check with the previous iteration of the oxidant flow rate being returned to the boiler (point C on recycle diagram) to determine if steady state has been achieved.

$$\Delta \dot{M}_{O_2\_Recycle} \leq 0.05\%$$

#### 4.4.5 Carbon Dioxide and Moisture Mass Balance

The carbon mass balance closure in the new model is functionally identical to how it was previously closed. A recycle rate is specified, the model is then iterated until the carbon molar flow rate in the stream sent to the CPU reaches steady state (this will be equal to the molar flow rate into the system from the fuel).

In the new model the user is asked to specify a Recycle Rate between 60 and 85%. This percentage was previously called the “Flue gas recirculation rate”, but this is not technically accurate as the bulk quantity of flue gas is changed (sulfur removed, water added and removed) depending upon the pollution treatment equipment involved. The presence of these intermediate processes make it impossible to identify a single location in the process flow diagram which could be used as the “absolute denominator” for determining what percentage of the “total” flue gas is sent to each of the recycle streams and the carbon processing unit. To avoid this confusion, and to allow the system to use primary and secondary recycle streams, it is better to think of the Recycle Rate simply as the percentage of carbon dioxide not sent to the carbon processing unit. Therefore, for each iteration of the model (1-Recycle Rate) is being sent to the carbon processing unit. I have named the stream sent to the carbon handling system the Z-stream. Also, the primary recycle stream is the X-stream and the secondary recycle is the Y-stream.

#### 4.4.5.1 Algorithm Setup

Unlike, the molar flow rate of water, the molar flow rate of carbon dioxide in the flue gas is not affected (to first order) by pollution control equipment. Because of this, it is possible to use the molar flow rate of carbon dioxide through the X, Y, and Z streams to properly configure how flue gas is divided in the system. Using the conceptual layout of two successive stream splits of percentage alpha and beta, as seen in Figure 4.4, the relation between the three streams can be expressed mathematically as:

$$Z = 1 - \text{Recycle Rate}$$

$$Y = \alpha * A$$

$$X = \beta * B$$

Where:

$A$  is the molar flow rate of carbon dioxide before the first split

$B$  is the molar flow rate of carbon dioxide before the second split

$\alpha$  is the fraction of A which becomes the molar flow rate of carbon dioxide in the Y-stream

$\beta$  is the fraction of B which becomes the molar flow rate of carbon dioxide in the X-stream

If we let A be unity and assume carbon dioxide molar flow is unaffected by intermediate processes, then:

$$A = 1$$

$$B = (1 - \alpha)$$

$$X = \beta * (1 - \alpha)$$

$$Z = (1 - \alpha) * (1 - \beta)$$

We want to fix the Z-stream value by specifying the Recycle Rate, so it is helpful to express beta as:

$$\beta = 1 - \frac{Z}{(1 - \alpha)}$$

This leaves us with alpha as the lone independent variable once the user specifies a Recycle Rate. Alpha can then be used as the indexed variable in the iterative process used to close the mass balance of gases in the oxyfuel plant.

#### 4.4.5.2 Algorithm

This is the procedure used to solve for Beta (and reaching steady state) for a given Recycle Rate for the warm recycle configuration. The amount of fuel moisture under stoichiometric combustion remains constant each iteration and is calculated:

$$\dot{m}_{H_2O, Fuel} = \left( (y_{H_2, Fuel} * 9) + y_{H_2O, Fuel} \right) * \dot{m}_{Fuel}$$

Initial Values: Recycle Index (RI) = 0, Alpha = Recycle Rate, and Beta = 0

**Begin:** Let the current iteration be (t) and the previous iteration be (t-1):

$$A(t) = \dot{B}oiler_{exit_{H_2O}}(t) = \dot{F}uel_{H_2O}(t) + \dot{B}oiler_{exit_{H_2O}}(t - 1)$$

Then

$$Y - \dot{s}tream_{H_2O}(t) = A(t) * \alpha(t)$$

Then pass the flue gas not fractioned of into the Y-stream through pollutant treatment and moisture removal. For Warm Recycle this quantity of flue gas is:

$$A(t) * (1 - \alpha(t))$$

Once this gas is passed through the SDA and the DCCPS it is B(t)

Then

$$X - \dot{s}tream_{H_2O}(t) = B(t) * \beta(t)$$

Then combine the primary and secondary streams with the oxidant from the ASU (no H<sub>2</sub>O will be present in this stream)

$$C_{ombined\_R}ecycle_{H_2O}(t) = X - \dot{s}tream_{H_2O}(t) + Y - \dot{s}tream_{H_2O}(t)$$

At this point we check to see if the Combined Recycle Moisture Constrains is met:

$$Y_{H_2O, C_{ombined\_R}ecycle}(t) \leq M_{aximum\ Recycle\ Moisture}$$

If yes: STOP indexing the recycle fractions and allow the system to attempt to reach steady state.

If no, set:

$$RI(t) = RI(t - 1) + 1$$

Then

$$\alpha(t) = R_{ecycle\ Rate} - (0.01 * RI(t))$$

$$\beta(t) = 1 - \frac{(1 - R_{ecycle\ Rate})}{(1 - \alpha(t))}$$

Then repeat from **Begin** until the Maximum Recycle Moisture Constraint is met.

#### 4.4.5.3 Algorithm Results

When followed through to completion, the algorithm for determining the alpha and beta fractions will usually look similar to the result presented in Figure 4.7. The alpha fraction will start at the Recycle Rate (65% in this case) and continue to iterate downward until the Maximum Recycle Moisture constraint is met (Fig. 4.8). While the alpha fraction is being decreased; the beta fraction is slowly increasing and the

amount of moisture in the combined recycle stream is being reduced.

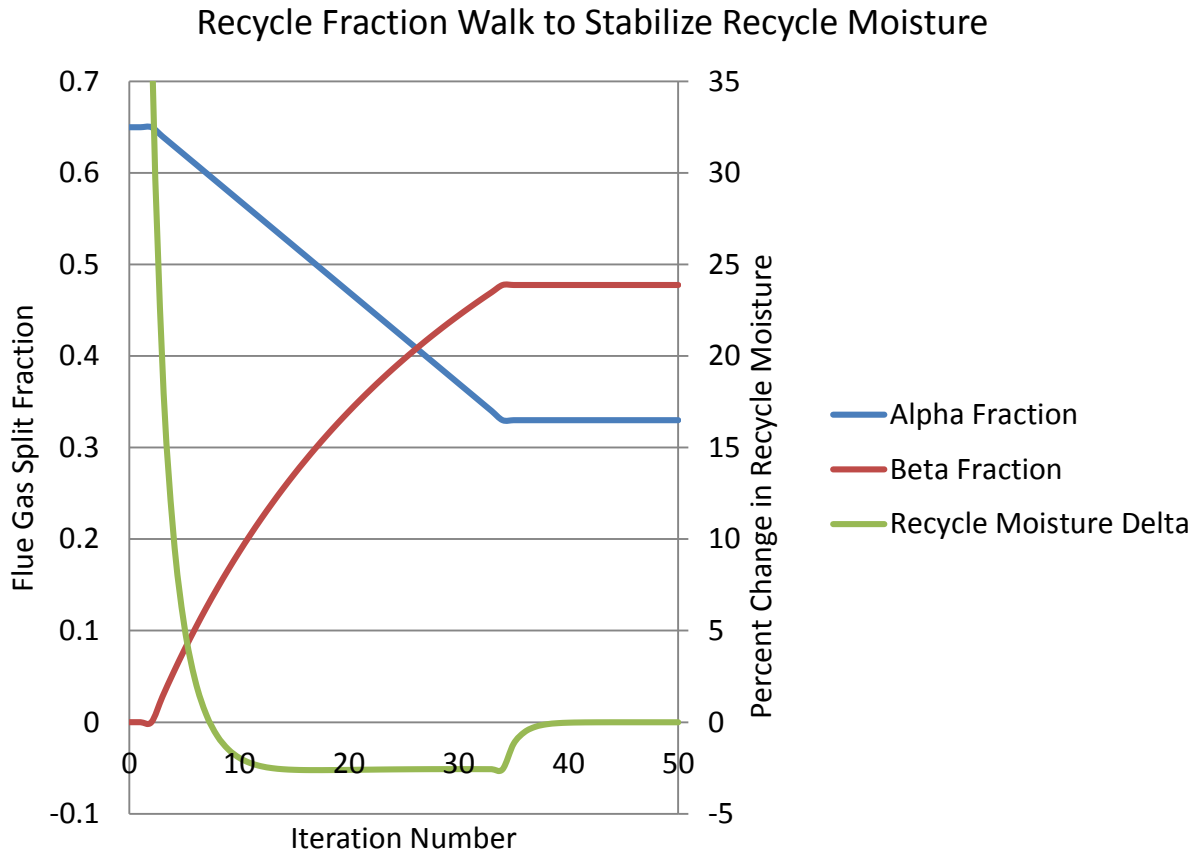


Figure 4.7 Walk of the recycle fractions (alpha and beta) as the recycle moisture constraint is met

After enough iterations have occurred and the Max Recycle Moisture constraint has been met, the system accepts the current alpha a beta recirculation fractions. Once this occurs (iteration 33 in this example) the system is allowed to reach steady state, which takes roughly an additional ten iterations in this example.

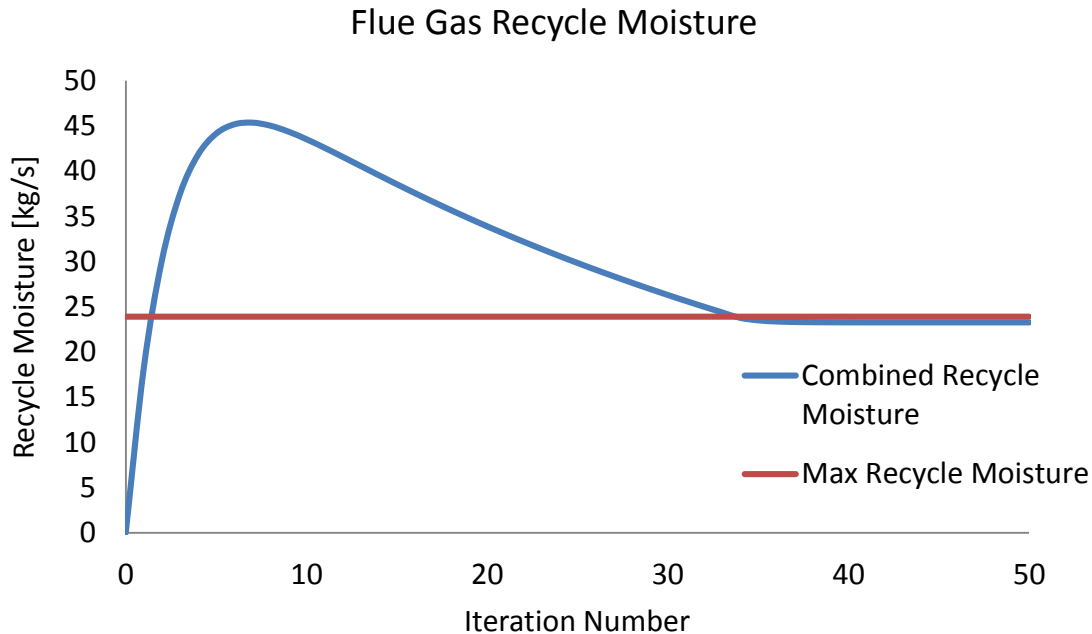


Figure 4.8 Trajectory of the mass flow rate of moisture in the recycle stream as the system works toward convergence.

#### 4.4.5.4 Steady State Operation

The pulverized coal oxyfuel model is a large set of mass balance equations which must satisfy the constraints developed for each compound before results can be reported in the IECM. Each plant modeled in the IECM produces results which are representative of steady state operation at the designed output capacity. Steady state in this context refers narrowly to a stable solution which meets all mass flow constraints. The quality of this stable solution is a function of the quality of the constraints only and there has been no attempt made to find an “optimized” or “best” plant. Optimization typically requires detailed environmental knowledge and specific cost information which is beyond the scope of the estimates intended to be produced by the IECM.

The steady state solution that the model converges to is a result of iteration until the mass balance constraints have been satisfied. The oxyfuel model is best conceived of as a set of algorithms designs to find a satisfactory solution, rather than an optimal solution. For criteria pollutants such as sulfur oxides and particulate matter the iterations are used to determine the required level of control for the WFGD/SDA and fabric filter, respectively. For the carbon balance, the incoming carbon with the coal must be matched by the outward flux of carbon in the carbon dioxide in the flue gas sent to the carbon handling system. As was discussed in Chapter 3, this constraint is both straight forward and absolute and is eventually met regardless of the absolute quantity of flue gas recycled.

The least straight forward of the mass constraints is the water vapor content returned to the boiler in the combined recycle stream. The constraint is formulated as a maximum allowable mass fraction which is determined by the mass fraction of moisture in the coal. The algorithm to achieve a viable solution always begins by over shooting the moisture content in the recycle stream, then slowly increases the quantity of moisture removed by the DCCPS until the combined recycle stream has a moisture content below the maximum recycle moisture constraint. This is accomplished by initially

recycling all the flue gas to be recycled through the secondary recycle stream. This causes the moisture content of the combined recycle stream to quickly exceed the MRM constraint (Fig. 4.8). The crossing of the constraint initially cannot be mistakenly identified as a local solution by the oxyfuel model because the derivative is very large at this point due to the rapid accumulation of moisture in the recycle stream. It is only through the gradual shifting of recycled gas from secondary to primary stream, and the associated removal of moisture, that the second crossing of the MRM constraint results in a converged steady state solution.

#### 4.4.6 Remaining Flue Gas Constraints

With the total amount of flue gas to be recirculated to the boiler known and the splits for both primary and secondary recycle determined, we turn our attention to the remaining mass flow constraints. If any of these criteria pollutant constraints are not initially met, they are adjusted using the outlined strategy for each in Section 3.4., and generally the removal efficiency is increased.

##### Sulfur Oxides

$$\Delta \dot{M}_{SO_2\_Recycle} \leq 0.05\%$$

and

$$\dot{M}_{SO_2\_Recycle} \leq NSPS\ Limit$$

##### Nitrogen Oxides

$$\Delta \dot{M}_{NOx\_Zstream} \leq 0.05\%$$

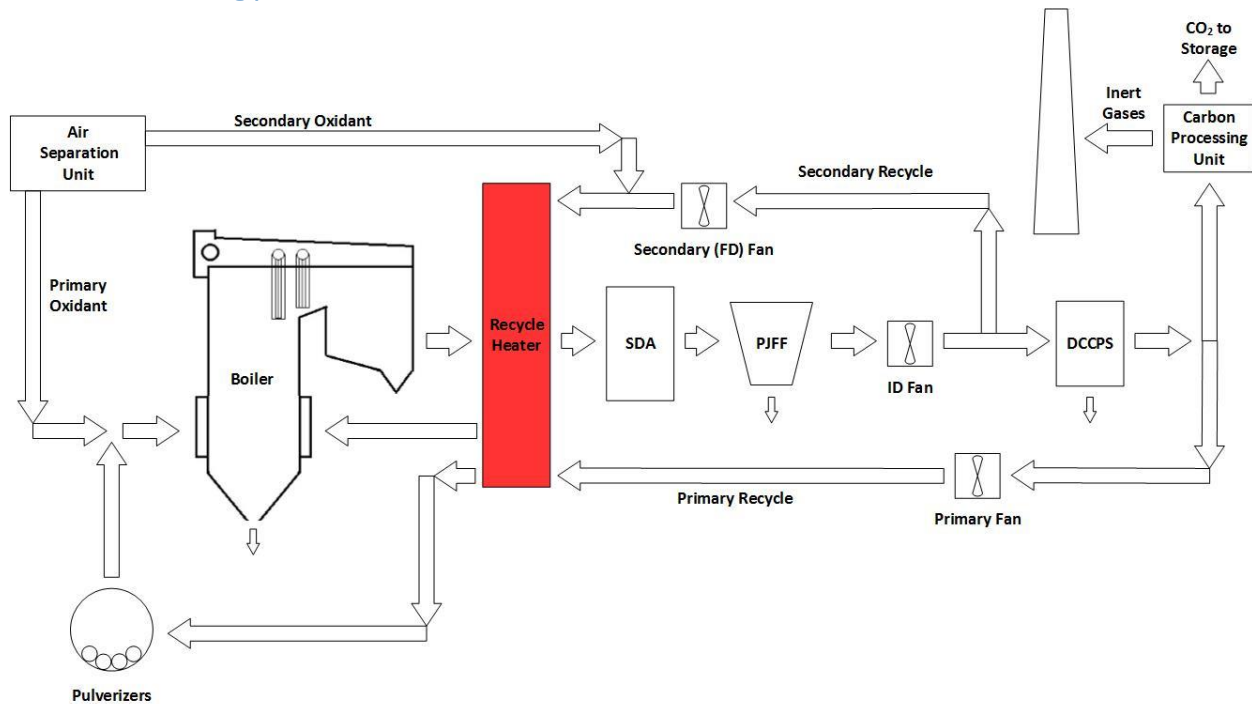
##### Total Suspended Particulates

$$\Delta \dot{M}_{PM\_Recycle} \leq 0.05\%$$

and

$$\dot{M}_{PM\_Recycle} \leq NSPS\ Limit$$

## 4.5 Energy Balance



Only after the mass balance has been determined and steady state has been reached does the oxyfuel model make any calculations or corrections for the energy balance of the overall plant. There are two specific energy balance calculations which need to be completed. The first of these is accounting for the recovery of heat energy from compression in the ASU and CPU which is used for boiler feedwater preheating. The second is an accounting of the enthalpy content of the flue gas being recycled to the boiler.

### 4.5.1 Gas Thermodynamic Property Calculations

In order to be able to account for the enthalpy content of the gases being recycled to the boiler, it was necessary to have the ability to calculate gas phase heat capacity, enthalpy, and entropy thermochemistry in the IECM. A common means of handling these calculations is the use of the Shomate Relations. The following equations can be used with the coefficients in Table 4-6 to calculate any of these thermoproperties at a known temperature.

$$c_p = A + B * t + C * t^2 + D * t^3 + E/t^2$$

$$h^\circ - h_{298.15}^\circ = A * t + B * t^2/2 + C * t^3/3 + D * t^4/4 - E/t + F - H$$

$$s^\circ = A * \ln(t) + B * t + C * t^2/2 + D * t^3/3 - E/(2 * t^2) + G$$

Where:

$$c_p = \text{heat capacity} \left[ \frac{J}{\text{mol} * K} \right]$$

$$h^\circ = \text{standard enthalpy} \left[ \frac{\text{kJ}}{\text{mol}} \right]$$

$$s^\circ = \text{standard entropy} \left[ \frac{\text{J}}{\text{mol} \cdot \text{K}} \right]$$

$$t = \text{temperature} \frac{[\text{K}]}{1000}$$

Table 4-6 Gas Phase Coefficients for the Shomate Relations (59)

Gas Species	Temperature Range [K]	A	B	C	D	E	F	G	H
Ar	298 - 6000	20.786	2.83E-07	-1.5E-07	1.09E-08	-3.7E-08	-6.19735	179.999	0
CO	298 - 1300	25.56759	6.09613	4.054656	-2.6713	0.131021	-118.0089	227.3665	-110.5271
	1300 - 6000	35.1507	1.300095	-0.20592	0.01355	-3.28278	-127.8375	231.712	-110.5271
CO2	298 - 1200	24.99735	55.18696	-33.6914	7.948387	-0.13664	-403.6075	228.2431	-393.5224
	1200 - 6000	58.16639	2.720074	-0.49229	0.038844	-6.44729	-425.9186	263.6125	-393.5114
H2	298 - 1000	33.06618	-11.3634	11.43282	-2.77287	-0.15856	-9.980797	172.707974	0
	1000 - 2500	18.56308	12.25736	-2.85979	0.268238	1.97799	-1.147438	156.288133	0
	2500 - 6000	43.41356	-4.29308	1.272428	-0.09688	-20.5339	-38.515158	162.081354	0
H2O	298 - 1700	30.092	6.832514	6.793435	-2.53448	0.082139	-250.881	223.3967	-241.8264
	1700 - 6000	41.96426	8.622053	-1.49978	0.098119	-11.1576	-272.1797	219.7809	-241.8264
N2	298 - 6000	26.092	8.218801	-1.97614	0.159274	0.044434	-7.98923	221.02	0
NO	298 - 1200	23.83491	12.58878	-1.13901	-1.49746	0.214194	83.35783	237.1219	90.29114
	1200 - 6000	35.99169	0.95717	-0.14803	0.009974	-3.00409	73.10787	246.1619	90.29114
NO2	298 - 1200	16.10857	75.89525	-54.3874	14.30777	0.239423	26.17464	240.5386	33.09502
	1200 - 6000	56.82541	0.738053	-0.14472	0.009777	-5.45991	2.846456	290.5056	33.09502
O2	298 - 6000	29.659	6.137261	-1.18652	0.09578	-0.21966	-9.861391	237.948	0
SO2	298 - 1200	21.43049	74.35094	-57.7522	16.35534	0.086731	-305.7688	254.8872	-296.8422
	1200 - 6000	57.48188	1.009328	-0.07629	0.005174	-4.0454	-324.414	302.7798	-296.8422
SO3	298 - 1200	24.02503	119.4607	-94.3869	26.96237	-0.11752	-407.8526	253.5186	-395.7654
	1200 - 6000	81.99008	0.622236	-0.12244	0.008294	-6.70369	-437.659	330.9264	-395.7654
CH4	298 - 1300	-0.70303	108.4773	-42.5216	5.862788	0.678565	-76.84376	158.7163	-74.8731
	1300 - 6000	85.81217	11.26467	-2.11415	0.13819	-26.4222	-153.5327	224.4143	-74.8731
C2H6	298 - 3000	14.4326	159.5815	-59.4614	7.835697	-0.42739	0	0	0
C3H8	298 - 1500	-4.78019	304.284	-156.131	31.29992	0.056218	0	0	0
HCL	298 - 1200	32.12392	-13.4581	19.86852	-6.85394	-0.04967	-101.6206	228.6866	-92.31201
	1200 - 6000	31.91923	3.203184	-0.54154	0.035925	-3.43853	-108.015	218.2768	-92.31201
NH3	298 - 1400	19.99563	49.77119	-15.376	1.921168	0.189174	-53.30667	203.8591	-45.89806
	1400 - 6000	52.02427	18.48801	-3.76513	0.248541	-12.458	-85.53895	223.8022	-45.89806

#### 4.5.1.1 Current NIST Coefficient Comparison

When the IECM base plant had originally been developed some provision to utilize some of the Shomate relations had been made. However, these had been removed from the IECM and needed to be replaced. The original coefficients for the thermo-property equations had not been well documented and their accuracy compared to current NIST values was unknown. The below table provides a summary of the comparison of calculated enthalpy values of three gases at 450 Kelvin.

Table 4-7 Comparison between previously NIST coefficients and current NIST coefficients.

Case	Gas Species	A	B	C	D	E	F	Enthalpy [kJ/mol]	Percent Difference
Existing IECM	N2	26.092	8.218801	-1.97614	0.159274	0.044434	-7.98923	4.427189	-
Current NIST 100-500	N2	28.98641	1.853978	-9.64746	16.63537	0.000117	-8.67191	4.436923	0.002199
Existing IECM	O2	29.659	6.137261	-1.18652	0.09578	-0.21966	-9.86139	4.559638	-
Current NIST 100-700	O2	31.32234	-20.2353	57.86644	-36.5062	-0.00737	-8.90347	4.542591	-0.00374
Existing IECM	Ar	20.786	2.83E-07	-1.5E-07	1.09E-08	-3.7E-08	-6.19735	3.15635	-
Current NIST	Ar	20.786	2.83E-07	-1.5E-07	1.09E-08	-3.7E-08	-6.19735	3.15635	8.44E-15

As was expected, there was little change in the NIST coefficients. The coefficients were left with the most recent values. The coding of the Shomate Relations restored the ability to handle the calculation of thermo-property data internal to the IECM.

#### 4.5.2 Combining the Recycle Streams

The primary and secondary recycle streams, along with their respective oxidant streams, must be combined into a single stream prior to entering the recycle heater energy balance model. To do this we assume ideal gas behavior and apply the Gibbs-Dalton law for calculating the combined enthalpy of the bulk recycle gas stream entering the recycle heater.

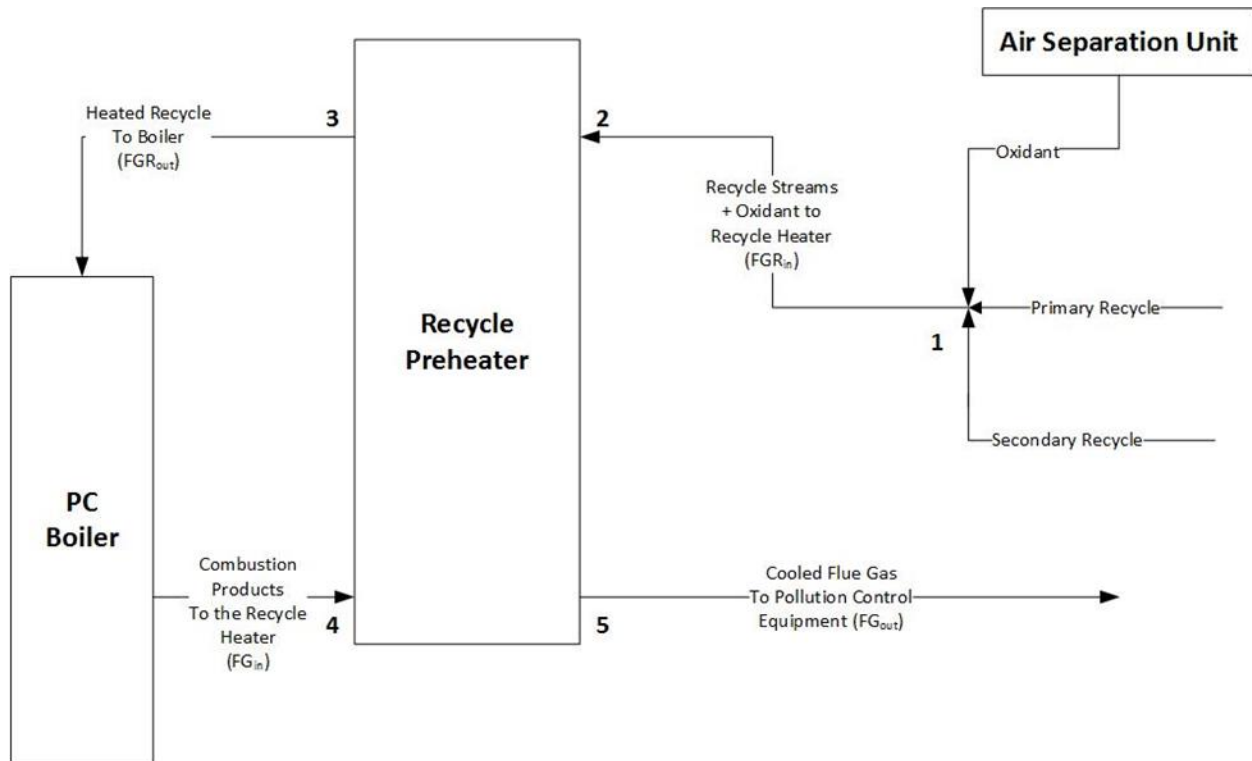


Figure 4.9 Diagram depicts the stream flows associated with the combining of the three feed streams which comprise the bulk recycle stream (1) and the heat exchange between the bulk recycle stream (2,3) and the flue gas (4,5).

For the low pressures involved in this mixing process, the gasses behave essentially as ideal gases. It was therefore assumed that the mixture obeys the Gibbs-Dalton law. The internal energy of ideal gases is solely a function of temperature. Thus, the final equilibrium temperature for the recycle stream prior to entering the recycle heater (2) depends on the internal energy of the mixture. We assume that there are no work or heat interactions for the mixing process; therefore the internal energy of the system does not change.

$$U_{Recycle} = U_{Oxidant} + U_{Primary} + U_{Secondary}$$

Alternatively, this relation can be written with respect to the enthalpies of the gas streams.

$$H_{Recycle} = H_{Oxidant} + H_{Primary} + H_{Secondary}$$

For an arbitrary enthalpy stream ( $H_m$ ), the total enthalpy is comprised of the sum of enthalpy values from each pure species which collectively make up the gas stream composition.

$$H_m = N_m h_m = N_1 h_1 + N_2 h_2 + \dots + N_k h_k = \sum_{i=1}^k N_i h_i$$

For this model (and in the IECM generally) the Shomate Relations are used for calculating thermodynamic properties for pure species.

$$h^\circ - h_{298.15}^\circ = A * t + B * t^2/2 + C * t^3/3 + D * t^4/4 - E/t + F - H$$

Where

$A - H$  are the Shomate Relation constants for the pure species being evaluated  
 $t$  is the temperature of the gas stream [K/1000]

#### 4.5.2.1 Ideal Mixing of the Recycle Streams

The mixing of the three feed streams (Oxidant, Primary and Secondary Recycle), which together create the bulk recycle to the boiler, begins with a molar balance to ensure mass is conserved. The mixing is assumed to take place in a steady-state control-volume where the pressures of the three incoming streams are equivalent. The total molar flow rate of the bulk recycle stream is the aggregate of the total molar flow rate of each pure species (i) across the three inlet streams.

$$\varphi_{i,Recycle} = \varphi_{i,Oxidant} + \varphi_{i,Primary} + \varphi_{i,Secondary}$$

$$\varphi_{Recycle} = \sum_{i=1}^k \varphi_{i,Oxidant} + \varphi_{i,Primary} + \varphi_{i,Secondary}$$

With both the total molar flow rate of the recycle stream and the molar flow rate of each species known, the mole fractions of the recycle stream are calculated and reported to the user in the model interface.

$$x_{i,Recycle} = \frac{\varphi_{i,Recycle}}{\varphi_{Recycle}}$$

Enthalpy is a state property and consequently meaningless absent a reference condition. For this work a reference state of 298.15K is used to calculate the energy flow [kJ/s] contained within a given stream. To better illustrate this methodology, the required calculation steps for determining the specific energy flow associated with the oxidant stream are presented below in long form. An identical strategy is used for the primary and secondary recycle streams, with the exception that the accounted pure species are dictated by the composition of the stream being evaluated.

#### Example Oxidant Energy Flow

Let:  $x_{Oxygen} = 0.95$ ,  $x_{Argon} = 0.03$ ,  $x_{Nitrogen} = 0.02$ ,  $T = 323K$  (50°C)

Table 4-8 Calculated enthalpy values for the example oxidant stream.

Gas Species	A	B	C	D	E	F	G	Enthalpy (T1) [kJ/mol]	Enthalpy (T2) [kJ/mol]	Enthalpy Delta
Ar	20.786	2.83E-07	-1.5E-07	1.09E-08	-3.7E-08	-6.19735	179.999	0	0.52	0.52
N2	26.092	8.218801	-1.97614	0.15927	0.044434	-7.98923	221.02	0	0.71	0.72
O2	29.659	6.137261	-1.18652	0.09578	-0.21966	-9.86139	237.948	0	0.71	0.73

Using the evaluated enthalpy values in Table 4-8 above the bulk specific enthalpy of the oxidant stream can be calculated:

$$h_{Oxidant} = \sum_{i=1}^k x_i (h_i^{323K} - h_i^{298K}) = [0.95(0.729) + 0.03(0.520) + 0.02(0.723)] = 0.723 \left[ \frac{kJ}{mol} \right]$$

If the primary and secondary recycle streams are defined as:

Primary:  $x_{O_2} = 0.0217$ ,  $x_{Ar} = 0.0285$ ,  $x_{N_2} = 0.0741$ ,  $x_{CO_2} = 0.6803$ ,  $x_{H_2O} = 0.1953$   $T = 346K$  (73°C)

$$h_{Primary} = \sum_{i=1}^k x_i (h_i^{346K} - h_i^{298K}) = 1.726 \left[ \frac{kJ}{mol} \right]$$

Secondary:  $x_{O_2} = 0.175$ ,  $x_{Ar} = 0.023$ ,  $x_{N_2} = 0.0598$ ,  $x_{CO_2} = 0.5493$ ,  $x_{H_2O} = 0.3502$ ,  $T = 423K$  (150°C)

$$h_{Secondary} = \sum_{i=1}^k x_i (h_i^{423K} - h_i^{298K}) = 4.562 \left[ \frac{kJ}{mol} \right]$$

The bulk specific enthalpy of the recycle stream can then be calculated:

$$h_{Recycle} = \frac{\sum_{m=1}^n \varphi_m * h_m}{\sum_{m=1}^n \varphi_m} = \frac{(H_{Oxidant} + H_{Primary} + H_{Secondary})}{\varphi_{Recycle}}$$

Where

$m$  is an arbitrary recycle feed stream

$n$  is the total number of feed streams being combined

Calculating the temperature of the bulk recycle stream cannot be easily calculated with a closed-form solution as the temperature and specific enthalpy calculations are physically coupled. Therefore determining the bulk recycle temperature is most easily handled through an iterative approach to arrive at a final temperature.

$$h_{Recycle} = \sum_{i=1}^k x_i (h_i^{Recycle Temp [K]} - h_i^{298K}) \quad Eq. A$$

For this example, suppose the normalized molar flow rate three feed streams are the following fractions: Oxidant = 0.25, Primary = 0.33, and Secondary = 0.42. Using these, the specific enthalpy of the bulk recycle stream can be calculated.

$$h_{Recycle} = 2.657 \left[ \frac{kJ}{mol} \right] = 0.25 * h_{Oxidant} + 0.33 * h_{Primary} + 0.42 * h_{Secondary}$$

Once our three example feed streams are combined into a single bulk recycle stream, they yield the resulting gas:

Bulk Recycle:  $x_{O_2} = 0.252$ ,  $x_{Ar} = 0.027$ ,  $x_{N_2} = 0.055$ ,  $x_{CO_2} = 0.456$ ,  $x_{H_2O} = 0.211$ ,  $T = 365.2K$  (102.2°C)

The final temperature of 365 Kelvin was determined by using the Newtonian Method to arrive at the bulk recycle temperature required to satisfy Equation A.

### 4.5.3 Recycle Preheater Energy Balance Model

Ideally, the fully characterized combined recycle flue gas stream would be used in the Recycle Preheater Energy Balance Model (Appendix B). Unfortunately, sufficient process data was not available to be able to calibrate the Recycle Preheater Energy Balance Model and its use had to be postponed at the current time. In the future, hopefully the availability of more thorough process flow data will allow this model to be added to the IECM. The second best workaround to allow for the enthalpy content of the combined recycle gas stream is discussed in the following section.

### 4.5.4 Recycle Heat Energy Correction

A design objective of the PC oxyfuel model has been to provide the capacity to vary a litany of parameters which will contribute towards producing a recycle stream which may vary substantially in both composition and thermal energy. To account for disparities in contained thermal energy in the recycle stream we adopted a two part strategy: first determining the anticipated the contained thermal energy in the recycle stream for arbitrary fuel composition and then accounting for disparities from this anticipated level by either debiting or crediting a representative amount of energy from the plant.

As has been previously discussed, the fuel moisture is the primary determinant of the required plant configuration to ensure proper operation and emissions performance. The amount of thermal energy contained in the recycle stream is a result of the required emissions control technologies and the primary to secondary recycle split necessitated by the fuel moisture. It then follows that the amount of fuel moisture would give a direct indication of the amount of thermal energy returned to the boiler in the recycle stream.

To construct a model which would allow both gross plant size and fuel composition to be arbitrary, it was necessary to develop a relation between thermal energy returned in the recycle stream and input thermal energy provided to the boiler from the fuel. The first step towards developing this relation was to use the methodology, outlined in Section 4.5.3, for calculating the specific enthalpy of the bulk recycle stream (Eq. A) to determine the amount of thermal energy contained in the recycle streams of the DOE case study plants<sup>4</sup> (36). This was accomplished finding the product of the bulk recycle molar flow rate and the specific enthalpy of the bulk recycle stream.

$$\text{Recycle Heat } \left[ \frac{kJ}{hr} \right] = (\varphi_{Oxidant} + \varphi_{Primary} + \varphi_{Secondary}) * h_{Recycle}$$

---

<sup>4</sup> The DOE study only examined sub-bituminous (S12) and lignite (L12) coals because of their low sulfur content and the previously discussed associated advantages.

Table 4-9 Thermal Input and Recycle Heat for the DOE Case Studies

Coal Type	Gross Electrical Output [kWe]	Thermal Input [kJ/hr]	Recycle Heat [kJ/hr]
Wyoming PRB	748,300	6,342,826,800	98,367,821
ND Lignite	751,000	6,541,944,550	72,587,940

The ratio of the recycle to input heat for these two coals was then plotted using the NCM of their respective coals as the independent variable. Some liberty had to be taken in assuming the presence of a linear relation, but due to a lack of available data, there was nothing to indicate a different functional relation was more appropriate. The result of plotting the calculated anticipated recycle to input heat ratios for other coals available in the IECM database is presented below.

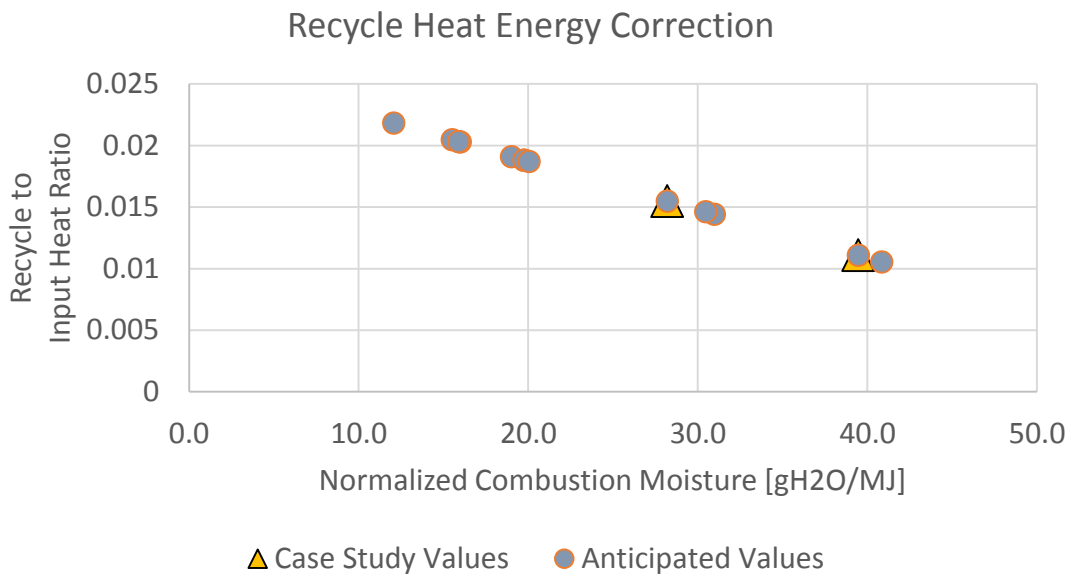


Figure 4.10 Recycle heat input ratio as a function of the normalized combustion moisture of the fuel being burned.

The trend here is that plants utilizing lower moisture fuels would be anticipated to recover a larger fraction of heat from the recycle stream. This relation reflects the physical reality of less moisture needing to be removed from the flue gas and the thermodynamically favorable state of having a proportionately large secondary recycle fraction which need not pass through the DCCPS. If the only fuel component affecting the recycle stream bulk enthalpy were moisture then this relation would predict the performance we would anticipate to see out of the model across fuel compositions. However, the PC oxyfuel model must also make sure that sulfur emissions and recycle limits are met. This necessitates that fuels with higher sulfur concentrations (typically fuels with low NCM) use a wet flue gas desulfurization unit. The effect on recycle heat of the WFGD can be substantial and result in a situation like that illustrated in Figure 4.11.

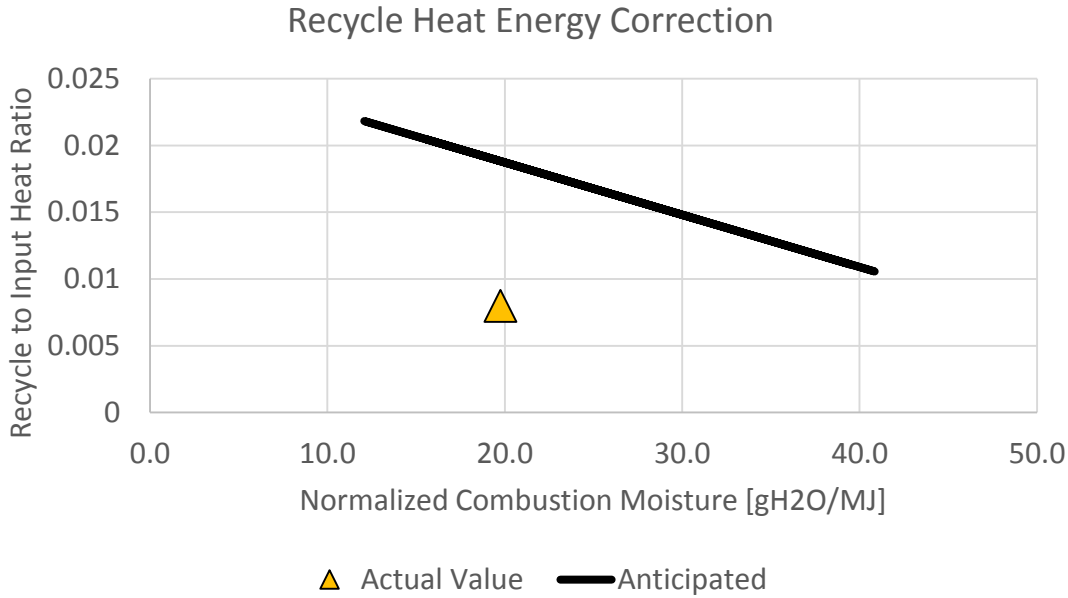


Figure 4.11 Example of the disparity in the recycle to input heat ratio (RIHR) which may result from the use of a wet flue gas desulfurization ratio.

This represents a situation where a high sulfur coal (Illinois #6) is anticipated to have a recycle to input heat ratio (RIHR) of 0.01882 and instead has a RIHR of 0.008 because of the extra cooling of the WFGD. If we take this to reflect the operation of a plant with a thermal input of 6 billion kilojoules per hour (roughly 500 [MW-net]), we can work out the amount of energy which needs to be debited from the calculation of net electrical output.

$$6,000,000,000 \left[ \frac{\text{kJ}}{\text{hr}} \right] * (RIHR_{Actual} - RIHR_{Anticipated}) = -65,000,000 \left[ \frac{\text{kJ}}{\text{hr}} \right]$$

Given

$$RIHR_{Anticipated} = 0.026566 - 0.000392 * NCM$$

$$RIHR_{Actual} = \frac{\text{Recycle Heat} \left[ \frac{\text{kJ}}{\text{hr}} \right]}{\text{Thermal Input} \left[ \frac{\text{kJ}}{\text{hr}} \right]}$$

$$\text{Thermal Input} \left[ \frac{\text{kJ}}{\text{hr}} \right] = 3600 * HHV_{fuel} * \dot{M}_{Fuel}$$

Where

$HHV_{Fuel}$  is the higher heating value of the fuel [kJ/kg]

$\dot{M}_{Fuel}$  is the fuel flow rate into the boiler [kg/s]

This 65 million kilojoules per hour is the thermal energy which is not present in the recycle stream which would have been predicted to be there from our fuel moisture model. In order to account for this lost energy without changing the fuel flow rate into the boiler (and thus creating a cascade of iterations) this

thermal energy must be converted into an equivalent amount of electrical output and then debited. A thermal to electrical conversion efficiency ( $\eta_{electric}$ ), default value of 42%, is used to approximate the electrical load lost. For our example the conversion works out as follows:

$$-65,000,000 \left[ \frac{kJ}{hr} \right] \div 3600 \left[ \frac{sec}{hr} \right] = -18,000 [kW_{thermal}]$$

$$\eta_{electric} = \frac{3600}{Gross\ Heat\ Rate}$$

Given

$$Gross\ Heat\ Rate = \frac{HR_{Steam}}{\eta_{Boiler}}$$

Where

3600 is the ideal heat rate expressed in [kJ/kWh]

*Gross Heat Rate* is the heat rate of the base plant in [kJ/kWh]

$$MW_{RHEC} = -18,000 [kW_{thermal}] * \eta_{electric} = -7.6 [MW_{electirc}]$$

#### 4.5.5 ASU and CPU Heat Integration

The effect of heat integration is to reduce the steam cycle heat rate [kJ/kWh] directly through reducing the amount of boiler feed water heating which must be done with primary energy from the coal. Heat integration may be performed at the main air compressor of the ASU and/or the CO2 product compressor, which is considered part of the CPU. The combined heat integration duty [GJ/hr] of all integrated heat sources is then combined to determine the reduction in steam cycle heat rate.

The total amount of heat integration will be dependent on whether a CPU or CoCapture is used as the means for processing the carbon dioxide product.

For a CPU equipped plant:

$$HIDuty_{Total} = ASU_{HIDuty} + CPU_{HIDuty}$$

For a CoCapture plant:

$$HIDuty_{Total} = ASU_{HIDuty} + CoCap_{HIDuty}$$

Regardless of configuration, the total heat integration duty can then be used to calculate the reduction in steam cycle heat rate. The relation between heat integration and steam cycle heat rate is presented in Figure 4.12 with data derived from the DOE oxyfuel case studies (37).

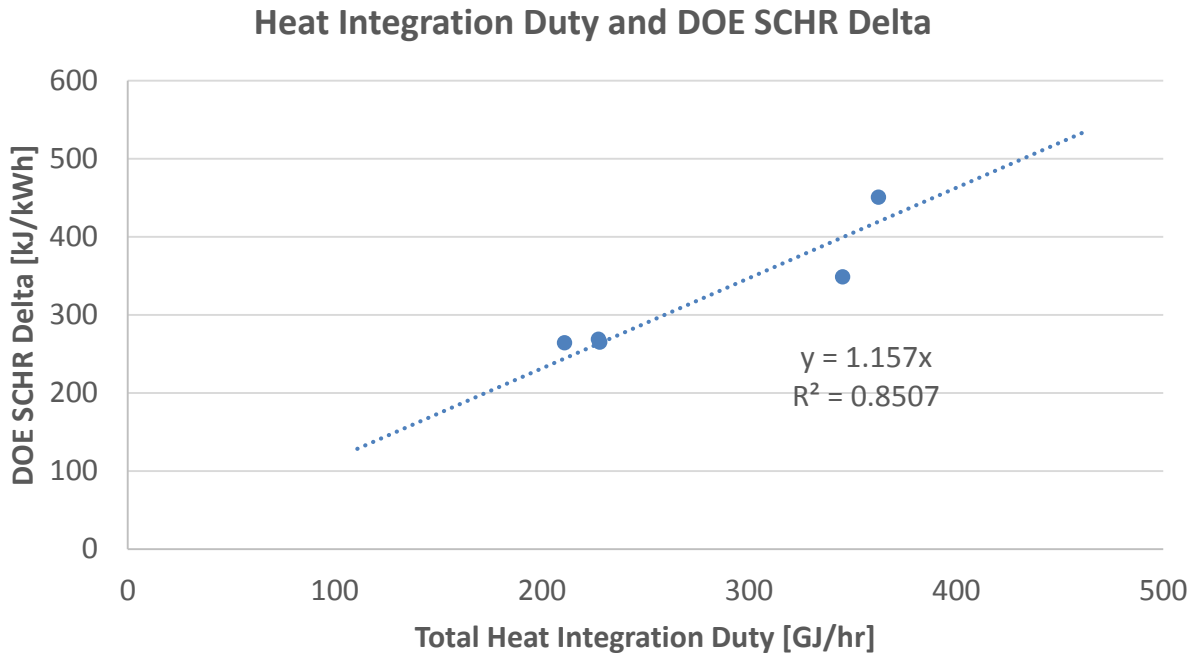


Figure 4.12 Plot of the steam cycle heat rate delta observed in the DOE cases as a function of the total reported heat integration duty.

The reduction in the steam cycle heat rate from heat integration can then be calculated:

$$HI_{SCHR} \left[ \frac{kJ}{kWh} \right] = 1.16 * HI_{Duty_{Total}} \left[ \frac{GJ}{hr} \right]$$

The problem with directly calculating the reduction in the steam cycle heat rate afforded by the heat integration is that it causes an iteration problem within the IECM. The iteration problem is a result of the base plant fuel mass flow rate (one of the initial calculations the model performs) being a function of the steam cycle heat rate. Therefore, because the heat integration duty can only be calculated after the entire plant comes to steady state, the change in steam cycle heat rate would require that the entire plant be reiterated until steady state was again reached and yet another steam cycle heat rate was calculated. This process would need to continue until the a priori steam cycle heat rate used to calculate the fuel flow rate would be equivalent to the calculated steam cycle heat rate (including heat integration). This would require more iteration than can reasonably be handled by the IECM and therefore the following simplified method will be used to approximate the effect of heat integration on the overall plant energy balance.

#### 4.5.5.1 Simplified Heat Integration Energy Credit Algorithm

This simplified methodology is based on evaluating the relative effects of heat integration on the gross electrical output of the steam turbine. The approach was to use the available DOE case studies and examine the reduction in electrical output which occurred when the steam cycle heat rates of the individual cases were substituted with the base case (S12A) super-critical steam cycle heat rate. Holding the mass flow rate of fuel into the boilers constant, the gross electrical output of each case was calculated using the base steam cycle heat rate. The delta between the original and modified gross

output for each case was the calculated and converted to exhibit the gross output percentage increase enabled by heat integration over the base steam cycle heat rate gross output. The gross output increase percentage was then plotted as a function of the extent of heat integration achieved in the combined ASU and CPU systems. This relation is presented in figure HH below and shows a split data set with the CPU equipped plants forming one grouping and the two co-capture plants comprising another at a higher extent of heat integration. For simplicity, and also because of a lack of additional data, a continuous, linear relation was assumed to be representative for both interpolation and extrapolation to other plant configurations inside the IECM.

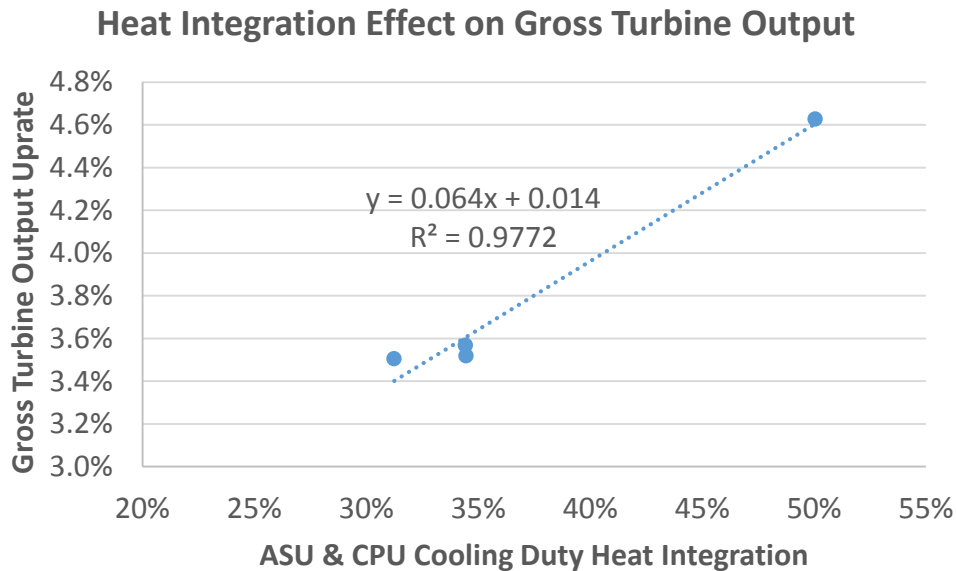


Figure 4.13 Simplified heat integration effect on gross turbine output for oxyfuel plants in the IECM. This relation allows the thermal benefits of heat integration with the ASU and CPU to be accounted for without needing to reiterate the mass balance across the entire plant.

In the final model, the impact of heat integration is calculated as an increase in electrical output produced by the turbine. It is calculated using the user specified gross electrical output of the plant and needs to be credited to the electrical balance of the plant.

$$MW_{HI} = MW_{Gross} * \left( 0.064 * \left( \frac{HIDuty_{Total}}{CoolingDuty_{Total} + HIDuty_{Total}} \right) + 0.014 \right)$$

Where

$MW_{Gross}$  is the user specified gross electrical output of the steam turbine [MW]

$HIDuty_{Total}$  is the sum of the ASU and either CPU or CoCap heat integration duty [GJ/hr]

$CoolingDuty_{Total}$  is the total sum of the bulk ASU and either CPU or CoCap cooling duty [GJ/hr]

For a CPU equipped plant:

$$CoolingDuty_{Total} \left[ \frac{GJ}{hr} \right] = ASU_{CoolingDuty} * A\dot{S}U_{Oxygen} + CPU_{CoolingDuty} * C\dot{o}mp_{CO2}$$

Or for a CoCapture equipped plant:

$$CoolingDuty_{Total} \left[ \frac{GJ}{hr} \right] = ASU_{CoolingDuty} * A\dot{S}U_{Oxygen} + CoCap_{CoolingDuty} * C\dot{o}mp_{CO2}$$

Where

$A\dot{S}U_{Oxygen}$  is the mass flow rate of oxygen produced by the air separation unit [t O2/hr]

$C\dot{o}mp_{CO2}$  is the mass flow rate of carbon dioxide in the compressed product stream [t CO2/hr]

## 4.6 Net Plant Performance

The net performance of the oxyfuel plant can be determined once the mass balance is closed and the thermal corrections have been calculated and converted to an electrical equivalent value. For a plant of arbitrary size, configuration, and fuel the procedure used to determine net performance is always the same. The first step is to find the sum of all parasitic loads. The parasitic electrical loads for the ASU, DCCPS, and CPU can be determined from the performance equations in their respective chapters, but there is one essential plant system not given a dedicated chapter.

### 4.6.1 Flue Gas Recycle Fan

The movement of flue gas through the plant is ensured through the use of flue gas fans. These fans provide the pressure increase required to overcome the various gas processing equipment head pressures. For modelling economy, the entire head pressure is assumed to be provided by a single unit. To maintain continuity across capture technologies and plant configurations in the IECM, the pre-existing Gas Fan Model has been used in the oxyfuel model. The electrical load requirement equation for this unit is as follows:

$$MW_{Fan} = 3.255 * 10^{-6} * \frac{\dot{V}_{fg} * \Delta P_{head}}{\eta_{Fan}}$$

Where:

$\dot{V}_{fg}$  flue gas flow rate [ft<sup>3</sup>/min]

$\Delta P_{head}$  total head pressure faced by the flue gas [psi]

$\eta_{Fan}$  fan efficiency [decimal], typically 0.75

Also:

$$V = 22.4 \text{ (m}^3\text{/kgmole)} \times 70,366 \text{ (lbmole/hr)} \times (\text{kg}/2.2 \text{ lb}) \times (311/298) \times (\text{hr}/60 \text{ min}) \times (\text{ft}^3/0.02832 \text{ m}^3) = 438,620 \text{ (ft}^3\text{/min)}$$

#### 4.6.2 Net Plant Electrical Output

Once the mass balance has been used to determine the electrical requirements of all the pollution control equipment and gas processing units the sum of all plant component electric loads can be determined. The two thermal corrections can also be computed and combined with the component sum in the following equation to determine net plant electrical output:

$$MW_{Net} = MW_{Gross} - \sum Components + \sum Thermal$$

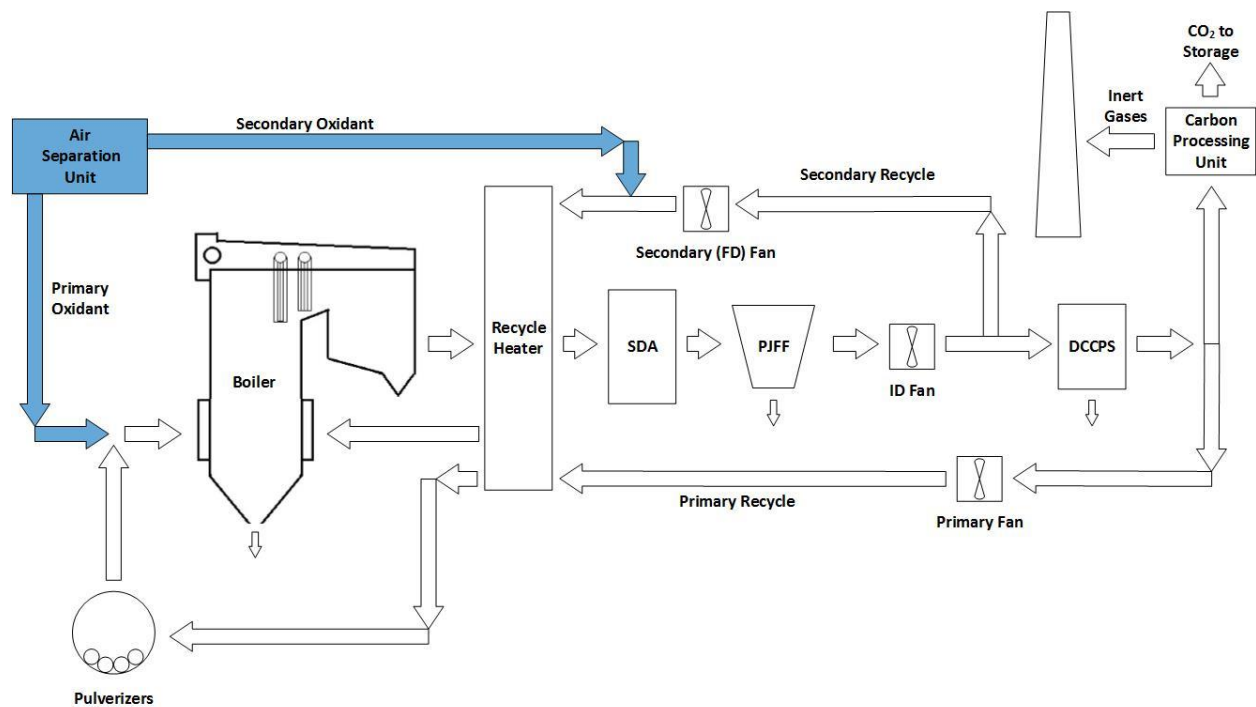
Where, for example, a low-sulfur coal utilizing a spray dry absorber, a fabric filter for TSP control, and producing a high-purity CO<sub>2</sub> product:

$$\sum Components = MW_{ASU} + MW_{SDA} + MW_{DCCPS} + MW_{Fan} + MW_{TSP} + MW_{CPU} + MW_{BasePlant}$$

And:

$$\sum Thermal = MW_{RHEC} + MW_{HI}$$

# Chapter 5 Air Separation Unit Performance Model



## 5.1 Application

The cryogenic separation of air to produce high purity oxygen is not a new idea; it has been happening commercially for roughly a century. The core principle of these systems is to pressurize atmospheric air, cool the pressurized gas, then rely on the Joule-Thompson Effect during expansion to provide the cooling required to reach cryogenic temperatures in a cold box where the constituent gases are then separated. The need for large quantities of high purity oxygen at power generation facilities is a development which has been largely driven by a desire to produce, and capture, concentrated carbon dioxide in the past few decades. Over that time period, a handful of capture technologies have been developed which would require an onsite air separation unit (ASU) to provide oxygen to support their operation. There are currently three such capture systems in the IECM which require an ASU. These include: integrated gasification combined cycle (IGCC), post-combustion chemical looping (PCCL), and oxyfuel.

Although there is some overlap in their specific demands, each of the capture technologies has different requirements for the purity and pressure at which the oxygen product needs to be delivered. Gasifiers require their oxygen to be highly pressurized (4 MPa), whereas PCCL and oxyfuel utilize a much lower pressure (<0.2 MPa) product. Each system also has performance and financial trade-offs which must be considered with respect to the purity of oxygen product utilized. The ASU's being developed to meet the specialized demands of these capture systems are novel in their capacity and ability to produce a

relatively low purity oxidant product compared to the 99%+ oxygen purity of traditional commercial ASU's for industrial gas production.

## 5.2 Modeling Approach and Development

The cryogenic separation of gases has been heavily studied and modeled. In light of this, our approach for developing an ASU model was not to develop a first principles, thermodynamic model; as many others have done previously. Rather, we decided it would be most beneficial to assemble a model which reflected the current state-of-the-art with respect to specific separation energy [kWh/tonne O<sub>2</sub>] and then handle the associated mass balance respective of the demand for oxidant. Given the interest in understanding the tradeoffs associated with oxidant purity, production capacity, and delivery pressure, it was imperative that we be able to locate quality data. Fortunately, there has been a significant amount of literature published on the performance of cryogenic air separation units for use with carbon capture systems. A summary of the publications with sufficient detail to be of use in constructing our ASU model is provided in Table 5-1. All of the published studies used in this analysis had ASU's which provided their oxidant product slightly above atmospheric pressure (~20 psi).

Table 5-1 Summary of ASU performance from recent literature

Case	Purity	Mass Flow [tonne/hr]	Specific Work [kWh/tonne O <sub>2</sub> ]
2010 IEAGHG	94.99	432.4	200.6
2007 DTI C1A1	95	319.3	231.9
2007 DTI C2A1	95	312.5	206.6
2007 DTI C3A1	95	364.1	221.6
2011 EPRI	96.5	444.9	200.3
2010 DOE S12D	94.95	489.5	193.4
2010 DOE S12E	94.95	478.8	196.8
2010 DOE S12F	94.95	481.1	196.8
2012 Cormos	95	138.7	225.0
2012 Huang Oxyfuel	95	667.9	177.3
2012 Huang 10% Air	95	601.1	179.8
2012 Huang 20% Air	95	534.3	183.0
2012 Huang 30% Air	95	467.5	187.1
2012 Huang 40% Air	95	400.8	192.6
2012 Huang 50% Air	95	334.0	200.3
2004 Dillon et al.	95	285.0	245.6
2002 Andersson & Maksinen	90	635.8	229.6
2002 Andersson & Maksinen	95	635.8	243.8
2002 Andersson & Maksinen	97	635.8	250.1

2001 Liljedahl et al.	99	371.8	257.6
2009 Amann et al.	85	271.7	221.3
2009 Amann et al.	90	255.7	239.2
2009 Amann et al.	95	241.4	260.2
2009 Amann et al.	97	236.8	268.7

Traditionally ASU's have been optimized to produce very high purity oxygen 99 [mol%] for the industrial gas market. In the past decade however, the possibility of using ASU's to produce oxidant for oxyfuel applications has engendered a move toward optimizing ASU's for per tonne of oxidant delivered efficiency rather than product purity. For this reason, we have selected studies which have been conducted with intent for use in power generation when constructing the updated model used in the IECM. Some of these studies have considered the use of an ASU capable of producing nearly 700 [tph] of oxidant. This size was deemed excessively optimistic compared to the current cold box size limitation of roughly 500 [tph] (33). Anticipating modest advancement, we have adopted a single train ASU size limit of 550 [tph] or 13,200 [tpd]. To develop a relation for the specific separation work [kWh/tonne O<sub>2</sub>] as a function of train size [tph], the 95 [mol%] oxygen purity data from literature was plotted. An exponential regression was found to best fit the specific separation work data which displays decreasing efficiency returns as the single train capacity is increased.

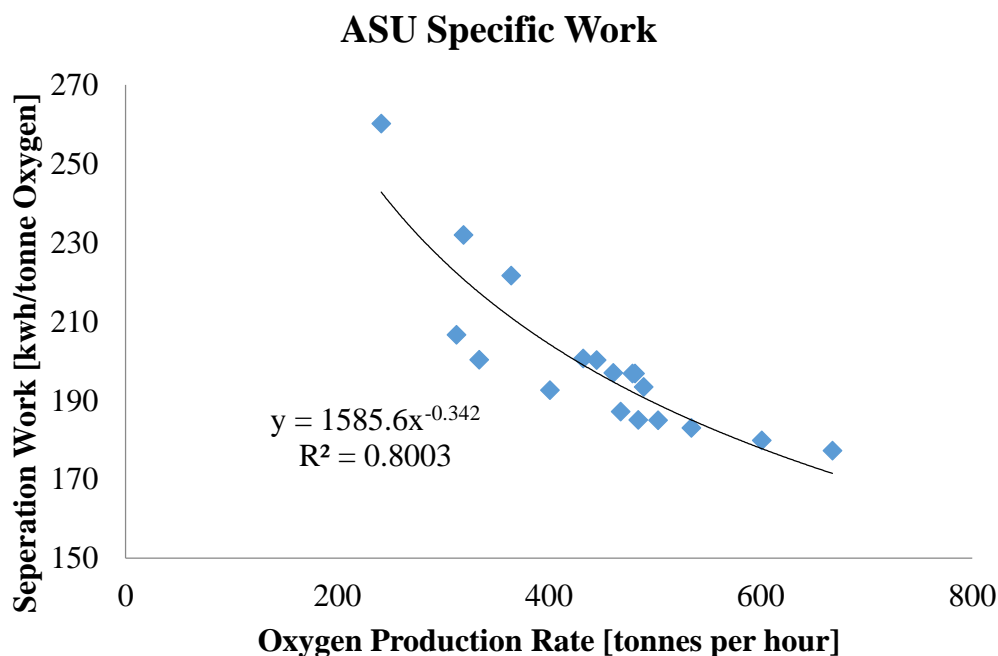


Figure 5.1 The relation between specific separation work and single train capacity is best represented with an exponential regression equation. This regression equation is used to predict the base work requirements of single train ASU's with a capacity between 200 and 550 [tph].

The traditional standard for an oxygen/oxidant stream in commercial gas production is 99.5 [mol%]. Implicit in the above specific work relation is the assumption that the purity of the oxidant produced by the ASU is a fixed value of 95 [mol%]. Determining the disparity in specific work required to produce a

tonne of oxidant at an oxygen purity of 95 [mol%] versus 99.5 [mol%] is far from straight forward due to the variation in ASU configurations available. We were fortunate to have access to a white paper (59) produced by the Praxair Corporation which provided information on the performance of their three column ASU design across oxidant purities. Table 5-2 below is a reproduction of the relative energy data from their paper along with an additional column of values which normalize the relative energy data to a 95% [mol%] oxidant purity.

**Table 5-2 Relative ASU Separation Energy across Oxidant Purity Levels**

<b>Oxygen Purity</b>	<b>Relative Energy</b>	<b>Normalized to 95 [mol%]</b>
50	0.35	0.45
60	0.5	0.65
70	0.63	0.81
80	0.7	0.90
90	0.75	0.97
95	0.775	1.00
97.5	0.79	1.02
98.1	0.87	1.12
99	0.99	1.28
99.5	1	1.29

In order to incorporate this data into our model, the relative separation energy from Praxair that was normalized to 95 [mol%] was first plotted. This can be seen in Figure 5.2 along with the two correlation equations which were used to fit the data in a piecewise fashion. The use of two correlations which coincide at a value of 97.5 [mol%] oxygen is dictated by the data, but also has solid backing from the separation of non-ideal gases. Unlike the ever increasing separation energy which would be expected as 100% separation was approached when two ideal gases are separated (basis of old IECM ASU model), there is an inflection point in the actual production of oxygen. The value of 97.5 [mol%] oxygen in the oxidant is of importance because it is the point at which all the nitrogen has boiled off and you are beginning to separate argon and oxygen. Argon and oxygen have very similar vapor pressures and boiling temperatures (90.2 and 87.3K, respectively) which makes them difficult to separate from one another cryogenically. However, this difficulty is resolved in a real separation process by adding more flash stages and having to increase the reflux rate at higher oxygen purity levels. This adds complexity and requires a larger cold box (i.e. increases capital cost) but has a fairly marginal effect of the amount of energy required as compared to the infinite increase predicted by ideal gas separation.

There is another important reason why the infinite increase in separation energy predicted by ideal gas separation is not exhibited by real systems. The assumption in ideal gas separation is that you are attempting to minimize the entropy of the two gas system by removing every last atom of gas A from gas B. In an actual cryogenic separation system, the retention rate of oxygen entering the main air compressor which ends up in the oxidant product is not 100 [mol%], but typically closer to 97.5 [mol%]. Intuitively it makes sense that at the extreme, it is easier to compress more air than it is to extract those last few atoms of oxygen from the balance of atmospheric gases in the cold box. This means that the

waste gas stream produced by an ASU optimized for oxidant production is not pure nitrogen, but if this stream is to be vented to the atmosphere it is without consequence.

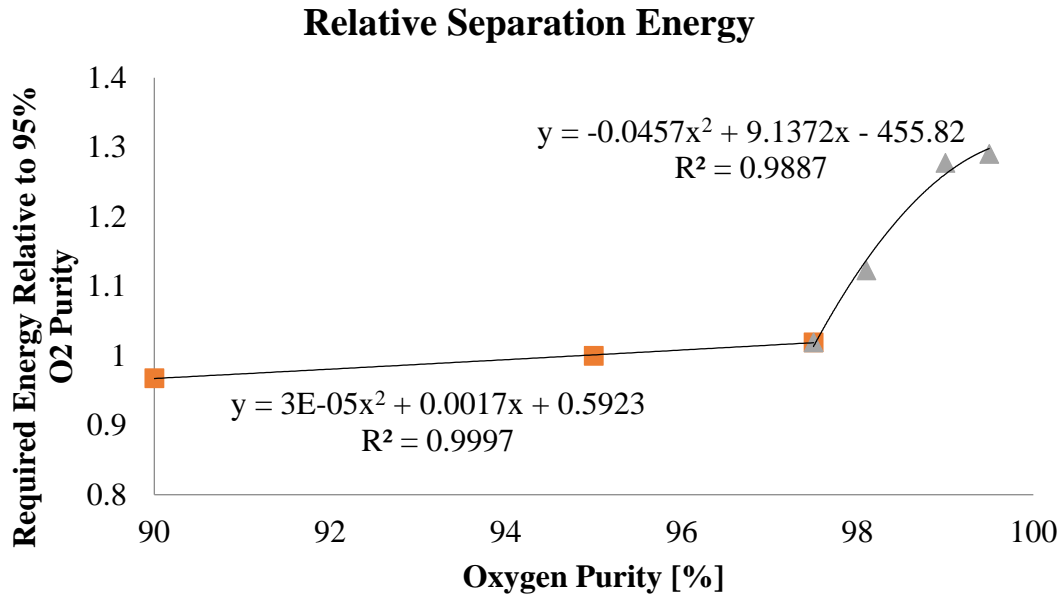


Figure 5.2 A piecewise correlation was developed for oxidant purity levels above and below the point where oxygen and argon are the two remaining atmospheric gases to be separated in the ASU. These correlation equations are used to adjust the specific work requirements to produce oxygen at a 95 [mol%] purity.

The result of incorporating this real separation system data from Praxair is that the shape of our oxidant delivery curve, as a function of purity, has changed dramatically from the previous ASU model in the IECM. In Figure 5.3 I have plotted the old ASU model along with the new ASU model for an oxyfuel plant with an oxidant demand of 400 [tph] (~450MW).

## Comparison of Oxyfuel ASU Models

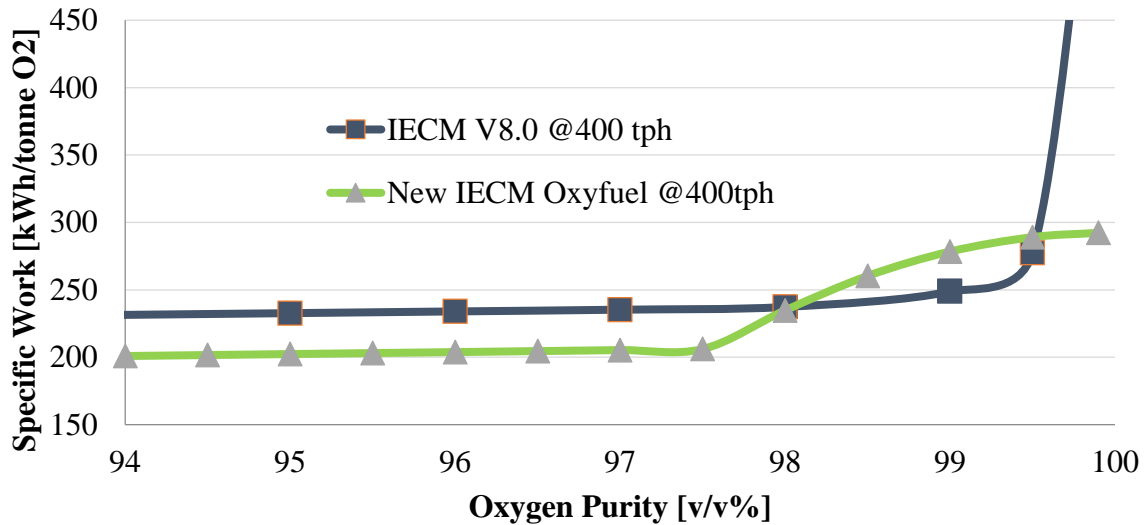


Figure 5.3 Comparison of the old and new ASU model performance across oxidant purity levels from a production rate of 400 tonnes of oxygen per hour.

There are two prominent trends which are illustrated in Figure 5.3. The first is that the ideal separation work basis for the old ASU model is starkly different than the new model. The old model has a very shallow slope from 95 to 99.5 [mol%] and then increases dramatically as the purity approaches 100 [mol%]. The new model increases gradually from 94 to 97.5 [mol%] and then the transition to argon separation results in a quick increase in specific work that plateaus as purity approaches 100%. The second major trend is that for purity levels below 98 [mol%] the specific separation work predicted by the new ASU model is roughly 40 [kWh/tonne O<sub>2</sub>] below the old ASU model. This disparity is a result of the advancements which have made technologically since the old ASU model was constructed. As the focus of ASU design has shifted from producing high-purity oxygen for industrial gases to large quantities of oxidant for power production, specific work requirements have fallen as a result of the refrigeration cycles within the ASU being optimized.

## 5.3 Summary of Input and Output Parameters

### Input Parameters

The key input parameters defining the performance of the ASU are as follows:

*User Specified*

*ORF*                                      Mass percentage of oxygen entering MAC entrained in oxidant [mass fraction]

*η<sub>Iisentropic</sub>*                                Isentropic efficiency of the oxidant compressor [decimal]

$HI_{ASU}$	Fraction of cooling duty which can be recovered in the steam cycle through BFW heating, Min = 0.0, Max = 1.0, Default = 0.0 (0.4 representative)
$\Delta T_{Water\_Max}$	Maximum allowable temperature increase of the cooling water [K]
<i>Passed from IECM</i>	
$\dot{A}SU_{Oxygen}$	Mass flow rate of oxygen to the boiler from the ASU [kg/hr]
$AAH$	Average ambient air humidity level [kg H2O/kg dry air]

### Output Parameters

The model will then calculate or report the following key output parameters:

$\dot{W}ater_{MAC\ Produced}$	Water produced by the main air compressor for the ASU [kg/hr]
$\dot{M}_{Vent}$	Mass flow rate of gases leaving the ASU vent stream [kg/hr]
$\dot{A}SU_{Oxidant}$	Mass flow rate of gases leaving the ASU in the oxidant stream [kg/hr]
$ASU_{CoolingDuty}$	Cooling duty of ASU in [GJ/tonne O2]
$\dot{A}SU_{Cooling\ Water}$	Mass flow rate of cooling water required for the ASU [kg/hr]
$ASU_{HIDuty}$	Heat integration duty from ASU in [GJ/hr]
$MW_{ASU}$	Electrical load required to power the air separation unit [MW]
$MW_{OxComp}$	Electrical load required to power the oxidant compressor (optional) [MW]

## 5.4 Mass and Energy Balance Calculations

The following sections run through the mass and energy accounting of all the streams highlighted in Figure 5.4. The cooling water in and out streams are representative of the bulk cooling duty which must be performed, but this cooling could be handled either by boiler feed water heating or through the use of cooling water from the base plant.

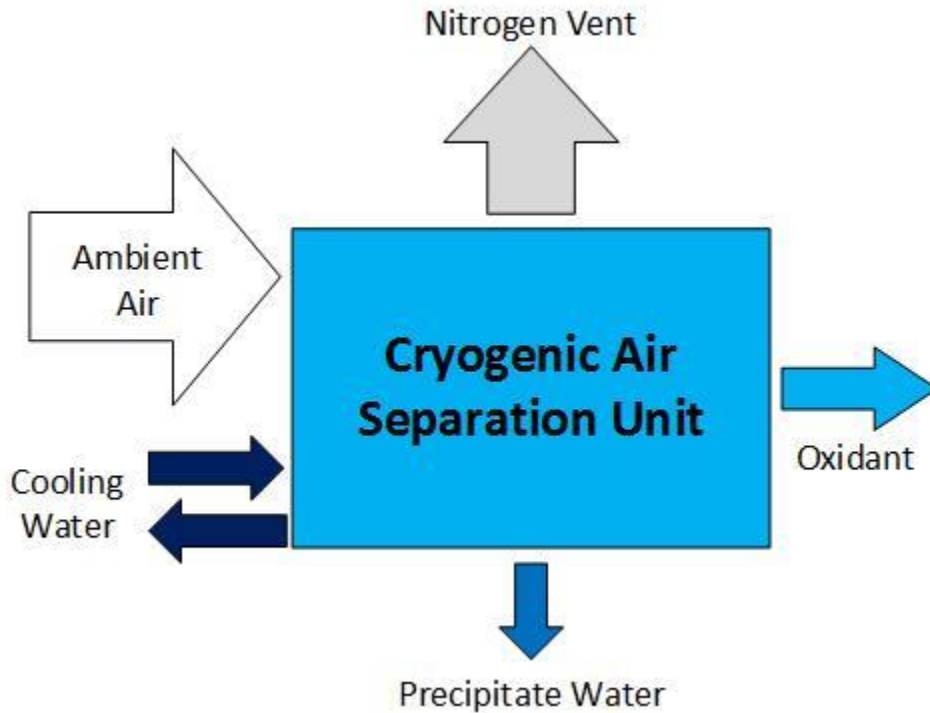


Figure 5.4 Process flow diagram of all the gas and liquid streams entering and exiting the air separation unit.

#### 5.4.1 Oxidant Production

The amount of oxidant required is calculated during the overall plant mass balance of whichever carbon capture technology is utilizing the ASU. The ASU model is provided a demand for oxidant production which must be met. For additional detail in how this demand is calculated for the oxyfuel model please see Section 4.4.4.

#### 5.4.2 Water Production from Compression

Once the required oxygen mass flow rate has been calculated by the overall plant mass balance algorithm, the amount of water produced by the main air compressor for the ASU can be calculated. By applying a 97.5% oxygen retention factor (ORF) (36) to our required oxygen mass flow rate we can calculate the oxygen flow rate that needs to enter the main air compressor (MAC). Using the ambient air conditions provided in the IECM, along with our calculated MAC oxygen flow rate, the mass flow rate of dry air through the MAC can be calculated. Because the ambient air conditions are not perfectly dry air, the humidity present will be precipitated out during the compression process. Dry air is assumed to be 23.2% oxygen, 1.3% argon, and 75.5% nitrogen by mass.

$$\dot{M}AC_{Dry\ Air} \left[ \frac{kg}{hr} \right] = \frac{ASU_{Oxygen} / ORF}{0.232}$$

Where:

$ASU_{Oxygen}$	Mass flow rate of oxygen to the boiler from the ASU [kg/hr]
$ORF$	Mass percentage of oxygen entering MAC entrained in oxidant [mass fraction]
$\dot{M}AC_{Dry\ Air}$	Mass flow rate of dry air compressed by MAC to meet oxygen demand [kg/hr]

Using the Ambient Air Humidity [kg H<sub>2</sub>O/kg dry air] the amount of water precipitated out by the MAC can then be calculated.

$$\dot{W}ater_{MAC\ Produced} \left[ \frac{kg}{hr} \right] = AAH * \dot{M}AC_{Dry\ Air}$$

Where:

$\dot{W}ater_{MAC\ Produced}$	Mass flow rate of water precipitated out of ambient air by the MAC [kg/hr]
$AAH$	Average ambient air humidity level [kg H <sub>2</sub> O/kg dry air]
$\dot{M}AC_{Dry\ Air}$	Mass flow rate of dry air compressed by MAC to meet oxygen demand [kg/hr]

### 5.4.3 Nitrogen Vent Stream and Oxidant Balance

The remaining mixture of atmospheric gases split off when the oxidant product is formed is vented from the cold box to the atmosphere. This stream is composed almost entirely of nitrogen, but may contain argon and oxygen depending on the specified retention factor for the ASU. The mass flow of gases in the vent stream can be calculated in the following manner where dry air is assumed to be 23.2% oxygen, 1.3% argon, and 75.5% nitrogen by mass.

The mass flow of oxygen in the vent stream:

$$\dot{V}ent_{Oxygen} \left[ \frac{kg}{hr} \right] = \dot{M}AC_{Dry\ Air} * (1 - ORF) * 0.232$$

Where:

$\dot{M}AC_{Dry\ Air}$	Mass flow rate of dry air compressed by MAC to meet oxygen demand [kg/hr]
$ORF$	Mass percentage of oxygen entering MAC entrained in oxidant [mass fraction]

The mass flow of nitrogen and argon is complicated by the variable composition of the oxidant produced by the ASU. For the following equations I use the mass fraction of these gases in the oxidant as variables, but please note that they are functions of the user selected oxidant composition.

The mass flow of argon in the oxidant stream:

$$Oxidant_{Argon} \left[ \frac{kg}{hr} \right] = \left( \frac{y_{Ox,Argon}}{y_{Ox,Oxygen}} \right) * ASU_{Oxygen}$$

Where:

$ASU_{Oxygen}$  Mass flow rate of oxygen to the boiler from the ASU [kg/hr]

$y_{Ox,Argon}$  is the mass fraction of argon in the oxidant product

$y_{Ox,Oxygen}$  is the mass fraction of oxygen in the oxidant product

The mass flow of nitrogen in the oxidant stream may be calculated in an analogous fashion:

$$Oxidant_{Nitrogen} \left[ \frac{kg}{hr} \right] = \left( \frac{y_{Ox,Nitrogen}}{y_{Ox,Oxygen}} \right) * ASU_{Oxygen}$$

Where:

$y_{Ox,Nitrogen}$  is the mass fraction of nitrogen in the oxidant product

The total mass flow rate of the oxidant stream may then be calculated:

$$ASU_{Oxidant} \left[ \frac{kg}{hr} \right] = ASU_{Oxygen} + Oxidant_{Nitrogen} + Oxidant_{Argon}$$

It follows then that the quantity of argon and nitrogen found in the vent stream must be equal to the mass flow rate of each which entered the ASU through the main air compressor, less what was entrained in the oxidant.

For argon:

$$Vent_{Argon} \left[ \frac{kg}{hr} \right] = (\dot{M}AC_{Dry Air} * 0.013) - Oxidant_{Argon}$$

For nitrogen:

$$Vent_{Nitrogen} \left[ \frac{kg}{hr} \right] = (\dot{M}AC_{Dry Air} * 0.755) - Oxidant_{Nitrogen}$$

Lastly, the mass flow of gases in the vent stream is:

$$\dot{M}_{vent} \left[ \frac{kg}{hr} \right] = \dot{V}_{ent_{Argon}} + \dot{V}_{ent_{Nitrogen}} + \dot{V}_{ent_{Oxygen}}$$

#### 5.4.4 Cooling and Heat Integration

The refrigeration load of the ASU is generated through the use of a large, intercooled air compressor which compresses and cools the incoming air with gas-to-liquid heat exchangers. A large amount of heat is generated during compression which must either be removed by the plant's cooling water system or by preheating boiler feed water through heat integration. Table 5-3 below presents values from several case studies in the DOE Oxyfuel Report (37) along with many of the calculations used to formulate the cooling relations for the new ASU model.

Table 5-3 ASU Cooling Duty Information from DOE Oxyfuel Report

	Case Studies from 2010 DOE Oxyfuel Report						
	S12C	S12D	S12E	S12F	L12F	S13F	L13F
ASU Cold Box Pre-Cooling [GJ/hr]	156	181.9	178	178.8	186	171.3	179.1
ASU BFW Enthalpy In [kJ/kg]	217.35	217.35	217.35	217.35	217.35	238.79	238.98
ASU BFW Enthalpy Out [kJ/kg]	591.45	591.45	591.45	591.45	591.45	590.93	590.93
ASU BFW Enthalpy Delta [kJ/kg]	374.1	374.1	374.1	374.1	374.1	352.14	351.95
ASU BFW Flow [kg/hr]	429,930	379,337	371,049	372,847	327,893	379,301	388,345
ASU BFW Duty [GJ/hr]	161	142	139	139	123	134	137
ASU Oxygen Flow [kg/hr]	481,647	489,547	478,852	481,191	503,007	460,773	484,169
Specific (BFW) ASU Cooling Duty [GJ/tO2]	0.334	0.290	0.290	0.290	0.244	0.290	0.282
Total Specific ASU Cooling Duty [GJ/tO2]	0.658	0.661	0.662	0.661	0.614	0.662	0.652
ASU Heat Integration [% Cooling Duty Recovered]	51%	44%	44%	44%	40%	44%	43%

##### 5.4.4.1 Cooling Duty

The following relation may be used to calculate the required specific cooling load of the ASU in units of [GJ/tonne O2]:

$$ASU_{CoolingDuty} \left[ \frac{GJ}{tO2} \right] = 0.65 * (1 - HI_{ASU})$$

Where:

$HI_{ASU}$  is the fraction of cooling duty which can be recovered in the steam cycle through BFW heating, Min = 0.0, Max = 1.0, Default = 0.0 (0.4 representative)

##### 5.4.4.2 Cooling Water Requirements

In the IECM, the cooling water requirements are handled on a plant wide basis. However, the following closely approximates the process used for calculating the required cooling water mass flow rate. For a

given maximum temperature rise allowed in the cooling water and an average heat capacity for water of 4.2 [kJ/kg-K]; a cooling water flow rate can be calculated:

$$A\dot{S}U_{Cooling\ Water} \left[ \frac{kg}{hr} \right] = A\dot{S}U_{Oxygen} * ASU_{CoolingDuty} \div (SH_{Water} * \Delta T_{Water\_Max})$$

Where:

$A\dot{S}U_{Cooling\ Water}$	Mass flow rate of cooling water required for the ASU [kg/hr]
$A\dot{S}U_{Oxygen}$	Mass flow rate of oxygen to the boiler from the ASU [kg/hr]
$ASU_{CoolingDuty}$	Required specific cooling duty for the ASU [kJ/kg O <sub>2</sub> ]
$SH_{Water}$	Average specific heat of cooling water [kJ/kg-K]
$\Delta T_{Water\_Max}$	Maximum allowable temperature increase of the cooling water [K]

#### 5.4.4.3 Heat Integration

The heat integration duty of the air separation unit may then be calculated:

$$ASU_{HIDuty} \left[ \frac{GJ}{hr} \right] = \left\{ 0.65 * (HI_{ASU}) \left[ \frac{GJ}{tO_2} \right] \right\} * A\dot{S}U_{Oxygen} \left[ \frac{tO_2}{hr} \right]$$

Where:

$HI_{ASU}$	is the fraction of cooling duty which can be recovered in the steam cycle through BFW heating, Min = 0.0, Max = 0.6, Default = 0.0 (0.4 representative)
$A\dot{S}U_{Oxygen}$	is the iteratively calculated flow rate of oxygen from the ASU [tonnes/hr]

The heat integration duty of the ASU is added to the chosen carbon handling systems' to provide the total heat integration duty of the oxyfuel plant. Details on calculating the effects on performance from heat integration can be found in Section 4.5.5 in the overall mass and energy balance plant details.

#### 5.4.5 Electrical Load Requirement

Calculating the amount of electrical power consumed by the air separation unit may require the total oxygen demand ( $A\dot{S}U_{Oxygen}$ ) to be split into multiple trains if the demanded mass flow rate exceeds the maximum single train capacity. When the oxygen demand exceeds the limit of 550 [tph] the demand is simply distributed evenly across however many trains are required to simultaneously meet demand and not violate the train size limit. With that having been established, the base (95 [mol%] oxygen) single train specific separation work may be calculated:

$$SW_{95\%} \left[ \frac{kWh}{tonne\ O_2} \right] = 1585.6 * OPR_{SingleTrain}^{-0.342}$$

Where:

$OPR_{SingleTrain}$  is the oxygen production rate of a single train,  $200 < [\text{tonnes } O_2/\text{hr}] < 550$

The base specific work equation is then modified according to the purity of the oxidant desired. This is done with two separate correlations: one fit to purity levels below 97.5%  $O_2$  and the other for oxidant purity levels above 97.5%. This adjustment to the base specific work is called the specific work multiplier (SWM).

For oxidant purity equal to or below 97.5 [mol%] oxygen:

$$SWM_{\leq 97.5\%} = (3.0 * 10^{-5} * OP^2 + 1.7 * 10^{-3} * OP + 0.5923)/1.02455$$

Where:

$OP$  is the purity of the oxidant produced by the ASU [ $O_2$  mol%]

For oxidant purity greater than 97.5 [mol%] oxygen:

$$SWM_{>97.5\%} = (-0.0457 * OP^2 + 9.1372 * OP - 455.82)/0.62318$$

The electrical requirement for a single train can then be calculated:

$$MW_{SingleTrain} = OPR_{SingleTrain} * SWM * SW_{95\%}$$

The electrical requirement for the ASU can then be calculated:

$$MW_{ASU} = MW_{SingleTrain} * ASU_{Trains}$$

Where:

$ASU_{Trains}$  is the number of single trains required to meet the total oxygen demand

#### 5.4.6 Oxidant Compressor Electrical Load Requirement

The base air separation unit in the IECM is assumed to produce the specified oxidant product at a pressure of 140 [kPa]. This pressure is sufficient for use with oxyfuel or delivery to the calciner in a post-combustion chemical looping system. However, the elevated pressure inside the gasifier unit of an IGCC plant requires that the oxidant be compressed. The typical pressure required for IGCC ASU units in the IECM is 4 [MPa]. There is a considerable amount of compression work, in the form of additional electric load, which needs to be accounted for to deliver oxidant at elevated pressure. The following is how this compression work is accounted for:

Assuming ideal gas behavior, the ideal, specific steady-flow work of the compressor is:

$$\omega_{OxComp\_Ideal} \left[ \frac{kJ}{kg} \right] = \frac{RT}{mw_{Ox}} * \ln \frac{P_{exit}}{P_{enter}}$$

Where:

$R$  is the universal gas constant, 8.314 [kJ/kmol K]

$T$  is the isothermal temperature of compression [Kelvin]

$mw_{Ox}$  is the molecular weight of the oxidant leaving the ASU [kg/kmol]

$P_{exit}$  is the desired exit pressure of the oxidant leaving the compressor [kPa]

$P_{enter}$  is the oxidant pressure entering the compressor from the ASU [kPa]

The ideal, specific compressor work is then modified using the specified isentropic efficiency:

$$\omega_{OxComp} \left[ \frac{kJ}{kg} \right] = \frac{\omega_{OxComp\_Ideal}}{\eta_{Isentropic}}$$

Where:

$\eta_{Isentropic}$  is the isentropic efficiency of the oxidant compressor [decimal]

The added electrical load of compressing the oxidant is then:

$$MW_{OxComp} = \frac{\omega_{OxComp} * A\dot{S}U_{Oxidant}}{1000}$$

Where:

$A\dot{S}U_{Oxidant}$  is the mass flow rate of oxidant through the compressor [kg/sec]



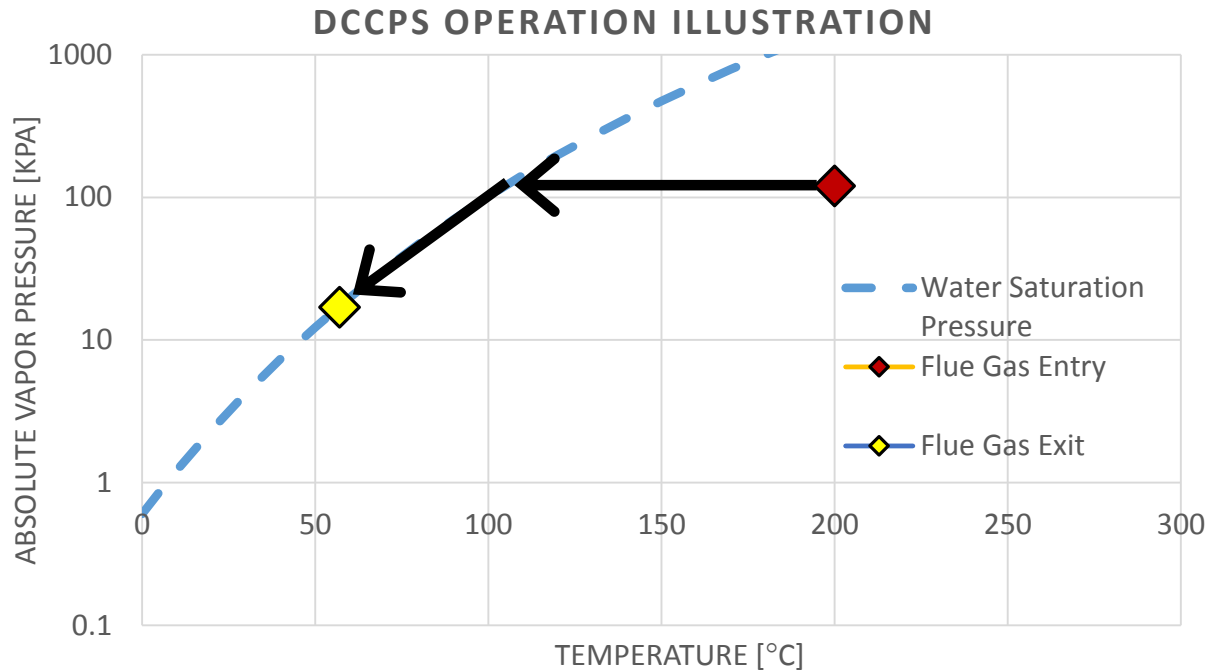


Figure 6.1 Illustration of the physical working process utilized in the direct contact cooler polishing scrubber.

Trace sulfur removal can be performed simultaneously via a chemical process by adding sodium hydroxide (commonly referred to as caustic soda) which reacts with the residual sulfur dioxide in the flue gas to form sodium sulfite. This combination of a chemical and physical process allows DCCPS systems to accomplish their three tasks of bulk flue gas cooling, trace sulfur removal, and water concentration reduction in the exiting gas stream.

## 6.2 Oxyfuel Application

The current generation of oxyfuel systems require the use of flue gas recirculation (FGR) to moderate temperature inside the boiler and to ensure that the heat transfer mechanisms are maintained closely to the air-fired conditions for which today's boilers were designed. To that end, the flue gas which is recycled to the boiler must have an acceptable temperature and water concentration to ensure proper thermal regulation and to allow uninterrupted performance of the downstream traditional pollution control equipment. This last consideration is especially important for oxyfuel systems utilizing either a sub-bituminous or lignite coal with a high moisture content. Such coal types typically have a low enough sulfur content to permit the use of a spray-dry absorption system for sulfur removal in lieu of a wet system. This is beneficial for plant heat rate. However, a direct contact cooler must then be used to reduce FGR water content to ensure that a sufficient approach temperature is maintained so that the SDA may continue to function at the desired level of sulfur removal.

## 6.3 Modelling Approach

The direct contact cooler and polishing scrubber model uses or calculates the nine inlet and outlet streams depicted in Figure 6-2. These process flow streams are delineated for ease of mass and energy accounting and calculation but are not necessarily reflective of real-world DCCPS operation. The entering flue gas stream is passed to the model from the IECM fully defined: meaning that the stream is fully defined with composition, temperature, and pressure data along with the mass flow rate. There are then two main parameters which need to be specified prior to the first calculation for cooling and condensing: an anticipated pressure drop across the contacting column and either a desired exit temperature for the flue gas exiting the DCCPS or a desired water concentration in the exiting flue gas. If sulfur polishing is desired, the concentration of sulfur dioxide exiting the DCCPS must also be specified in units of parts per million.

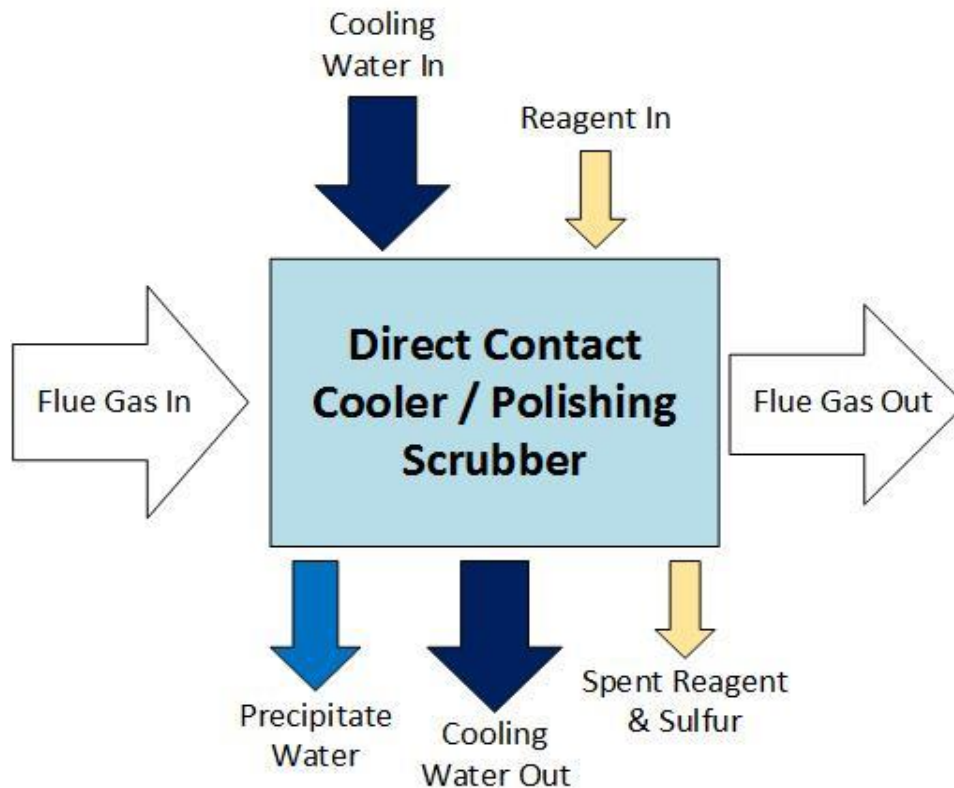


Figure 6.2 Block flow diagram representing the stream flows accounted for in the direct contact cooler and polishing scrubber model.

The model then steps through a series of calculations involving the saturation pressure curve of water to determine the non-specified value of either exit flue gas temperature or exit water concentration in the flue gas. From there, the model calculates the mass balance of all streams in the model along with the composition of gases, liquids, and/or solids in each stream. The energy balance is then completed in a two-step calculation process. First, changes in latent and sensible heat for each stream are calculated using a combination of the Shomate relations, heat capacity data, and the latent heat of condensation

model (Section 3.7.1.2). Secondly, the amount of cooling load required to offset the total latent and sensible heat increase is calculated treating the DCCPS as an adiabatic heat exchanger. Lastly, the amount of cooling water can be calculated from the required cooling load and reported along with the rest of the fully defined process flow streams.

There were a number of simplifying assumptions made in the creation of this model. Specifically, the separate reagent and cooling water inlet streams would in practice be a premixed solution entering the top of the contacting column. Similarly, the cooling water out, precipitate water, and spent reagent streams would in practice be a single admixture at the bottom of the contacting column. Furthermore, many studies involving a DCCPS of the size required for a coal plant equipped with carbon capture (26) (60) have indicated that it is desirable from both a cost and simplicity standpoint to construct a dedicated cooling system and water handling services for the contacting tower(s). This is in part due to the issues previously raised about the reagent stream and cooling water being combined in practice. Thus having a dedicated system to handle the caustic-doped water and precipitated solids (sodium sulfite) would be desirable. There are also balance of plant and layout considerations from the volume of cooling water required which bolster the case for a dedicated cooling water system.

Treating the DCCPS system as an adiabatic heat exchanger for purposes of calculating the heat balance is another simplification. Weather conditions (including ambient water and air temperature, and associated maximum cooling water delta) will affect the quantity of cooling water required and associated parasitic load of pumping and processing that cooling water. However, absent very detailed weather data, anticipating the effect of the weather is beyond the capabilities of this analysis. Instead, a heat transfer efficiency factor  $\alpha_{Cooling}$  has been provided to allow the user to enter what amounts to a cooling water safety factor into an analysis to account for non-adiabatic conditions.

## 6.4 Saturation Pressure of Water

The maximum concentration of water vapor which can be contained in a gas mixture is a function of the gas temperature and pressure. This relationship is illustrated by the water vapor saturation pressure curve presented in Figure 6.3. There are numerous scientific methods for describing the relationship between vapor pressure and temperature for pure components. For this work we have chosen to use the Antoine Equation, which is derived from the Clausius-Clapeyron relation.

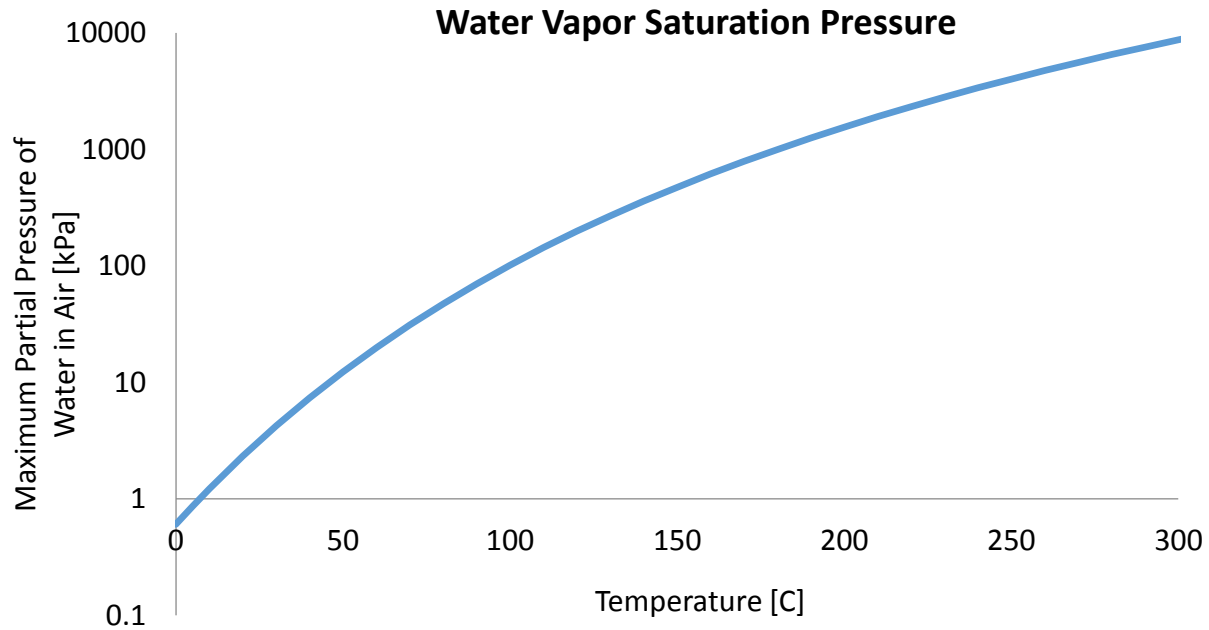


Figure 6.3 Saturation pressure of water vapor in air as a function of temperature between 0 and 300 degrees centigrade.

The units of pressure of the Antoine coefficients (A, B, and C) are reported in millimeters of mercury [mmHG]. A conversion factor ( $\gamma$ ) allows for the Antoine equation to report pressures in units of kilopascals rather than millimeters of mercury using the relation.

$$\gamma = 0.133322368$$

$$P_{saturation} = p_{H_2O} = 10^{\left[A - \frac{B}{(C + T)}\right]}$$

The Antoine equation reports a saturation pressure which is here interpreted as the maximum partial pressure of water vapor in the flue gas mixture. The partial pressure of any given component of a gas mixture can be calculated directly given the total pressure of the gas stream and the molar fraction using Dalton's Law of Partial Pressures.

## 6.5 Latent Heat of Water Condensation

A reduction in the concentration of water in the flue gas is accomplished by causing the water vapor to change phase and condense out as liquid water. The amount of heat required to cause a liquid to vaporize is known as the latent heat of vaporization (LHOV). The latent heat of condensation (LHOC) is equivalent in magnitude to the (LHOV) for a pure component, but of the opposite sign. In the case of water vapor in the DCCPS, we are concerned with the amount of heat which must be removed in order to induce a change of phase from vapor to liquid. The LHOC is temperature dependent for water. More specifically, the LHOC of water displays a gradual decline in magnitude as temperature is increased (Fig. 6.4). However, as the triple point is approached, the LHOC rapidly converges toward zero.

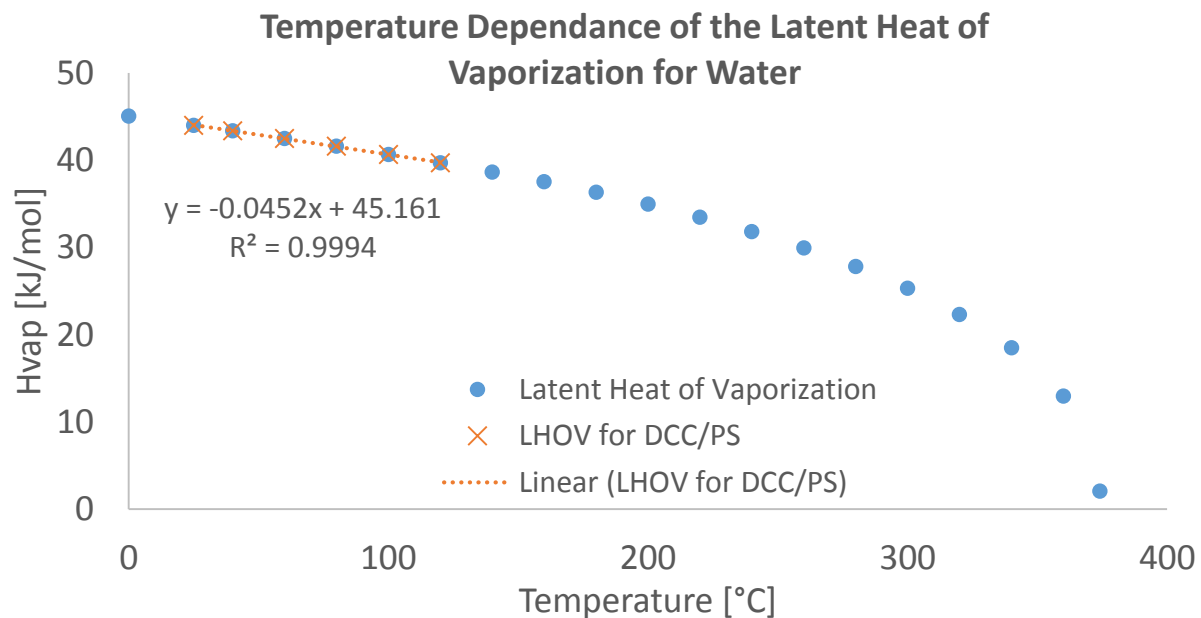


Figure 6.4 The latent heat of vaporization of water is temperature dependent. The decline in LHOV magnitude is very linear over the temperature window expected during operation of the DCCPS

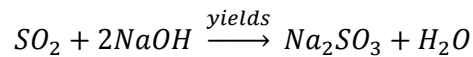
Flue gas temperatures entering the DCCPS rarely exceed 170°C and the temperature zone where water condensation occurs from these entry conditions will typically be below 120°C. This operational temperature window allows us to simplify the LHOV relation of water to the linear region. A linear regression taken from 20 - 120°C provides a nearly perfect fit ( $R^2 > 0.99$ ) over our condensation regime.

$$\text{Latent Heat of Condensation} \left[ \frac{\text{kJ}}{\text{mol}} \right] = -45.161 + 0.0452 * T_{\text{Condensation}}$$

In practice, the phase change to liquid water would not occur at a single temperature, but across a range defined by the interplay between maximum partial pressure and temperature. In our model we use a mean temperature for  $T_{\text{Condensation}}$  in the above equation for calculating the LHOC for water. This mean temperature is the average between the DCCPS exit temperature ( $T_{\text{sat\_exit}}$ ) and the temperature at which the inlet flue gas first encounters the water vapor saturation curve during cooling ( $T_{\text{sat\_enter}}$ ).

## 6.6 Sulfur Removal Calculation

Deep sulfur scrubbing with sodium hydroxide (NaOH) can be enabled as a concurrent process to flue gas cooling in the updated DCCPS model. The amount of sodium hydroxide, also referred to as caustic soda or caustic, required for polishing is determined on a strictly mass balance basis according to the mass of sulfur to be removed from the flue gas. The kinetics are assumed to be sufficiently fast as to not preempt the completion of the following reaction:



The heat of reaction from the formation of solid sodium sulfite ( $Na_2SO_3$ ) and water is also neglected in determining the required cooling load of the DCCPS unit. However, the water formed has been assumed to be in the gaseous state and is therefore accounted for in the latent heat removal.

A desired exiting sulfur concentration, in parts per million (ppm), may be specified when using the DCCPS model. This volumetric concentration, along with the entering flue gas composition, is then used to determine the mass of sulfur which must be removed from the flue gas stream per unit time. Because the quantity of sulfur in the DCCPS exit stream is much less than the total quantity of gas in the exit stream, the number of sulfur moles can be calculated with sufficient accuracy based upon the balance of gas moles in the exit stream.

## 6.7 Summary of Input and Output Parameters

### Input Parameters

The key input parameters defining the performance of the DCCPS are as follows:

$\dot{M}_{fg\_enter}$	Mass flow rate of flue gas entering the contacting tower [kgmol/hr]
$x_{i,fg\_enter}$	Mole fraction of all species (i) in the entering flue gas
$P_{fg\_enter}$	Absolute pressure [kPa] of the entering flue gas
$P_{drop\_DCCPS}$	Absolute pressure drop across the contacting tower [kPa]
$x_{SO_2,fg\_exit}$	Molar concentration of sulfur dioxide in exiting flue gas [ppm]
$PMC$	Moisture content in the sodium sulfite slurry [mass fraction]
$\alpha_{cooling}$	Heat transfer efficiency of the DCCPS system (unity being ideal heat transfer)
$\Delta T_{max,cooling\ water}$	Largest acceptable cooling water temperature increase [ $^{\circ}C$ ]

*Additionally, one of the following two parameters must be specified about the exit flue gas stream:*

$T_{fg\_exit}$	Temperature of exiting flue gas [ $^{\circ}C$ ]
----------------	---

$x_{H2O,fg\_exit}$  Mole fraction of water vapor in exiting flue gas

### Output Parameters

The model will then calculate or report the following key output parameters:

$\dot{M}_{fg\_exit}$	Mass flow rate of flue gas exiting the contacting tower [kgmol/hr]
$x_{i,fg\_exit}$	Mole fraction of all species (i) in the exiting flue gas
$P_{fg\_exit}$	Absolute pressure [kPa] of the exiting flue gas
$T_{fg\_exit}$	Temperature of exiting flue gas [°C]
$\varphi_{H2O\_Condensed}$	Molar flow rate of water condensed out of flue gas [mol/sec]
$\varphi_{Na2SO3,precipitant}$	Molar flow rate of sodium sulfite produced from sulfur treatment [mol/sec]
$\varphi_{H2O,precipitant}$	Molar flow rate of water produced for sulfur treatment [mol/sec]
$\dot{M}_{NaOH}$	Mass flow rate of sodium hydroxide required for sulfur treatment [kg/sec]
$\dot{M}_{Slurry}$	Mass flow rate of sodium sulfite slurry produced by sulfur treatment [kg/sec]
$Cooling\ Load_{total}$	Total cooling load requirement of DCCPS [kJ/sec]
$\dot{M}_{Cooling\ water}$	Mass flow rate of cooling water required for DCCPS cooling [kg/sec]
$\dot{M}_{water\_generated}$	Mass flow rate of water generated during DCCPS operation [kg/sec]

## 6.8 Mass and Energy Balance Calculations

The DCCPS model has been designed so that either a desired water concentration of the exiting flue gas or a desired exiting flue gas temperature may be specified by the user. These two variables are co-dependent and cannot be specified independently. Regardless of starting information, the Antoine Equation is then utilized to determine either the exit concentration or exit temperature of the flue gas leaving the DCCPS.

Table 6-1. The constants used in the Antoine Equation are temperature dependent across the range of expected operation of the DCCPS.

Antoine Constants for Water [°C and mmHG]		
	1 – 100 °C	99 – 374 °C
A	8.07131	8.14019
B	1730.63	1810.94
C	233.426	244.485

Starting equations given: fully defined inlet (pressure, temperature, composition, mass flow rate), pressure drop across DCCPS, and desired flue gas exit composition.

$$p_{H_2O,fg\_exit} = x_{H_2O,fg\_exit} * (P_{fg\_enter} - P_{drop\_DCCPS})$$

$$T_{fg\_exit} = T_{sat\_exit} = \frac{B}{A - (\log_{10}(p_{H_2O,fg\_exit}/\gamma))} - C$$

Starting equations given: fully defined inlet, pressure drop across DCCPS, desired flue gas exit temperature.

$$p_{H_2O,fg\_exit} = \gamma \left[ 10^{\left( A - \frac{B}{(C + T_{fg\_exit})} \right)} \right]$$

$$x_{H_2O,fg\_exit} = \frac{p_{H_2O,fg\_exit}}{(P_{fg\_enter} - P_{drop\_DCCPS})}$$

Once one of the above sequences has been followed, the temperature at which the incoming flue gas reaches the water vapor saturation curve during cooling must be calculated:

$$T_{sat\_enter} = \frac{B}{A - (\log_{10}(p_{H_2O,fg\_enter}/\gamma))} - C$$

### 6.8.1 Gas Stream Flow Rate Calculations

At this point, the temperature, pressure, and composition of the flue gas has been either calculated or specified at the three important states of the DCCPS. The mass flows through the system must now be balanced:

Inlet stream needs to be in [mol/sec] for each compound. This conversion can be accomplished utilizing the following if total mass flow is in [kgmol/hr]:

$$\varphi_{i,fg\_enter} = x_{i,fg\_enter} * \frac{\dot{M}_{fg\_enter}}{3.6}$$

Where:

$\varphi_{i,fg\_enter}$  is the molar flow rate [mol/sec] of species i in the entering flue gas

$x_{i,fg\_enter}$  is the mole fraction of species (i) in the entering flue gas

$\dot{M}_{fg\_enter}$  is the total mass flow rate [kgmol/hr] of flue gas into the DCCPS

The flue gas exit molar flow rate can then be calculated using the below for all gaseous species other than water and sulfur dioxide:

$$\varphi_{i,fg\_exit} = \varphi_{i,fg\_enter}$$

For water the following is used to determine the exit flue gas molar flow rate:

$$\varphi_{H_2O,fg\_exit} = \frac{x_{H_2O,fg\_exit} * \sum_j \varphi_{i,fg\_exit}}{1 - x_{H_2O,fg\_exit}}$$

Where:

$\sum_j \varphi_{i,fg\_exit}$  is the total flow rate of all non-water gas species in the exiting flue gas (neglecting sulfur)

The molar flow rate of water condensed out of the DCCPS is then calculated by subtracting the outlet flue gas flow rate from the inlet flow rate

$$\varphi_{H_2O\_Condensed} = \varphi_{H_2O,fg\_enter} - \varphi_{H_2O,fg\_exit}$$

The sulfur dioxide molar flow rate in the exiting flue gas is then defined by:

$$\varphi_{SO_2,fg\_exit} = x_{SO_2,fg\_exit} [ppm] * \frac{\sum_k \varphi_{i,fg\_exit}}{1,000,000}$$

Where:

$\sum_k \varphi_{i,fg\_exit}$  is the total flow rate of all gas species in the exiting flue gas (neglecting sulfur)

$x_{SO_2,fg\_exit} [ppm]$  is the desired concentration of sulfur dioxide in the exiting flue gas in ppm

The mass flow rate [kgmol/hr] of the exiting flue gas stream can now be calculated by taking the sum across all component gas molar flow rates and multiplying by their respective molecular weights.

$$\dot{M}_{fg\_exit} = 3.6 * \sum (\varphi_{i,fg\_exit} * MW_i)$$

Where:

$\varphi_{i,fg\_exit}$  is the molar flow rate [mol/sec] of species (i) in the exiting flue gas

$MW_i$  is the molecular weight of species (i) [g/mol]

$\dot{M}_{fg\_exit}$  is the total mass flow rate [kgmol/hr] of flue gas exiting the DCCPS

## 6.8.2 Reagent Stream Flow Rate Calculations

The amount of sodium hydroxide (NaOH) added for sulfur removal in the DCCPS model is assumed to be equal to the stoichiometric requirement. In practice, a surplus quantity of caustic would be supplied to the DCCPS in the recycled cooling water to ensure sufficient availability to achieve the stipulated exiting sulfur dioxide concentration. For ease of calculation however, we have assumed that the stoichiometric quantity of caustic closely approximates steady state behavior for caustic consumption in the DCCPS model.

$$\varphi_{NaOH} = 2 * (\varphi_{SO_2,fg\_enter} - \varphi_{SO_2,fg\_exit})$$

The mass flow rate of required sodium hydroxide added as reagent is then

$$\dot{M}_{NaOH} \left[ \frac{kg}{sec} \right] = 0.04 \left[ \frac{kg}{mol} \right] * \varphi_{NaOH}$$

## 6.8.3 Precipitant Stream Flow Rate Calculations

The precipitant stream is assumed to be comprised of only water and the sodium sulfite solid created by the removal of sulfur from the incoming flue gas. The quantity of sodium sulfite can be calculated based upon the difference in sulfur dioxide flow rate between the entering and exiting flue gas. This is true because SO<sub>2</sub> and Na<sub>2</sub>SO<sub>3</sub> are equimolar in reaction (A). Additionally, an equivalent number of moles of water are generated in the production of sodium sulfite which must be added to the molar flow rate of precipitate water.

$$\varphi_{Na_2SO_3,precipitant} = \varphi_{SO_2,fg\_enter} - \varphi_{SO_2,fg\_exit} = \varphi_{H_2O\_SO_2removal}$$

The molar flow rate of all precipitate water can then be calculated by adding the water generated by the creation of sodium sulfite to the condensed water calculated previously.

$$\varphi_{H_2O,precipitant} = \varphi_{H_2O\_Condensed} + \varphi_{H_2O\_SO_2removal}$$

For reporting mass flow rates from the model, it is necessary to convert the molar flow rates of the above streams. In practice, a fraction of the water produced in the formation of sodium sulfite remains with the solid to form a slurry. This fraction, denoted as Precipitant Moisture Content [mass fraction], may be specified by the user but carries a default value of 25%. A lower limit of 14.3% is stipulated for Precipitant Moisture Content (PMC) because this represents the equimolar mixture of sodium sulfite and water which would be produced simultaneously when sodium hydroxide reacts with sulfur. Therefore, absent drying, a PMC of less than 14.3% is not possible. For PMC's greater than 14.3% additional water from the DCCPS is entrained with the precipitant slurry. For a generic PMC the resulting precipitant slurry mass flow rate is defined by:

$$\dot{M}_{Slurry} \left[ \frac{kg}{sec} \right] = 0.126 \left[ \frac{kg}{mol} \right] * \varphi_{Na_2SO_3,precipitant} + 0.018 \left[ \frac{kg}{mol} \right] * \left( \frac{PMC}{14.3} \right)$$

Because the sodium sulfite is produced in a slurry, rather than as a dry product, there is no excess water created from the removal of sulfur which can be returned to the DCCPS. In fact, for all PMC's greater than the minimum value, the sulfur removal process is water negative. The required slurry water must be subtracted from the overall water balance and is calculated as follows:

$$\dot{M}_{Slurry\_water} \left[ \frac{kg}{sec} \right] = 0.018 \left[ \frac{kg}{mol} \right] * \varphi_{H2O\_SO2removal} * \left( \frac{PMC}{14.3} - 1 \right)$$

#### 6.8.4 Calculating the Required Cooling Load

To determine the amount of cooling which must be provided to the DCCPS, we define the system as an adiabatic heat exchanger. This allows us to neglect any second order effects of environmental temperature fluctuations and focus on the primary bulk fluid heat transfer required. The cooling load is made up of a sensible heat component (temperature change) and a latent heat component (phase change). The sensible heat change of each of the non-reactive gas species is calculated using the Shomate equation (Section 4.5.1) to determine the enthalpy of each component at the entering and exiting states of the DCCPS. To then calculate the change in sensible heat of all the non-reactive gas (NRG) species we assume ideal gas behavior and apply the Gibbs-Dalton law for calculating the combined enthalpy of a gas stream.

$$H = mh = m_1h_1 + m_2h_2 + \dots + m_kh_k = \sum_{i=1}^k m_ih_i$$

The difference in enthalpy of each component of the entering and exiting flue gas can then be multiplied by their respective mass flow rates to calculate the total sensible heat which must be removed from the non-reactive gas species while in the DCCPS.

$$\Delta \text{Sensible Heat}_{NRG} = H_{enter\_NRG} - H_{exit\_NRG}$$

The sensible heat delta calculation for sulfur dioxide is calculated using the same formula as the non-reactive gases. Theoretically, there should be some accounting for the reduction in moles of SO<sub>2</sub> gas as the flue gas passes through the DCCPS which would result in a slightly lower value for the sensible heat of SO<sub>2</sub> than calculated using the non-reactive gases methodology. However, due to the diminutive mass flow rate of SO<sub>2</sub> even before removal, the reduction in the system heat balance through precise mass accounting is negligible (<0.1%). We therefore chose to use the following relation to calculate the sensible heat delta of the sulfur dioxide gas in the flue gas stream.

$$\Delta \text{Sensible Heat}_{SO2} = \varphi_{SO2,fg\_enter} * [h_{SO2}(T_{fg\_enter}) - h_{SO2}(T_{fg\_exit})]$$

The sensible heat delta from water in the flue gas is calculated in three parts. Two of which correspond to the vapor and liquid phase of the condensing water, while the third accounts for the bulk cooling of the non-condensing water vapor (NCV) in the flue gas. The third part is the most straightforward and is calculated in identical fashion to the sensible heat of sulfur dioxide save that the molar flow rate used is the exiting, rather than entering, gas flow rate of water vapor from the DCCPS.

$$\Delta \text{Sensible Heat}_{H2O\_NCV} = \varphi_{H2O\_NCV,fg\_exit} * [h_{H2O}(T_{fg\_enter}) - h_{H2O}(T_{fg\_exit})]$$

The remaining two sensible heat components for water relate to the vapor (CV) and then liquid water (CL) which is condensed out of the incoming flue gas. The vapor phase of the condensate water sensible heat change is calculated in a similar fashion to the non-reactive gaseous components using the Shomate relations. The specific calculation varies in that the final temperature of the water vapor is not assumed to be the exit temperature of the DCCPS, but rather the average condensation temperature as defined below:

$$T_{Condensation} = \frac{T_{sat\_enter} + T_{sat\_exit}}{2}$$

$$\Delta \text{Sensible Heat}_{H2O\_CV} = \varphi_{H2O\_Condensed} * [h_{H2O}(T_{fg\_enter}) - h_{H2O}(T_{Condensation})]$$

The liquid phase of the condensate sensible heat change is calculated using the heat capacity of liquid water.

$$Cp_{H2O\_liquid} \left[ \frac{kJ}{mol * K} \right] = 0.075$$

The heat capacity of liquid water is close enough to constant over the range of temperature involved within the DCCPS to allow us to safely assume a fixed specific heat for liquid water. The sensible heat change of the liquid water can be calculated using the change in temperature of the condensate and the molar flow rate.

$$\Delta \text{Sensible Heat}_{H2O\_CL} = \varphi_{H2O\_Condensed} * Cp_{H2O\_liquid} * (T_{Condensation} - T_{fg\_exit})$$

### 6.8.5 Latent Heat of Water

Calculating the latent heat required to be removed from a gas stream in order to have a specified fraction of a component condense is not a straight-forward calculation to obtain an exact answer. In order to simplify the calculation of the latent heat of cooling,  $T_{Condensation}$  was assumed to be the temperature at which all water vapor was condensed out of the flue gas within the DCCPS. This assumption preempts the use of a much more computationally intensive, iterative method which could capture continuous changes in water vapor concentration as a function of temperature. It was determined that this degree of precision was not appropriate given the inherent uncertainty of the electrical generation unit as a whole and therefore a decision was made in favor of computational economy.

The total latent heat of condensation for the water condensed out of the flue gas is calculated for the new DCCPS model using the molar flow rate of the precipitated water and the molar flow rate of water created by the sulfur removal process chemistry. The water created by the formation of sodium sulfite is very small in comparison (typically 3 orders of magnitude less) but is included here as the sole means of thermally accounting for the exothermic removal of sulfur in the model. The sum of these two molar flow rates is then combined with the latent heat of condensation correlation detailed earlier to calculate the required cooling load for the latent heat of water condensation.

$$\Delta \text{ Latent Heat} = (\varphi_{H2O\_Condensed} + \varphi_{H2O\_SO2removal}) * (45.161 - 0.0452 * T_{Condensation})$$

## 6.9 Cooling Water Requirement Calculation

At this point all of the mass and energy streams have been calculated with the exception of the cooling water flow rate. The required flow rate of cooling water is a function of four parameters:

$\alpha_{Cooling}$	heat transfer efficiency of the DCCPS system (unity being ideal heat transfer)
$Cooling\ Load_{total}$	sum of all latent and sensible cooling loads in the DCCPS system
$\Delta T_{max,Cooling\ water}$	largest acceptable temperature increase of cooling water
$Cp_{Cooling\ water}$	specific heat of cooling water, default value of 4.2 [kJ/kg K]

The total cooling load is the first piece of information which is required to be calculated. It can be found by taking the sum of all the latent and sensible heat deltas calculated in the previous section to get a total cooling load in kilojoules per second.

$$Cooling\ Load_{total} \left[ \frac{kJ}{SEC} \right] = \Delta SH_{NRG} + \Delta SH_{SO2} + \Delta SH_{H2O\_NCV} + \Delta SH_{H2O\_CV} + \Delta SH_{H2O\_CL} + \Delta LH$$

The required mass flow of cooling water can then be calculated:

$$\dot{M}_{Cooling\ water} \left[ \frac{kg}{SEC} \right] = \frac{Cooling\ Load_{total}}{\alpha_{Cooling} * Cp_{Cooling\ water} * \Delta T_{max,Cooling\ water}}$$

### 6.9.1 Water Balance

One of the primary functions of the DCCPS is to reduce the moisture content in the entering flue gas. It follows logically then that a substantial amount of liquid water ( $\varphi_{H2O\_Condensed}$ ) is produced during normal operation. However, as discussed previously, the reaction to sodium sulfite can be a water consuming process if a water-rich slurry is specified. However, the creation of sodium sulfite slurry is a secondary process compared to the precipitation of flue gas moisture under typical operating conditions and has correspondingly little effect on the net water produced during operation.

$$\dot{M}_{water\_generated} \left[ \frac{kg}{SEC} \right] = \left( 0.018 \left[ \frac{kg}{mol} \right] * \varphi_{H2O\_Condensed} \right) - \dot{M}_{Slurry\_water} \left[ \frac{kg}{SEC} \right]$$

## 6.9.2 Auxiliary Electrical Load Requirements

### 6.9.2.1 Pneumatic Head

The required pneumatic head to overcome the pressure loss across the contacting tower is provided by a combination of the main induced draft fan and the primary forced draft fan unit. The electrical load required for their operation is calculated outside this component model and is included in the base plant energy use calculations performed by the IECM.

### 6.9.2.2 Cooling Water Pumping

The electrical load required to pump the above quantity of cooling water is calculated using a pre-existing IECM relation for pumping:

$$MW_{fg\_cooling} = 4.7 * 10^{-5} * CoolingWater_{fg}[gpm]$$

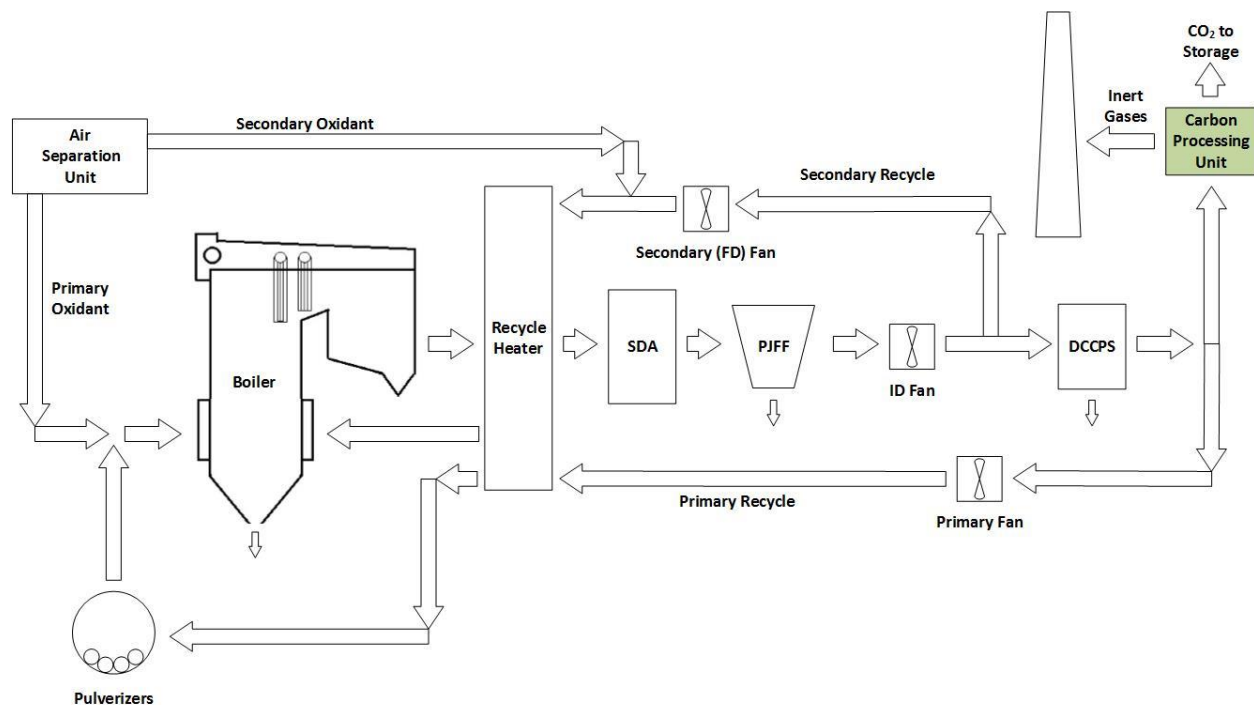
The cooling water flowrate was in units of [kg/sec], so we must use the following relation to convert from volume to mass flowrate:

$$1 \text{ gallon water} = 3.79 \text{ kg water}$$

With this, and correcting for the time unit disparity, the electrical use of the DCCPS pumps can be expressed as:

$$MW_{DCCPS,pump} = 7.44 * 10^{-4} * \dot{M}_{Cooling\ water} \left[ \frac{kg}{sec} \right]$$

# Chapter 7 Carbon Processing Unit Performance Model



## 7.1 Model Objectives

Carbon capture technologies which are not based on absorption or adsorption, such as oxyfuel, produce a carbon dioxide product gas that is far from pure without enrichment. Before the flue gas can be sent beyond the plant gate, it must be purified and pressurized to meet pipeline specifications. The piece of equipment responsible for completing this task is called the carbon processing unit (CPU). This designation is slightly complicated by the fact that a CPU is both a specific unit which produces high-purity carbon dioxide gas and the umbrella term for equipment which performs carbon handling on the back end of an oxyfuel plant. To avoid confusion in this chapter when referencing the various systems I will refer to CPU systems which capture all the flue gas in the carbon dioxide product stream as co-capture systems and reserve the term CPU for cryogenic systems which separate the carbon dioxide from the balance of gases in the flue gas.

Regardless of whether a co-capture system or a CPU is used, the performance and cost metrics of interest do not change. The main objectives for either carbon handling model are to be able to explore trade-offs associated with carbon dioxide capture rate and carbon dioxide product purity. Integral to this goal is accurately accounting for the energy and mass flow requirements of each system; including cooling water requirements and heat integration opportunities. Additionally, the carbon handling models created need to be flexible enough to work with all relevant carbon dioxide capture technologies in the IECM.

## 7.2 Carbon Handling System Configurations

### Co-Capture

For plant designs where the sole intent is to sequester the carbon dioxide product, simply compressing the entire flue gas stream may be the most attractive alternative. This design benefits from not having the additional complexity of a cold-box system for cryogenic purification of the flue gas and therefore has lower capital intensity. Conversely, because the entirety of the flue gas is being compressed to pipeline pressure, the specific energy use is greater. Unique to this configuration is the ability to capture 100% of the carbon dioxide produced by the plant, but also eliminate all other criteria pollutant emissions as they would be sequestered along with the carbon dioxide.

### High-Purity Carbon Processing Unit

If injection regulations forbid the simultaneous sequestration of impurities and inert gases along with carbon dioxide, or if there is an economic case for selling a high-purity carbon dioxide product, a cryogenic CPU must be used. The use of a CPU is very common amongst studies which compare the performance of oxyfuel to other capture technologies such as amine absorption. This is because the purity of the carbon dioxide product from the oxyfuel plant must be increased to a purity of 99.5 [mol%] in order to compare the systems on an apples-to-apples basis. Furthermore, if there is a desire to produce saleable carbon dioxide for enhanced oil recovery, the oxygen content of the carbon dioxide product must be reduced to meet safety requirements. At the time of writing, a cryogenic carbon processing unit was the only proven technology capable of providing the flow rates necessary to produce high-purity carbon dioxide product gas from an oxyfuel plant.

## 7.3 Carbon Handling Bypass

There are times when a user may want to specify a carbon capture rate which is lower than would be permitted inside the base configuration of their chosen carbon handling system. To achieve lower carbon dioxide rates a bypass may be used with either CoCapture or a CPU to route a fraction of the flue gas from the direct contact cooler polishing scrubber (DCCPS) directly to the stack for emission to the atmosphere. The flow diagram for bypass is depicted in Figure 7.1. The fraction of flue gas from the DCCPS sent to the carbon handling system is denoted by  $\gamma$ , whereas the fraction sent directly to the stack for emission to the atmosphere is  $\delta$ .

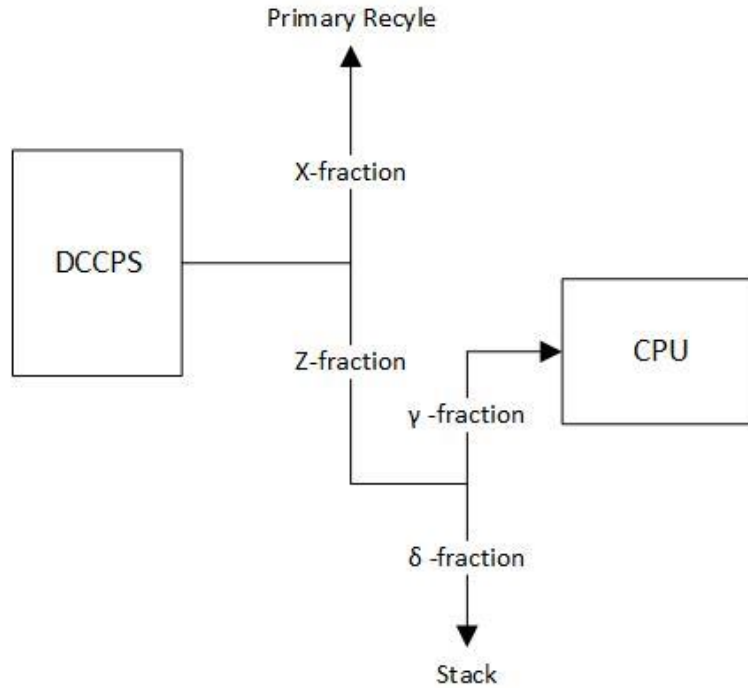


Figure 7.1 Process flow diagram of the carbon handling system bypass.

### 7.3.1 CoCapture Bypass

In a co-capture system all the carbon dioxide present in the stream sent to compression is contained. For this reason, calculating the fraction of the gas stream ( $\gamma_{CoCap}$ ) exiting the direct contact cooler and polishing scrubber which must be sent to compression to achieve a desired carbon dioxide avoided percentage ( $CAP$ ) is relatively straight forward.

$$\gamma_{CoCap} = \frac{CAP}{100}$$

$$\delta_{CoCap} = 1 - \frac{CAP}{100}$$

Where:

$CAP$  plant level carbon dioxide avoided percentage

$\gamma_{CoCap}$  mass fraction of the flue gas stream exiting the DCCPS sent to compression

$\delta_{CoCap}$  mass fraction of the flue gas stream exiting the DCCPS sent directly to the stack

### 7.3.2 CPU Bypass

In those systems which utilize a cryogenic carbon processing unit, calculating the fraction of flue gas from the DCCPS ( $\gamma_{CPU}$ ) which must be sent to the CPU is dependent on the performance parameters of the CPU. The bypass fractions for oxyfuel systems utilizing a CPU are calculated using the following two formulas:

$$\gamma_{CPU} = \frac{CAP}{CRR}$$

$$\delta_{CPU} = 1 - \gamma_{CPU}$$

Where:

$CAP$	plant level carbon dioxide avoided percentage
$CRR$	carbon dioxide recovery rate achievable in the CPU [%]
$\gamma_{CPU}$	mass fraction of the flue gas stream exiting the DCCPS sent to CPU
$\delta_{CPU}$	mass fraction of the flue gas stream exiting the DCCPS sent directly to the stack

The carbon recovery rate of the CPU places an upper bound on the plant level carbon dioxide avoided percentage. For instance, if the cold-box system of the CPU is only able to retain 90% of the carbon dioxide which enters in the carbon dioxide product; then a CAP value of 90% would only be possible if 100% of the flue gas from the DCCPS was routed to the CPU. This scenario would have a ( $\gamma_{CPU}$ ) value of 1. If this same CPU was used in a system with a ( $\gamma_{CPU}$ ) value of 0.9, then the CAP would be set to 81%. Figure BB is a matrix of gamma values which correspond to CRR, CAP value pairs. There is a large region of the matrix where the gamma values are greater than one. These scenarios represent instances where the CRR is less than the CAP. In these cases the mass balance of the system is violated and they are not feasible bypass configurations.

## Carbon Recovery Rate (CRR) of CPU

	99.5	98	96.5	95	92.5	90	87	84	81	75	70	60	50
0	0	0	0	0	0	0	0	0	0	0	0	0	0
10	0.101	0.102	0.104	0.105	0.108	0.111	0.115	0.119	0.123	0.133	0.143	0.167	0.200
20	0.201	0.204	0.207	0.211	0.216	0.222	0.230	0.238	0.247	0.267	0.286	0.333	0.400
25	0.251	0.255	0.259	0.263	0.270	0.278	0.287	0.298	0.309	0.333	0.357	0.417	0.500
30	0.302	0.306	0.311	0.316	0.324	0.333	0.345	0.357	0.370	0.400	0.429	0.500	0.600
35	0.352	0.357	0.363	0.368	0.378	0.389	0.402	0.417	0.432	0.467	0.500	0.583	0.700
40	0.402	0.408	0.415	0.421	0.432	0.444	0.460	0.476	0.494	0.533	0.571	0.667	0.800
45	0.452	0.459	0.466	0.474	0.486	0.500	0.517	0.536	0.556	0.600	0.643	0.750	0.900
50	0.503	0.510	0.518	0.526	0.541	0.556	0.575	0.595	0.617	0.667	0.714	0.833	1.000
55	0.553	0.561	0.570	0.579	0.595	0.611	0.632	0.655	0.679	0.733	0.786	0.917	1.100
60	0.603	0.612	0.622	0.632	0.649	0.667	0.690	0.714	0.741	0.800	0.857	1.000	1.200
65	0.653	0.663	0.674	0.684	0.703	0.722	0.747	0.774	0.802	0.867	0.929	1.083	1.300
70	0.704	0.714	0.725	0.737	0.757	0.778	0.805	0.833	0.864	0.933	1.000	1.167	1.400
75	0.754	0.765	0.777	0.789	0.811	0.833	0.862	0.893	0.926	1.000	1.071	1.250	1.500
80	0.804	0.816	0.829	0.842	0.865	0.889	0.920	0.952	0.988	1.067	1.143	1.333	1.600
81	0.814	0.827	0.839	0.853	0.876	0.900	0.931	0.964	1.000	1.080	1.157	1.350	1.620
82	0.824	0.837	0.850	0.863	0.886	0.911	0.943	0.976	1.012	1.093	1.171	1.367	1.640
83	0.834	0.847	0.860	0.874	0.897	0.922	0.954	0.988	1.025	1.107	1.186	1.383	1.660
84	0.844	0.857	0.870	0.884	0.908	0.933	0.966	1.000	1.037	1.120	1.200	1.400	1.680
85	0.854	0.867	0.881	0.895	0.919	0.944	0.977	1.012	1.049	1.133	1.214	1.417	1.700
86	0.864	0.878	0.891	0.905	0.930	0.956	0.989	1.024	1.062	1.147	1.229	1.433	1.720
87	0.874	0.888	0.902	0.916	0.941	0.967	1.000	1.036	1.074	1.160	1.243	1.450	1.740
88	0.884	0.898	0.912	0.926	0.951	0.978	1.011	1.048	1.086	1.173	1.257	1.467	1.760
89	0.894	0.908	0.922	0.937	0.962	0.989	1.023	1.060	1.099	1.187	1.271	1.483	1.780
90	0.905	0.918	0.933	0.947	0.973	1.000	1.034	1.071	1.111	1.200	1.286	1.500	1.800
91	0.915	0.929	0.943	0.958	0.984	1.011	1.046	1.083	1.123	1.213	1.300	1.517	1.820
92	0.925	0.939	0.953	0.968	0.995	1.022	1.057	1.095	1.136	1.227	1.314	1.533	1.840
93	0.935	0.949	0.964	0.979	1.005	1.033	1.069	1.107	1.148	1.240	1.329	1.550	1.860
94	0.945	0.959	0.974	0.989	1.016	1.044	1.080	1.119	1.160	1.253	1.343	1.567	1.880
95	0.955	0.969	0.984	1.000	1.027	1.056	1.092	1.131	1.173	1.267	1.357	1.583	1.900
96	0.965	0.980	0.995	1.011	1.038	1.067	1.103	1.143	1.185	1.280	1.371	1.600	1.920
97	0.975	0.990	1.005	1.021	1.049	1.078	1.115	1.155	1.198	1.293	1.386	1.617	1.940
98	0.985	1.000	1.016	1.032	1.059	1.089	1.126	1.167	1.210	1.307	1.400	1.633	1.960
99	0.995	1.010	1.026	1.042	1.070	1.100	1.138	1.179	1.222	1.320	1.414	1.650	1.980

Figure 7.2 Matrix of gamma fractions corresponding to CRR and CAP values for the CPU system with bypass. White cells represent the feasible region; red cells violate mass balance constraints.

## 7.4 CoCapture Performance Model

The process of co-capturing all the flue gas into the carbon product stream is relatively straight forward in design compared to a cryogenic CPU. The equipment necessary is limited to the compressor train required to compress the flue gas stream from the direct contact cooler polishing scrubber (DCCPS) to pipeline pressure. During compression and intercooling all the moisture is precipitated out of the flue gas. The remaining carbon dioxide product is roughly 85 [mol%] carbon dioxide, depending upon the coal composition and recycle rate specified.

### 7.4.1 Summary of Input and Output Parameters

#### Input Parameters

The key input parameters defining the performance of the ASU are as follows:

##### *User Specified Variables*

$CAP$	plant level carbon dioxide avoided percentage [%]
$\alpha_{Cooling}$	heat transfer efficiency of CoCap system (unity being ideal heat transfer)
$\Delta T_{max, Cooling\ water}$	largest acceptable temperature increase of cooling water [K]
$P_{Pipeline}$	desired pipeline pressure of the product gas [kPa]
$\eta_{Comp}$	isentropic efficiency of the compression process [decimal]

##### *Passed From IECM*

$\varphi_{to\_CoCap}$	molar flow rate of flue gas from the DCCPS [mol/sec]
$P_{DCCPS\_exit}$	pressure of the product gas leaving the DCCPS [kPa]

#### Output Parameters

The model will then calculate or report the following key output parameters:

$\dot{M}_{precip\_water}$	mass flow rate of the removed water stream [kg/hr]
$\dot{M}_{CP}$	mass flow rate of the carbon product stream produced [kg/hr]
$CoCap_{CoolingDuty}$	specific cooling duty of the co-capture system [GJ/tonne CO <sub>2</sub> ]
$CoCap_{HIDuty}$	heat integration duty of the co-capture system [GJ/hr]
$MW_{CoCap}$	electrical power requirement of the co-capture system [MW]

## 7.4.2 Mass and Energy Balance Calculations

The following sections run through the mass and energy accounting of all the streams highlighted in Figure 7.3. The cooling water in and out streams are representative of the bulk cooling duty which must be performed, but this cooling could be handled either by boiler feed water heating or through the use of cooling water from the base plant.

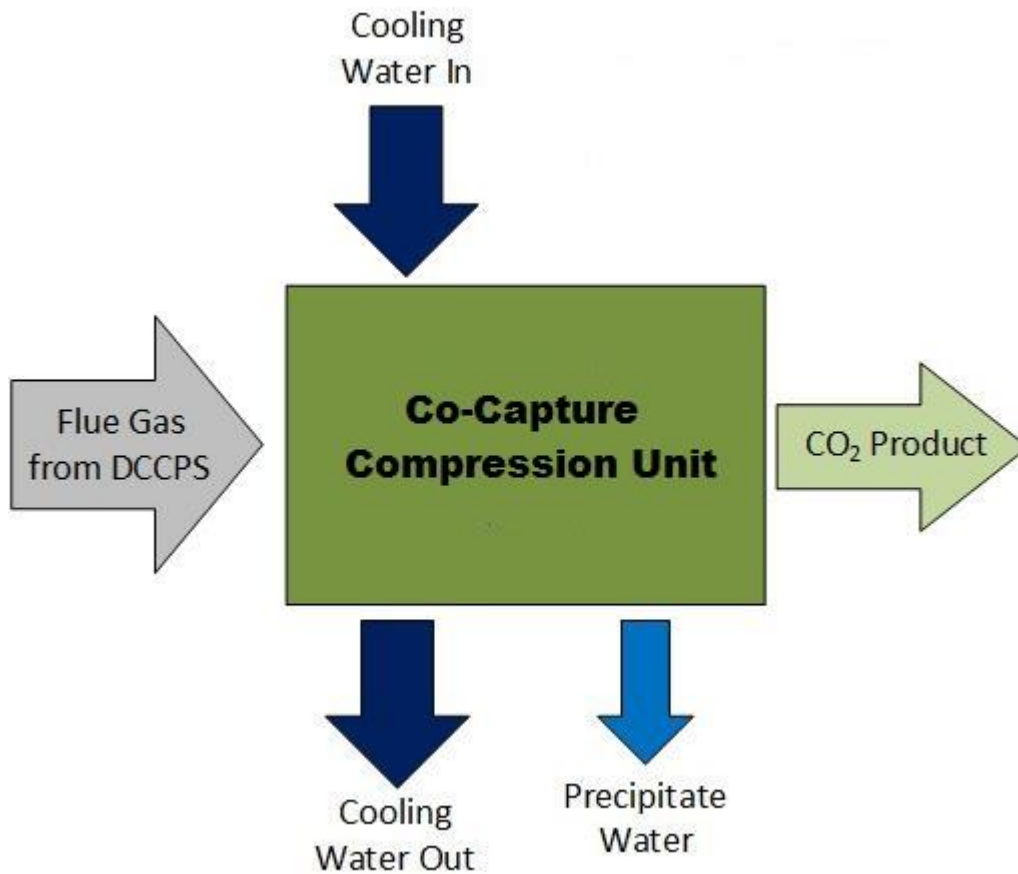


Figure 7.3 Process flow diagram of all the gas and liquid streams entering and exiting the CoCapture unit.

### 7.4.2.1 Carbon Dioxide Product

In the parlance of the overall oxyfuel model in the IECM, the total molar flow rate of flue gas sent to the co-capture system from the direct contact cooler and polishing scrubber (DCCPS) can be defined as:

$$\varphi_{to\_CoCap} = \sum \varphi_{i,to\_CoCap} = (1 - \beta) * \sum \varphi_{i,fg\_exit}$$

Where the following comes from the DCCPS Model:

$\varphi_{i,fg\_exit}$  is the molar flow rate [mol/sec] of species (i) in the exiting flue gas

$(1 - \beta)$  is the fraction of the flue gas exiting the DCCPS which is sent to co-capture

It follows then that the total molar flow rate of carbon dioxide sent to the co-capture system from the DCCPS can be calculated in the following manner:

$$\varphi_{CO_2, to\_CoCap} = (1 - \beta) * \varphi_{CO_2, fg\_exit}$$

In those instances where co-capture is the chosen carbon handling system, but less than 100% capture of the carbon dioxide is required, the bypass relations discussed in the bypass section must be utilized. The quantity of this carbon dioxide entrained in the carbon dioxide product gas produced by the co-capture system is directly proportional to the carbon dioxide avoided percentage (CAP):

$$\varphi_{CO_2, CoCap} = \left(\frac{CAP}{100}\right) * \varphi_{CO_2, to\_CoCap}$$

Where:

$CAP$  is the plant level carbon dioxide avoided percentage [%]

The molar flow rate of carbon dioxide which is vented from the system can then be calculated as:

$$\varphi_{CO_2, vent} = \left(1 - \frac{CAP}{100}\right) * \varphi_{CO_2, to\_CoCap}$$

For energy accounting purposes, all water is assumed to be removed by the compression process in the co-capture unit. This means that the volume of the water gas must be accounted for when calculating the compression work of the co-capture system. The molar flow rate of the flue gas sent to the co-capture compressor can be calculated as:

$$\varphi_{CoCap} = \varphi_{to\_CoCap} * \frac{CAP}{100}$$

The mass flow rate of the flue gas into the co-capture compressor can then be calculated:

$$\dot{M}_{CoCap} \left[ \frac{kg}{hr} \right] = \varphi_{CoCap} * 3.6 * mw_{CoCap}$$

Where:

$\varphi_{CoCap}$  is the total molar flow rate of flue gas sent to the co-capture compressor [mol/sec]

$mw_{CoCap}$  is the molecular weight of the flue gas from the DCCPS [g/mol]

#### 7.4.2.2 Precipitate Water Production

In order to prevent water from precipitating out of the carbon dioxide product gas once it is in the pipeline and potentially causing corrosion problems; the bulk moisture remaining in the flue gas must be removed. An assumption has been made for calculation purposes that all of the water in the flue gas can be removed through compression with after cooling. This is not entirely accurate as it is not possible to remove 100% of the water through compression and cooling alone. However, to the first

order, it is sufficient for closing the mass balance in this instance because there is not an immediate concern from any residual trace moisture. The calculations for determining the mass flow rate of precipitate water are provided below. The cooling water required to condense out the precipitate water during compression is accounted for in the following section on cooling water requirements.

The flue gas passed to the CPU is assumed to have the same characteristics as the flue gas had upon exiting the direct contact cooler (DCCPS). The molar fraction of water in this flue gas is determined by the operational characteristics of the DCCPS and can be altered by the user. The co-capture system needs to remove all of the remaining water left after the flue gas has been processed by the DCCPS. Thus calculating the quantity of water which needs to be removed by compression is rather straight forward once the incoming flue gas stream from the DCCPS is known because all of the water must be removed as precipitate.

The molar flow rate of water is:

$$\varphi_{H2O,to\_CoCap} = (1 - \beta) * \varphi_{H2O,fg\_exit}$$

And the mass flow rate of water which is removed in the form of precipitate by the compressor is:

$$\dot{M}_{precip\_water} \left[ \frac{kg}{hr} \right] = 3.6 * \varphi_{H2O,to\_CoCap} * mw_{H2O}$$

Where:

$mw_{H2O}$  is the molecular weight of water [g/mol]

$\varphi_{H2O,to\_CoCap}$  is the molar flow rate of water to the co-capture system [mol/sec]

$\dot{M}_{precip\_water}$  is the mass flow rate of the removed water stream [kg/hr]

With the mass flow rate of water being precipitated out during compression calculated; it is then possible to determine the mass flow rate of the carbon dioxide product gas leaving the co-capture unit for storage.

$$\dot{M}_{CP} \left[ \frac{kg}{hr} \right] = \dot{M}_{CoCap} - \dot{M}_{precip\_water}$$

#### 7.4.2.3 Cooling and Heat Integration

The relations developed for calculating the cooling duty of the co-capture unit are based on a combination of DOE Case Studies (36) and the pre-existing carbon dioxide compression module in the IECM. This method separates the cooling duty of compression from the other cooling requirements of co-capture; which allows us to keep the compression cooling code the same across all CCS systems in the IECM. Table GG below presents values from several case studies in the DOE Oxyfuel Report along with many of the calculations used to formulate the cooling relations. The two co-capture case studies presented are S12C and S12D with the difference between them being the absence of a DCCPS in case S12C.

Table 7-1 Co-Capture Cooling Duty Information

	Case Studies from 2010 DOE Oxyfuel Report						
	S12C	S12D	S12E	S12F	L12F	S13F	L13F
CO2 Cooling [GJ/hr]	300.6	134.8	227.7	227.4	239.2	275	291.4
CPU BFW Enthalpy In [kJ/kg]	217.35	217.35	217.35	217.35	217.35	238.79	238.79
CPU BFW Enthalpy Out [kJ/kg]	616.44	616.44	616.44	616.44	616.44	615.94	615.94
CPU BFW Enthalpy Delta [kJ/kg]	399.09	399.09	399.09	399.09	399.09	377.15	377.15
CPU BFW Flow [kg/hr]	505,327	509,083	221,510	221,541	221,130	224,795	226,048
CPU BFW Duty [GJ/hr]	201.67	203.17	88.40	88.41	88.25	84.78	85.25
CO2 Product Flow [kg/hr]	665,626	671,065	537,511	530,281	559,208	507,975	510,554
CO2 Yi [wt%]	0.878	0.884	98.26	99.96	99.96	99.96	99.96
CO2 Flow [t/hr]	584.3	593.4	528.2	530.1	559.0	507.8	510.3
Specific (BFW) Cooling Duty [GJ/tCO2]	0.345	0.342	0.167	0.167	0.158	0.167	0.167
Specific Cooling Duty [GJ/tCO2]	0.515	0.227	0.431	0.429	0.428	0.542	0.571
Total CPU Cooling Duty [GJ/hr]	528.27	365.57	343.10	343.01	366.45	359.78	376.65
Total Specific CPU Cooling Duty [GJ/tCO2]	0.904	0.616	0.650	0.647	0.656	0.709	0.738
Total Specific CPU, less Comp. Cooling Duty [GJ/tCO2]	0.390	0.389	0.218	0.218	0.228	0.167	0.167
KO Water [GJ/hr]	26	27.6	27	27.2	39	25.8	37.5
CPU Heat Integration [% Cooling Duty Recovered]	38%	56%	26%	26%	24%	24%	23%

The ability to recoup heat energy from the large compressor in the co-capture system can be key to reducing the steam cycle heat rate and consequently increasing the overall efficiency of the plant. With this in mind, the relations were constructed to calculate the total cooling duty requirement for each carbon handling system regardless of the extent of heat integration. This allows the extent of heat integration to be a user specified variable in the IECM while utilizing just one set of cooling duty relations in order to determine the amount of cooling water needed to provide residual cooling to the compression units. Keeping accordance with the commonly used unit system in industry, the cooling duty relation for co-capture was created on a gigajoule of cooling duty per tonne of carbon dioxide throughput basis.

Equation for the specific cooling duty of the co-capture system:

$$CoCap_{CoolingDuty} \left[ \frac{GJ}{tCO_2} \right] = 0.62 * (1 - HI_{CoCap})$$

Where:

$HI_{CoCap}$  is the fraction of cooling duty which can be recovered in the steam cycle through BFW heating

Min = 0.0, Max = 0.6, Default = 0.0 (0.45 representative)

### Cooling Water Requirements

The total amount of cooling water required to provide the calculated cooling duty is determined by a function of four parameters:

$\alpha_{Cooling}$  heat transfer efficiency of CoCap system (unity being ideal heat transfer)

Cooling Duty total cooling duty [GJ/tonne CO2]

$\Delta T_{max, Cooling\ water}$  largest acceptable temperature increase of cooling water [K]  
 $Cp_{Cooling\ water}$  specific heat of cooling water, default value of 0.0042 [GJ/t K]

The required mass flow of cooling water can then be calculated:

$$\dot{M}_{Cooling\ water} \left[ \frac{tonne}{tonne\ CO2} \right] = \frac{Cooling\ Duty}{\alpha_{Cooling} * Cp_{Cooling\ water} * \Delta T_{max, Cooling\ water}}$$

### Heat Integration

The heat integration of the co-capture unit is calculated in a similar fashion to the cooling duty above being that it is simply the fraction of the overall cooling duty which does not need to be met with cooling water. For ease of combining the heat integration duty from the carbon handling system with that of the ASU, the relations have been altered to produce values with common units of [GJ/hr]. For a plant equipped with a co-capture unit:

$$CoCap_{HIDuty} \left[ \frac{GJ}{hr} \right] = 0.62 * \dot{M}_{CO2} * (HI_{CoCap})$$

Where

$HI_{CoCap}$  is the fraction of cooling duty which can be recovered in the steam cycle through BFW heating

Min = 0.0, Max = 0.6, Default = 0.0 (0.45 representative)

$\dot{M}_{CO2}$  is the mass flow rate of carbon dioxide through the compressor [tonnes/hr]

The heat integration duty of the co-capture system is added with the heat integration duty of the ASU to provide the total heat integration duty of the oxyfuel plant. Details on calculating the effects on performance from heat integration can be found in Section 4.5.5 in the overall mass and energy balance plant details.

#### 7.4.2.4 Electrical Load Requirements

The compression model used for co-capture is the same compressor model used throughout the IECM for compressing the CO<sub>2</sub> product of all carbon capture technologies. This model assumes ideal gas behavior in an isothermal process. The assumption for this process is that there is no temperature change during compression and thus the steady-flow mechanical work for such a process can be expressed as:

$$\omega_{sf} = \int v dP = \int \frac{RT}{P} dP = RT \ln \frac{P_2}{P_1} = RT \ln \frac{v_1}{v_2}$$

The user must then provide an isentropic efficiency value ( $\eta_{comp}$ ) before the compression work for the co-capture process can be calculated using the following:

$$MW_{CoCap} = \frac{\dot{M}_{CoCap} * \left( \frac{RT}{mw_{CoCap}} * \ln \frac{P_{Pipeline}}{P_{DCCPS\_exit}} \right)}{\eta_{comp} * 1000}$$

Where:

$\dot{M}_{CoCap}$	is the mass flow rate of the product gas from the DCCPS [kg/sec]
$R$	is the universal gas constant [kJ/kmol-K]
$T$	is the temperature of the product gas from the DCCPS [K]
$mw_{CoCap}$	is the molecular weight of the product gas from the DCCPS [kg/kmol]
$P_{Pipeline}$	is the desired pipeline pressure of the product gas [kPa]
$P_{DCCPS\_exit}$	is the pressure of the product gas leaving the DCCPS [kPa]
$\eta_{Comp}$	is the isentropic efficiency of the compression process [decimal]

## 7.5 High-Purity Carbon Processing Unit Performance Model

### 7.5.1 General Application

Carbon capture technologies which produce a gas comprised of more than just carbon dioxide and water may require the enrichment of carbon dioxide in their produced gas stream. This is especially true if the carbon dioxide product must either meet sequestration specifications or be saleable for enhanced oil recovery. The value of a carbon dioxide processing unit (CPU) is that the carbon dioxide fraction of a feed stream can be increased to nearly 100%. There are sizeable energy and financial costs incurred through the use of a CPU. However, if pipeline specifications or injection regulations require high-CO<sub>2</sub> purity, CPU's are presently the only means of making these alternative carbon capture technologies viable.

Carbon processing units today utilize cryogenic separation to increase the purity of the carbon dioxide in the product stream. Section 2.3.5 discusses in detail proposed and patented designs for specific capture rates and product purities achievable through various cryogenic configurations. The specific sequence of operations and equipment involved in these systems vary, but the underlying physical principle utilized for enrichment of carbon dioxide is the same. The feed gas stream is cooled to a very low temperature (~-55°C), just above the triple point in Figure 7-4. Due to the elevated operating pressure of the CPU, the carbon dioxide gas then begins to condense out as liquid and separates from the remaining inert gas mixture (Argon, Oxygen, and Nitrogen). The cooling load required to reach cryogenic temperatures is provided through compressing the feed stream, removing heat through indirect contact gas/liquid heat exchangers, then expanding the feed stream to achieve the required cooling through the Joule-Thompson Effect.

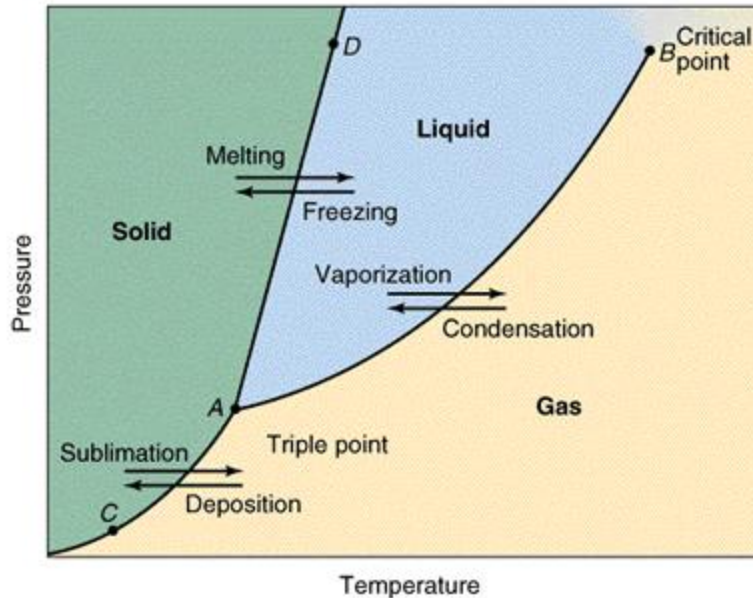


Figure 7.4 Phase diagram of carbon dioxide which shows the path taken by carbon dioxide gas in the carbon processing unit, cooled at an elevated pressure and condensed out as a liquid, as the temperature approaches the triple point

Operation at cryogenic temperatures necessitates that all water be removed from the feed stream prior to entering the cold box of the CPU in order to prevent ice build-up and possible mechanical failure. The bulk moisture is removed from the feed stream during preliminary compression. Residual moisture is then removed by a desiccant bed drying system which allows for at least one bed to be operational while another bed is being regenerated with the inert gas stream produced by the cold box.

### 7.5.2 Oxyfuel Application

For carbon dioxide product purity levels greater than ~85% the current generation oxyfuel systems require the use of a carbon processing unit. Presently, the concept of co-sequestering the inert gases along with the carbon dioxide has not become ubiquitously accepted as a preferred practice and considerable uncertainty remains regarding its legality. This, combined with the general comparison benchmarks (adopted from amine systems) of 90% capture and 99%+ purity in the carbon dioxide product stream for capture systems, ensures that the “typical” oxyfuel system will utilize a CPU. Consequently, the performance and cost of the CPU plays a large role in determining the competitiveness of oxyfuel systems.

### 7.5.3 Modelling Approach

Creating a performance model for the carbon processing unit was challenging for a number of reasons. The most prominent being that data and case studies which provide adequate performance detail to construct and test a performance model are extremely limited. Secondly, because of the importance of the CPU to most oxyfuel configurations, we wanted to create a robust performance model to provide sufficient granularity for examining differences in separation performance resulting from changes in feed stream composition or product stream requirements. There were also concessions made in order

to allow the model to have additional value inside the IECM. Because other systems which produced feed stream conditions outside the range produced by an oxyfuel system would be utilizing the model; it needed to be able to accommodate feed streams down to only 50% carbon dioxide. Also, compression and separation needed to be handled separately (integrated processes in a CPU) so that differences in the isentropic compressor efficiency for carbon dioxide product compression could be handled on an apples-to-apples basis when comparing two different capture systems (i.e. oxyfuel to amine). Ultimately, the decision was made to utilize a parallel approach. Compression of the CO<sub>2</sub> product stream would be handled by the existing compression framework in the IECM and separation would be handled by a first principles, thermodynamic model to ensure that sensible results could be generated for any arbitrary feed stream composition.

#### 7.5.4 Model Structure and Theoretical Foundation

The performance model for the carbon processing unit breaks into two separate processes: compression and separation of the gas stream. This approach has been used for computational economy and is not directly reflective of the real world process in which the entire feed gas stream is compressed, dehydrated, compressed further, cooled, expanded in the cold box, separated into inert and product streams, and finally the product stream is compressed to pipeline pressure for transport. However, from a thermodynamics perspective, the approach we have adopted provides acceptable accuracy given the constraints we placed on the model and the limited amount of performance data available for validation.

The performance data available at the time of writing treats the CPU like the black box depicted in Figure 7.5. A fully characterized (pressure, temperature, and composition) feed stream enters the device and three fully characterized streams (precipitate water, non-condensable/inert gases, and CO<sub>2</sub> product) leave the opposite side. Work is done on the feed stream in this process and reported in units of kWh/tonne contained CO<sub>2</sub> [kWh/t CO<sub>2</sub>] in the CO<sub>2</sub> product stream.

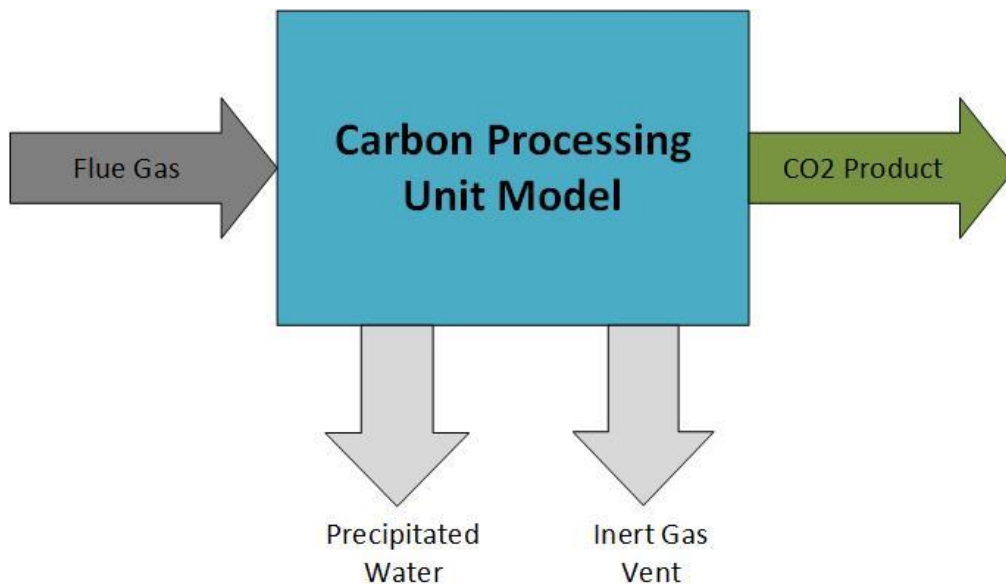


Figure 7.5 Flow diagram of the CPU which represents how stream data is handled and presented in literature.

The performance model we constructed breaks this black box into two operations: separation and compression. This was done so that the compression of the CO<sub>2</sub> product stream could be handled in an analogous fashion between the various carbon capture systems in the IECM and also so that the user could specify a desired CO<sub>2</sub> product pressure. This assumption is defensible because although some proposed CPU configurations may produce CO<sub>2</sub> product streams at elevated pressures (49) or in liquid state (47), many yield a CO<sub>2</sub> product stream exiting the cold box which has characteristics similar to those found exiting the regenerator in an amine absorption system. To model the separation process; we began by debiting the required compression work for the CO<sub>2</sub> product stream from the CPU performance data. This left us the proportion of CPU work involved with the gas separation process (Fig 7.6).

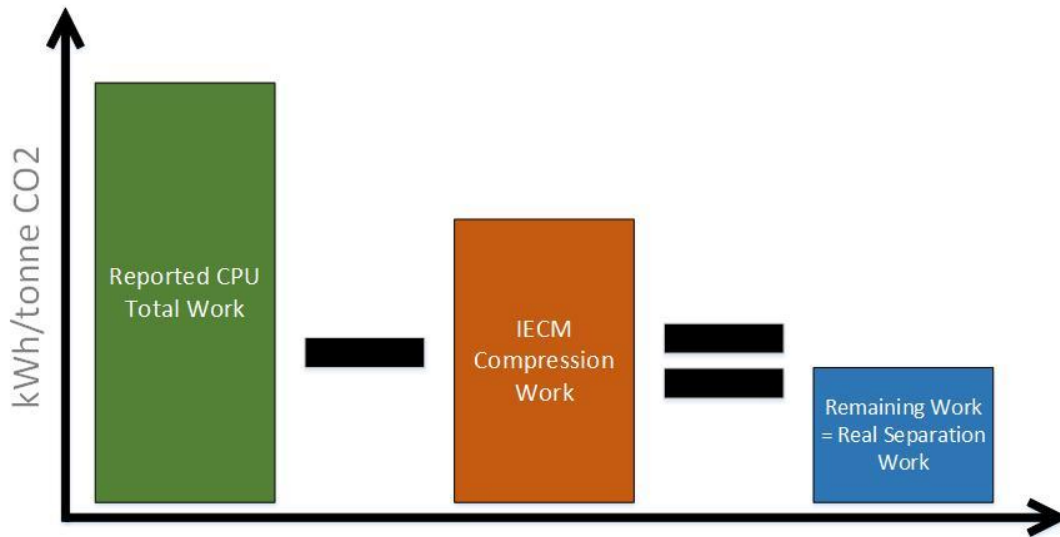


Figure 7.6 Depiction of the debiting of compression work required to produce the reported CO<sub>2</sub> product stream from the reported CPU work data. This yielded the fraction of reported work assumed to be associated with the separation of gases in the feed stream.

With the fraction of CPU work dedicated to separation calculated for the available systems (Real Separation Work or RSW), we needed to create a model capable of characterizing the separation work required to separate an arbitrary feed stream which could be calibrated using the newly created RSW data set. The approach we adopted was to use a second law analysis, along with our RSW data set, to create a model capable of handling a wide range of feed stream compositions. At the most basic level, a second law analysis tells you how efficient a process is at getting a stream from state 1 to state 2 relative to the minimum work required to go from state 1 to 2. Our separation model is predicated on the idea of calculating the minimum work required to separate the feed stream into the product streams specified by the user then applying a calculated 2<sup>nd</sup> law efficiency to predict the real separation work.

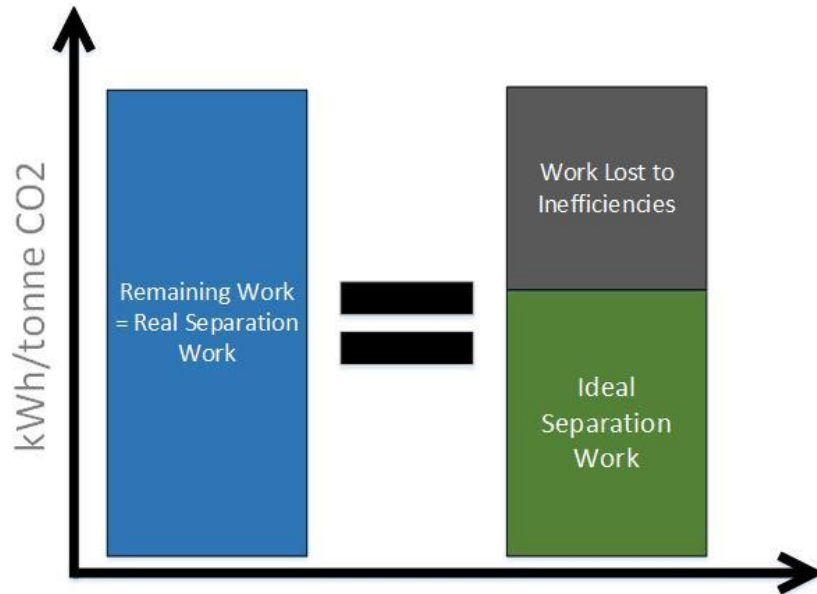


Figure 7.7 The real separation work is the difference between the black box CPU work and the compression work on a per tonne entrained CO<sub>2</sub> basis. The real separation work is comprised of the minimum work required to move from state 1 to 2 along with all work lost to process inefficiencies.

Our model for determining the minimum separation work starts with an expression of the 1<sup>st</sup> Law for defining the internal energy of a control-volume system.

$$dU = \delta Q - \delta W$$

Any net increase in the internal energy,  $U$  must be reflected, in terms of heat,  $\delta Q$  entering the system and the work,  $\delta W$  done by the system. Internal energy,  $U$  is a state property of the system and correspondingly changes in this value are represented by an exact differential,  $d$ . State properties depend solely on the original and final state of the system and are independent of the path (or process) taken to achieve the change in state. Heat and work are not state functions however and changes in their values are represented by Greek deltas,  $\delta$ . Without knowing the exact process involved in shifting the system from state 1 to 2 it is impossible to say how much of the energy went out of the system as heat or work. This is because work is a path-dependent quantity and is therefore a thermodynamic process function. However, if we assume that the separation process is ideal (both reversible and adiabatic) this serves as a specification of process pathway and it can be determined that the integral amount of process work depends solely on the initial and final states of the system. In our CPU model we refer to this reversible and adiabatic differential between the initial and final states as the “Ideal Work”.

The above simplified formulation of the first law presupposes that there are no changes to the composition of the system, which is not the case in our separation process because we are separating a feed stream in to a precipitate water stream, non-condensable gas stream, and a CO<sub>2</sub> product stream. In this case we need to employ a more general formulation, Gibbs free energy.

$$G = H - Ts$$

Where

$G$  is Gibbs free energy

$T$  is the absolute temperature of the system [K]

$s$  is the entropy of the system

$H$  is the enthalpy of the system

And

$$H = U + pV$$

Utilizing the Gibbs free energy relation we can identify the maximum ability for a system to do work (or minimum work required to be done upon it) by a change from state 1 to 2. A common methodological framework which utilizes the Gibbs free energy concept is a second law, or exergy, analysis. The exergy content of a stream of matter is defined by the work which can ideally be extracted when the stream is brought into equilibrium with the environment. The exergy of a stream can be further decomposed into four parts: physical molar exergy ( $\varepsilon_{ph}$ ), chemical molar exergy ( $\varepsilon_{ch}$ ), potential molar exergy ( $\varepsilon_{pot}$ ), and kinetic molar exergy ( $\varepsilon_{kin}$ ).

$$\varepsilon_{total} = \varepsilon_{ph} + \varepsilon_{ch} + \varepsilon_{pot} + \varepsilon_{kin}$$

For the purposes of this work, both the kinetic and potential terms can be ignored as they are orders of magnitude lower in value than the chemical and physical terms. The physical molar exergy of a given stream can be calculated from the molar enthalpy ( $h$ ) and molar entropy ( $s$ ) of the stream at actual conditions and the molar enthalpy ( $h^0$ ) and molar entropy ( $s^0$ ) of the stream at the environmental temperature ( $T^0$ ) and pressure ( $P^0$ ):

$$\varepsilon_{ph} = (h_{T,P} - h_{T^0,P^0}) - T^0(s_{T,P} - s_{T^0,P^0})$$

The chemical molar exergy of an ideal gas stream can be calculated from the standard chemical exergies of the components ( $\varepsilon_{0,i}$ ) and the mole fraction they comprise in the stream ( $x_i$ ).

$$\varepsilon_{ch} = \sum_i x_i \varepsilon_{0,i} + RT^0 \sum_i x_i \ln x_i$$

In the above,  $R$  is the molar gas constant. The standard chemical exergies are defined based on atmospheric concentrations of the reference substances comprising the stream. If a substance is present in a stream which is not found in the reference state, or if a phase change occurs during the separation process, these reactions must be accounted.

For species formation:

$$\varepsilon_{ch,j}^0 = \Delta_f G_j^0 - \sum_k v_f \varepsilon_{ch,k}^0$$

In which  $\varepsilon_{ch,j}^0$  denotes the standard exergy of any species j,  $\varepsilon_{ch,k}^0$  denotes the standard chemical exergy of the element k in species j, and  $v_f$  denotes the stoichiometric coefficient of element k in species j.

For a species j in its phase  $\alpha$  can be calculated from the value in phase  $\beta$ :

$$\varepsilon_{ch,j}^{0,\alpha} = \varepsilon_{ch,j}^{0,\beta} + \Delta_{\beta \rightarrow \alpha} G_j^0$$

Where

$$\Delta_{\beta \rightarrow \alpha} G_j^0 = \Delta_f G_j^{0,\alpha} - \Delta_f G_j^{0,\beta}$$

The total exergy of any stream ( $E_{tot}$ ) can then be calculated by multiplying the total molar exergy ( $\varepsilon_{tot}$ ) by the molar flow rate ( $\varphi$ ):

$$E_{tot} = \varphi * \varepsilon_{tot}$$

The rational exergy efficiency ( $\psi$ ), also known as the second law efficiency, is a measure of the thermodynamic perfection of the process which can be calculated by dividing the ideal exergy change by the total used (real) exergy:

$$\psi = \frac{\Delta E^{Ideal}}{\Delta E^{Real}}$$

The definition of the ideal exergy change for the CPU can be calculated by subtracting the exergy contents of the separation products from the exergy content of the feed stream. The total real exergy is given by the specific work input to the CPU ( $E^{RSW}$ ), which is represented by the reported specific work of separation reported by CPU vendors.

$$2^{nd} \text{ Law Efficiency} = \psi = \frac{E^{Feed\_Inlet} - (E^{Water\_Prod} + E^{Inert\_Prod} + E^{CO2\_Prod})}{E^{RSW}}$$

The above quantity is evaluated on a kilowatt-hours required to separate a tonne of entrained carbon dioxide basis. This convention reflects the units used in industry both for the production of carbon dioxide from a CPU but also for oxygen production from an air separation unit. This relation can be arranged to calculate a real separation work value from the ideal work and 2<sup>nd</sup> Law Efficiency:

$$E^{RSW} = \frac{E^{Feed\_Inlet} - (E^{Water\_Prod} + E^{Inert\_Prod} + E^{CO2\_Prod})}{\psi}$$

The CPU model relies upon the ability to calculate a 2<sup>nd</sup> Law efficiency value from the published case studies and then predict the real separation work from the ideal separation work. The following section elaborates upon the process of calculating 2<sup>nd</sup> Law efficiency values as well as constructing the model for evaluating the ideal exergy change for an arbitrary feed stream.

## 7.5.5 MATLAB CPU Exergy Analysis Model

Computationally intensive processes involving access to detailed thermodynamic property data have historically been handled externally to the IECM. Reduced order models (ROMs) of these MATLAB or ASPEN models have then been created and embedded into the IECM to ensure computational efficiency is maintained. This ROM approach was adopted for the CPU model. The remainder of this section describes the MATLAB CPU Exergy Analysis used for calculating the ideal separation work and its adaptation to a model for use in the IECM.

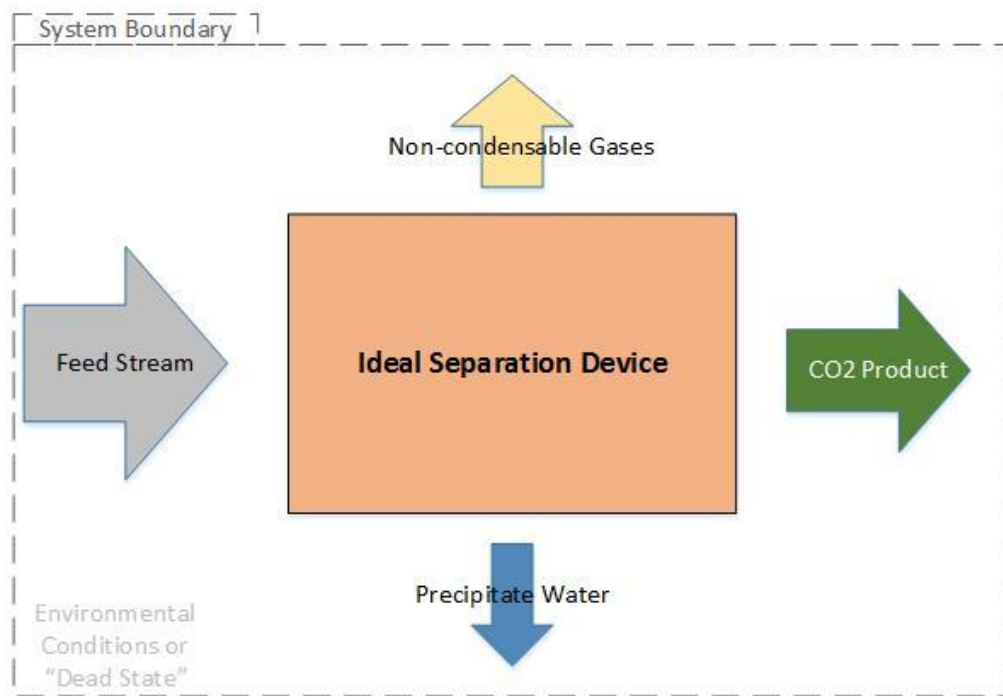


Figure 7.8 Diagram of the system used to conduct the exergy analysis as coded in MATLAB.

### 7.5.5.1 Approach

Utilizing an exergy analysis allows us to calculate the ideal separation work for arbitrary input and output streams while making the most of the extremely limited process flow information which is present in reports and literature. The exergy analysis across the three streams shown in the Figure EE, when completed across a variety of inlet flue gas compositions, CO<sub>2</sub> product purities, and CO<sub>2</sub> capture efficiencies was used to populate several sets of data tables that were then used to produce a reduced order model for the IECM. The last step was then to calculate the rational exergy efficiency for the systems for which we have stream information available. These few data points all yield similar exergetic efficiency values and allow us to make a general assumption about the efficiency of current separation equipment that can be used to adjust the minimum exergy tables to yield a specific work of

separation for any combination of flue gas composition, CO<sub>2</sub> product composition, and CO<sub>2</sub> capture efficiency.

#### 7.5.5.2 Assumptions

The MATLAB model assumes an inlet pressure of 90 kPa and temperature of 330K. This inlet temperature is assured by the overall mass/energy balance loop of the oxyfuel boiler and traditional pollution control systems through the use of a gas heater/cooler directly upstream of the carbon processing model. The outlet conditions for the three product streams are also assumed to be constant for all CPU scenarios investigated. Stream 2 and 3 below are directly reported as the exit states of each respective stream from the CPU in the IECM, but stream 1 exit conditions are an intermediate state prior to compression of the carbon dioxide product.

```
%State CPU CO2 Product (Outlet 1) Conditions
```

```
T1 = 298;  
P1 = 103000;
```

```
%State CPU Inerts (Outlet 2) Conditions
```

```
T2 = 298;  
P2 = 103000;
```

```
%State CPU Water (Outlet 3) Conditions
```

```
T3 = 330;  
P3 = oneatm;
```

The MATLAB code was created to account for only the change in physical and chemical exergy between the inlet and total product streams. All exergy changes resulting from the interaction of gases have been ignored because of the assumption of ideal gas behavior. Also, the code was set up to calculate the minimum separation work for a single kilogram of carbon dioxide entering into the separation system. The results of this calculation were then scaled to the actual mass flow rate processed by the CPU model. Hence there is no effect of scaling efficiency expressed in the CPU model directly. However, the process used for predicting the second law efficiency of the separation system does include the performance of the separation system at scale, thus there is some indirect inclusion of efficiency gains through equipment scaling. It is important to note however that, unlike the ASU where more data was available, the final IECM CPU model does not account for changes in system efficiency (i.e. specific separation work) associated with larger or smaller train sizes.

#### 7.5.5.3 MATLAB Exergy Analysis Code

For the complete code used for calculating minimum separation work please see Appendix C.

#### 7.5.5.4 *Generating Ideal Separation Work Response Surfaces*

The first step in producing a CPU ROM for the IECM was to exercise the MATLAB mode across a variety of representative inlet gas stream compositions and desired product compositions. The input parameters into the MATLAB model are as follows:

CO2inlet	Concentration of CO2 in CPU inlet stream [%]
N2inlet	Concentration of N2 in CPU inlet stream [%]
O2inlet	Concentration of O2 in CPU inlet stream [%]
Arinlet	Concentration of Argon in CPU inlet stream [%]
H2Oinlet	Concentration of Water in CPU inlet stream [%]
CRR	Carbon Dioxide Recovery Rate [%]
CPP	Carbon Product Purity [%]

These seven parameters were then run across CRR from 90 to 99.5% and CPP values from 95 to 100% for the nine inlet gas stream conditions presented in Table 7-2.

**Table 7-2 Composition of the inlet gas streams used in MATLAB Exergy Analysis**

<b>Carbon Dioxide</b>	<b>Oxygen</b>	<b>Argon</b>	<b>Nitrogen</b>	<b>Water</b>
50.0	4.2	5.0	12.5	28.3
60.0	3.3	4.0	10.0	22.7
68.0	6.0	7.0	12.0	7.0
70.0	2.5	3.0	7.5	17.0
75.0	6.0	4.0	8.0	7.0
80.0	1.7	2.0	5.0	11.3
81.0	5.0	5.0	8.0	1.0
85.0	2.0	3.0	6.0	4.0
90.0	0.8	2.0	2.5	4.7

Because the assumption of ideal gas behavior was used in the exergy analysis there is no functional difference between separating nitrogen from carbon dioxide or oxygen from carbon dioxide. If real gas behavior was assumed however, the similar fugacity values of carbon dioxide and oxygen would result in higher specific work values of separation for an oxygen and carbon dioxide mixture than for a mixture of nitrogen and carbon dioxide. This is an area where future work could improve upon this analysis and for completeness, the following product gas compositions in Table 7-3 were assumed for product streams of various CPP's.

Table 7-3 Composition of CO2 Product Streams for Various CPP Values

CO2 Purity	Oxygen	Argon	Nitrogen
95	0.925	1.7	2.4
96	0.74	1.36	1.92
97	0.555	1.02	1.44
98	0.37	0.68	0.96
99	0.185	0.34	0.48
100	0	0	0

For each set of input gas stream conditions a table of ideal separation work values was then populated across the feasible CPP and CRR values<sup>5</sup>. Table 7-4 presents the results of this exercise for an inlet stream composed of 70% carbon dioxide flue gas.

Table 7-4 Ideal separation work values as calculated by the MATLAB model [kWh/tonne CO2].

		CO2 Product Purity						
		99.98	99.5	99	98	97	96	95
Carbon Recovery Rate	99.5	20.47						
	98	20.1	19.65	19.27				
	96.5	19.92	19.47	19.1	18.45	17.88		
	95	19.82	19.37	19	18.37	17.82	17.31	
	92.5	19.77	19.33	18.97	18.36	17.82	17.33	16.88
	90	19.82	19.39	19.04	18.44	17.92	17.45	17.02
	87	19.82	19.39	19.04	18.44	17.92	17.45	17.02
	84	19.82	19.39	19.04	18.44	17.92	17.45	17.02
	81	19.82	19.39	19.04	18.44	17.92	17.45	17.02
	75	19.82	19.39	19.04	18.44	17.92	17.45	17.02
	70	19.82	19.39	19.04	18.44	17.92	17.45	17.02
	60	19.82	19.39	19.04	18.44	17.92	17.45	17.02
	50	19.82	19.39	19.04	18.44	17.92	17.45	17.02

An important trend to note from the above is that for carbon recovery rates below 90% the ideal separation work remains unchanged. This is because for these lower recovery rates a fraction of the flue gas would be routed around the CPU in a flue gas bypass rather than being processed through the cold box. Consequently, the ideal separation work for each tonne of captured carbon dioxide does not change. However, because fewer tonnes of carbon dioxide are being captured, the overall electrical power consumption of the CPU would be lowered.

To better visualize the behavior of the separation system, and also to demonstrate the effect of bypass on lower carbon dioxide recovery rates, the values for ideal separation work were recomputed on a

<sup>5</sup> Because the separation system was assumed to be a once through system it is not possible to achieve carbon recovery rates which are higher than the purity of the produced product stream.

tonne of carbon dioxide sent to the CPU basis and plotted. The resulting 3D graph for the 70% carbon dioxide inlet stream values is presented in Figure 7.9.

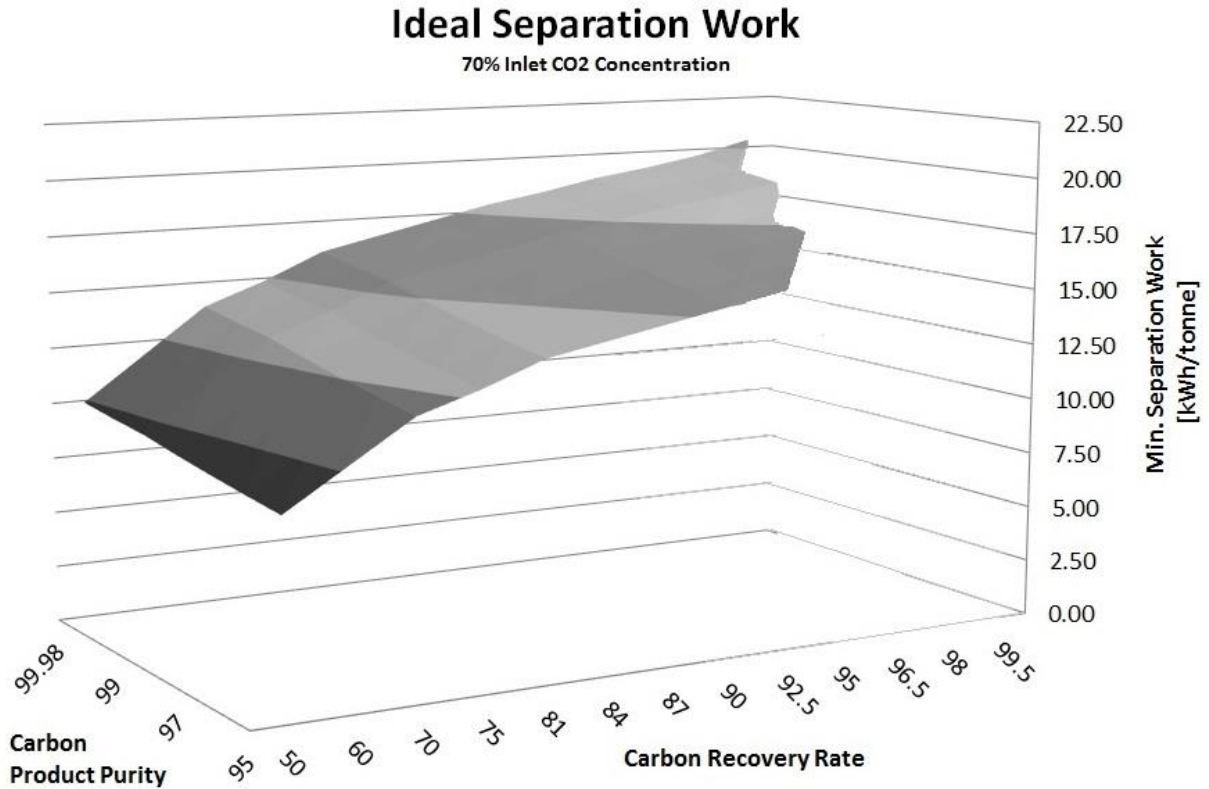


Figure 7.9 Three dimensional plot of the ideal separation data from the MATLAB model for a 70% carbon dioxide inlet stream converted to a flowrate to the CPU basis [kWh/tonne].

A similar process as demonstrated for the 70% carbon dioxide inlet stream was used for the remaining eight inlet compositions. The data generated for the nine inlet compositions comprised a data set of 702 observations. This minimum separation work data then needed to be reduced into a single, master model capable of being run quickly and simply in the IECM.

#### 7.5.5.5 Reduced Order Model Development

The calculation of separation energy in the IECM has been greatly simplified through the use of a reduced order model based upon hundreds of thermodynamic calculations performed using the GRI 3.0 database in MATLAB. These ideal separation work (ISW) calculations encompassed a wide range of expected carbon recovery rates and carbon product purities across several different anticipated inlet gas compositions. When a regression of these ideal calculations was completed using DataFit 9.0.59 Software to obtain a best fit equation for predicting minimum separation work based upon the seven input variables (CO<sub>2</sub>inlet, O<sub>2</sub>inlet, Arinlet, N<sub>2</sub>inlet, H<sub>2</sub>Oinlet, CRR, CPP) an R-squared value of 97.8% was obtained. This ideal separation work equation is exponential in form and includes six regression coefficients.

$$\text{Ideal Separation Work} = e^{a*X_1+b*X_2+c*X_3+d*X_4+e*X_5+f*X_6+g}$$

Where:

$X_1 = \text{CO}_2\text{inlet}$  Concentration of CO<sub>2</sub> in CPU inlet stream [%], range 50 – 100

$X_2 = \text{O}_2\text{inlet}$  Concentration of O<sub>2</sub> in CPU inlet stream [%], range 0 – 50

$X_3 = \text{Arinlet}$  Concentration of Argon in CPU inlet stream [%], range 0 – 50

$X_4 = \text{H}_2\text{Oinlet}$  Concentration of Water in CPU inlet stream [%], range 0 – 50

$X_5 = \text{CRR}$  Carbon Dioxide Recovery Rate [%], range: 50.0 – 99.5, default: 90

$X_6 = \text{CPP}$  Carbon Product Purity [%], range: 95.0 - 99.98, default: 99.5

With the Regression Coefficients:

$a = -0.0851$

$b = -0.0284$

$c = -0.159$

$d = -0.0491$

$e = 0.0141$

$f = 0.0422$

$g = 4.68$

Plotting the exponential regression model against the actual data demonstrates the functional form of the relation and provides a visual representation of the fit of reduced order model to the raw data.

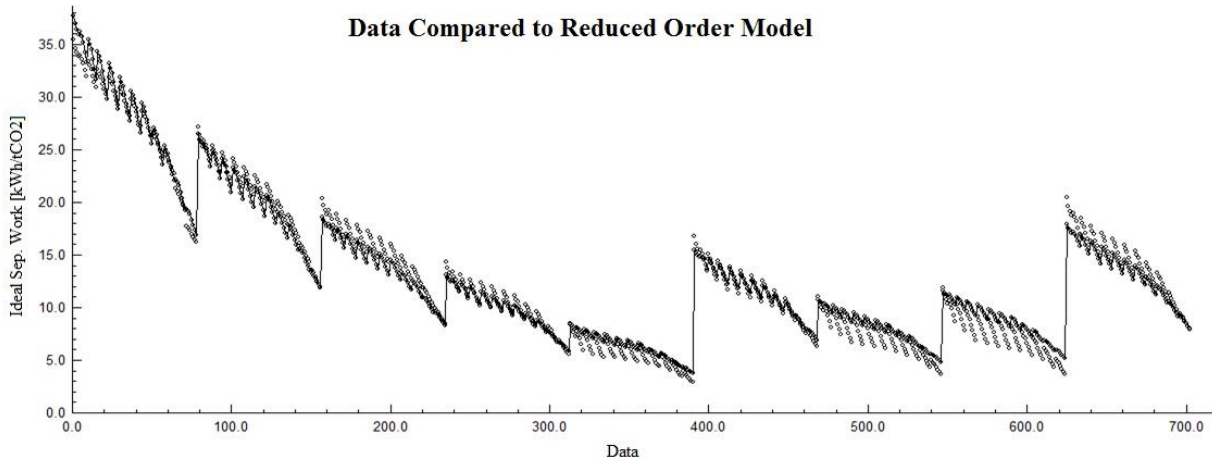


Figure 7.10 Plot of the reduced order model for ideal separation work along with the raw data from the MATLAB model.

It is clear from visual inspection and from the high R-squared value of 97.8% that the reduced order model does a respectable job of capturing the large trends in the ideal separation work data. However, there is considerable noise around the reduced order model for each of the nine inlet gas composition data sets where it appears the more subtle variances are not being particularly well reproduced by the reduced order model. A plot of the residual errors between the raw data and the reduced order model clearly shows the loss of fidelity internal to each of the nine inlet gas compositions.

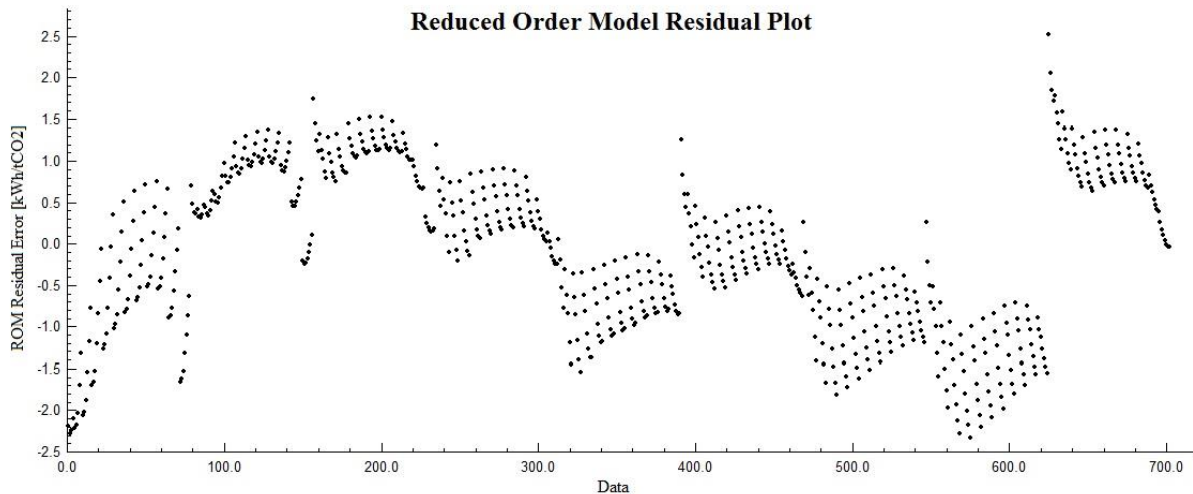


Figure 7.11 Residual error plot of the raw data from the MATLAB exergy analysis model and the exponential reduced order model generated using DataFit Software.

Examining the residual plot provides two prominent observations. The first is that the reduced order model does indeed lose the ability to accurately predict most of the fine grained differences in ISW internal to each inlet composition. The second is that because the intra-inlet composition differences are so small in magnitude, it is unlikely that losing this fine-grain fidelity is particularly important to the overall CPU model. The largest discrepancies between the raw data and the ROM occur with either very

high (>80%) or very low (<60%) CO<sub>2</sub> inlet concentrations. For the very high CO<sub>2</sub> inlet concentration cases there are a few instances where the predicted ISW value varies by nearly 2.5 [kWh/tonne CO<sub>2</sub>] and the magnitude of the ISW is only 10 [kWh/tonne CO<sub>2</sub>]. Admittedly, this is not ideal. However, these are very unlikely conditions to be present in an actual plant and even a difference of 2.5 [kWh/tonne CO<sub>2</sub>] only translates to an error of about 1.2 [MW] for the electrical load demand of the CPU at a capture rate of 500 tonnes CO<sub>2</sub> per hour (~550 [MWe]).

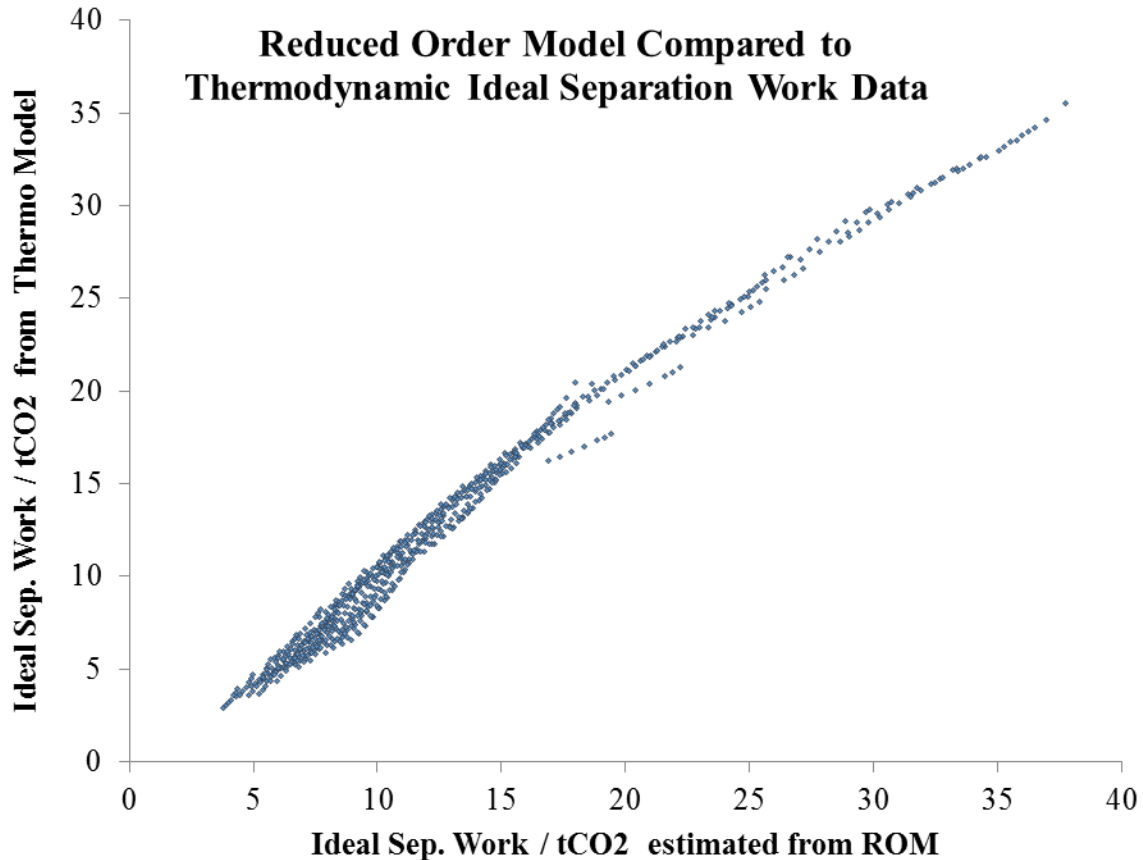


Figure 7.12 Comparison of ROM predicted ideal separation work values to the raw data generated from the MATLAB thermodynamic model shows that the overall fit is very good, but lacks some accuracy at very low values.

Although the reduced order model has some difficulty in capturing fine grained differences in ISW for varying CPP and CRR values for a given inlet CO<sub>2</sub> concentration and it has some difficulty in accurately predicting ISW values for very high CO<sub>2</sub> purity inlet streams, the overall fit of the ROM is very good. For the expected inlet CO<sub>2</sub> concentrations found under pulverized-coal oxyfuel conditions (near 70%), the ROM does an excellent job of forecasting the ISW. For the purposes of work conducted within the IECM modeling framework, the reduced order model provides a favorable compromise in favor of computational efficiency while still capturing the overall behavior and magnitude of the separation process modelled in MATLAB.

#### 7.5.5.6 Generating Real Separation Work Response Surfaces

Having produced a reduced order model to accurately predict the separation work required for an ideal separation device given a carbon dioxide capture rate and product purity, it is necessary to then be able

to translate that to a real separation device. In this work the assumed real separation device is a cryogenic carbon purification unit. As was outlined in *Theoretical Foundation* section at the beginning of this sub-chapter, the approach we adopted was to use the few case studies available to us to calibrate our ideal separation model to the real CPU systems in the NETL/DOE Oxyfuel case studies (36).

The seven parameters used in the MATLAB exergy analysis were extracted from each of the applicable case studies and input in the MATLAB model. An ideal separation work value for each case study was calculated and entered into Table 7-5 below along with all the other pertinent information from each case including a standard CO<sub>2</sub> compression allowance which was debited from the CPU specific work [kWh/tonne CO<sub>2</sub>] of all cases to calculate what we defined as the real separation work.

Table 7-5 DOE Case Studies with Ideal Separation Work Values from MATLAB Exergy Analysis

	<b>S12E</b>	<b>S12F</b>	<b>L12F</b>	<b>S13F</b>	<b>L13F</b>
<b>CPU [kWe]</b>	62,100	64,740	67,140	62,090	65,780
<b>CRR [%]</b>	90.9	89.5	90.8	90.8	90.8
<b>CPP [%]</b>	97.71	99.98	99.98	99.98	99.98
<b>CO<sub>2</sub> Product Flow [kg/hr]</b>	537,511	530,281	559,208	507,975	510,554
<b>CO<sub>2</sub> Yi [wt%]</b>	98.26	99.96	99.96	99.96	99.96
<b>CO<sub>2</sub> Flow [t/hr]</b>	528.2	530.1	559.0	507.8	510.3
<b>Specific Cooling Duty [GJ/tCO<sub>2</sub>]</b>	0.167	0.167	0.158	0.167	0.167
<b>Ideal Sep. Work [kWh/tCO<sub>2</sub>]</b>	18.23	19.88	19.27	19.82	20.62
<b>CPU Specific Work [kWh/tCO<sub>2</sub>]</b>	117.58	122.14	120.11	122.28	128.89
<b>Comp. Allowance [kWh/tCO<sub>2</sub>]</b>	89.4	89.4	89.4	89.4	89.4
<b>Real Separation Work [kWh/tCO<sub>2</sub>]</b>	28.18	32.74	30.71	32.88	39.49
<b>CO<sub>2</sub>/O<sub>2</sub> Feed Ratio</b>	31.22	31.37	30.92	31.66	19.19
<b>2nd Law Efficiency [%]</b>	64.69	60.73	62.75	60.28	52.21

Using the performance of several case studies, a benchmark for performance was established for each case study examined relative to the ideal performance predicted by the ideal model. In this fashion a metric for 2<sup>nd</sup> law efficiency (a comparison of the ideal vs. the real work required by a system) for the carbon processing units was established. A linear correlation was fit to the 2<sup>nd</sup> law efficiency data; which revealed a decreasing process efficiency as the desired product purity was increased. This relationship was expected. The ideal separation calculation has no mechanism for taking into account the work associated with high reflux rates which are necessary for reaching very high product purities. Therefore, it is necessary to use the below equation to predict the 2<sup>nd</sup> law efficiency of the separation system based upon CPP rather than use a set efficiency value.

$$2nd\ Law\ Separation\ Efficiency\ [\%] = -152.72 * CPP + 213.97$$

A further adjustment to 2<sup>nd</sup> law separation efficiency is done to account for the difficulty of separating gases with very similar volatilities. For example, because of the similarity in vapor pressure between carbon dioxide and oxygen as compared to water, it is much more difficult to separate an 80/20 mixture of CO<sub>2</sub>/O<sub>2</sub> than one of CO<sub>2</sub>/H<sub>2</sub>O. Due to the availability of NETL cases which were modeled at near

identical CPP and CRR rates but with different coal types (i.e. inlet flue gas compositions), a relative 2<sup>nd</sup> law efficiency equation could be constructed.

$$\text{Relative 2nd Law Separation Efficiency [\%]} = 1.21 * \frac{CO_2}{O_2} + 62.71$$

When the two 2<sup>nd</sup> law separation efficiency equations are computed and multiplied together, the resulting efficiency value can then be used to adjust the ideal separation work response surface to an expected real separation work surface. The surface below is real separation work surface for a 70% CO<sub>2</sub> inlet flue gas composition.

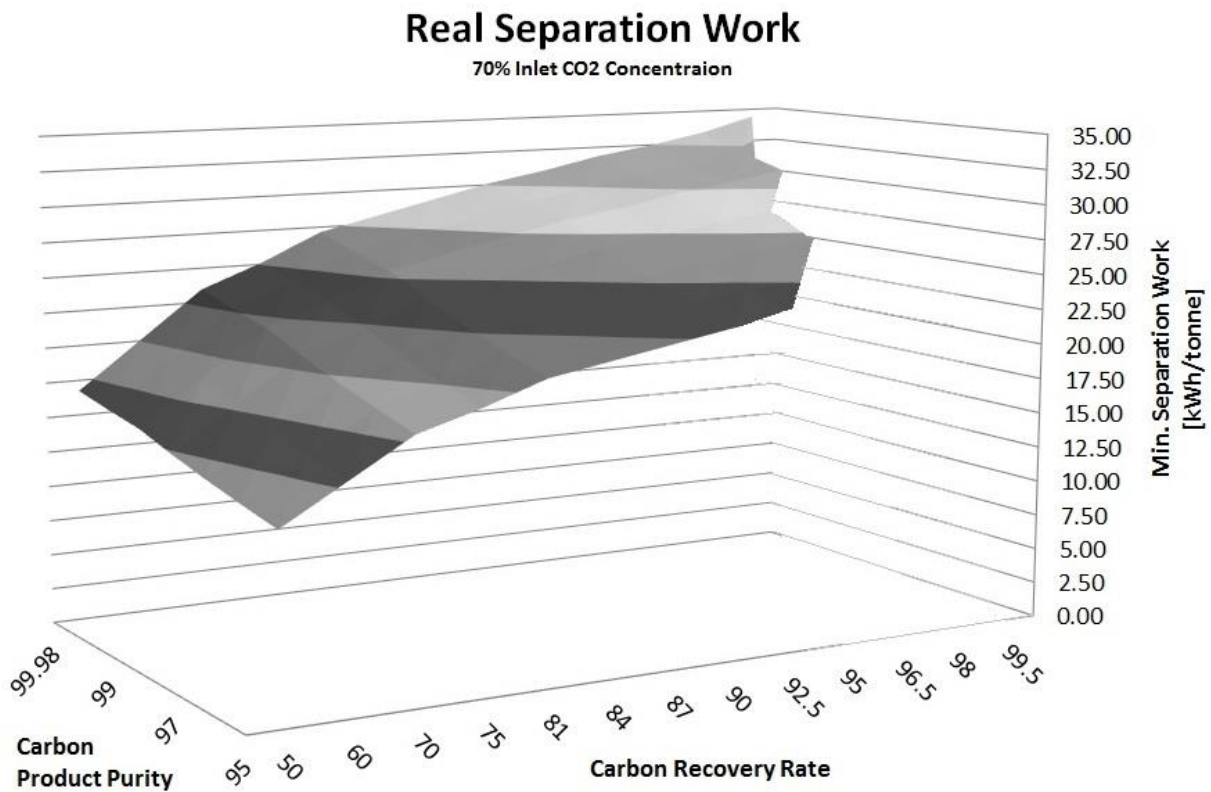


Figure 7.13 Three dimensional plot of the real separation work data from the MATLAB model for a 70% carbon dioxide inlet stream converted to a flowrate to the CPU basis [kWh/tonne] with the 2nd Law efficiency relation applied.

The response surface for the real separation work is greater in magnitude than the ideal separation work surface and is now notably tilted in favor of low CO<sub>2</sub> product purities as real systems which produce higher carbon dioxide purity are less efficient, on a second law efficiency basis, than are low purity systems. The contrast between ideal and real work is most easily visualized by superimposing the real and ideal work response surfaces onto one another as has been done in Figure 7.14.

## CPU Separation Work Surfaces

70% Inlet CO<sub>2</sub> Concentraion, Blue: Real, Red: Ideal

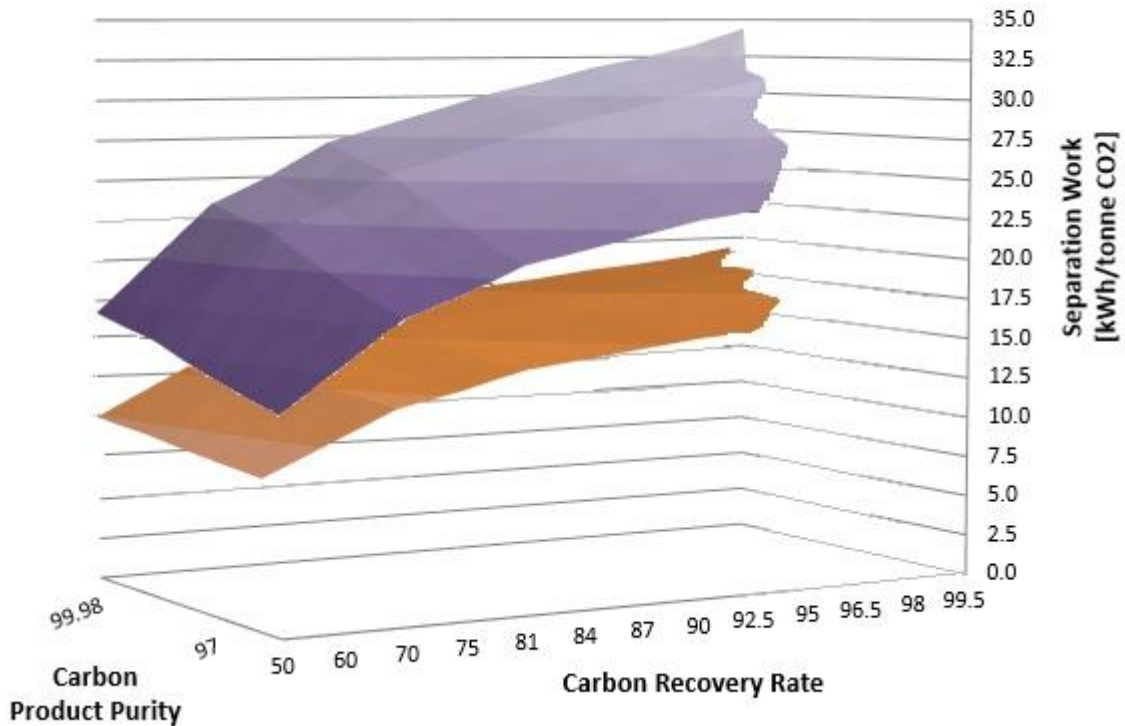


Figure 7.14 Three dimensional plot of the real (blue) and ideal (red) separation work response surfaces for a 70% carbon dioxide inlet stream

The final result of the complete exercise of calculating the ideal separation work using our created ROM, adjusting the ideal work using the second law separation efficiency values calculated from literature, then adding the compression work to raise the CO<sub>2</sub> product to pipeline pressure from the existing IECM compression model is that a total specific work [kWh/tonne CO<sub>2</sub>] value for the CPU model in the IECM can be calculated. We are able to closely replicate the CPU specific work values from literature using this process, but we have gained the ability for users to adjust CO<sub>2</sub> product pressure, CO<sub>2</sub> product purity, and CO<sub>2</sub> capture rate. Additionally, because of the addition of sound thermodynamic underpinnings, the CPU model can now be used confidently over a much greater variety of inlet stream compositions. This will allow the CPU model to be used not only for pulverized coal oxyfuel combustion, but for other carbon technologies which need product stream enrichment, such as chemical looping.

## 7.5.6 Summary of Input and Output Parameters

### Input Parameters

The key input parameters defining the performance of the CPU are as follows:

#### *User Specified Variables*

CPP	Carbon Product Purity [%], range: 95.0 - 99.98, default: 99.5
CRR	Carbon Dioxide Recovery Rate [%], range: 50.0 – 99.5, default: 90
$\eta_{Separation}$	2 <sup>nd</sup> Law Efficiency for the Separation Process [%], range: 0.01 – 100.00

#### *Passed From IECM*

CO2inlet	Concentration of CO2 in CPU inlet stream [%], range 50 – 100
N2inlet	Concentration of N2 in CPU inlet stream [%], range 0 – 50
O2inlet	Concentration of O2 in CPU inlet stream [%], range 0 – 50
Arinlet	Concentration of Argon in CPU inlet stream [%], range 0 – 50
H2Oinlet	Concentration of Water in CPU inlet stream [%], range 0 – 50
$\dot{M}_{inlet}$	Mass flow rate of the CPU inlet stream
$\dot{M}_{CO2}$	Mass flow rate of CO2 in the CPU inlet stream

### Output Parameters

The model will then calculate or report the following key output parameters:

$MW_{CPU}$	Total electric load for the carbon processing unit [kW]
$\varphi_{CP}$	Molar flow rate of carbon dioxide product stream [mol/sec]
$\varphi_{inerts}$	Molar flow rate of the non-condensable, inert gas stream [mol/sec]
$\dot{M}_{precip\_water}$	Mass flow rate of removed water stream [tonnes/hr]
CO2/O2	Ratio of inlet conc. of CO2 and O2, used for correcting the 2 <sup>nd</sup> law sep. efficiency

## 7.5.7 Mass and Energy Balance Calculations

The following sections run through the mass and energy accounting of all the streams highlighted in Figure 7.15. The cooling water in and out streams are representative of the bulk cooling duty which must be performed, but this cooling could be handled either by boiler feed water heating or through the

use of cooling water from the base plant. Lastly, the terms “non-condensable gases” and “inerts” are used interchangeably throughout this document for shorthand when writing equations.

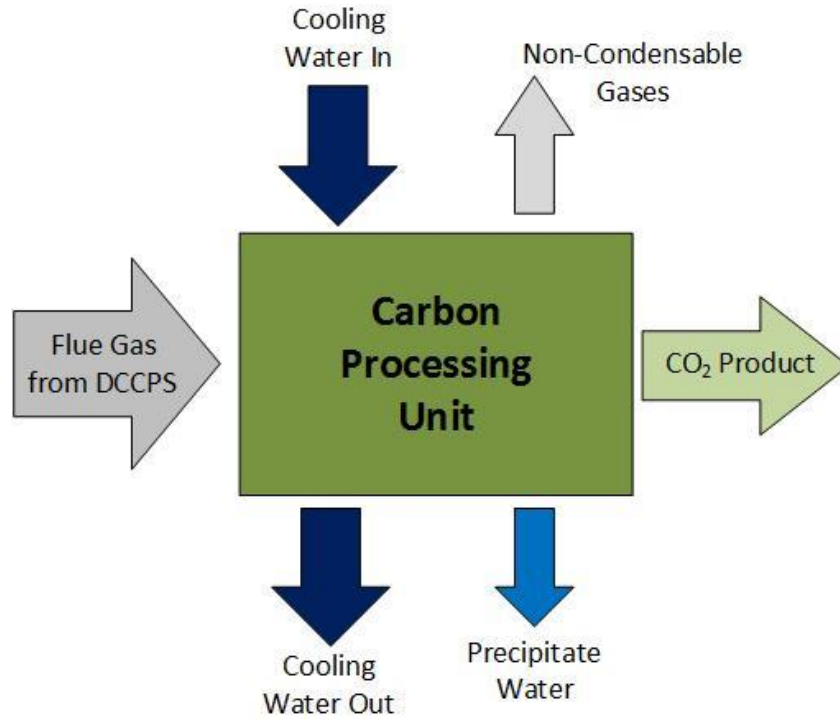


Figure 7.15 Process flow diagram of all the gas and liquid streams entering and exiting the CPU.

#### 7.5.7.1 Carbon Dioxide Product and Inert Gas Streams

In the parlance of the overall oxyfuel model in the IECM, the total molar flow rate of flue gas sent to the CPU from the direct contact cooler and polishing scrubber (DCCPS) can be defined as:

$$\varphi_{to\_CPU} = \sum \varphi_{i,to\_CPU} = (1 - \beta) * \sum \varphi_{i,fg\_exit}$$

Where the following comes from the DCCPS Model:

$\varphi_{i,fg\_exit}$  is the molar flow rate [mol/sec] of species (i) in the exiting flue gas

$(1 - \beta)$  is the fraction of the flue gas exiting the DCCPS which is sent to the CPU

It follows then that the total molar flow rate of carbon dioxide sent to the CPU from the DCCPS can be calculated in the following manner:

$$\varphi_{CO2,to\_CPU} = (1 - \beta) * \varphi_{CO2,fg\_exit}$$

The quantity of this carbon dioxide entrained in the carbon dioxide product gas produced by the CPU is directly proportional to the carbon recovery rate (CRR):

$$\varphi_{CO2,CP} = \left( \frac{CRR}{100} \right) * \varphi_{CO2,to\_CPU}$$

The quantity of carbon dioxide which is vented from the CPU along with the non-condensable inert gases can then be calculated as:

$$\varphi_{CO_2,inerts} = \left(1 - \frac{CRR}{100}\right) * \varphi_{CO_2,to\_CPU}$$

In order to determine the molar flow rate of Argon, Nitrogen, and Oxygen entrained in the carbon dioxide product stream the following relations need to be used to calculate the molar fraction of each gas:

$$x_{Argon\_CP} = -\left(0.3393 * \frac{CPP}{100}\right) + 0.3393$$

$$x_{Nitrogen\_CP} = -\left(0.4802 * \frac{CPP}{100}\right) + 0.4802$$

$$x_{Oxygen\_CP} = -\left(0.185 * \frac{CPP}{100}\right) + 0.185$$

The molar flow rate of these three gases in the carbon dioxide product stream can then be calculated as:

$$\varphi_{Argon\_CP} = \frac{(100 * \varphi_{CO_2\_CP} * x_{Argon\_CP})}{CPP}$$

$$\varphi_{Nitrogen\_CP} = \frac{(100 * \varphi_{CO_2\_CP} * x_{Nitrogen\_CP})}{CPP}$$

$$\varphi_{Oxygen\_CP} = \frac{(100 * \varphi_{CO_2\_CP} * x_{Oxygen\_CP})}{CPP}$$

The total molar flow rate of the carbon dioxide product stream, for a given CPP and CO<sub>2</sub> molar flow rate, is simply the following sum:

$$\varphi_{CP} = \varphi_{CO_2,CP} + \varphi_{Argon\_CP} + \varphi_{Nitrogen\_CP} + \varphi_{Oxygen\_CP}$$

The total molar flow rate of the inert stream can then be calculated:

$$\varphi_{inerts} = \sum_k (\varphi_{i,to\_CPU} - \varphi_{i,CP})$$

Where

$k$  is all gas species excluding water

$\varphi_{i,to\_CPU}$  is the molar flow rate of species (i) to the CPU [mol/sec]

$\varphi_{i,CP}$  is the molar flow rate of species (i) entrained in the CO<sub>2</sub> product [mol/sec]

Water has been specifically excluded from the inert stream because it must be completely removed prior to the flue gas entering the cold box of the CPU. The removal of water from the flue gas sent to the CPU is dealt with explicitly in the following section.

### 7.5.7.2 Precipitate Water Production

In the carbon processing units which we evaluated in literature the most common method for removing residual moisture from the flue gas stream produced by the direct contact cooler was a two-step procedure. The remaining bulk moisture was removed from the flue gas through compression with after cooling to precipitate out nearly all remaining water. The remaining trace moisture was then removed with a desiccant based, fixed bed dryer. The desiccant drying is necessary to prevent icing in the cold box of the carbon processing unit which could result in equipment failure. In practice the desiccant dryer is typically comprised of two or three beds which allow for at least one bed to be in service while another is being regenerated using the produced inert gas stream from the cold box to remove moisture from the desiccant.

In our CPU model we did not have adequate performance information to model the desiccant dryer in great detail. Furthermore, we did not identify this as a high priority as these systems are a fully mature technology in the gas processing industry and their performance and cost does not have a large impact on the overall performance or cost of the CPU system. However, it is still necessary to account for the sizable mass flow rate of the precipitate water removed upstream of the cold box in addition to the cooling which must be provided. The calculations for determining the mass flow rate of precipitate water are provided below. The cooling water required to condense out the precipitate water during compression is accounted for in the following section on cooling water requirements.

The flue gas passed to the CPU is assumed to have the same characteristics as the flue gas had upon exiting the direct contact cooler (DCCPS). The molar fraction of water in this flue gas is determined by the operational characteristics of the DCCPS and can be altered by the user. The CPU needs to remove all of the remaining water left after the flue gas has been processed by the DCCPS. Thus calculating the quantity of water which needs to be removed the CPU is rather straight forward once the incoming flue gas stream from the DCCPS is known because all of the water must be removed as precipitate.

The molar flow rate of water is:

$$\varphi_{H2O,to\_CPU} = (1 - \beta) * \varphi_{H2O,fg\_exit}$$

And the mass flow rate of water which is removed in the form of precipitate by the CPU is:

$$\dot{M}_{precip\_water} \left[ \frac{\text{tonnes}}{\text{hr}} \right] = 0.0036 * \varphi_{H2O,to\_CPU} * mW_{H2O}$$

Where:

$mW_{H2O}$  is the molecular weight of water [g/mol]

$\varphi_{H2O,to\_CPU}$  is the molar flow rate of water to the CPU [mol/sec]

$\dot{M}_{precip\_water}$  is the mass flow rate of the removed water stream [tonnes/hr]

### 7.5.7.3 Cooling and Heat Integration

The relations developed for calculating the cooling duty of the carbon processing unit are based on a combination of DOE Case Studies (36) and the pre-existing carbon dioxide compression module in the IECM. This method separates the cooling duty of compression from the other cooling requirements of

the CPU which allows us to keep the compression cooling code the same across all CCS systems in the IECM. Table 7-6 below presents values from several case studies in the DOE Oxyfuel Report along with many of the calculations used to formulate the cooling relations.

Table 7-6 CPU Cooling Duty Information

	Case Studies from 2010 DOE Oxyfuel Report						
	S12C	S12D	S12E	S12F	L12F	S13F	L13F
CO2 Cooling [GJ/hr]	300.6	134.8	227.7	227.4	239.2	275	291.4
CPU BFW Enthalpy In [kJ/kg]	217.35	217.35	217.35	217.35	217.35	238.79	238.79
CPU BFW Enthalpy Out [kJ/kg]	616.44	616.44	616.44	616.44	616.44	615.94	615.94
CPU BFW Enthalpy Delta [kJ/kg]	399.09	399.09	399.09	399.09	399.09	377.15	377.15
CPU BFW Flow [kg/hr]	505,327	509,083	221,510	221,541	221,130	224,795	226,048
CPU BFW Duty [GJ/hr]	201.67	203.17	88.40	88.41	88.25	84.78	85.25
CO2 Product Flow [kg/hr]	665,626	671,065	537,511	530,281	559,208	507,975	510,554
CO2 Yi [wt%]	0.878	0.884	98.26	99.96	99.96	99.96	99.96
CO2 Flow [t/hr]	584.3	593.4	528.2	530.1	559.0	507.8	510.3
Specific (BFW) Cooling Duty [GJ/tCO2]	0.345	0.342	0.167	0.167	0.158	0.167	0.167
Specific Cooling Duty [GJ/tCO2]	0.515	0.227	0.431	0.429	0.428	0.542	0.571
Total CPU Cooling Duty [GJ/hr]	528.27	365.57	343.10	343.01	366.45	359.78	376.65
Total Specific CPU Cooling Duty [GJ/tCO2]	0.904	0.616	0.650	0.647	0.656	0.709	0.738
Total Specific CPU, less Comp. Cooling Duty [GJ/tCO2]	0.390	0.389	0.218	0.218	0.228	0.167	0.167
KO Water [GJ/hr]	26	27.6	27	27.2	39	25.8	37.5
CPU Heat Integration [% Cooling Duty Recovered]	38%	56%	26%	26%	24%	24%	23%

The ability to recoup heat energy from the large compressors in the ASU and CPU can be key to reducing the steam cycle heat rate and consequently increasing the overall efficiency of the plant. With this in mind, the relations were constructed to calculate the total cooling duty requirement for each piece of equipment regardless of the extent of heat integration. This allows the extent of heat integration to be a user specified variable in the IECM while utilizing just one set of cooling duty relations in order to determine the amount of cooling water needed to provide residual cooling to the compression units. Keeping accordance with the commonly used unit system in industry, the cooling duty relations for the CPU were created on a gigajoule of cooling duty per tonne of carbon dioxide throughput basis.

$$CPU_{CoolingDuty} \left[ \frac{GJ}{tCO_2} \right] = \left( 0.22 + \left\{ \frac{Comp_{CoolingDuty}}{\dot{M}_{CO_2}} \right\} \right) * (1 - HI_{CPU})$$

Where

$HI_{Cpu}$  is the fraction of cooling duty which can be recovered in the steam cycle through BFW heating

Min = 0.0, Max = 0.6, Default = 0.0 (0.25 representative)

$Comp_{CoolingDuty}$  is the cooling duty [GJ/hr] currently being calculated in the IECM for compression

$\dot{M}_{CO_2}$  is the mass flow rate of carbon dioxide through the compressor [tonnes/hr]

### Cooling Water Requirements

In plant configurations with a CPU the total amount of cooling water required to provide the calculated cooling duty is determined by a function of four parameters:

$\alpha_{Cooling}$	heat transfer efficiency of CPU system (unity being ideal heat transfer)
$Cooling\ Duty$	total cooling duty [GJ/tonne CO <sub>2</sub> ]
$\Delta T_{max,Cooling\ water}$	largest acceptable temperature increase of cooling water [K]
$Cp_{Cooling\ water}$	specific heat of cooling water, default value of 0.0042 [GJ/t K]

The required mass flow of cooling water can then be calculated:

$$\dot{M}_{Cooling\ water} \left[ \frac{tonne}{tonne\ CO_2} \right] = \frac{Cooling\ Duty}{\alpha_{Cooling} * Cp_{Cooling\ water} * \Delta T_{max,Cooling\ water}}$$

### Heat Integration

The heat integration of the carbon processing unit is calculated in a similar fashion to the cooling duty above being that it is simply the fraction of the overall cooling duty which does not need to be met with cooling water. For ease of combining the heat integration duty from the carbon handling system with that of the ASU, the relations have been altered to produce values with common units of [GJ/hr]. For a plant equipped with a carbon processing unit:

$$CPU_{HIDuty} \left[ \frac{GJ}{hr} \right] = ((0.22 * \dot{M}_{CO_2}) + Comp_{CoolingDuty}) * HI_{CPU}$$

Where

$HI_{CPU}$  is the fraction of cooling duty which can be recovered in the steam cycle through BFW heating

Min = 0.0, Max = 0.6, Default = 0.0 (0.25 representative)

$Comp_{CoolingDuty}$  is the cooling duty [GJ/hr] currently being calculated in the IECM for compression

$\dot{M}_{CO_2}$  is the mass flow rate of carbon dioxide through the compressor [tonnes/hr]

The heat integration duty of the carbon processing unit is added with the heat integration duty of the ASU to provide the total heat integration duty of the oxyfuel plant. Details on calculating the effects on performance from heat integration can be found in Section 4.5.5 of the overall mass and energy balance plant details.

#### 7.5.7.4 Electrical Load Requirement

Calculating the electrical power required to operate the CPU only requires a few steps at this point. The first is to use the reduced order model generated from the DataFit Software to calculate the ideal separation work for the system conditions:

$$\text{Ideal Separation Work} \left[ \frac{kWh}{\text{tonne CO}_2} \right] = e^{a*X_1+b*X_2+c*X_3+d*X_4+e*X_5+f*X_6+g}$$

Where:

$X_1 = \text{CO}_2\text{inlet}$  Concentration of CO<sub>2</sub> in CPU inlet stream [%], range 50 – 100

$X_2 = \text{O}_2\text{inlet}$  Concentration of O<sub>2</sub> in CPU inlet stream [%], range 0 – 50

$X_3 = \text{Arinlet}$  Concentration of Argon in CPU inlet stream [%], range 0 – 50

$X_4 = \text{H}_2\text{Oinlet}$  Concentration of Water in CPU inlet stream [%], range 0 – 50

$X_5 = \text{CRR}$  Carbon Dioxide Recovery Rate [%], range: 50.0 – 99.5, default: 90

$X_6 = \text{CPP}$  Carbon Product Purity [%], range: 95.0 - 99.98, default: 99.5

With the Regression Coefficients:

$a = -0.0851$

$b = -0.0284$

$c = -0.159$

$d = -0.0491$

$e = 0.0141$

$f = 0.0422$

$g = 4.68$

Then the real separation work can be calculated from the combined second law efficiency equation and the ideal separation work:

$$Real\ Sep.\ Work\ \left[ \frac{kWh}{tonne\ CO_2} \right] = \frac{Ideal\ Sep.\ Work}{\eta_{separation}}$$

With:

$$\eta_{separation} = \left( -1.5272 * \left( \frac{CPP}{100} \right) + 2.1397 \right) * \left( 0.0121 * \left( \frac{CO_2}{O_2} \right) + 0.6271 \right)$$

Where:

$\frac{CO_2}{O_2}$  is the molar ratio of carbon dioxide and oxygen sent to the CPU

With the above calculations completed for calculating the expected real separation work [kWh/tonne CO<sub>2</sub>], the mass flow of carbon dioxide through the system must be taken into account in order to determine the energy demand of the separation process.

$$\dot{M}_{CO_2, to\ CPU} \left[ \frac{tonnes}{hr} \right] = 0.0036 * \varphi_{CO_2, to\ CPU} * mw_{CO_2}$$

Where:

$mw_{CO_2}$  is the molecular weight of carbon dioxide [g/mol]

$\varphi_{CO_2, to\ CPU}$  is the molar flow rate of CO<sub>2</sub> sent to the CPU [mol/sec]

$\dot{M}_{CO_2}$  is the mass flow rate of the CO<sub>2</sub> sent to the CPU [tonnes/hr]

$$MW_{CPU} = \dot{M}_{CO_2} * Real\ Sep.\ Work$$

## Chapter 8 Pulverized Coal Oxyfuel Cost Model

The economic portion of the update to the pulverized coal oxyfuel model is essential to ensuring that case studies produced from the IECM are representative of current technology and the evolution in the design of oxyfuel systems which has occurred in the past decade. Where possible, an effort has been made to utilize cost estimates which allow the creation of cost models which are a function of the mass flowrate processed by the technical component. For other important cost areas, the most recent cost estimates have been used to supplant the previously existing reference cases.

The integrated nature of oxyfuel requires that many of the pre-existing technical components: sulfur removal, particulate removal, waste water treatment, and the entirety of the base plant are exercised when any techno-economic estimate is produced in the IECM. Substantial documentation for all of these components exists and has been referenced, where appropriate, so that the reader may easily obtain additional information on the cost estimation of all these supporting technical areas.

The system cost areas, specific to oxyfuel, may be broadly divided into four categories. Three of these categories are defined by large pieces of equipment while the fourth is a catch-all which includes costs associated with flue gas recirculation and increases in boiler costs. The three major equipment areas are the air separation unit, direct contact cooler and polishing scrubber, and the carbon handling system. The following sections describe the overall methodology for producing cost estimates in the IECM as well as outlining the calculation of the respective process facility costs (PFC) and variable operations and maintenance costs (VOM) for each of the novel oxyfuel components.

### 8.1 Plant Costing Method

The methodology used for producing financial estimates in the IECM is reflective of the methodology prescribed by the Electric Power Research Institutes' (EPRI) Technical Assessment Guide (62). To help the reader better understand this methodology, this first section is devoted to providing a high level overview of the costing methodology.

#### 8.1.1 Cost Model Terminology

**Process Facilities Capital** is the total cost of all on-site processing and generating units with direct and indirect constructed costs accounted. For each overall plant configuration, the PFC should be divided into major unit components such as individual pollution control technologies, pumps, compressors, etc. Where sufficient information is available, each major unit will be subdivided further into materials, construction labor, and indirect field costs. It is not uncommon that fine resolution detail on materials, construction labor, etc. is not available for the unit components which make up an overall plant configuration. This is especially true with novel or proprietary technologies such as air separation or carbon processing units.

**General Facilities Capital** is the total construction cost of general support facilities and includes: roads, office buildings, shops, labs, etc. This cost is treated as an adder and is normally in the range of 5-20% of the process facilities capital.

**Engineering & Home Office** fees account for the cost of engineering and office overhead for the purpose of actually producing the estimate for the cost of the unit in question. These fees typically comprise an adder of 7-15% of the process facilities capital.

**Contingencies** are used in the creation of cost estimates to account for uncertainty in the cost estimate.

- **Project Contingency** covers the uncertainty in the cost estimate which inherently results from the cost estimate lacking detailed design information from a definite project at an actual sight. This contingency value is used to reflect the degree of design effort put into the project and ranges from 5-10% for finalized designs to 30-50% for simplified designs. Most designs in the IECM fall under the Preliminary design category and carry project contingency values of 15-30%.
- **Process Contingency** covers the uncertainty in the technical performance of the unit whose cost is being estimated. This contingency value can be a relatively small adder on the PFC of less than 5% for mature technology units such as sub-critical boilers where there is extensive experience from completed projects to draw from. Conversely, for immature or novel technologies (most carbon capture specific units) the project contingency adder can range from 5-40+% of PFC depending upon the degree of development.

**Allowance for Funds Used During Construction (AFUDC)** is a financial adjustment factor which takes into account the time value of money during the construction period. Because the costs of construction are incurred over several years, rather than at a single moment in time, the overnight cost (TPC) does not capture the true cost of erecting the plant. The total capital expenditure (TCE) is a mixed-year dollar expression of the TPC over the construction period. Once capital is spent in any given year during construction, interest begins to accumulate on those funds. Incurred interest costs, along with an adjustment for the annual escalation rate for the cost of plant equipment, are used to calculate the total plant investment (TPI) at the in-service date. The disparity between TPI and TCE is known as the AFUDC.

**Owners Costs** are a broad, catch-all type category to account for the remaining costs which need to be incorporated in assessing the total cost of a project.

- **Prepaid Royalties** may apply to those plant components utilizing new and/or proprietary technologies or processes. If the applicable royalty fee is known it should be explicitly accounted for, but for proprietary processes with an uncertain royalty, a value of 0.5% of PFC is recommended.
- **Preproduction Costs**, or start-up costs as they are alternatively known when combined with the following category, cover operator training, extra maintenance, and inefficient use of consumables during startup.
- **Initial Cost for Catalyst and Chemicals** contained in the process equipment in the plant, but not that held in inventory, is to be included.

- **Inventory Capital** is the value of all fuel, consumable, and by-product inventories along with an allowance for spare parts. EPRI outlines specific inventory levels depending upon the intended function of the plant.
- **Land** costs vary and are extremely site-specific. However, depending upon the level of cost detail, either a specific or nominal value for the cost of land is to be included.

### 8.1.2 Total Capital Requirement

The total capital requirement for a plant (either a specific piece of equipment or the entire facility) is calculated using the same formulation. Provided in the following paragraph and in Figure AA are two supporting explanations of the TCR formulation. If greater detail on the specific financial mathematics involved in the calculation of TCR is required, please reference the EPRI Technical Assessment Guide.

The total plant cost (TPC) is the sum of the process facilities capital (PFC), general facilities capital, engineering and home office fees, and contingencies (project and process). The project contingency is a capital cost factor covering the cost of additional equipment or other costs that would result from a more detailed design at an actual site. The process contingency is a capital cost factor applied to a technology to reflect its level of maturity. TPC is developed on the basis of instantaneous (“overnight”) construction occurring at a single point in time, and is generally expressed in mid-year dollars of a (user-specified) reference year. The total capital requirement (TCR) includes all the capital necessary to complete the entire project, including interest during construction (AFUDC) and owner costs, which include: royalties, startup costs, land, and inventory capital.

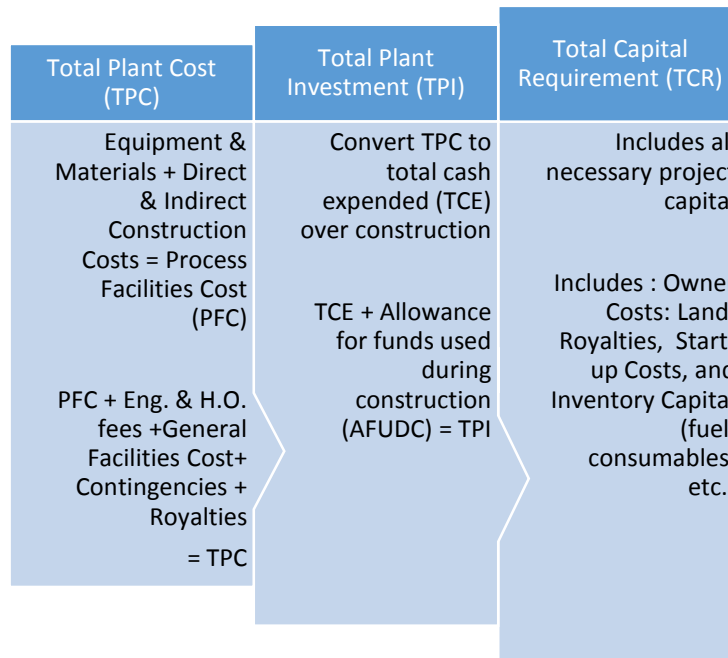


Figure 8.1 Flow chart of how cost estimates get built up from the equipment cost to the total capital required for both plant components and the overall plant.

The calculation of the total capital requirement in the IECM is handled using the procedure outlined above and the capital cost elements (A, C-M for component or B-M for overall plant) outlined in Table AA below.

**Table 8-1 Capital Cost Elements and Valuation in the IECM**

	<b>Capital Cost Elements</b>	<b>Equation or Value</b>
A	Process Facilities Capital (PFC)	$PFC_i$
B	Engineering and Home Office	= 7% PFC
C	General Facilities	= 10% PFC
D	Project Contingency	= 15% PFC
E	Process Contingency	= 5% PFC
F	Total Plant Cost (TPC) = sum of above	= A + B + C + D + E
G	AFUDC (interest during construction)	Calculated
H	Royalty Fees	= 0.5% PFC
I	Pre-production	= 1 month's fixed O&M cost
J	Pre-production	= 1 month's variable O&M cost
K	Inventory Cost	= 0.5% TPC
L	Total Capital Requirement (TCR)	= F + G + H + I + J + K

The values of capital cost elements B-E, H, and K are simply representative values for a mature technology component such as a flue gas desulfurization unit. As discussed in the terminology section above, the values for royalties and contingencies can vary from component to component depending on commercial maturation, the quality of the cost estimate, and whether a technology is proprietary. With the exception of capital cost elements A, G, and L the remaining elements can be found on the Capital Cost tab under Set Parameters (SET PARAMETERS/Component (i)/Capital Cost) for each major cost component in the IECM. Each major cost component is also designated a construction time which allows for elements G and L to be calculated. Once the total capital requirement for each component has been calculated individually, the sum value is presented as the total capital requirement for the overall plant (GET RESULTS/Overall Plant/Total Cost).

### 8.1.3 General Component Size and Cost Year Adjustment

The PFC calculations for most components in the oxyfuel model comprise some metric which accounts for the size (mass/volumetric flow) of the component. For those component areas where sufficient cost detail across sizes is not available, costs are scaled using a 0.6 cost scaling index. The cost scaling index is applied to a ratio of the relevant scaling parameter (X), which is typically a throughput flow rate or power consumption. All PFC values are also adjusted to the cost year specified by the IECM user using the Chemical Engineering Plant Cost Index (PCI).

$$PFC_i = PFC_{i,reference} * \left( \frac{X_i}{X_{i,reference}} \right)^{0.6} * \left( \frac{PCI}{PCI_{reference}} \right)$$

Where:

- $PFC_i$  cost value of cost area (i) for a user's case study
- $PFC_{i,reference}$  reference cost for cost area (i), given a specific reference case
- $X_i$  value of relevant scaling parameter (i) for user's case study
- $X_{i,reference}$  value of scaling parameter (i) for reference case study
- $PCI$  plant cost index for year of user's case study
- $PCI_{reference}$  plant cost index of reference year in which costs were reported

The Chemical Engineering Plant Cost Indices in Table 8-2 cover all the base years for which original cost estimates were produced for equipment modeled in the IECM. It is considered good practice to not index costs over a span of more than 8-10 years. A concerted effort has been made to ensure that all major cost components are as recent as possible. The majority of reference cost years are within 4-5 years with only a few minor components having original base years which are greater than 10 years old.

Table 8-2 Plant cost index (CEPCI (63)) for all years in which reference cost estimates were performed

Year	PCI		Year	PCI
2012	584.6		2002	395.6
2011	585.7		2001	394.3
2010	539.1		2000	394.1
2009	522		1999	390.6
2008	575.4		1998	389.5
2007	525.4		1997	386.5
2006	499.6		1996	381.7
2005	468.2		1995	381.1
2004	444.2		1994	368.1
2003	402		1993	359.2

### 8.1.4 General Operations and Maintenance Cost

For any given process component there are a litany of costs associated with its operations and maintenance. Although there are certain cost areas for each technology which are unique to that individual process, there are a number of cost areas which it will share with all other components under the EPRI TAG guidelines. The first of these is the cost of labor for operating, maintaining, and the administration overseeing operations. Labor is considered to be a fixed cost (FOM) in the TAG and is formulated in the following fashion:

$$FOM_i = FOM_{labor,i} + FOM_{maint,i} + FOM_{admin,i} \quad (1)$$

$$FOM_{labor,i} = wage \left[ \frac{\$}{hr} \right] * N_{labor,i} \left[ \frac{jobs}{shift} \right] * N_{shifts,i} \left[ \frac{shifts}{day} \right] * 40 \left[ \frac{hrs}{week} \right] * 52 \left[ \frac{weeks}{year} \right] \quad (2)$$

$$FOM_{maint,i} = fom_{maint,i} * TPC_i \quad (3)$$

$$FOM_{admin,i} = fom_{admin,i} * (FOM_{labor,i} + fom_{maintlab,i} * FOM_{maint,i}) \quad (4)$$

Where:

- i* a given process area (ASU, CPU, etc.)
- wage* hourly wage paid to labor [\$/hr]
- N<sub>labor,i</sub>* number of operating labor required per shift
- N<sub>shifts,i</sub>* number of labor shifts per day
- fom<sub>maint,i</sub>* annual maintenance cost expressed as fraction of TPC for given process area
- fom<sub>maintlab,i</sub>* fraction of maintenance cost allocated to labor
- fom<sub>admin,i</sub>* administrative labor cost expressed as a fraction of the total labor cost

In the IECM, FOM cost elements A-E can be found on the O&M tab of the component in question under set parameters (SET PARAMETERS/Component (i)/O&M Cost). Equations 1-4 are used to determine the total FOM for each component once values are provided by the user or the defaults are accepted.

Table 8-3 O&M Cost Elements for a WFGD Unit in the IECM v9

	O&M Cost Elements	Default Value
<b>Fixed O&amp;M Costs</b>		
A	Total Maintenance Cost (% TPC)	4.269
B	Number of Operating Jobs (jobs/shift)	6.670
C	Number of Operating Shifts (shifts/day)	4.750
D	Maintenance Cost Allocated to Labor (% total)	40.00
E	Admin. & Support Labor Cost (% total labor)	30.00
<b>Variable O&amp;M Costs</b>		
F	Limestone Cost (\$/tonne)	25.76
G	Lime Cost (\$/tonne)	112.0
H	Stacking Cost (\$/tonne)	8.559
I	Waste Disposal Cost (\$/tonne)	14.68
J	Electricity Price (Internal) (\$/MWh)	45.20

#### 8.1.4.1 *Price of Internal Electricity Use*

The first common variable operations and maintenance cost (VOM) is the auxiliary power consumption required to operate the component. By default, all energy costs are handled internally in the model by de-rating the overall power plant based on the calculated electrical load. Each component is then charged for the total electricity production foregone because of the electrical load consumed. The unit cost of internal electricity is, by default, estimated by the base plant module (62). This value may be overridden by a user-specified value if the electricity is assumed to be supplied from an external source. For energy intense process, such as those common to CO<sub>2</sub> capture, the cost of electricity use is one of the biggest variable O&M cost items. It is important to note that the way in which the cost of electricity is accounted is extremely important for determining common metrics of comparison; such as the mitigation cost.

#### 8.1.4.2 *Wastewater Treatment*

The second common VOM is the treatment of water produced by technical components. An assumption has been made that the water produced by all components in the pulverized coal oxyfuel model needs to be treated before it may be reused or introduced back to the environment. It is assumed that the produced water from each component is aggregated with that from all relevant technical components and sent to the plant-wide water treatment facility. The cost of treatment is calculated on a mass flow basis and details for this calculation are handled by the wastewater treatment model.

## 8.2 Base Plant

The calculation of costs associated with the base plant: fuel cost, boiler, coal conveyors and mills, air preheater, stack, etc. are handled in common fashion with all pulverized coal plants modeled inside the IECM. For details on these specific calculations please refer to the base IECM model documentation (64) (65). Revisions and updates to this documentation may be found in Volume 4 of the revised documentation (66)

One notable exception to the above is for the process contingency cost values used for calculating the total capital requirement of the boiler and recycle preheater. Although the oxyfuel version of these pieces of equipment do not vary substantially from their air-fired counterparts, an increased value for process contingency of 15% (37) has been used to reflect the lack of demonstration of the technology at commercial scale.

## 8.3 Criteria Pollution Control Units

Costs associated with the removal of criteria pollutants are handled internal to the individual techno-economic models developed for each pollution control technology. Detailed economic calculations for the Spray Dry Absorber and Wet Flue Gas Desulfurization Unit may be found in Chapter 6 of the Base IECM Technical Documentation (65). Details on the Electrostatic Precipitator are outlined in Chapter 4 and Fabric Filters are covered in Chapter 5.

## 8.4 Air Separation Unit

The cost model for the air separation unit has been developed from the case studies (Table 5-1) which utilize 95 [mol%] oxygen for power generation with oxyfuel. Figure 8.2 below is a plot of the process facility costs of the ASU's of various sizes presented in 2010 dollars.

### 8.4.1 Capital Cost

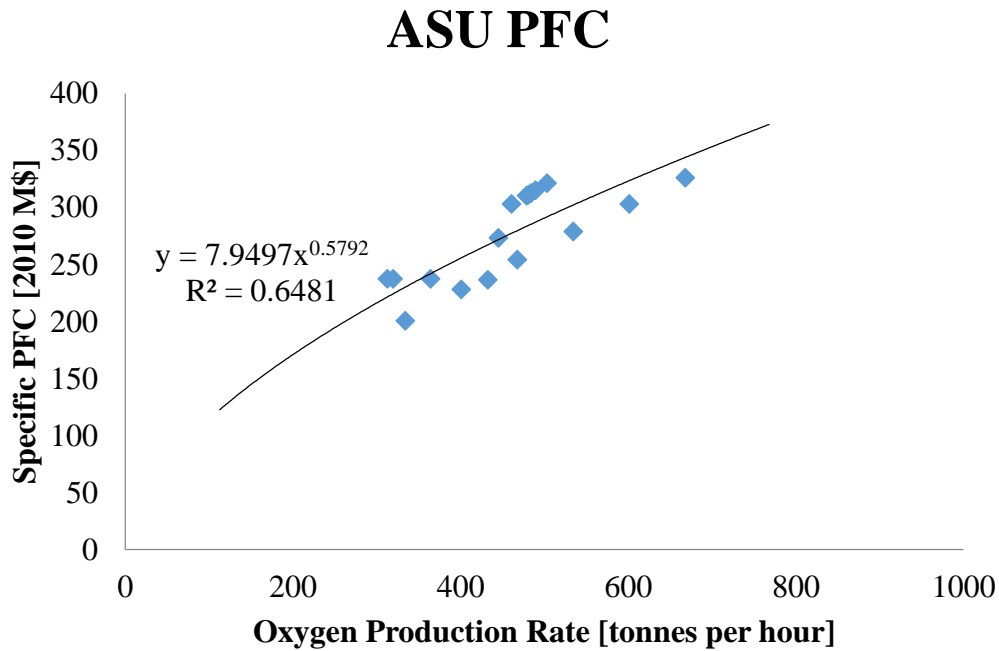


Figure 8.2 Process facility cost of ASU's across various oxygen production rates presented in 2010 dollars. The correlation coefficient is relatively weak ~0.65, however the data is relatively well represented by a 6/10ths scaling law

The cost equations presented below are not a function of purity, as sufficient recent cost detail was unavailable across the oxidant purity range. The maximum single train size for a cryogenic air separation unit has been limited to 550 [tph] in the IECM. For oxygen production rates great than the single train size, the oxygen demand should be divided equally into the smallest integer value which allows the single train production constraint to be met. The cost equation for a single train is:

$$PFC_{ASU,singletrain} [M\$] = 7.95 * \left( \frac{ASU_{Oxygen}}{1000} \right)^{0.58} * \left( \frac{PCI}{PCI_{2010}} \right)$$

Where:

$ASU_{Oxygen}$                       Mass flow rate of oxygen to the boiler from the ASU [kg/hr]

The total process facilities cost may then be calculated:

$$PFC_{ASU} [M\$] = N_{ASU} * PFC_{ASU,singletrain}$$

Where:

$N_{ASU}$  number of equal sized trains which comprise the air separation unit [integer]

## 8.4.2 Fixed and Variable Operations and Maintenance Cost

The fixed O&M costs which are specific to the cryogenic air separation unit are calculated using a combination of equations 1-4 from Section 8.1.4 and the values presented in Table 8-4. The internal cost of electricity is calculated internal to the IECM using the base plant COE as the default (case specific) but may also be specified by the user.

Table 8-4 Default O&M Parameters for the ASU Model

	O&M Cost Elements	Default Value
<b>Fixed O&amp;M Costs</b>		
A	Electricity Price (Internal) (\$/MWh)	Case Specific
B	Total Maintenance Cost (% TPC)	2
C	Number of Operating Jobs (jobs/shift)	6.670
D	Number of Operating Shifts (shifts/day)	4.750
E	Maintenance Cost Allocated to Labor (% total)	40.00
F	Admin. & Support Labor Cost (% total labor)	30.00

The electrical load required for operation of the ASU is calculated in the performance model and is debited from the gross plant output. The cost of electricity use is assessed to the ASU model by multiplying the internal cost of electricity [\$/MWh] by the load [MW].

$$VOM_{ASU,electric} \left[ \frac{\$}{hr} \right] = MW_{ASU} * COE_{internal}$$

Additionally, the quantity of water precipitated out during the compression of atmosphere by the main air compressor is sent to the wastewater treatment facility where the associated cost is determined on a mass flow basis.

$$VOM_{ASU,wwt} \left[ \frac{\$}{hr} \right] = Water_{MAC Produced} \left[ \frac{kg}{hr} \right] * 10^{-3} * WWT \left[ \frac{\$}{tonne} \right]$$

Where:

$WWT$  cost of wastewater treatment in \$/tonne

## 8.5 Oxidant Compressor

The requisite oxidant pressure for the PC boiler is 20 psia for the design scenarios examined in the creation of the PC oxyfuel model. However, because the ASU module in the IECM is also used by the integrated gasification combined cycle module, which requires oxidant at an elevated pressure, a downstream compressor was modeled to supply oxidant at elevated pressures. The physical model of the compressor is detailed in Section 5.4.6. The cost model was developed using data from a 2002 DOE report on cost estimation (67) and capital costs were verified using project costs from Rolls Royce and MAN Turbo reported by IEA-GHG (68).

### 8.5.1 Capital Cost

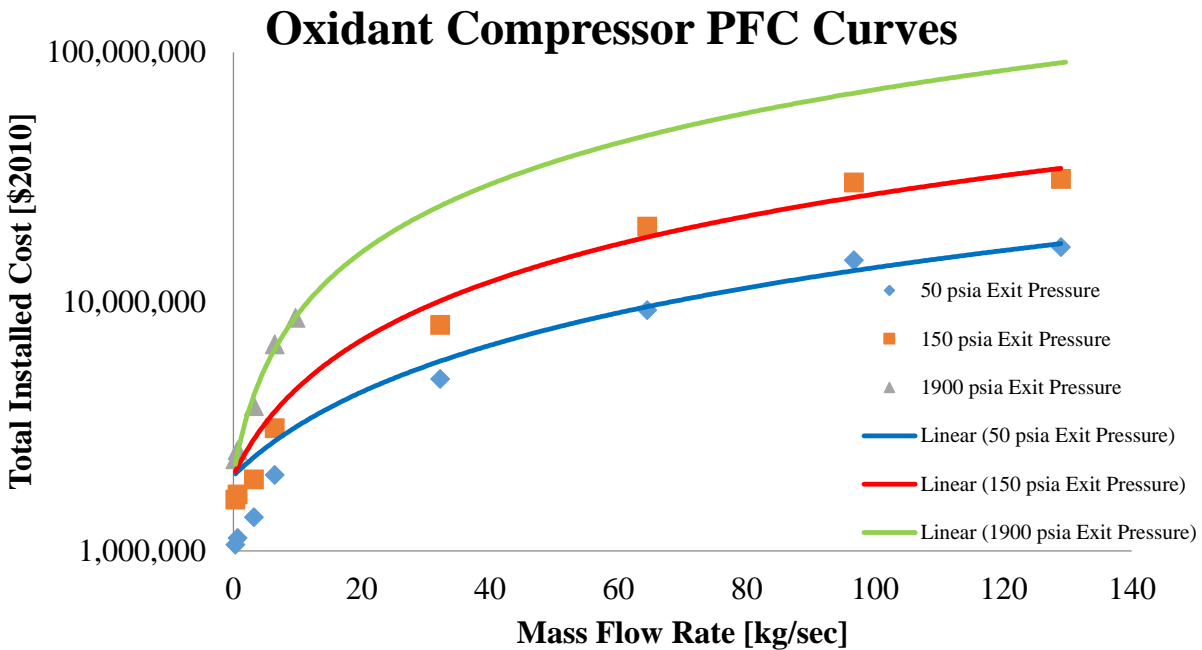


Figure 8.3 Oxygen compressor process facility cost curves for various exit pressures

The data used to create these process facility cost curves was then fit to an exponential regression with an  $R^2$  value of .98 for exit pressures between 50 and 1900 [psia]. This regression equation was then used to generalize the curves in Figure 8.3 to accommodate any required oxidant exit pressure. However, it should be noted that the required pressure of oxidant for gasifiers (~4000 [psi]) requires extrapolation beyond the range used to develop the PFC relation. The generalized oxidant compressor process facility cost is given by:

$$PFC_{OxComp} [\$M] = 8200 * P^{0.47} * A\dot{S}U_{Oxidant} + 2 * 10^6 * \left( \frac{PCI}{PCI_{2011}} \right)$$

Where:

$P$  desired pressure of oxidant leaving the compressor [psia]

$A\dot{S}U_{Oxidant}$  oxidant mass flow from the ASU [kg/sec]

## 8.5.2 Fixed and Variable Operations and Maintenance Cost

In instances where an oxidant compressor is required it is assumed that no other O&M costs are directly incurred with the exception of the additional electrical load consumed by the compressor. The O&M costs of the ASU and oxidant compressor as a system are increased through the addition of the PFC specific to the oxidant compressor to the total PFC of the system. Consequently the FOM costs, which are based upon the total PFC of the system, are increased proportionally.

The electrical load required for operation of the oxidant compressor is calculated in the performance model and is debited from the gross plant output. The cost of electricity use is assessed to the ASU model by multiplying the internal cost of electricity [\$/MWh] by the oxidant compressor load [MW].

$$VOM_{OxComp,electric} \left[ \frac{\$}{hr} \right] = MW_{OxComp} * COE_{internal}$$

## 8.6 Direct Contact Cooler and Polishing Scrubber

Available cost information for DCCPS is currently very limited. This is largely a result of the private vendors who produce cost estimates for DOE, and other publicly available information organizations, rolling the cost of the DCCPS into the cost quote for an entire system; be that oxyfuel or post-combustion scrubbing. Consequently, it is impossible to discern the proportion of costs which should be ascribed to the DCCPS. A concerted effort was made to contact representatives of the vendors responsible for producing said system estimates. But at the time of writing, no new cost information has been garnered. The only reliable cost quote available was produced by the Alstom Corporation in 2001 for an evaluation study for the State of Ohio Department of Development. The accuracy of applying this, slightly dated, point estimate is perhaps poor. However, the overall cost contribution of the DCCPS is fairly small and any inaccuracy in this specific estimate is well within the margin of error of the overall plant cost estimate.

### 8.6.1 Capital Cost

The PFC of the DCCPS is scaled on the basis of the flue gas flow rate entering the contacting tower. The reference cost of the DCCPS is \$17.6 million in 2001 USD (69), corresponding to a treated flue gas flow rate of 810,000 acfm. A single train limit of 2,000,000 acfm is enforced and is adopted from flue gas

desulfurization train limits (70). Actual cubic feet per minute (acfm) of gas flow can be calculated using the ideal gas law and the molar flow rate of flue gas entering the DCCPS.

$$\dot{V} \left[ \frac{m^3}{s} \right] = \frac{\varphi_{total\_FG} * RT}{P}$$

Where

$\dot{V}$	flue gas velocity [ $m^3/sec$ ] entering the DCCPS
$\varphi_{total\_FG}$	total molar flow rate [ $mol/sec$ ] of all gases entering the DCCPS
$R$	the universal gas constant [ $J/mol\ K$ ] ( $R = 8.314$ )
$T$	bulk gas temperature [ $Kelvin$ ]
$P$	bulk gas pressure [ $Pascals$ ]

The reference cost information and train size limit are both in units of actual cubic feet per minute, so it is necessary to convert prior to calculating a PFC for the DCCPS being examined.

$$\dot{V}[acfm] = \dot{V} \left[ \frac{m^3}{s} \right] * 35.314 \left[ \frac{ft^3}{m^3} \right] \div 60 \left[ \frac{s}{min} \right]$$

The PFC can then be calculated using the following set of operations:

If  $\dot{V} > 2,000,000\ acfm$ , divide the stream into equal parts which are each less than 2,000,000 acfm. The total PFC of the DCC will be given by:

$$PFC_{DCCPS}[\$M] = Number\ of\ Trains * pfc_{DCCPS\_single}$$

The PFC for a single train is calculated based upon the reference cost and associated volumetric flow rate. The cost estimate must also be adjusted to the base financial year selected by the user using the chemical engineering plant cost index (PCI).

$$pfc_{DCCPS\_single}[\$M] = 17.6 * \left( \frac{\dot{V}}{810,000} \right)^{0.6} * \left( \frac{PCI}{PCI_{2001}} \right)$$

## 8.6.2 Fixed and Variable Operations and Maintenance Cost

The fixed O&M costs which are specific to the direct contact cooler and polishing scrubber are calculated using a combination of equations 1-4 from Section 8.1.4 and the values presented in table 8-5. The internal cost of electricity is calculated internal to the IECM using the base plant COE as the default (case specific) but may also be specified by the user.

Table 8-5 Default O&M Parameters for the DCCPS Model

	O&M Cost Elements	Default Value
<b>Fixed O&amp;M Costs</b>		
A	Electricity Price (Internal) (\$/MWh)	Case Specific
B	Total Maintenance Cost (% TPC)	2
C	Number of Operating Jobs (jobs/shift)	2.000
D	Number of Operating Shifts (shifts/day)	4.750
E	Maintenance Cost Allocated to Labor (% total)	40.00
F	Admin. & Support Labor Cost (% total labor)	30.00

The electrical load required for operation of the DCCPS is limited to the pumping required to circulate the water in the contacting column. The electric load of the pump is calculated in the performance model and is debited from the gross plant output. The cost of electricity use is assessed to the DCCPS model by multiplying the internal cost of electricity [\$/MWh] by the pumping load [MW].

$$VOM_{DCCPS,electric} \left[ \frac{\$}{hr} \right] = MW_{DCCPS,pump} * COE_{internal}$$

When the ability to perform polishing scrubbing is being utilized, sodium hydroxide (NaOH), also known as caustic, is consumed. The mass consumed is calculated by the performance model and is reported to the cost model where it is multiplied by the unit cost.

$$VOM_{DCCPS,caustic} \left[ \frac{\$}{hr} \right] = NaOH \left[ \frac{\$}{tonne} \right] * 3.6 * \dot{M}_{NaOH} \left[ \frac{kg}{sec} \right]$$

With the consumption of caustic, the DCCPS generates sodium sulfate (Na<sub>2</sub>SO<sub>3</sub>) as part of a slurry which must be treated and/or disposed of as solid waste. The disposal cost is assumed to be equivalent to the waste disposal cost of solids produced by the flue gas desulfurization system.

$$VOM_{DCCPS,solidwaste} \left[ \frac{\$}{hr} \right] = Waste\ Disposal\ Cost \left[ \frac{\$}{tonne} \right] * 3.6 * \dot{M}_{Slurry} \left[ \frac{kg}{sec} \right]$$

The quantity of water produced by the DCCPS is affected by whether or not polishing scrubbing is being performed; as a fraction of the produced water is entrained in the sodium sulfate slurry. Regardless, the DCCPS performance model reports the quantity of water generated to the cost model which must be treated by the wastewater treatment model.

$$VOM_{DCCPS,wwt} \left[ \frac{\$}{hr} \right] = \dot{M}_{water\_generated} \left[ \frac{kg}{sec} \right] * 3.6 * WWT \left[ \frac{\$}{tonne} \right]$$

## 8.7 Carbon Processing Unit

Both the CPU and the CoCapture (no CPU) systems below are scaled from the mass flow of CO<sub>2</sub> product exiting the system. This directly correlates with the cold box volume and/or compression equipment required by the compression and self-refrigeration systems, which represent the primary drivers of capital cost for either the CPU or Co-capture system.

### 8.7.1 Capital Cost

#### 8.7.1.1 Carbon Processing Unit

Prior to starting to calculate the process facilities cost (PFC) for the CPU a calculation to determine the number of trains required, and the size of each, must be completed. Knowing the mass flow rate of carbon dioxide entering the CPU, along with the selected carbon recovery rate (CRR), allows us to determine the mass throughput. A single train size limit of 600 tph must then be enforced due to limitations (currently 550 tph) on the construction size of cold boxes (33), but practical design configurations would additionally benefit from the operational flexibility of multiple smaller trains. In the CPU model, trains should be sized to evenly handle the required mass flow. The calculated carbon dioxide throughput for each train  $\dot{CO}_{2, single\ train} [\frac{tonnes}{hr}]$  can then be used in the following:

$$pf_{CPU\_single}[\$M] = 2.126 * (\dot{CO}_{2, single} [tonnes/hr])^{0.586} * \left( \frac{PCI}{PCI_{2010}} \right)$$

This power based correlation yielded an R<sup>2</sup> value of 98.8%. This quality of fit is likely due to the use of the 6/10ths scaling law by the authors who originally constructed the case studies. Then the final CPU process facilities cost can be calculated by accounting for the number of trains used.

$$PFC_{CPU}[\$M] = Number\ of\ Trains * pf_{CPU\_single}$$

#### 8.7.1.2 Product Compression

The compression of the carbon dioxide product produced by a cryogenic CPU is handled by the common IECM carbon dioxide compression model. For cost details of this model, please see the Amine Capture System Documentation (71). In addition to the PFC of the compression unit, the performance model reports the electrical load to the cost model which multiplies the load by the internal cost of electricity.

$$VOM_{CO_2\ compression} \left[ \frac{\$}{hr} \right] = MW_{CO_2\ compression} * COE_{internal}$$

#### 8.7.1.3 CoCapture System

There is extremely limited financial data on CoCapture systems; therefore the cost equation uses the 6/10ths power rule in absence of more robust information. The relationship is based on a system with a

PFC of 100 million dollars at a flow rate of 585 metric tonnes of CO2 being processed per hour. In order to calculate single train cost for different flow rates the six-tenths power law is used.

$$CoCap_{Single\ Train}[M\$] = CoCap_{Single\ Train\_Base\ Cost} [2010\ M\$] * \left(\frac{tph_{Actual\ Size}}{585\ [tph]}\right)^{0.6} * \left(\frac{PCI}{PCI_{2010}}\right)$$

The single train size restriction for a co-capture compressor has been assumed to be 600 [tph] (same as for the CPU) in the IECM. This size limitation should be imposed on the co-capture system just as it is for the cryogenic CPU CO2 compression system. Once the number of required trains has been calculated, the total CoCapture PFC equation will be of the following form:

$$CoCap_{Total\ PFC}[M\$] = Number\ of\ Trains * CoCap_{Single\ Train}$$

### 8.7.2 Fixed and Variable Operations and Maintenance Cost

The fixed O&M costs for either the CoCapture or CPU are calculated using a combination of equations 1-4 from Section 8.1.4 and the values presented in Table 8-6. The internal cost of electricity is calculated internal to the IECM using the base plant COE as the default (case specific) but may also be specified by the user.

Table 8-6 Default O&M Parameters for the DCCPS Model

	O&M Cost Elements	Default Value
<b>Fixed O&amp;M Costs</b>		
A	Electricity Price (Internal) (\$/MWh)	Case Specific
B	Total Maintenance Cost (% TPC)	2
C	Number of Operating Jobs (jobs/shift)	2.000
D	Number of Operating Shifts (shifts/day)	4.750
E	Maintenance Cost Allocated to Labor (% total)	40.00
F	Admin. & Support Labor Cost (% total labor)	30.00

The electrical load required for operation of either carbon handling system is reported from the performance models to the cost model. The electric load of the equipped carbon handling system in the IECM is debited from the gross plant output. The cost of electricity use is then assessed to either the CPU or CoCapture model by multiplying the internal cost of electricity [\$/MWh] by the calculated load [MW].

For the cryogenic carbon processing unit:

$$VOM_{CPU,electric} \left[ \frac{\$}{hr} \right] = MW_{CPU} * COE_{internal}$$

For the CoCapture system:

$$VOM_{CoCap,electric} \left[ \frac{\$}{hr} \right] = MW_{CoCap} * COE_{internal}$$

Regardless of the carbon handling system chosen for a case study in the IECM, each performance model reports the mass flow of water precipitated out of the flue gas during compression to the cost model. The mass flow of produced water must then be processed by the wastewater treatment model. The relation for the CoCapture model is identical to that for the CPU below.

$$VOM_{CPU,wwt} \left[ \frac{\$}{hr} \right] = \dot{M}_{precip\_water} \left[ \frac{tonnes}{hr} \right] * WWT \left[ \frac{\$}{tonne} \right]$$

There is an additional VOM term for the CPU model to account for the consumption of desiccant and various chemicals which are consumed during normal operation. This cost has been normalized on the basis of carbon dioxide throughput and is expressed as dollars per tonne of CO2 captured. The relation was developed for the original pulverized oxyfuel model (28).

$$VOM_{CPU,chemicals} \left[ \frac{\$}{hr} \right] = UC_{chemicals} \left[ \frac{\$}{tonne} \right] * \dot{M}_{CO2} * \frac{CRR}{100}$$

Where:

$\dot{M}_{CO2}$  mass flow rate of carbon dioxide in the CPU inlet stream [t/hr]

$CRR$  carbon dioxide recovery rate of the CPU [%]

## 8.8 Balance of Oxyfuel Plant

There are two remaining minor cost components which round out a cost estimate for a pulverized coal oxyfuel plant. These are related to the recirculation of flue gas to the boiler and include specifically the flue gas recycle fan and the ducting required to contain and transport the recycle flue gas. The original models developed by Anand Rao were deemed to be of acceptable accuracy given the uncertainty of design and their relatively small contribution to overall system cost. For additional detail on the following two models please reference the original oxyfuel model documentation (72).

### 8.8.1 Flue Gas Recycle Fan

The cost of the fan required for recycling part of the flue gas is scaled on the basis of the flow rate of the flue gas being recycled. The reference cost for the fan is 2 M\$, corresponding to a flue gas flow rate of  $6.474(10)^5$  [ft<sup>3</sup>/min (actual)].

$$PFC_{FGRfan} = PFC_{FGRfan,ref} * \left( \frac{\dot{V}_{FGR}}{\dot{V}_{FGR,ref}} \right)^{0.6} * \left( \frac{PCI}{PCI_{ref}} \right)$$

$$PFC_{FGRfan} [\$M] = 2.0 * \left( \frac{\dot{V}_{FGR}}{6.474 * 10^5} \right)^{0.6} * \left( \frac{PCI}{PCI_{1998}} \right)$$

The electrical load of the FGR fan is calculated by the performance model and passed to the cost model where it is multiplied by the internal cost of electricity to determine the VOM associated with operating the FGR fan.

$$VOM_{Fan,electric} \left[ \frac{\$}{hr} \right] = MW_{Fan} * COE_{internal}$$

## 8.8.2 Flue Gas Recycle Ducting

In comparison to a traditional PC plant additional ducting is necessary to recycle part of the flue gas in the oxyfuel combustion system. The cost of this ducting is assumed to be a function of the flow rate of recycled flue gas. The reference cost is 10 M\$, corresponding to a flue gas flow rate of 6.474(10)<sup>5</sup> ft<sup>3</sup>/min (actual).

$$PFC_{FGRducting} = PFC_{FGRducting,fg} * \left( \frac{\dot{V}_{FGR}}{\dot{V}_{FGR,ref}} \right)^{0.6} * \left( \frac{PCI}{PCI_{ref}} \right)$$

$$PFC_{FGRducting} [\$M] = 10.0 * \left( \frac{\dot{V}_{FGR}}{6.474 * 10^5} \right)^{0.6} * \left( \frac{PCI}{PCI_{2001}} \right)$$

## 8.9 Plant Water Usage and Cooling

The performance and cost models for cooling water requirements, wastewater treatment, and makeup water requirements are handled in detail in Volumes 1-3 of the IECM update documentation (66). The component models pass their cooling duty and water usage requirements to the water use models which determine the capital and variable costs associated with a system sized to meet the demand of the aggregated component models.

## 8.10 Carbon Dioxide Transport and Storage

The transportation of the carbon dioxide product stream is assumed to be transported by pipeline to the location where it will be used or stored. The cost of the transport is calculated using a rigorous model

developed for the IECM which accounts for many variables including distance, injection pressure, pipe material properties, etc. In distilled form, the cost of transport may be reduced to a single equation which presents the levelized unit cost of transport.

$$VOM_{Transport} \left[ \frac{\$}{yr} \right] = UTC * \dot{M}_{CP} * CF * 8760$$

Where:

*UTC* unit transport cost calculated from transport model [\$/tonne]

$\dot{M}_{CP}$  mass flow rate of carbon product produced [tonne/hr]

*CF* capacity factor of the plant [decimal] (0.75 typical)

The cost associated with the storage of the produced carbon product may be positive or negative (enhanced oil recovery offtake agreement) depending upon the chosen method of disposal or storage. The IECM now includes a complex storage model to determine the cost associated with storage based upon a multitude of variables for site selection, storage volume, monitoring, etc. As with the transport model, the storage cost may be represented by the following simplified equation:

$$VOM_{Storage} \left[ \frac{\$}{yr} \right] = USC * \dot{M}_{CP} * CF * 8760$$

Where:

*USC* unit storage cost calculated from storage model [\$/tonne]

$\dot{M}_{CP}$  mass flow rate of carbon product produced [tonne/hr]

*CF* capacity factor of the plant [decimal] (0.75 typical)

The details of calculating the unit storage and transport are covered in Volume 5 of the IECM Update Documentation (66).

## 8.11 Incremental Cost of Electricity

Once the total capital requirement has been calculated and the fixed and variable operations and maintenance costs are known, the levelized cost of electricity may be calculated (LCOE). Additional financial parameters are required related to financing terms and fuel cost, but the LCOE may be estimated as follows:

$$[\$/MWh] = \frac{(TCR)(FCF) + FOM}{(CF)(8760)(MW_{Capacity})} + VOM + (HR)(FC)$$

Where:

<i>TCR</i>	total capital requirement [\$]
<i>FCF</i>	fixed charge factor [fraction]
<i>FOM</i>	fixed operations & maintenance cost [\$/yr]
<i>VOM</i>	variable operations & maintenance cost [\$/MWh]
<i>HR</i>	net power plant heat rate [MJ/MWh]
<i>FC</i>	unit fuel cost [\$/MJ]
<i>CF</i>	annual average capacity factor [decimal]
<i>MW<sub>Capacity</sub></i>	net power plant electrical output [MW]

The fixed charge factor is a calculated factor which annualizes the total capital requirement of the plant. It is a function of the assumed useful lifetime of the plant and the applicable interest rate for borrowed capital. For more details on how this factor is calculated please reference the EPRI TAG (62).

When trying to determine the incremental cost of adding carbon capture it is important to first establish what exactly you are attempting to calculate. There are a handful of varying methodologies for calculating the incremental cost of electricity. Much of the disparity is related to whether the analysis is to determine the incremental cost of adding carbon capture to an existing plant or whether the analysis is to determine the cost of building a carbon capture plant in lieu of an alternative electricity generation unit. The incremental cost determination used in this work is based upon the later definition of erecting one plant type in lieu of another.

To begin, a reference plant capable of meeting all of the same criteria pollutant standards as the capture plant must be modeled. The IECM will then produce a cost of electricity estimate for the base plant (say 60 [\$/MWh] for 500 [MW-net] output). Next, a carbon capture plant which has the same net electrical output (500 [MW] in this case) must be modeled and a cost of electricity estimate obtained (100 [\$/MWh]). At this point, assuming all financial and non-GHG environmental performance parameters have been held constant, the reference cost of electricity may be subtracted from the capture plant COE. The difference in COE values, 40 [\$/MWh] is the incremental cost of electricity.

## 8.12 Cost of Carbon Dioxide Captured and Avoided

The cost of implementing environmental controls is often expressed in terms of cost of unit mass of pollutant-X removed. With respect to carbon capture for the electricity sector however, what is ultimately important is the cost of producing a megawatt of electricity at some specified carbon

intensity. Consequently, “avoidance cost” which is an all-in metric which accounts for all costs to produce electricity with a specified carbon intensity is the economic indicator that is widely used in evaluating carbon capture systems.

$$Avoidance\ Cost\ \left[ \frac{\$}{tCO_2} \right] = \frac{[\$/MWh]_{Capture} - [\$/MWh]_{Reference}}{[tCO_2/MWh]_{Reference} - [tCO_2/MWh]_{Capture}}$$

There are instances when knowing the cost of capture, rather than the avoidance cost may be preferred. For example, a company that is considering expanding its enhanced oil recovery operations but needs to secure carbon dioxide as a commodity will not be most interested in the avoidance cost. In this example the capture cost would be the economic metric of interest so that the company could compare the cost of procuring carbon dioxide through power generation with carbon capture versus paying for its extraction from geological formations.

The cost per unit of CO<sub>2</sub> removed or captured is simply the additional expenses incurred in the capture of CO<sub>2</sub>, divided by the total quantity of CO<sub>2</sub> captured. This is calculated in the IECM as the difference between the total annualized cost of the plants [M\$/yr] with and without CO<sub>2</sub> control, divided by the total quantity of CO<sub>2</sub> captured [tonne CO<sub>2</sub>/yr], with the net power generated by the two plants remaining equal.

# Chapter 9 Applications of the Pulverized Coal Oxyfuel Model in the IECM

The purpose of this chapter is to illustrate the model's functionality in the Integrated Environmental Control Model (IECM), displaying the sensitivity of component models, conducting uncertainty analysis of the integrated oxyfuel model, and demonstrating its capabilities across a variety of case studies. First, Section 9.1 elaborates the sensitivity of the various technical component models to changes in key design parameters. Following this, the remainder of this chapter presents results for integrated plant designs based on results of the component-level analysis.

## 9.1 Technical Component Sensitivity

This section is devoted to showing the sensitivity of the individual technological components which comprise the oxyfuel system. For each component this includes the response across expected operating conditions in terms of performance and cost. Where applicable, additional information related to secondary effects from performance changes will be illustrated and discussed. All of the following sensitivity figures have been generated using the oxyfuel model in the IECM set up with an Illinois #6 Coal and net electrical output of 500 [MW] as specified in Section 9.3. All costs and financial metrics are reported in constant 2012 dollars.

### 9.1.1 Air Separation Unit

The air separation unit (ASU) generates nearly all the oxygen needed for combustion of the fuel selected for the oxyfuel plant. It's location at the front end of the oxyfuel system means that it is largely isolated from the downstream performance of other technical components. The main system parameters which affect the ASU are examined here along with select environmental parameters which have an appreciable effect on ASU performance.

#### 9.1.1.1 Water Production

Cryogenic air separation systems begin the oxygen enrichment process by compressing a large quantity of atmospheric air. To prevent the formation of ice in the cold box, which could lead to equipment failure, all water from the compressed atmosphere must be removed. The quantity of water which must be removed is a function of the relative humidity and the dry bulb temperature of the air. This removed water is referred to as produced water and its relation to relative humidity and temperature can be seen in the following figure.

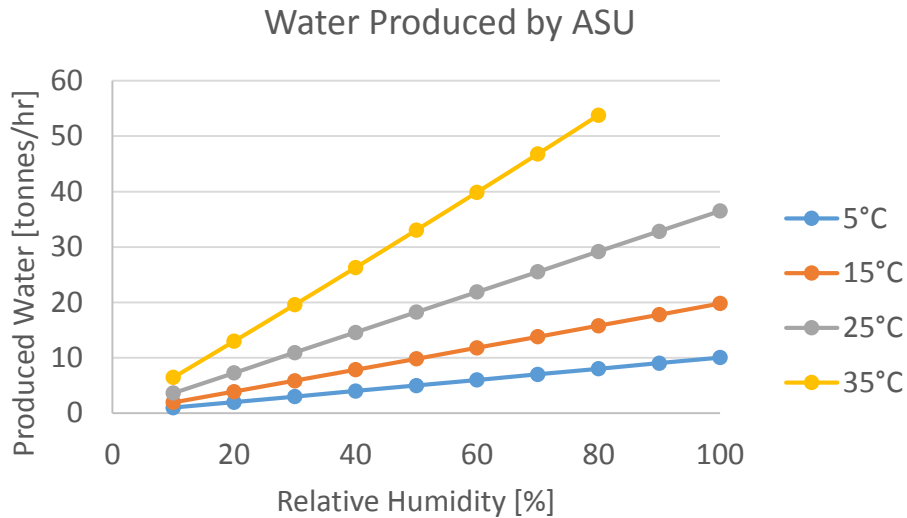


Figure 9.1. Water produced by the main air compressor of the air separation unit across relative humidity levels for various ambient temperatures

The quantity of produced water from the ASU is not a staggeringly large flow rate. However, under the default IECM conditions (25°C, 50% Relative Humidity) the produced water could offset over 15% of the makeup water required for the steam cycle. In localities where access to water is plentiful this is unlikely to be seen as a substantial advantage, but in water-tight circumstances the ability to produce water as a byproduct could be beneficial.

#### 9.1.1.2 Air Ingress and Excess Air

Air ingress is a term which comes from air-fired generation and is a measure of the amount of atmospheric air which finds its way into the boiler due to negative draft being maintained during firing. In the oxyfuel model, the term is used to denote the quantity of atmosphere which enters the flue gas after it leaves the boiler. For mass balance purposes, all air ingress is assumed to occur at the recycle heater directly downstream of the boiler. The quantity of air ingress is defined in terms to the rate of oxygen entering the flue gas relative to the stoichiometric oxygen requirement of combustion. Other atmospheric gases enter the system along with the oxygen and contribute to increasing the total mass flow of flue gas through the system. The only effect of air ingress for the ASU however, is that less oxygen needs to be provided to the boiler by the ASU. For the base oxyfuel plant, the relation of power savings as air ingress increases is shown below.

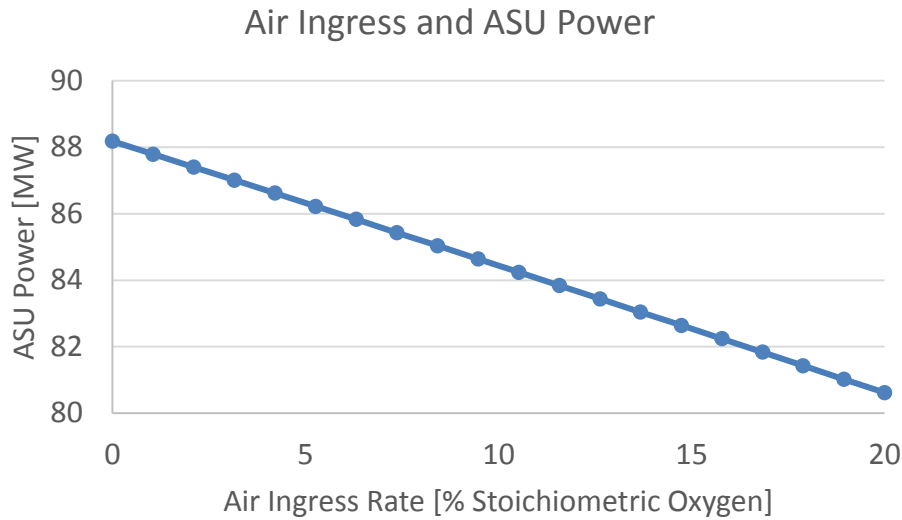


Figure 9.2. ASU electrical power consumption across air ingress rates (5% typical) to the recycled flue gas stream

As would be expected, the electrical load required by the ASU decreases as less oxygen is required to be produced for the boiler. The reduction in electrical load is not substantial and, as will be shown later, is not great enough to offset the negative downstream effects caused by increased air ingress rates.

The quantity of oxygen required to completely oxidize a fuel under ideal conditions is known as the stoichiometric requirement. In practice, due to residence time and mixing limitations inside a real boiler, elevated levels of oxygen are used to ensure complete fuel burn out. Excess air is the term used in the IECM to denote the percent of oxygen required during combustion that is greater than the stoichiometric level. The following figure shows the increase in ASU load as excess air is increased.

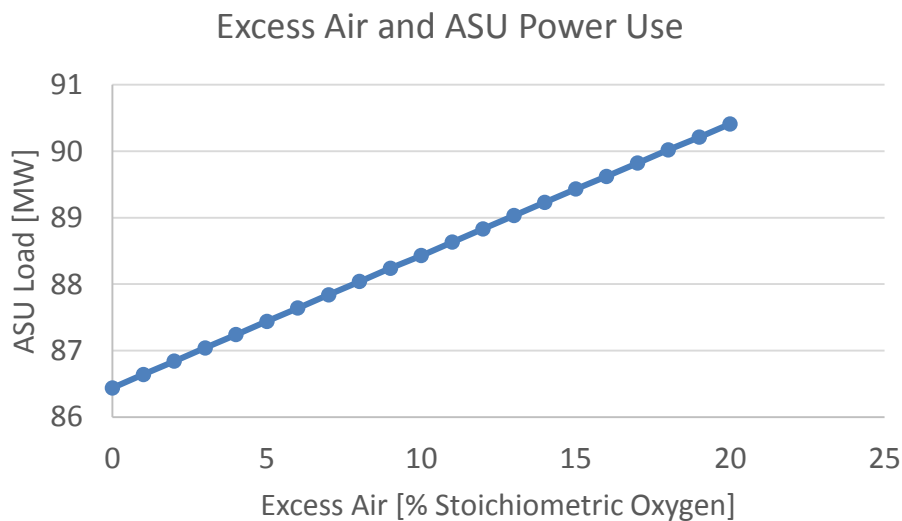


Figure 9.3. Electrical use of the ASU across excess air requirements (5% typical) for combustion in the boiler

The typical value for excess oxygen assumed in the IECM is 5%. Small variations from this value do not have a large effect of the ASU load as an increase in excess air requirement of 1% increases ASU load only by about 200 kW. Furthermore, excess air is typically a boiler design variable and consequently is unlikely to change significantly during the course of plant operation.

### 9.1.1.3 Oxidant Purity

One of the primary drivers in the performance of the ASU is the purity of the oxidant required for plant operation. Figure 9.4 shows the relation between specific separation energy and oxidant purity for the ASU model in the IECM. Chapter 5 discusses the physical reasons which underpin the shape of the purity response in greater detail.

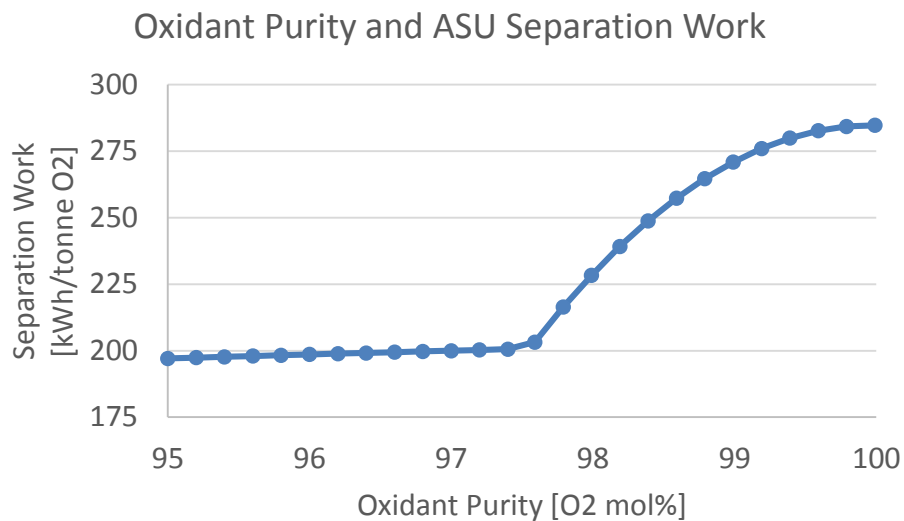


Figure 9.4. Specific oxygen separation work of the ASU as a function of oxidant purity

There is a dramatic increase in specific separation work for oxidant purity levels higher than 97.5% oxygen [mol %]. The increase in separation work derivative then decays to nearly zero as oxidant purity approaches 100%. This is starkly different behavior than was present in the previous version of an ASU in the IECM. The older model's specific separation energy would continue to increase at higher purities; with the derivative increasing as oxidant purity approached 100%. A comparison of the specific separation work of the old and new ASU model is presented in the following figure.

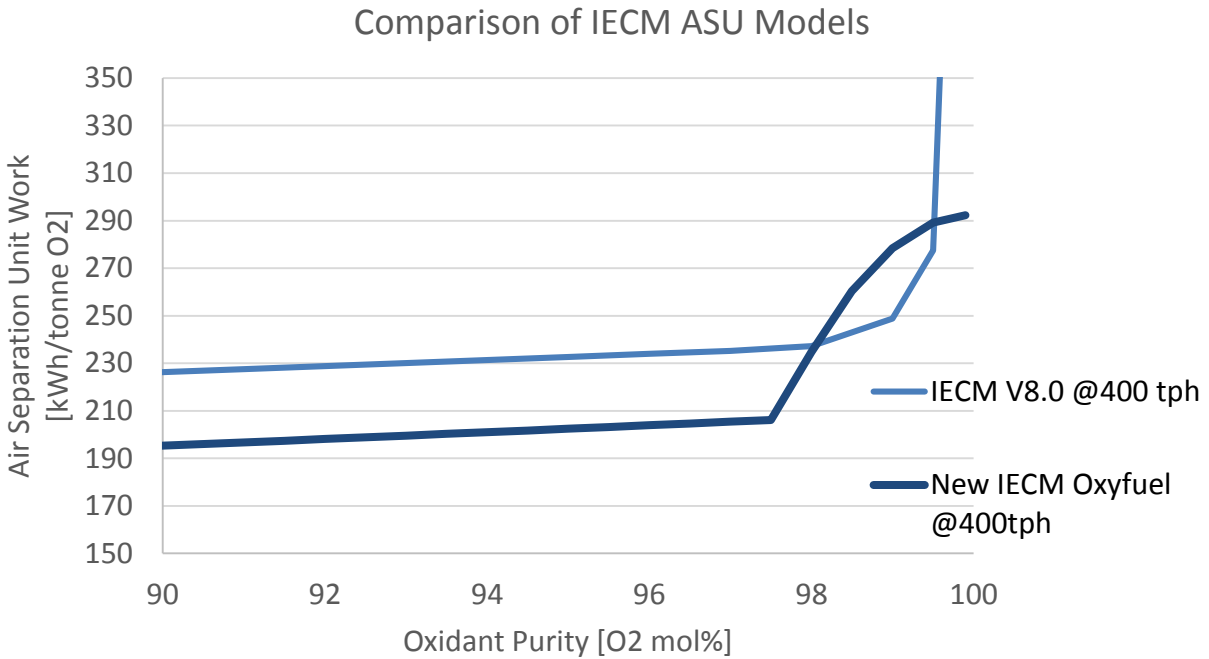


Figure 9.5. Comparison of the pre-existing ASU model with the updated ASU model which reflects the real world specific separation work across oxidant purity levels

In addition to the changes in behavior at high oxidant purity, the new ASU model has lower unit work for all oxidant purities below about 98 [O2 mol%]. This can be attributed to advancements in developing ASU's specifically to produce large quantities of oxidant at reduced purity level for power generation. Previous ASU's, on the other hand, had been optimized to create high purity gas streams for industrial gas production.

Despite the advances made to optimize ASU's more specifically for use with electricity generation the substantial increase in unit work at higher oxidant purity levels still has a substantial negative effect on net plant efficiency.

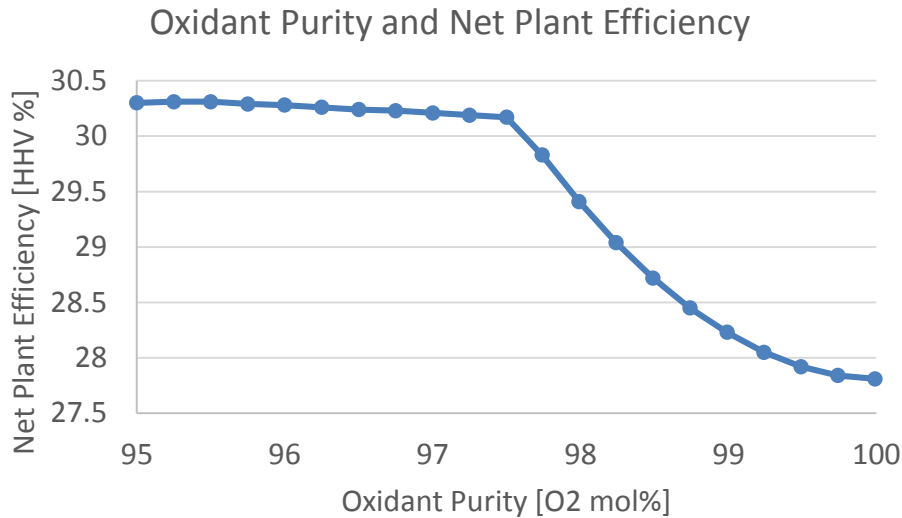


Figure 9.6 As the ASU transitions from removing nitrogen to separating oxygen from argon the net plant efficiency decreases substantially due to the large increase in ASU unit work.

A decrease in net plant efficiency of nearly two and a half percentage points is substantial. The associated increase in the levelized cost of electricity produced from a plant utilizing 99.5 [O2 mol%] oxidant compared to 95-97.5 [O2 mol%] is roughly 10%.

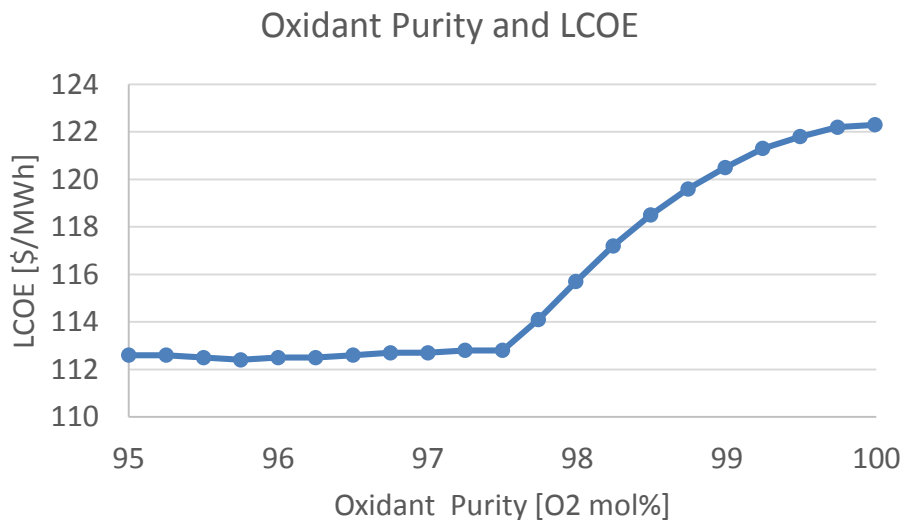


Figure 9.7 The levelized cost of electricity increases markedly in reverse proportion to the decrease in net plant efficiency at high oxidant purity levels.

#### 9.1.1.4 Oxidant Pressure

If the oxidant produced by the ASU needs to be delivered at an elevated pressure, to a gasifier for example, then a compressor is required. The amount of electrical load required to raise the oxidant pressure is a function of the final delivery pressure. The specific compression work from compressing

the oxidant is added to the specific separation work to get a total value for the unit work of a pressurized product ASU. The relationship between ASU specific work and oxidant delivery pressure is presented in the following figure for the base oxyfuel plant and 95 [O<sub>2</sub> mol%] oxidant.

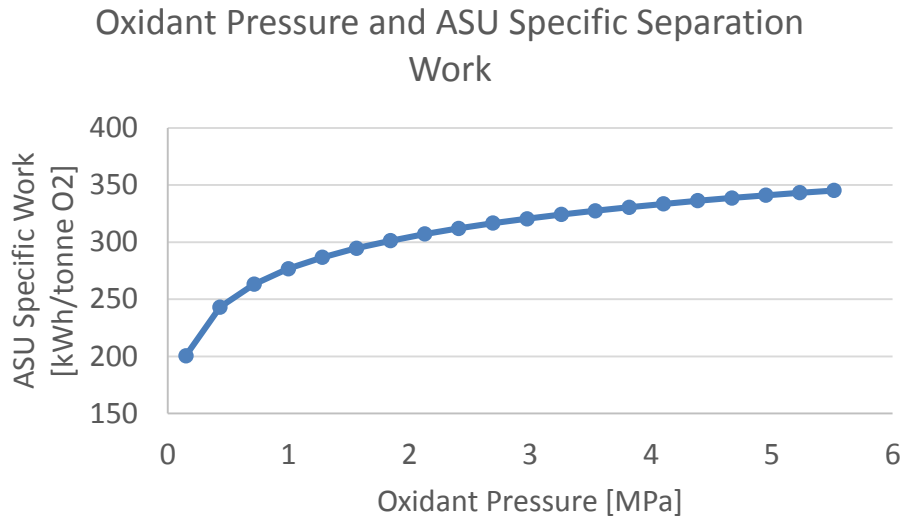


Figure 9.8. Effect of required oxidant delivery pressure on the ASU specific work

#### 9.1.1.5 Gross Plant Size Effects

The gross electrical output of the plant directly affects the size of the ASU. The gross plant size also determines the number of ASU trains which must be used to meet oxidant flow requirements. The maximum train size for an ASU in the IECM is 550 tonnes of entrained oxygen per hour. For the base oxyfuel plant configuration a second train was required once gross output eclipsed 800 [MW](Fig. 9.9).

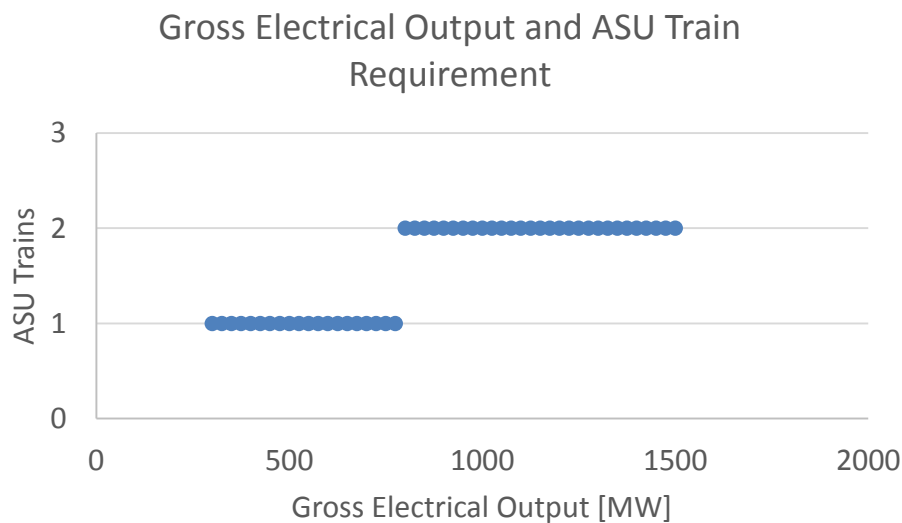


Figure 9.9. Number of ASU trains required across gross electrical output of the base plant

The specific separation work of the ASU system also changes as a function of gross plant output because there are efficiencies at scale for cold boxes and the main air compressor of each individual train. Demonstrated in the below figure is the decline of specific work intensity as the single train size limit is approached. Once the second train is required average specific work decreases at half the rate it did with a single train system. This reciprocal decrease in the specific work derivative would hold for any number of equally-sized trains in the plant.

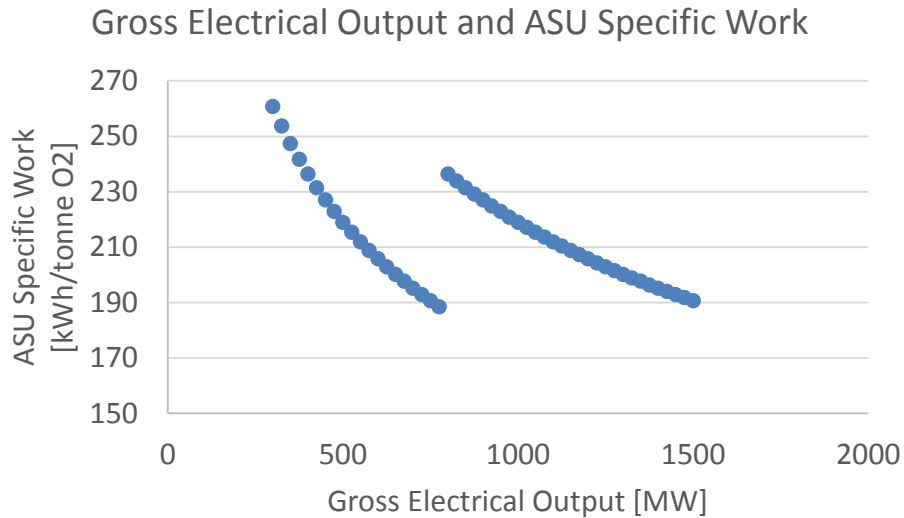


Figure 9.10. Specific oxygen separation work of the ASU across gross electrical output of the base plant

An opportunity for future work could be to optimize the size of the size of the ASU trains working in tandem. While not addressed here, an opportunity for savings and or increased operational flexibility could exist through using asymmetrically sized trains.

The total ASU load across gross plant size can be seen in Figure 9.11. The load is discontinuous where the second train is added to the system, but otherwise is a smooth curve which has a slightly decreasing derivative.

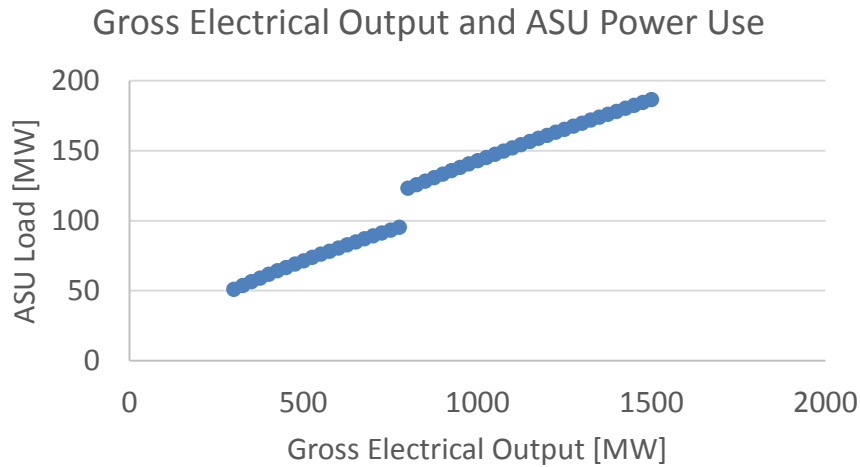


Figure 9.11. Electrical load of the ASU across the gross electrical output of the base plant

The process facility cost of the ASU system is very similar in shape to the ASU load relation. Two curves with slightly decreasing derivatives separated by a discontinuity where a second train is added to the system. The capital cost of the ASU is a major contributor to the cost of capture for oxyfuel systems, representing over half the total capital investment for capture on the chosen base plant.

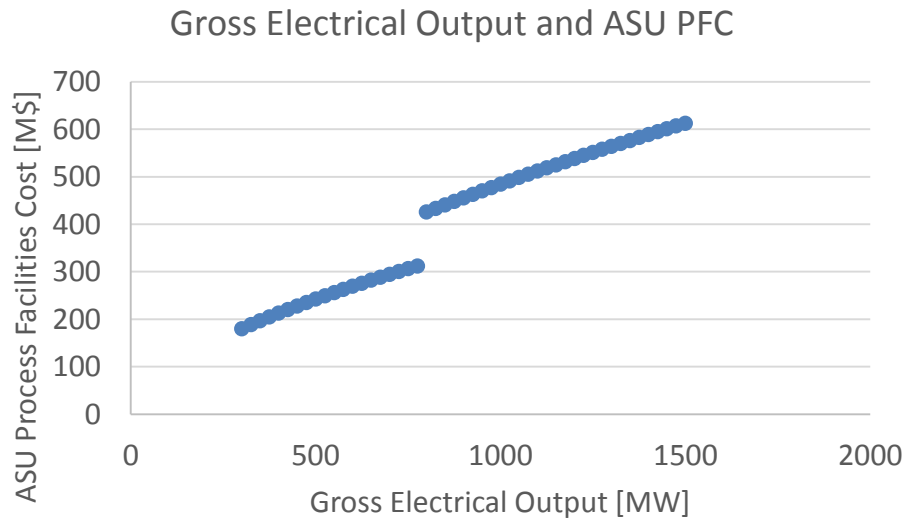


Figure 9.12. Process facilities cost of the ASU across the gross electrical output of the base plant

The operations and maintenance costs for the ASU are largely a summation of adder functions calculating a percentage of the PFC to annual costs. It follows then that the operations and maintenance costs (Fig. 9.13) look nearly identical aside from the cost units of [M\$/yr] rather than [M\$].

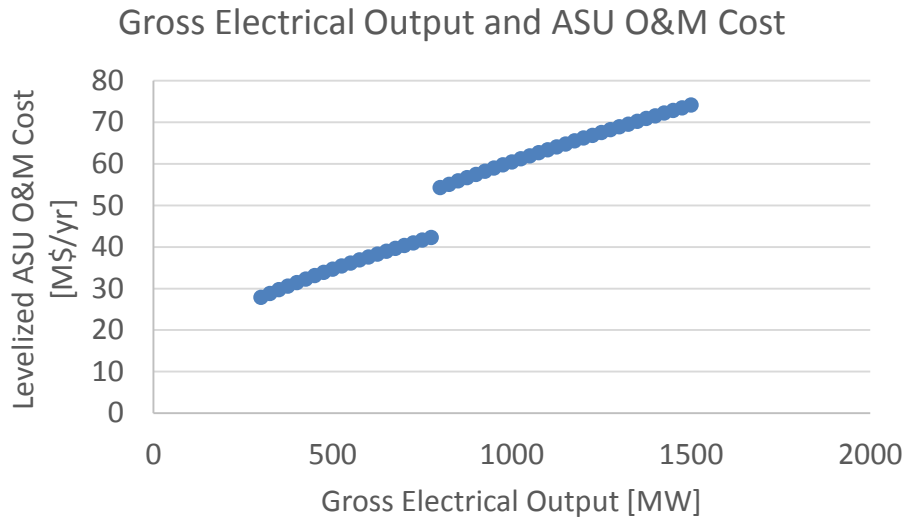


Figure 9.13. Annual operations and maintenance costs for the ASU across gross electrical output of the base plant

## 9.1.2 Direct Contact Cooler and Polishing Scrubber

The direct contact cooler and polishing scrubber (DCCPS) removes moisture and residual sulfur oxides from the flue gas. The following sensitivity studies examine the performance and economic trade-offs which are present for the main parameters of the DCCPS. Additionally, the performance of the DCCPS has a large effect of the overall mass and energy balance of the oxyfuel plant. The integral nature of this piece of equipment will be covered partly in this section and revisited in others where appropriate.

### 9.1.2.1 Operating Temperature Effects

The quantity of moisture which is removed from the flue gas passed through the DCCPS is a direct function of the operating temperature (temperature at the exit or top of the contacting column). The saturation temperature of water is a function of pressure as well, but this variable is fixed once a plant configuration has been chosen. Therefore, the quantity of water vapor present in the flue gas is a function just of the operating temperature of the DCCPS as is shown in the below figure.

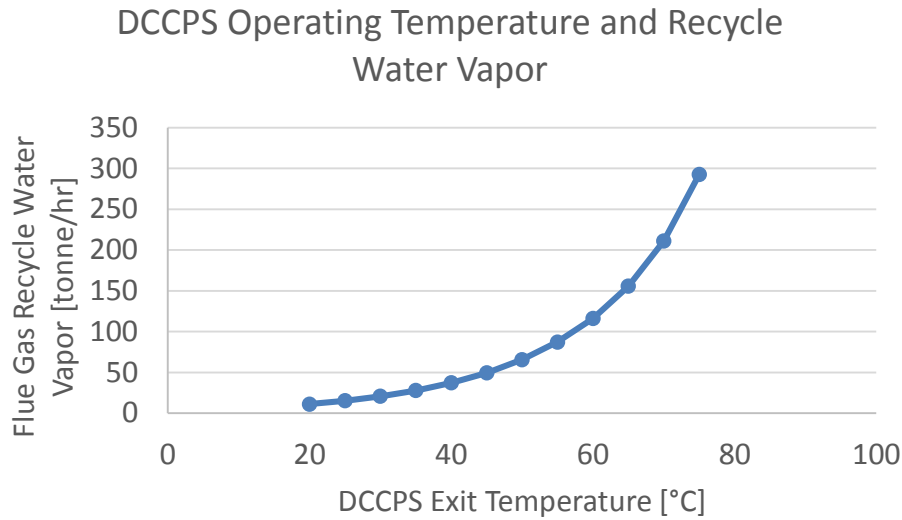


Figure 9.14. Mass flow rate of water in the flue gas stream exiting the DCCPS as a function of operating exit temperature

In order to keep the DCCPS operating temperature at the specified value, the requisite quantity of cooling water must be provided to the contacting tower in order to cool the flue gas. The absolute flow rate of cooling water is a function of a number of parameters specific to the cooling water (base temperature, allowable temperature delta, etc.). However, the overall behavior of cooling water flow rate is captured in the below figure showing the relationship between DCCPS operating temperature and required cooling water.

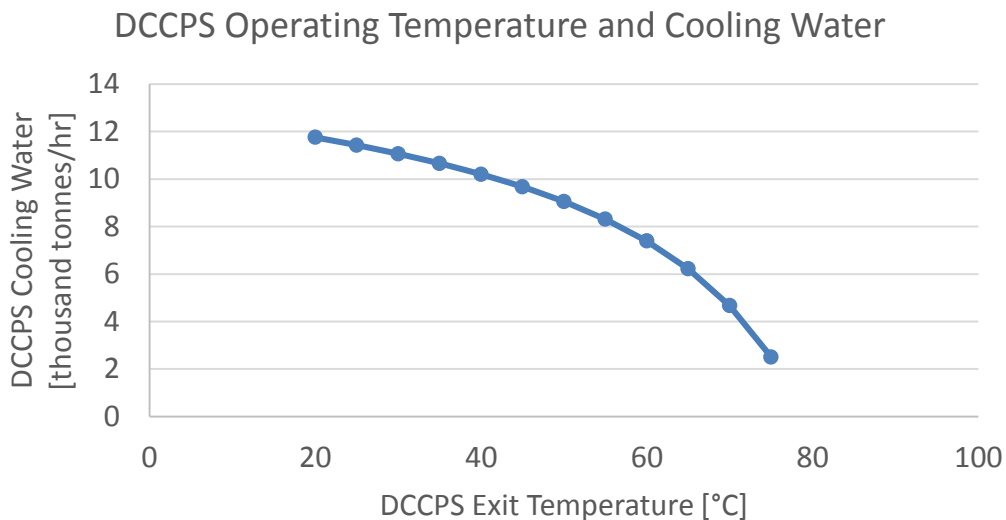


Figure 9.15. Cooling water flow rate requirement for the DCCPS as a function of operating exit temperature

The flow rate of cooling water drops off precipitously at higher operating temperatures as less heat transfer is required to maintain the specified operating temperature. However, as operating temperatures above 65 [°C] are specified, the reduction in flue gas moisture becomes so small that the rationale for using a DCCPS is largely undermined. The default DCCPS operating temperature in the

IECM has been set at 55 [°C], a value which provides an acceptable compromise between moisture removal and enthalpy reduction in the recycle flue gas stream.

The electrical load consumed by the DCCPS is almost exclusively limited to the quantity of cooling water required to maintain the specified operating temperature. The below figure presents the relationship for DCCPS electrical load as a function of operating temperature.

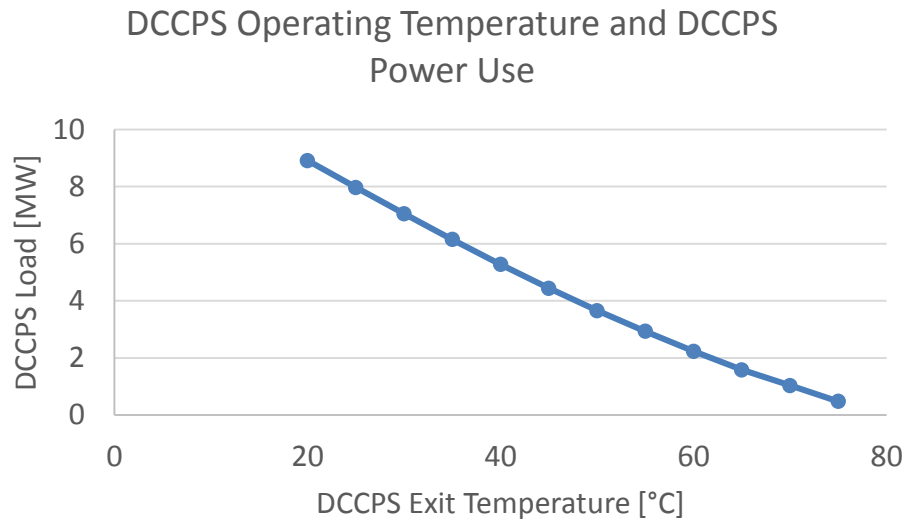


Figure 9.16. Electrical load required to operate the DCCPS across operating exit temperature

As is the case with many flue gas handling components, the capital cost of an individual DCCPS train is a function of the volumetric flow rate of flue gas it must process. It logically follows from this that higher operating temperatures will necessitate the use of a larger contacting tower and will have higher process facility costs than their lower operating temperature counterparts. Figure 9.17 shows the sensitivity of the base plant's DCCPS PFC to variations in operating temperature.

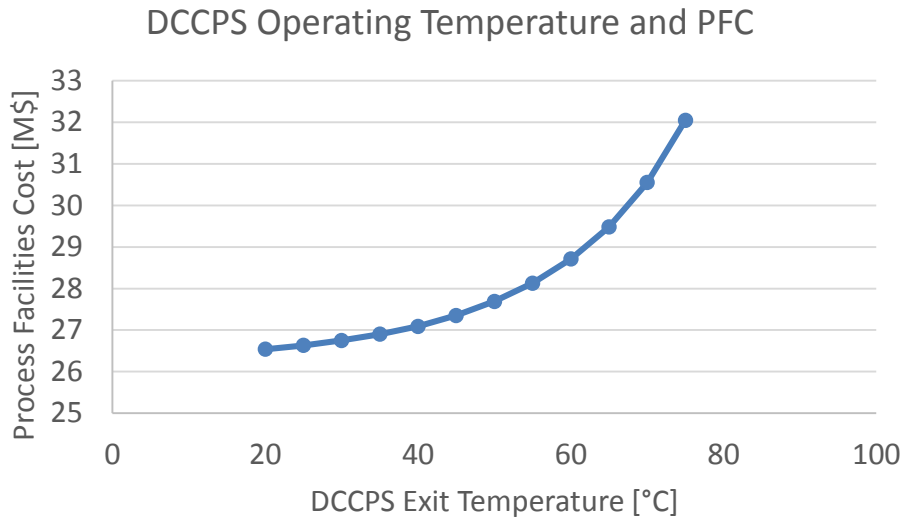


Figure 9.17. Process facilities cost of the DCCPS as a function of operating exit temperature

It is fairly straight-forward to deduce from the shape of many of the performance response curves that there must be some “optimum” trade-off present between cost and performance for a stand-alone DCCPS system. We have identified this “optimum” as being about 55 [°C] and have designated this as the default operating temperature in the IECM. When part of an integrated oxyfuel system with various coal properties, flue gas recirculation rates, and trade-offs in carbon handling performance; the choice of an operating temperature becomes more nuanced. It was outside of the scope of this work to attempt to optimize DCCPS operating temperature for each of the case studies examined. However, opportunity remains for future work on this subject and potential improvements in thermal and economic performance appear likely.

In concert with increasing contacting column size at higher operating temperatures, the quantity of flue gas which must be moved through the DCCPS is increased. Motivation of the flue gas through the contacting column is achieved through the use of a forced draft fan.

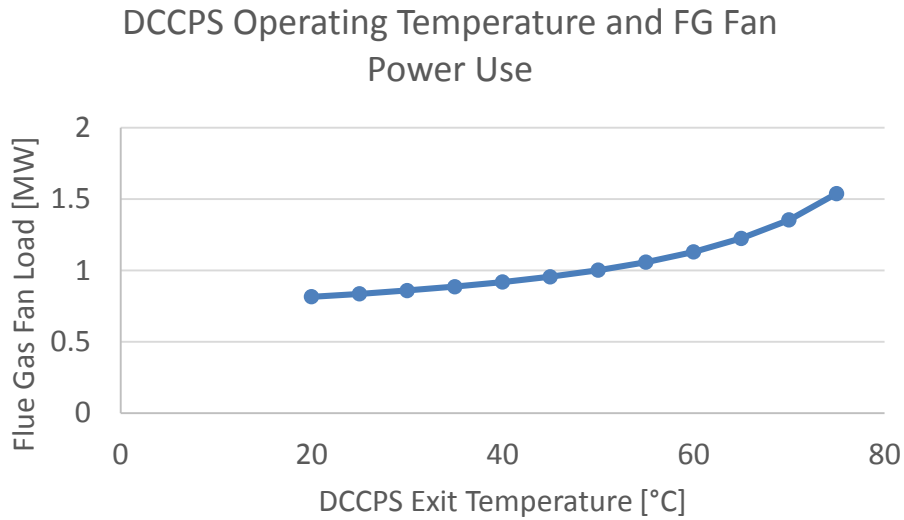


Figure 9.18. Flue gas recirculation fan load across DCCPS operating exit temperature

Across the range of viable operating temperatures for the DCCPS, the electrical load of the flue gas fan nearly doubles. In absolute terms the electrical load of the flue gas fan comprises a rather small portion of overall parasitic load. However, the flue gas fan makes up 10-15% of the electrical load required by the DCCPS unit.

#### 9.1.2.2 Gross Plant Size Effects

The number of DCCPS trains required is a function of the flue gas flow rate which must pass through the contacting column. More specifically, the single train size limit is based on the volumetric flow rate of the flue gas entering the column. There are a number of variables which affect the flue gas volumetric flow rate; including recycle rate and temperature. The primary driver, gross plant size, is shown in the following figure.

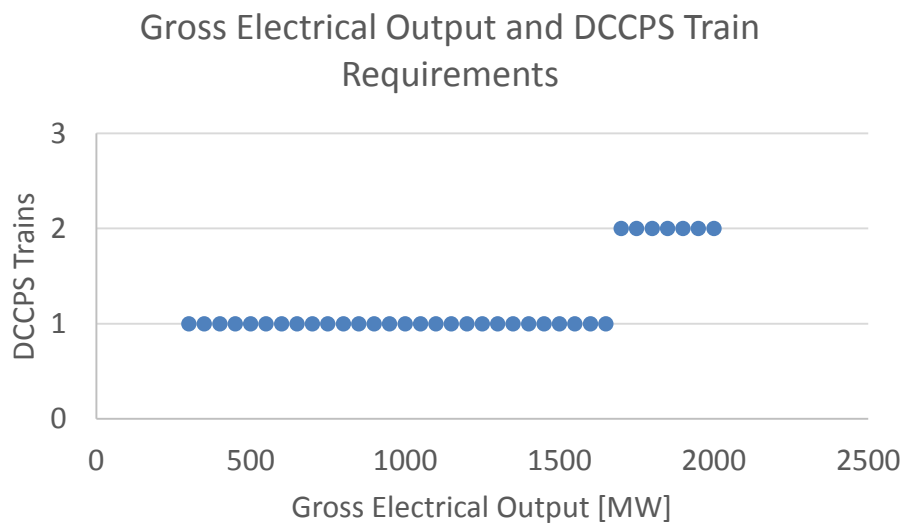


Figure 9.19. Required DCCPS trains across gross electrical output.

For the chosen base plant, a low moisture bituminous coal (Illinois #6), the maximum gross electrical output which can be accommodated by a single DCCPS train is very high (1,700 [MW]). There are cases where a higher recycle rate combined with a higher moisture coal would reduce the maximum gross output serviceable with a single train. However, for nearly all configurations, a single train DCCPS would be adequate.

The process facilities cost reflects the need for multiple trains at gross electrical outputs above 1700 [MW]. There are also economies of scale for larger single train units. Overall, the DCCPS represents only about 5% of the carbon dioxide control capital expenditure in an oxyfuel plant.

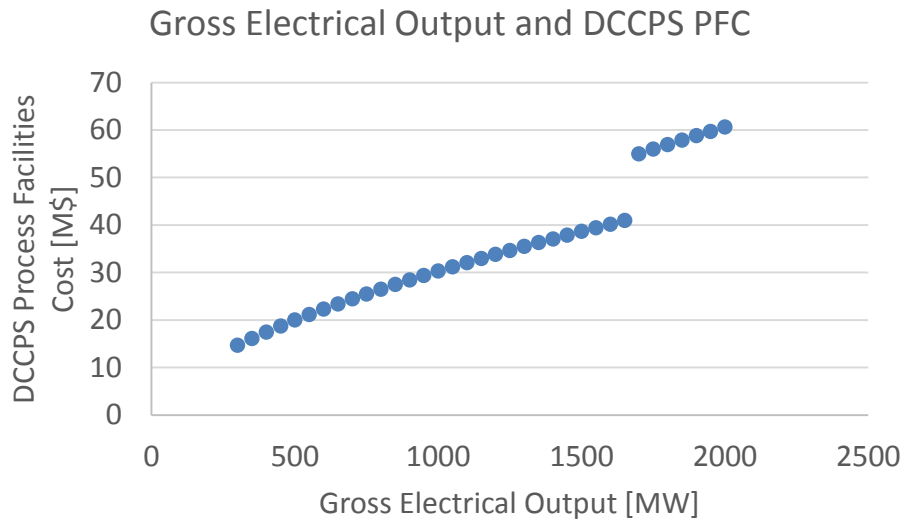


Figure 9.20 Process facilities cost of the DCCPS as a function of the gross electrical output.

The operations and maintenance costs associated with the DCCPS are tabulated and reported along with the other technical components which fall under the umbrella of “Flue Gas Recycle and Purification” in the IECM. The total O&M cost for this category can be found in the following section on the sensitivity of the carbon processing unit.

### 9.1.3 Carbon Processing Unit

The carbon processing unit (CPU) is responsible for removing the remaining moisture in the flue gas left by the DCCPS then producing a concentrated carbon dioxide product stream. The performance of the CPU is driven primarily by two parameters: carbon dioxide product purity (CPP) and carbon dioxide recovery rate (CRR). The effects of these two parameters is investigated in this section along with interactions with the DCCPS and a litany of other factors which affect CPU cost and performance.

#### 9.1.3.1 Carbon Dioxide Product Purity Effects

The CPU model in the IECM is capable of producing performance estimates for carbon dioxide product purity levels between 90 and 99.99 [CO<sub>2</sub> mol%]. The sensitivity analysis presented here focuses on the region above 95 [CO<sub>2</sub> mol%] because these purity levels best align with the purity levels achieved by

competing carbon capture technologies. The unit (specific separation and compression) work across this range of CPP's is not exactly linear, but is very close as can be seen in the following figure.

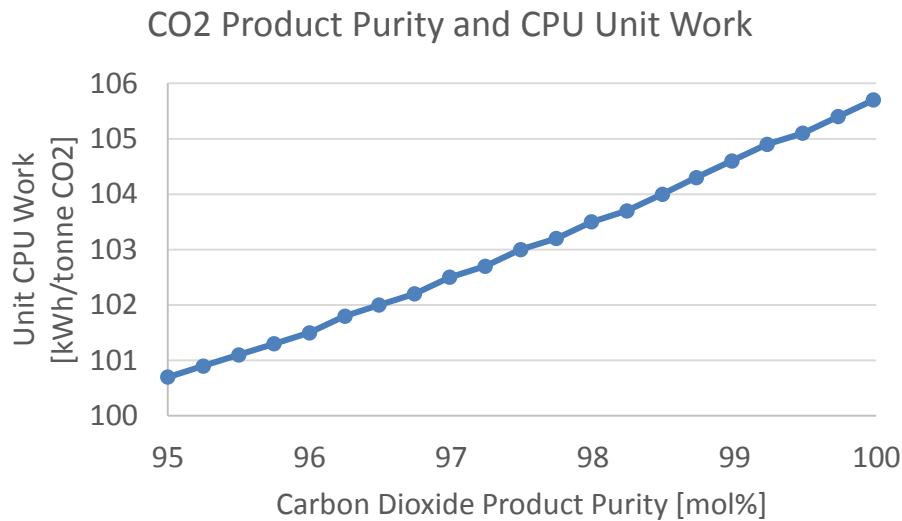


Figure 9.21. Unit carbon purification work of the CPU across carbon dioxide purity levels of the product stream.

The deviation from linearity is a result of the reduced order model (ROM) developed for the CPU not having a linear functional form. However, with a constant input stream composition, the relation is approximately linear above CPP values of 95 [CO<sub>2</sub> mol%]. The effect of an increase in unit work is reflected in the total electrical load consumed by the CPU in the below figure.

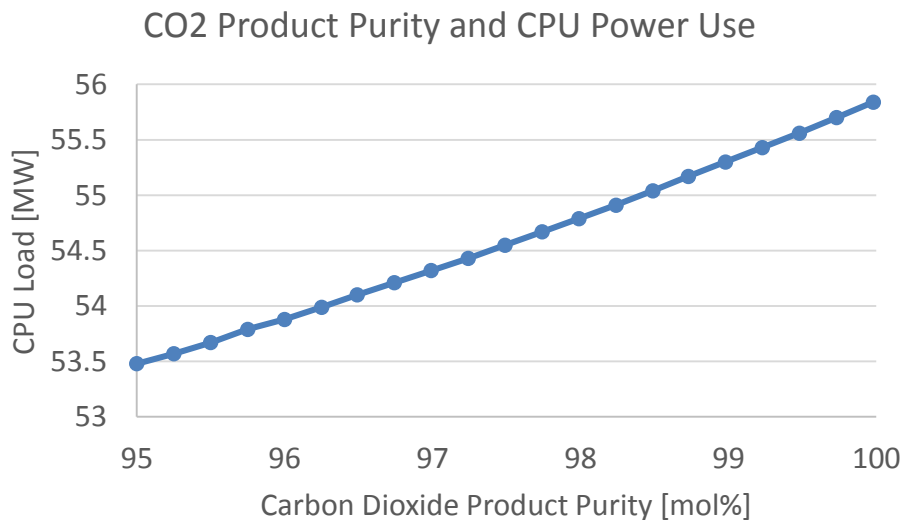


Figure 9.22 Effect of CPP on the total load of the CPU for the base plant.

The electrical load of the CPU increases by only about 2 [MW] across the CPP range considered here. This represents a change in total electrical load requirement of less than 5%. As will be demonstrated later in this section, there are a number of parameters which can have a greater effect on CPU load than

CPP if they are allowed to vary. That does not mean that there are no additional consequences for the oxyfuel plant system as a result of changes to the CPP. The reduction in net electrical output of the plant, as a result of the increase in unit work, is shown in the following figure.

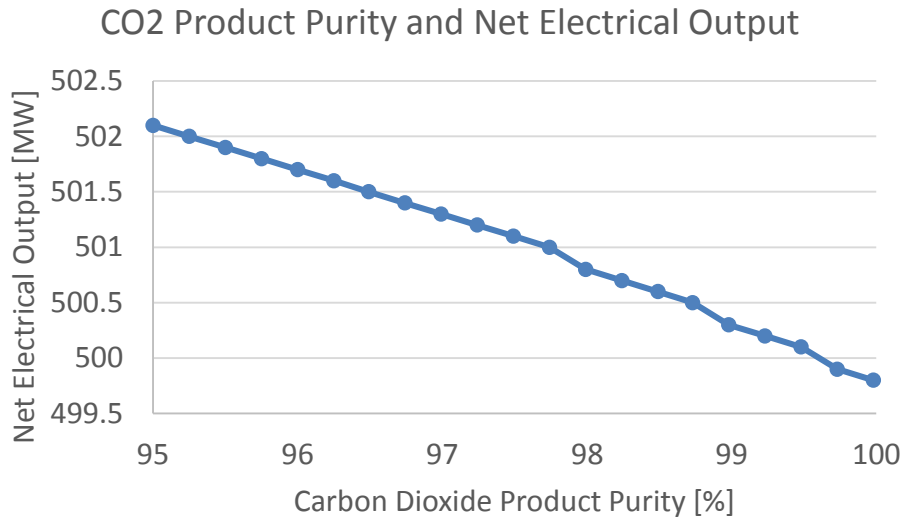


Figure 9.23 Net electrical output of the base plant is decreased as the CPP is increased.

Also affected by variations in the CPP is the transportation and storage of the carbon dioxide product. As CPP is increased, the flow rate of the carbon dioxide product stream is reduced. Consequently, the required pipeline and injection infrastructure may be downsized. The levelized cost curve (Fig. 9.24) is not smooth due to the discrete sizes in which pipe is offered and procured in the IECM T&S model.

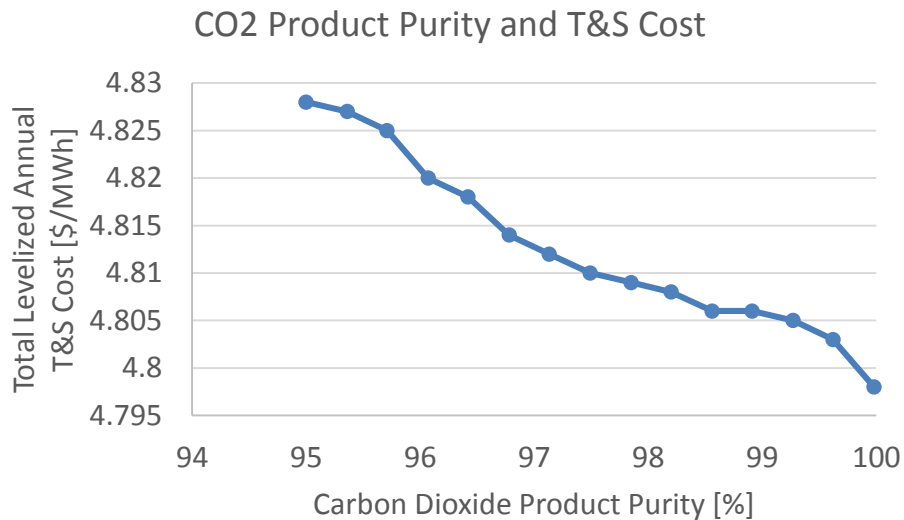


Figure 9.24 The levelized annual cost of transport and storage declines slightly in erratic fashion with increasing CPP for the base plant.

The reduction in levelized annual cost is rather small (~0.03 [\$/MWh]) across the chosen CPP range for the base plant. This works out to about \$100,000 annually or 3 million dollars over the financial lifetime of the plant. This is likely not a significant enough financial incentive to dominate the decision about which CPP to operate the CPU. However, the effects on T&S from CPP are sizeable enough that they should be considered in the development of any real-world system.

### 9.1.3.2 Carbon Dioxide Recovery Rate Effects

The carbon dioxide recovery rate (CRR) of the carbon processing unit determines the percentage of carbon dioxide that is ultimately contained in the product stream upon entering the unit. An upward sloping curve would be expected from gas separation dynamics and this is the shape produced across the CRR range.

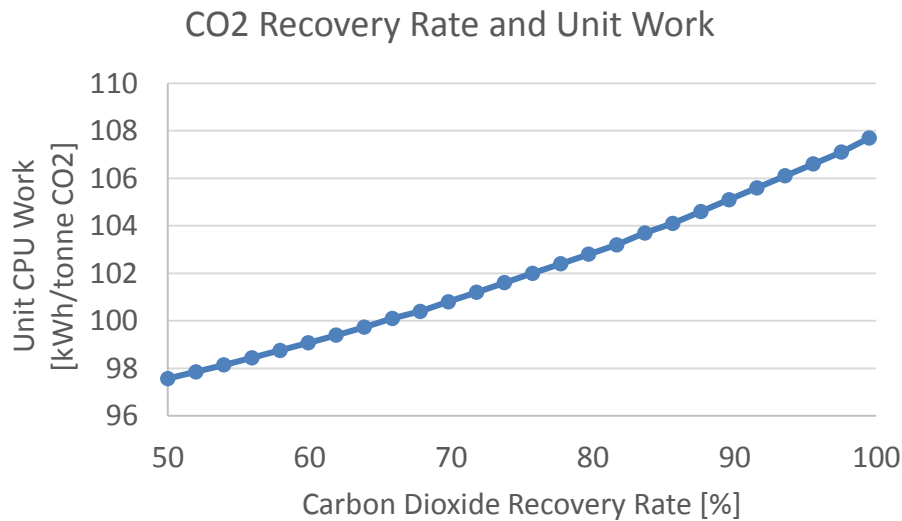


Figure 9.25 Accelerating increase in the CPU unit work as the CRR is increased.

The effect of this change in unit work becomes even more apparent when examining the change in net electrical output across CRR's. Because the quantity of carbon dioxide being captured in the CPU is increasing along with the increasing specific work, the total change across the CRR range is roughly 30 [MW].

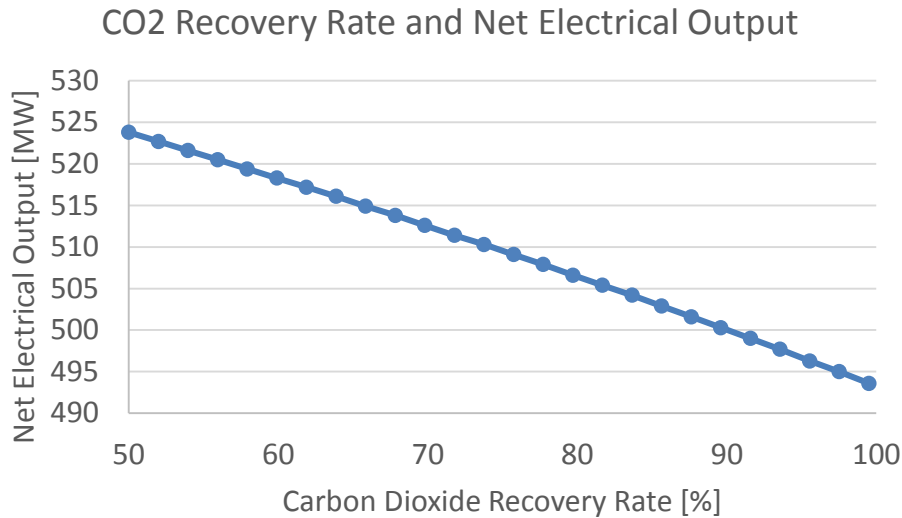


Figure 9.26 Steady decrease in the net electrical output of the base plant and the CRR is increased.

It is worth thinking about the above result in comparison with how other carbon capture technologies would fare if specified to capture half the carbon dioxide present in the flue gas. In post combustion capture processes the energy penalty is almost entirely bound to the quantity of carbon dioxide you are stripping from the flue gas. More specifically, the capture energy is determined by how much energy is required to regenerate the solvent responsible for capturing the carbon dioxide. If you are capturing half the CO<sub>2</sub>, you need only regenerate half as much solvent, and you have essentially halved your total energy penalty. Oxyfuel, by contrast, requires that you pay over half the capture energy penalty up front just to run the air separation unit. If you then chose to only purify half the flue gas, you have at best (assuming purification was 50% of energy penalty) only reduced your overall energy penalty for capture by 25%. For the base plant used for this sensitivity analysis, reducing the capture rate to 50% only reduces the capture energy penalty by about 20%.

Directly tied to CRR is the carbon intensity of the electricity produced by the oxyfuel plant. The relationship is linear and decreases from about half a tonne of CO<sub>2</sub> per megawatt-hour at 50% CRR with a slope of ~10 [kg/MWh] per point of CRR.

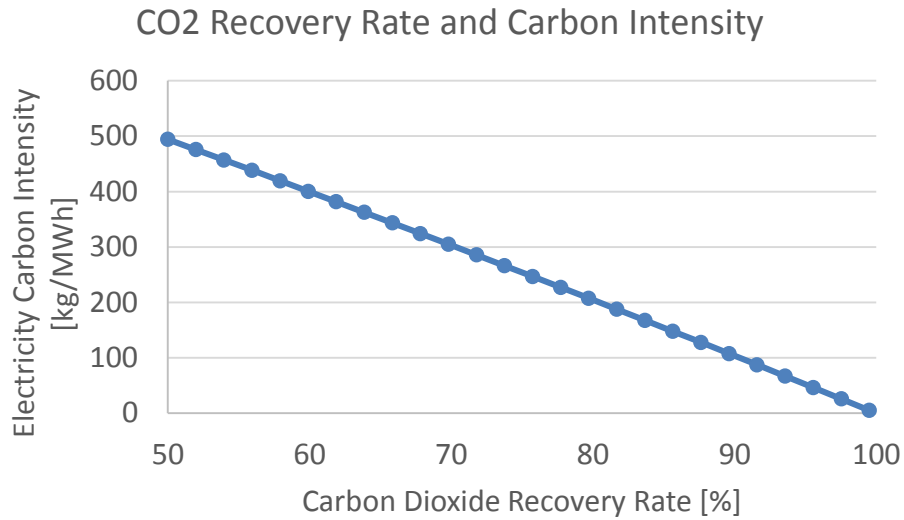


Figure 9.27 Intuitively, the carbon intensity of electricity generated by the base plant decreases as the CRR of the CPU is increased.

For a carbon capture plant, a decrease in carbon intensity is synonymous with an increase in the absolute quantity of carbon dioxide being captured. The consequence of this for the base plant's transport system across increasing CRR's is that the process facilities cost will increase as the system is enlarged to handle the increased volumetric flow.

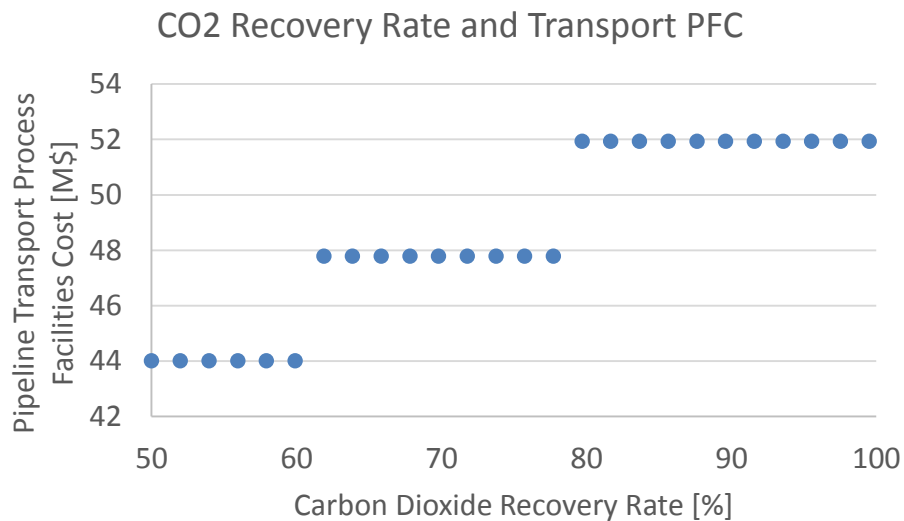


Figure 9.28 The PFC of the pipeline transport system for the base plant increases discretely as the CRR of the CPU is increased.

There are discontinuities followed by areas of no change in the PFC of the transport cost in the above figure. This is the result of the transport model having to jump from one discrete pipe diameter to the next as the flowrate of carbon dioxide product is increased. The utilization of each pipe size's maximum

flow right is highest just before the next larger diameter pipe is required. Consequently, the levelized cost, per tonne transported basis, is typically higher immediately after a pipe size increase than it was previously. This relationship can be seen in blue in Figure 9.29. The blue data, per tonne basis, corresponds to the left vertical axis and the red data, per megawatt-hour basis, corresponds to the right vertical axis.

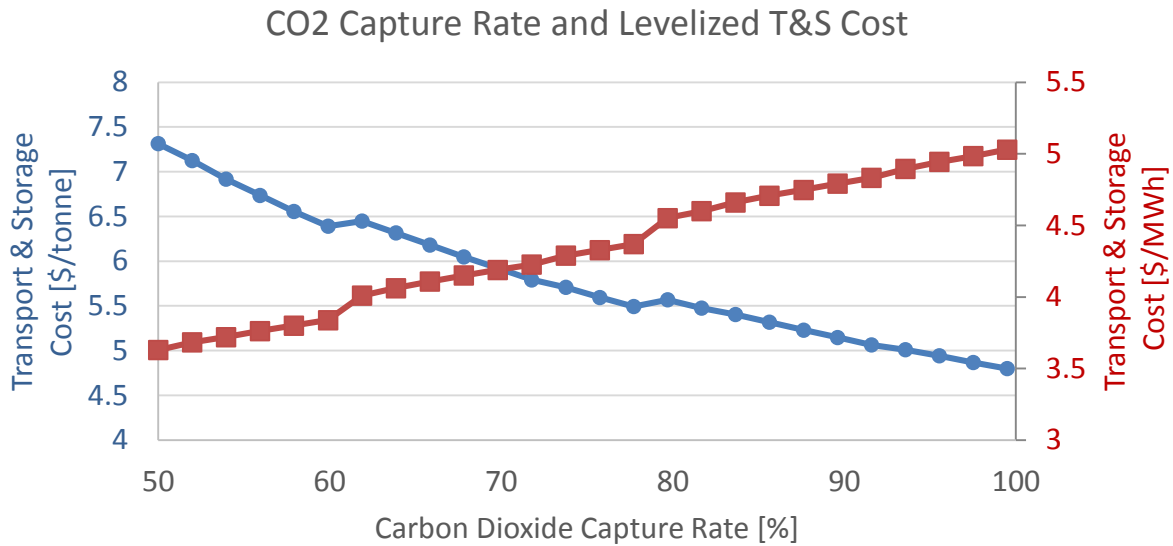


Figure 9.29 Transport and storage costs measured by two different metrics as a function of CPU CRR.

The overall trend of the blue data is that as more tonnes of carbon dioxide are transported and stored the bigger base lowers the average cost. Whereas the red data shows that the costs per megawatt-hour are highest whenever the most carbon dioxide is being transported and stored. Which of these metrics is most important is determined by the business model for an individual facility, but in general, per tonne transport and storage costs are sought to be minimized. It is also important to note that regardless of which metric is considered, transport and storage accounts for less than 5% of the overall cost of electricity regardless of carbon dioxide recovery rate for the base plant.

### 9.1.3.3 DCCPS Operating Temperature Effects

The operating temperature of the direct contact cooler and polishing scrubber (DCCPS) determines the amount of moisture which is removed from the flue gas before it is sent to the carbon processing unit (CPU). Moisture that is not removed from the flue gas by the DCCPS must be removed by the CPU before the flue gas may enter the cold box to prevent ice formation and equipment failure. The moisture is primarily removed through compression and intercooling in the CPU. This means that extra energy is used to compress the additional gaseous water then move additional cooling water through the CPU. The following figure shows the change in CPU load which is produced at the operating temperature of the DCCPS is varied along the operational range.

### DCCPS Operating Temperature and CPU Power Use

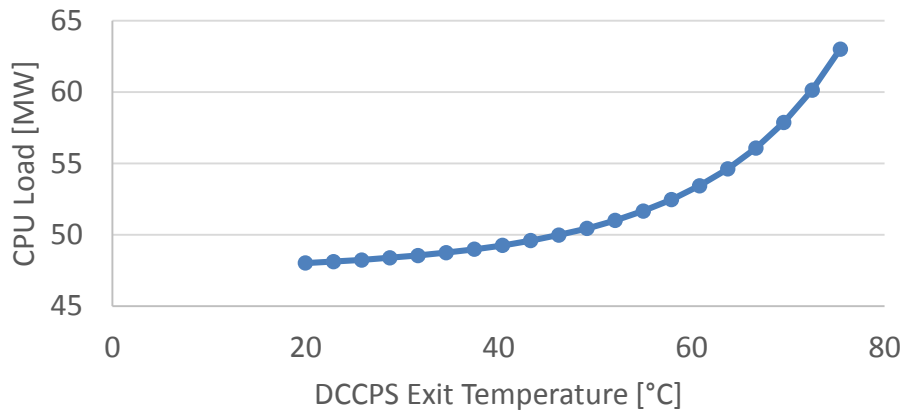


Figure 9.30 CPU load increases dramatically as the operating temperature of the DCCPS gets towards the high end of the spectrum.

In section 9.3.2 on the sensitivity of the DCCPS it was intimated that the interactions of the DCCPS load and CPU load across operating exit temperatures would produce a relation which had a minimum total load. Figure 9.31 presents the total electrical load of the Flue Gas Recirculation and Purification System; which includes the DCCPS, CPU, and flue gas recirculation fan.

### DCCPS Operating Temperature and Flue Gas Recycle & Purification Power Use

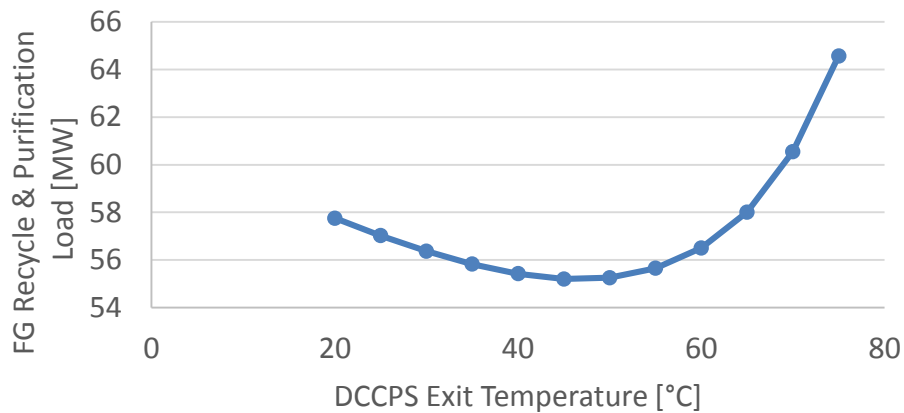


Figure 9.31 The total electrical load of the flue gas recirculation and purification has a knee at around 50 centigrade for the base plant.

The temperature which minimizes the electrical load of the combined Flue Gas Recirculation and Purification System is approximately 45 [°C]. The temperature range of 35-55 [°C] for the base plant configuration has very similar performance however. When the remainder to the plant is included the following relation of net plant output is produced:

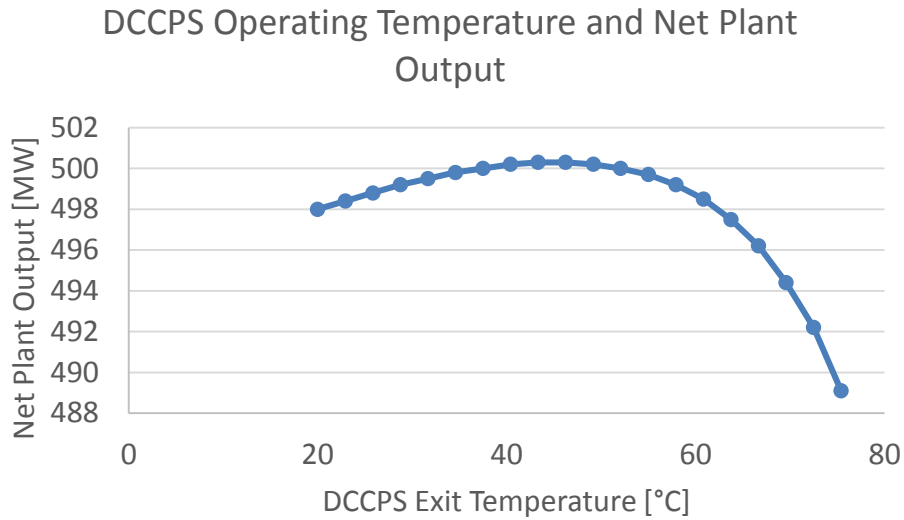


Figure 9.32 The net electrical output of the plant reflects the knee identified in the flue gas recirculation and purification load as a function of DCCPS operating temperature.

The overall plant output reaffirms that there is a wide operating temperature for this plant configuration which produces comparable performance. It should be noted that other oxyfuel plant configurations may have a much more dramatic peak with respect to DCCPS operating temperature and net plant output.

#### 9.1.3.4 Carbon Dioxide Product Compression Effects

The user has the ability to stipulate a desired pressure for the carbon dioxide product produced by the CPU. The IECM default is 13.79 [MPa] but a range of 7.5 to 15.2 [MPa] is examined in the following figure. The required product pressure is typically a function of the depth of the formation into which the carbon dioxide is to be injected for sequestration or use in enhanced oil recovery. The plant gate pressure may be higher than the injection pressure in instances where booster pumps are not going to be used and the gate pressure is expected to overcome the pneumatic pressure in the transport pipeline.

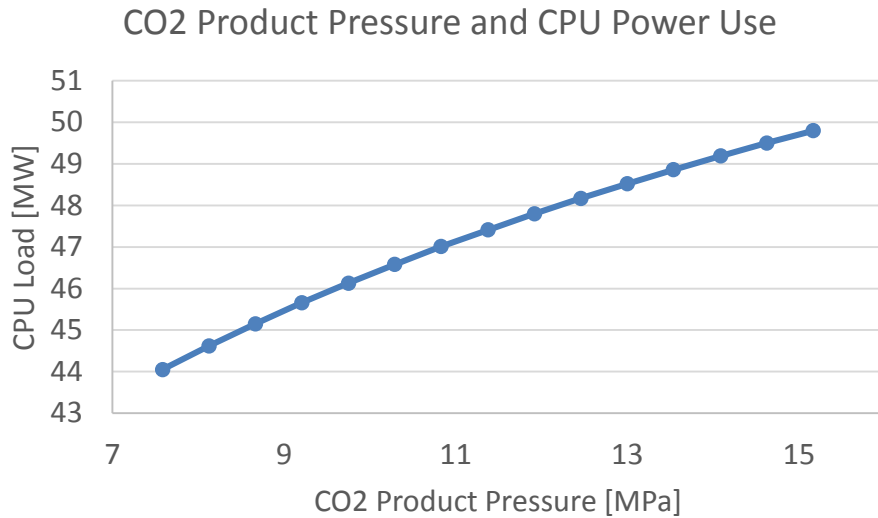


Figure 9.33 CPU load increase about 10% as the product pressure is increased from 7 to 15 MPa.

There is an increase in CPU load of about 6 [MW] as the product pressure is doubled from 7.5 to 15 [MPa]. This represents a roughly 15% variance in CPU load across the product pressure range. It is apparent that, all else being equal, operating at the lowest acceptable product pressure will result in the lowest electrical load for the CPU.

The user is also prompted to provide an efficiency value for the carbon dioxide compressor. The default value in the IECM is 85%. A range of reasonable compressor efficiency values are evaluated for their effect on CPU load in the below figure.

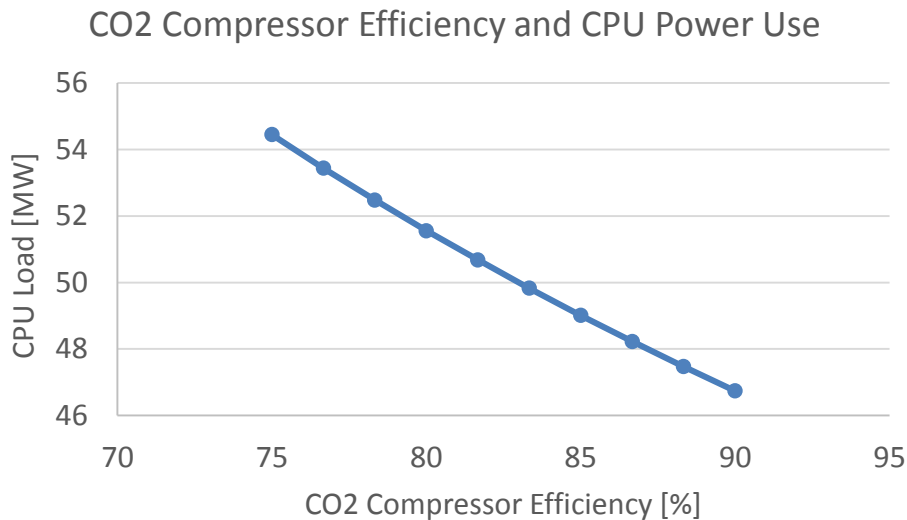


Figure 9.34 CPU load decreases as the CO2 compressor efficiency is increased.

For the base plant, the slope of the relation is approximately 500 [kW] of additional load for each percentage reduction in compressor efficiency. Here again, it is straight forward to deduce that the CPU which has the most efficient compressor will require the lowest electrical load.

#### 9.1.3.5 Effects of Air Ingress and Excess Air

The mass flow rate of the gas stream entering the cold box of the CPU along with the concentration of carbon dioxide of that gas stream have a dramatic effect of the power consumed by the CPU. The amount of air which enters the flue gas stream at the recycle preheater is known as air ingress. Air ingress is defined by the quantity of atmospheric oxygen which enters the flue gas relative to the quantity of oxygen required to completed stoichiometric combustion of the fuel. Atmosphere, being comprised of less than 21% oxygen, brings a large amount of other gases into the flue gas stream. These gases dilute the concentration of carbon dioxide in the flue gas stream while also increasing the mass flow rate.

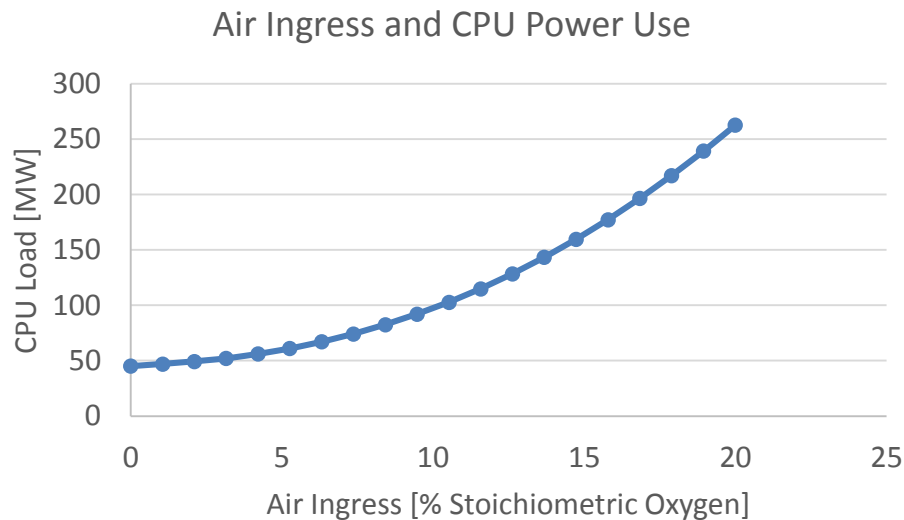


Figure 9.35 The electrical power consumption of the CPU increases dramatically once the air ingress rate exceeds ~10%.

The above figure shows the dramatic effect which air ingress can have on the power consumption of the CPU. As the amount of air ingress increases beyond 5% the CPU load begins to increase dramatically as a result of the combined effects of a larger, more CO<sub>2</sub> dilute, flue gas stream. The severity of load increase at elevated air ingress levels is why it is imperative that the boiler and flue gas handling systems be specifically designed and diligently maintained to minimize leaks and ensure peak performance. This is also a large factor in why the concept of retrofitting existing boilers for oxycombustion, which commonly have air ingress rates near 10%, has lost favor.

To a much lesser extent than air ingress, excess air also affects the electrical load requirements of the CPU. The term “excess air” is a bit of a misnomer for oxycombustion because the fuel is being combusted with oxygen rich oxidant rather than air. However, there is general acceptance and familiarity with the term “excess air” and given that it is measured relative to stoichiometric oxygen, it is easiest to simply adopt the convention of air-fired units.

In practice, boilers require some degree of excess air to ensure proper burnout of fuel. For the base plant, 105% of stoichiometric oxygen requirement (5% excess air) is supplied to the boiler. As can be seen in Figure 9.36, increasing the percentage of excess air causes an increase in the electrical load requirement of the CPU.

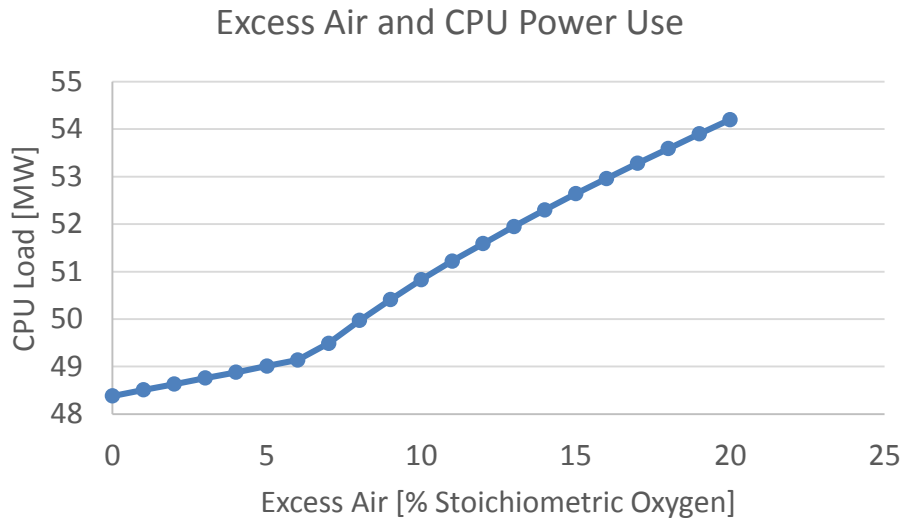


Figure 9.36 CPU load increased as excess air is provided to the boiler due to dilution of the flue gas. There is a knee in this curve that is the result of the carbon dioxide to oxygen ratio causing a change in the second law separation efficiency of the CPU.

For the base configuration, there is an inflection point in this relationship at about 6% excess air where the slope suddenly increases. The reason for this behavior is that the second law separation efficiency begins to decrease with the increasing concentration of oxygen in the CPU. Consequently, after 6% excess air, both separation efficiency reductions and increasing gas flow rates are causing the CPU electrical load to increase.

The separation efficiency of the CPU is a function of the ratio of carbon dioxide to oxygen in the flue gas entering the CPU. A more thorough discussion of the gas separation physics which underlie the importance of the carbon dioxide to oxygen ratio can be found in Chapter 7. This ratio is most affected by coal composition, oxidant purity, air ingress, and excess air and typical second law efficiencies are calculated to be between 50 and 60%.

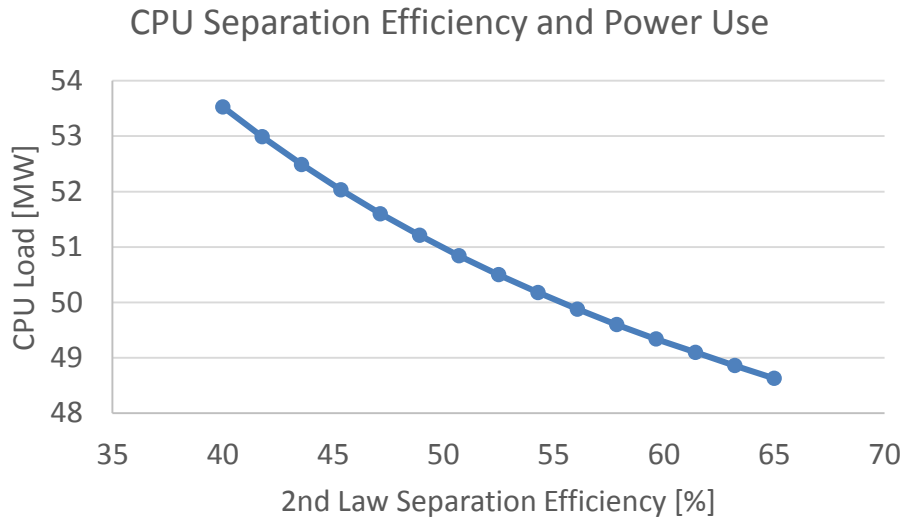


Figure 9.37 Effect of 2nd Law Separation efficiency on the CPU load.

The effect of separation efficiency on the overall power consumption of the CPU is not dramatic by comparison to air ingress. The reason for this is that the CPU work is dominated by the need to compress large quantities of flue gas to high pressures. By comparison, the separation work component is rather small. The result is demonstrated in the above figure: separation efficiency has an appreciable impact on CPU load, but it is a secondary effect compared to increases from increased volumetric flow.

#### 9.1.3.6 Gross Plant Size Effects

The gross electrical output of the oxyfuel plant equipped with a carbon processing unit (CPU) directly affects the electrical load consumed by the CPU. The below figure demonstrates CPU load across a gross electrical output range from 300 to 1500 [MW].

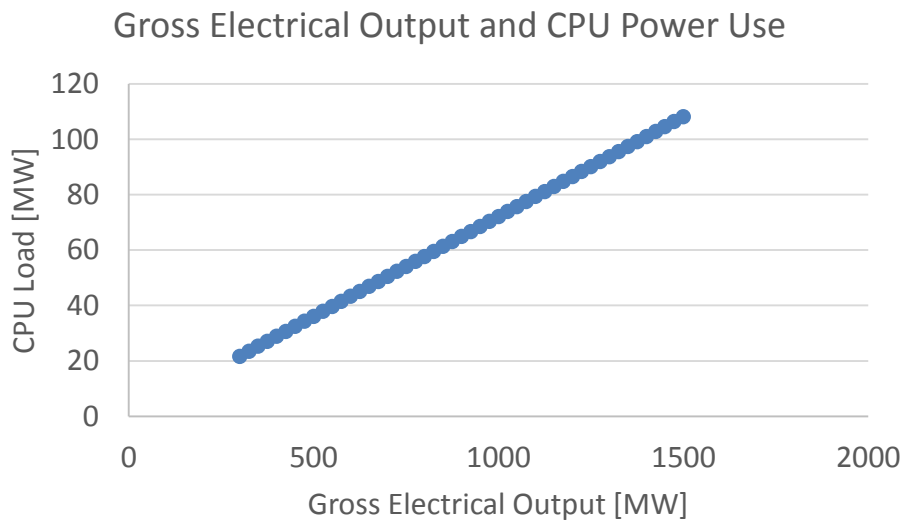


Figure 9.38 CPU load is a linear function of plant size.

The relation between CPU load and gross electrical output is assumed to be linear based on a specific work per tonne basis and scaled by the mass throughput. Not enough performance information was available across various gas processing rates to be able to create a more detailed performance relationship with throughput as a performance parameter.

There was greater availability of information regarding the size limits of cold boxes which allowed for an economic model capable of calculating the number of CPU trains required for a specified carbon dioxide throughput. The below figure depicts the CPU train requirements across the gross electrical output of the base oxyfuel plant.

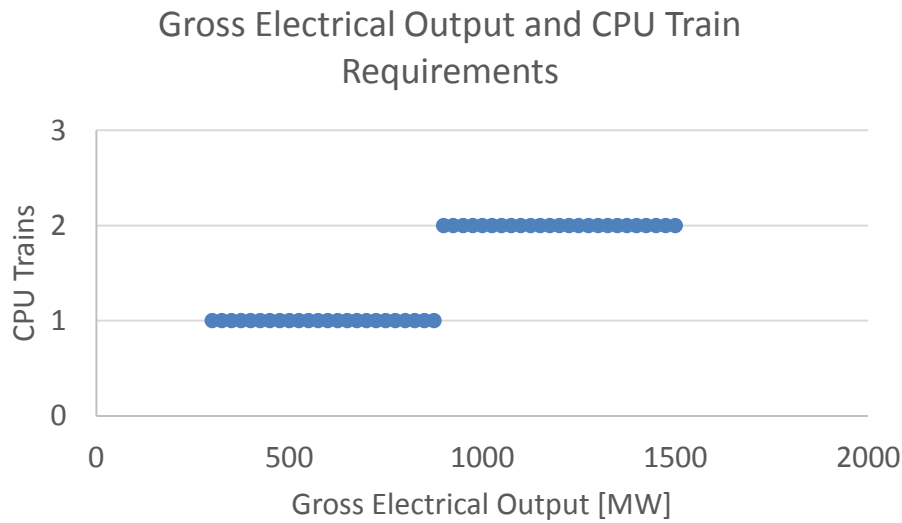


Figure 9.39 The required number of CPU trains increased to two once the gross electrical output exceeds 900 [MW].

For the base oxyfuel plant a gross electrical output of 900 [MW] is required before multiple CPU trains are necessitated to handle the gas flow. For practical purposes, this indicates that a single train CPU system would be capable of providing carbon dioxide enrichment for all but the largest steam turbines currently in the U.S. pulverized coal generation fleet.

The process facilities cost of the CPU system is determined by the gas flowrate it must be able of processing. As the gross electrical output of the base plant is increased, the PFC of the CPU increases smoothly across the range aside from the discontinuity where a second train is added.

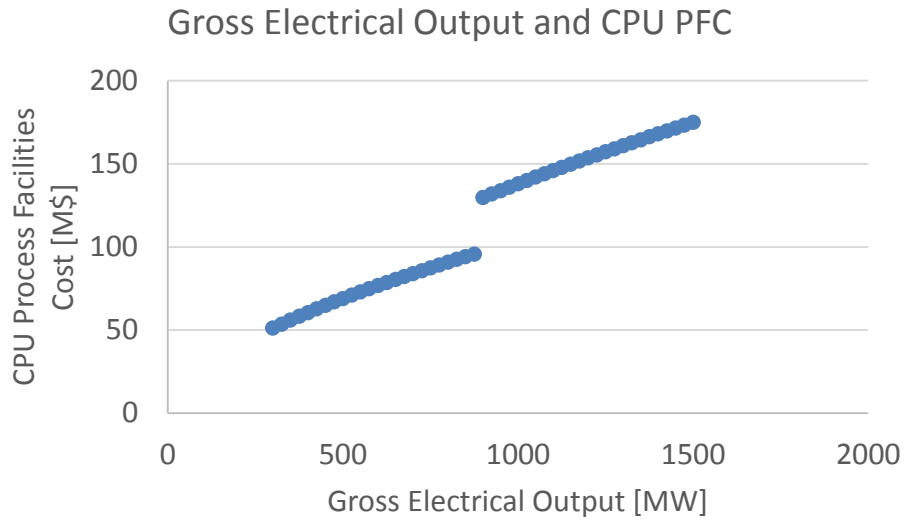


Figure 9.40 PFC of the CPU has a discontinuity from the inclusion of a second train when gross electrical output exceeds 900 [MW].

The operations and maintenance costs of the CPU are tallied along with the balance of equipment (DCCPS, flue gas fan) which comprises the Flue Gas Recycle and Purification System. The levelized O&M costs for this system are calculated largely based upon the original capital requirement of the system. This is why the Figure 9.41 shows a discontinuity in the cost curve stemming from the addition of a second CPU train as the gross electrical output of the plant is increased.

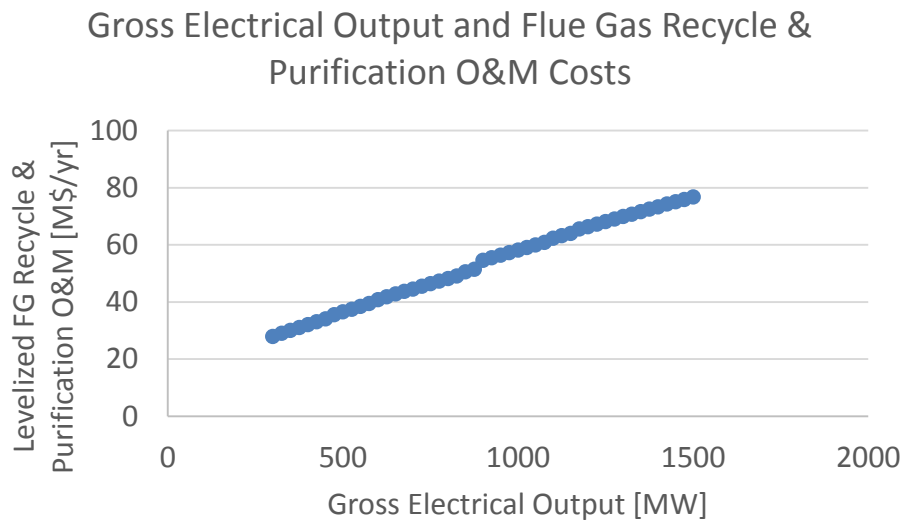


Figure 9.41 Levelized flue gas recirculation and purification costs are a muted reflection of the gross PFC for this umbrella system.

It is worth noting that there would be an additional discontinuity in the operations and maintenance cost curve above where the gross electrical output large enough to warrant a second DCCPS train. It just so happens that the base plant does not have a high enough volumetric flow rate even at 1500 [MW] to necessitate such an investment.

### 9.1.4 CoCapture System

When a carbon processing unit is not being used to increase the purity of the carbon dioxide product a combined capture (CoCapture) system must handle the entire flue gas stream. This includes removing all the residual moisture left in the flue gas by the DCCPS in addition to compressing the entire gas stream to the stipulated plant gate pressure. The CoCapture system performance model is sensitive to the mass flow rate and temperature of the flue gas. These two parameters will be evaluated in the following sub-sections along with effects of gross plant size.

#### 9.1.4.1 Effects of Air Ingress and Excess Air

Increasing the quantity of excess air used in the boiler will increase the total amount of flue gas handled by the oxyfuel plant. The relationship between CoCapture load and excess air is apparent, but it is not dramatic (Fig. 9.42). The slope of the load change is rather mild with only a +/- of 1 [MW] as excess air is varied from 0 to 10% around the default of 5%.

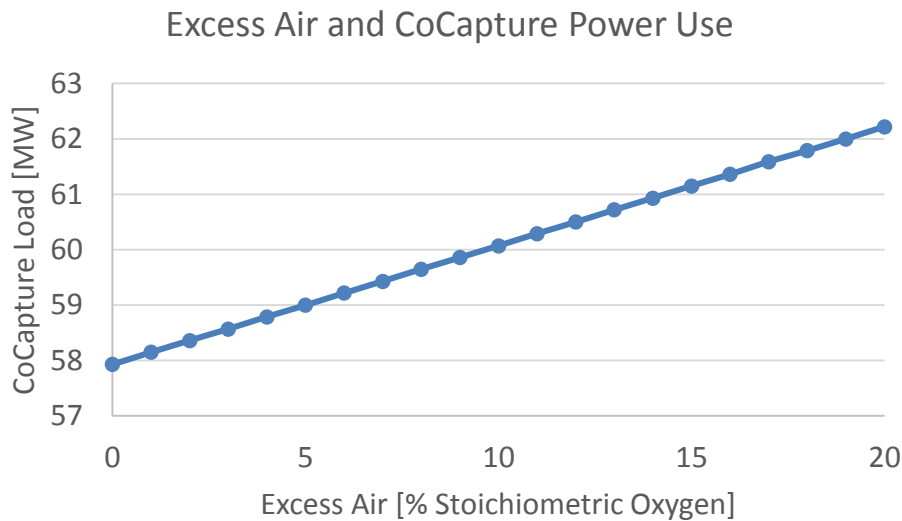


Figure 9.42 Excess air has little effect of the overall load of the CoCapture system.

In Fig. 9.43 we evaluate the impact of the air ingress rate on CoCapture power use. The slope of the line is very dramatic compared to the relationship for excess air. This is because of the disparity in oxygen concentration between oxidant and atmosphere. You are adding equivalent amounts of oxygen to the flue gas at a 10% air ingress rate and at 10% excess air, however the former is 20 [O<sub>2</sub> mol%] and the latter is 95 [O<sub>2</sub> mol%].

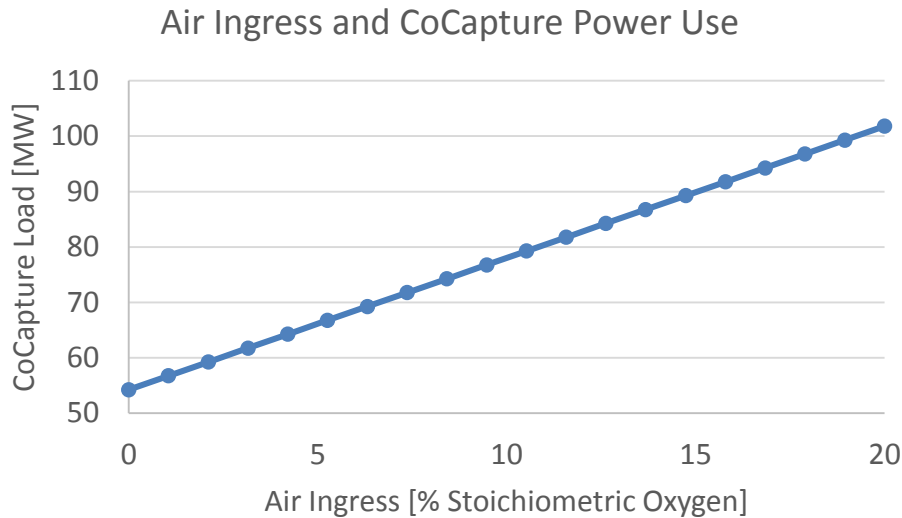


Figure 9.43 The effect of air ingress on CoCapture load is dramatic as a result of the added gas which must be compressed.

The effect of high air ingress rates on CoCapture electric load consumption are non-trivial and have a substantial impact of the net plant efficiency of the overall plant. In the following figure the net plant efficiency of the overall plant, on a higher heating value basis, is shown across an air ingress range from 0 to 20%.

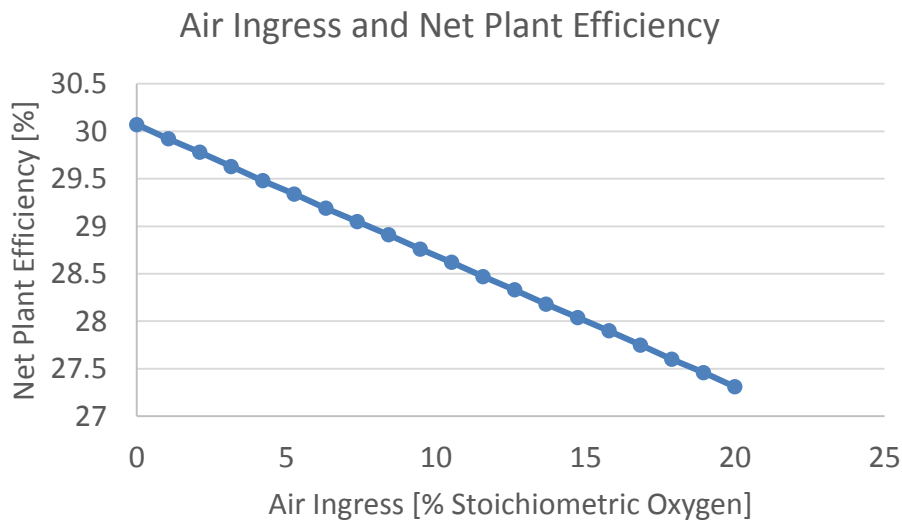


Figure 9.44 Reduction in overall plant efficiency is just shy of 1.5 percentage points for an air ingress rate of 10%.

Net plant efficiency for a CoCapture plant is a strong function of the air ingress rate. The reduction in net plant efficiency translates to higher levelized cost of electricity values at air ingress increases (Fig. 9.45). The increase in LCOE is mainly a result of higher variable operations and maintenance costs (fuel and consumables) which comes with a higher heat rate. It is worth noting that traditionally air-fired units tend to have increased air ingress rates as they age. The current lack of long-term oxyfuel plant

operation studies does little to assuage concerns that air ingress rates will increase and bring higher operating costs for plant owner/operators as the plant ages.

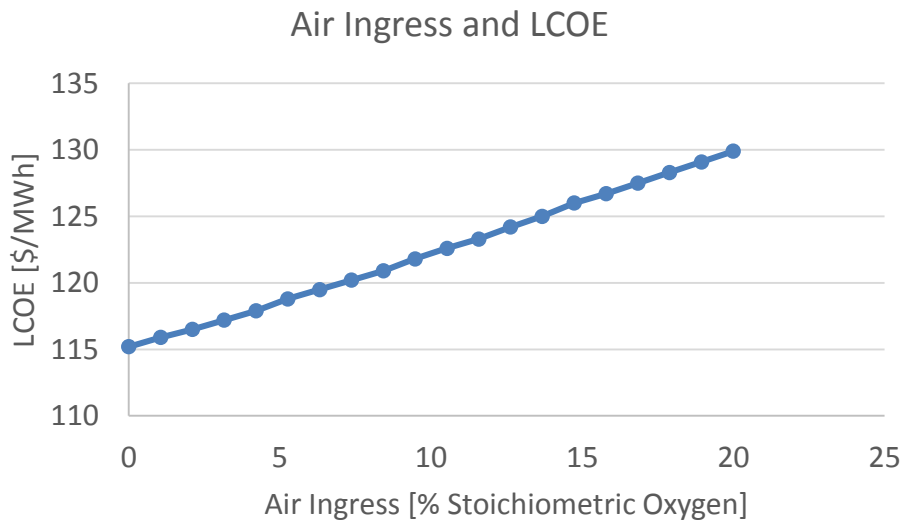


Figure 9.45 Marked increased in LCOE result from increases in the air ingress rate. This is of potential concern as oxyfuel plants age and leaks form.

An interesting moderating element to the LCOE cost increases presented in the above figure is that as air ingress increases, the quantity of oxygen which must be provided by the ASU to the boiler decreases. The consequence of this is that if you were planning on an elevated, but constant, air ingress rate you could down-size the ASU. Because the capital intensity of the ASU is very high relative to the other components of the CoCapture system, the overall PFC of the CO<sub>2</sub> control equipment actually decreases as the air ingress rate is increased.

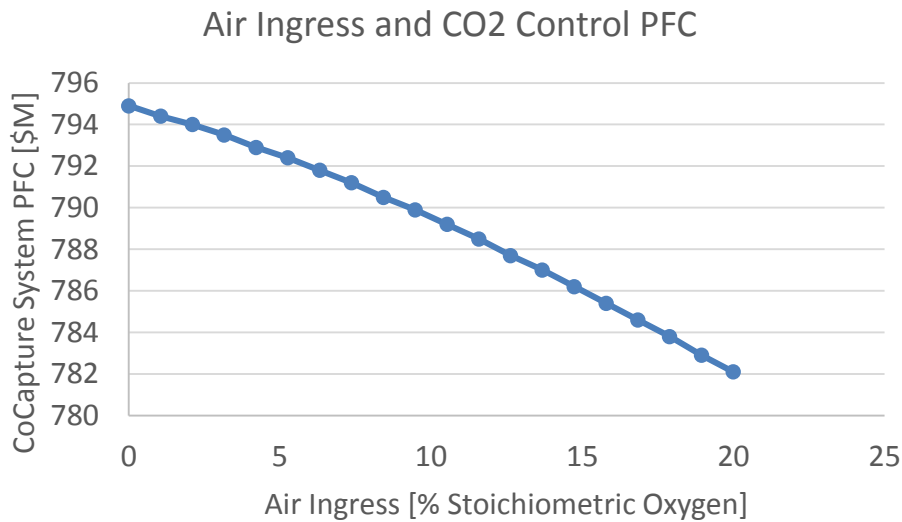


Figure 9.46 The overall PFC of the CoCapture system is actually decreased at high air ingress rates. This is because it allows for the ASU, the most capital intensive component, to be undersized.

The decrease in capital cost from the CO<sub>2</sub> control equipment is not substantial enough to overcome the increase in O&M cost on a levelized basis however. Thus, it is still preferable to minimize the air ingress rate to ensure the overall performance of an oxyfuel plant with CoCapture.

#### 9.1.4.2 DCCPS Operating Temperature Effects

The operating temperature of the direct contact cooler and polishing scrubber (DCCPS) controls two very important parameters which affect the performance and cost of the CoCapture system. The exit temperature of the DCCPS determines the mass flow rate and moisture concentration of the flue gas passed to the CoCapture system. As the operating temperature of the DCCPS is increased, less flue gas moisture is precipitated out (Fig. 9.47).

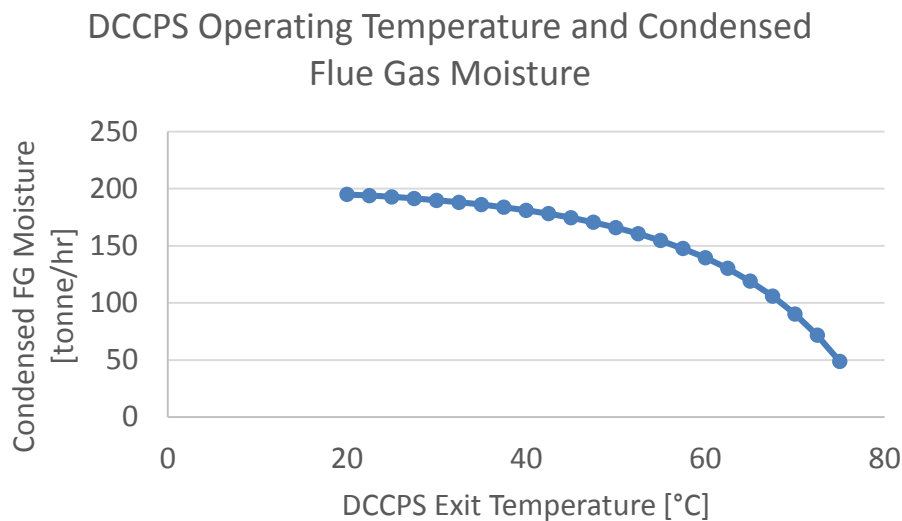
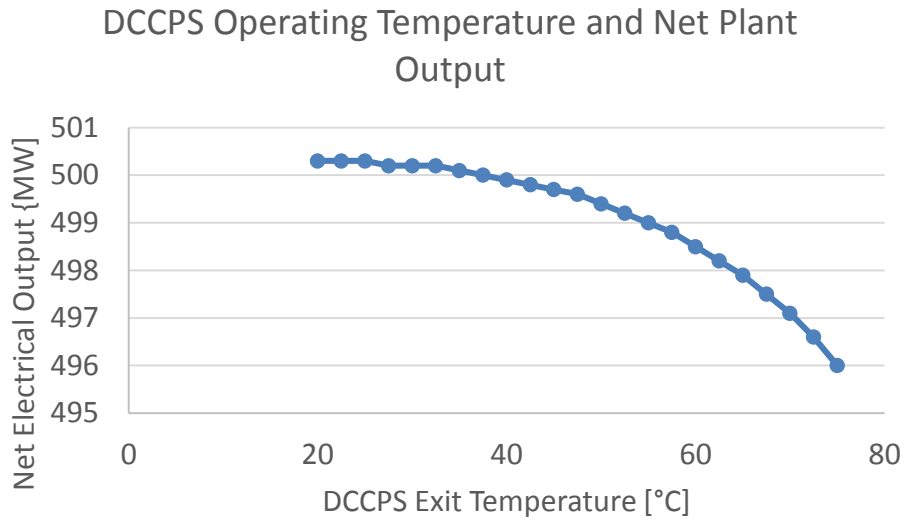


Figure 9.47 Condensed flue gas moisture is reduced to a quarter of its value at 20 centigrade when operating at 75 centigrade.

Less moisture being removed by the DCCPS means that this moisture must then be removed by the CoCapture system. The DCCPS removes moisture through the use of a temperature swing near atmospheric pressure. By contrast, the CoCapture system removes moisture through a temperature swing process only after the entire gas stream has been pressurized. The former is a more thermodynamically efficiency process to remove moisture as long as you have access to cooling water at a sufficiently low temperature to provide the cooling load. The base plant is not constrained by cooling water availability and consequently we would anticipate net plant efficiency (and electrical output) to suffer at high DCCPS operating temperatures.



**Figure 9.48** Operating the DCCPS at elevated temperatures results in a decrease in the net electrical output of the base plant.

Figure 9.48 displays the expected relationship for net electrical output across DCCPS operating temperature. Using the CoCapture system to remove moisture from the flue gas is not as thermodynamically efficient as the DCCPS.

#### 9.1.4.3 Gross Plant Size Effects

The performance and cost of the CoCapture system is determined largely by the mass flow rate of the flue gas throughput it must be able to process. Flue gas flowrate is strongly a function of the gross plant size. The performance model for CoCapture does not have total flowrate as a performance parameter because data on performance across flowrates was not available. Consequently, like the CPU system, the specific performance of the CoCapture system is multiplied by the mass flow rate to arrive at a total performance figure. This is the reason why the relation between CoCapture load and gross electrical output in the following figure is a straight line.

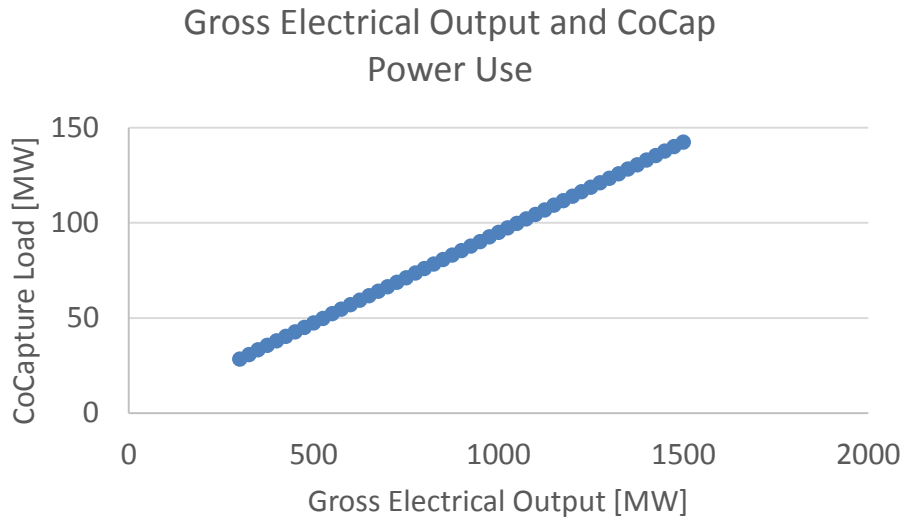


Figure 9.49 CoCapture power use increases steadily as a function of plant size.

Data on the size limitations for a single train size were available which allowed the development of an economic model which considered mass flow rate. In the following figure the number of CoCapture trains required to service a plant of gross electrical output from 300 to 1500 [MW] is presented. For the base plant, a second CoCapture train would be required for any gross electrical output above 800 [MW].

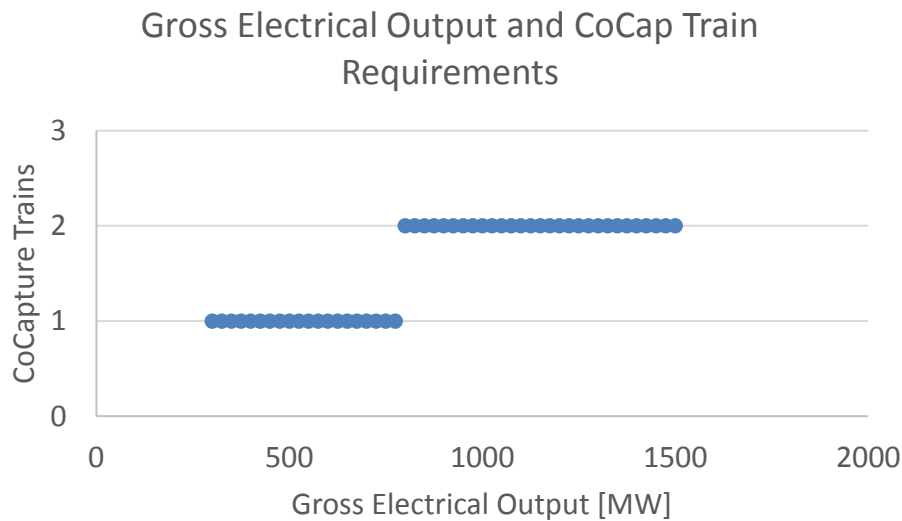


Figure 9.50 The number of required CoCapture trains increases to two at a gross plant output of 800 [MW].

The process facilities cost of the CoCapture system across gross electrical output is presented in Figure 9.51. The PFC of a single train system decreases in accordance with the 6/10ths scaling law for plant equipment. After the jump to a second train, the rate of cost decrease is halved as the size of the two complementary units is then increased at half the previous rate.

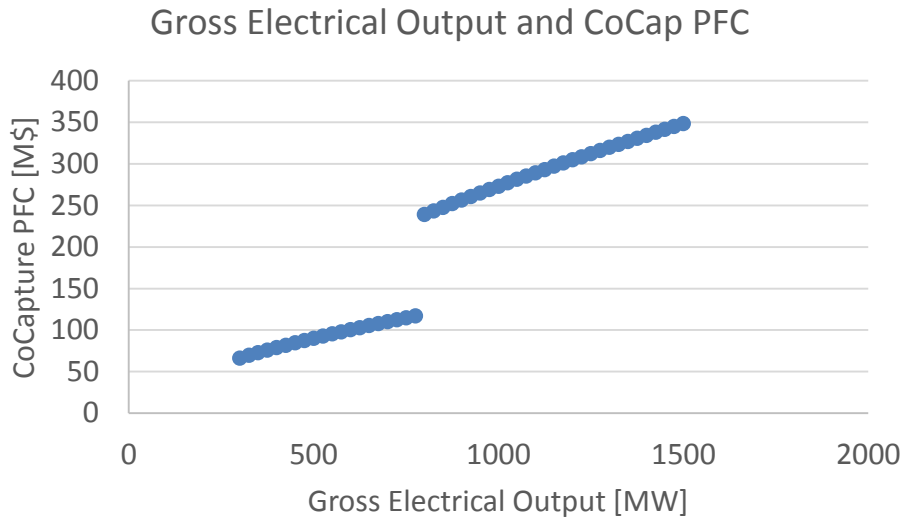


Figure 9.51 Process facilities cost of the CoCapture carbon handling system across gross electrical output.

Operations and maintenance costs for the CoCapture system are calculated along with the flue gas recirculation fan and the DCCPS. There is no purification of the carbon dioxide product gas occurring under this scenario; otherwise the title “Flue Gas Recycle & Purification” would have been retained. Here, the equivalent equipment has been labeled “Total CoCap System”. However, the two are functionally the same for purposes of comparing across oxyfuel carbon handling technologies.

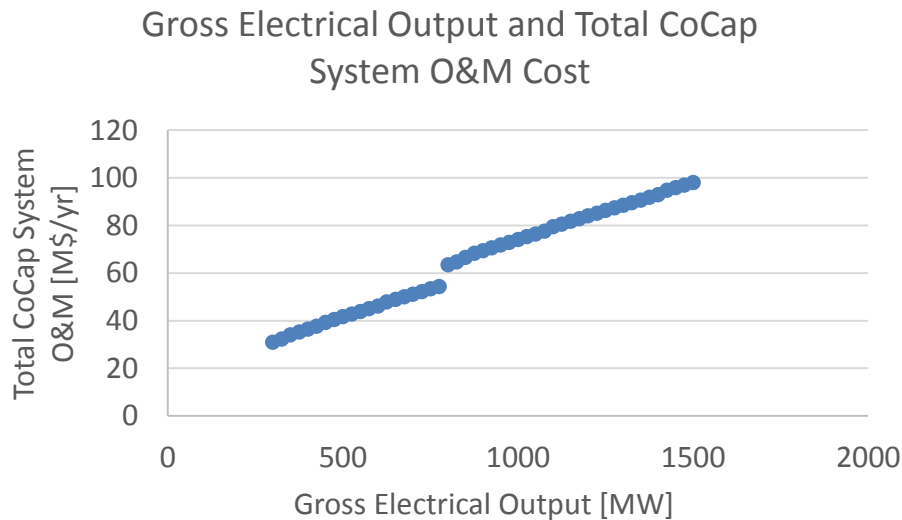


Figure 9.52 The operations and maintenance costs associated with the total CoCapture system display a discontinuity in an otherwise constantly increasing function of plant size where the second train is added.

Operations and maintenance costs increase as gross electrical output is increased. This is predominately because the majority of O&M costs in the IECM are calculated as a percentage of the capital cost for each process area.

### 9.1.5 Flue Gas Recirculation Rate

The oxyfuel model in the IECM is capable of determining how the recycled flue gas is to be divided in order to meet emission and performance constraints for any overall flue gas recirculation rate specified by the user within the range of 60-85%. Adjusting the total flue gas recirculation rate does cause some changes in the plant design which impacts the cost and performance of the overall plant. As the flue gas recirculation rate is increased, the volumetric flow rate of flue gas which must be handled by all of the plant components increases as well. The result of this upsizing can be seen in the below figure where a fairly smooth increase in total capital requirement occurs across the range of flue gas recirculation rates.

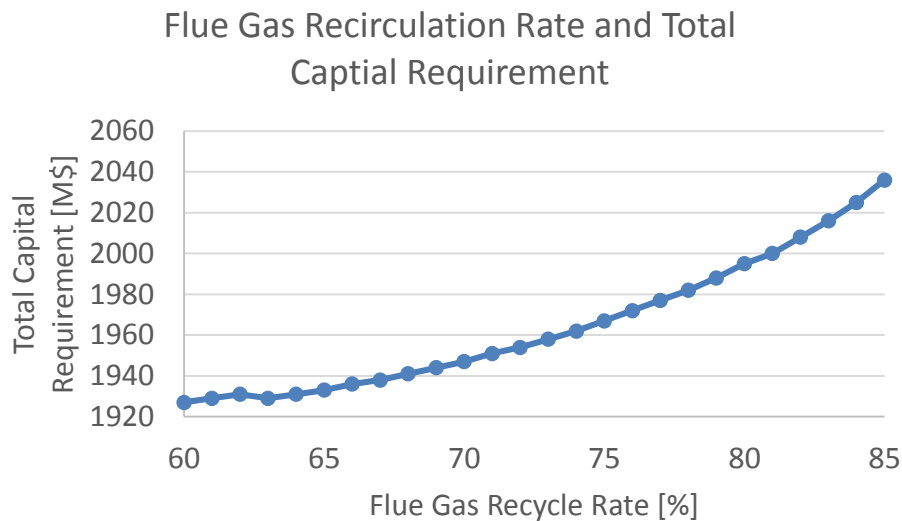


Figure 9.53 Total capital requirement of the base plant as the flue gas recycle rate is increased. There are two perturbations in the curve resulting from alterations to the TSP and FGD system to accommodate the change in gas volume.

There are a few perturbations in the total capital requirement curve (at 63 and 81% FGR rate) which require explanation. Conceptually, an increase in the flue gas recirculation rate affects the boiler, DCCPS, and the criteria pollution control equipment. The boiler is a single unit which is scaled and therefore would not produce any discontinuities in the capital cost requirement; and we have shown earlier that a single train DCCPS is capable of handling much larger flue gas volumetric flow rates than are present here. That leaves the pollution control equipment as the plausible explanation.

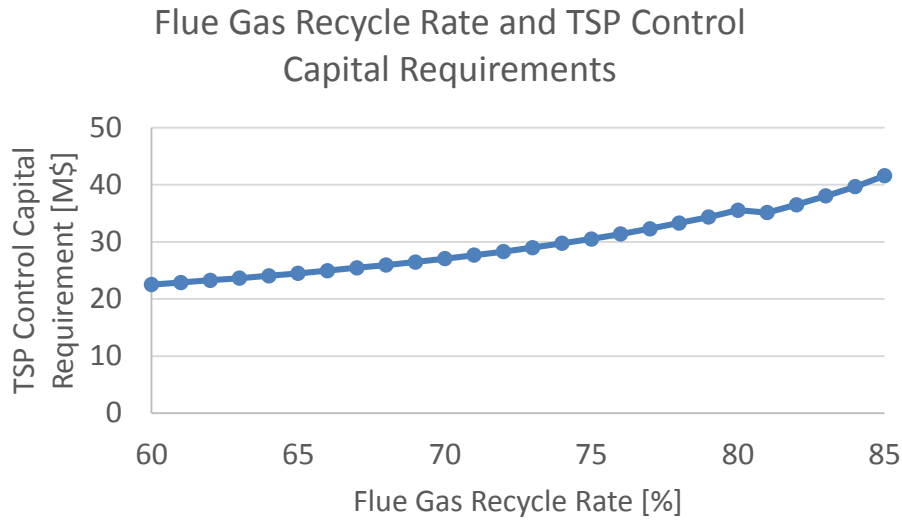


Figure 9.54 Capital requirement of the TSP system as a function of flue gas recycle rate for the base plant.

The discontinuity at 80% can be attributed to the upsizing of the pulse-jet fabric filter system for total suspended particulate (TSP) control; see above figure. The second discontinuity, at 62%, can be attributed to a change in the size of the wet flue gas desulfurization (WFGD) unit for sulfur dioxide control.

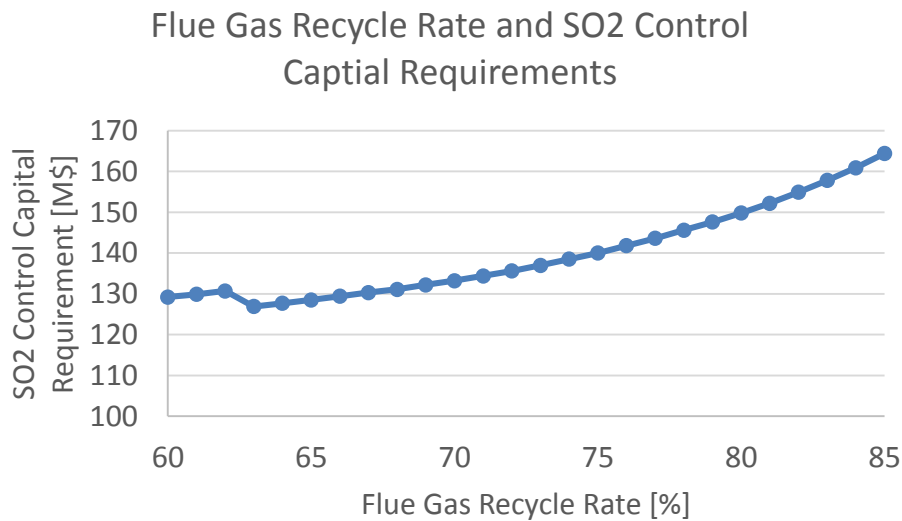


Figure 9.55 Capital requirement of the FGD system as a function of the flue gas recycle rate for the base plant.

The upsizing of the fabric filter and WFGD account for an increase of roughly 20 [M\$] and 35 [M\$], respectively across the range of flue gas recycle rates evaluated. The remainder of the 120 [M\$] total increase in capital requirement comes from upsizing the DCCPS, boiler, flue gas fan, and flue gas duct work.

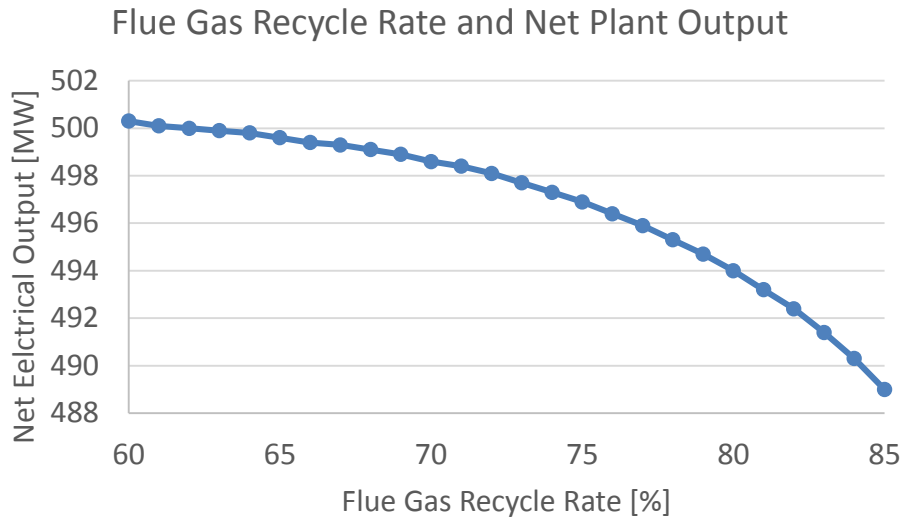


Figure 9.56 Increasing electrical loads to operate the gas handling and processing equipment at higher flue gas recycle rates reduces the net electrical output of the base plant.

The increase in equipment size also means that more electrical load is dedicated to operate each of the flue gas handling components. The result (Fig. 9.56) is that at a flue gas recirculation rate of 85% the net electrical output has fallen to 489 [MW] from 500 [MW] at the default flue gas recirculation rate of 65%. This reduction in net electrical output, along with the increased capital cost, combines to increase the leveled cost of energy as the flue gas recirculation rate is increased (Fig. 9.57).

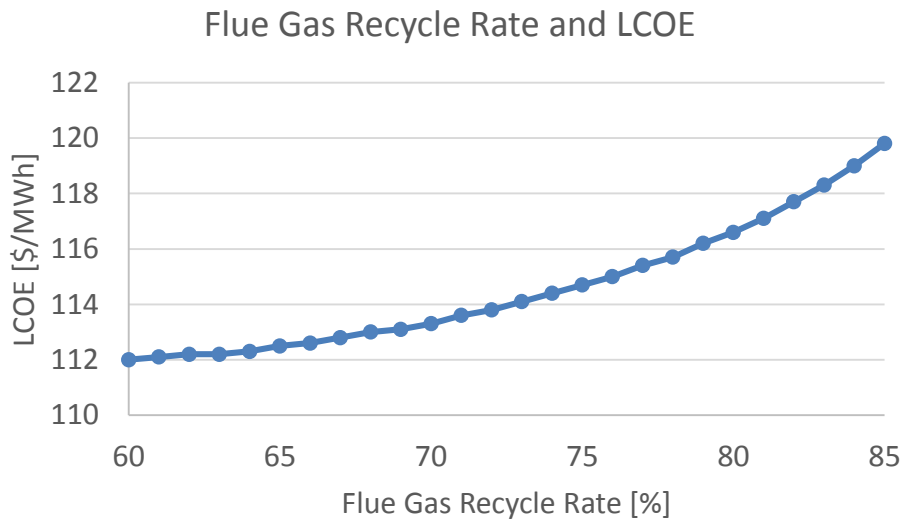


Figure 9.57 LCOE increases at an increasing rate for the base plant as the flue gas recirculation rate is increased.

From the preceding, using the lowest recycle rate possible would seem to provide the most favorable plant economics. Within the context of the IECM oxyfuel model, this deduction is correct. A variable

not accounted for in the above is how alterations in the flue gas recirculation rate affect the heat transfer capabilities between the boiler and steam cycle. Unfortunately, this level of detail is beyond the scope of the current model. The selection of flue gas recirculation rates well beyond the default value (65%) should be used cautiously.

### 9.1.6 Transport and Storage

The quantity of carbon dioxide product produced by an oxyfuel plant with a carbon processing unit (CPU) is a strong function of the gross plant output. The transport and storage systems mated to the plant are tasked with handling the carbon dioxide product and consequently their size and cost is largely determined by gross plant output.

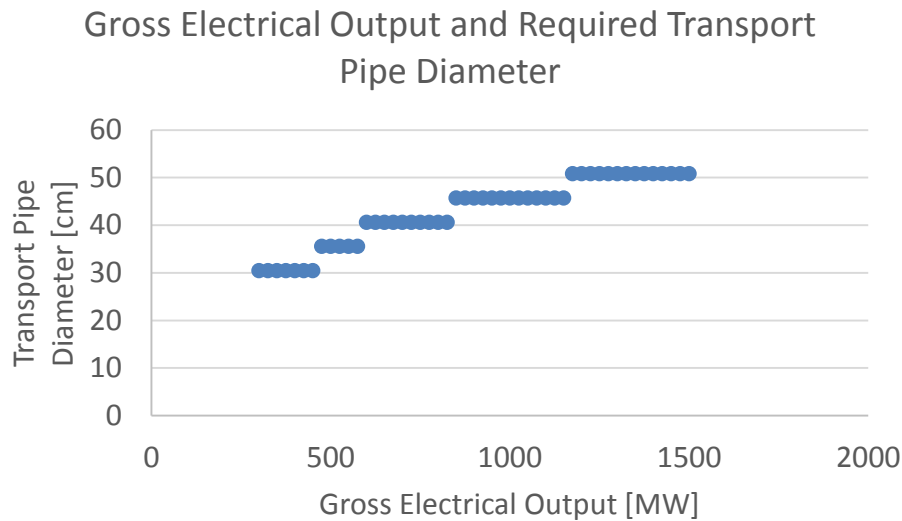


Figure 9.58 Required discrete pipe diameters required to handle the mass flow of carbon dioxide product as a function of gross electrical output.

The max hourly flowrate of carbon dioxide product through the transport system determines the diameter of pipe which must be used during construction. The above figure presents the diameter of pipe chosen by the transport model as a function of gross electrical output for our base plant with a CPU. Pipes are not commercially available in continuous sizes to accommodate any arbitrary flow rate. Consequently, for each discrete pipe diameter, there is a band of gross plant sizes within which their carbon dioxide product flowrates can most economically be handled.

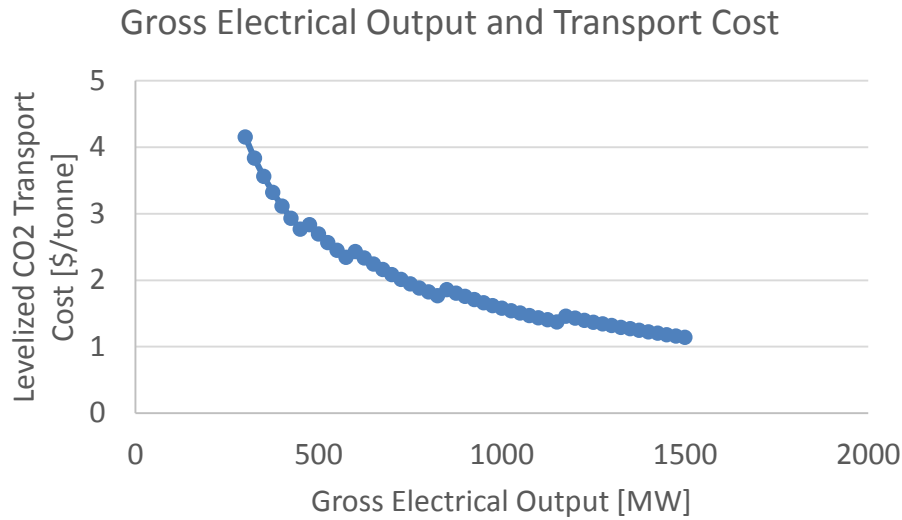


Figure 9.59 The levelized cost of transporting the captured carbon dioxide decreases in a stepwise fashion as gross plant size is increased.

As the larger end of the gross plant size band for a given pipe diameter, the average transport cost is decreased. This is a result of higher pipeline utilization and essentially increasing the number of tonnes of carbon dioxide product over which the same capital investment is divided. This interplay is continued for each pipe diameter across the range of gross electrical output. The result is a decaying function (Fig. 9.59) with discontinuities caused by the jump between discrete pipeline diameters.

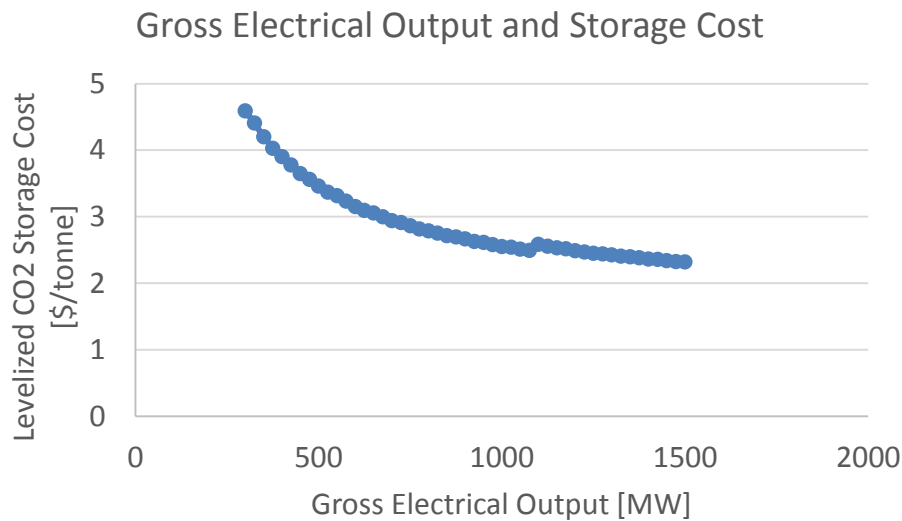


Figure 9.60 Levelized storage costs reduce with increasing plant size primarily due to high fixed operating costs which can only be reduced by spreading them over a larger base.

The initial investment in a storage facility is very large and represents the largest cost associated with storage. There are also substantial fixed operations and maintenance costs (monitoring, verification, etc.) which remain approximately the same regardless of the number of tonnes of carbon dioxide

product being stored. This results in a decaying levelized storage cost curve (Fig. 9.60) across gross electrical output. Levelized costs fall fairly rapidly from ~\$4.5 for a 300 [MW] plant to ~\$2.5 for a 1000 [MW] facility. Further cost reductions above 1000 [MW] are not substantial however because of high fixed costs.

### 9.1.7 Plant Size and Financial Parameters

Many of the previous component sections have shown that there are economies of scale from building a larger facility. The effect on the overall specific capital requirement (Fig. 9.61) shows the cumulative effects of the process components for plants with a gross electrical output from 300-1500 [MW].

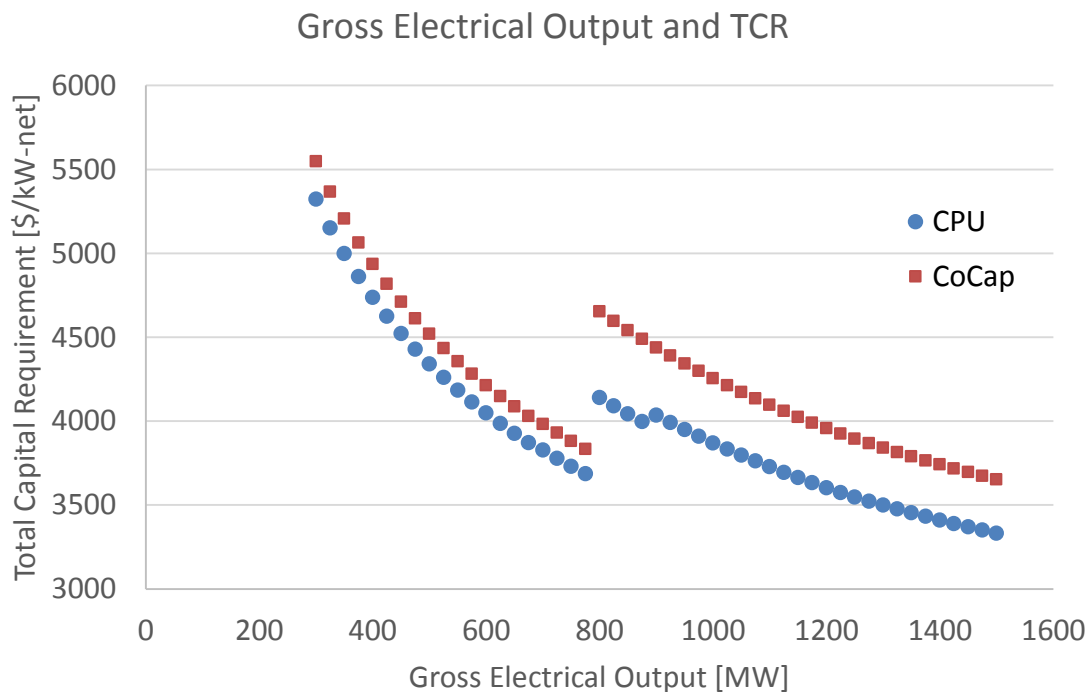


Figure 9.61 Specific total capital requirement of two plants with either carbon handling system as a function of gross electrical output.

The large discontinuity in both plants' specific TCR is a result of a second ASU train being added. The process facilities cost of the ASU alone is increasing by \$115M (Fig. 9.12) and the unit work of separation increases from 190 to 235 [kWh/tonne O<sub>2</sub>] (Fig. 9.10). The combination of these two factors creates a large jump in TCR resulting from a substantial increase in overall cost and a decrease in net electrical output. A very similar trend would be anticipated for the LCOE of both the CoCapture and CPU plants due to the capital intensity of either project. Figure 9.62 displays the LCOE of two plants with either carbon handling system. The CPU system is the cheaper option across the gross electrical output range for the nominal plant configurations.

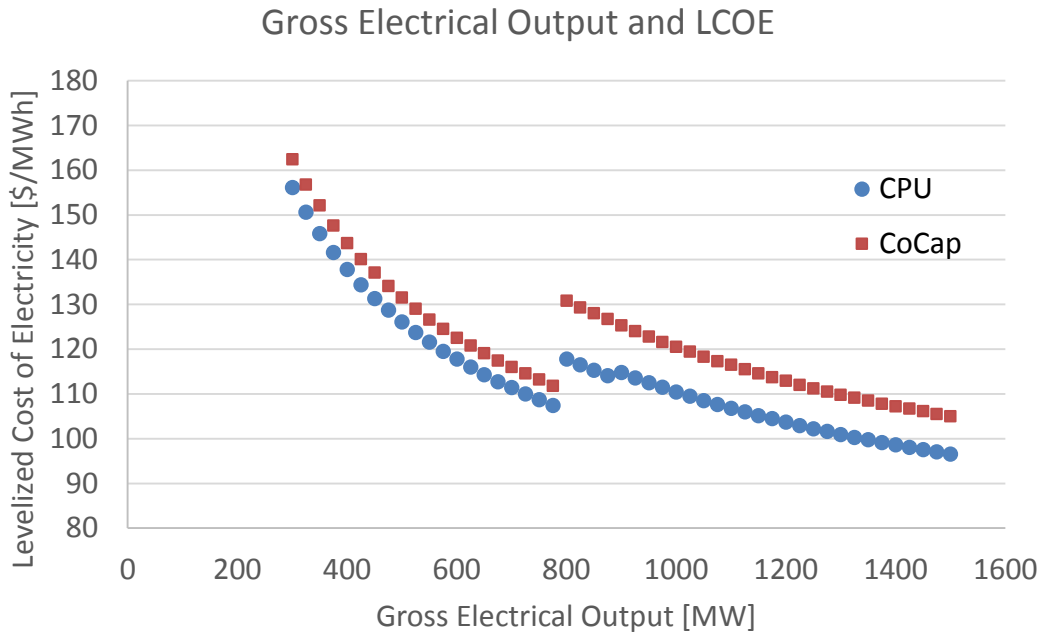


Figure 9.62 Levelized cost of electricity for two plants with either carbon handling system as a function of the gross electrical output. The CPU system has the lower LCOE across the range examined for the nominal plant configurations.

#### 9.1.7.1 Important Financial Parameters

The fixed charge factor (FCF) is a parameter which represents the cost of borrowing money for the entity considering building the oxyfuel plant. For a capital intense project such as building an electricity generation unit, the cost of borrowing money plays a major role in determining the levelized cost of electricity. For the nominal CPU oxyfuel plant increasing the FCF from 0.10 to 0.18 results in an LCOE increase of roughly 50%.

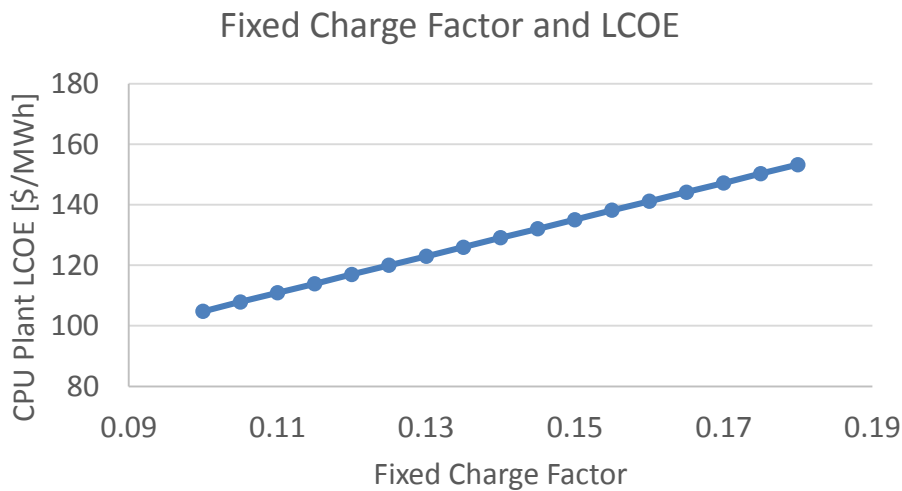


Figure 9.63 The fixed charge factor plays an important role in determining the LCOE from a project.

The cost of fuel utilized also has a major effect on the LCOE of our nominal oxyfuel plant with CPU as fuel makes up the dominant share of the variable operations and maintenance cost. Varying the cost of Illinois #6 coal from 30 to 70 [\$/tonne] for the nominal plant results in an increase in LCOE of approximately 20%.

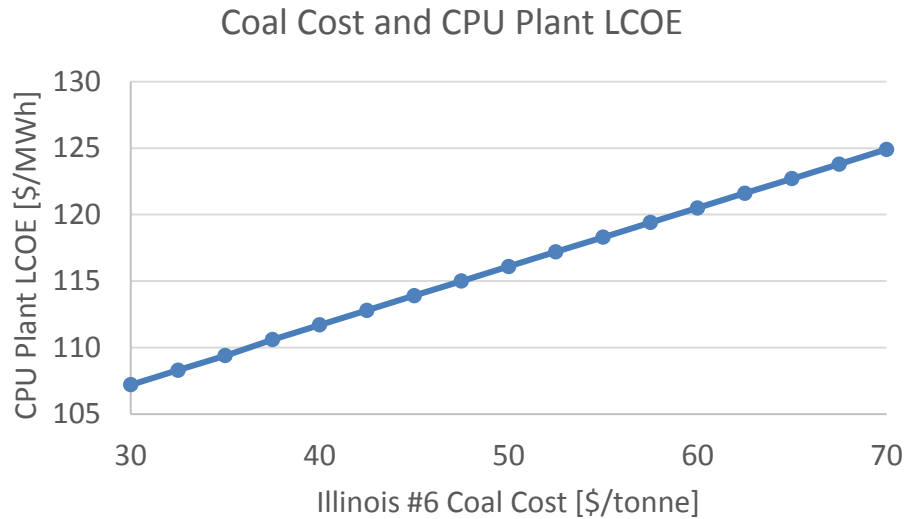


Figure 9.64 Assumed fuel cost can have a large effect on the LCOE of the nominal plant. In this instance, an increase in LCOE of 20% was observed as coal prices ranged from 30 to 70 [\$/tonne].

## 9.2 Total Plant Analysis: Reference Air Fired Plants

Here we now employ the IECM and the new oxyfuel models to analyze the performance and cost of a complete power plant to identify least-cost alternatives and performance opportunities. First, however, it is necessary to assemble and detail the reference plants without carbon capture to which the plants with oxyfuel capture are to be compared. The base coal steam cycle has been chosen to be a supercritical performance level with a steam cycle heat rate of 7764 [kJ/kWh]. Case studies with a “b” notation utilize a sub critical steam cycle with a heat rate of 8219 [kJ/kWh] and those with a “c” utilize an ultra-super critical steam cycle with a heat rate of 7074 [kJ/kWh].

The coal types selected for Cases 1-4 have been selected based on differences in their coal compositions and heating values. Each of these coals generates a unique oxyfuel plant configuration for criteria air pollutant emissions to be controlled and to maintain proper boiler operation. The last reference plant is a natural gas combined cycle unit (which will be utilized in Chapter 10 when oxyfuel is compared to other fossil fueled electricity generation units). Due to the discrete nature of gas turbines commercially available, the net electrical output of Case 6 (580.9 MW) does not perfectly align with the balance of case studies. For the purposes of this analysis however, this discrepancy is not significant as the performance data will be utilized on a specific [x/kWh] basis.

Provided below is a summary table of the cost and performance data for case studies 1-6 modeled in the IECM. The more important financial and performance categories are presented in bold font for each case study. With the exception of Cases 4 and 5, which utilize PRB coal, the revenue requirement or levelized cost of electricity across all the case studies is essentially equivalent. Even the NGCC plant [ \$ 6.5/GJ] comes in with a revenue requirement in the low 60's [\$/MWh].

**Table 9-1 Summary of cost and performance data for air fired pulverized coal and natural gas combined cycle reference plants. All costs are reported in constant 2012 dollars.**

	Case 1a	Case 1b	Case 1c	Case 2	Case 3	Case 4	Case 5	Case 6
<b>Plant Type</b>	PC Supercrit	PC Subcrit	PC USC	PC Supercrit	PC Supercrit	PC Supercrit	PC USC	NGCC
<b>Fuel Type</b>	Illinois #6	Illinois #6	Illinois #6	App. Low Sulfur	ND Lignite	PRB	PRB	Nat. Gas
<b>Fuel Flow Rate</b>								
Coal (tonnes/hr)	172.3	183.4	156.0	150.0	362.0	249.8	226.2	
Natural Gas (tonnes/hr)								80.0
<b>Gross Electrical Output (MWe)</b>	535.5	538.6	532.2	528.3	541.9	534.9	531.5	596.7
<b>Auxiliary Electrical Loads (MWe)</b>								
Base Plant	17.3	18.7	15.7	15.9	28.0	21.7	19.62	11.9
Hot Side SCR	2.6	2.8	2.4	2.5	3.1	2.8	2.59	
Fabric Filter	0.3	0.3	0.3	0.3	0.3	0.3	0.3	
Wet FGD / SDA	8.5	9.1	7.8	2.9	3.7	3.3	3.0	
Cooling Tower	6.7	7.6	6.1	6.6	6.8	6.7	6.1	3.9
<b>Net Electrical Output (MWe)</b>	500.0	500.0	500.0	500.0	500.0	500.0	500.0	580.9
<b>Plant Efficiency (% HHV)</b>	38.5	36.1	42.5	39.4	35.5	37.1	41.0	50.0
<b>Annual Power Generation (BkWh/yr)</b>	3.29	3.29	3.29	3.29	3.29	3.29	3.29	3.82
<b>CO2 Emissions (kg/kWh)</b>	0.815	0.868	0.738	0.789	0.930	0.882	0.799	0.364
Base Plant (TCR) (2012 \$M)	796.8	705.7	905.7	779.7	885.9	821.6	932.2	429.2
Cooling Tower (TCR) (2012 \$M)	46.8	51.9	39.0	46.2	47.3	46.7	38.9	29.6
Nox Control (TCR) (2012 \$M)	34.3	35.4	32.5	33.3	35.8	36.1	34.3	
TSP Control (TCR) (2012 \$M)	30.0	31.5	27.8	26.3	32.1	28.6	26.5	
SO2 Control (TCR) (2012 \$M)	134.8	138.7	133.5	75.8	91.8	79.9	75.9	
<b>Total Plant Capital Requirement (2012 \$M)</b>	1043.0	963.3	1139.0	965.4	1096.0	1016.0	1108	458.8
<b>Total Plant O&amp;M Costs/Year (2012\$/yr)</b>	92.7	95.2	88.3	67.9	58.5	58.4	53.5	190.4
<b>Capital Required (\$/kW-net)</b>	2086	1927	2277	1931	2192	2031	2215	789
<b>Revenue Required (\$/MWh)</b>	64.0	62.0	65.9	63.4	66.1	52.6	54.3	63.4

## 9.3 Base Oxyfuel Plants for Sensitivity Analysis

The plant design used for all component model sensitivity testing was a cool recycle unit with wet flue gas desulfurization fired with Illinois #6 Coal. Case 8 utilizes a carbon purification unit (CPU) that in the default configuration is capturing 90% of the carbon dioxide and producing a product stream which is 99.5% carbon dioxide by volume. Case 9 is operating as a CoCapture process where all the combustion gases are compressed along with the carbon dioxide to compose the product stream. The purity of this stream is about 88 [mol%] carbon dioxide and all carbon dioxide is being captured.

In analogous fashion to the air-fired cases, the base coal steam cycle has been chosen to be a supercritical performance level with a steam cycle heat rate of 7764 [kJ/kWh]. Case studies with a “b” notation utilize a sub critical steam cycle with a heat rate of 8219 [kJ/kWh] and those with a “c” utilize an ultra-super critical steam cycle with a heat rate of 7074 [kJ/kWh]. The corresponding air-fired reference plant from Case 1 has been matched to Cases 8 and 9 when calculating economic performance metrics such as avoidance cost.

A complete IECM configuration of the supercritical base oxyfuel plant is available in Appendix E. For the following analysis, the summary table of Cases 8 and 9 below gives sufficient detail of the default cost and performance of each configuration to establish a baseline for the examination of the sensitivity of individual process components in Section 9.1.

**Table 9-2. Cost and performance summary for CPU (Case 8) and CoCapture (Case 9) oxyfuel reference plants with Illinois #6 Coal across steam cycle performance levels (Sub Critical, Super Critical, and Ultra-Super Critical). All costs are reported in constant 2012 dollars.**

	Case 8a	Case 8b	Case 8c	Case 9a	Case 9b	Case 9c
<b>Plant Type</b>	Oxy Supercrit	Oxy Subcrit	Oxy USC	Oxy Supercrit	Oxy Subcrit	Oxy USC
<b>Coal Type</b>	Illinois #6	Illinois #6	Illinois #6	Illinois #6	Illinois #6	Illinois #6
<b>CO2 Capture Rate (%) /CO2 Product Purity (mol%)</b>	90/99.5	90/99.5	90/99.5	90/99.5	90/99.5	90/99.5
Coal (tonnes/hr)	218.8	236.0	194.4	222.6	240.4	197.4
Natural Gas (tonnes/hr)						
<b>Gross Electrical Output (MWe)</b>	680.1	692.8	663.2	691.8	705.7	673.4
<b>Auxiliary Electrical Loads (MWe)</b>						
Base Plant	22.0	24.1	19.5	22.4	24.6	19.8
Hot Side SCR						
Fabric Filter	0.2	0.2	0.2	0.2	0.2	0.2
Wet FGD / SDA	6.4	6.8	5.7	6.5	7.0	5.7
Cooling Tower	8.5	9.8	7.6	8.6	10.0	7.7
Air Separation Unit	87.4	91.9	80.9	88.4	93.0	81.7
CO2 Separation & Comp.	55.6	59.9	49.4	65.7	70.9	58.3
<b>Net Electrical Output (MWe)</b>	500.0	500.0	500.0	500.0	500.0	500.0
<b>Plant Efficiency (% HHV)</b>	30.3	28.1	34.1	29.8	27.6	33.6
<b>Annual Power Generation (BkWh/yr)</b>	3.29	3.29	3.29	3.29	3.29	3.29
<b>CO2 Emissions (kg/kWh)</b>	0.104	0.112	0.092	0.000	0.000	0.000

Base Plant (TCR) (2012 \$M)	959.8	858.1	1075.0	972.6	870.5	1088.0
Capture System (TCR) (2012 \$M)	744.0	776.2	696.2	794.0	829.4	741.9
Cooling Tower (TCR) (2012 \$M)	69.3	76.0	58.7	70.3	77.1	59.5
Nox Control (TCR) (2012 \$M)	9.9	10.1	9.6	10.0	10.2	9.8
TSP Control (TCR) (2012 \$M)	22.4	23.7	20.4	22.7	24.0	20.7
SO <sub>2</sub> Control (TCR) (2012 \$M)	130.2	134.6	123.8	131.2	135.7	124.6
<b>Capture O&amp;M/Year (2012\$M/yr)</b>	83.7	85.0	80.4	90.9	92.5	87.1
BOP O&M/Year (2012\$M/yr)	68.1	72.6	62.4	66.5	71.1	60.7
<b>Total Plant Capital Requirement (2012 \$M)</b>	1936	1879	1984	2001	1947	2045
<b>Total Plant O&amp;M Costs/Year (2012\$M/yr)</b>	151.8	157.6	142.8	157.4	163.6	147.8
<b>Capital Required (\$/kW-net)</b>	3871	3757	3968	4002	3894	4089
<b>Revenue Required (\$/MWh)</b>	112.6	112.4	111.5	116.5	116.6	115.1
<b>Added Cost of CCS (\$/MWh)</b>	48.6	50.4	45.6	52.6	54.5	49.2
<b>Cost of CO<sub>2</sub> Avoided (\$/tonne)</b>	68.3	66.6	70.5	64.5	62.8	66.6
<b>Cost of CO<sub>2</sub> Captured (\$/tonne)</b>	46.8	45.0	49.3	39.4	37.9	41.4

As would be expected the more efficient steam cycles with less flue gas to process require smaller carbon dioxide control systems and in turn cost less to procure and operate. The savings from the carbon dioxide control system is essentially negated however by the increased cost of the base plant for the more efficient steam cycles. The net result is that the revenue requirement for both Case 8 and 9 is essentially the same (<1% difference) across the three levels of steam cycle performance.

The net plant efficiency of the CoCapture plants (Case 9) are always just slightly below the comparable CPU equipped plants (Case 8) for this plant design. The relationship of least to most efficient, which would be predicted by the steam cycle performance, is also evident across both Cases 8 and 9.

## Illinois #6 Oxyfuel Plant Efficiency

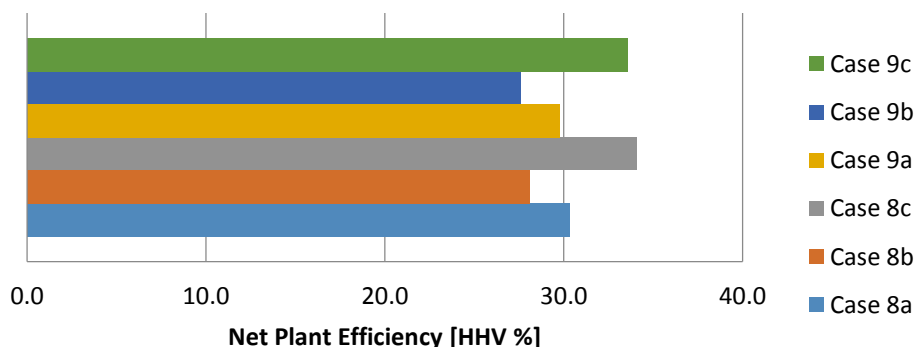


Figure 9.65. Net plant efficiency [HHV %] across steam cycle performance levels (Sub Critical, Super Critical, and Ultra-Super Critical) for both CPU (Case 8) and CoCapture (Case 9) with Illinois #6 Coal. All costs are reported in constant 2012 dollars.

Compared to their corresponding air-fired reference plant in Case 1, the net efficiency of the capture equipped plants is about 8% points lower on a HHV basis. This represents an efficiency penalty of about 21% for a plant with a super critical steam cycle (Cases 8a and 9a).

The unit, or specific, emissions of the plants in Case 8 express the anticipated behavior with those plants with the least efficient steam cycles producing the most emissions on a kilowatt hour basis. Less efficient plants produce more emissions per unit electricity (by definition) than a more efficient plant. Therefore, capturing 90% of the original emissions still results in a proportionally higher emission rate for the less efficient plant relative to the more efficient plant.

### Illinois #6 Oxyfuel Specific Emissions

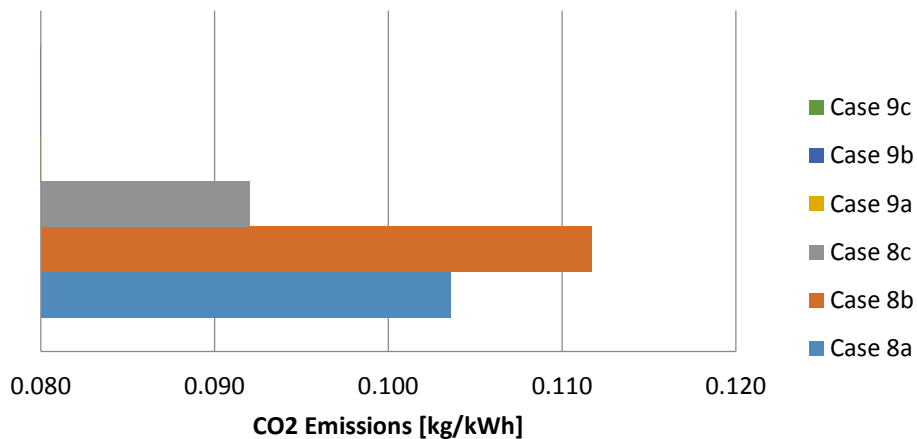


Figure 9.66. Specific carbon dioxide emissions for CPU (Case 8) and CoCapture (Case 9) for Illinois #6 Coal across steam cycle performance levels (Sub Critical, Super Critical, and Ultra-Super Critical). All costs are reported in constant 2012 dollars.

The specific emission levels for Case 9 are zero for each CoCapture plant configuration. The complete capture of carbon dioxide emissions removes the aforementioned proportionality of emission reduction found when capturing 90% of a plant’s emissions. As the next two figures show, this has some interesting effects on traditional techno-economic performance metrics used when evaluating carbon capture systems.

## Illinois #6 Oxyfuel Avoidance Cost

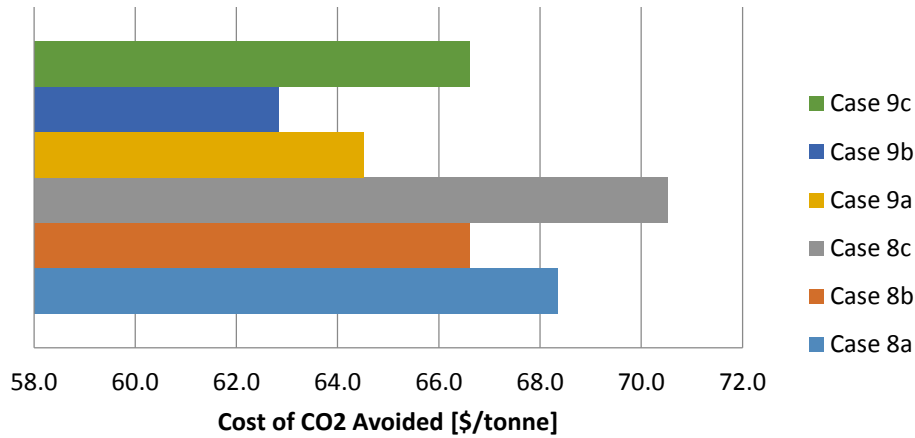


Figure 9.67. Cost of carbon dioxide avoidance cost for Illinois #6 Coal across steam cycle performance levels (Sub Critical, Super Critical, and Ultra-Super Critical) for CPU (Case 8) and CoCapture (Case 9). All costs are reported in constant 2012 dollars.

Thanks to a larger quantity of carbon dioxide being captured by the CoCapture system, the avoidance costs are about 5 [\$/tonne] cheaper in Case 9 compared to Case 8. The reason for this can be seen by examining the denominator of the avoidance cost formulation.

$$Avoidance\ Cost\ \left[ \frac{\$}{tCO_2} \right] = \frac{[\$/MWh]_{capture} - [\$/MWh]_{reference}}{[tCO_2/MWh]_{reference} - [tCO_2/MWh]_{capture}}$$

The capture plant carbon intensity is subtracted from the reference plant's carbon intensity and the difference provides the denominator. It is straight forward then that if you are subtracting zero you have the largest possible denominator (save negative carbon intensity). Additionally, the least efficient plants have the lowest avoidance and capture costs because their reference carbon intensity is so high that it dictates that the denominator will be the largest. Absent a large disparity in the LCOE delta between case studies (not present here), the least efficient plant will have the lowest cost of avoidance or capture.

## Illinois #6 Oxyfuel Capture Cost

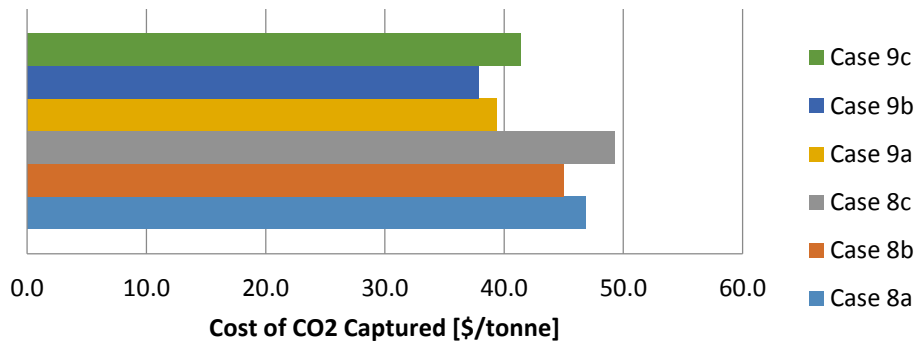


Figure 9.68. Cost of carbon dioxide capture cost for Illinois #6 Coal across steam cycle performance levels (Sub Critical, Super Critical, and Ultra-Super Critical) for CPU (Case 8) and CoCapture (Case 9). All costs are reported in constant 2012 dollars.

The cost of capture is a metric typically reserved for evaluations of whether a carbon capture project would be cost effective for enhanced oil recovery (EOR) or some other industrial use of the carbon dioxide. The cost of capture values for Case 9 are roughly \$8 lower across all steam cycle efficiencies, however the product gas produced by CoCapture is low purity (~88 [mol%] in this case) and would not be suitable for EOR. The take away from this is that with oxyfuel systems, the process details are often more important than the techno-economic metrics. Without knowing the intent of the project developer, it is not possible to say whether CoCapture or a CPU system would be economically preferred. More discussion on matching oxyfuel systems with owner/operator objectives can be found in Chapter 11.

## 9.4 Coal Composition Effects

The goal of this section is to demonstrate the possible variation in performance between fuel blends within the same recycle system configuration for the pulverized coal oxyfuel model in the IECM. The recycle system utilized in this section is the cool recycle with a spray dry absorber unit for sulfur oxide control. The two fuels chosen from the IECM fuel database for this analysis are Appalachian Low Sulfur (App. Low) and North Dakota Lignite (ND Lignite). Although these two fuels both meet the elemental sulfur mass requirement ( $0.5 < [S \text{ wt\%}] < 1.5$ ); they could hardly be more disparate. ND Lignite has a higher heating value of about 14,000 [kJ/kg] and is 33% moisture as received whereas App. Low has a higher heating value of just over 30,000 [kJ/kg] with a moisture content of only 5.6%. The disparity in as received moisture will be a major determinate in how the primary and secondary recycle streams are parsed.

Both of the fuels were modeled in the IECM for an oxyfuel system producing a 99.5 [CO<sub>2</sub> mol%] carbon dioxide product from the CPU and capturing 90% of the carbon dioxide in the flue gas stream. The complete characterization of these two systems can be found in Appendix D. Table 9-3 presents a

truncated version of the system characterization for each of the two coals; highlighting the important cost and performance results.

**Table 9-3 Important parameters and results for Appalachian Low Sulfur and North Dakota Lignite modeled in the cool recycle configuration and utilizing a spray dry absorber. All costs are reported in constant 2012 dollars.**

	<b>Case 10</b>	<b>Case 11</b>
<b>Plant Type</b>	Oxy Supercritical	Oxy Supercritical
<b>Coal Type</b>	App. Low Sulfur	ND Lignite
<b>Recycle System</b>	Cool SDA	Cool SDA
<b>Coal (tonnes/hr)</b>	184.7	462.8
<b>Gross Electrical Output (MWe)</b>	650.7	693.2
<b>Net Electrical Output (MWe)</b>	500	500
<b>Plant Efficiency (% HHV)</b>	32.02	27.78
<b>Annual Power Generation (BkWh/yr)</b>	3.287	3.287
<b>CO2 Emissions (kg/kWh)</b>	0.097	0.119
<b>Capital Required (\$/kW-net)</b>	3506	4059
<b>Revenue Required (\$/MWh)</b>	104.7	115.5
<b>Added Cost of CCS (\$/MWh)</b>	41.26	49.44
<b>Cost of CO2 Avoided (\$/tonne)</b>	59.65	60.99
<b>Cost of CO2 Captured (\$/tonne)</b>	41.65	41.37
<b>Primary Recycle (acfm)</b>	1559	11890
<b>Secondary Recycle (acfm)</b>	15910	5360
<b>Recycle Moisture (mass %)</b>	12.51	7.79
<b>Temperature (°C)</b>	90.11	66.61

The most glaring disparity between these two coals is how the flue gas is divided between the primary and secondary recycle streams. The high moisture content of ND Lignite requires that a large portion of the moisture in the combustion gases be removed prior to being recycled to the boiler. As has been discussed previously, limiting the recycled moisture is essential to maintain consistent boiler heat transfer and to ensure that the spray dry absorber operates at sufficiently high sulfur removal efficiency. In the case of ND Lignite, this is accomplished by sending over 2/3 of the total recycle gas through the DCCPS in the primary recycle stream.

By contrast, the App. Low plant need only send about 10% of the total recycle gas through the DCCPS in the primary recycle stream. The small primary recycle fraction is achievable because the as received moisture content of the fuel is very low. The upshot for the App. Low plant is that the temperature of the combined recycle stream is nearly 35 [°C] warmer than the combined recycle stream of the ND Lignite plant. For the App. Low plant the higher enthalpy content of the combined recycle stream translates to reduced coal consumption and ultimately, a higher net efficiency.

The net efficiency disparity between the two plants is primarily not a result of the recycle temperature however. The primary driver of this disparity is the boiler efficiency. App. Low has a boiler efficiency of nearly 90% in the IECM, whereas ND Lignite is about 84%. The disparity in net plant efficiency between the two coals is then exacerbated by the increased size of the base plant to manage the increased mass flow rate of fuel necessitated by the low specific energy content.

Despite all the disparity between the recycle splits, the fuel flow rates, and the net plant efficiency values, the avoidance cost is nearly identical for both plants. The cost of CO<sub>2</sub> avoided is about \$60 for each of the systems; however the carbon intensity of the electricity produced by the ND Lignite facility is 20% higher. If asked to choose, the lower carbon intensity alone may not be reason enough to select the App. Low plant as the fuel of choice in this scenario, however the 10 [\$/MWh] lower revenue requirement would probably cement the decision.

## 9.5 Recycle Configuration Effects

In this section the effects of using the three new oxyfuel recycle configurations will be examined for Wyoming Powder River Basin coal. This coal was chosen from the IECM fuel database because of its prominence and because it possess a low enough sulfur composition (0.37 [S wt%]) to be used with any of the recycle configurations. Each of the three configurations was modeled in the IECM for an oxyfuel system producing a 99.5 [CO<sub>2</sub> mol%] carbon dioxide product from the CPU and capturing 90% of the carbon dioxide in the flue gas stream. The complete characterization of these three systems can be found in Appendix D. Table 9-4 presents a truncated version of the system characterization for each of the system configurations; highlighting the important cost and performance results.

Table 9-4 Important parameters and results for Powder River Basin coal utilizing the three (Cases 12-14) new oxyfuel recycle configurations. Case 15 explores the thermodynamic limits of the warm recycle configuration. All costs are reported in constant 2012 dollars.

	<b>Case 12</b>	<b>Case 13</b>	<b>Case 14</b>	<b>Case 15</b>
<b>Plant Type</b>	Oxy Supercritical	Oxy Supercritical	Oxy Supercritical	Oxy Supercritical
<b>Coal Type</b>	PRB	PRB	PRB	PRB
<b>Recycle System</b>	Cool WFGD	Cool SDA	Warm	Warm
<b>Coal (tonnes/hr)</b>	316.5	314.7	310.4	270.9
<b>Gross Electrical Output (MWe)</b>	678	674	664.9	580.1
<b>Net Electrical Output (MWe)</b>	500	500	500	500
<b>Plant Efficiency (% HHV)</b>	29.31	29.48	29.89	34.26
<b>Annual Power Generation (BkWh/yr)</b>	3.287	3.287	3.287	3.287
<b>CO2 Emissions (kg/kWh)</b>	0.112	0.111	0.11	0.096
<b>Capital Required (\$/kW-net)</b>	3870	3770	3726	3377
<b>Revenue Required (\$/MWh)</b>	98.44	95.95	94.88	86.85
<b>Added Cost of CCS (\$/MWh)</b>	45.84	43.35	42.28	34.25
<b>Cost of CO2 Avoided (\$/tonne)</b>	59.51	56.22	54.73	43.55
<b>Cost of CO2 Captured (\$/tonne)</b>	40.43	38.28	37.73	33.8
<b>Primary Recycle (acfm)</b>	8920	7968	6116	5210
<b>Secondary Recycle (acfm)</b>	8000	9452	12990	9959
<b>Recycle Moisture (mass %)</b>	9.52	9.62	9.683	9.487
<b>Temperature (°C)</b>	64.06	75.5	113.5	111.1

The increase in efficiency from configuration cases 12 to 14 is not dramatic, but it is non-trivial. Net plant efficiency increases 6/10ths of a percent and both the LCOE and avoidance costs are reduced by about \$4. The largest disparities are to be found in how the flue gas streams are divided and the resulting temperature of the combined recycle stream. Passing all the flue gas through flue gas desulfurization in the cool recycle configurations (Cases 12 & 13) actually increases that mass of moisture in the flue gas which must be removed by the DCCPS to maintain steady state. The result for the cool recycle configurations is that they must pass a larger primary recycle fraction as compared to the warm recycle configuration. The disparity of the secondary split between the three cases appears magnified in Table 9-4 due to the temperature disparity of the secondary recycle stream and its effect of flue gas volume.

The temperature of the recycled gas stream increases by 50 C from Case 12 to Case 14, resulting in a predicted increase of 0.6% in net plant efficiency. Due to the lack of any available data or other studies on the magnitude of thermal differences of the recycle configurations, corroborating the results produced in Table 9-4 was not possible. If this information were to become available, the model used to convert between combined recycle stream enthalpy content and electric debit/credit could be better calibrated. As it stands, the thermal to electrical conversion model utilizes a conservative set of assumptions and thus is likely underestimating the thermal efficiency benefit of increasing the combined recycle stream temperature.

### 9.5.1 Ideal Gas Separation Oxyfuel

There is ultimately only so much efficiency which can be gained through the manipulation of the recycle gas streams given the constraints of current oxyfuel boilers and pollutant control equipment. More substantial efficiency increases could be made, with first generation oxyfuel boilers and pollutant control equipment, by reducing the parasitic load of the gas separation and processing units. The premise of this section is to examine the effects on cost and performance of the current state-of-the-art oxyfuel system (Case 14) if tremendous strides in gas separation and processing were made.

Table 9-5 Thermodynamic limit gas separation values (73) for the air separation unit and carbon processing unit.

Parameter	Units	Value
Unit Separation ASU Energy	kWh/tonne O <sub>2</sub>	42
Oxidant Purity	O <sub>2</sub> mol%	99
Unit CPU Energy	kWh/tonne CO <sub>2</sub>	65

The thermodynamic limit unit separation energy values for the CPU and ASU were used to override the calculated values in the IECM to produce the results for Case 15 in Table 9-4. The effect on plant performance is rather dramatic, as would be expected when the two largest parasitic loads are reduced drastically. The reduction in electrical load from the ideal ASU and CPU allows for a reduction in the gross plant size of 85 [MW] and a net plant efficiency increase of about 4.5 percentage points.

While the financial ramifications of ideal gas separation are sizeable, they are not large enough to be considered transformative. For instance, the LCOE of Case 15 was calculated to be 87 [\$/MWh], a reduction of about 10% from the 95 [\$/MWh] of Case 14. This is a step in the right direction, but even 87 [\$/MWh] remains a 65% increase in the cost of electricity relative to the base plant (52.6 [\$/MWh]). Furthermore, this cost is at the theoretical limit of thermodynamic performance for the ASU and CPU, values we are unlikely to achieve in practice.

When coal is very cheap, efforts to save every last tonne of fuel through process efficiency improvements have very little (if any) payoff. Given that even ideal gas separation cannot reduce the LCOE by more than 10% from current levels, it is clear that marginal thermal efficiency gains will never provide the “step change” required to increase the economic viability of CCS systems.

## 9.6 Uncertainty Analysis

The sensitivity studies performed in the first half of this chapter provide useful insight into the cost and performance interplay of one system (occasionally more) as a single parameter is varied. To acquire a better understanding of how variations in several parameters may affect the overall system performance, an uncertainty analysis should be performed. To illustrate the comparative magnitude of their individual effects upon overall plant performance, parameters relating to financial and performance uncertainty have been separated in the following two sections. In the last section of this chapter the total uncertainty of all identified parameters for a warm recycle oxyfuel system is considered.

### 9.6.1 Financial Uncertainty

The identified financial uncertainty parameters, along with their assigned distributions, can be found in Table 9-6. The choice of these six parameters was made because they most fully capture the irreducible uncertainty which would be faced by a new build oxyfuel project. The base plants used for the uncertainty analysis are Cases 14 and 16. The cumulative distribution functions produced in the following section are the result of 200 samples taken using the uncertainty editor in the IECM. The number of samples was limited to 200 due to the extended amount of time required for each oxyfuel configuration to reach convergence.

Table 9-6 Financial uncertainty parameters and their chosen distributions.

Uncertainty Parameter	Units	Warm Oxyfuel 90% Capture	Warm Oxyfuel 100% Capture	Reference
Levelized Capacity Factor	Fraction	Uniform (0.65, 0.85)	Uniform (0.65, 0.85)	Rubin and Zhai 2011 (74)
Fuel Cost	2012 \$	Uniform (8, 20)	Uniform (8, 20)	Author's Estimate
Oxyfuel Equipment Cost	2012 \$	Uniform (default, 0.7x, 1.3x)	Uniform (default, 0.7x, 1.3x)	Authors Estimate
Project Contingency Cost	% PFC	Normal (default, 20%)	Normal (default, 20%)	Berkenpas et al. 1999 (44)
Process Contingency Cost	% PFC	Normal (default, 30%)	Normal (default, 30%)	Berkenpas et al. 1999
Fixed Charge Factor	Fraction	Uniform (0.10, 0.180)	Uniform (0.10, 0.180)	GCCSI (75) & Rubin and Zhai 2011

The levelized cost of electricity (LCOE) cumulative distribution function (CDF) resulting from the sampling of the financial parameter distributions is presented in Figure 9.69. For a given probability, the CPU plant always has a slightly lower expected LCOE. The CPU configuration had CDF with a 95% Confidence Interval (CI) of 85 to 147 [\$/MWh] and the CoCapture 95% CI was 90 to 153 [\$/MWh].

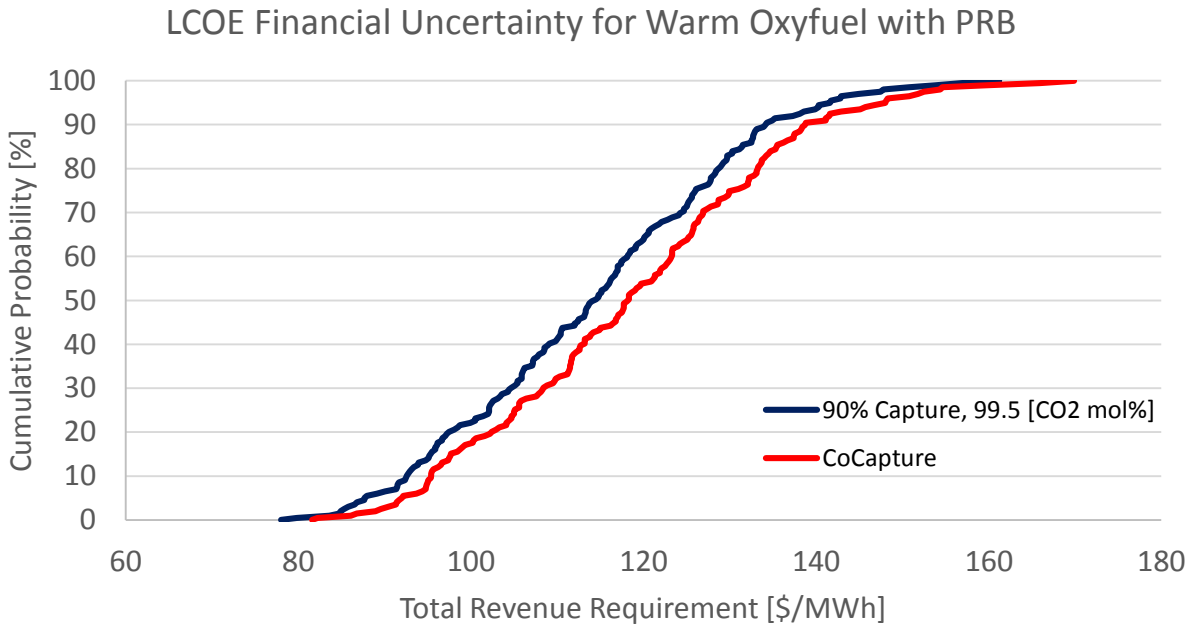


Figure 9.69 Cumulative distribution function of total revenue requirement (LCOE) for warm recycle oxyfuel using PRB coal. Revenue requirement for CPU system is below the CoCapture system for all probabilities. All costs are reported in constant 2012 dollars.

The CDF for carbon dioxide avoidance cost for financial uncertainty (Fig. 9.70) presents the opposite relationship as was the case for total revenue requirement. Namely, the CoCapture configuration has the lower expected cost across the cumulative probability range. The reason for the switch is that CoCapture configurations produce no carbon dioxide emissions. Consequently, in the following equation the denominator is larger for CoCapture configurations than their CPU counterparts.

$$Avoidance\ Cost\ \left[ \frac{\$}{tCO_2} \right] = \frac{[\$/MWh]_{Capture} - [\$/MWh]_{Reference}}{[tCO_2/MWh]_{Reference} - [tCO_2/MWh]_{Capture}}$$

The numerator is similar between the two oxyfuel plant configurations (Fig. 9.69) and any small increase in cost between a CPU system and CoCapture is swamped by the 10-15% increase in the denominator.

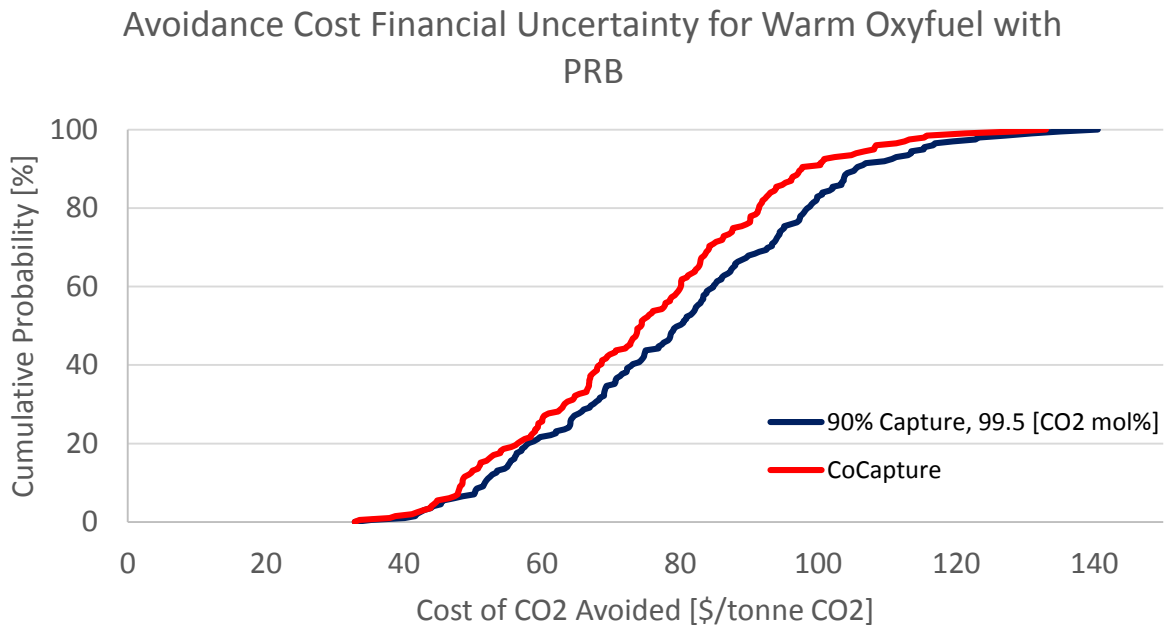


Figure 9.70 Cumulative distribution function of CO2 avoidance cost for warm recycle oxyfuel using PRB coal. Avoidance cost for CPU system is above the CoCapture system for all probabilities. All costs are reported in constant 2012 dollars.

## 9.6.2 Performance Uncertainty

The identified performance uncertainty parameters, along with their assigned distributions, can be found in Table 9-7. The choice of these five parameters was made because they most fully capture the irreducible uncertainty which would be faced by operating an oxyfuel project. The base plants used for the uncertainty analysis are Cases 14 and 16. The cumulative distribution functions produced in the following section are the result of 200 samples taken using the uncertainty editor in the IECM. The number of samples was limited to 200 due to the extended amount of time required for each oxyfuel configuration to reach convergence. Uniform distributions were used due to a lack of available process performance data from real projects. The upper and lower bound of each distribution has been carefully selected as a result of the author's time spent assessing case studies and reported performance estimates. There was insufficient information available to justify a distribution shape other than uniform for the performance parameters.

Table 9-7 Performance uncertainty parameters and their chosen distributions.

Uncertainty Parameter	Units	Warm Oxyfuel 90% Capture	Warm Oxyfuel 100% Capture	Reference
Performance				
Unit Separation ASU Energy	kWh/tonne O <sub>2</sub>	Uniform (180, 220)	Uniform (180, 220)	Author's Estimate
Unit CPU Energy	kWh/tonne CO <sub>2</sub>	Uniform (90, 120)	N/A	Author's Estimate
CO <sub>2</sub> Compressor Efficiency	%	Uniform (0.75, 0.85)	Uniform (0.75, 0.85)	Author's Estimate
Excess Air	% Stoich. O <sub>2</sub>	Uniform (2, 10)	Uniform (2, 10)	Author's Estimate
Leakage Air (Ingress)	% Stoich. O <sub>2</sub>	Uniform (0, 6)	Uniform (0, 6)	Author's Estimate

The cumulative probability functions of the CPU and CoCapture for performance uncertainty reflect the underlying uniform distributions of the parameters. The two nearly parallel lines formed by the two functions show CoCapture being expected to be roughly 8 [\$/MWh] more expensive than the CPU counterpart for any given probability.

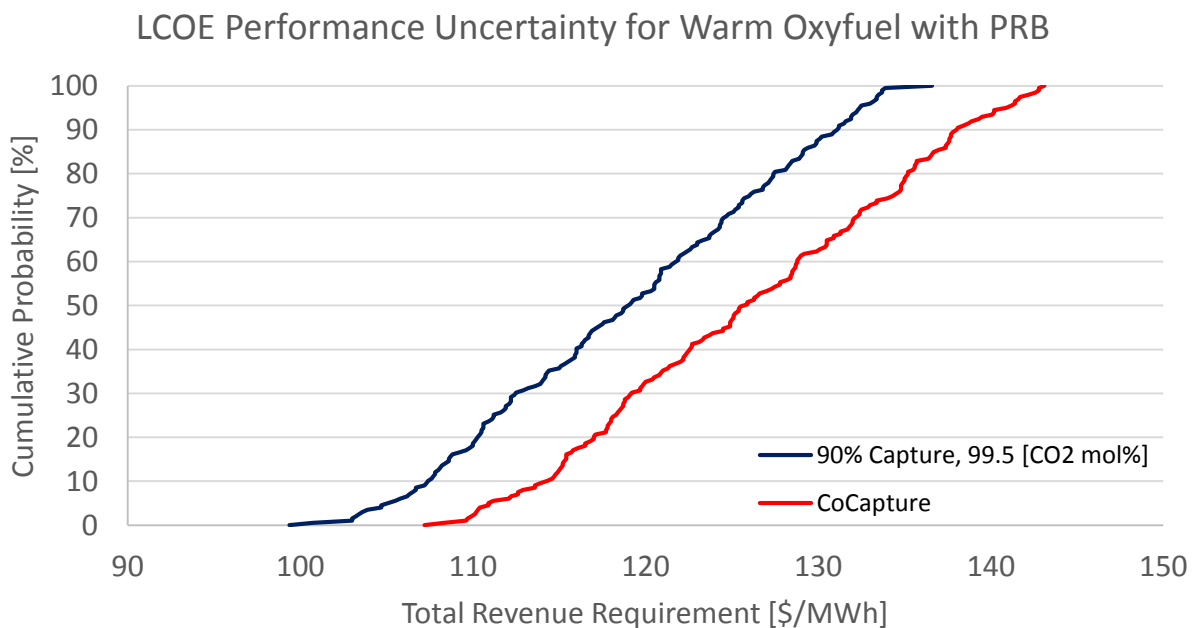


Figure 9.71 Cumulative distribution function of total revenue requirement (LCOE) for warm recycle oxyfuel using PRB coal. Revenue requirement for CPU system is below the CoCapture system by approximately 8 [\$/MWh] for all probabilities. All costs are reported in constant 2012 dollars.

LCOE for the CPU system has a 95% CI of 103 to 133 [\$/MWh] while the CoCapture system has a 95% CI of 110 to 143 [\$/MWh]. The carbon dioxide avoidance cost (Fig. 9.72) 95% CI ranges from about 66 to 105 [\$/tonne CO<sub>2</sub>] for the CPU system and the CoCapture system outperforms it slightly at the high end with a 95% CI that goes from about 65 to 101 [\$/MWh]. Here again, we observe the CoCapture system swapping with the CPU system for which system has the lowest expected cost between metrics.

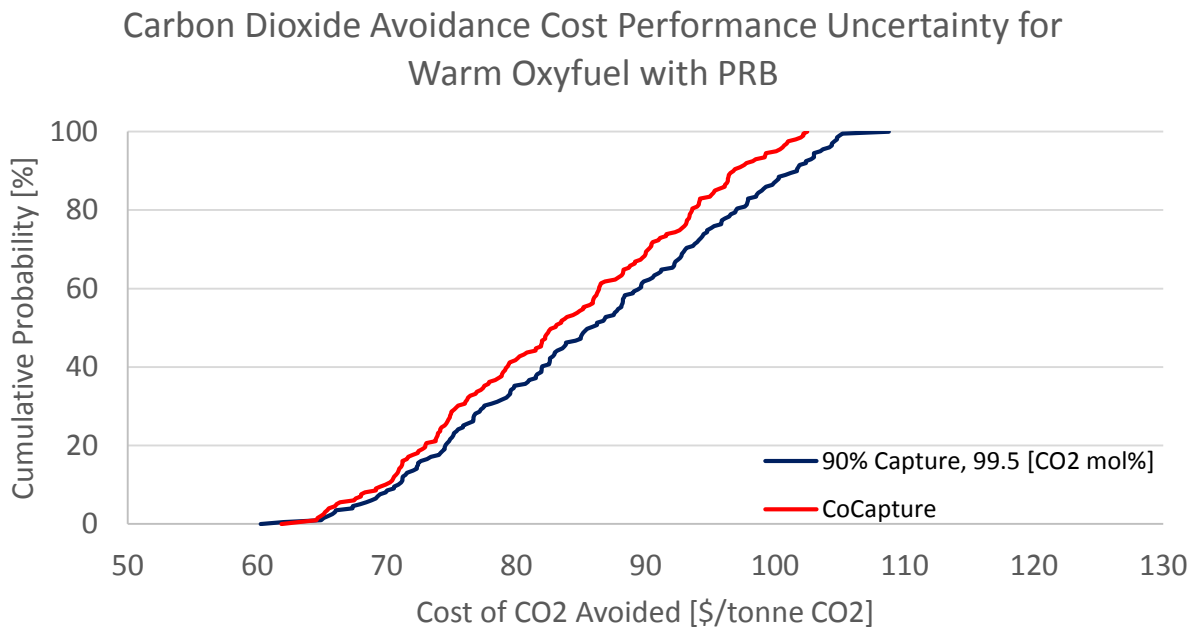


Figure 9.72 Cumulative distribution function of CO<sub>2</sub> avoidance cost for warm recycle oxyfuel using PRB coal. Avoidance cost for CPU system is above the CoCapture system for most all probabilities, but are indistinguishable for the high performing systems sampled. All costs are reported in constant 2012 dollars.

The uncertainty distributions resulting from the performance parameters alone tend to be a bit narrower compared to those produced by the financial parameters. For example, the LCOE distribution for the performance parameters is fairly tight ranging from about 100 to 135 [\$/MWh]. Compare this to the distribution for LCOE resulting from the financial parameters of approximately 80 to 160 [\$/MWh]. It appears, given the assigned distributions, that the chosen financial parameters have a greater effect on the financial metrics used to gauge plant performance than do the performance parameters. A combined assessment of these uncertainty parameters is performed in the following section.

### 9.6.3 Total Uncertainty

The identified financial and performance uncertainty parameters, along with their assigned distributions, can be found in Tables 9-6 and 9-7, respectively. As before, the base plants used for the uncertainty analysis are Cases 14 and 16. A modified version of each of these deterministic cases (alpha rev "a") which replaces the IECM default fixed charge factor (FCF) of 0.1128 with 0.14 has also been provided to better illustrate the importance of the assumed FCF. The cumulative distribution functions produced in the following section are the result of 200 samples taken using the uncertainty editor in the IECM. The number of samples was limited to 200 due to the extended amount of time required for each oxyfuel configuration to reach convergence.

Table 9-8 Deterministic cases used to compare the uncertainty analysis results. The default IECM fixed charge factor (FCF) is 0.113 and has been used in all the base case studies. Cases 14 and 16 were duplicated with a FCF of 0.14 to demonstrate the importance of this parameter in the uncertainty analysis and are denoted Cases 14a and 16a. All costs are reported in constant 2012 dollars.

	Case 14	Case 14a	Case 16	Case 16a
Plant Type	Oxy Supercritical	Oxy Supercritical	Oxy Supercritical	Oxy Supercritical
Coal Type	PRB	PRB	PRB	PRB
CO2 Emissions (kg/kWh)	0.1097	0.1097	0	0
Fixed Charge Factor	0.113	0.14	0.113	0.14
Revenue Required (\$/MWh)	94.88	110.8	98.42	114.9
Cost of CO2 Avoided (\$/tonne)	54.73	75.29	51.94	70.58

For reference, the PRB base plant was also included in this uncertainty analysis for LCOE (Fig. 9.67). The base plant was not subject to any performance parameters and the produced cumulative probability function is purely a function of the financial parameters of Table 9-6.

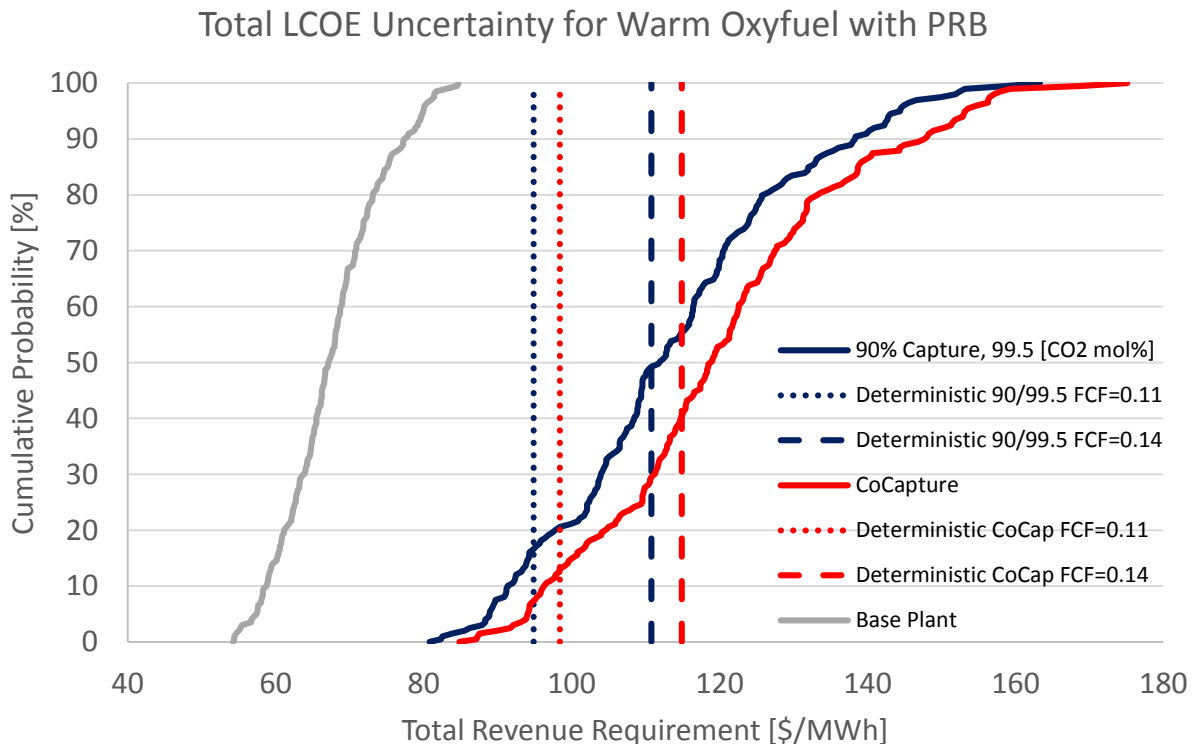


Figure 9.73 Total uncertainty plot of the base, CPU, and CoCapture plant configurations for levelized cost of electricity (LCOE). Deterministic results have been shown for reference and indicate that the case studies generated in this work are optimistic. All costs are reported in constant 2012 dollars.

The resultant cumulative probability distributions for the base, CPU, and CoCapture plants are presented in Figure 9.73. The CPU system holds a slight cost of electricity edge over the CoCapture system with a LCOE 95% CI that ranges from about 86 to 150 [\$/MWh] and has a median value of around 112 [\$/MWh]. The CoCapture system's 95% CI is from about 92 to 157 [\$/MWh] with a median value of about 119 [\$/MWh]. Both capture systems, as expected, have considerably higher LCOE values than the base plant range which has a range from 55 to 85 [\$/MWh] and a median value near 67 [\$/MWh]. The deterministic case studies using the default IECM fixed charge factor (FCF) represent the low end of both the CPU and CoCapture system distributions falling at a cumulative probability of only about 16 and 11%, respectively. The deterministic cases with a FCF of 0.14 fell closer to the 50<sup>th</sup> percentile for CPU and 40<sup>th</sup> percentile for the CoCapture system.

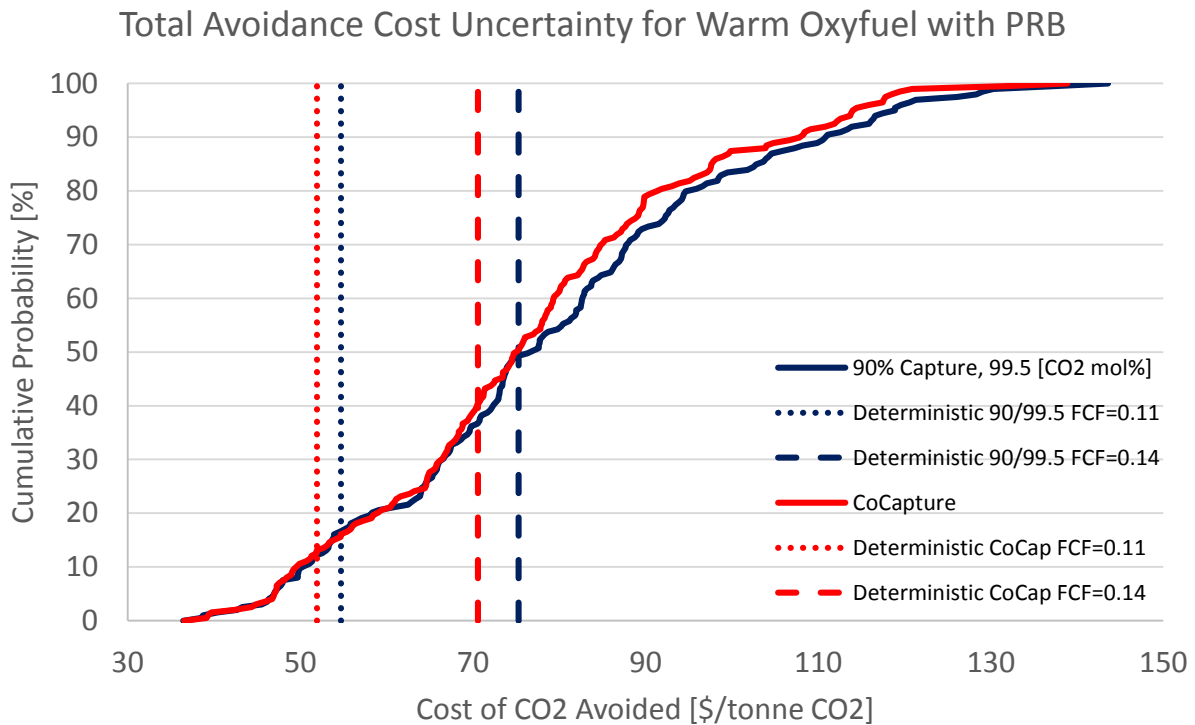


Figure 9.74 Total uncertainty plot of the base, CPU, and CoCapture plant configurations for carbon dioxide avoidance cost. Deterministic results have been shown for reference and indicate that the case studies generated in this work are optimistic. All costs are reported in constant 2012 dollars.

The cumulative probability functions produced for both the capture systems are nearly identical until up until the 40<sup>th</sup> percentile when the CoCapture system begins to hold a slight edge over the CPU system. It should be noted here that these distributions were produced independently from one another, and the base plant performance was taken to be static for all samples. These factors may contribute to the large ranges produced for the capture system distributions stemming from alterations of key parameters such as leveled capacity factor. A more rigorous, paired analysis technique should be adopted if a more exact quantitative understanding of the variance between the systems is required.

As was posited in the previous sections on uncertainty for the carbon dioxide avoidance cost; the equation used for calculating avoidance cost tips the scales in favor of CoCapture thanks to the low carbon intensity of electricity produced from CoCapture systems.

$$Avoidance\ Cost\ \left[ \frac{\$}{tCO_2} \right] = \frac{[\$/MWh]_{Capture} - [\$/MWh]_{Reference}}{[tCO_2/MWh]_{Reference} - [tCO_2/MWh]_{Capture}}$$

Despite the similarity in the avoidance cost distributions of the capture systems at low probabilities, the dynamic produced by the avoidance cost calculation suggests that the expected avoidance cost for CoCapture systems will be lower than that of CPU systems.

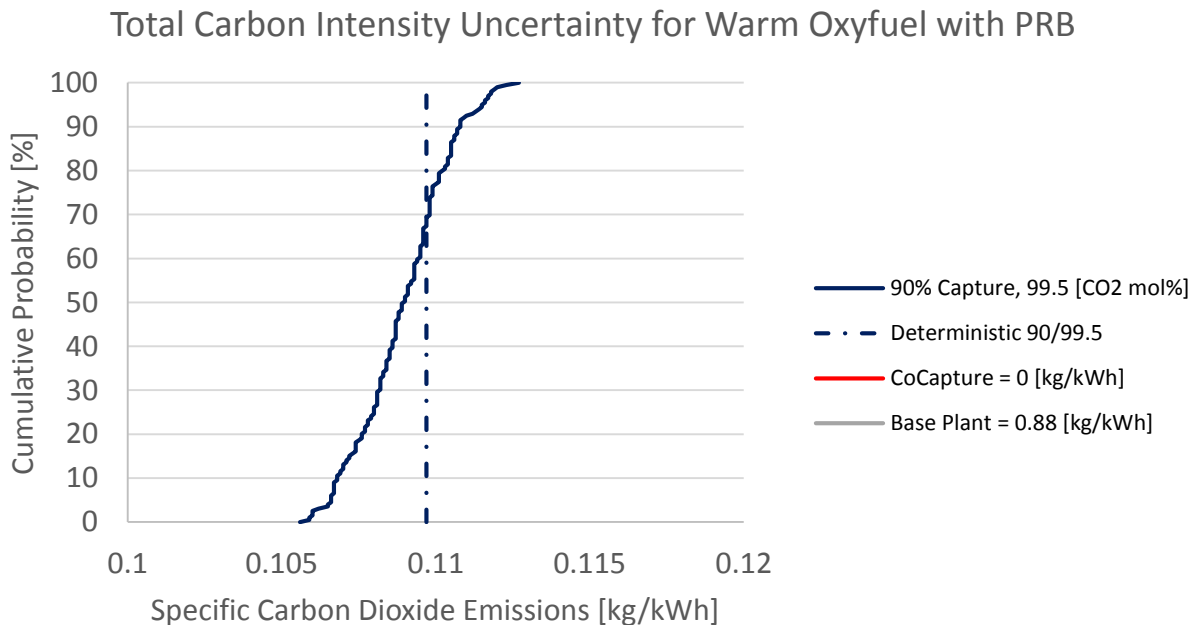


**Figure 9.75** The uncertainty distributions for carbon intensity of the capture systems suggest that most of the variability in the cost metric of avoidance cost is due to cost parameters.

The distribution of carbon intensity for produced electricity is rather narrow across the ranges considered for the CPU system; ranging from 0.106 to 0.113 [kg/kWh] with a median value of 0.109 [kg/kWh]. The carbon intensity of produced electricity from the CoCapture system remains at zero for all configurations sampled as it is a design variable for such systems. Also, the base plant carbon intensity of 0.88 [kg/kWh] has been assumed to be fixed in this analysis. The carbon intensity of the deterministic CPU Case 16 and 16a results is also a fixed value of 0.11 [kg/kWh] and intersects the cumulative probability distribution near the 70<sup>th</sup> percentile, indicating that the majority of CPU configurations sampled produce a lower carbon intensity than our deterministic case configuration. The relatively high carbon intensity of the deterministic CPU case also lends further credence to the assertion that the majority of variation in the carbon dioxide avoidance cost distributions is a result of financial uncertainty rather than performance uncertainty.

The overall takeaway from this analysis is that oxyfuel systems configured with a carbon processing unit (CPU) are more likely to have a slightly lower levelized cost of electricity than CoCapture systems.

Conversely, the CoCapture systems, thanks to their lower carbon intensity, are more likely to achieve lower carbon dioxide avoidance costs than CPU systems. A more rigorous, paired Monte Carlo simulation would need to be conducted to determine the expected magnitude of cost disparity between the two systems with respect to avoidance cost and levelized cost of electricity.

### 9.6.4 Magnitude of Uncertainty Sources

The Monte Carlo uncertainty analysis in the preceding section uses distributions on a number of key parameters which have a pronounced effect on the levelized cost of electricity for oxyfuel systems. In the following series of five cumulative probability distribution functions (CDFs) a few major parameter groups will be presented to showcase their contribution to overall uncertainty. The first parameter group (Fig. 9.76) includes all the performance parameters presented in Table 9-7.

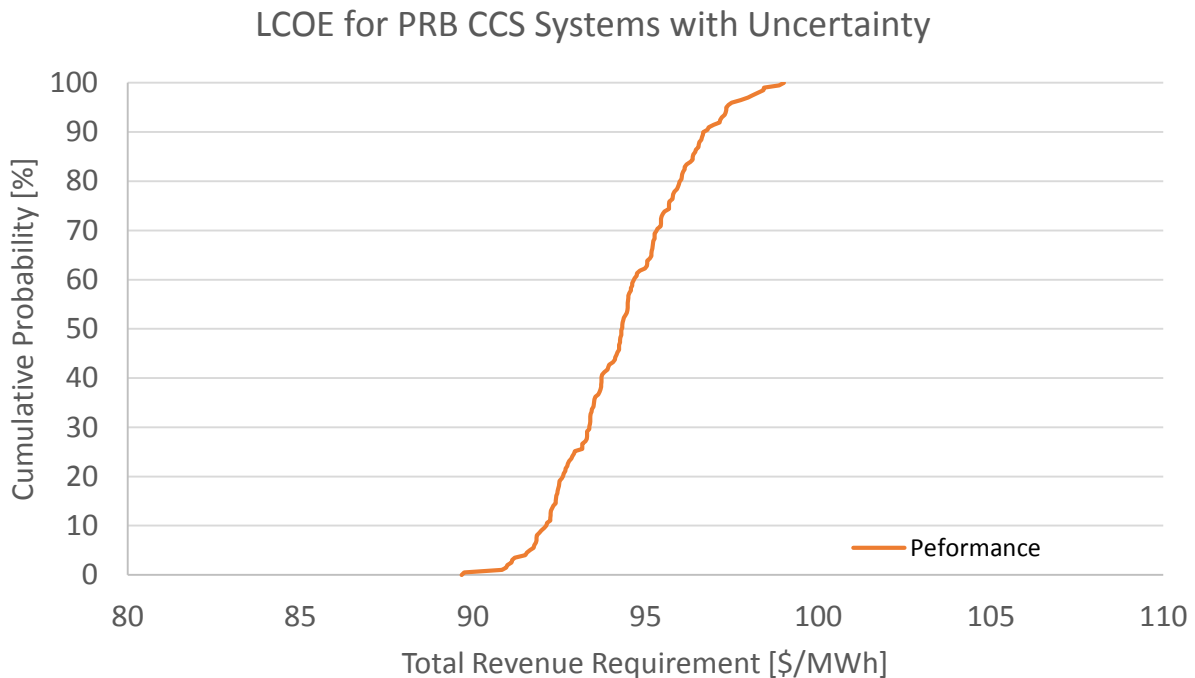
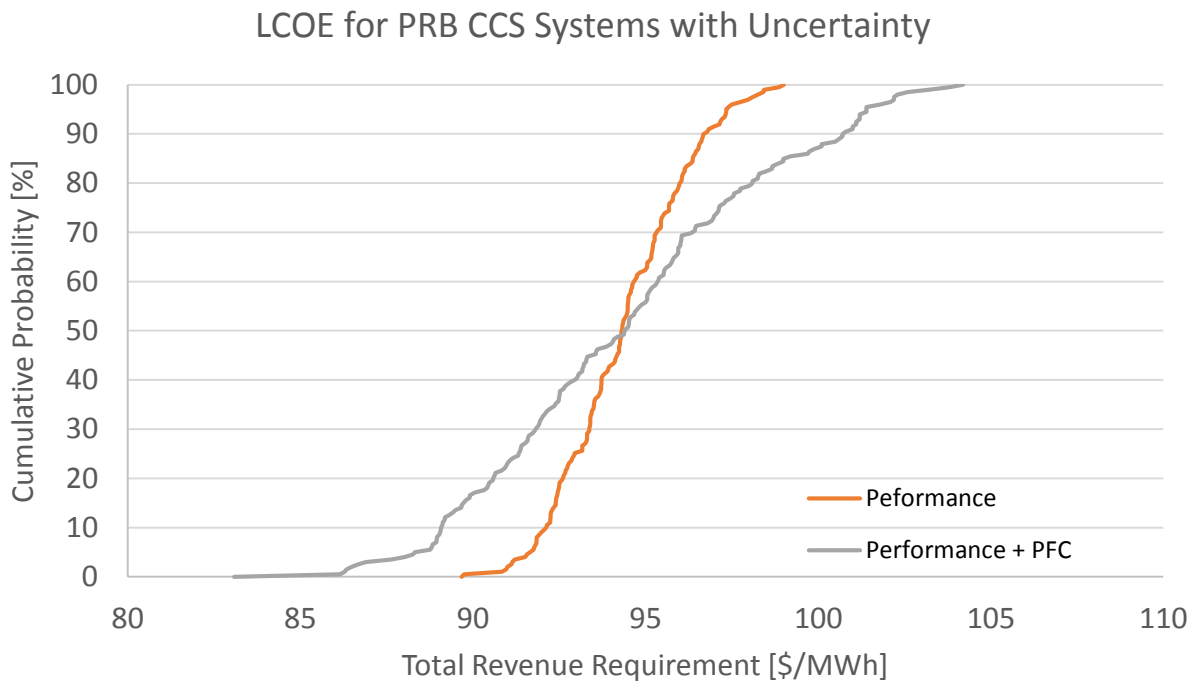


Figure 9.76. Cumulative probability distribution for the PRB oxyfuel system for just the physical performance parameters produced by the Monte Carlo simulations. All costs are reported in constant 2012 dollars.

Despite the broad range of performance assumed for the individual gas separation component (ASU and CPU) and an expansive range for air ingress, the LCOE variation attributed to the physical performance parameters is relatively small (+/- ~5%) from the median value of 95 [\$/MWh]. This is a somewhat surprising result from this analysis. The implication is that the physical performance of the system is responsible for a fairly small amount of the overall uncertainty in the LCOE of oxyfuel systems.

We then add in the process and project contingency and the process facility cost (capital cost) parameters to the Monte Carlo simulation of the plant performance parameters. The inclusion of these three financial parameters for the cost of plant components produces a CDF with over twice the range of the CDF for just the performance parameters.



**Figure 9.77. Cumulative probability distribution function for PRB systems including process and project contingency and capital cost uncertainty in addition to performance parameters. All costs are reported in constant 2012 dollars.**

The range of LCOE has increased, from 90 to 100 [\$/MWh] with just the performance parameters, to 83-105 [\$/MWh] with the inclusion of the three PFC parameters. This indicates that the variability we have assumed as plausible for the cost of the plant components has just as much, if not more, effect on the LCOE of oxyfuel systems than the physical performance of those same plant components.

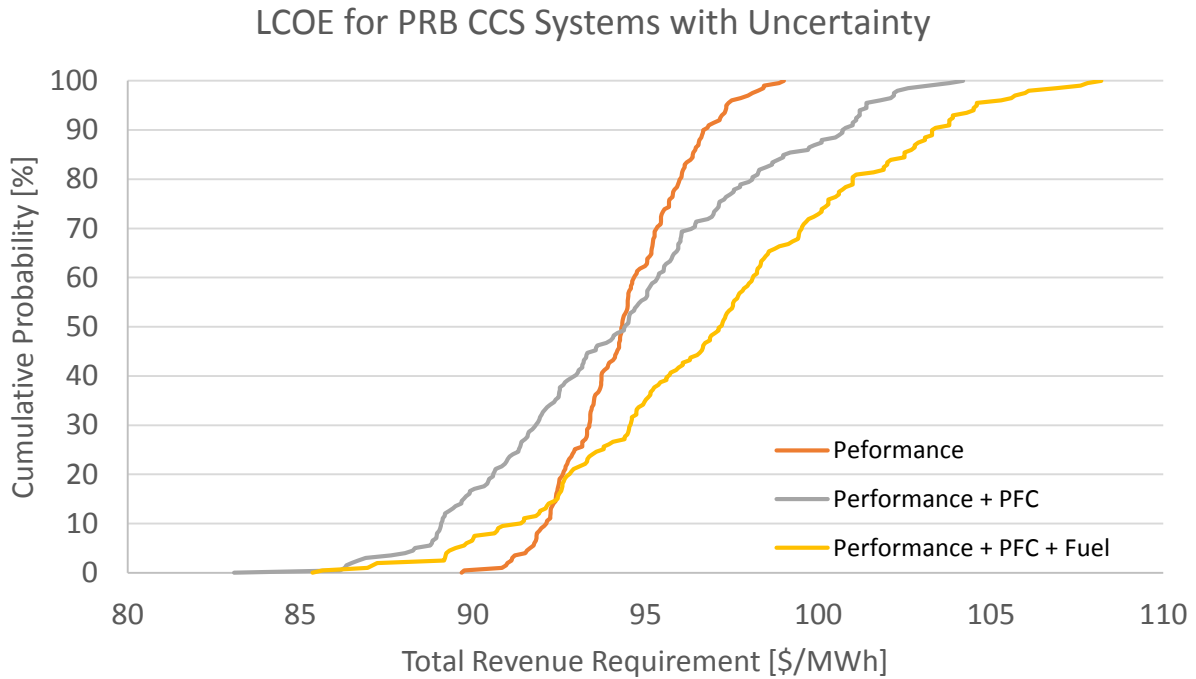


**Figure 9.78.** Cumulative probability distribution function for PRB systems including fuel cost uncertainty along with PFC and performance parameters. All costs are reported in constant 2012 dollars.

When the uncertainty in the price of coal is accounted for, the LCOE CDF shifts to the right due to the range of coal prices used being relatively high compared to the deterministic value (\$9.5/tonne). The high end of the price range for PRB coal (\$20/tonne) represents a plant which must pay to transport coal a long distance, whereas the low end (\$8/tonne) represents a mine-mouth facility.

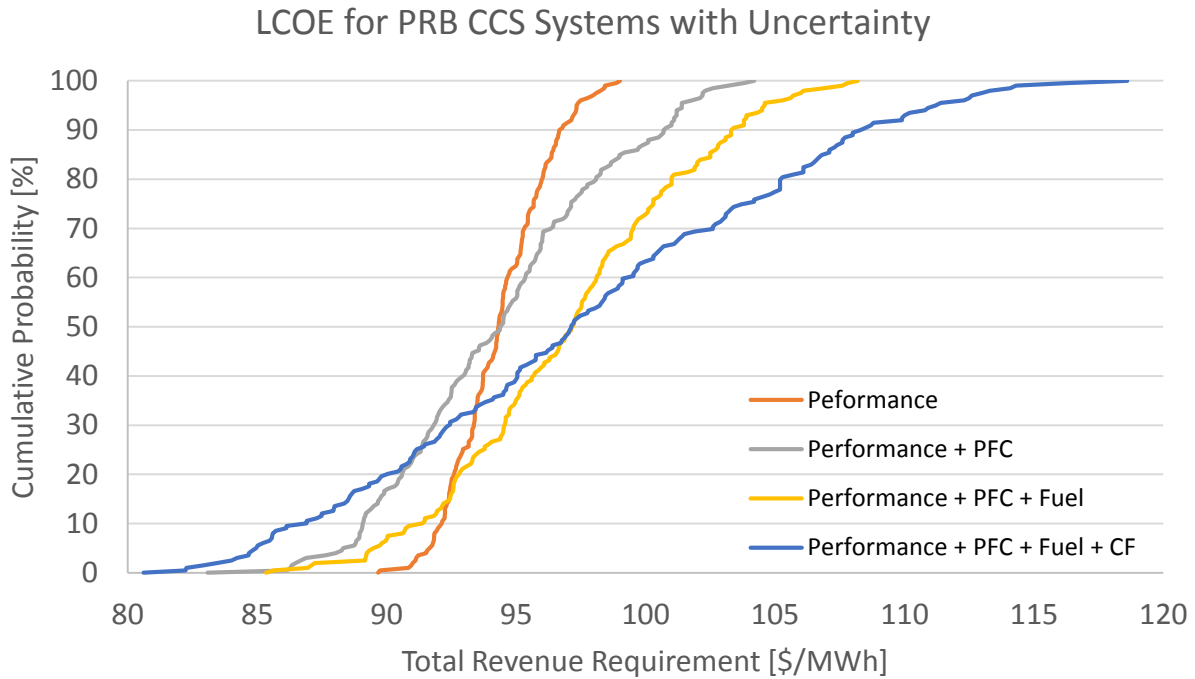


Figure 9.79. Cumulative probability distribution function for PRB systems including capacity factor in addition to fuel cost, PFC, and performance parameters. All costs are reported in constant 2012 dollars.

The fraction of time which the plant is operating each year (levelized) is known as the capacity factor. For the deterministic cases examined in this work a capacity factor of 75% has been used. For the uncertainty distributions, a uniform distribution of 65 to 85% has been sampled from to produce the blue CDF in Figure 9.79. The capacity factor produces a large increase in the range of the CDF (80-120 [\$/MWh]) due to the large change in the quantity of electricity generated annually. Cost sensitivity to variation in the capacity factor is expected and displayed for any electricity generating plant. Sensitivity to capacity factor is further exaggerated for projects with high capital intensity such as oxyfuel carbon capture.

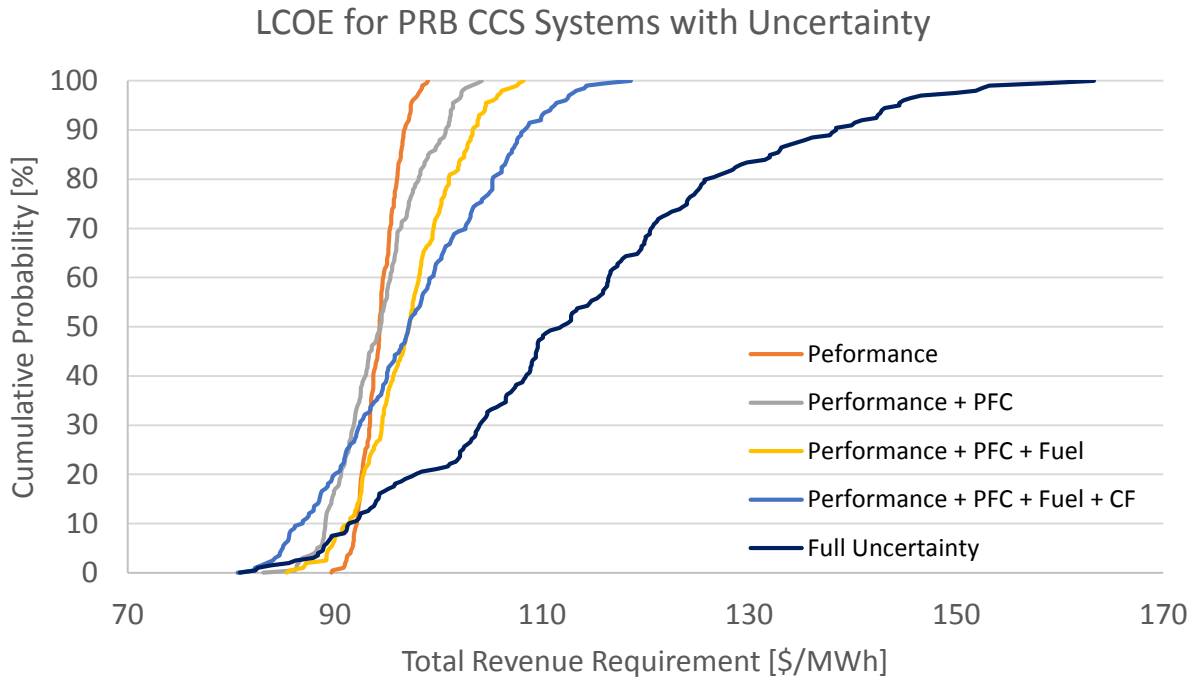


Figure 9.80. Cumulative probability distribution function for PRB systems including the cost of borrowing money (FCF) in addition to capacity factor, fuel cost, PFC, and performance parameters. All costs are reported in constant 2012 dollars.

The last parameter added to the Monte Carlo simulation is the fixed charge factor (FCF). This is a lumped financial parameter which represents the cost of borrowing money to build the project. The value for the deterministic FCF is just over 0.11 and represents an investment which has low risk. New build projects for proven generation technologies may be below 0.10 depending upon financial markets, but a uniform distribution from 0.10 to 0.18 has been assumed for FCF of the oxyfuel projects. A FCF of near 0.10 would represent an N<sup>th</sup> of a kind plant after the technology has been proven and the financial risk of the project has been reduced substantially. A FCF value closer to 0.18 would represent a high risk, first of a kind type of facility where significant uncertainty remains about scaling up oxyfuel technology to commercial scale.

The cost of borrowing money has a significant effect on the CDF for LCOE (Fig. 9.80). High FCF values stretch the CDF to higher values and can dominate the uncertainty distribution. It is apparent from the near doubling of the range of the CDF when FCF is included that it is the single most important parameter for determining the financial viability of an oxyfuel facility. In practice there would never be such a large range of uncertainty on the FCF for any singular project. Depending upon location, state of technology development, and financial markets the cost of borrowing money will be more precisely known. However, the purpose of this exercise has been to illustrate what we believe to be the plausible range for oxyfuel LCOE for projects in future and current states of development.

# Chapter 10 Comparison of PC Oxyfuel to Alternative Low-Carbon Fossil Fuel Generators

This chapter examines how oxyfuel systems compare to other low carbon fossil fuel generation options for electricity production. The first section presents an uncertainty analysis comparing oxyfuel and post-combustion amine-based absorption systems, both designed to produce a high-purity carbon dioxide product at 99.5 [CO<sub>2</sub> mol%] while capturing 90% of the carbon dioxide in the flue gas stream of a 500 [MW] power plant fired by Powder River Basin (PRB) sub-bituminous coal. The second section of this chapter examines the carbon dioxide intensity of electricity generated by six different fossil fuel generating options. The six generation options are evaluated on both a direct emissions and life cycle inventory basis.

## 10.1 Oxyfuel and Amine Capture Under Uncertainty

The identified performance uncertainty parameters, along with their assigned distributions, can be found in Table 10-1. The choice of these financial and performance parameters was made because of their importance for determining the performance of each capture system with respect to the metric of interest, levelized cost of electricity (LCOE) and avoidance cost. The base plants used for the uncertainty analysis are Cases 14 and 17. Full details on the characterization of both systems can be found in Appendix D. The cumulative distribution functions produced in the following section are the result of 200 samples taken using the uncertainty editor in the IECM. The number of samples was limited to 200 due to the extended amount of time required for each oxyfuel configuration to reach convergence.

Table 10-1 Uncertainty parameters and their chosen distributions for the comparison between warm recycle oxyfuel and post-combustion amine capture systems.

Uncertainty Parameter	Units	PRB Base Plant	Warm Oxyfuel 90% Capture	Amine 90% Capture	Reference
<b>Financial</b>					
Levelized Capacity Factor	Fraction	Uniform (0.65, 0.85)	Uniform (0.65, 0.85)	Uniform (0.65, 0.85)	Rubin and Zhai 2011
Fuel Cost	2012 \$	Uniform (8, 20)	Uniform (8, 20)	Uniform (8, 20)	Author's Estimate
CO2 Absorber Cost	2012 \$	N/A	N/A	Uniform (default, 0.7x, 1.3x)	Versteeg 2012 (76)
Oxyfuel Equipment Cost	2012 \$	N/A	Uniform (default, 0.7x, 1.3x)	N/A	Authors Estimate
Project Contingency Cost	% PFC	Normal (default, 20%)	Normal (default, 20%)	Normal (default, 20%)	Berkenpas et al. 1999
Process Contingency Cost	% PFC	Normal (default, 30%)	Normal (default, 30%)	Normal (default, 30%)	Berkenpas et al. 1999
Fixed Charge Factor	Fraction	Uniform (0.130, 0.180)	Uniform (0.130, 0.180)	Uniform (0.10, 0.180)	GCCSI & Rubin and Zhai 2011
<b>Performance</b>					
CO2 Regeneration Heat Requirement	kJ/kg CO2	N/A	N/A	Normal (default, 10%)	Versteeg 2012
Unit Separation ASU Energy	kWh/tonne O2	N/A	Uniform (180, 220)	N/A	Author's Estimate
Unit CPU Energy	kWh/tonne CO2	N/A	Uniform (90, 120)	N/A	Author's Estimate
CO2 Compressor Efficiency	%	N/A	Uniform (0.75, 0.85)	Uniform (0.75, 0.85)	Author's Estimate
Excess Air	% Stoich.	N/A	Uniform (2, 10)	N/A	Author's Estimate
Leakage Air (Ingress)	% stoich.	N/A	Uniform (0, 6)	N/A	Author's Estimate

### 10.1.1 Wyoming Powder River Basin Sub-bituminous Coal

The probability distribution function for the amine-based system has a 95% Confidence Interval (CI) from about 90 to 152 [\$/MWh] with a median value of roughly 119 [\$/MWh]. This is slightly higher than the distribution generated for the warm oxyfuel system which had a 95% CI from 86 to 150 [\$/MWh] with a median value of approximately 112 [\$/MWh]. It should be noted here that these distributions were produced independently from one another and the base plant performance was taken to be static for all samples. As noted in Chapter 9, a more rigorous, paired analysis technique should be adopted if a more exact quantitative measure of the variance between the two systems is required. The yellow CDF represents an amine based capture plant which is identical to the red system aside from a lower high end FCF value of 0.16 rather than 0.18. This reflects the maturity advantage held by PCC over oxyfuel.

## LCOE for PRB CCS Systems with Uncertainty

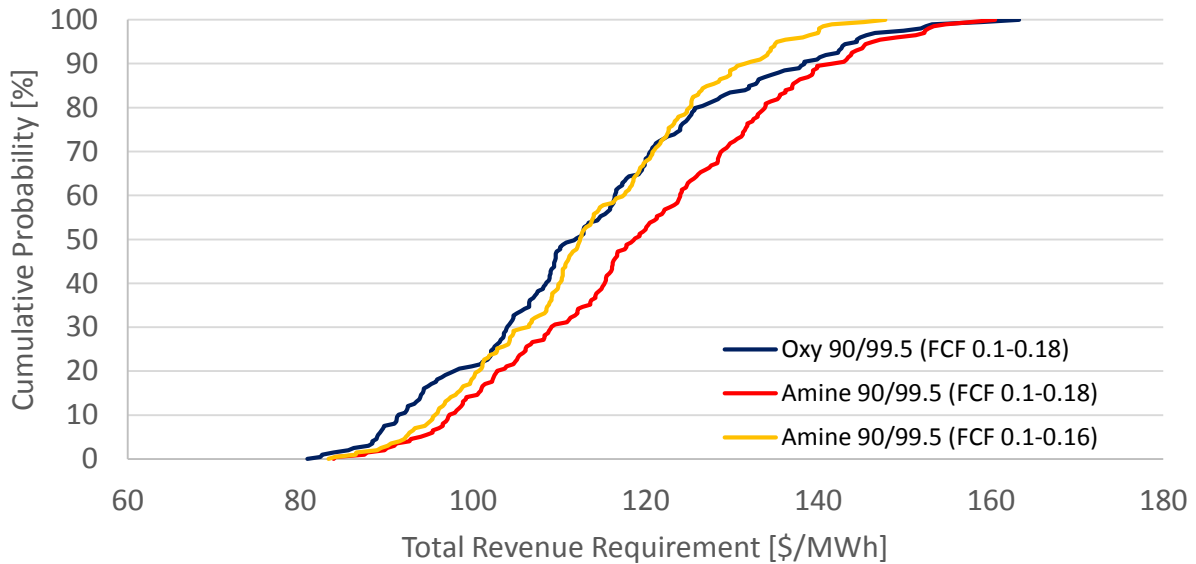


Figure 10.1 Cumulative probability functions for the warm oxyfuel and amine plants have similar LCOE ranges. The warm oxyfuel plant distribution has a longer tail than the amine system, displaying a skew toward higher LCOE values. All costs are reported in constant 2012 dollars.

For all but the last 10% of the distribution, the warm oxyfuel system is likely to produce lower LCOE values by 5-10 [\$/MWh] when the FCF range is the same between technologies. Again, a paired Monte Carlo analysis would be required to place a more precise expected value on the savings, but this analysis indicates that the total cost (LCOE) of the two systems is roughly comparable, with the oxyfuel system having a slightly lower cost for this case. The yellow amine system is near cost parity with the oxyfuel system for PRB coal.

## Avoidance Cost for PRB CCS Systems with Uncertainty

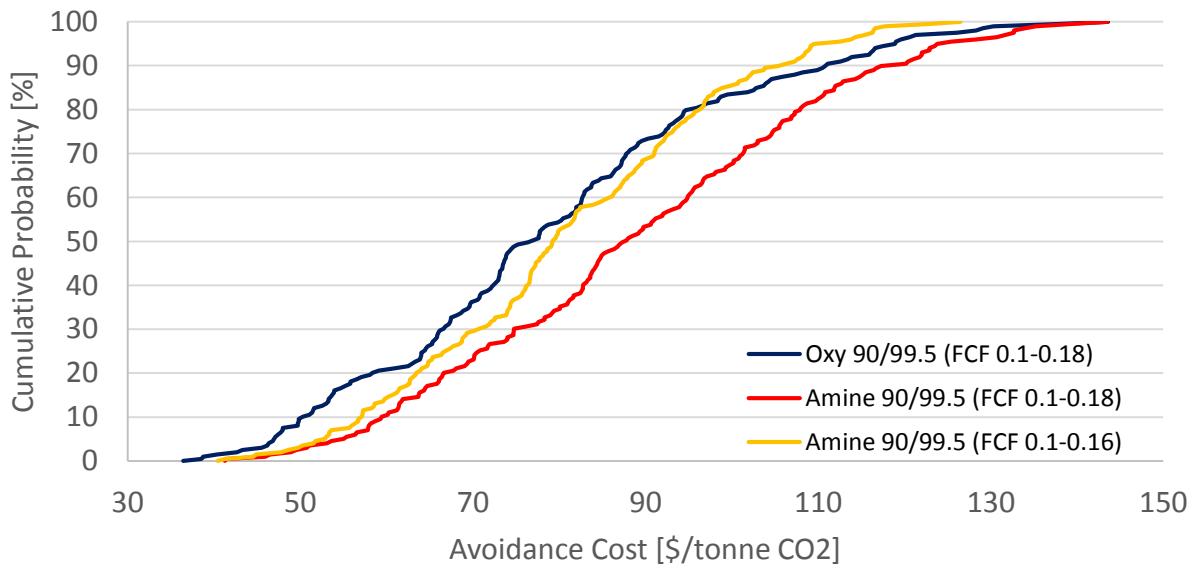


Figure 10.2 Cumulative probability functions for the warm oxyfuel and post-combustion amine system for carbon dioxide avoidance cost. The warm oxyfuel system has a lower expected avoidance cost across the distribution. All costs are reported in constant 2012 dollars.

The warm oxyfuel system cumulative probability distribution has lower expected avoidance costs than the amine system across the distribution. Oxyfuel avoidance costs have a 95% CI from 43 to 126 [\$/tonne CO<sub>2</sub>] with a median of about 76 [\$/tonne CO<sub>2</sub>] whereas the amine avoidance cost CDF has a 95% CI from 49 to 133 [\$/tonne CO<sub>2</sub>] with a median value of 87 [\$/tonne CO<sub>2</sub>]. The relatively wider gap between the two capture technologies distributions for avoidance cost than LCOE is a result of the disparity in carbon intensity between the two technologies and the avoidance cost formulation.

$$\text{Avoidance Cost} \left[ \frac{\$}{tCO_2} \right] = \frac{[\$/MWh]_{\text{capture}} - [\$/MWh]_{\text{reference}}}{[tCO_2/MWh]_{\text{reference}} - [tCO_2/MWh]_{\text{capture}}}$$

Using nominal (base case) assumptions, the carbon intensity of electricity produced by the amine-based system (0.128 [kg/kWh]) is approximately 15% higher than that of the oxyfuel system (0.11 [kg/kWh]) despite both systems having a 90% capture designation. This disparity is a result of the oxyfuel net plant efficiency (~30%) being considerably higher than that of the amine system (~25.5%). The lower carbon intensity of oxyfuel system (Fig 10.3) across the distribution produces a considerable advantage (~10 [\$/tonne CO<sub>2</sub>]) in expected avoidance cost.

The lower net plant efficiency also is a contributing factor to the greater uncertainty for carbon intensity produced by the amine-based system. The greater absolute mass flow of carbon dioxide through the carbon dioxide processing equipment (absorber/stripper and compressor) results in the performance uncertainties of these components being magnified compared to their oxyfuel counterparts. Alterations in the heat of generation for the amine-based system also has significant secondary effects on the mass flow rate of carbon dioxide which needs to be processed due to the significant impact this parameter has on the gross plant heat rate.

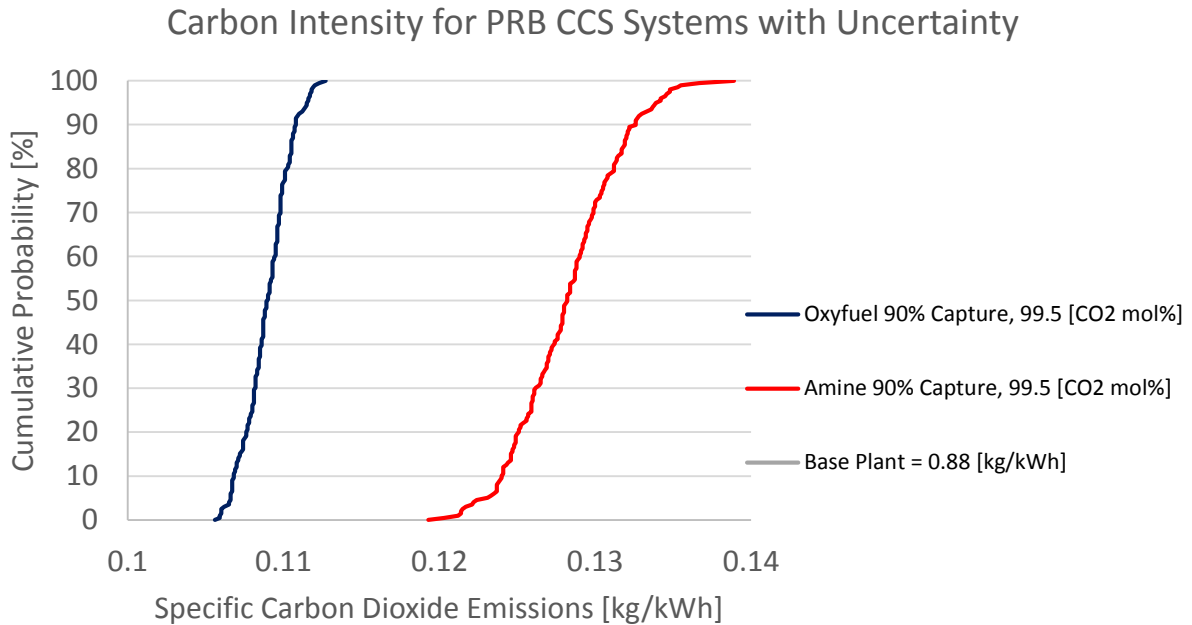


Figure 10.3 Cumulative probability functions for the carbon dioxide intensity of electricity produced from the warm oxyfuel and amine systems. The expected emissions from the warm oxyfuel system are approximately 15% lower than the amine system.

#### 10.1.2 Illinois #6 Bituminous Coal

The stochastic dominance displayed by oxyfuel compared to the amine based post combustion capture system for PRB is again present for Illinois #6 bituminous coal when the system have similar FCF ranges. The gap between the CDF's has narrowed to the point where the systems are nearly at cost parity from a stochastic point of view however. The yellow amine CDF, with the lower FCF top end, is stochastically dominate over the oxyfuel system for Illinois #6 across nearly the entire uncertainty distribution.

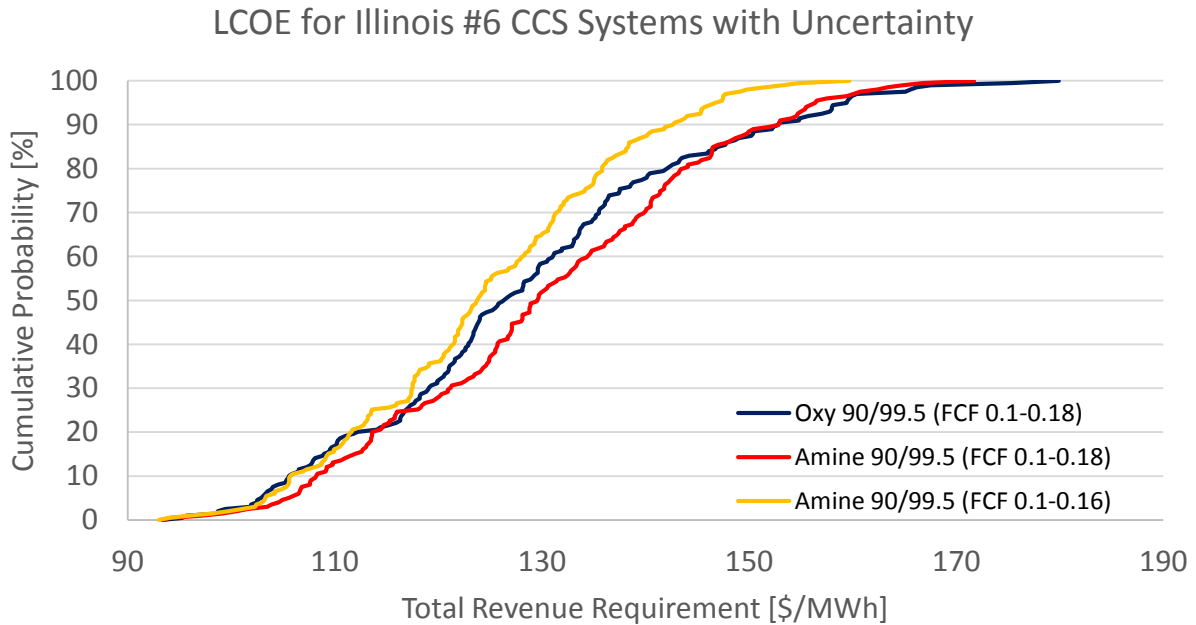


Figure 10.4. Cumulative probability distribution functions for the warm oxyfuel system and amine based capture for Illinois #6 Bituminous Coal. The systems are at near cost parity for this coal when the FCF ranges are similar. All costs are reported in constant 2012 dollars.

The avoidance cost cumulative probability distributions for the Illinois #6 bituminous coal are nearly identical for the oxyfuel and amine based systems with the same FCF range. The yellow amine based system CDF, which has a FCF range which reflects the advancement of PCC over oxyfuel, is stochastically dominant over the oxyfuel system for all but the lowest 20% of the probability distribution function. The change from PRB coal to Illinois #6 coal has not qualitatively changed the result of oxyfuel being the stochastically dominant carbon capture option, however the disparity between the two systems has been reduced for both the LCOE and avoidance cost CDFs.

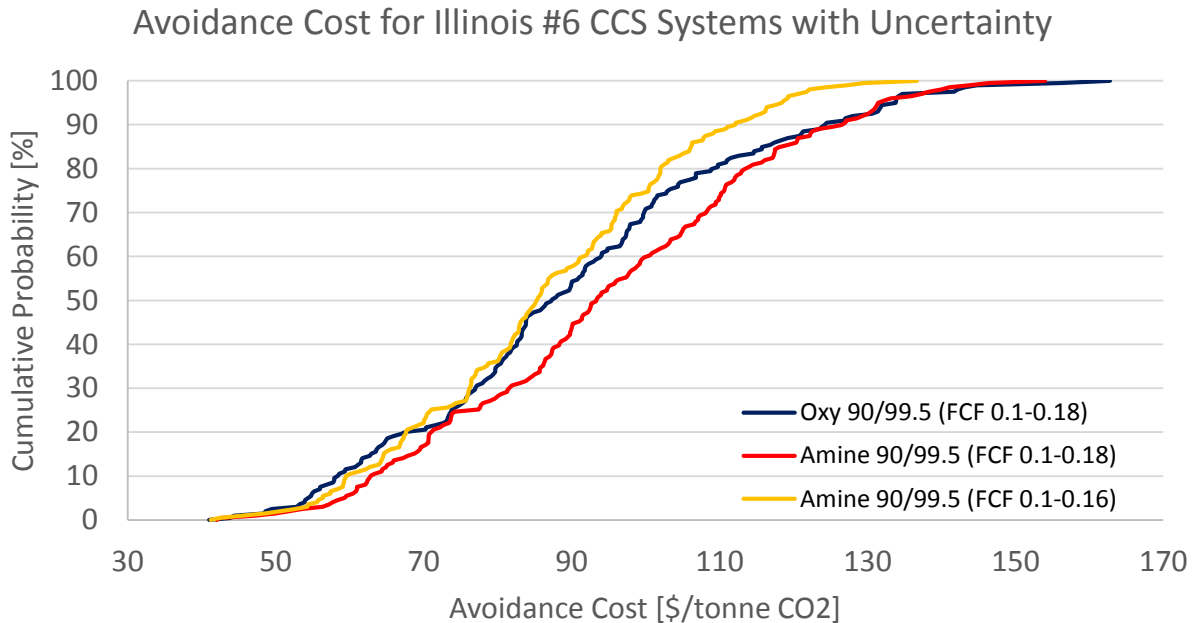


Figure 10.5. Cumulative probability distribution functions for the warm oxyfuel system and amine based capture for Illinois #6 Bituminous Coal. The avoidance cost of the oxyfuel system is stochastically dominate until about 85<sup>th</sup> percentile where amine and oxyfuel are essentially the same. All costs are reported in constant 2012 dollars.

### 10.1.3 North Dakota Lignite

The stochastic dominance displayed by oxyfuel compared to the amine based post combustion capture system for PRB is again present for North Dakota Lignite when the system have similar FCF ranges. The gap between the CDF's has widened to the point where the oxyfuel system is clearly stochastically dominant over both the red and yellow CDFs for amine based capture. With FCF ranges equivalent between the systems, the median value of the oxyfuel LCOE CDF is nearly 15 [\$/MWh] less expensive than the median value of 145 [\$/MWh] for the amine based system. The range of the two systems distributions are very similar, but the oxyfuel system is stochastically dominant across the range.

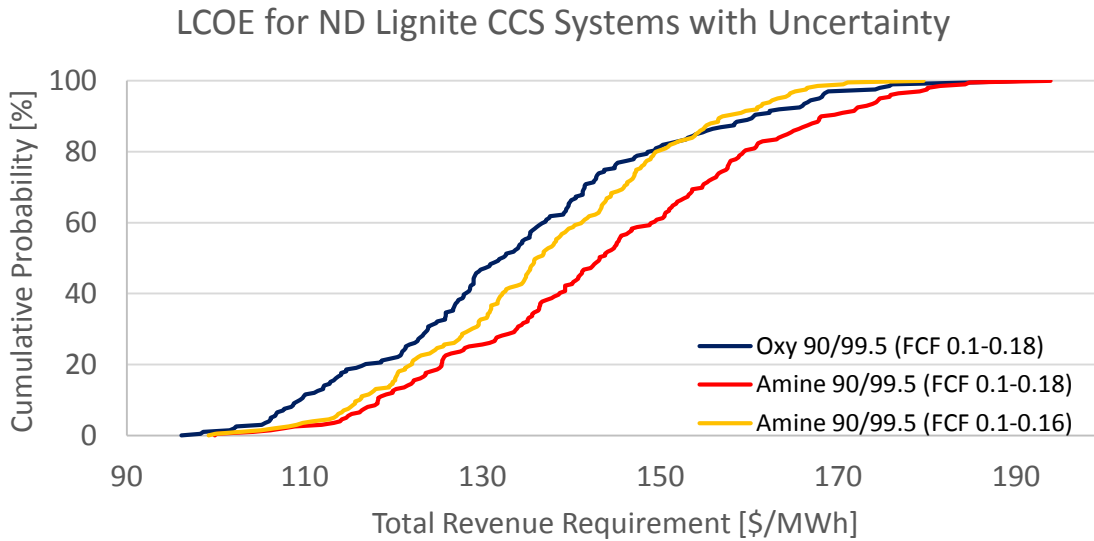


Figure 10.6. Cumulative probability distribution functions for the cool recycle oxyfuel system and equivalent post combustion capture amine based systems for North Dakota Lignite. The oxyfuel system is stochastically dominant over amine based capture for the ND Lignite. All costs are reported in constant 2012 dollars.

The avoidance cost distributions for ND Lignite are even starker in the stochastic dominance of oxyfuel over amine based capture than the LCOE CDFs. This is because the generally low efficiency of lignite boilers further magnifies the efficiency advantage that oxyfuel holds over post combustion capture. The result is a median avoidance cost advantage of nearly 20 [\$/tonne CO<sub>2</sub>] for oxyfuel.

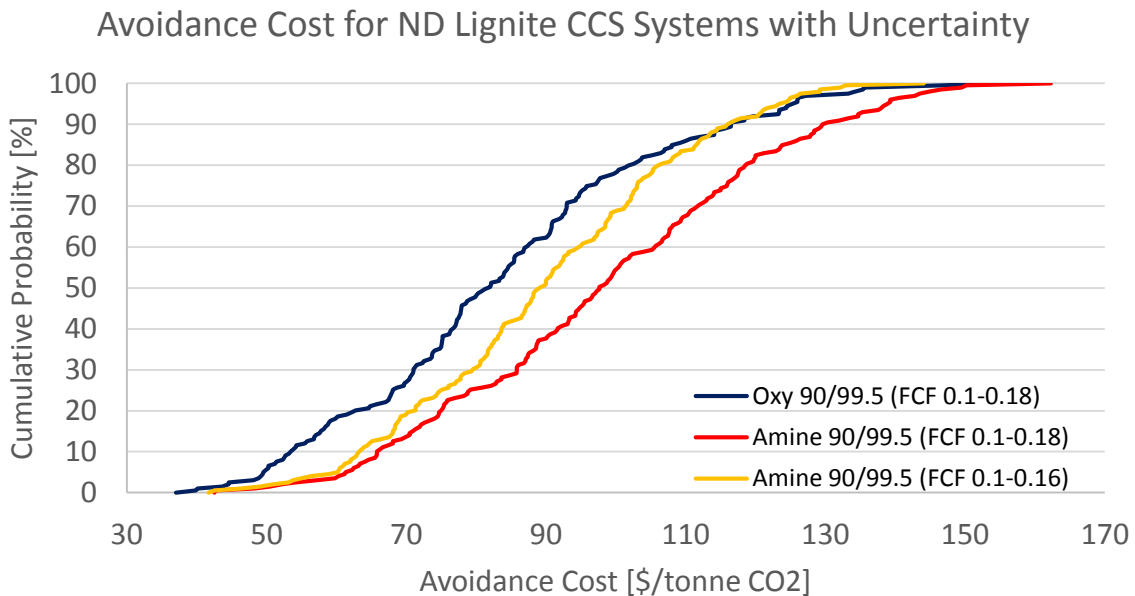


Figure 10.7. Cumulative probability distribution functions for cool oxyfuel and comparable amine based post combustion capture systems for North Dakota Lignite. The efficiency advantage of oxyfuel produces a significant advantage for oxyfuel over amine based PCC. All costs are reported in constant 2012 dollars.

## 10.2 Generation Alternatives: A Comparison including a Life-Cycle Perspective

Carbon emission reduction in the U.S. electrical mix as a result of fuel switching has produced great excitement among supporters of natural gas. However, a life-cycle perspective may not be quite so rosy. Fugitive emissions of methane, a much more powerful greenhouse gas (GHG) than carbon dioxide, are a non-trivial concern in traditional natural gas production (77). Recent work on shale gas production (78) suggests that we should give pause before anointing shale gas as GHG-friendly. Fugitive emissions of methane as well as other GHG emissions from plant consumables must be characterized, understood, and addressed.

Further insight from the life-cycle perspective for CCS technologies suggests that the upstream emissions from plant consumables (limestone, ammonia, amines, etc.) begin to be a dominant source of GHG's as carbon capture rates in excess of 90% are achieved with post-combustion capture from pulverized coal (79). This may result in an advantage for oxyfuel-based pulverized coal plants, which require far fewer consumables than their amine-based counterparts.

The goal of this analysis is to consider the impact of upstream emissions from the major plant consumables (fuel, lime/limestone, ammonia, and amines) in addition to the direct "smoke stack" carbon dioxide emissions of low-carbon fossil fuel generators. The generators being considered are: Ultra-Supercritical Coal, Supercritical Coal with Amine Capture, Natural Gas Combined Cycle (NGCC), NGCC with Amine Capture, Warm Oxyfuel with CPU, and Warm Oxyfuel with CoCapture. All of these plants were modeled in the IECM with a levelized capacity factor of 75%. An effort was made to set the net power output of all plants to 500 megawatts, or as close to it as possible. Full characterization of all the cases can be found in Appendix D, but Table 10-2 presents the cost and performance highlights for each.

Table 10-2. Cost and performance highlights from the low carbon fossil fuel case studies. All costs are reported in constant 2012 dollars.

	<b>Case 5</b>	<b>Case 14</b>	<b>Case 16</b>	<b>Case 17</b>	<b>Case 6</b>	<b>Case 7</b>
<b>Plant Type</b>	USC	Oxy Supercritical	Oxy Supercritical	Amine Supercritical	NGCC	Amine NGCC
<b>Fuel Type</b>	PRB	PRB	PRB	PRB	Nat. Gas	Nat. Gas
<b>Fuel Cost (\$/GJ)</b>	0.5	0.5	0.5	0.5	6.5	6.5
<b>Coal (tonnes/hr)</b>	226.2	310.4	314.9	361.9	N/A	N/A
<b>Natural Gas (tonnes/hr)</b>	N/A	N/A	N/A	N/A	79.99	79.99
<b>Net Electrical Output (MWe)</b>	500	500	500	500	580.9	501.6
<b>Plant Efficiency (% HHV)</b>	41.02	29.89	29.47	25.64	49.99	43.16
<b>CO2 Emissions (kg/kWh)</b>	0.7987	0.1097	0	0.1281	0.3642	0.0422
<b>Capital Required (\$/kW-net)</b>	2215	3726	3851	3850	789.8	1439
<b>Revenue Required (\$/MWh)</b>	54.27	94.88	98.42	99.12	63.39	88.07
<i>Consumables (x/kWh)</i>						
<b>Lime/Limestone</b>	2.2E-03	3.1E-03	3.1E-03	7.9E-03	N/A	N/A
<b>Sorbent</b>	N/A	N/A	N/A	1.2E-04	N/A	3.9E-05
<b>Ammonia</b>	3.6E-04	N/A	N/A	5.7E-04	N/A	N/A
<b>Coal</b>	0.452	0.621	0.630	0.724	N/A	N/A
<b>Natural Gas</b>	N/A	N/A	N/A	N/A	0.1377	0.160

The direct carbon dioxide emissions for each of the low-carbon fossil fuel generators are plotted against their respective levelized cost of electricity in Figure 10.4. The inclusion of Ultra-Supercritical Coal as a low-carbon generation technology is likely a contestable point for some; however it does represent an evolutionary increase in net plant efficiency. Furthermore, it provides a logical benchmark with which to judge the cost and performance of the other technologies.

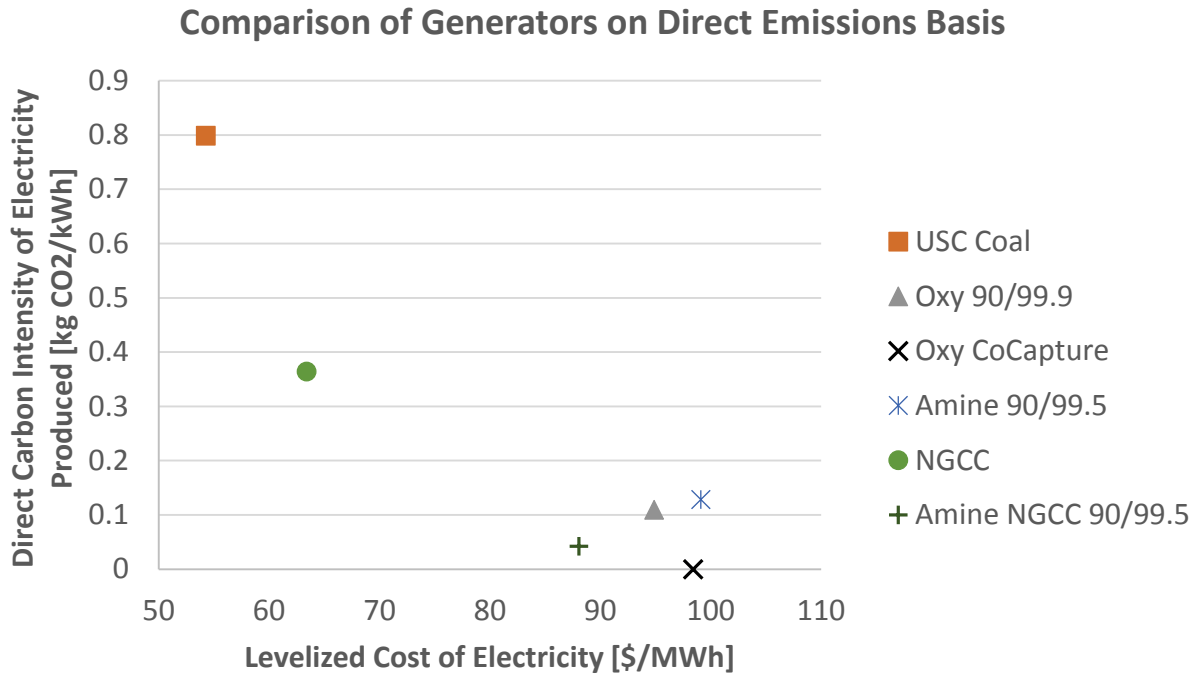


Figure 10.8 Comparison of direct carbon dioxide emission intensity for the six low-carbon fossil fuel generators. All costs are reported in constant 2012 dollars.

The spread of these six plants across the quadrant is nearly total. The red square in the upper left hand portion of the graph is the USC Coal plant; representing high carbon dioxide intensity but at a relatively low cost. By contrast, the four carbon capture plants are clustered in the lower right hand portion of the graph; representing low carbon dioxide intensity but at a cost premium. Variations in the fuel price would have no effect on the carbon intensity of electricity produced. The location of the marker would simply shift to the left if fuel price was reduced and to the right with an increase in fuel cost. At the assumed natural gas price of 6.5 [\$/GJ] the NGCC plant represents a sizeable carbon intensity reduction at a moderate cost increase over the USC Coal plant.

Of the four carbon dioxide capture technologies, the NGCC with Amine Capture unit possesses the lowest LCOE value and the second lowest carbon dioxide intensity. The Supercritical Coal with Amine Capture unit has both the highest direct carbon intensity and the highest LCOE; making it the least attractive of the four capture plants. The two oxyfuel units are somewhere in-between and the choice of one over the other would need to be determined based upon preference, circumstances, and perhaps business model.

## 10.2.1 Upstream Emissions Inventory

Direct emissions don't tell the whole story. Aside from the combustion of fuel, they omit all the material flows which were required to produce that kilowatt of electricity. Understanding the emissions associated with these material flows, and their contribution to the total carbon dioxide intensity, is the purpose of this section.

**Table 10-3 Emission factors used for converting from consumable flow rates to 100 Year Global Warming Potential [CO<sub>2</sub>e].**

<b>Consumable</b>	<b>100 Year CO<sub>2</sub> Equivalency by Mass</b>
Lime/Limestone (78)	2.501E-02
Solvent (Amine) (78)	7.631E+00
Ammonia (78)	4.421E-01
Coal (78)	1.756E-01
Study 1 (79) Coal	4.999E-02
Study 2 (80) Coal	2.734E-02
Study 3 (81) Coal	5.012E-02
Study 4 (82) Coal (Avg.)	9.444E-03
Study Average for Coal	3.422E-02
Natural Gas (1% Leakage)	3.400E-01
Natural Gas (3% Leakage)	1.020E+00
Natural Gas (5% Leakage)	1.700E+00

The scope of this life cycle inventory assessment is intentionally very narrow. The main objective is to evaluate the potential effects of fugitive methane emissions from the production and handling of the fuels. Consequently, only the upstream and combustion (if applicable) emissions associated with the consumables are being evaluated. No consideration has been given to disposal of waste streams within the plant or the embodied carbon of facilities, etc.

The Environmental Input-Output Life Cycle Assessment model (EIO-LCA) was used to generate the 100 year carbon dioxide equivalency emissions factors for each of the four plant consumables being considered (Table 10-3). Four studies which evaluated the release of methane from surface coal mining, during and after coal removal, in addition to carbon dioxide and methane emissions from coal handling were also considered. All methane releases were converted to 100 year global warming potential (CO<sub>2</sub>e basis) using a factor of 34 (83) and the sum of all emissions vectors considered in each of the four studies has been reported. Lastly, a range of natural gas fugitive emission rates has been adopted and applied to provide a range for the effects from fugitive methane emissions.

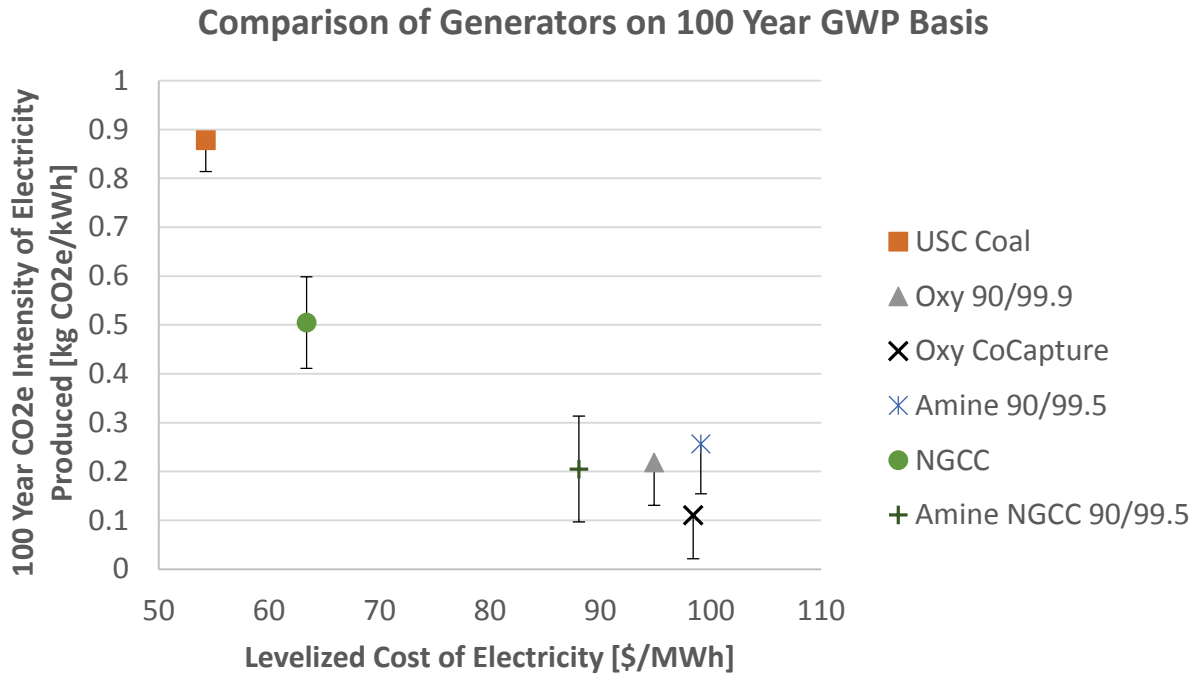


Figure 10.9 Comparison of the 100 year CO<sub>2</sub>e intensity of the six low-carbon fossil fuel generators. All costs are reported in constant 2012 dollars.

The error bars for the natural gas consuming plants are representative of varying the fugitive emission rate from 1-5% with 3% being the point value. The error bars for the coal consuming plants represent the use of the study average emission factor for consumed coal rather than the EIO-LCA emission factor, which is the point value. The fairly obvious assessment is that none of the carbon intensities were reduced by including the associated emissions from plant consumables. The second observation is that the fugitive emission rate applied to the natural gas consumed by a plant has a dramatic effect of the CO<sub>2</sub>e intensity. A NGCC facility was considered to provide a 60% reduction in direct carbon dioxide intensity compared to the USC Coal plant, but at a 5% fugitive methane emission rate would reduce the CO<sub>2</sub>e intensity reduction to only about 25%.

## Comparison of CCS Technologies on 100 Year GWP Basis

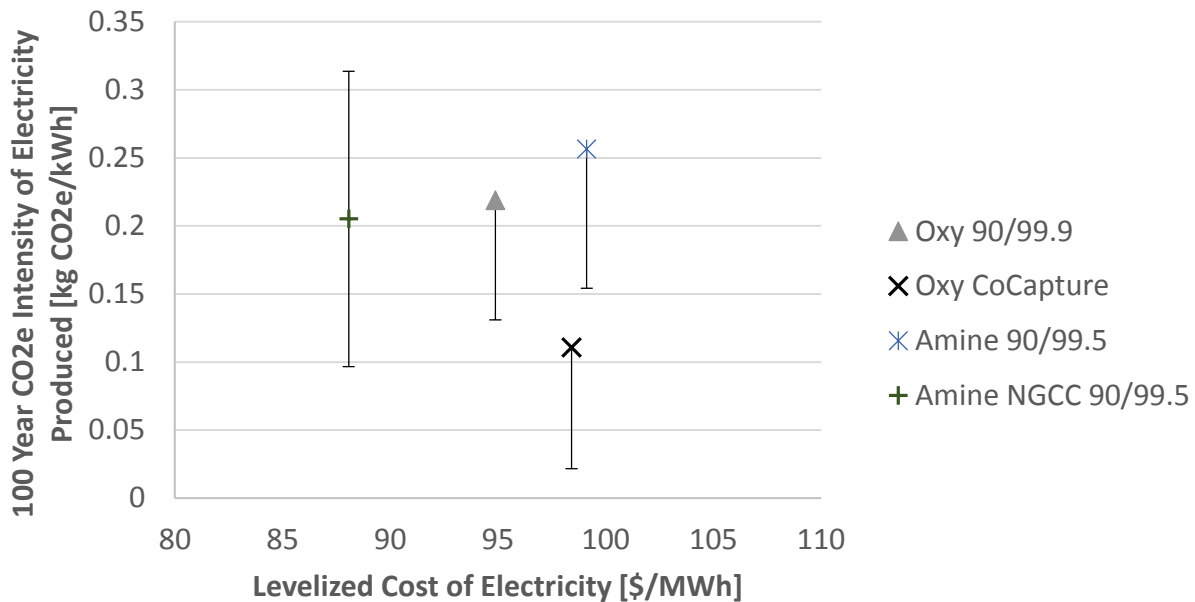


Figure 10.10 The rate of fugitive emissions assumed for the NGCC with Amine Capture facility determines whether it has the lowest or the highest CO<sub>2</sub>e intensity of any of the capture facilities. All costs are reported in constant 2012 dollars.

Focusing in on just the capture plants, (Fig. 10.6) the effects of including the associated emissions for plant consumables has a dramatic effect on the CO<sub>2</sub>e intensity for all of the plants. The CO<sub>2</sub>e intensity of the Warm Oxyfuel with CPU and Supercritical Coal with Amine Capture both incur an increase of 20-100% over their direct emission carbon dioxide intensities. The CO<sub>2</sub>e intensity of the Warm Oxyfuel with CoCapture plant goes from being accounted as 0 to 0.11 [kg/kWh]. By the numbers, this would be the only plant actually capable of achieving 90% capture on a CO<sub>2</sub>e basis. Also, the Warm Oxyfuel with CoCapture plant has lowest carbon intensity of any capture plant unless a very low (<1 %) fugitive emission rate is assumed for the NGCC with Amine Capture plant and the EIO-LCA value is used for upstream coal emissions.

The NGCC with Amine Capture case is the most interesting of all the capture technologies because it can either be the least CO<sub>2</sub>e intensive technology or the most depending upon the fugitive methane emission rate. Even with a fugitive emission rate of just 1.5%, the potency of methane as a greenhouse gas essentially eliminates any CO<sub>2</sub>e intensity advantage held by NGCC over Warm Oxyfuel with CPU. For a fugitive emission rate of about 2.5% the CO<sub>2</sub>e intensity of all the non-CoCapture carbon capture technologies fall within the same band of CO<sub>2</sub>e intensity of about 0.15 to 0.2 [kg CO<sub>2</sub>e/kWh]. The only capture technology which provides a uniquely low level of carbon intensity is Warm Oxyfuel with CoCapture.

# Chapter 11 Policy Analysis and Implications

This chapter will briefly cover a few of the policy related issues related to carbon capture systems generally as well as the performance of oxyfuel systems relative to other carbon capture systems such as post combustion capture with amines. The first section will focus on the proposed EPA 111(b) and which carbon capture systems are capable of meeting the standard most cost effectively. The second section focuses on the social valuation of carbon dioxide emissions and what the implications of this valuation are for carbon capture systems. The last section of this chapter briefly presents and discusses the policy paper in Appendix A. The proposed Low Carbon Capacity Standard (LCCS) would provide an alternative means of procuring low carbon energy to the previously passed renewable portfolio standards in PJM.

## 11.1 New Source Performance Standards

In June of 2012 the U.S. Environmental Protection Agency proposed a rule for the carbon dioxide emission performance of new electricity generation sources (NSPS). The rule for coal is that sources must limit emissions to 1,100 [lbs CO<sub>2</sub>/MWh-gross] for a 12 month monitoring period (8). In oxyfuel systems, the majority of separation work and added capture cost is a result of separating the oxygen to operate the boiler. Consequently, the notion of designing an oxyfuel system to capture any lower percentage than is optimal for operation of the CPU will just result in substantially higher LCOE values as the majority of equipment required for 90% capture is still necessitated at lower capture rates. Post combustion capture systems, by contrast, can be designed to capture a lower percentage of the carbon dioxide in the flue gas stream. This can be done by using a bypass stream and downsizing the absorber and regenerator. This results in a significant decrease in capital cost and the operations and maintenance costs associated with capturing a lower percentage of the carbon dioxide. The 111(b) standard requires that 45.2% of the carbon dioxide be captured for a supercritical coal plant burning PRB sub-bituminous coal.

**Table 11-1. Carbon capture plants capable of meeting or exceeding the carbon dioxide new source performance standard proposed by the Environmental Protection Agency. All costs are reported in constant 2012 dollars.**

<b>Plant Type</b>	<b>Oxyfuel Supercrit</b>	<b>Amine Supercrit</b>	<b>Amine Supercrit</b>
<b>Coal Type</b>	PRB	PRB	PRB
<b>Capture Performance (Cap. %/Purity %)</b>	90/99.5	90/99.5	45.2/99.5
<b>Coal (tonnes/hr)</b>	310.4	361.9	303.6
<b>Gross Electrical Output (MWe)</b>	664.9	632.8	590.3
<b>Net Electrical Output (MWe)</b>	500	500	500
<b>Plant Efficiency (% HHV)</b>	29.89	25.64	30.56
<b>Annual Power Generation (BkWh/yr)</b>	3.287	3.287	3.287
<b>CO2 Emissions (kg/kWh)</b>	0.1097	0.1281	0.589
<b>Revenue Required (\$/MWh)</b>	94.88	99.12	77.4
<b>Added Cost of CCS (\$/MWh)</b>	42.28	46.52	21.27
<b>Cost of CO2 Avoided (\$/tonne)</b>	54.73	61.69	69.13
<b>Cost of CO2 Captured (\$/tonne)</b>	37.73	35.87	37.03

The LCOE (revenue requirement) of the amine system (77 [\$/MWh]) specifically designed to meet the NSPS is about 20 [\$/MWh] lower than either of the full capture systems in Table 11-1. This reduced cost of compliance may have been the EPA’s intention when formulating the NSPS. However, be that the case or not, there are other social and market pressures which may result in the capture plant designed specifically to just meet the NSPS not being the best choice for a new build facility.

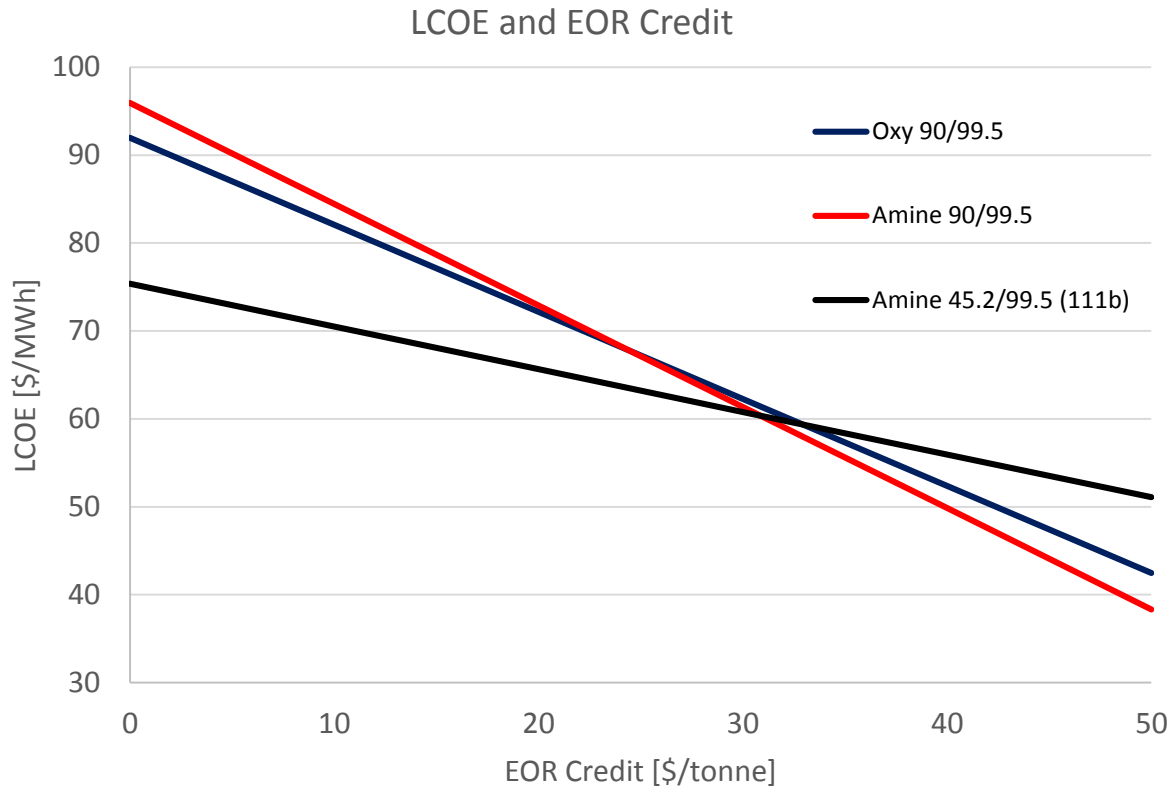


Figure 11.1. NSPS compliant carbon capture plants and their LCOE's as a function of enhanced oil recovery revenue. All costs are reported in constant 2012 dollars.

Most of the carbon capture facilities being built currently rely upon revenue generated from selling their captured carbon dioxide to oil companies for use in enhanced oil recovery. Figure 11.1 examines what the levelized cost of electricity would be across various carbon dioxide prices [\$/tonne CO<sub>2</sub>] for the three carbon capture plants in Table 11-1. The general trend is that LCOE values fall as revenue from carbon dioxide sales is increased. At the y-axis the LCOE values correspond to the values reported in Table 11-1 with the amine facility designed specifically to barely meet the NSPS providing the cheapest new source option.

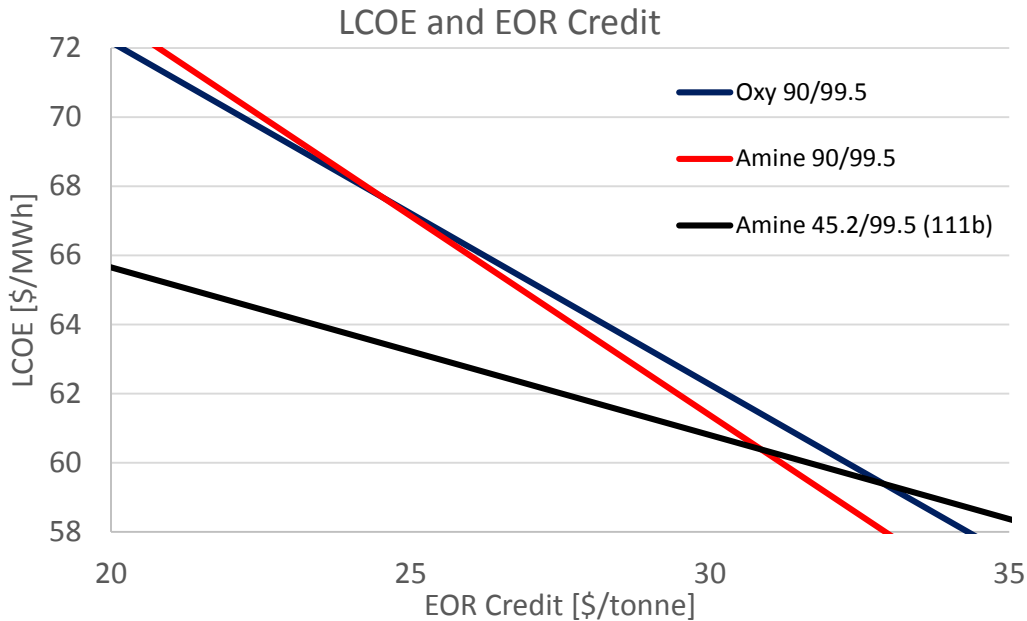


Figure 11.2. A closer look at the interplay between EOR revenue and the three NSPS compliant carbon capture facilities. All costs are reported in constant 2012 dollars.

Looking more closely at where the LCOE lines cross for the three carbon capture facilities, the first interesting qualitative change occurs at an EOR credit of about 25 [\$/tonne CO<sub>2</sub>]. At this point the full capture amine plant becomes a less expensive option than full capture oxyfuel. The changeover occurs because the lower efficiency of the amine based system results in more carbon dioxide being produced and ultimately sold to generate more and more revenue as carbon dioxide prices rise. The second qualitative change occurs at an EOR credit of about 31 [\$/tonne CO<sub>2</sub>] in this example. Here, the NSPS designed facility is no longer the cheaper option as the revenue from carbon dioxide sales from the full capture amine based post combustion capture facility is making up for the extra capital and O&M costs. The rule of thumb has been that carbon dioxide usually can be sold for 2-3% of the price of crude oil per MCF. This equates to about \$35/tonne of CO<sub>2</sub> at a crude price of \$95/barrel. Oil markets in the beginning of 2015 would therefore not incentivize the construction of a full capture facility, however the crude prices of the preceding decade would have made the investment look more attractive.

## 11.2 Valuing Carbon Dioxide

The ultimate objective of carbon dioxide capture systems is to limit the emission of carbon dioxide to the atmosphere in order to slow the accumulation of greenhouse gases. There are a myriad of policies which have been proposed over the years to formulate a system for the reduction of carbon dioxide from stationary generation sources in the United States. One of the most prominent of these proposals has been the idea of applying a tax [\$/tonne CO<sub>2</sub>] to the emission of carbon dioxide. Another prominent idea which has been progressed concurrently is the notion of carbon dioxide not being emitted to the atmosphere having a value to society. The idea is that the social value should then be

the cost which society is willing to pay to have carbon dioxide emissions avoided. The social cost of carbon is estimated to be 37 [\$/tonne CO<sub>2</sub>] (85) by the United States government currently.

**Table 11-2. Air fired and carbon capture plants evaluated on their economic value under a potential carbon dioxide tax. All costs are reported in constant 2012 dollars.**

<b>Plant Type</b>	<b>PC Supercrit</b>	<b>Oxyfuel Supercrit</b>	<b>Amine Supercrit</b>	<b>Amine Supercrit</b>
<b>Coal Type</b>	PRB	PRB	PRB	PRB
<b>Capture Performance (Cap. %/Purity %)</b>	N/A	90/99.5	90/99.5	45.2/99.5
<b>Coal (tonnes/hr)</b>	249.8	310.4	361.9	303.6
<b>Gross Electrical Output (MWe)</b>	534.9	664.9	632.8	590.3
<b>Net Electrical Output (MWe)</b>	500	500	500	500
<b>Plant Efficiency (% HHV)</b>	37.14	29.89	25.64	30.56
<b>Annual Power Generation (BkWh/yr)</b>	3.287	3.287	3.287	3.287
<b>CO<sub>2</sub> Emissions (kg/kWh)</b>	0.882	0.101	0.128	0.589
<b>Revenue Required (\$/MWh)</b>	52.6	94.88	99.12	77.4
<b>Added Cost of CCS (\$/MWh)</b>	N/A	42.28	46.52	21.27
<b>Cost of CO<sub>2</sub> Avoided (\$/tonne)</b>	N/A	54.73	61.69	69.13
<b>Cost of CO<sub>2</sub> Captured (\$/tonne)</b>	N/A	37.73	35.87	37.03

To help visualize how these new plants would perform economically compared to one another, their levelized cost of electricity was plotted as a function of carbon dioxide tax. Also, the social cost of carbon dioxide that the United States government is currently using is plotted for comparison.

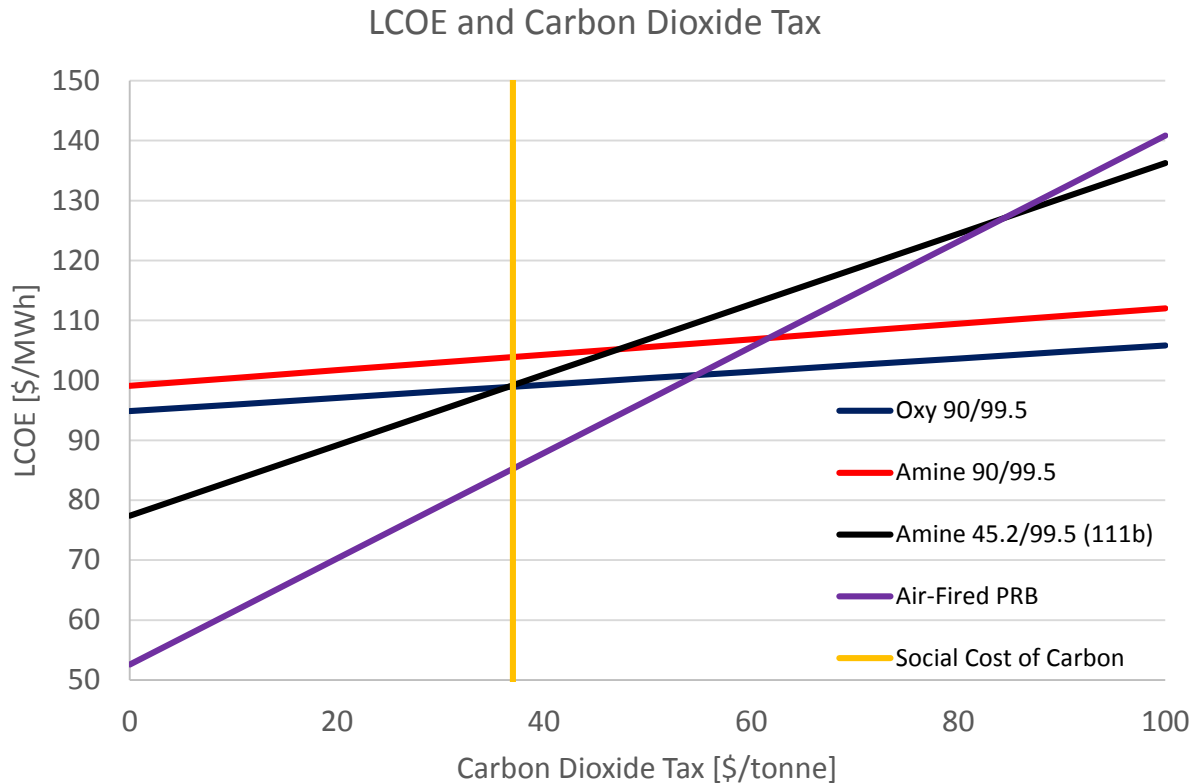


Figure 11.3. Levelized cost of electricity for the generation sources evaluated under a carbon dioxide tax. The U.S. social cost of carbon has also been plotted for comparison. All costs are reported in constant 2012 dollars.

The overall trend is that the tax on carbon dioxide causes the LCOE of all generation options to rise as the tax is increased. Those generators which have a higher carbon dioxide emission intensity, air-fired coal and the NSPS designed amine capture plant, are more severely affected by the increase in carbon dioxide tax rate. At a tax rate of 0 [\$/tonne CO<sub>2</sub>] the air-fired plant is about 25 [\$/MWh] cheaper than the NSPS facility, which is about 20 [\$/MWh] cheaper than the two full capture facilities.

In Figure 11.4, a zoomed in perspective on where the LCOE curves for each of the facilities intersect, the carbon dioxide tax rates where there is a qualitative change in the lowest cost system can be more clearly observed. At a tax of about 55 [\$/tonne CO<sub>2</sub>] the oxyfuel facility becomes the cheapest option, surpassing the air-fired facility which is incurring a heavy tax burden. The NSPS amine based facility remains the cheapest carbon capture option until a tax of about 35 [\$/tonne CO<sub>2</sub>] when the oxyfuel facility surpasses it. What is noteworthy about this crossing is that it is very close to (a bit below) the social cost of carbon dioxide that the United States government has calculated. The result suggests that if we truly valued carbon dioxide emissions at 37 \$/tonne CO<sub>2</sub>, we would require a higher removal efficiency for CO<sub>2</sub> capture (i.e., a lower emission rate from new power plants), and/or penalize a partial-capture facility such as the NSPS compliant amine based system. That would raise its overall cost to approximately that of a full-capture oxyfuel system, which would then be competitive as a compliance option—as might other advanced post-combustion options with 90% or more capture. At the present time, however, EPA’s proposed 111(b) standard does not incorporate the government’s estimated social cost of carbon and thus renders full-capture oxyfuel uncompetitive as a compliance option.

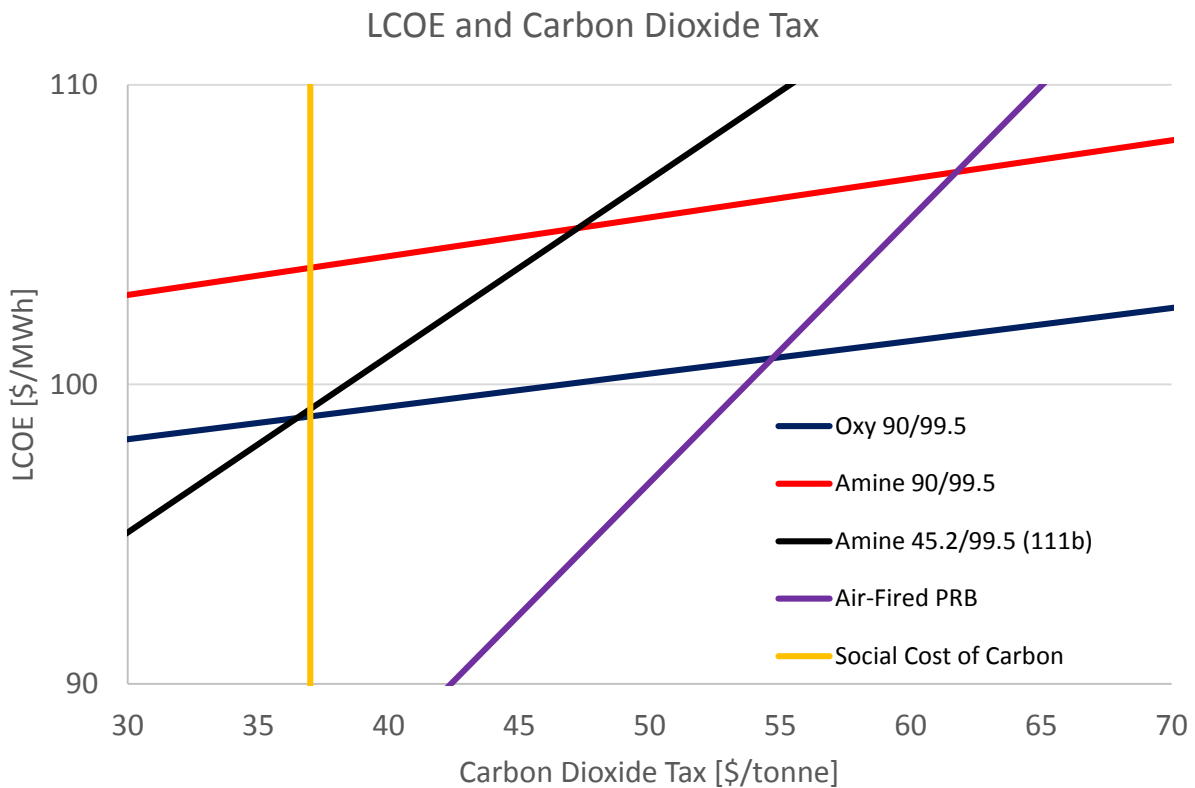


Figure 11.4. A zoomed in look at the levelized cost of electricity for the generation sources evaluated under a carbon dioxide tax. The U.S. social cost of carbon has also been plotted for comparison. All costs are reported in constant 2012 dollars.

There are a few other takeaways from Figure 11.3 which are worth noting. A carbon dioxide tax of at least 45-50 [\$ / tonne CO<sub>2</sub>] would be required to get a NSPS designed amine based capture plant to convert to full capture. Also, the social cost of carbon dioxide 37 [\$ / tonne CO<sub>2</sub>] is significantly lower than the lowest tax value (55 [\$ / tonne CO<sub>2</sub>]) which would be required to incent the use of carbon dioxide capture technologies absent the 111(b) NSPS becoming law.

Lastly, it should be noted that this, and the previous, sections have been based upon a series of case studies using Wyoming Powder River Basin sub-bituminous coal and the nominal plant assumptions for the IECM. The results presented here are unique to these assumptions and inferring general policy positions from this limited analysis should be kept solely to qualitative deductions. It is also worth noting that substantial uncertainty exists in the LCOE curves presented in Figures 11-1 to 11-4. Care should therefore be exercised in ascribing too much weight to the particular values reported for a particular carbon dioxide tax value where a qualitative plant decision occurs. The exercises presented have been shown to demonstrate the nature of the trade-offs involved with carbon dioxide capture and the effects which valuing carbon dioxide can have on the preferred facility to be built.

### 11.3 Low Carbon Capacity Standard

In the paper attached in Appendix A, a potential policy for encouraging the development of carbon capture in restructured electricity markets is presented. This policy, which we dubbed a Low Carbon Capacity Standard (LCCS), would seek to provide a more balanced supply of low carbon energy and capacity. We evaluated our proposed policy compared to the existing renewable portfolio standards which have been passed by 11 of the 13 PJM member states. The renewable generation sources (wind and solar) have a poor correlation to system load and consequently have low equivalent load carrying capability ratings, a measure of capacity reliability. For the comparison, we assumed that the amount of energy produced by low-carbon generation would be equivalent under either the renewable portfolio standards or LCCS.

The financial metric we used in our comparison is adopted from Brattle and is called Net Cost of New Entry (Net CONE). This metric is intended to calculate the cost of building new electricity generation; while taking into account the profits anticipated to be made in the energy market. Our results are presented as a function of the price which could be had for carbon dioxide sold for enhanced oil recovery (Fig. 11.5).

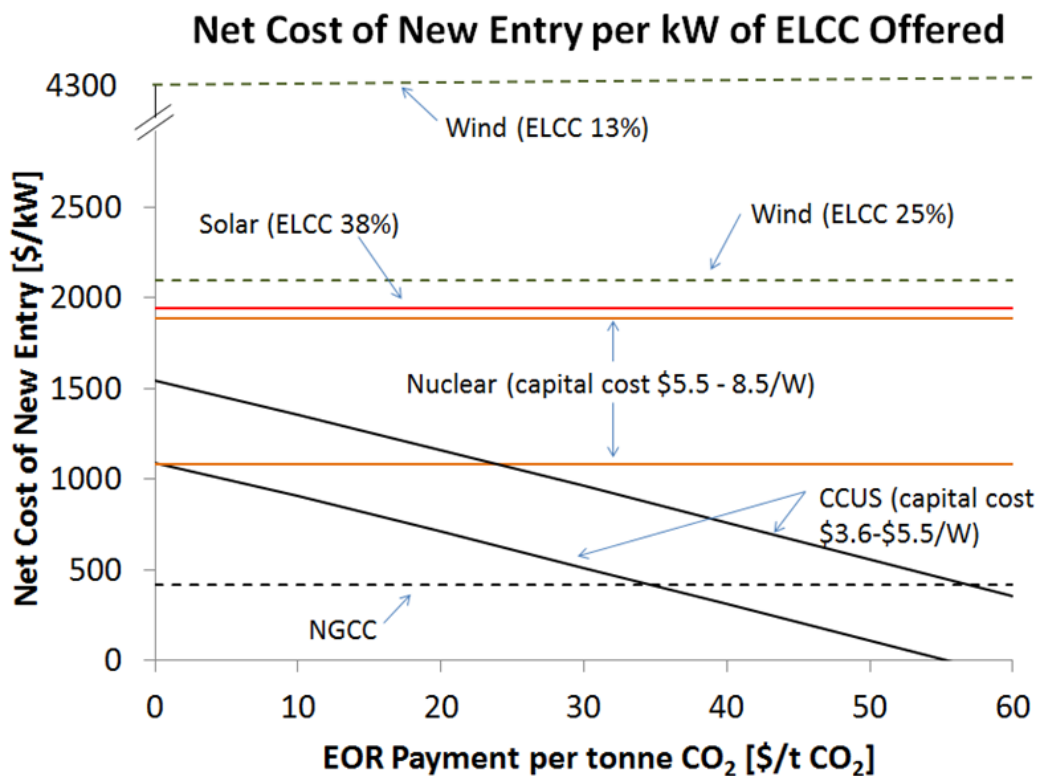


Figure 11.5. Summary of Net Cost of New Entry (Net CONE) calculations for electricity generation sources evaluated for the low carbon capacity standard (23).

Due to the poor match of renewable generation to system load, the low ELCC values for wind and solar result in Net CONE values of greater than 2000 \$/kW. These compare poorly to the Net CONE values for CCUS which ranged from about 1000-1500 \$/kW depending upon the assumed capital cost for

CCUS. The CCUS Net CONE values were more competitive than nuclear, especially if an EOR payment of greater than 20 [\$/tonne CO<sub>2</sub>] is guaranteed. Natural gas combine cycle (NGCC) units compare favorably to all other generators evaluated, but the carbon dioxide emissions associated with NGCC are significantly greater than the other generators. Evaluating the cost and carbon dioxide emission disparity between the individual generating options was beyond the scope of our analysis, but for additional information on these results, please consult Appendix A.

# Chapter 12 Summary and Conclusions

## 12.1 Thesis Summary

The work completed here is intended to be a starting point for those seeking to estimate the cost and performance of oxyfuel carbon dioxide capture for pulverized coal. The new models and design options that have been developed and implemented in the publicly-available Integrated Environmental Control Model (IECM) can help policy analysts, researchers, and technology to be better informed about the cost and performance of carbon capture systems.

Chapter 1 presented a brief introduction into electricity generation in the United States, established the connection between stationary emissions and climate change, and discussed the development of carbon capture technologies capable of reducing emissions from electricity generators. Chapter 1 also limited the scope of this thesis to the creation of a techno-economic model of oxyfuel carbon capture which would be implemented in the IECM and used to investigate the performance and economics of oxyfuel amongst other low-carbon electricity generation options.

Chapter 2 provided an evaluation of proposed oxyfuel system configurations, technological components, and established the operational similarities and differences between oxyfuel and traditional air-fired generators. Also covered was the rationale for designing or updating technical components for the oxyfuel performance and cost models.

Chapters 3 and 4 covered the design, possible configurations, and mass and energy balance algorithms which tie the technical components comprising an oxyfuel plant into a complete system. These two chapters also discussed the challenges and solutions involved in creating a recursive system in the traditionally once-through framework of the IECM.

Chapters 5, 6, and 7 covered modeling of the air separation unit (ASU), direct contact cooler/polishing scrubber (DCCPS), and carbon handling systems (CPU and CoCapture). These four new component models have been implemented in the IECM v9. They provide a level of flexibility and robustness of design which allows them to be utilized in various power plant and oxyfuel system configurations to estimate system performance and cost based on the most recently available public information.

Chapter 8 provided the economic modelling to accompany the technical performance models covered in Chapters 3-7. An outline of the costing methodology was provided to describe how key cost metrics such as total capital requirement, operating and maintenance costs, levelized cost of electricity, and carbon dioxide avoidance costs are calculated for the IECM oxyfuel model.

Chapter 9 then demonstrated applications of the completed PC oxyfuel model in the IECM. Component-level sensitivity studies were first performed to identify tradeoffs in cost and performance for parameters such as: steam cycle heat rate, air ingress, oxidant purity, gross plant size, etc. Important findings from sensitivity studies are as follows: default oxidant purity should be 97% [O<sub>2</sub> mol%] to maximize plant performance; DCCPS operating temperature should be kept near 50 [°C] to minimize the electrical load of the flue gas recirculation and purification system; the lowest flue gas recirculation rate which provides safe operating conditions should be utilized to improve system performance and reduce

gas handling costs; and finally that elevated air ingress rates (> 3%) have a substantial negative impact on the overall system performance.

The effects of altering coal composition within an oxyfuel recycle configuration were examined for the cool recycle system with a spray dry absorber. The oxyfuel model's ability to properly divide and recombine the flue gas to maintain moisture and sulfur levels was demonstrated. The dramatic disparity in volumetric flows for the primary and secondary recycle streams of North Dakota Lignite (70/30 split) and Appalachian Low Sulfur Bituminous (10/90) demonstrates the importance of properly configuring the recycle system to the fuel being fired.

The consequences of utilizing each of three different oxyfuel recycle configurations was then evaluated using Powder River Basin sub-bituminous for each configuration. A small but significant increase in net plant efficiency (6/10ths of a point) was observed between the cool recycle with WFGD to the warm recycle configuration. The more substantial gains were a result of equipment downsizing which produced a reduction in carbon dioxide avoidance cost of approximately 4 [\$/tonne CO<sub>2</sub>].

The last exercise of Chapter 9 also included an uncertainty analysis of the warm recycle configuration for both a CPU system producing a 99.5 [CO<sub>2</sub> mol%] carbon dioxide product while capturing 90% of flue gas carbon dioxide and a CoCapture system capturing 100% of the flue gas CO<sub>2</sub>. For the uncertainty parameters selected, the 95% Confidence Interval (CI) of levelized cost of electricity for the CPU system was found to be 86 to 150 [\$/MWh] and 92 to 157 [\$/MWh] for the CoCapture system. The carbon dioxide avoidance cost distribution for the CPU system had a 95% CI from 44 to 126 [\$/tonne CO<sub>2</sub>] and the CoCapture system had a 95% CI from 44 to 118 [\$/tonne CO<sub>2</sub>]. The shape of the CoCapture plant distribution further suggests that its expected avoidance costs would be slightly lower than with a CPU.

Chapter 10 showed results of an uncertainty analysis comparing a warm oxyfuel system with an amine-based post-combustion capture system, both producing a 99.5 [CO<sub>2</sub> mol%] carbon dioxide product while capturing 90% of flue gas carbon dioxide. The cumulative probability distribution function (PDF) of LCOE for oxyfuel had a 95% CI from 86 to 150 [\$/MWh] while the amine system 95% CI ranged from 90 to 153 [\$/MWh]. The oxyfuel distribution has a long tail towards higher costs, but the bulk of the distribution suggests that oxyfuel-based plant would have a LCOE slightly lower than amine-based capture plant. The results from the avoidance cost distributions were similar, with oxyfuel ranging from 44 to 126 [\$/tonne CO<sub>2</sub>] and amine from 50 to 133 [\$/tonne CO<sub>2</sub>]. Here again, there was a longer tail for the oxyfuel PDF, but most of the distribution suggested oxyfuel to have the advantage in avoidance cost.

The second half of the chapter compared oxyfuel to a selection of alternative low-carbon fossil fuel generators. Both the direct carbon intensity and 100 year GWP (CO<sub>2</sub>e) intensity were considered for the selected generators. The two warm oxyfuel plants considered compared favorably to amine capture for pulverized coal; the oxyfuel plants were strictly dominant with respect to emission intensity and LCOE. The inclusion of upstream emissions from consumables produced some interesting results regarding the performance of systems firing natural gas. Even with a fugitive emission rate of just 1.5%, the potency of methane as a greenhouse gas essentially eliminates any CO<sub>2</sub>e intensity advantage held by NGCC over Warm Oxyfuel with CPU. For a fugitive emission rate of about 2.5% the CO<sub>2</sub>e intensity of all the non-CoCapture carbon capture technologies fall within the same band of CO<sub>2</sub>e intensity of about 0.15 to 0.2 [kg CO<sub>2</sub>e/kWh]. The only capture technology which provides a uniquely low level of carbon

intensity is Warm Oxyfuel with CoCapture which was calculated as having a CO<sub>2</sub>e intensity of 0.11 [kg/kWh].

Chapter 11 presented three scenarios where oxyfuel and carbon capture are regulated by or are incented by policy. The first scenario explored the sale of captured carbon dioxide to oil companies for use in enhanced oil recovery. Findings from this exercise implicated that capture plants designed to specifically meet the EPA 111(b) standard would not be economically preferred to full capture facilities for CO<sub>2</sub> EOR prices greater than 35 [\$ /tonne CO<sub>2</sub>]. The second scenario established that a carbon tax of greater than 55 [\$ /tonne CO<sub>2</sub>] would be required to have oxyfuel supplant the air-fired coal plant as the lowest cost PRB coal option. Also shown in this scenario was the discordant nature of the U.S. Government's stated social cost of carbon with the EPA's current proposed new source performance standard. The last scenario summarized the findings from the proposed low carbon capacity standard (LCCS) in Appendix A. Under the assumptions examined, CCUS was determined to have the lowest Net CONE in PJM.

## 12.2 Future Research for Oxyfuel Systems

There are a number of ways in which the oxyfuel model described in this thesis could be improved. For example, increasing the accuracy with which the thermal benefits from heat integration and higher temperature recycle configurations are accounted. Also, the constraints used to determine the maximum allowable moisture fraction could be more precisely tuned to each coal to improve plant performance and decrease the iterations required for model convergence. Lastly, the economic cost models could be further refined for different options and configurations. The issue, however, is that all of these require data and information which is currently unavailable, given the current state of technology development. Thus, while there is certainly room for improvements in the oxyfuel model, further advancements in modeling are currently hampered by the lack of available data and information.

With respect to advancing the technology of oxyfuel more broadly, the analysis of oxyfuel with ideal gas separation described in Chapter 9 provides one important insight. The takeaway from that analysis is that since coal is very cheap, the goal of reducing fuel use through a research focus on efficiency improvements has only limited payoffs. Given that the performance advantage gained by ideal gas separation cannot reduce the LCOE by more than 10% from current levels, it is clear that marginal thermal efficiency gains will never provide the "step change" required to increase the economic viability of CCS systems. Thus, future technical research would be better directed predominately towards reducing the capital intensity of capture equipment and gas separation technologies.

The last suggestion for future research would be to focus efforts to reduce system costs through the process of "learning by doing" that historically accompanies the installation of new capacity. This would apply to gas-based power plants as well as the coal-based plants that are the main focus of this thesis. A large source of complexity and cost for oxyfuel systems is the presence of elements such as sulfur and mercury which need to be removed from the flue gas. Natural gas is distinct from coal in that it is a relatively clean fuel. It is free of ash and most other elemental compounds native to coals. This means that the emissions cleanup equipment for natural gas-fired power plants would be far less extensive, and expensive, than in coal-based power plants. The two major components of an oxyfuel system, an

air separation unit and a carbon dioxide purification unit, are large scale distillation-based processes which are relatively well developed but have yet to be built at commercial scale for electricity generation. Thus, if oxyfuel natural gas combustion combined cycle plants (OC3) were developed and provided an economic incentive, the experience and technological developments gained through capacity additions might also bring down the system costs for future pulverized coal installations which would rely on similar equipment.

## 12.3 Concluding Remarks

Uncertainty analysis, along with deterministic case studies, performed in this thesis indicate that a full-scale oxyfuel facility would be expected to have a levelized cost of electricity and carbon dioxide avoidance cost comparable to or slightly lower than that of a post-combustion amine-based capture system. It also has been demonstrated that oxyfuel capture plants can be designed to comply with the emission levels stipulated in EPA's proposed Rule for New Stationary Sources limiting CO<sub>2</sub> emission from new coal-fired power plants (8). This work has also shown that, of the current available technologies for carbon capture, oxyfuel plants with CoCapture have the unique ability to capture 100% of the direct carbon dioxide emissions. Applying this theoretical advantage in practice, however, would face major regulatory uncertainty. As of the time of writing, only two Class VI well permits for the injection of captured CO<sub>2</sub> has been issued in the United States and there exists no regulatory precedent for commercial injection of a mixed flue gas product with the CO<sub>2</sub> purity level (~85 [ CO<sub>2</sub> mol%]) produced by CoCapture systems.

It is the author's opinion that because of the uncertainty surrounding carbon dioxide products with low CO<sub>2</sub> purity, policies for the advancement of carbon capture should focus on technologies which produce saleable-quality CO<sub>2</sub>. This also opens a potential source of revenue through the sale of carbon dioxide for enhanced oil recovery. The EOR market would allow plant owners to partially recoup the cost of capture. In the policy piece in Appendix A, we posit a policy called a Low Carbon Capacity Standard (LCCS). Under this standard we found that when accounting for both the energy and capacity services supplied by coal plants with carbon capture, the net cost of new entry (Net CONE) for CCUS facilities was robustly lower than the competing low carbon generators. We also found that the inclusion of substantial (> 35 [\$ /tonne CO<sub>2</sub>]) EOR payments could reduce the Net CONE of CCUS facilities to below that of NGCC units. Perhaps then the best near term option to advance the development of carbon capture may be to see carbon dioxide not simply as a pollutant but also as a commodity able to reduce net costs in conjunction with enhanced oil recovery.

## REFERENCES

1. **IPCC Working Group III.** *Special Report on Carbon Dioxide Capture and Storage.* Cambridge : Cambridge University Press, 2005.
2. **International Energy Association.** *Energy Technology Perspectives.* Paris : www.iea.org, 2008.
3. **EIA.** *International Energy Outlook.* s.l. : DOE/EIA, 2011.
4. *Understanding the pitfalls of CCS cost estimates.* **Rubin, E. S.** 2012, International Journal of Greenhouse Gas Control, pp. 181-190.
5. *Carbon Capture and Storage: How Green Can Black Be?* **Haszeldine, S.R.** 2009, Science, Vol. 325, pp. 1647-1652.
6. **NETL/DOE.** *Cost and Performance Baseline for Fossil Energy Power Plants. Volume 1: Bituminous Coal and Natural Gas to Electricity.* s.l. : NETL/DOE, 2010.
7. **IECM Online.** [Online] 2012. <http://iecm-online.com>.
8. **EPA.** Standards of Performance for Greenhouse Gas Emissions for New Stationary Sources: Electric Utility Generating Units. *Federal Register.* s.l. : United States, June 18, 2014. Vol. 79 FR 34829, pp. 34829-34958.
9. **U.S. Environmental Protection Agency.** Carbon Pollution Emission Guidelines for Existing Stationary Sources: Electric Utility Generating Units. *Federal Register.* June 18, 2014. Vol. 79.
10. **EIA.** EIA Electricity Data. [Online] March 22, 2015. [http://www.eia.gov/electricity/monthly/epm\\_table\\_grapher.cfm?t=epmt\\_1\\_1](http://www.eia.gov/electricity/monthly/epm_table_grapher.cfm?t=epmt_1_1).
11. **Rocky Mountain Institute.** RMI. [Online] 2011. [http://www.rmi.org/rfgraph-us\\_capacity\\_electricity\\_generation\\_by\\_energy](http://www.rmi.org/rfgraph-us_capacity_electricity_generation_by_energy).
12. **EIA.** [Online] 2015. [Cited: March 22, 2015.] <http://www.eia.gov/dnav/ng/hist/n3045us3m.htm>.
13. —. Monthly Energy Review. [Online] March 2015. [Cited: March 22, 2015.] <http://www.eia.gov/totalenergy/data/monthly/index.cfm#environment>.
14. **U.S. Energy Information Administration.** *Annual Energy Outlook 2014 with projections to 2040.* s.l. : DOE/EIA, 2014.
15. **Linde.** [Online] [Cited: March 21, 2015.] <http://www.captureready.com/EN/Channels/OverViews/showDetail.asp?ClassID=1>.
16. **GCCSI.** GCCSI Project Database. [Online] March 2015. <http://www.globalccsinstitute.com/project/>.
17. **DOE/NETL.** *The United States Carbon Utilization and Storage Atlas IV.* s.l. : US Department of Energy, NETL, Office of Fossil Energy, 2012.

18. *How a "Low Carbon" Innovation can Fail - Tales from a "Lost Decade" for Carbon Capture, Transport, and Sequestration.* Von Hirschhausen, C. 2012, *Economics of Energy & Environmental Policy*, pp. 115-123.
19. *Stabilization Wedges: Solving the Climate Problem for the Next 50 Years with Current Technologies.* Pacala, S. and Socolow, R. s.l. : [www.sciencemag.org](http://www.sciencemag.org), August 13, 2004, *Science*, Vol. 305, pp. 968-972.
20. GCCSI. *Economic Assessment of Carbon Capture and Storage Technologies.* s.l. : GCCSI, 2011.
21. MIT. *The Future of Coal: Options for a Carbon-Constrained World.* s.l. : MIT, 2007.
22. *Use of experience curves to estimate to future cost of power plants with CO2 capture.* Rubin, Edward S., et al. s.l. : Elsevier, 2007, *International Journal of Greenhouse Gas Control*, Vol. 1, pp. 188-197.
23. *Could Low Carbon Capacity Standards be More Cost Effective at Reducing CO2 than Renewable Portfolio Standards?* Moore, Jared T., Borgert, Kyle J. and Apt, Jay. s.l. : Elsevier, 2014, *Energy Procedia*, Vol. 63, pp. 7459-7470.
24. Advanced Resources International, Inc. *U.S. Oil Production Potential From Accelerated Deployment of Carbon Capture and Storage.* Arlington, VA : ARI, 2010.
25. EIA. EIA. [Online] March 2015. [Cited: March 22, 2015.] [http://www.eia.gov/dnav/pet/pet\\_pri\\_spt\\_s1\\_d.htm](http://www.eia.gov/dnav/pet/pet_pri_spt_s1_d.htm).
26. Babcock & Wilcox Power Generation Group. *Engineering and Economic Evaluation of Oxy-Fired 1100F (593C) Ultra-Supercritical Pulverized Coal Power Plant with CO2 Capture.* Palo Alto : EPRI, 2011. 1021782.
27. Doosan Babcock. *Demonstration of an Oxyfuel Combustion System.* 2011.
28. Rao, Anand B., Rubin, Edward S. and Berkenpas, Michael B. *Oxygen-based Combustion Systems (Oxyfuels) with Carbon Capture and Storage (CCS).* 2007.
29. IEA-GHG. *2010/07 Oxyfuel Combustion of Pulverized Coal .* s.l. : ieaghg, 20120.
30. *Emission control of nitrogen osides in the oxy-fuel process.* Normann, F, et al. 5, October 2009, *Progress in Energy and Combustion Science*, Vol. 35, pp. 385-397.
31. *NO emission during oxy-fuel combustion of lignite.* Andersson, K, et al. 6, March 19, 2008, *Industrial & Engineering Chemisty Research*, Vol. 47, pp. 1835-1845.
32. *Current status of ceramic-based membranes for oxygen separation from air.* Hashim, S.M., Mohamed, A.R. and Sudhash, B. 160, s.l. : Elsevier, 2010, *Advances in Colloid and Interface Science*, pp. 88-100.
33. *Assessment of carbon capture thermodynamic limitation on coal-fired power plant efficiency.* Moullec, Yann Le. 2012, *International Journal of Greenhouse Gas Control* 7, pp. 192-201.

34. *Oxygen Supply for Oxycoal CO<sub>2</sub> Capture*. Higginbotham, Paul, et al. 2011, Energy Procedia 4, pp. 884-891.
35. *Air Separation and Flue gas purification units for oxycoal combustion systems*. Darde, A, et al. 2009, Energy Procedia 1, pp. 527-534.
36. *Exergy analysis of two cryogenic air separation processes*. Van der Ham, L.V. and Kjelstrup, S. 35, 2010, Energy, pp. 4731-4739.
37. DOE/NETL. *Cost and Performance for Low-Rank Pulverized Coal Oxycombustion Energy Plants*. 2010.
38. IEAGHG. *Water Usage and Loss Analysis of Bituminous Coal Fired Power Plants with CO<sub>2</sub> Capture, 2010/05*. 2011.
39. *Integrated assessment of iGCC power generation technology with carbon capture and storage (CCS)*. Cormos, Calin-Cristian. s.l. : Elsevier, 2012, Energy.
40. *Natural gas combined cycle power plant modified into an O<sub>2</sub>/CO<sub>2</sub> cycle for CO<sub>2</sub> capture*. Amann, J.-M, Kanniche, M. and Bouallou, C. 2009, Energy Conversion and Management 50, pp. 510-521.
41. *Hybrid coal-fired power plants with CO<sub>2</sub> capture: A technical and economic evaluation based on computational simulations*. Huang, Y., et al. 2012, Fuel 101, pp. 244-253.
42. *Integration of Evaporative Gas Turbine with Oxy-fuel Combustion for Carbon Dioxide Capture*. Hu, Y., Li, H. and Yan, J. 2010, International Journal of Green Energy 7, pp. 615-631.
43. Department for Business Enterprise & Regulatory Reform. *Future CO<sub>2</sub> Capture Technology Options for the Canadian Market Report No. COAL R309 BERR/Pub URN 07/1251*. 2007. p. 219.
44. Berkenpas, Michael and al., et. *Integrated Environmental Control Model Technical Documentation*. s.l. : DOE, 1999.
45. *Purification of Oxyfuel Derived CO<sub>2</sub> for Sequestration or EOR*. White, V. USA : s.n., 2007. 2nd Workshop of the International Oxy-Combustion Research Network.
46. *Proceedings of the 8th International Conference on Greenhouse Gas Control Technologies*. Allam, V.W. Norway : s.n., 2006.
47. Allam. *Purification of Carbon Dioxide*. 7416716 B2 United States, August 26, 2008.
48. White. *Purification of Carbon Dioxide*. 2008/0176174 A1 United States, July 24, 2008.
49. —. *Purification of Carbon Dioxide*. 2008/0173584 A1 United States, July 24, 2008.
50. —. *Purification of Carbon Dioxide*. 2008/0173585 A1 United States, July 24, 2008.
51. *Sour compression process for the removal of SO<sub>x</sub> and NO<sub>x</sub> for oxyfuel-derived CO<sub>2</sub>*. Torrente Murciano, Laura, Petrocelli, Francis and Chadwick, David. 2011, Energy Procedia 4, pp. 908-916.
52. Fogash, K.B. *Flue Gas Purification Utilizing SO<sub>x</sub>/NO<sub>x</sub> Reactions During Compression of CO<sub>2</sub> Derived from Oxyfuel Combustion*. Allentown, PA : Air Products and Chemicals, 2010.

53. IEAGHG. *Rotating machinery for CO2 compression in CCS systems 2011/07*. 2011.
54. Hailong, Li. *Thermodynamic Properties of CO2 Mixtures and Their Applications in Advanced Power Cycles with CO2 Capture Processes*. Stockholm, Sweden : Royal Institute of Technology, 2008.
55. IEA GHG. *Corrosion and Materials Selection in CCS Systems*. 2010.
56. *Impacts of Non-condensable Components on CO2 Compression/Purification, Pipeline Transport and Geologic Storage*. Vatenfall. Cottbus, Germany : s.n., 2009. 1st IEA Oxyfuel Combustion Conference.
57. *2011/04 Effects of Impurities on Geological Storage of CO2*. IEA GHG. 2011.
58. U.S. Environmental Protection Agency. Federal Requirements Under the Underground Injection Control (UIC) Program for Carbon Dioxide Geological Sequestration Wells. *Federal Register*. 2010. Vol. 75, 237.
59. Marsh, K.N. *Recommended Reference Materials for the Realization of Physicochemical Properties*. Oxford : Blackwell, 1987.
60. Shah, Minish M. *Oxy-Fuel Combustion for CO2 Capture from PC Boilers*.
61. NETL. *Cost and Performance Baseline for Fossil Energy Plants, Volume 1: Bituminous Coal and Natural Gas to Electricity*. s.l. : U.S. Department of Energy, 2013.
62. EPRI. *Technical Assessment Guide - Power Generation and Storage Technology Options*. s.l. : EPRI, 2009.
63. Chemical Engineering Magazine. *Chemical Engineering*. [Online] March 2015. <http://www.chemengonline.com/pci-home>.
64. al., Rubin et. *Modeling of Integrated Environmental Control Systems for Coal-Fired Power Plants*. 1991.
65. Rubin, Edward S, Berkenpas, Michael B. and Frey, H. Christopher. *Integrated Environmental Control Model Technical Documentation*. 1999.
66. al., Rubin et. *IECM Technical Documentation Update*. 2009.
67. NETL/DOE. *Process Equipment Cost Estimation*. Pittsburgh : DOE/NETL, 2002.
68. IEA GHG. *Rotating machinery for CO2 compression in CCS systems*. 2011. p. 321.
69. Alstom, et al. *Engineering feasibility and economics of CO2 capture on an existing coal-fired power plant*. 2001. Final report prepared by ALSTOM Power Inc., ABB Lummus Global Inc., ALSTOM Power Environmental Systems and American Electric Power (AEP).
70. Black & Veatch. *Wisconsin Public Service: Weston Unit 4 Flue Gas Desulfurization*. 2004. pp. 3-4.
71. Rao, Anand B, Rubin, Edward S and Berkenpas, Michael B. *Amine-Based CO2 Capture and Storage Systems for Fossil Fuel Power Plant*. 2004.

72. Rao, Anand B, Berkenpas, Michael B and Rubin, Edward S. *Technical Documentation: Oxygen-base Combustion Systems (Oxyfuels) with Carbon Capture and Storage (CCS)*. 2007.
73. *Assessment of carbon capture thermodynamic limitation on coal-powered plant efficiency*. Le Moulec, Yann. s.l. : Elsevier, 2012, International Journal of Greenhouse Gas Control, Vol. 7, pp. 192-201.
74. *The Cost of CCS for Natural Gas-Fired Power Plants*. Rubin, E.S and Zhai, H. Pittsburgh, PA : s.n., 2011. 10th Annual Conference on Carbon Capture and Storage.
75. GCCSI prepared by Worley Parsons and Schlumberger. *Economic assessment of carbon capture and storage technologies: 2011 update*. Global CCS Institute. Canberra, Australia : GCCSI, 2011.
76. Versteeg, Peter L. *Advanced Amine and Ammonia Systems for Greenhouse Gas Control at Fossil Fuel Power Plants*. 2012.
77. *Comparative Life-Cycle Air Emissions of Coal, Domestic Natural Gas, LNG, and SNG for Electricity Generation*. Jaramillo, P., Griffin, W.M. and Matthews, H.S. November 17, 2007, Environmental Science & Technology, Vol. 41, pp. 6290-6296.
78. *Methane and greenhouse-gas footprint of natural gas from shale formations*. Howarth, R.W., Santoro, R. and Ingraffea, A. March 13, 2011, Climatic Change.
79. *Life cycle GHG assessment of fossil fuel power plants with carbon capture and storage*. Odeh, N.A. and Cockerill, T.T. 2008, Energy Policy, pp. 367-380.
80. *Comparison of Liquid Amine and Solid Sorbent Carbon Dioxide Capture Systems for New, Supercritical Coal-Fired Power Plants: A Life Cycle Assessment*. Glier, Justin C. and Versteeg, Peter. Tacoma, Washington : s.n., 2012. LCA XII.
81. *Emissions reduction potential from CO<sub>2</sub> capture: A life-cycle assessment of Brazilian col-fired power plant*. Castelo Branco, David A., et al. 2013, Energy Policy, Vol. 61, pp. 1221-1235.
82. *A Tier 3 method to estimate fugitive gas emissions from surface coal mining*. Saghafi, Abouna. 2012, International Journal of Coal Geology, Vol. 100, pp. 14-25.
83. Irving, William and Tailakov, Oleg. *IPCC Guidelines for National Greenhouse Gas Inventories CH<sub>4</sub> Emissions: Coal Mining and Handling*. s.l. : IPCC, 2006.
84. *An Improved Inventory of Methan Emissions from Coal Mining in the United States*. Kirchgessner, David A., Piccot, Stephen D. and Masemore, S. 2000, Journal of the Air & Waste Management Association, pp. 1904-1919.
85. *5th Assessment Report - Anthropogenic and Natural Radiative Forcing*. IPCC. 2013.
86. U.S. Office of Management and Budget. Whitehouse.gov. [Online] [Cited: April 22, 2015.] <https://www.whitehouse.gov/blog/2013/11/01/refining-estimates-social-cost-carbon>.
87. *Impurity impacts on the purification process in oxy-fuel combustion based CO<sub>2</sub> capture and storage system*. Li, H., Yan, J. and Anheden, M. 86, 2009, Applied Energy, pp. 202-213.

**88. Marsh, K.N. *Recommended Reference Materials for the Realization of Physicochemical Properties.* Oxford : Blackwell, 1987.**

**89. *Why Conventional Tools for Policy Analysis are Often Inadequate for Problems of Global Change.* Morgan, M.G., et al. 1999, *Climatic Change*, Vol. 41, pp. 271-281.**





Available online at [www.sciencedirect.com](http://www.sciencedirect.com)

**ScienceDirect**

Energy Procedia 63 (2014) 7459 – 7470

Energy  
**Procedia**

GHGT-12

# Could Low Carbon Capacity Standards be More Cost Effective at Reducing CO<sub>2</sub> than Renewable Portfolio Standards?

Jared Moore<sup>a,b</sup>, Kyle Borgert<sup>b,c,\*</sup>, and Jay Apt<sup>a,b,d</sup>

*a Carnegie Mellon Electricity Industry Center, Carnegie Mellon University, 5000 Forbes Ave, Pittsburgh, PA, USA*

*b Department of Engineering and Public Policy, Carnegie Mellon University*

*c National Energy Technology Laboratory-Regional University Alliance (NETL-RUA)*

*d Tepper School of Business, Carnegie Mellon University*

## Abstract

We examine the implications of lowering electricity sector CO<sub>2</sub> emissions in PJM through a Low Carbon Capacity Standard (LCCS) instead of a renewables portfolio standard (RPS). An LCCS would create a requirement for load-serving entities to procure new low carbon capacity (GW). The LCCS would provide a greater balance of energy and capacity supply than a renewable portfolio standard, which requires only the supply of energy (and excludes non-renewable low carbon generators). Approximately 25 GW of PJM generation capacity is scheduled to retire by 2019 and the RPSs currently in place in PJM will supply only 5 GW of Equivalent Load Carrying Capability (ELCC). An LCCS, providing the same amount of low carbon energy, would supply 13 to 16 GW of ELCC. We estimate the required reduction of capacity prices required to cover the investment cost premium low carbon capacity would require from consumers. For example, if the energy from an LCCS costs on average \$20/MWh more than energy from an RPS, the annual premium would be approximately \$2.2 B. In order for consumers to be better off with an LCCS in this example, capacity prices would have to decrease by \$40/MW-day. We find that if an LCCS were adopted, coal fired power plants with carbon capture, utilization, and sequestration (CCUS) would likely have the lowest cost per MW of capacity of all low carbon technologies, based on net Cost of New Entry (CONE) estimates.

© 2014 The Authors. Published by Elsevier Ltd. This is an open access article under the CC BY-NC-ND license (<http://creativecommons.org/licenses/by-nc-nd/3.0/>).

Peer-review under responsibility of the Organizing Committee of GHGT-12

**Keywords:** cost effectiveness, renewable portfolio standards, restructured markets, capacity markets, carbon capture utilization and sequestration

\* Corresponding author. Tel.: 269-251-7663.

E-mail address: [kborgert@andrew.cmu.edu](mailto:kborgert@andrew.cmu.edu)

## 1. Introduction

The U.S. Environmental Protection Agency (EPA) has begun a rulemaking process to regulate greenhouse gas emissions from existing power plants through Section 111(d) of the Clean Air Act [1]. The proposed rule would establish EPA approved State Implementation Plans (SIPS) as the default mechanism for achieving federally mandated emission reductions in the electricity sector. For many states, a renewable portfolio standard could be used as the primary policy mechanism to achieve a substantial portion of reductions in the SIP. Here, we examine the implications of lowering CO<sub>2</sub> emissions from the electricity sector in the PJM regional transmission organization area with a Low Carbon Capacity Standard (LCCS) instead of an RPS.

### Nomenclature

CCUS	Carbon Dioxide Capture, Utilization, and Sequestration
CONE	Cost of New Entry
ELCC	Equivalent Load Carrying Capability
EOR	Enhanced Oil Recovery
EPA	Environmental Protection Agency
LCCS	Low Carbon Capacity Standard
LSE	Load Serving Entities
PJM	Pennsylvania-New Jersey-Maryland Interconnection
RPS	Renewable Portfolio Standard
SIPS	State Implementation Plans

Twenty nine of the United States have an RPS; 11 out of 13 PJM member states have one<sup>1</sup> [2]. In a restructured utility market such as PJM, an RPS serves as a requirement levied on the load-serving entities (LSEs) to annually procure a specified quantity of energy (GWh) derived from sources defined as renewable. We propose, and here evaluate in PJM, a requirement on load-serving entities to procure new low carbon capacity (GW). The LCCS would seek to provide greater balance of energy and capacity supply than an RPS, which requires only the supply of energy.

In most areas where wholesale markets exist in the United States, market clearing prices in energy markets are currently low due to low natural gas prices and demand which is below pre-recession levels. Stakeholders maintain that these low prices do not provide enough revenue to stimulate new capacity [3]. The addition of renewables tends to reduce wholesale energy prices [4], further discouraging new capacity investments. By capacity, we mean the capacity available at times of peak load, as computed by the metric equivalent load carrying capability (ELCC) [5]. Renewables are inherently variable, and the capacity they supply is generally a significantly smaller fraction of their nameplate capacity than for thermal plants. In PJM, the ELCC of wind is 13% [6] [7]; out of 100 MW of nameplate capacity, wind would qualify for only 13 MW of capacity. Electricity markets require a balanced supply of both services, energy and capacity, to meet demand with an acceptable loss of load probability (LOLP) [8].

In 2007, PJM introduced a capacity market known as the “Reliability Pricing Model” to drive investment in new capacity [9]. To date, prices have been moderate (~\$85/MW-day) and sufficient capacity has been supplied to the region. In 2013, the average total wholesale cost of energy in PJM was \$54/MWh [10]. The energy portion of this cost was \$39/MWh (73%) and the capacity portion was \$7/MWh (13%) [10].

Although the capacity market has been successful in meeting many of its stated objectives [9], it has been volatile; ranging from a price of \$16/MW-day to a price of \$174/MW-day [11]. The supply curve in the capacity market is quite steep, increasing by as much as \$300/MW-day over the last 10 GW offered [9]. Therefore, even a modest change in supply may cause large changes in capacity prices. For example, in the most recent PJM annual capacity auction, capacity prices doubled from \$60/MW-day to \$120/MW-day even as demand for supply decreased

<sup>1</sup>Of these 11, Ohio recently put a “freeze” on its RPS [40].

by 2 GW [11]. The price increase was “driven by supply-side effects” as imports and demand side management decreased 4.5 GW [11].

Prices in PJM’s capacity market could rise significantly if more power plants retire or demand increases. New environmental regulations [12], post-Fukushima nuclear safety regulations [13], and low energy prices are accelerating coal and nuclear retirements [14] [15]. PJM estimates that 25 GW of coal capacity will retire between 2011 and 2019 with an additional 15 GW of capacity at risk of retirement [14]. Exelon has already suggested that they will be forced to close nuclear generators if energy and capacity prices remain low [16].

We examine the implications of lowering electricity sector CO<sub>2</sub> emissions in PJM through an LCCS. We quantify the energy and capacity produced by RPS requirements enacted by states within PJM and contrast against the energy and capacity produced by an LCCS. We gauge the required suppression of capacity prices necessary to cover the investment cost premium low carbon capacity would require from consumers. We also examine the competitiveness (on a per MW basis) of capacity offered for solar, wind, nuclear, natural gas, and coal with carbon capture, utilization, and sequestration (CCUS).

We find that if CCUS was on average \$20/MWh more expensive than wind on a levelized cost of electricity (LCOE) basis, an LCCS would be more cost effective for consumers if it lowered capacity market prices by just \$40/MW-day.

## 2. Methods

### 2.1. *Quantity of Capacity Needed, Supplied by Standards*

The collective RPS’s in PJM states require 14% of generation to be supplied by renewable resources by 2026 [17]. To meet this collective RPS, approximately 105,000 GWh of renewable electricity per year are required [17]. If the renewable portfolio is filled exclusively with wind, it would require 40 GW of nameplate wind capacity assuming a capacity factor of 30% [14]. With an ELCC rating of 13%, this would generate approximately 5 GW of ELCC.

This 5 GW of ELCC created by the RPS is likely to be less than the capacity of units that are expected to be retired this decade. Between 2011 and 2019, 25 GW of capacity is scheduled to be retired in PJM, with an additional 15 GW of capacity at risk of retirement<sup>2</sup> [14]. Capacity could be further shortened if the modest growth in demand, 1% per year through 2030 [18], is realized.

Ideally, demand side management (DSM) would supply the shortfall. However, it appears likely that DSM supply in PJM may have reached a plateau. Offers peaked at 21 GW in 2015/2016 auction and dropped to 16 GW in the 2016/2017 auction and then to 13 GW in the most recent (2017/2018) auction [11].

In theory, PJM’s capacity market is the financial mechanism that should procure the generators needed to satisfy the shortfall. However, for the capacity market to procure significant amounts of new build capacity, prices must rise substantially. PJM estimates that the gross Cost of New Entry (CONE) for a combined cycle<sup>3</sup> gas fired power plants is \$390/MW-day [19]. When profits from energy and ancillary service markets are taken into account, PJM estimates the net CONE to be \$335/MW-day<sup>4</sup> [20]. Net CONE is the net cost of capacity given the energy and ancillary service market value of the power plant. Essentially, capacity prices would have to increase to \$335/MW-day to incent new (gas) power plants. Historically, capacity prices have averaged ~\$85/MW-day [11].

<sup>2</sup> The average capacity-weighted forced outage rate (FOR) of steam power plants in PJM is 10% [13]. The ELCC of the coal plants scheduled for retirement or at risk of retirement would be 22.5 GW, and 13.5 GW, respectively.

<sup>3</sup> Brattle’s CONE estimates show that combined cycle units’ capital costs are now only slightly more expensive than simple cycle turbines. Because of the small difference in capital costs and the revealed preference of developers to build combined cycle units [10], we focus this research on NGCC’s as the default option for new generators.

<sup>4</sup> Energy and Ancillary Services (E&AS) estimates are based on the performance of generators for the three previous years. For the 2017/2018 auction, the years of 2011 through 2013 were used to estimate E&AS revenue [13].

If capacity prices increase from ~\$85/MW-day to \$335/MW-day to incent new capacity, the costs to consumers will increase by approximately \$15B. This would amount to an increase of \$20 per MWh delivered in the PJM region, or about a 40% increase in the total wholesale cost per MWh delivered.

## 2.2. Quantifying the Costs and Required Capacity Benefits of an LCCS

If generators that ran at a constant output (nuclear for example), were exclusively used to fulfill the RPS, approximately 13 GW of capacity would be supplied in addition to 105,000 GWh of carbon free electricity per year (assumed capacity factor of 90%). However, coal fired power plants with CCUS theoretically have the ability to temporarily boost output by shutting down the sequestration process [21]. This would boost peak electrical output by approximately 25% [22]. If the RPS was filled exclusively with CCUS plants, then the capacity delivered could be as high as 16 GW<sup>5</sup>.

Estimating how this capacity supply would affect capacity markets is not straightforward. Capacity market models do not exhibit a high degree of accuracy because the market is so volatile. Instead of modeling the market, we estimate how much prices in capacity markets must decrease in order to make up for the premium paid for low carbon capacity. In Table 1 below, we show an example for quantifying the premium paid for low carbon capacity.

Table 1: Example for Costs and Capacity Supplied by RPS and LCCS

	RPS	LCCS
LCOE [\$/MWh]	100	120
Energy Supplied [GWh]	105,000	105,000
Cost for Energy [2012 USD]	\$ 10.5 B	\$ 12.6 B
ELCC Supplied [GW]	5	13 - 16

Note: We assume the cost of wind is \$100/MWh including variability and transmission costs. We assumed a cost of \$120/MWh for the cost of the new low carbon source. The ELCC supplied from the low carbon source varies because of the ability of CCUS plants to temporarily pause the sequestration process and boost output. ELCC supply of the RPS was calculated assuming a 13% ELCC.

Using the assumptions in Table 1, the LCCS would cost approximately \$2.1 B more but supply approximately 8 to 11 more GW of capacity than an RPS. Figure 1 below shows the supply and demand curves for the 2014/2015 auction year. To save consumers the \$2.2 B from our example in Figure 1, the extra capacity supply would have to drive down capacity prices by \$40/MW-day (assume 165 GW of capacity demand).

<sup>5</sup> Coal plants with post-combustion capture typically are designed to capture 90% of the emissions from the plant. In this research we neglect these emissions noting that the variability of wind power plants decreases the amount of carbon emissions off-set as well [41][42][43].

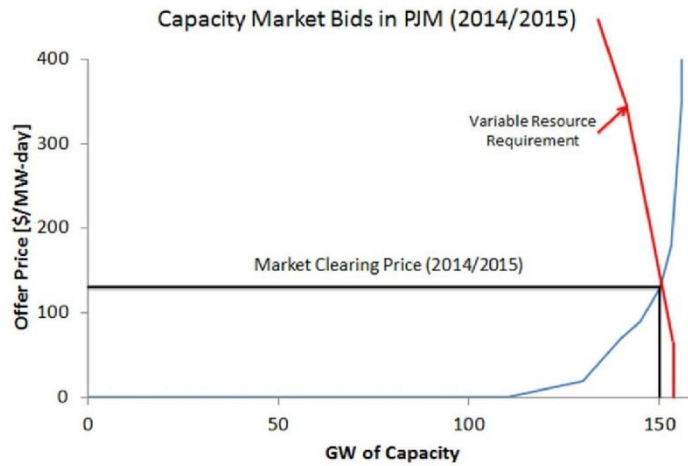


Figure 1. Supply and demand of capacity in the 2014/2015 PJM capacity auction. The Variable Resource Requirement is the downward sloping demand curve constructed by B. Hobbs [23]. The VRR is designed to reduce the volatility of capacity markets.

The costs in Table 1 above are just an example. As described well in the literature, the LCOE of renewables is dependent on the values of the analyst [24]. This is particularly true for nuclear, where LCOE is largely a function of capital cost, years needed for construction, and the discount rate assumed [25]. CCUS costs are uncertain because the first large scale plants are just now under construction [26].

Because the LCOE of low carbon energy is uncertain, we present our results as a function of the difference between and LCCS and RPS. For example, if energy from the low carbon capacity source is \$20/MWh more expensive than energy from wind, how much would capacity prices have to decrease in order for technology agnostic, cost minimizing consumers to be indifferent between the two policy scenarios?

In Figure 2 below, we show how much capacity prices must decrease in order to make up for the premium paid for low carbon capacity. We assume that the cost seen by consumers for either renewables or low carbon capacity would be equivalent to the LCOE. Table 1 above is an example of these quantifications.

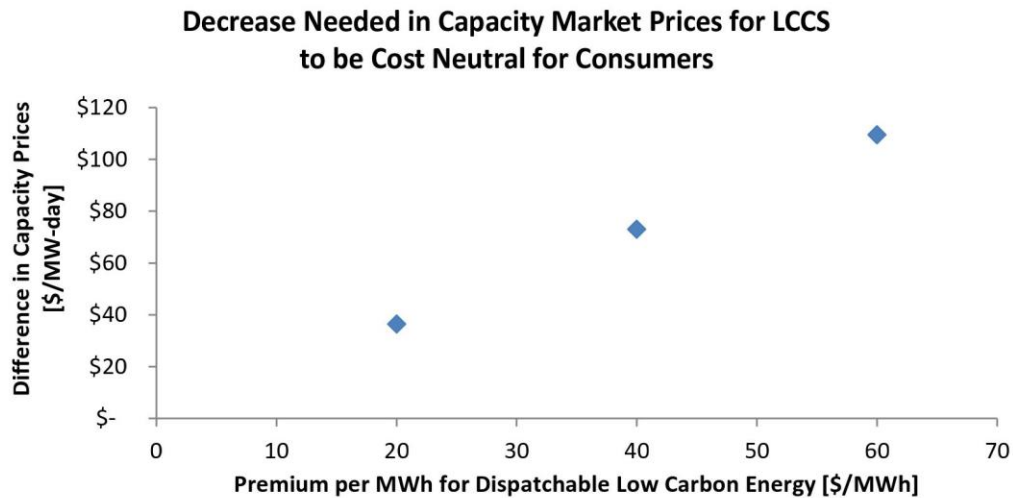


Figure 2: Savings in capacity prices that must be realized in order for consumer costs to be unaffected. An LCCS that provides the same amount of energy as the RPSs required in PJM would decrease capacity prices by supplying  $\geq 10$  GW more capacity than an RPS.

### 2.3. Ensuring that Low Carbon Energy is Supplied in Addition to Capacity with an LCCS

When comparing the costs of policies, we assumed that the cost of energy to consumers of both renewable energy and dispatchable energy would be equal to the LCOE. Furthermore, we assumed that power plants would be dispatched according to their technological capability (i.e. dispatchable plants would achieve a capacity factor of  $\sim 90\%$ ). In this section, we describe how low carbon capacity might be procured with an LCCS and the implied risks for the energy generated.

Typically with an RPS in restructured markets, renewable energy is procured through renewable energy certificates (REC) [27]. The REC market fosters competition to encourage the development of the lowest cost renewable energy possible. The sum of the revenue received by developers through energy markets, subsidies, and REC's should be approximately equal to the levelized cost of the energy, in the absence of a market failure.

The market mechanism we examine to directly procure capacity for an LCCS would be a new low carbon capacity market. This market would directly procure a fixed amount of low carbon capacity very much like the capacity market currently in place in PJM except that it would be limited to new low carbon generators. This market mechanism utilizes market forces to procure the lowest cost capacity given a generator's value in energy markets.

However, an issue for this market structure that directly pays only for capacity is that additional policies are needed to ensure that the LCCS plant dispatches before carbon emitting power plants. We assume in this research a gas price of  $\$6/\text{MMBTU}$ , and the relatively low marginal energy costs of the low carbon generators would assure that the generator would dispatch. However, the marginal costs of CCUS plants may be higher than some existing carbon emitting power plants because the sequestration process is inherently energy intensive. If gas prices are low ( $\sim \$4/\text{MMBTU}$ ) and EOR revenue is not available, we estimate that the CCUS plant would be dispatched rarely and have a capacity factor of only 35%.

A number of policies could be used to ensure that LCCS power plants dispatch and supply low carbon energy generation regardless of market conditions. For example, some system operators consider wind power "must run" unless the wind power needs to be curtailed for grid stability reasons [28]. Also, wind plants receive energy subsidies, such as the federal production tax credit. This effectively ensures that wind energy is dispatched, even when energy market clearing prices are (slightly) negative [28].

One potential policy mechanism for ensuring LCCS plants are dispatched is the use of contracts for differences (CfD). A contract of this sort redirects some of the financial risk for the plant owner/operator onto the state which agrees to monetarily “fill in” any disparity in the wholesale price for electricity and the marginal cost of energy supply. When the converse is true and the marginal cost of energy supply is below the market clearing price, the owner/operator is obligated to pay the difference to the state. The major benefit of this arrangement is that the plant will always be dispatched and the state bears the risk to ensure low carbon energy is supplied. The risk to the state is relatively small because the marginal costs of a CCUS plant are only slightly higher than carbon emitting power plants. We find that a small EOR payment or subsidy (\$10/MWh) would place CCUS plants ahead in the dispatch stack of carbon emitting power plants.

Because several mechanisms can be used to reduce the relatively small risk that LCCS plants do not dispatch, we assumed plants dispatched according to their technical capability. Furthermore, we assumed that the cost of the LCCS energy could be approximated by the LCOE. The revenue received by LCCS generators from energy market revenues, necessary energy subsidies, and capacity payments would be approximately equal to the LCOE of the energy supplied by the LCCS.

#### 2.4. Quantifying the Competitiveness of Low Carbon Capacity Options – Net Cost of New Entry (Net CONE)

Per current practice in PJM’s capacity market, the metric we will use to evaluate the economic competitiveness of a low carbon power plant’s capacity is net Cost of New Entry (net CONE) [20]. We assume that capacity would be procured through an auction where low carbon generators bid their net CONE (defined below). The net CONE is quantified by fixed costs (PJM refers to these as “avoidable costs” [14]) less profits made in energy markets [14]. We estimate the net CONE on a per MW basis using the equation below.

$$CapBid = NetCONE \left[ \frac{\$}{MW_{ELCC}} \right] = \frac{\text{Present Value (Owner's Fixed Costs - Energy Market Profits)}}{\text{Present Value}(MW_{ELCC})} \quad (1)$$

Owners fixed costs are a sum of construction, accrued interest, and fixed O&M. Energy market profits are a function of revenue made in energy service markets less marginal costs (variable O&M and fuel costs). We do not take into account ancillary service market revenue. We estimate costs using the financial assumptions from Brattle for PJM’s official Cost of New Entry (CONE) estimates: 8% after tax weighted average cost of capital, 20 year MACRS depreciation schedule, a federal tax rate of 35%, and a state tax rate of 10% [19].

To estimate how generators would profit in energy markets, we used an hourly economic dispatch model of the generators in PJM. Marginal power plant costs (fuel and variable O&M) and carbon intensities for each region were obtained from Ventyx Velocity Suite. The dispatch model calculates marginal costs for all generators, then dispatches the least expensive generators to meet load. The dispatch model does not take into account transmission, thermal, and security constraints.

Because we are examining a plausible near future, we removed 18 GW of coal capacity from the dispatch stack. To decide which generators to remove, we relied on the PJM 40/400 rule for the power plants most at risk of retirement (over 40 years old and small than 400 MW) [12]. More information on the dispatch model for PJM is given in the previous chapter.

#### 2.5. Assumptions for New Power Plants

Table 2 below shows our assumptions for estimating the owner’s fixed costs and profits made in energy markets. The assumptions are based on the most recent data available from literature cited in the table below. Like all economic analyses, the preferences of the analyst can lead to a wide range of results [24]. Our goal is to quantify (to first order) the net cost of capacity given the market value of the energy contribution for competing technologies.

The assumptions have a mix of point estimates and a range estimates. We varied the parameter(s) which had the greatest effect on their cost per MW of capacity offered. The price of natural gas alone can dominate energy profit estimates because it sets market clearing prices in energy markets. However, we did not vary the price of gas because higher or lower market clearing prices would help or hurt all of the technologies studied. We assumed the price of natural gas was fixed at \$6/MMBTU, the EIA estimate for 2020 [29]. Of course, natural gas plants would be greatly affected by variation in natural gas prices. However, we do not show results sensitive to natural gas because it is known that gas plants have the lowest cost of new entry. We show NGCC plants here for reference.

For renewables, a wide range of ELCC can be assumed. In some regions with low penetration, the ELCC of wind can be approximated by its capacity factor [5]. However, wind does not correlate well with load in the USA, and wind in PJM had an ELCC rating of 13%. We assumed a fixed cost for the capital costs of renewables because the ELCC rating has the most pronounced effect.

For CCUS, there are multiple uncertain assumptions. Capital costs are currently unknown because the first large scale plants are now under construction [26]. Our assumptions are based on estimates from the literature [30], but these are for  $n^{\text{th}}$  of a kind plants. Early examples of new pollutant control technologies tend to increase in cost after the first of a kind [31] before asymptotically approaching the  $n^{\text{th}}$  of a kind cost. Given the uncertain price of oil, it is also unknown how much revenue should be assumed for enhanced oil recovery. A rule of thumb is that the price of each MCF of CO<sub>2</sub> is around 2-3% of the price of a barrel of oil [32] which equates to ~\$35/tonne at \$95/barrel. We assume a range from \$0 to \$60/t CO<sub>2</sub>. We discuss the overall net emissions from CCUS after we present the results for net CONE.

Table 2: Assumptions used for (\$2012 USD)

	NGCC [20]	Wind [33]	Solar PV [34]	Nuclear [25]	Coal with CCUS [35] [36]
Capital Costs \$/kW <sub>Nameplate</sub>	1,200	1,940	3,000	5,500 – 8,500	3,600-5,500
Fixed Maintenance Costs (\$/kW-year)	17	25	17	60	100
Fuel Costs (\$/MWh)	40	0	0	7	27
Total Marginal Costs (\$/MWh)	43	0	0	7	-25 - 30*
Financial Lifetime of Plant (Years)	20	20	20	30	30
Construction Time (Years)	3	2	2	7	4
ELCC*	.95	0.13 – .25	0.38	.975	.9 – 1.1
Energy Market Profits (\$/kW-year)	\$15	\$108	\$82	\$245	\$67 - \$500*

Notes: \*Marginal costs and energy market profits from CCUS plants vary with EOR payments. Without EOR revenue, marginal cost of CCUS would be approximately \$30/MWh. We varied EOR payments from 0 to \$60/tCO<sub>2</sub>, which would allow CCUS plants to have a marginal cost as low as -\$25/MWh. This would substantially increase energy market profits as shown in the table. ELCC estimates were estimated.

Below in Figure 3, we show the net CONE of various low carbon technologies according to the assumptions from Table 2.

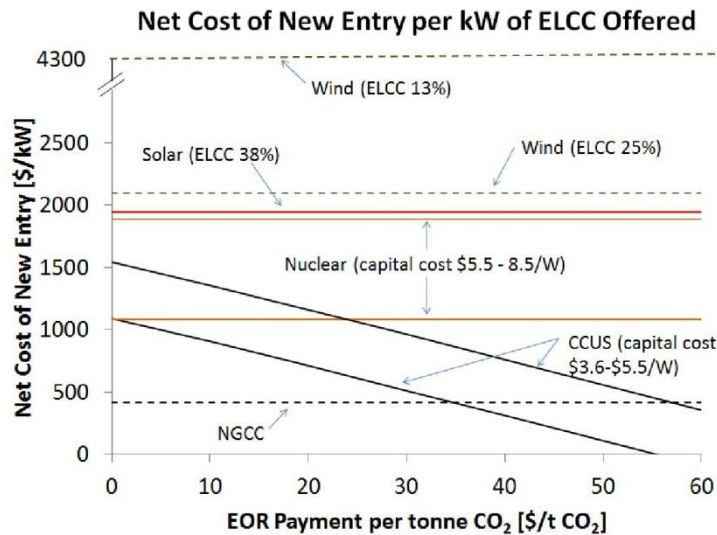


Figure 3: Net CONE of various low carbon technologies as a function of EOR revenue.

Figure 3 shows that CCUS is likely to be the most competitive technology given our assumptions. Costs of renewables are dominated by the assumed ELCC. It should be noted that ELCC of wind and solar diminishes with increasing penetrations [37].

### 2.6. Note on Emissions from Coal Plants with CCUS

In the analysis above, we assumed an LCCS could achieve the same emissions reductions as an RPS because eligible plants would generate substantial amounts low carbon electricity. An issue for CCUS as a carbon mitigation strategy is that CO<sub>2</sub>-flood EOR may have greater net emissions than other low carbon power plants because it increases the overall oil supply [38]. Here, we do not account for the emissions produced by combusting the oil because we are exploring this policy as a means to meet EPA mandated emission reductions for the power sector, comparing an RPS to an LCCS. Section 111(d) regulates power plant emissions, and we assume that emissions reductions from the transportation sector are achieved through other regulations, such as Corporate Average Fuel Economy (CAFE) standards. Current U.S. policy of emissions accounting is not based on where carbon is supplied but where it is combusted [39]. Therefore, we assumed that CCUS is an eligible technology to help fulfill SIPS even though its impact on overall emissions is unclear.

### 3. Discussion

We examined the implications of lowering the CO<sub>2</sub> emissions in PJM with a Low Carbon Capacity Standard (LCCS) instead of an RPS. An LCCS requires LSE's to procure a certain amount of low carbon capacity as a means to ensure that both capacity and low carbon energy is supplied. We examined this policy as an alternative to an RPS that does not supply capacity that is commensurate with the amount of energy supplied.

We quantified the amount of capacity supplied by the RPSs in PJM and showed that capacity could become undersupplied before 2020. 25 GW of capacity are scheduled to retire by 2019 and we estimated that the RPS will supply only 5 GW of capacity. An RPS would not necessarily cause an increase in capacity prices to net CONE, but it would increase the likelihood of capacity market clearing price increases by way of undercutting profits in energy markets while supplying little capacity. If new generators are needed to supply capacity, capacity market prices will

likely rise from current prices, ~\$85/MW-day, to PJM's projection of net CONE, \$335/MW-day. We estimate that raising capacity prices to this level would cost consumers \$15 B annually and raise the wholesale cost of electricity in PJM by 40%.

An LCCS would lower dependence on capacity markets by requiring LSE's to procure capacity through "self-supply" [14]. However, energy from CCUS and nuclear plants is at present higher cost than from wind generators. We quantified the cost differences between the policies, by estimating the LCOE. If the energy from an LCCS costs on average \$20/MWh more than energy from an RPS, then the annual premium would be approximately \$2.2 B. In order for consumers to be better off with an LCCS in this example, capacity prices would have to decrease by \$40/MW-day. The LCCS could reduce capacity prices by supplying at least ~10 GW more capacity than an RPS. Given the steepness of the supply curve for capacity, it is reasonably likely that 10 GW of capacity would lower capacity prices an appreciable amount. The supply curve for capacity in PJM typically increases by over \$300/MW-day over the last 10 GW of capacity offered [9].

We then showed that if an LCCS were enacted, CCUS plants would likely have the lowest cost per MW of capacity based on net CONE estimates, if the revenue from EOR exceeds \$30-45/ton of CO<sub>2</sub>. Despite uncertainty in EOR revenue, our analysis shows CCUS to be strictly dominant compared to solar and wind on both a gross and net CONE basis across the range of capital cost and EOR revenue assumptions. Net CONE estimates for CCUS were lower than for nuclear in all but those scenarios with high CCUS capital expense and low EOR revenues, and were cost-competitive with NGCC under the most favorable (\$3600/kW and EOR credit >\$35/t) scenarios examined.

The ability to switch off carbon capture for purposes of temporarily increasing capacity is a topic which requires further analysis to properly evaluate cost effectiveness. However, our first order analysis indicates that this ability reduces net CONE by roughly \$300-400/MW-day for CCUS facilities. We also acknowledge that there are complex market dynamics of implementing a LCCS over an RPS, or vice versa, which are beyond the scope of our analysis.

Our purpose has been to highlight the potential system costs (energy and capacity) of implementing an LCCS instead of an RPS in the PJM market. We have shown that net CONE (a metric that includes the value of capacity) is more useful in evaluating the all-in system costs of policies than LCOE. We have noted throughout this work that the assumptions and values of the analyst can heavily influence the outcome of any cost estimate. However, this work suggests that, at a minimum, the costs of supplying adequate capacity to ensure acceptable loss of load should be accounted when analyzing alternative emission reduction scenarios and that the use of more comprehensive metrics such as net CONE should be preferred where data are available.

### **Acknowledgements**

This work was supported in part by grants from the Doris Duke Charitable Foundation, the R.K. Mellon Foundation, EPRI, and the Heinz Endowments to the RenewElec program at Carnegie Mellon University, and the U.S. National Science Foundation under Award no. SES-0949710 to the Climate and Energy Decision Making Center. The balance of support for this work was provided by the National Energy Technology Laboratory's Regional University Alliance (NETL-RUA), collaborative initiative with technical efforts performed under contract number 24905.913.ER.1041723.

### **Disclaimer**

This project was funded by the Department of Energy, National Energy Technology Laboratory, an agency of the United States Government, through a support contract with URS Energy & Construction, Inc. Neither the United States Government nor any agency thereof, nor any of their employees, nor URS Energy & Construction, Inc., nor any of their employees, makes any warranty, expressed or implied, or assumes any legal liability or responsibility for the accuracy, completeness, or usefulness of any information, apparatus, product, or process disclosed, or represents that its use would not infringe privately owned rights. Reference herein to any specific commercial product, process, or service by trade name, trademark, manufacturer, or otherwise, does not necessarily constitute or imply its endorsement, recommendation, or favoring by the United States Government or any agency thereof. The views and opinions of authors expressed herein do not necessarily state or reflect those of the United States Government or any agency thereof.

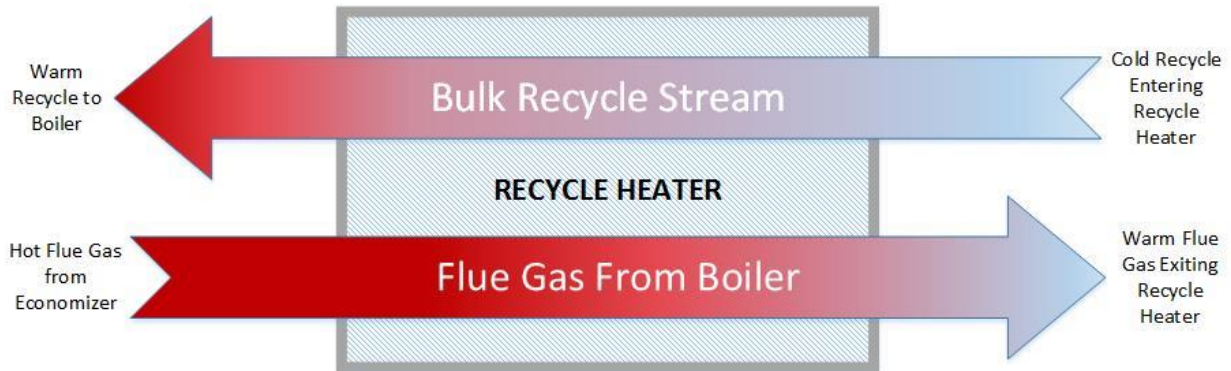
## References

- [1] The White House. Presidential Memorandum -- Power Sector Carbon Pollution Standards. [Online]. <http://www.whitehouse.gov/the-press-office/2013/06/25/presidential-memorandum-power-sector-carbon-pollution-standards>
- [2] PJM. Renewable Energy in PJM. [Online]. <http://www.pjm.com/about-pjm/learning-center/renewable-resources/renewable-energy-in-pjm.aspx?faq=%7BCD4EAC51-2867-47D7-9B32-0C563056EBAD%7D>
- [3] Michael Hogan, Jan Raczka, Frederick Weston, and Edith Bayer, "Market Mechanisms for Resource Adequacy and System Security: Framing the Issues," 2014.
- [4] Cliff Chen, Ryan Wiser, and Mark Bolinger, "Weighing the Costs and Benefits fo State Renewable Portfolio Standards: A Comparative Analysis of State Level Policy Impact Projections," Lawrence Berkeley National Laboratory, LBNL-61580, 2007.
- [5] Kevin Porter and Michael Milligan, "The Capacity Value of Wind in the United States: Methods and Implementation," *The Electricity Journal*, vol. 19, no. 2, pp. 1040-6190, 2006.
- [6] GE Energy, "PJM Renewable Integration Study," 2012.
- [7] PJM System Planning Department, "PJM Manual 21," 2014. [Online]. <http://www.pjm.com/~media/documents/manuals/m21.ashx>
- [8] North American Electric Reliability Corporation, "Methods to Model and Calculate Capacity Contributions of Variable Generation for Resource Adequacy Planning," 116-390, 2011.
- [9] Johannes Pfeifenberger, Newell, Spees, Hajos, and Madjarov, "Second Performance Assessment of PJM's Reliability Pricing Model," 2011.
- [10] PJM. (2014, February) Executive Report. [Online]. <http://www.pjm.com/~media/committees-groups/committees/mc/20140227/20140227-item-06-markets-report.ashx>
- [11] PJM, "2017/2018 RPM Base Residual Auction Results," 794597 , 2013. [Online]. <http://www.pjm.com/~media/markets-ops/rpm/rpm-auction-info/2017-2018-base-residual-auction-report.ashx>
- [12] PJM Interconnection, "Coal Capacity at Risk for Retirement in PJM;," 2011.
- [13] Nancy Thompson. (2014, April) U.S. response to the nuclear accident at Fukushima Daiichi. [Online]. [http://www.eia.gov/forecasts/AEO/nuclear\\_fuk.cfm](http://www.eia.gov/forecasts/AEO/nuclear_fuk.cfm)
- [14] Monitoring Analytics, LLC, "2013 State of the Market Report for PJM," 2014.
- [15] Julie Johnsson. ( 2013, May) Exelon Falls Most in Three Years on PJM Auction Results. [Online]. <http://www.bloomberg.com/news/2013-05-28/exelon-falls-most-in-three-years-on-pjm-auction-results.html>
- [16] Steve Daniels. (2014, May) Chicago Business.com. [Online]. <http://www.chicagobusiness.com/article/20140301/ISSUE01/303019987/exelon-warns-state-it-may-close-3-nukes#>
- [17] Gene Hinkle, "PJM Renewable Integration Study," 2014.
- [18] PJM. (2014) PJM Load Forecast Report. [Online]. <http://www.pjm.com/~media/documents/reports/2014-load-forecast-report.ashx>
- [19] Johannes Pfeifenberger, Samuel Newell, Kathleen Spees, Ann Murray, and Ioanna Karkatsouli, "Third Triennial Review of PJM's Variable Resource Requirement Curve," 2014.
- [20] Samuel Newell, J. Michael Hagerty, Kathleen Spees, Johannes Pfeifenberger, and Quincy Liao, "Cost of New Entry Estimates for Combustion Turbine and Combined Cycle Plants in PJM," 2014.
- [21] David Luke Oates, Peter Versteeg, Eric Hittinger, and Paulina Jaramillo, "Profitability of CCS with flur gas bypass and solvent storage," *International Journal of Greenhouse Gas Control*, vol. 27, pp. 279-288, 2014.
- [22] Stuart M. Cohen, Gary T. Rochelle, and Michael E. Webber, "Optimal operation of flexible post-combustion CO2 capture in response to volatile electricity prices," *Energy Procedia*, vol. 4, pp. 2604-2611, 2011.
- [23] Ben Hobbs, "A Dynamic Analysis of a Demand Curve-Based Capacity Market Proposal: The PJM Reliability Pricing Model," *IEEE Transactions on Power Systems*, vol. 22, no. 1, pp. 0885-8950, 2007.
- [24] Severin Borenstein, "The Private and Public Economics of Renewable Electricity Generation," EI @ Haas WP 221R, 2011.
- [25] LAZARD, "Levelized Cost of Electricity Analysis Version 7.0," 2013.
- [26] MIT. Carbon Capture and Sequestration Project Database. [Online]. <http://sequestration.mit.edu/tools/projects/>
- [27] U.S. DOE: Energy Efficiency and Renewable Energy. (2014) Renewable Energy Certificates (RECs). [Online]. <http://apps3.eere.energy.gov/greenpower/markets/certificates.shtml?page=0>
- [28] Mark Andor, Kai Flinkerbusch, Matthias Janssen, Bjorn Liebau, and Magnus Wobben, "Rethinking Feed-in Tariffs and Priority Dispatch for Renewables," Foundation for Reserach on Market Design and Energy Trading, 2010. [Online]. <http://www.hks.harvard.edu/hepg/Papers/2010/Rethinking%20feed-in%20tariffs.pdf>

- [29] EIA. (2013, May) ANNUAL ENERGY OUTLOOK 2013. [Online]. [http://www.eia.gov/forecasts/aeo/MT\\_electric.cfm](http://www.eia.gov/forecasts/aeo/MT_electric.cfm)
- [30] International Energy Agency, "Cost and Performance of Carbon Dioxide Capture from Power Generation," 2011.
- [31] Edward S. Rubin and et al., "The Effect of Government Actions on Environmental Technology Innovation: Applications to the Integrated Assessment of Carbon Sequestration Technologies," 2004.
- [32] Klaas van't Veld and Owen R. Phillips, "Pegging Input Prices to Output Prices in Long-Term Contracts: CO2 Purchase Agreements in Enhanced Oil Recovery," Department of Economics & Finance, University of Wyoming, 2009.
- [33] Department of Energy: Energy Efficiency and Renewable Energy, "2012 Wind Technologies Market Report," 2013.
- [34] Galen Barbose, Naim Darghouth, Samantha Weaver, and Ryan Wiser, "An Historical Summary of the Installed Price of Photovoltaics in the United States from 1998 to 2012," LBNL-5919E, 2013. [Online]. <http://emp.lbl.gov/sites/all/files/LBNL-5919e-REPORT.pdf>
- [35] International Energy Agency, "Cost and Performance of Carbon Dioxide Capture from Power Generation," OECD/IEA, 2011.
- [36] NETL, "Cost and Performance Baseline for Fossil Energy Plants Volume 1: Bituminous Coal and Natural Gas to Electricity," DOE, DOE/NETL-2010/1397, 2013.
- [37] M Milligan and K Porter, "Determining the Capacity Value of Wind: An Updated Survey of Methods and Implementation," NREL/CP-500-43433, 2008.
- [38] Paulina Jaramillo, Michael W. Griffin, and Sean T. McCoy, "Life Cycle Inventory of CO2 in an Enhance Oil Recovery System," *Environmental Science and Technology*, vol. 43, no. 21, pp. 8027-8032, 2009.
- [39] Peter Erickson and Michael Lazarus, "Accounting for Greenhouse Gas Emissions Associated with the Supply of Fossil Fuels," 2013. [Online]. <http://www.sei-international.org/publications?pid=2419>
- [40] ECOWatch, Ohio Becomes First State to Roll Back Renewable Energy Mandate. [Online]. <http://ecowatch.com/2014/05/28/ohio-renewable-energy-mandate/>
- [41] Warren Katzenstein and Jay Apt, "Air Emissions Due to Wind and Solar Power," *Environmental Science and Technology*, vol. 43, no. 2, pp. 253-258, 2009.
- [42] L. Valentino, V Valenzuela, A. Botterud, Z. Zhou, and G Conzelmann, "System wide emissions implications of increased wind power penetration," *Environmental Science and Technology*, vol. 46, no. 7, pp. 4200-4206, 2012.
- [43] D.L. Oates and P. Jaramillo, "Production cost and air emissions impacts of coal cycling in power systems with large-scale wind penetration," *Environmental Research Letters*, vol. 8, 2013.

## Appendix B Recycle Preheating and Energy Balance

There are currently no case studies available which provide enough detail on the operation of the recycle preheater to accurately benchmark the performance of a model for the recycle preheater. However, when this information does become available the strategy presented in this section will be a robust method for providing another degree of control for users of the IECM. The performance of the recycle preheater can most simplistically be modeled as a counter-flow heat exchanger with the hot flue gas from the boiler interacting with the comparatively cold bulk recycle stream.



The inputs and outputs in the above diagram correspond to variables either already calculated or specified in the IECM. The Cold Recycle Entering Recycle Heater is defined by the bulk recycle gas calculated in the prior section. The Hot Flue Gas from Economizer is defined by the “Gas Temperature Exiting the Economizer (120, 370, 650°C)” parameter and the Warm Flue Gas Exiting Recycle Heater is defined by “Gas Temperature Exiting the Recycle Heater (66, 150, 260°C)” (formerly Air Preheater) in the IECM. For the purposes of the remainder of this section however, shorthand designations will be used to identify the four states. The hot stream will be denoted the Flue Gas (FG) streams and the cool stream will be denoted as the Recycle (Recycle) stream. Each stream is then parsed into the incoming (in) stream and the outgoing (out) stream.

The general heat exchange relation used in this model is the change in specific enthalpy equation and the corresponding calculation for specific heat capacity [kJ/mol] which is one of the Shomate Relations.

$$\Delta h_i = c_{p,i}(T) * \Delta T$$

$$c_{p,i} = A + B * t + C * t^2 + D * t^3 + E/t^2$$

Where

$A - E$  are the Shomate Relation constants for the pure species being evaluated

$t$  is the temperature of the pure species [K/1000]

$T$  is the temperature of the pure species [K]

In an adiabatic heat exchanger the heat transfer between the two gas streams can be defined as:

$$\begin{aligned} \varphi_{Recycle} * [(c_{p,Recycle\_out} * T_{Recycle\_out}) - (c_{p,Recycle\_in} * T_{Recycle\_in})] \\ = \varphi_{FG} * [(c_{p,FG\_in} * T_{FG\_in}) - (c_{p,FG\_out} * T_{FG\_out})] \end{aligned}$$

For such a large heat exchanger, truly adiabatic conditions are unlikely. In order to keep as much user control as possible for the model, a heat exchanger effectiveness ( $\epsilon_Q$ ) was created for adjusting the effectiveness of the heat exchanger. The relation for calculating the unknown temperature of the recycle gas entering the boiler is then:

$$\begin{aligned} c_{p,Recycle\_out} * T_{Recycle\_out} \\ = (c_{p,Recycle\_in} * T_{Recycle\_in}) \\ + \frac{\epsilon_Q * \{\varphi_{FG} * [(c_{p,FG\_in} * T_{FG\_in}) - (c_{p,FG\_out} * T_{FG\_out})]\}}{\varphi_{Recycle}} \end{aligned}$$

The specific heat capacity of the recycle stream exiting the heat exchanger has been left on the same side of relation as the exiting recycle temperature because both quantities are a function of the exit temperature and thus must be solved for concurrently and iteratively.

#### Example

Continuing from the example calculations performed in the previous section we have the following recycle gas entering the recycle heater:

Recycle In:  $x_{O_2} = 0.252$ ,  $x_{Ar} = 0.027$ ,  $x_{N_2} = 0.055$ ,  $x_{CO_2} = 0.456$ ,  $x_{H_2O} = 0.211$ ,  $T = 365K$  (102°C)

$$c_{p,Recycle\_in} * T_{Recycle\_in} = \sum_{i=1}^k x_i (h_i^{365K} - h_i^{298K}) = 2.657 \left[ \frac{kJ}{mol} \right]$$

Using an example flue gas composition from the IECM and default temperatures for the entrance and exit of the recycle heater we have:

Flue Gas In:  $x_{O_2} = 0.012$ ,  $x_{Ar} = 0.035$ ,  $x_{N_2} = 0.05$ ,  $x_{CO_2} = 0.692$ ,  $x_{H_2O} = 0.211$ ,  $T = 643K$  (370°C)

$$c_{p,FG\_in} * T_{FG\_in} = \sum_{i=1}^k x_i (h_i^{643K} - h_i^{298K}) = 13.803 \left[ \frac{kJ}{mol} \right]$$

Flue Gas Out:  $x_{O_2} = 0.012$ ,  $x_{Ar} = 0.035$ ,  $x_{N_2} = 0.05$ ,  $x_{CO_2} = 0.692$ ,  $x_{H_2O} = 0.211$ ,  $T = 423K$  (150°C)

$$c_{p,FG\_out} * T_{FG\_out} = \sum_{i=1}^k x_i (h_i^{423K} - h_i^{298K}) = 4.655 \left[ \frac{kJ}{mol} \right]$$

If we then let  $\epsilon_Q = 0.95$  and assume  $\frac{\varphi_{FG}}{\varphi_{Recycle}} = 1.5$  (corresponds to a recycle fraction of 66%) the heat exchanger relation can now be reduced to the following:

$$c_{p,Recycle\_out} * T_{Recycle\_out} = 2.657 + 0.95 * \{1.5 * [(13.803) - (4.655)]\} = 15.693 \left[ \frac{kJ}{mol} \right]$$

There is a problem here unfortunately. When the recycle stream temperature leaving the heat exchanger is calculated, a temperature of 713K is found. This is physically impossible because the maximum temperature of the recycle stream can be no higher than the temperature of the hot flue gas entering the recycle heater (643K). A few rare circumstances from our example assumptions led to a situation where an unrealistic temperature is calculated. Specifically a relatively low recycle fraction of 2/3 and a high feed temperature for the recycle stream entering the recycle heater. Because it is possible to create feed conditions which result in a violation of physics given our simplified heat exchange methodology, it is necessary to establish a temperature limit constraint for the recycle temperature exiting the recycle heater.

$$T_{Recycle\_out} \leq T_{FG\_in}$$

When, as in the case of our example, an impossibly high temperature is calculated for the exiting recycle stream the temperature should instead be set to the temperature of the entering flue gas.

Applying this constraint to our example yields the following state for the exiting recycle stream:

Recycle Out:  $x_{O_2} = 0.252$ ,  $x_{Ar} = 0.027$ ,  $x_{N_2} = 0.055$ ,  $x_{CO_2} = 0.456$ ,  $x_{H_2O} = 0.211$ ,  $T = 643K$  (370°C)

$$c_{p,Recycle\_out} * T_{Recycle\_out} = \sum_{i=1}^k x_i (h_i^{643} - h_i^{298K}) = 12.830 \left[ \frac{kJ}{mol} \right]$$

## Appendix C Matlab Code for Carbon Processing Unit

```
%Automated Carbon Purification Unit for finding the ideal separation work
%required to purify a tonne of carbon dioxide
%
%User must provide the following (all before line 79):

%Temperature [K] and Pressure [Pa] for: dead state, initial stream into CPU,
CO2
%Product stream, and the Inert Gas stream

%Molar Fractions [decimal form] for the initial stream into the CPU

%Desired Carbon Dioxide Product Purity (CPP) [decimal form] and Carbon
Dioxide Recovery Rate (CRR) [decimal form].
%Note: CRR must be less than CPP!!!

%
%
%

%State desired Carbon Dioxide Capture Rate (CRR) and CO2 Product Purity
%(CPP) as decimal

CPP = .95
CRR = .9

%Universal gas constant
Ru = 8.314*1000; %J/kmol/K (Necessary for Cantera)

%Standard enthalpy of vaporization for water [J/kmol]
enthalpy_H2Ovap = 40680000;

%Molar mass of pure elements (grams/mol)

molmass_Ar = 40;
molmass_O2 = 32;
molmass_CO2 = 44;
molmass_N2 = 28;
molmass_H2O = 18;

%State Environmental (dead state) Conditions

To = 298.15;
Po = oneatm;

%State mole fractions of assumed atmosphere and also relative humidity

Xo_Ar = 0.0093;
Xo_CO2 = 0.0004;
Xo_H2O = 0.0064;
```

```

Xo_N2 = 0.7758;
Xo_O2 = 0.2081;

rel_humidity = 0.7; %enter as fraction, not percent

%Calculate Environmental (dead state) Exergies assuming pure components

phichemo_Ar = Ru*To*log(Xo_Ar);
phichemo_CO2 = Ru*To*log(Xo_CO2);
phichemo_N2 = Ru*To*log(Xo_N2);
phichemo_O2 = Ru*To*log(Xo_O2);

phichemo_H2O = Ru*To*log(rel_humidity);

%State CPU Inlet Conditions

Ti = 330;
Pi = 90000;

%State CPU CO2 Product (Outlet 1) Conditions

T1 = 298;
P1 = 103000;

%State CPU Inerts (Outlet 2) Conditions

T2 = 298;
P2 = 103000;

%State CPU Water (Outlet 3) Conditions

T3 = 330;
P3 = oneatm;

%State mole fractions of Inlet Stream

Xi_Ar = 0.07;
Xi_CO2 = 0.68;
Xi_H2O = 0.07;
Xi_N2 = 0.12;
Xi_O2 = 0.06;

%Calculate molar mass of Inlet Stream

molmass_inlet = Xi_Ar * molmass_Ar + Xi_CO2 * molmass_CO2 + Xi_H2O *
molmass_H2O + Xi_O2 * molmass_O2 + Xi_N2 * molmass_N2;

%
%Calculations to determine the concentrations of the inert and product
%streams (all calcs based on 1 mol entry into system)
%

%Calculate required minimum product CO2 mass

```

```

CO2_mass_initial = Xi_CO2 * molmass_CO2;
CO2_mass_product_req = CO2_mass_initial * CRR;

%Use regression equations for CO2 product mole fractions: derived from 2010
DOE

X1_Ar = (-0.3392*CPP) + 0.3393;
X1_CO2 = CPP;
X1_N2 = (-0.4802*CPP) + 0.4802;
X1_O2 = (-0.185*CPP) + 0.185;

%Calculate molar mass of CO2 Product Stream

molmass_CO2product = X1_Ar * molmass_Ar + X1_CO2 * molmass_CO2 + X1_O2 *
molmass_O2 + X1_N2 * molmass_N2;

%Calculate mass fractions of 1 mol of this CO2 product

y1_Ar = (X1_Ar * molmass_Ar)/molmass_CO2product;
y1_CO2 = (X1_CO2 * molmass_CO2)/molmass_CO2product;
y1_N2 = (X1_N2 * molmass_N2)/molmass_CO2product;
y1_O2 = (X1_O2 * molmass_O2)/molmass_CO2product;

%Calculate actual mass of CO2 product constituents given specified CRR
%[theoretical grams]

CO2product_moles = CO2_mass_product_req / (y1_CO2 * molmass_CO2product);

mass1_Ar = (y1_Ar * molmass_CO2product) * CO2product_moles;
mass1_CO2 = CO2_mass_product_req;
mass1_N2 = (y1_N2 * molmass_CO2product) * CO2product_moles;
mass1_O2 = (y1_O2 * molmass_CO2product) * CO2product_moles;

%Calculate mass fractions of 1 mol of initial gas stream

yi_Ar = (Xi_Ar * molmass_Ar)/molmass_inlet;
yi_CO2 = (Xi_CO2 * molmass_CO2)/molmass_inlet;
yi_N2 = (Xi_N2 * molmass_N2)/molmass_inlet;
yi_O2 = (Xi_O2 * molmass_O2)/molmass_inlet;

%Calculate actual mass of initial gas stream [theoretical grams]

massi_Ar = yi_Ar * molmass_inlet;
massi_CO2 = yi_CO2 * molmass_inlet;
massi_N2 = yi_N2 * molmass_inlet;
massi_O2 = yi_O2 * molmass_inlet;

%Calculate actual mass of inert stream [theoretical grams]

mass2_Ar = massi_Ar - mass1_Ar;
mass2_CO2 = massi_CO2 - mass1_CO2;
mass2_N2 = massi_N2 - mass1_N2;
mass2_O2 = massi_O2 - mass1_O2;

```

```

mass2_total = mass2_Ar + mass2_CO2 + mass2_N2 + mass2_O2;

y2_Ar = mass2_Ar/mass2_total;
y2_CO2 = mass2_CO2/mass2_total;
y2_N2 = mass2_N2/mass2_total;
y2_O2 = mass2_O2/mass2_total;

%Convert calculated Inerts Stream mass fractions to aquire mole fractions

mol2_Ar = y2_Ar / molmass_Ar;
mol2_CO2 = y2_CO2 / molmass_CO2;
mol2_N2 = y2_N2 / molmass_N2;
mol2_O2 = y2_O2 / molmass_O2;

mol2_total = mol2_Ar + mol2_CO2 + mol2_N2 + mol2_O2;

X2_Ar = mol2_Ar / mol2_total;
X2_CO2 = mol2_CO2 / mol2_total;
X2_N2 = mol2_N2 / mol2_total;
X2_O2 = mol2_O2 / mol2_total;

%Calculate molar mass of Inert Stream

molmass_inert = X2_Ar * molmass_Ar + X2_CO2 * molmass_CO2 + X2_O2 *
molmass_O2 + X2_N2 * molmass_N2;

inertproduct_moles = mass2_total / molmass_inert;

%Calculate Water Stream moles

waterproduct_moles = Xi_H2O;

%State mold fractions of Water Stream

X3_H2O = 1;

%
%INLET CALCULATIONS
%

%Calculate Inlet Stream Exergies assuming pure components

phichemi_Ar = Ru*To*log(Xi_Ar);
phichemi_CO2 = Ru*To*log(Xi_CO2);
phichemi_H2O = Ru*To*log(Xi_H2O);
phichemi_N2 = Ru*To*log(Xi_N2);
phichemi_O2 = Ru*To*log(Xi_O2);

%Calculate total chemical exergy (neglecting sulfur as it has negligible
%effect and is not part of the GRI30 database)

```

```

phicheminlet = Xo_Ar*phichemo_Ar + Xo_CO2*phichemo_CO2 + Xo_H2O*phichemo_H2O
+ Xo_N2*phichemo_N2 + Xo_O2*phichemo_O2 + Xi_Ar*phichemi_Ar +
Xi_CO2*phichemi_CO2 + Xi_H2O*phichemi_H2O + Xi_N2*phichemi_N2 +
Xi_O2*phichemi_O2;

```

```

%Calculate physical exergy
%To and Po

```

```

gas = GRI30;
set(gas, 'T', To, 'P', Po, 'MoleFractions', 'AR:1');
ho_Ar = enthalpy_mole(gas);
so_Ar = entropy_mole(gas);

```

```

gas = GRI30;
set(gas, 'T', To, 'P', Po, 'MoleFractions', 'CO2:1');
ho_CO2 = enthalpy_mole(gas);
so_CO2 = entropy_mole(gas);

```

```

gas = GRI30;
set(gas, 'T', To, 'P', Po, 'MoleFractions', 'H2O:1');
ho_H2O = enthalpy_mole(gas);
so_H2O = entropy_mole(gas);

```

```

gas = GRI30;
set(gas, 'T', To, 'P', Po, 'MoleFractions', 'N2:1');
ho_N2 = enthalpy_mole(gas);
so_N2 = entropy_mole(gas);

```

```

gas = GRI30;
set(gas, 'T', To, 'P', Po, 'MoleFractions', 'O2:1');
ho_O2 = enthalpy_mole(gas);
so_O2 = entropy_mole(gas);

```

```

%Ti and Pi

```

```

gas = GRI30;
set(gas, 'T', Ti, 'P', Pi, 'MoleFractions', 'AR:1');
hi_Ar = enthalpy_mole(gas);
si_Ar = entropy_mole(gas);

```

```

gas = GRI30;
set(gas, 'T', Ti, 'P', Pi, 'MoleFractions', 'CO2:1');
hi_CO2 = enthalpy_mole(gas);
si_CO2 = entropy_mole(gas);

```

```

gas = GRI30;
set(gas, 'T', Ti, 'P', Pi, 'MoleFractions', 'H2O:1');
hi_H2O = enthalpy_mole(gas);
si_H2O = entropy_mole(gas);

```

```

gas = GRI30;
set(gas, 'T', Ti, 'P', Pi, 'MoleFractions', 'N2:1');
hi_N2 = enthalpy_mole(gas);
si_N2 = entropy_mole(gas);

```

```

gas = GRI30;
set(gas, 'T', Ti, 'P', Pi, 'MoleFractions', 'O2:1');
hi_O2 = enthalpy_mole(gas);
si_O2 = entropy_mole(gas);

%Calculate total physical exergy

phiphysinlet = (Xi_Ar*((hi_Ar - ho_Ar) - To*(si_Ar - so_Ar))) +
(Xi_CO2*((hi_CO2 - ho_CO2) - To*(si_CO2 - so_CO2))) + (Xi_H2O*((hi_H2O -
ho_H2O) - To*(si_H2O - so_H2O))) + (Xi_N2*((hi_N2 - ho_N2) - To*(si_N2 -
so_N2))) + (Xi_O2*((hi_O2 - ho_O2) - To*(si_O2 - so_O2)));

%Calculate Total Inlet Exergy [KJ/mol]

Inlet_Exergy = (phicheminlet + phiphysinlet)/10^6;

%
%OUTLET CALCULATIONS
%

%Calculate CO2 Product Stream Exergies assuming pure components

phichem1_Ar = Ru*To*log(X1_Ar);
phichem1_CO2 = Ru*To*log(X1_CO2);
phichem1_N2 = Ru*To*log(X1_N2);
phichem1_O2 = Ru*To*log(X1_O2);

%Calculate Inert Stream Exergies assuming pure components

phichem2_Ar = Ru*To*log(X2_Ar);
phichem2_CO2 = Ru*To*log(X2_CO2);
phichem2_N2 = Ru*To*log(X2_N2);
phichem2_O2 = Ru*To*log(X2_O2);

%Calculate Water Stream Exergies assuming pure components

phichem3_H2O = Ru*To*log(X3_H2O);

%Calculate total chemical exergy of CO2 Product Stream

phichem1 = Xo_Ar*phichemo_Ar + Xo_CO2*phichemo_CO2 + Xo_H2O*phichemo_H2O +
Xo_N2*phichemo_N2 + Xo_O2*phichemo_O2 + X1_Ar*phichem1_Ar +
X1_CO2*phichem1_CO2 + X1_N2*phichem1_N2 + X1_O2*phichem1_O2; %You must remove
components with mole fractions of zero else a NaN error is produced

%Calculate total chemical exergy of Inerts Stream

phichem2 = Xo_Ar*phichemo_Ar + Xo_CO2*phichemo_CO2 + Xo_H2O*phichemo_H2O +
Xo_N2*phichemo_N2 + Xo_O2*phichemo_O2 + X2_Ar*phichem2_Ar +
X2_CO2*phichem2_CO2 + X2_N2*phichem2_N2 + X2_O2*phichem2_O2;

```

```
%Calculate total chemical exergy of Water Stream
```

```
phichem3 = Xo_Ar*phichemo_Ar + Xo_CO2*phichemo_CO2 + Xo_H2O*phichemo_H2O +  
Xo_N2*phichemo_N2 + Xo_O2*phichemo_O2 + X3_H2O*phichem3_H2O;
```

```
%Calculate physical exergy
```

```
%To and Po
```

```
gas = GRI30;  
set(gas, 'T', To, 'P', Po, 'MoleFractions', 'AR:1');  
ho_Ar = enthalpy_mole(gas);  
so_Ar = entropy_mole(gas);
```

```
gas = GRI30;  
set(gas, 'T', To, 'P', Po, 'MoleFractions', 'CO2:1');  
ho_CO2 = enthalpy_mole(gas);  
so_CO2 = entropy_mole(gas);
```

```
gas = GRI30;  
set(gas, 'T', To, 'P', Po, 'MoleFractions', 'H2O:1');  
ho_H2O = enthalpy_mole(gas);  
so_H2O = entropy_mole(gas);
```

```
gas = GRI30;  
set(gas, 'T', To, 'P', Po, 'MoleFractions', 'N2:1');  
ho_N2 = enthalpy_mole(gas);  
so_N2 = entropy_mole(gas);
```

```
gas = GRI30;  
set(gas, 'T', To, 'P', Po, 'MoleFractions', 'O2:1');  
ho_O2 = enthalpy_mole(gas);  
so_O2 = entropy_mole(gas);
```

```
%T1 and P1
```

```
gas = GRI30;  
set(gas, 'T', T1, 'P', P1, 'MoleFractions', 'AR:1');  
h1_Ar = enthalpy_mole(gas);  
s1_Ar = entropy_mole(gas);
```

```
gas = GRI30;  
set(gas, 'T', T1, 'P', P1, 'MoleFractions', 'CO2:1');  
h1_CO2 = enthalpy_mole(gas);  
s1_CO2 = entropy_mole(gas);
```

```
gas = GRI30;  
set(gas, 'T', T1, 'P', P1, 'MoleFractions', 'N2:1');  
h1_N2 = enthalpy_mole(gas);  
s1_N2 = entropy_mole(gas);
```

```
gas = GRI30;  
set(gas, 'T', T1, 'P', P1, 'MoleFractions', 'O2:1');  
h1_O2 = enthalpy_mole(gas);
```

```

s1_O2 = entropy_mole(gas);

%T2 and P2

gas = GRI30;
set(gas, 'T', T2, 'P', P2, 'MoleFractions', 'AR:1');
h2_Ar = enthalpy_mole(gas);
s2_Ar = entropy_mole(gas);

gas = GRI30;
set(gas, 'T', T2, 'P', P2, 'MoleFractions', 'CO2:1');
h2_CO2 = enthalpy_mole(gas);
s2_CO2 = entropy_mole(gas);

gas = GRI30;
set(gas, 'T', T2, 'P', P2, 'MoleFractions', 'N2:1');
h2_N2 = enthalpy_mole(gas);
s2_N2 = entropy_mole(gas);

gas = GRI30;
set(gas, 'T', T2, 'P', P2, 'MoleFractions', 'O2:1');
h2_O2 = enthalpy_mole(gas);
s2_O2 = entropy_mole(gas);

%T3 and P3

gas = GRI30;
set(gas, 'T', T3, 'P', P3, 'MoleFractions', 'H2O:1');
h3_H2O = enthalpy_mole(gas);
s3_H2O = entropy_mole(gas);

%Calculate physical exergy of CO2 Product Stream

phiphysCO2product = X1_Ar*((h1_Ar - ho_Ar)-To*(s1_Ar - so_Ar)) +
X1_CO2*((h1_CO2 - ho_CO2) - To*(s1_CO2 -so_CO2)) + X1_N2*((h1_N2 - ho_N2) -
To*(s1_N2 -so_N2)) + X1_O2*((h1_O2 - ho_O2) - To*(s1_O2 -so_O2));

%Calculate physical exergy of Inert Stream

phiphysinert = X2_Ar*((h2_Ar - ho_Ar)-To*(s2_Ar - so_Ar)) + X2_CO2*((h2_CO2 -
ho_CO2) - To*(s2_CO2 -so_CO2)) + X2_N2*((h2_N2 - ho_N2) - To*(s2_N2 -so_N2))
+ X2_O2*((h2_O2 - ho_O2) - To*(s2_O2 -so_O2));

%Calculate physical exergy of Water Stream

phiphyswater = X3_H2O*((h3_H2O - ho_H2O)-To*(s3_H2O - so_H2O));

%Calculate phase change exergy of Water Stream

%phiphasewater = enthalpy_H2Ovap;

```

```

%Calculate Total CO2 Product Exergy [KJ/mol]
CO2product_Exergy = (phichem1 + phiphysCO2product)/10^6;

%Calculate Total Inert Stream Exergy [KJ/mol]
Inert_Exergy = (phichem2 + phiphysinert)/10^6;

%Calculate Total Water Stream Exergy [KJ/mol]
Water_Exergy = (phichem3 + phiphyswater)/10^6; %removed phiphasewater

%Calculate Total CPU Output Exergy [KJ/mol]
Output_Exergy = (CO2product_Exergy + Inert_Exergy + Water_Exergy)/10^6;

%
%Stream flow conversions for reporting on mass basis: desire output unit of
%KJ/Kg CO2 in CO2 product stream.
%

%Use necessary mass flow of carbon dioxide in product to determine molal
%flow of all streams.

molal_multiplier = 1000/CO2_mass_product_req;

%Determine required inlet molar flow for 1 Kg CO2 output

molarflow_inlet = molal_multiplier;
molarflow_inert = molal_multiplier * inertproduct_moles;
molarflow_CO2product = molal_multiplier * CO2product_moles;
molarflow_water = molal_multiplier * waterproduct_moles;
%
%Calculate net exergy flow through separation system [kJ/kg CO2]
%

Net_Exergy = (molarflow_inlet * Inlet_Exergy) - (molarflow_inert *
Inert_Exergy + molarflow_CO2product * CO2product_Exergy + molarflow_water *
Water_Exergy)

%Convert to [kWh/tonne CO2]

Minimum_Separation_Work = Net_Exergy/3.6

```

## Appendix D Case Studies

	Case 1a	Case 1b	Case 1c	Case 2	Case 3
Plant Type	PC Supercritical	PC Subcritical	PC USC	PC Supercritical	PC Supercritical
Coal Type	Illinois #6	Illinois #6	Illinois #6	App. Low Sulfur	ND Lignite
Fuel Flow Rate					
Coal (tonnes/hr)	172.3	183.4	156	150	362
Natural Gas (tonnes/hr)					
Gross Electrical Output (MWe)	535.5	538.6	532.2	528.3	541.9
Auxiliary Electrical Loads (MWe)					
Auxiliary Power Produced (MWe)					
Base Plant	17.3	18.74	15.66	15.89	27.98
Hot Side SCR	2.607	2.775	2.363	2.479	3.093
Fabric Filter	0.3031	0.3227	0.2745	0.2551	0.3168
Wet FGD / SDA	8.5484	9.132	7.784	2.906	3.652
Cooling Tower	6.694	7.594	6.061	6.604	6.774
Air Separation Unit					
CO2 Separation & Comp.					
Net Electrical Output (MWe)	500	500	500	500	500
Plant Efficiency (% HHV)	38.48	36.14	42.5	39.44	35.51
Annual Power Generation (BkWh/yr)	3.287	3.287	3.287	3.287	3.287
CO2 Emissions (kg/kWh)	0.8148	0.8675	0.7379	0.7887	0.9295
Base Plant (TCR) (2012 \$M)	796.8	705.7	905.7	779.7	885.9
Capture System (TCR)					
Cooling Tower (TCR)	46.75	51.88	38.95	46.15	47.29
Nox Control (TCR)	34.268	35.443	32.54	33.264	35.841
TSP Control (TCR)	29.99	31.5	27.76	26.26	32.06
SO2 Control (TCR)	134.8	138.7	133.5	75.82	91.78
Capture O&M/Year					
BOP O&M/Year	92.67	95.23	88.33	67.89	58.45
Total Plant Capital Requirement	1043	963.3	1139	965.4	1096
Total Plant O&M Costs/Year	92.67	95.23	88.33	67.89	58.45
Capital Required (\$/kW-net)	2086	1927	2277	1931	2192
Revenue Required (\$/MWh)	63.97	62.02	65.93	63.41	66.07
Added Cost of CCS (\$/MWh)					
Cost of CO2 Avoided (\$/tonne)					
Cost of CO2 Captured (\$/tonne)					

	Case 4	Case 5	Case 6	Case 7	Case 8a
Plant Type	PC Supercritical	USC	NGCC	Amine NGCC	Oxy Supercritical
Coal Type	PRB	PRB	Nat. Gas	Nat. Gas	Illinois #6
Fuel Flow Rate					
Coal (tonnes/hr)	249.8	226.2			218.8
Natural Gas (tonnes/hr)			79.99	79.99	
Gross Electrical Output (MWe)	534.9	531.5	596.7	540.8	680.1
Auxiliary Electrical Loads (MWe)					
Auxiliary Power Produced (MWe)					
Base Plant	21.68	19.62	11.93	10.82	21.97
Hot Side SCR	2.834	2.59			
Fabric Filter	0.2893	0.2619			0.2018
Wet FGD / SDA	3.285	2.975			6.355
Cooling Tower	6.686	6.053	3.877	2.871	8.501
Air Separation Unit					87.44
CO2 Separation & Comp.				81.48	55.57
Net Electrical Output (MWe)	500	500	580.9	501.6	500
Plant Efficiency (% HHV)	37.14	41.02	49.99	43.16	30.3
Annual Power Generation (BkWh/yr)	3.287	3.287	3.819	3.298	3.288
CO2 Emissions (kg/kWh)	0.8822	0.7987	0.3642	0.04218	0.1036
Base Plant (TCR) (2012 \$M)	821.6	932.2	429.2	407.4	959.8
Capture System (TCR)		0		272.5	744
Cooling Tower (TCR)	46.7	38.9	29.64	41.93	69.29
Nox Control (TCR)	36.11	34.25			9.866
TSP Control (TCR)	28.64	26.51			22.36
SO2 Control (TCR)	79.92	75.87			130.2
Capture O&M/Year				29.5	83.71
BOP O&M/Year	58.37	53.48	190.4	179.5	68.09
Total Plant Capital Requirement	1016	1108	458.8	721.8	1936
Total Plant O&M Costs/Year	58.37	53.48	190.4	209	151.8
Capital Required (\$/kW-net)	2031	2215	789.8	1439	3871
Revenue Required (\$/MWh)	52.6	54.27	63.39	88.07	112.6
Added Cost of CCS (\$/MWh)					48.6
Cost of CO2 Avoided (\$/tonne)					68.34
Cost of CO2 Captured (\$/tonne)					46.82

	Case 8b	Case 8c	Case 9a	Case 9b	Case 9c
Plant Type	Oxy Subcritical	Oxy USC	Oxy Supercritical	Oxy Subcritical	Oxy USC
Coal Type	Illinois #6	Illinois #6	Illinois #6	Illinois #6	Illinois #6
Fuel Flow Rate					
Coal (tonnes/hr)	236	194.4	222.6	240.4	197.4
Natural Gas (tonnes/hr)					
Gross Electrical Output (MWe)	692.8	663.2	691.8	705.7	673.4
Auxiliary Electrical Loads (MWe)					
Auxiliary Power Produced (MWe)					
Base Plant	24.11	19.52	22.35	24.56	19.82
Hot Side SCR					
Fabric Filter	0.2176	0.1793	0.2053	0.2217	0.182
Wet FGD / SDA	6.847	5.654	6.464	6.975	5.741
Cooling Tower	9.768	7.553	8.648	9.95	7.669
Air Separation Unit	91.89	80.89	88.43	93.01	81.71
CO2 Separation & Comp.	59.93	49.38	65.68	70.92	58.25
Net Electrical Output (MWe)	500	500	500	500	500
Plant Efficiency (% HHV)	28.1	34.1	29.79	27.59	33.59
Annual Power Generation (BkWh/yr)	3.287	3.287	3.287	3.288	3.287
CO2 Emissions (kg/kWh)	0.1117	0.09201	0	0	0
Base Plant (TCR) (2012 \$M)	858.1	1075	972.6	870.5	1088
Capture System (TCR)	776.2	696.2	794	829.4	741.9
Cooling Tower (TCR)	75.97	58.66	70.29	77.05	59.48
Nox Control (TCR)	10.05	9.621	10.04	10.24	9.769
TSP Control (TCR)	23.69	20.43	22.65	24.03	20.67
SO2 Control (TCR)	134.6	123.8	131.2	135.7	124.6
Capture O&M/Year	85.04	80.44	90.91	92.51	87.09
BOP O&M/Year	72.56	62.36	66.49	71.09	60.71
Total Plant Capital Requirement	1879	1984	2001	1947	2045
Total Plant O&M Costs/Year	157.6	142.8	157.4	163.6	147.8
Capital Required (\$/kW-net)	3757	3968	4002	3894	4089
Revenue Required (\$/MWh)	112.4	111.5	116.5	116.6	115.1
Added Cost of CCS (\$/MWh)	50.36	45.56	52.55	54.52	49.15
Cost of CO2 Avoided (\$/tonne)	66.61	70.53	64.51	62.83	66.6
Cost of CO2 Captured (\$/tonne)	45.04	49.25	39.39	37.89	41.42

	Case 10	Case 11	Case 12	Case 13	Case 14
Plant Type	Oxy Supercritical				
Coal Type	AppLow	ND Lignite	PRB	PRB	PRB
Fuel Flow Rate					
Coal (tonnes/hr)	184.7	462.8	316.5	314.7	310.4
Natural Gas (tonnes/hr)					
Gross Electrical Output (MWe)	650.7	693.2	678	674	664.9
Auxiliary Electrical Loads (MWe)					
Auxiliary Power Produced (MWe)	18.12	19.76	17.28	18.94	24.63
Base Plant	19.57	35.79	27.48	27.31	26.95
Hot Side SCR					
Fabric Filter	0.2033	0.2603	0.2601	0.2374	0.1478
Wet FGD / SDA	2.239	2.895	7.635	2.592	1.615
Cooling Tower	8.134	8.665	8.475	8.425	8.311
Air Separation Unit	84.6	94.09	90.25	89.88	89.08
CO2 Separation & Comp.	54.06	71.27	61.49	64.53	62.85
Net Electrical Output (MWe)	500	500	500	500	500
Plant Efficiency (% HHV)	32.02	27.78	29.31	29.48	29.89
Annual Power Generation (BkWh/yr)	3.287	3.287	3.287	3.287	3.287
CO2 Emissions (kg/kWh)	0.09714	0.1188	0.112	0.1111	0.1097
Base Plant (TCR) (2012 \$M)	917.1	1071	987.9	983.3	973
Capture System (TCR)	672.3	758.8	727.7	724.2	715.7
Cooling Tower (TCR)	63.08	74.43	71.07	69.73	67.99
Nox Control (TCR)	9.439	10.06	9.835	9.777	9.645
TSP Control (TCR)	22.36	27.95	26.65	24.89	39.38
SO2 Control (TCR)	68.87	87.1	111.5	72.97	57.24
Capture O&M/Year	81.52	93.22	77.95	78.5	77.67
BOP O&M/Year	64.88	57.58	27.45	24.3	24.13
Total Plant Capital Requirement	1753	2030	1935	1885	1863
Total Plant O&M Costs/Year	146.4	150.8	105.4	102.8	101.8
Capital Required (\$/kW-net)	3506	4059	3870	3770	3726
Revenue Required (\$/MWh)	104.7	115.5	98.44	95.95	94.88
Added Cost of CCS (\$/MWh)	41.26	49.44	45.84	43.35	42.28
Cost of CO2 Avoided (\$/tonne)	59.65	60.99	59.51	56.22	54.73
Cost of CO2 Captured (\$/tonne)	41.65	41.37	40.43	38.28	37.73

	Case 14a	Case 15	Case 16	Case 16a	Case 17
Plant Type	Oxy Supercritical	Oxy Supercritical	Oxy Supercritical	Oxy Supercritical	PC Supercritical
Coal Type	PRB	PRB	PRB	FCF=.14	PRB
Fuel Flow Rate					
Coal (tonnes/hr)	310.4	270.9	314.9	314.9	361.9
Natural Gas (tonnes/hr)					
Gross Electrical Output (MWe)	664.9	580.1	674.4	674.4	632.8
Auxiliary Electrical Loads (MWe)					142
Auxiliary Power Produced (MWe)	24.63	3.582	25.54	25.54	
Base Plant	26.95	23.51	27.33	27.33	30.17
Hot Side SCR					
Fabric Filter	0.1478	0.1238	0.1499	0.1499	0.4754
Wet FGD / SDA	1.615	1.35	1.638	1.638	18.9
Cooling Tower	8.311	7.251	8.43	8.43	17.72
Air Separation Unit	89.08	16.37	89.91	89.91	
CO2 Separation & Comp.	62.85	34.62	71.91	71.91	61.43
Net Electrical Output (MWe)	500	500	500	500	500
Plant Efficiency (% HHV)	29.89	34.26	29.47	29.47	25.64
Annual Power Generation (BkWh/yr)	3.287	3.287	3.287	3.287	3.287
CO2 Emissions (kg/kWh)	0.1097	0.0957	0	0	0.1281
Base Plant (TCR) (2012 \$M)	973	875	983.8	983.8	1043
Capture System (TCR)	715.7	659.1	765.7	765.7	561.4
Cooling Tower (TCR)	67.99	60.45	68.8	68.8	80.49
Nox Control (TCR)	9.645	8.415	9.783	9.783	45.67
TSP Control (TCR)	39.38	33.97	39.78	39.78	40.28
SO2 Control (TCR)	57.24	51.78	57.71	57.71	153.6
Capture O&M/Year	77.67	52.24	83.91	83.91	51.92
BOP O&M/Year	24.13	42.83	22.49	22.49	56.78
Total Plant Capital Requirement	1863	1689	1926	1926	1925
Total Plant O&M Costs/Year	101.8	95.07	106.4	106.4	108.7
Capital Required (\$/kW-net)	3726	3377	3851	3851	3850
Revenue Required (\$/MWh)	110.8	86.85	98.42	114.9	99.12
Added Cost of CCS (\$/MWh)	58.17	34.25	45.82	62.27	46.52
Cost of CO2 Avoided (\$/tonne)	75.29	43.55	51.94	70.58	61.69
Cost of CO2 Captured (\$/tonne)	53.3	33.8	32.69	45.61	35.87

## Appendix E Illinois #6 IECM Base Plant: Full IECM Configuration

Parameter	Value
<b>Configure Session</b>	
Fuel Type	Coal
NOx Control	In-Furnace Controls
NOx Control	Hot-Side SCR
Particulates	Fabric Filter
SO2 Control	Wet FGD
Mercury	Carbon Injection
CO2 Capture	None
Cooling System	Wet Cooling Tower
Wastewater	Ash Pond
Flyash Disposal	No Mixing
<b>Set Parameters/ Overall Plant/ Performance</b>	
Gross Electrical Output (MWg)	535.5
Capacity Factor (%)	75
Ambient Air Temperature (Dry Bulb Average) (deg. C)	25
Ambient Air Pressure (Average) (MPa)	0.1014
Relative Humidity (Average) (%)	50
Ambient Air Humidity (Average) (kg H2O/kg dry air)	9.88E-03
Oxygen Content in Air/Oxidant (vol %)	20.63
<b>Set Parameters/ Overall Plant/ Regulations &amp; Taxes</b>	
Sulfur Dioxide Emission Constraint (mg/KJ)	0.258
Nitrogen Oxide Emission Constraint (mg/KJ)	6.45E-02
Particulate Emission Constraint (mg/KJ)	1.29E-02
Total Mercury Removal Efficiency (%)	70
<b>Set Parameters/ Overall Plant/ Financing</b>	
Year Cost Reported	2012
Constant or Current Dollars?	Constant
Discount Rate (Before Taxes)	7.09E-02
Fixed Charge Factor (FCF)	0.1128
<b>Set Parameters/ Overall Plant/ Fuel Cost</b>	
As-Delivered Coal Cost (\$/tonne)	42.09
Natural Gas Cost (\$/mscm)	264
Real Escalation Rate (fuel) (%/yr)	0
Internal Cost of Electricity for Component Allocations	Base Plant
Internal Electricity Price (\$/MWh)	47.12
<b>Set Parameters/ Overall Plant/ O&amp;M Cost</b>	
Activated Carbon Cost (\$/tonne)	2453
Alum Cost (\$/tonne)	413.8
Ammonia Cost (\$/tonne)	152.1
Caustic (NaOH) Cost (\$/tonne)	506.5
Dibasic Acid Cost (\$/tonne)	648.7
Flocculant Polymer Cost (\$/tonne)	4858
Lime Cost (\$/tonne)	112
Limestone Cost (\$/tonne)	25.76
MEA/Amines Cost (\$/tonne)	2657
SCR Catalyst Cost (\$/cu m)	6092
Urea Cost (\$/tonne)	567.7
Water Cost (\$/kliter)	0.3027
Operating Labor Rate (\$/hr)	34.65
Real Escalation Rate (for all above) (%/yr)	0
<b>Set Parameters/ Base Plant/ Base Plant Performance</b>	

Gross Electrical Output (MWg)	535.5
Unit Type	Supercritical
Steam Cycle Heat Rate, HHV (kJ/kWh)	7764
Boiler Firing Type	Tangential
Boiler Efficiency (%)	88.89
Excess Air For Furnace (% stoich.)	20
Leakage Air at Preheater (% stoich.)	10
Gas Temperature Exiting Economizer (deg. C)	371.1
Gas Temperature Exiting Air Preheater (deg. C)	148.9
Percent Water in Bottom Ash Sluice (%)	0
Coal Pulverizer (% MWg)	0.55
Steam Cycle Pumps (% MWg)	0.2
Force/Induced Draft Fans (% MWg)	1.51
Miscellaneous (% MWg)	0.97
<b>Set Parameters/ Base Plant/ Steam Cycle Performance</b>	
Seam Energy Added in Boiler (kJ/kg)	2680
Boiler Blowdown (%)	6
Miscellaneous Steam Losses (%)	0.4
Demineraliser Underflow (%)	8.5
Cooling Water Temperature Rise (deg. C)	11.11
Auxillary Heat Exchanger Load (%)	1.41
<b>Set Parameters/ Base Plant/ Capital Cost</b>	
Construction Time (years)	3
General Facilities Capital (%PFC)	10
Engineering & Home Office Fees (E) (%PFC)	6.5
Process Contingency Cost (C) (%PFC)	2
Project Contingency Cost %(PFC+E+C)	10
Royalty Fees (%PFC)	0.07
Fixed Operating Cost (mnths)	1
Variable Operating Cost (mnths)	1
Miscellaneous Capital Cost (%TPI)	2
Inventory Capital (%TPC)	0.06
% TCR Amortized (%)	0
<b>Set Parameters/ Base Plant/ O&amp;M Cost</b>	
As-Delivered Coal Cost (\$/tonne)	42.09
Waste Disposal Cost (\$/tonne)	10.32
Water Cost (\$/kliter)	0.3027
Electricity Price (Internal) (\$/MWh)	47.12
Number of Operating Jobs	20
Number of Operating Shifts (shifts/day)	4.75
Operating Labor Rate (\$/hr)	34.65
Total Maintenance Cost (%TPC)	1.881
Maintenance Cost Allocated to Labor (%TMC)	35
Administrative & Support Cost (% total labor)	7
<b>Set Parameters/ NOx Control/ In-Furnace Controls/ Performance</b>	
Actual Nox Removal Efficiency (%)	39.06
Maximum Nox Removal Efficiency (%)	50
<b>Set Parameters/ NOx Control/ In-Furnace Controls/ Capital Cost</b>	
Combustion Modification (\$/kw-gross)	8.913
<b>Set Parameters/ Nox Control/ Hot-Side SCR/ Performance</b>	
Actual Nox Removal Efficiency (%)	61.7
Maximum Nox Removal Efficiency (%)	90
Particulate Rmoval Efficiency (%)	0

Number of SCR Trains	2
Number of Spare SCR Trains	0
<i>Number of Catalyst Layers</i>	
Dummy Layers	1
Initial Layers	3
Reserve Layers	0
Catalyst Replacement Interval (hours)	10000
Catalyst Space Velocity (1/hr)	3496
Ammonia Stoichiometry (mol NH <sub>3</sub> /mol Nox)	0.6248
Steam to Ammonia Ratio (mol H <sub>2</sub> O/mol NH <sub>3</sub> )	19
Total Pressure Drop Across SCR (cm H <sub>2</sub> O gauge)	22.86
Oxidation of SO <sub>2</sub> to SO <sub>3</sub> (vol %)	0.8579
Hot-Side SCR Power Requirement (% MWg)	0.4869
<i>Reference Parameters</i>	
Space Velocity (1/hr)	2500
Catalyst Replacement Interval (hours)	5694
Ammonia Slip (ppmv)	2
Temperature (deg. K)	644.4
Nox Removal Efficiency (%)	80
Nox Concentration (ppmw)	500
<i>Reference Catalyst Activity</i>	
Minimum Activity (fraction)	0.5
Reference Time (hours)	1.00E+04
Activity at Reference Time (fraction)	0.85
Ammonia Deposition on Preheater (%)	5
Ammonia Deposition on Fly Ash (%)	50
Ammonia in High Concentration Wash Water (mg/liter)	310
Ammonia in Low Concentration Wash Water (mg/liter)	40
Ammonia Removed from Wash Water (%)	67
<b>Set Parameters/ Nox Control/ Hot-Side SCR/ Capital Cost</b>	
Construction Time (years)	2
General Facilities Capital (%PFC)	10
Engineering & Home Office Fees (E) (%PFC)	10
Process Contingency Cost (C) (%PFC)	6.965
Project Contingency Cost (%(PFC+E+C))	15
Royalty Fees (%PFC)	0
<i>Pre-Production Costs</i>	
Months of Fixed O&M (months)	1
Months of Variable O&M (months)	1
Miscellaneous Capital Cost (%TPI)	2
Inventory Capital (%TPC)	0.5
%TCR Amortized (%)	0
<b>Set Parameters/ Nox Control/ Hot-Side SCR/ O&amp;M Cost</b>	
Catalyst Cost (\$/cu m)	6092
Ammonia Cost (\$/tonne)	152.1
Electricity Price (internal) (\$/MWh)	47.12
Number of Operation Jobs (jobs/shift)	0.46
Number of Operating Shifts (shifts/day)	4.75
Operating Labor Rate (\$/hr)	34.65
Total Maintenance Cost (%TPI)	2
Maintenance Cost Allocated to Labor (% total)	40
Administrative & Support Cost (% total labor)	30
<b>Set Parameters/ TSP Control/ Config</b>	

Fabric Filter Type	PJ (Pulse-jet)
<b>Set Parameters/ TSP Control/ Performance</b>	
Particulate Removal Efficiency (%)	99.56
Actual SO3 Removal Efficiency (%)	90
Solids Loading Out (grains/scm)	0.5297
Number of Baghouse Units	2
Number of Compartments per Unit	14
Number of Bags per Compartment	230
Bag Length (meters)	6.096
Bag Diameter (meters)	0.3048
Bag Life (years)	3
Air to Cloth Ratio (acmm/sq m)	1.113
Total Pressure Drop Across Fabric Filter (cm H2O gauge)	17.87
Percent Water in Fabric Filter Discharge (%)	0
Fabric Filter Power Requirement (% MWg)	5.66E-02
<b>Set Parameters/ TSP Control/ Capital Cost</b>	
Construction Time (years)	3
General Facilities Capital (%PFC)	1
Engineering & Home Office Fees (E) (%PFC)	5
Process Contingency Cost (C) (%PFC)	5
Project Contingency Cost (%(PFC+E+C))	15
Royalty Fees (%PFC)	0
<i>Pre-Production Costs</i>	
Months of Fixed O&M (months)	1
Months of Variable O&M (months)	1
Miscellaneous Capital Cost (%TPI)	2
Inventory Capital (%TPC)	0.5
%TCR Amortized (%)	0
<b>Set Parameters/ TSP Control/ O&amp;M Cost</b>	
Fabric Filter Bag Cost (\$/bag)	130.8
Waste Disposal Cost (\$/tonne)	19.07
Electricity Price (internal) (\$/MWh)	47.12
Number of Operating Jobs (jobs/shifts)	1.33
Number of Operating Shifts (shifts/day)	4.75
Operating Labor Rate (\$/hr)	34.65
Total Maintenance Cost (%TPC)	1.807
Maintenance Cost Allocated to Labor (% total)	40
Administrative & Support Cost (% total labor)	30
<b>Set Parameters/ SO2 Control/ Config</b>	
Reagent	Limestone
Flue Gas Bypass Control	No Bypass
<b>Set Parameters/ SO2 Control/ Performance</b>	
Maximum SO2 Removal Efficiency (%)	98
Scrubber SO2 Removal Efficiency (%)	85.45
Scrubber SO3 Removal Efficiency (%)	50
Particulate Removal Efficiency (%)	50
Absorber Capacity (% acmm)	100
Number of Operating Absorbers (integer)	1
Number of Spare Absorbers	0
Liquid-to-Gas Ratio (lpm/kacmm)	1.20E+04
Reagent Stoichiometry (mol Ca/mol S rem)	1.03
Reagent Purity (wt %)	92.4
Reagent Moisture Content (wt %)	0

Total Pressure Drop Across FGD (cm H2O gauge)	25.4
Temperature Rise Across FGD (deg. C)	7.778
Gas Temperature Exiting Scrubber (deg. C)	54.83
Gas Temperature Exiting Reheater (deg. C)	54.83
Entrained Water Past Demister (% evap H2O)	0.79
Oxidation of CaSO3 to CaSO4 (%)	90
Wet FGD Power Requirement (% MWg)	1.603
<b>Set Parameters/ SO2 Control/ Additives</b>	
Chlorine Removal Efficiency (%)	90
<b>Set Parameters/ SO2 Control/ Capital Cost</b>	
Construction Time (years)	2
General Facilities Capital (%PFC)	10
Engineering & Home Office Fees (E) (%PFC)	10
Process Contingency Cost (C) (%PFC)	2
Project Contingency Cost (%(PFC+E+C))	15
Royalty Fees (%PFC)	0.5
<i>Pre-Production Costs</i>	
Months of Fixed O&M (months)	1
Months of Variable O&M (months)	1
Miscellaneous Capital Cost (%TPI)	2
Inventory Capital (%TPC)	0.3641
%TCR Amortized (%)	0
<b>Set Parameters/ SO2 Control/ O&amp;M Cost</b>	
Bulk Reagent Storage Time (days)	60
Limestone Cost (\$/tonne)	25.76
Lime Cost (\$/tonne)	112
Stacking Cost (\$/tonne)	8.559
Waste Disposal Cost (\$/tonne)	14.68
Electricity Price (internal) (\$/MWh)	47.12
Number of Operating Jobs (jobs/shift)	6.67
Number of Operating Shifts (shifts/day)	4.75
Operating Labor Rate (\$/hr)	34.65
Total Maintenance Cost (%TPC)	4.253
Maintenance Cost Allocated to Labor (% total)	40
Administrative & Support Cost (% total labor)	30
<b>Set Parameters/ Mercury/ Removal Efficiency</b>	
Furnace Removal (total)(%)	7
Fabric Filter (total w/o control)(%)	39
Fabric Filter (oxidized)(%)	39
Fabric Filter (elemental)(%)	39
Wet FGD (oxidized)(%)	95
Wet FGD (elemental)(%)	0
Wet FGD (particulate)(%)	0
<i>Percent Increase in Speciation</i>	
In-furnace Nox (oxidized)(%)	0
SNCR (oxidized)(%)	0
Hot-Side SCR (oxidized)(%)	35
<b>Set Parameters/ Mercury/ Carbon Injection</b>	
Carbon Injection Rate (kg C/Macmm)	0
Carbon Injection Power Reqmt (% MWg)	1.01E-02
<b>Set Parameters/ Mercury/ Capital Cost</b>	
Construction Time (years)	1
General Facilities Capital (%PFC)	5

Engineering & Home Office Fees (E) (%PFC)	10
Process Contingency Cost (C) (%PFC)	5
Project Contingency Cost %(PFC+E+C)	15
Royalty Fees (%PFC)	0
<i>Pre-Production Costs</i>	
Months of Fixed O&M (months)	1
Months of Variable O&M (months)	1
Miscellaneous Capital Cost (%TPI)	2
Inventory Capital (%TPC)	0.5
%TCR Amortized (%)	0
<b>Set Parameters/ Mercury/ O&amp;M Cost</b>	
Activate Carbon Cost (w. shipping)(\$/tonne)	2453
Disposal Cost (\$/tonne)	19.07
Electricity Price (internal) (\$/MWh)	47.12
Number of Operating Jobs (jobs/shift)	0.175
Number of Operating Shifts (shifts/day)	4.75
Operating Labor Rate (\$/hr)	34.65
Total Maintenance Cost (%TPC)	1.48E-02
Maintenance Cost Allocated to Labor (% total)	40
Administrative & Support Cost (% total labor)	25
<b>Set Parameters/ Water Systems/ Config</b>	
Air Flow Draft Control Type	Forced
Slip Stream Treatment System	No
Makeup Water Treatment System	No
<b>Set Parameters/ Water Systems/ Performance</b>	
Ambient Air Temperature (Dry Bulb Average) (deg. C)	25
Air Wet Bulb Temperature (Average) (deg. C)	18.11
Cooling Water Inlet Temperature (deg. C)	32.22
Cooling Water Temperature Drop (deg. C)	11.11
Cycles of Concentration	4
Tower Drift Loss (%)	1.00E-03
Auxiliary Cooling Load (%)	1.41
Tower Overdesign Factor (% total load)	0
Power Requirement (% MWg)	1.25
<b>Set Parameters/ Water Systems/ Capital Cost</b>	
Construction Time (years)	3
General Facilities Capital (%PFC)	10
Engineering & Home Office Fees (E) (%PFC)	10
Process Contingency Cost (C) (%PFC)	0
Project Contingency Cost %(PFC+E+C)	15
Royalty Fees (%PFC)	0.5
<i>Pre-Production Costs</i>	
Months of Fixed O&M (months)	1
Months of Variable O&M (months)	1
Miscellaneous Capital Cost (%TPI)	2
Inventory Capital (%TPC)	0.5
%TCR Amortized (%)	0
<b>Set Parameters/ Water Systems/ O&amp;M Cost</b>	
Water Cost (\$/kliter)	0.3027
Waste Disposal Cost (\$/tonne)	0
Electricity Price (internal) (\$/MWh)	47.12
Number of Operating Jobs (jobs/shift)	1
Number of Operating Shifts (shifts/day)	4.75

Operating Labor Rate (\$/hr)	34.65
Total Maintenance Cost (%TPC)	2
Maintenance Cost Allocated to Labor (% total)	40
Administrative & Support Cost (% total labor)	30
<b>Set Parameters/ By-Prod. Mgmt/ Bottom Ash Performance</b>	
Water Content of Residue (%)	39.3
<b>Set Parameters/ By-Prod. Mgmt/ Wastewater Treatment Perf.</b>	
Fireside Cleaning Wastewater (lpd/MW)	10.98
Air Preheater Cleaning Wastewater (lpd/MW)	54.89
Floor & Yard Drain Wastewater (lpd/MW)	151.4
Average Annual Rainfall (cm/yr)	101.6
Coal Pile Height (meters)	3.048